INTERNATIONAL CERAMICS AND COMPOSITE MATERIALS SYMPOSIUM

November 15-16, 2024

Süleyman Demirel University, Isparta, Türkiye

PROCEEDINGS BOOK

EDITORS
Assoc. Prof. Dr. Serap ÜNAL
Dr. Ethem İlhan ŞAHİN

ISBN: 978-625-378-045-6

PROCEEDINGS BOOK

INTERNATIONAL CERAMICS AND COMPOSITE MATERIALS SYMPOSIUM

November 15-16, 2024

Süleyman Demirel University, Isparta, Türkiye

Editors

Assoc. Prof. Dr. Serap ÜNAL

Dr. Ethem İlhan ŞAHİN

Institute Of Economic Development And Social Researches Publications®
(The Licence Number of Publicator: 2014/31220)
TÜRKİYE

www.iksadkongre.com/ceramic
E posta: konferanstanitim@gmail.com

All rights of this book belong to IKSAD Publishing House
Authors are responsible both ethically and jurisdically
Iksad Publications - 2024©
Issued Date: 20.12.2024

ISBN: 978-625-378-045-6

https://doi.org/10.5281/zenodo.14537144

CONGRESS ID

TITLE OF CONGRESS

INTERNATIONAL CERAMICS AND COMPOSITE MATERIALS SYMPOSIUM

PARTICIPATION

Keynote & Invited

DATE - PLACE

November 15-16, 2024

Süleyman Demirel University, Isparta, Türkiye

ORGANIZATION

Süleyman Demirel University, Isparta, Türkiye

&

IKSAD-Institute of Economic Development and Social Researches

Head of Organizing Committee

Assoc. Prof. Dr. Serap ÜNAL *(Süleyman Demirel University)*

Organizing Committee and Members

Prof. Dr. Ayşe ÖNDÜRÜCÜ, *Süleyman Demirel University*
Prof. Dr. Ayşegül UYGUN ÖKSÜZ, *Süleyman Demirel University*
Prof. Dr. Bilgehan İlker HARMAN, *Süleyman Demirel University*
Prof. Dr. Gülcan ÖZKAN, *Süleyman Demirel University*
Prof. Dr. Mehmet AVCAR, *Süleyman Demirel University*
Prof. Dr. Mustafa GENÇ, *Süleyman Demirel University*
Prof. Dr. Recai Fatih TUNAY, *Süleyman Demirel University*

Prof. Dr. Serdal TERZİ, *Süleyman Demirel University*
Assist. Prof. Dr. Ekinhan EİŞKİN, *Süleyman Demirel University*
Res. Assist. Ayşe Melike BİRCAN, *Süleyman Demirel University*

Congress Science & Advisory Board

Prof. Dr. Ahmet YILDIZ - *Afyon Kocatepe University, Türkiye*
Prof. Dr. Ali Fatih YETİM - *Erzurum Technical University, Türkiye*
Prof. Dr. António Mendes FERREİRA - *University of Porto, Portugal*
Prof. Dr. Atila GÜL - *Süleyman Demirel University, Türkiye*
Prof. Dr. Ayşe ÖNDÜRÜCÜ - *Süleyman Demirel University, Türkiye*
Prof. Dr. Ayşegül Uygun Öksüz - *Süleyman Demirel University, Türkiye*
Prof. Dr. Bilgehan İlker HARMAN - *Süleyman Demirel University, Türkiye*
Prof. Dr. Candan Terwiel - *Hacettepe University, Türkiye*
Prof. Dr. Demet YILMAZ - *Süleyman Demirel University, Türkiye*
Prof. Dr. Enis Kemal SAGULAR - *Süleyman Demirel University, Türkiye*
Prof. Dr. Ertuğrul DURAK - *Süleyman Demirel University, Türkiye*
Prof. Dr. Esengül KIR - *Süleyman Demirel University, Türkiye*
Prof. Dr. Funda Cengiz ÇALLIOĞLU - *Süleyman Demirel University, Türkiye*
Prof. Dr. Gençağa PÜRÇEK - *Karadeniz Technical University, Türkiye*
Prof. Dr. Gülcan ÖZKAN - *Süleyman Demirel University, Türkiye*
Prof. Dr. Lazreg HADJİ *University of Sidi Bel Abbes, Algeria*
Prof. Dr. Hasan KÖSEOĞLU - *Süleyman Demirel University, Türkiye*
Prof. Dr. İbrahim ÜÇGÜL - *Süleyman Demirel University, Türkiye*
Prof. Dr. Mehmet AVCAR - *Süleyman Demirel University, Türkiye*
Prof. Dr. Mehmet Cengiz KAYACAN - *Süleyman Demirel University, Türkiye*
Prof. Dr. Mehmet ÖZÇELİK - *Süleyman Demirel University, Türkiye*
Prof. Dr. Mehmet ÖZHANLI - *Süleyman Demirel University, Türkiye*
Prof. Dr. Michele BACCİOCCHİ - *University of the Republic of San Marino, San Marino*
Prof. Dr. Murat FIRAT - *Süleyman Demirel University, Türkiye*
Prof. Dr. Mustafa GENÇ - *Süleyman Demirel University, Türkiye*
Prof. Dr. Mustafa Gürhan YALÇIN - *Akdeniz University, Türkiye*
Prof. Dr. Mustafa Reşit USAL - *Süleyman Demirel University, Türkiye*
Prof. Dr. Nevzat Özgü YİĞİT - *Süleyman Demirel University, Türkiye*
Prof. Dr. Nicholas FANTUZZİ - *University of Bologna, Italy*
Prof. Dr. Ömer CİVALEK - *Akdeniz University, Türkiye*
Prof. Dr. Ömer ELİTOK - *Süleyman Demirel University, Türkiye*
Prof. Dr. Pham Van VİNH - *Le Quy Don Technical University, Vietnam*
Prof. Dr. Pınar GENÇ - *Retired Professor, Türkiye*
Prof. Dr. Recai Fatih TUNAY - *Süleyman Demirel University, Türkiye*
Prof. Dr. Sema YURDAKUL - *Süleyman Demirel University, Türkiye*
Prof. Dr. Şemsettin CARAN - *Süleyman Demirel University, Türkiye*
Prof. Dr. Şemsettin KILINÇARSLAN - *Süleyman Demirel University, Türkiye*
Prof. Dr. Serdal TERZİ - *Süleyman Demirel University, Türkiye*
Prof. Dr. Shahzada AHMAD - *Basque Center for Materials Applications & Nanostructures, Spain*
Prof. Dr. Sibel KAPLAN - *Süleyman Demirel University, Türkiye*
Prof. Dr. Soner GENÇ - *Retired Professor, Türkiye*
Prof. Dr. Tahir TİLKİ - *Süleyman Demirel University, Türkiye*

Prof. Dr. Ümran ESENDEMIR - *Süleyman Demirel University, Türkiye*
Prof. Dr. Yuze NİAN - *Jiangsu University of Science and Technology, China*
Prof. Dr. Lazreg HADJİ - *University of Sidi Bel Abbes, Algeria*
Prof. Dr. Ergün YILDIZ - *Atatürk University, Türkiye*
Prof. Dr. Erdal EROĞLU - *Süleyman Demirel University, Türkiye*
Assoc. Prof. Dr. Babak SAFAEİ - *Doğu Akdeniz University, TRNC*
Assoc. Prof. Dr. Barış Gürel - *Süleyman Demirel University, Türkiye*
Assoc. Prof. Dr. Candan GÜNGÖR - *Dokuz Eylül University, Türkiye*
Assoc. Prof. Dr. Derya Yüksel İMER - *Istanbul Technical University, Türkiye*
Assoc. Prof. Dr. Esin EREN - *Süleyman Demirel University, Türkiye*
Assoc. Prof. Dr. Feyza AKARSLAN KODALOĞLU - *Süleyman Demirel University, Türkiye*
Assoc. Prof. Dr. Mehmet Fahri Saraç - *Süleyman Demirel University, Türkiye*
Assoc. Prof. Dr. Murat KALELİ - *Süleyman Demirel University, Türkiye*
Assoc. Prof. Dr. Savaş ÖZÜN - *Süleyman Demirel University, Türkiye*
Assoc. Prof. Dr. Serap ÜNAL - *Süleyman Demirel University, Türkiye*
Assoc. Prof. Dr. Şule Sultan UĞUR - *Süleyman Demirel University, Türkiye*
Assoc. Prof. Dr. Vinh Pham Van Peter *the Great St. Petersburg Polytechnic University, Russia / Le Quy Don Technical University, Vietnam*
Assoc. Prof. Dr. Taner YILDIZ - *Samsun 19 Mayıs University, Türkiye*
Assoc. Prof. Dr. Doç. Dr. Zeynep BAŞAOĞLU DEMİREKİN - *Süleyman Demirel University, Türkiye*
Assist. Prof. Dr. Aman GARG - *The NorthCap University, India*
Assist. Prof. Dr. Ekinhan ERİŞKİN - *Süleyman Demirel University, Türkiye*
Assist. Prof. Dr. Aman GARG - *Huazhong University of Science and Technology, China / The NorthCap University, India*
Assist. Prof. Dr. Yuze Nian Jiangsu *University of Science and Technology, China / University of California, USA*
Lect. Dr. Murat ŞENTÜRK - *Süleyman Demirel University, Türkiye*

PARTICIPATING COUNTRIES (13)

Türkiye, Azerbaijan, Germany, China, Poland, Romania, Morocco, Algeria, India, Iran, Pakistan, Vietnam, Nigeria

TOTAL ACCEPTED ARTICLE: 65

The number of accepted article from foreign countries: **34**

The number of accepted article from Türkiye: **31**

Number of rejected papers: **65**

LANGUAGES

Turkish, English

PRESENTATION

Online

Congress Topics

Ceramic Topics

- Discovery and Analysis of Ancient Ceramics
- Ceramic Production Techniques in Early Civilizations
- Ottoman and Seljuk Ceramics
- Use and Importance of Ceramics in Archaeological Excavations
- Cultural and Historical Development of Ceramics
- Traditional Ceramic Arts and Modern Applications
- Use and Meaning of Ceramics in Different Cultures
- Trends and Developments in Contemporary Ceramic Art
- The Role and Importance of Ceramic Art in Education
- Use of Ceramics and Clay in Art Therapy
- Ceramic Production Techniques: Past to Present
- Properties and Applications of Ceramic Materials
- Ceramic Formulations and Material Science
- Advanced Technology Ceramics and Applications
- 3D Printing and Digital Technologies in Ceramic Production
- Sustainable Ceramic Production Methods

Ceramic Composite Materials Topics

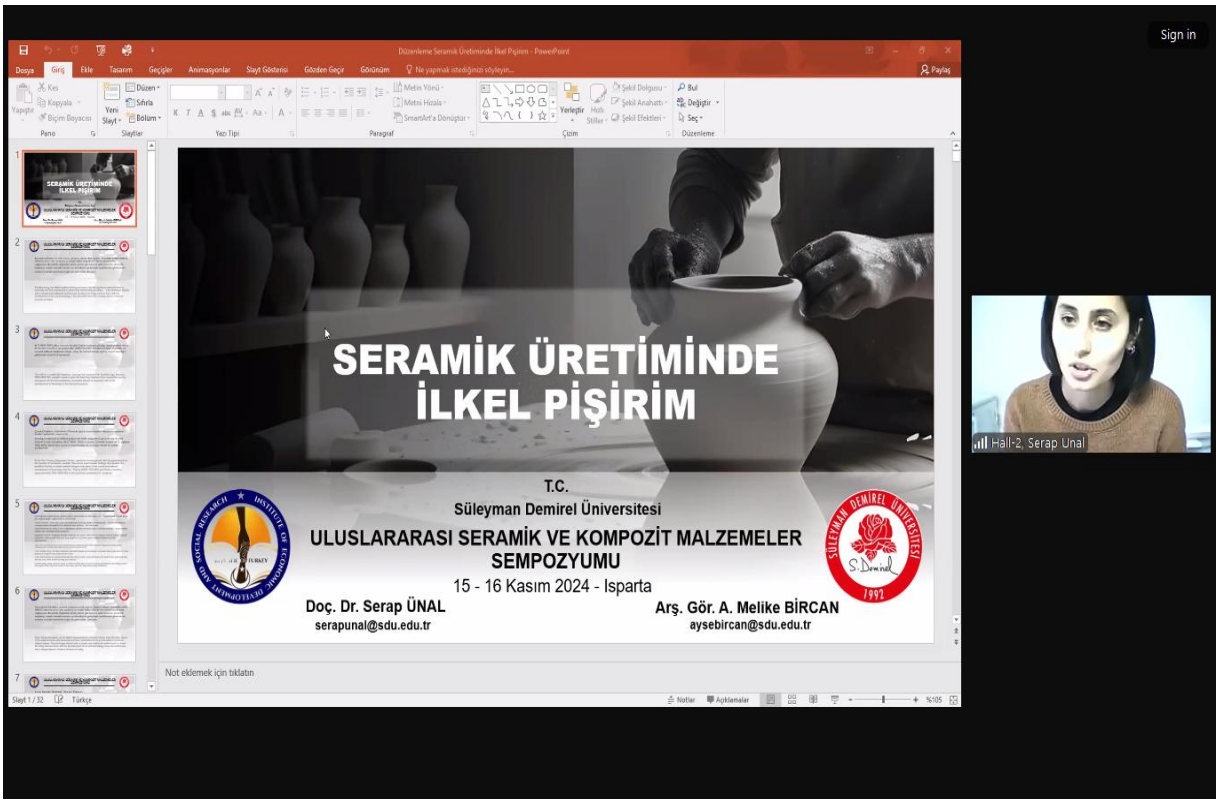
- Refractory Materials: Properties and Applications
- Advanced Ceramics: Properties and Applications
- Ceramic Matrix Composites (CMC): Production and Application Areas
- Ceramics in Electronic and Optoelectronic Applications
- Ceramics in Medical and Biomedical Applications
- The Role of Ceramics in Energy and Environmental Technologies
- Nano-Ceramics and Ceramic Applications in Nanotechnology
- Characterization Techniques for Advanced Ceramics
- Innovative Ceramic Products and Prototype Development
- Recycling and Waste Management of Ceramics
- Environmental Impacts and Sustainability in Ceramic Materials
- Industry 4.0 and Digitalization in Ceramic Production
- Use of Ceramics in Construction and Architecture

- **Advanced Ceramics in the Aerospace Industry**
- **Ceramic Applications in the Automotive Industry**
- **Ceramic Materials in the Electrical and Electronics Sector**
- **Ceramic Armor and Protective Materials in the Defense Industry**
- **Ceramics in the Chemical and Petrochemical Industry**
- **Ceramic Applications in Medicine and Dentistry**

Other Composite Materials Topics

- **Development and Applications of Polymer Composites**
- **Mechanical Properties of Polymer Matrix Composites**
- **Polymer Nanocomposites: Fabrication Methods and Properties**
- **Use and Advantages of Natural Fibers in Polymer Composites**
- **Role of Polymer Composites in the Automotive Industry**
- **Sustainability and Environmental Impact of Polymer Composites**
- **Use of Polymer Composites in Aerospace Applications**
- **Recycling and Reprocessing of Polymer Composites**
- **Smart Polymer Composites: Future Applications**
- **Thermal and Electrical Properties of Polymer Composites**
- **Manufacturing and Applications of Metal Matrix Composites**
- **Mechanical Performance of Carbon Fiber Reinforced Composites**
- **Biocomposite Materials: Fabrication, Properties, and Applications**
- **Composite Materials Incorporating Carbon Nanotubes**
- **Metal and Ceramic Reinforced Polymer Composites**
- **Hybrid Structures in Composite Materials: Metal-Ceramic Combinations**
- **Use of Kevlar Reinforced Composites in Structural Applications**
- **Composite Materials in Energy Storage Systems**
- **Metal Matrix Composites for High-Temperature Applications**
- **Matrix-Reinforcement Interactions and Strength in Composite Materials**

PHOTO GALLERY





Kaydediliyor...

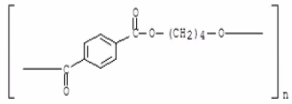
Hall-1 Zeynep Sıla Tırpancı ekranını görüntülüyorsunuz | Seçenekleri Görüntüle

Görüntüle

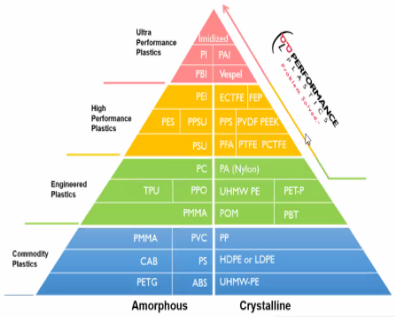
epsan
agile innovation for polymers

Polibutilen tereftalat Nedir?

- Polibutilen tereftalat (PBT), bütandiol ve tereftalik asidin polimerizasyonuyla üretilen yarı kristalin termoplastik bir polimerdir.



Şekil 1: PBT'nin kimyasal yapısı



Şekil 2: Yüksek performanslı pol

Özellikler

- ✓ Yüksek mukavemet ve tokluk
- ✓ Kolay İşlenebilirlik
- ✓ Mükemmel boyutsal kararlılık
- ✓ Yüksek mekanik dayanım
- ✓ İyi elektriksel iletkenlik
- ✓ Mükemmel kimyasal direnç
- ✓ Düşük su emilimi

app.zoom.us ekranınızı paylaşıyor. Paylaşmayı durdur Gizle

3

Hall-1 Zeynep Sıla Tırpancı

Observer Hall-1

Observer Hall-1

F

Salon-1, Ferhat Çeçen

Hafize Nagehan...

Hafize Nagehan KÖYSÜREN

Görkem Yumuşak

Sesi aç | Videoyu Başlat | Katılımcılar 5 | Sohbet | Ekranı paylaş | Kaydı Duraklat/Durdur | Ara Odalar | Reaksiyonlar | Uygulamalar | Beyaz Tahtalar | Odadan Çık

Kaydediliyor...

Görüntüle

Zoom Toplantı - Hall-1

Hall-1 Zeynep Sıla Tırpancı

Observer Hall-1

Observer Hall-1

Dr. Sercan Basit

Görkem Yumuşak

F

Salon-1, Ferhat Çeçen

Hafize Nagehan...

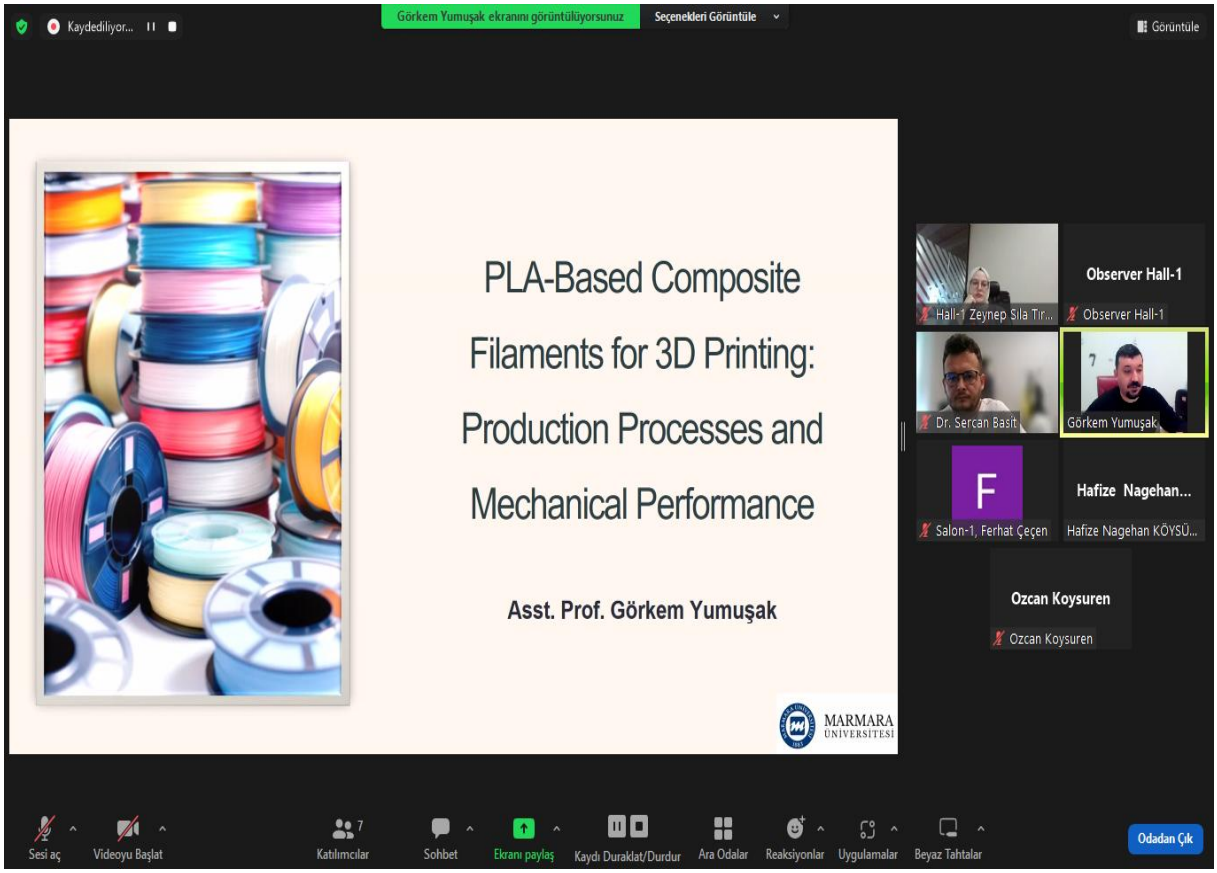
Hafize Nagehan KÖYSÜREN

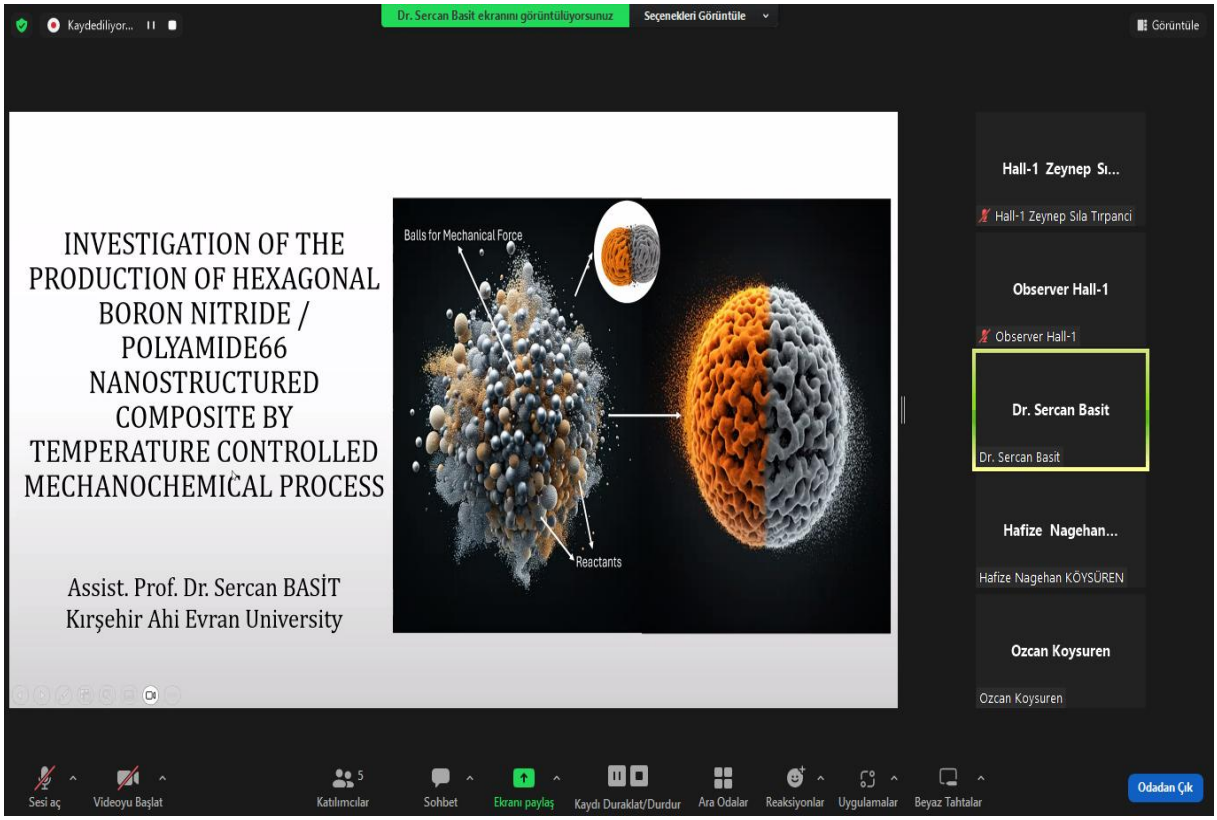
Ozcan Koysuren

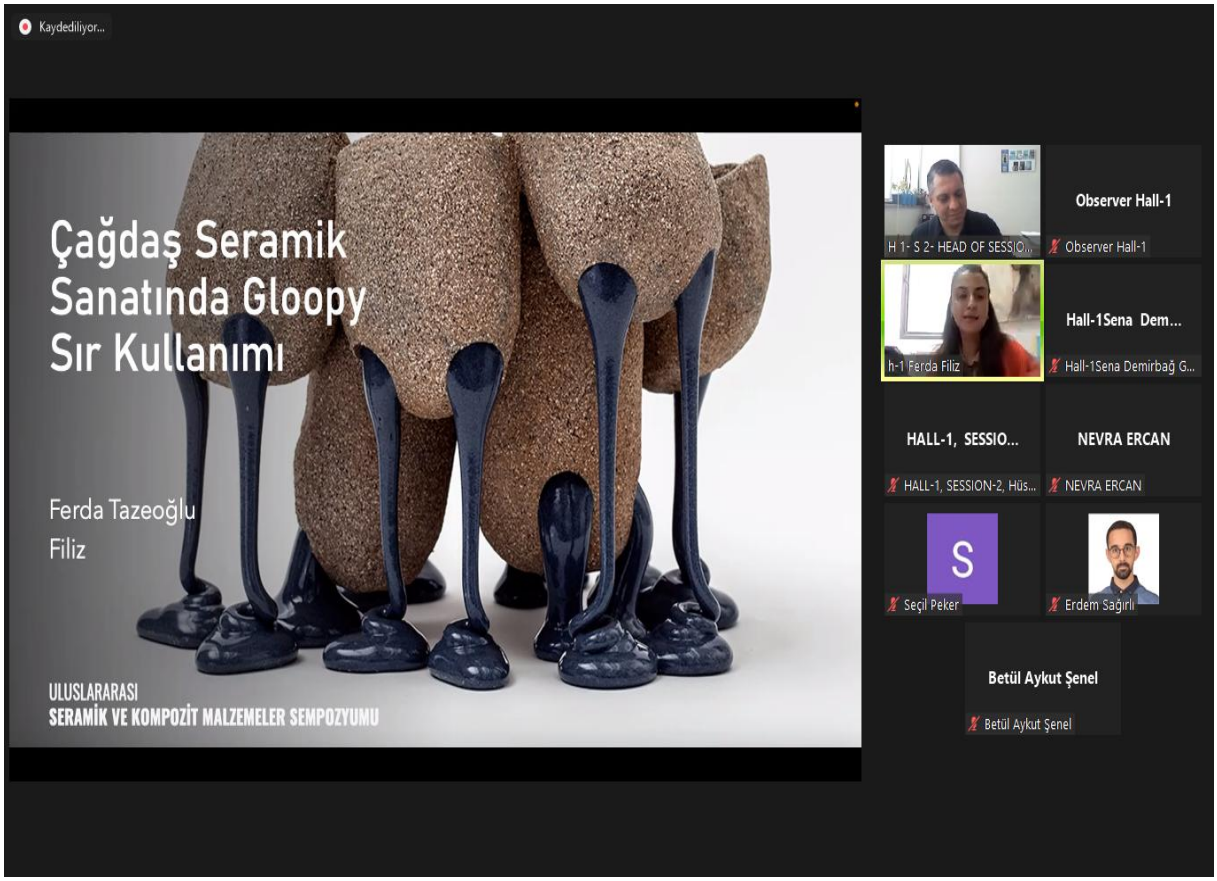
Ozcan Koysuren

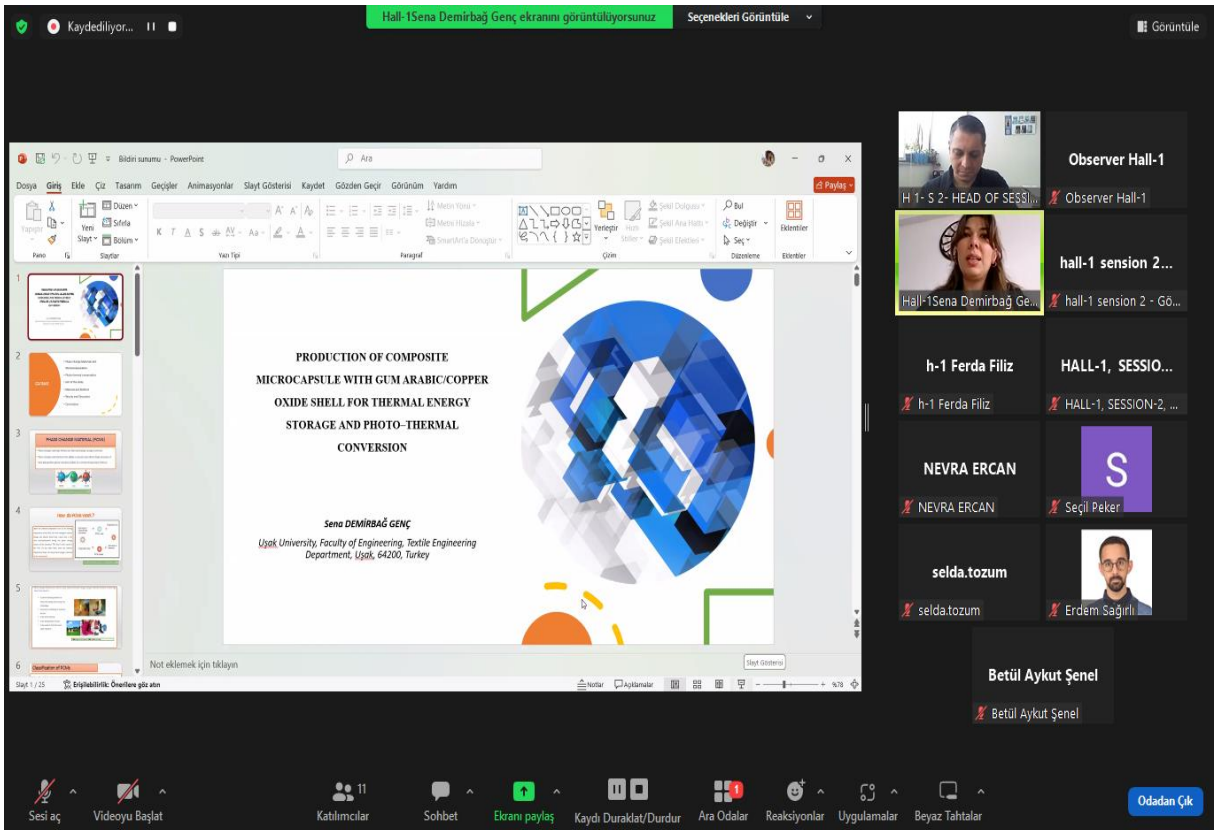
Sesi aç | Videoyu Başlat | Katılımcılar 7 | Sohbet | Ekranı paylaş | Kaydı Duraklat/Durdur | Ara Odalar | Reaksiyonlar | Uygulamalar | Beyaz Tahtalar | Odadan Çık

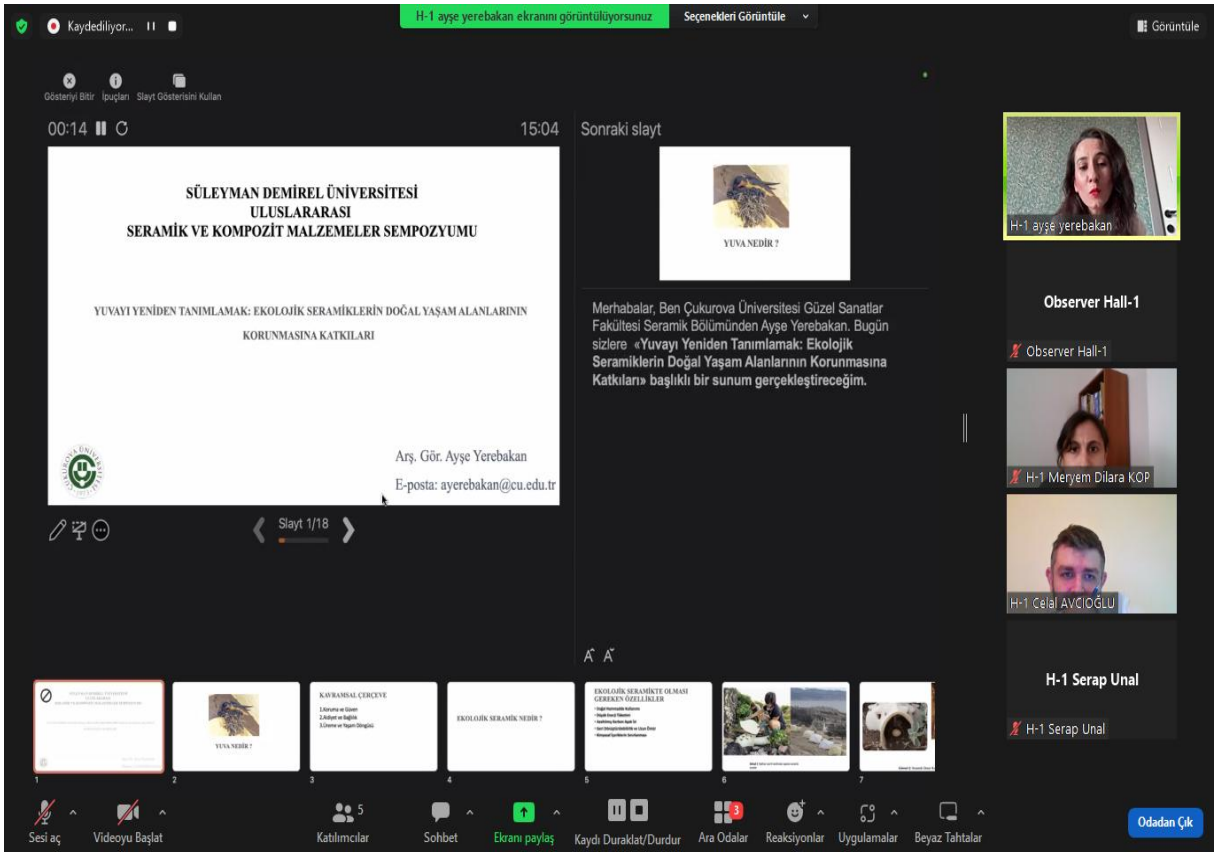
10:17
15.11.2024

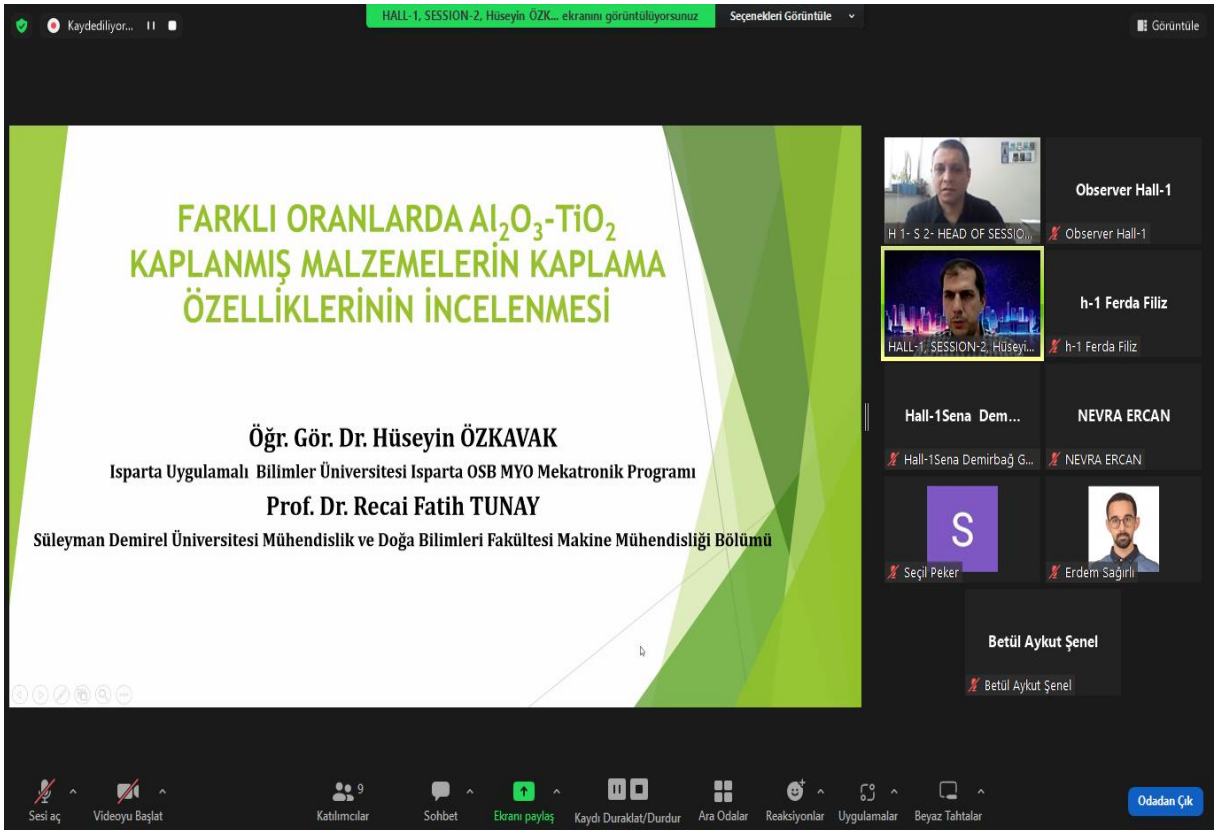

Kaydediliyor...
Görkem Yumuşak ekranını görüntülüyorsunuz
Seçenekleri Görüntüle
Görüntüle
PLA-Based Composite Filaments for 3D Printing: Production Processes and Mechanical Performance
Asst. Prof. Görkem Yumuşak
MARMARA ÜNİVERSİTESİ
Observer Hall-1
Hall-1 Zeynep Sıla Tır...
Observer Hall-1
Dr. Sercan Basit
Görkem Yumuşak
F
Salon-1, Ferhat Çeçen
Hafize Nagehan...
Hafize Nagehan KÖYSÜ...
Ozcan Koysuren
Ozcan Koysuren
Sesi aç
Videoyu Başlat
Katılımcılar
Sohbet
Ekranı paylaş
Kaydı Duraklat/Durdur
Ara Odalar
Reaksiyonlar
Uygulamalar
Beyaz Tahtalar
Odadan Çık

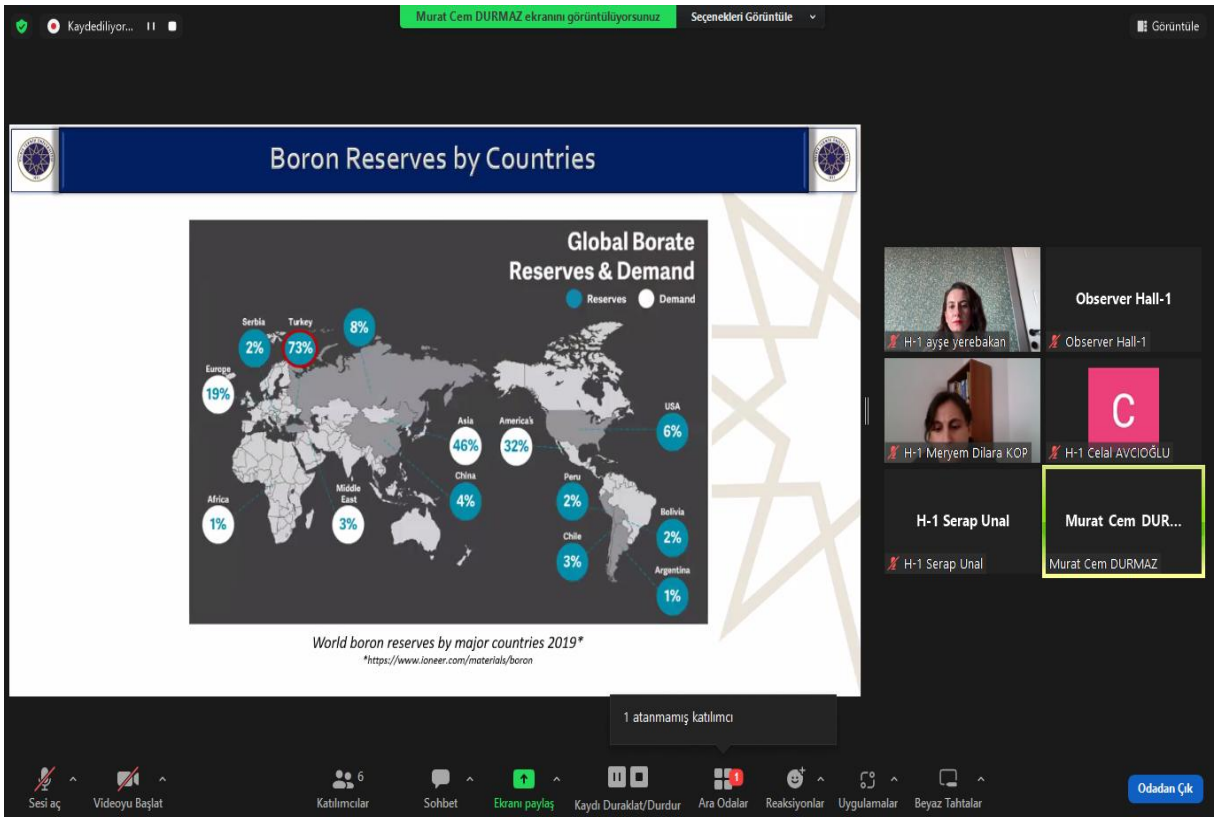

Kaydediliyor...
Dr. Sercan Basit ekranını görüntülüyorsunuz
Seçenekleri Görüntüle
Görüntüle
INVESTIGATION OF THE PRODUCTION OF HEXAGONAL BORON NITRIDE / POLYAMIDE66 NANOSTRUCTURED COMPOSITE BY TEMPERATURE CONTROLLED MECHANOCHEMICAL PROCESS
Assist. Prof. Dr. Sercan BASİT
Kırşehir Ahi Evran University
Balls for Mechanical Force
Reactants
Hall-1 Zeynep Sı...
Hall-1 Zeynep Sıla Tırpancı
Observer Hall-1
Observer Hall-1
Dr. Sercan Basit
Dr. Sercan Basit
Hafize Nagehan...
Hafize Nagehan KÖYSÜREN
Ozcan Koysuren
Ozcan Koysuren
Sesi aç
Videoyu Başlat
Katılımcılar
Sohbet
Ekranı paylaş
Kaydı Duraklat/Durdur
Ara Odalar
Reaksiyonlar
Uygulamalar
Beyaz Tahtalar
Odadan Çık

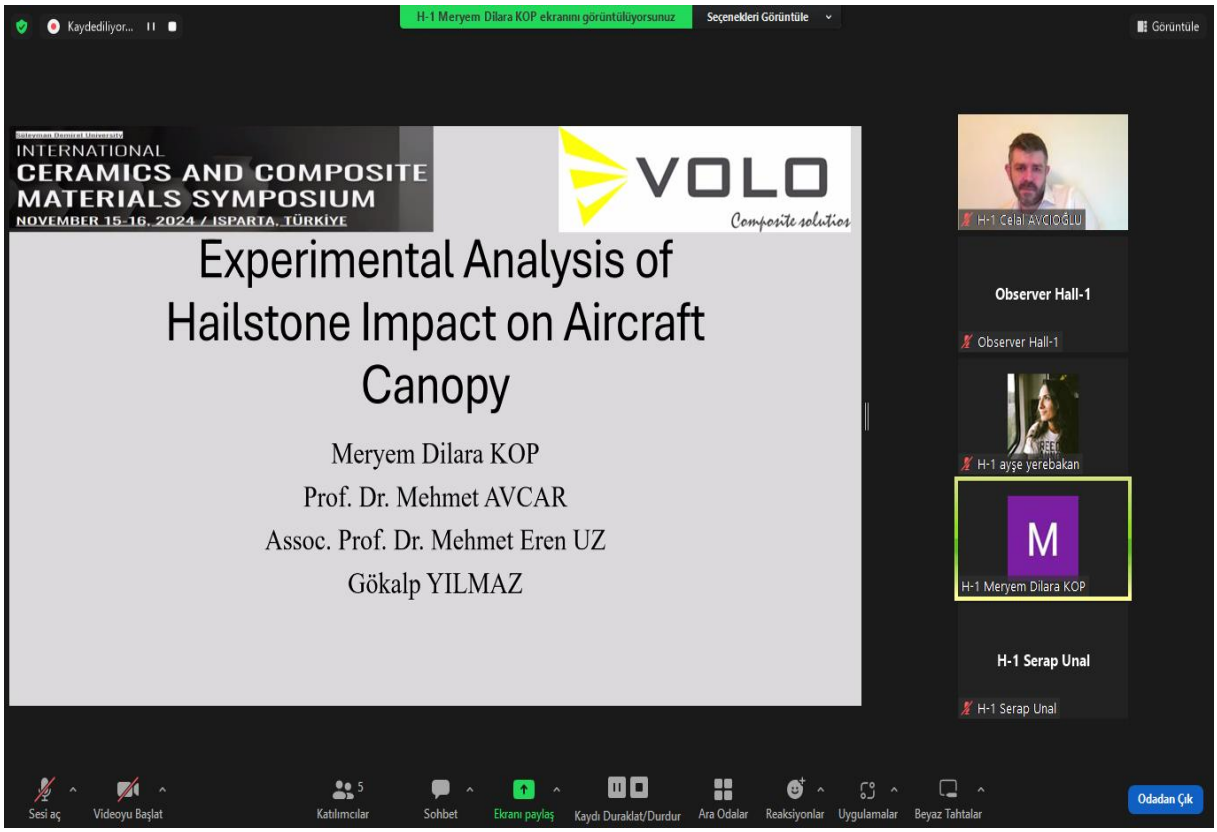

Kaydediliyor...
Çağdaş Seramik Sanatında Gloopy Sır Kullanımı
Ferda Tazeoğlu
Filiz
ULUSLARARASI
SERAMİK VE KOMPOZİT MALZEMELER SEMPOZYUMU
H 1- S 2- HEAD OF SESSIO...
Observer Hall-1
Observer Hall-1
h-1 Ferda Filiz
Hall-1Sena Dem...
Hall-1Sena Demirbağ G...
HALL-1, SESSIO...
HALL-1, SESSION-2, Hüs...
NEVRA ERCAN
NEVRA ERCAN
S
Seçil Peker
Erdem Sağırlı
Betül Aykut Şenel
Betül Aykut Şenel

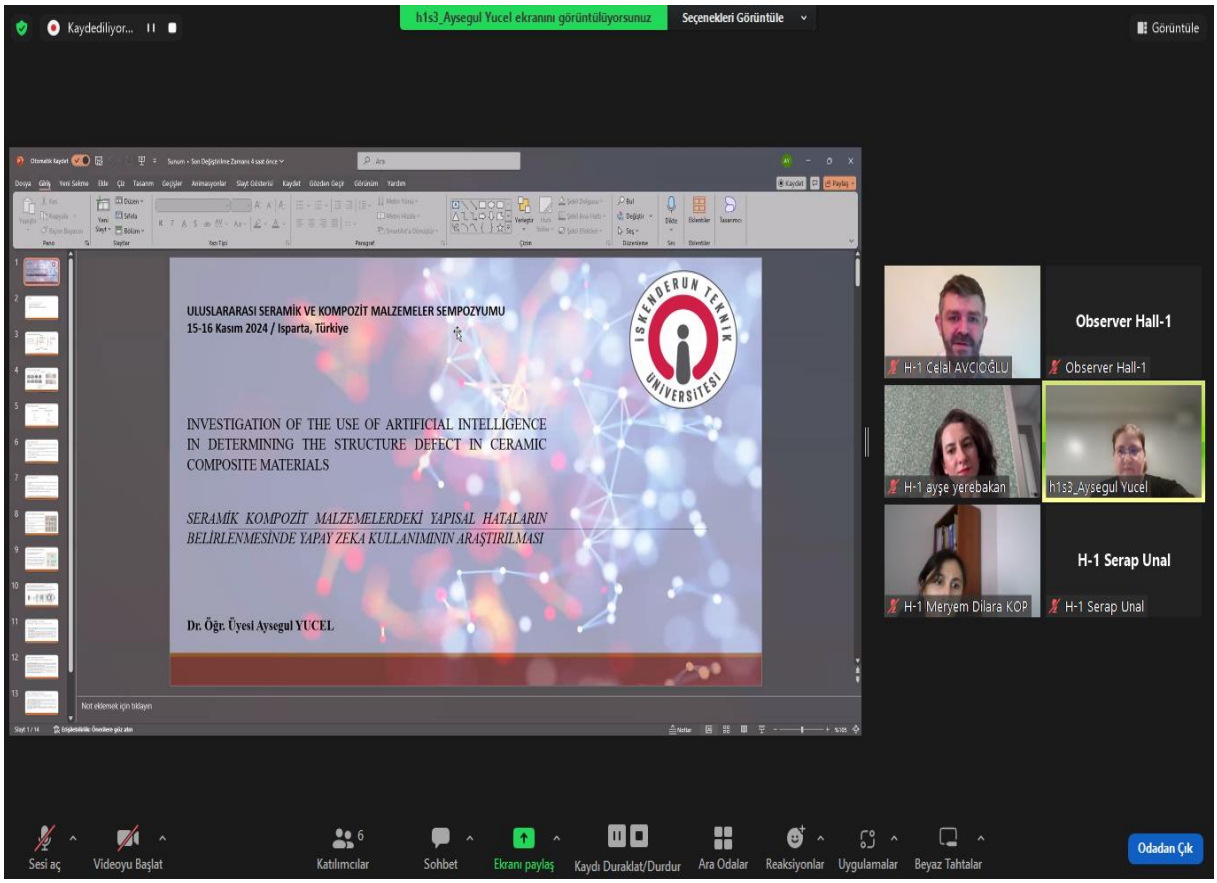

Kaydediliyor...
Hall-1Sena Demirbağ Genç ekranını görüntülüyorsunuz
Seçenekleri Görüntüle
Görüntüle
PRODUCTION OF COMPOSITE MICROCAPSULE WITH GUM ARABIC/COPPER OXIDE SHELL FOR THERMAL ENERGY STORAGE AND PHOTO-THERMAL CONVERSION
Sena DEMİRBAĞ GENÇ
Uşak University, Faculty of Engineering, Textile Engineering Department, Uşak, 64200, Turkey
H 1- S 2- HEAD OF SESSI...
Observer Hall-1
Observer Hall-1
Hall-1Sena Demirbağ Ge...
hall-1 sension 2...
hall-1 sension 2 - Gö...
h-1 Ferda Filiz
h-1 Ferda Filiz
HALL-1, SESSIO...
HALL-1, SESSION-2, ...
NEVRA ERCAN
NEVRA ERCAN
S
Seçil Peker
selda.tozum
selda.tozum
Erdem Sağırlı
Betül Aykut Şenel
Betül Aykut Şenel
Sesi aç
Videoyu Başlat
Katılımcılar
Sohbet
Ekranı paylaş
Kaydı Duraklat/Durdur
Ara Odalar
Reaksiyonlar
Uygulamalar
Beyaz Tahtalar
Odadan Çık


Kaydediliyor...
H-1 ayşe yerebakan ekranını görüntülüyorsunuz
Seçenekleri Görüntüle
Görüntüle
Gösteriyi Bitir
İpuçları
Slayt Gösterisini Kullan
00:14
15:04
SÜLEYMAN DEMİREL ÜNİVERSİTESİ
ULUSLARARASI
SERAMİK VE KOMPOZİT MALZEMELER SEMPOZYUMU
YUVAYI YENİDEN TANIMLAMAK: EKOLOJİK SERAMİKLERİN DOĞAL YAŞAM ALANLARININ KORUNMASINA KATKILARI
Arş. Gör. Ayşe Yerebakan
E-posta: ayerebakan@cu.edu.tr
Slayt 1/18
Sonraki slayt
YUVA NEDİR ?
Merhabalar, Ben Çukurova Üniversitesi Güzel Sanatlar Fakültesi Seramik Bölümünden Ayşe Yerebakan. Bugün sizlere «Yuvayı Yeniden Tanımlamak: Ekolojik Seramiklerin Doğal Yaşam Alanlarının Korunmasına Katkıları» başlıklı bir sunum gerçekleştireceğim.
H-1 ayşe yerebakan
Observer Hall-1
Observer Hall-1
H-1 Meryem Dilara KOP
H-1 Celal AVCIOĞLU
H-1 Serap Unal
H-1 Serap Unal
Sesi aç
Videoyu Başlat
Katılımcılar
Sohbet
Ekranı paylaş
Kaydı Duraklat/Durdur
Ara Odalar
Reaksiyonlar
Uygulamalar
Beyaz Tahtalar
Odadan Çık

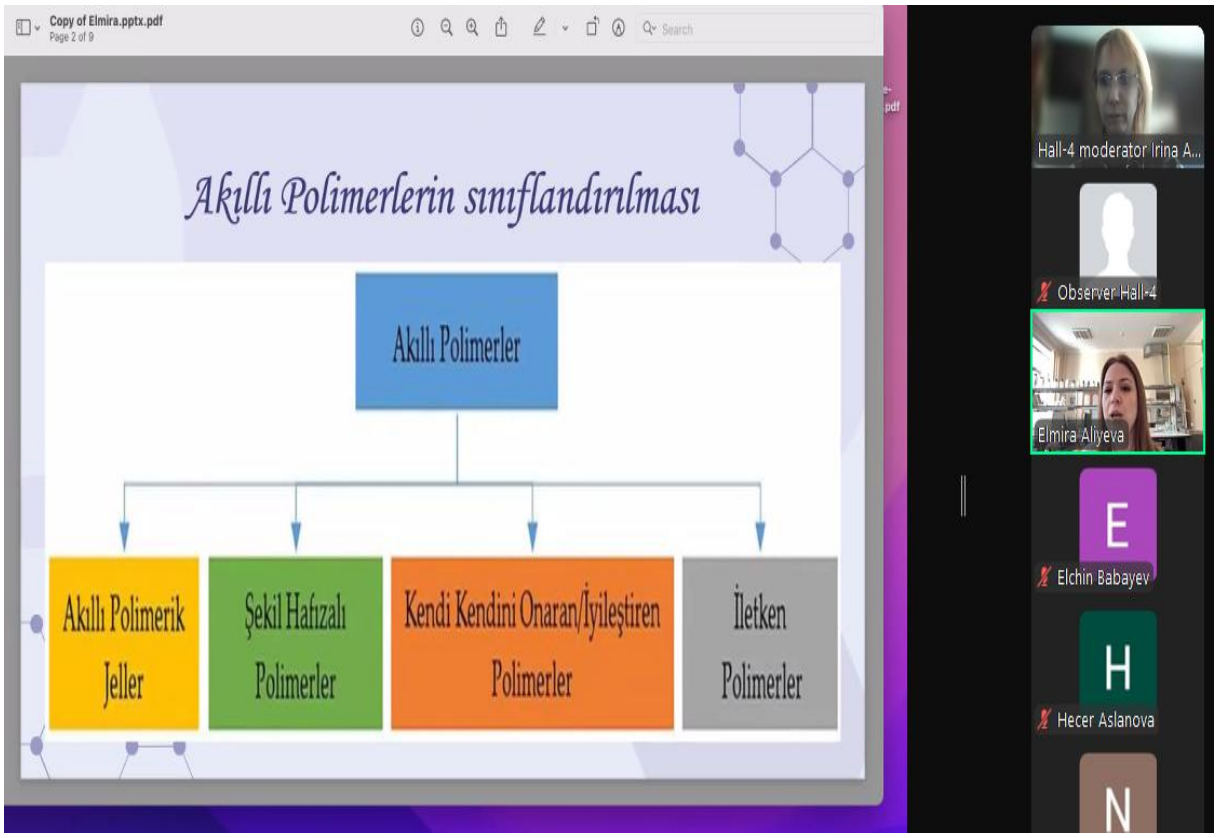

Kaydediliyor...
HALL-1, SESSION-2, Hüseyin ÖZK... ekranını görüntülüyorsunuz
Seçenekleri Görüntüle
Görüntüle
FARKLI ORANLARDA Al_2O_3-TiO_2 KAPLANMIŞ MALZEMELERİN KAPLAMA ÖZELLİKLERİNİN İNCELENMESİ
Öğr. Gör. Dr. Hüseyin ÖZKAVAK
Isparta Uygulamalı Bilimler Üniversitesi Isparta OSB MYO Mekatronik Programı
Prof. Dr. Recai Fatih TUNAY
Süleyman Demirel Üniversitesi Mühendislik ve Doğa Bilimleri Fakültesi Makine Mühendisliği Bölümü
H 1- S 2- HEAD OF SESSIO...
Observer Hall-1
Observer Hall-1
HALL-1, SESSION-2, Hüseyi...
h-1 Ferda Filiz
h-1 Ferda Filiz
Hall-1Sena Dem...
Hall-1Sena Demirbağ G...
NEVRA ERCAN
NEVRA ERCAN
S
Seçil Peker
Erdem Sağırlı
Betül Aykut Şenel
Betül Aykut Şenel
Sesi aç
Videoyu Başlat
Katılımcılar
Sohbet
Ekranı paylaş
Kaydı Duraklat/Durdur
Ara Odalar
Reaksiyonlar
Uygulamalar
Beyaz Tahtalar
Odadan Çık

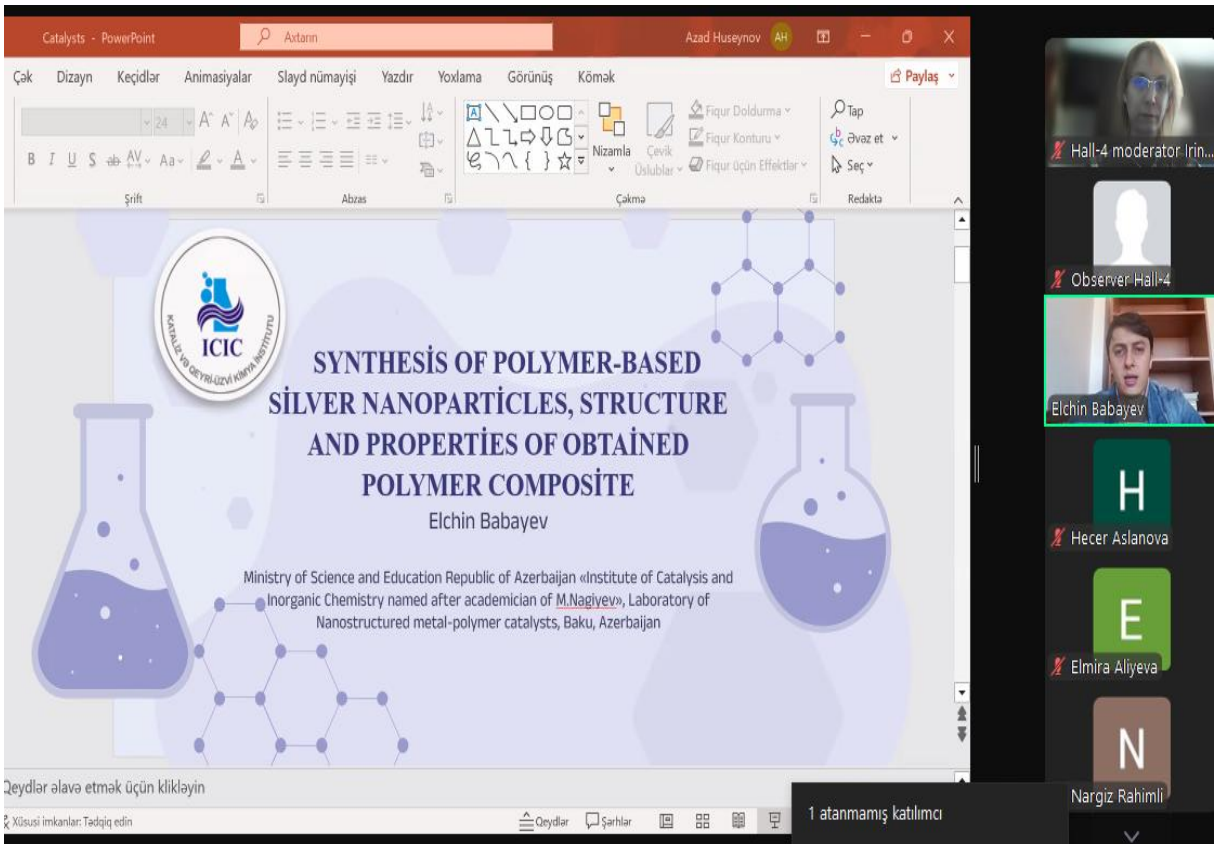

Kaydediliyor...
Murat Cem DURMAZ ekranını görüntülüyorsunuz
Seçenekleri Görüntüle
Görüntüle
Boron Reserves by Countries
Global Borate Reserves & Demand
Reserves
Demand
Serbia 2%
Turkey 73%
8%
Europe 19%
Asia 46%
America's 32%
USA 6%
China 4%
Peru 2%
Bolivia 2%
Chile 3%
Argentina 1%
Africa 1%
Middle East 3%
World boron reserves by major countries 2019*
*https://www.ioneer.com/materials/boron
Observer Hall-1
H-1 ayşe yerebakan
H-1 Meryem Dilara KÖP
H-1 Celal AVCIOĞLU
H-1 Serap Unal
Murat Cem DUR...
Murat Cem DURMAZ
1 atanmamış katılımcı
Sesi aç
Videoyu Başlat
Katılımcılar
Sohbet
Ekranı paylaş
Kaydı Duraklat/Durdur
Ara Odalar
Reaksiyonlar
Uygulamalar
Beyaz Tahtalar
Odadan Çık


Kaydediliyor...
H-1 Meryem Dilara KÖP ekranını görüntülüyorsunuz
Seçenekleri Görüntüle
Görüntüle
INTERNATIONAL
CERAMICS AND COMPOSITE MATERIALS SYMPOSIUM
NOVEMBER 15-16, 2024 / ISPARTA, TÜRKİYE
VOLO
Composite solutions
Experimental Analysis of Hailstone Impact on Aircraft Canopy
Meryem Dilara KOP
Prof. Dr. Mehmet AVCAR
Assoc. Prof. Dr. Mehmet Eren UZ
Gökalp YILMAZ
H-1 Celal AVCIOĞLU
Observer Hall-1
H-1 ayşe yerebakan
M
H-1 Meryem Dilara KÖP
H-1 Serap Unal
Sesi aç
Videoyu Başlat
Katılımcılar
Sohbet
Ekranı paylaş
Kaydı Duraklat/Durdur
Ara Odalar
Reaksiyonlar
Uygulamalar
Beyaz Tahtalar
Odadan Çık


Kaydediliyor...
h1s3_Aysegul Yucel ekranını görüntülüyorsunuz
Seçenekleri Görüntüle
Görüntüle
ULUSLARARASI SERAMİK VE KOMPOZİT MALZEMELER SEMPOZYUMU
15-16 Kasım 2024 / Isparta, Türkiye
INVESTIGATION OF THE USE OF ARTIFICIAL INTELLIGENCE IN DETERMINING THE STRUCTURE DEFECT IN CERAMIC COMPOSITE MATERIALS
SERAMİK KOMPOZİT MALZEMELERDEKİ YAPISAL HATALARIN BELİRLENMESİNDE YAPAY ZEKA KULLANIMININ ARAŞTIRILMASI
Dr. Öğr. Üyesi Aysegul YUCEL
H-1 Celal AVCIOĞLU
Observer Hall-1
H-1 ayşe yerebakan
h1s3_Aysegul Yucel
H-1 Meryem Dilara KOP
H-1 Serap Unal
Sesi aç
Videoyu Başlat
Katılımcılar
Sohbet
Ekranı paylaş
Kaydı Duraklat/Durdur
Ara Odalar
Reaksiyonlar
Uygulamalar
Beyaz Tahtalar
Odadan Çık


LACOMOFA
From Ornament to Structure: The Dual Role of Ceramics in Ottoman Architecture
Prepared by:
Melik Sami
Dr.Sara Khelil
Dr. Tallal Abdel Karim Bouzir
Affiliation : Mohamed Khider Biskra University /Member of LACOMOFA Biskra laboratory
International Ceramics And Composite Materials Symposium
November 15-16, 2024 / Isparta, Türkiye
Hall-4 moderator Irina A...
Observer Hall-4
Elmira Aliyeva
Elchin Babayev
Hecer Aslanova
H-2-sami melik


Copy of Elmira.pptx.pdf
Page 2 of 9
Akıllı Polimerlerin sınıflandırılması
Akıllı Polimerler
Akıllı Polimerik Jeller
Şekil Hafızalı Polimerler
Kendi Kendini Onaran/İyileştiren Polimerler
İletken Polimerler
Hall-4 moderator Irina A...
Observer Hall-4
Elmira Aliyeva
Elchin Babayev
Hecer Aslanova


Catalysts - PowerPoint
Axtarın
Azad Huseynov
ICIC
SYNTHESİS OF POLYMER-BASED SİLVER NANOPARTİCLES, STRUCTURE AND PROPERTİES OF OBTAİNED POLYMER COMPOSİTE
Elchin Babayev
Ministry of Science and Education Republic of Azerbaijan «Institute of Catalysis and Inorganic Chemistry named after academician of M.Nagiyev», Laboratory of Nanostructured metal-polymer catalysts, Baku, Azerbaijan
Hall-4 moderator Irin...
Observer Hall-4
Elchin Babayev
Hecer Aslanova
Elmira Aliyeva
Nargiz Rahimli
1 atanmamış katılımcı

RATHINAM TECHNICAL CAMPUS (AUTONOMOUS)

CGPA Score - 3.45

FOR CSE, IT & ECE DEPARTMENTS

Ecological Friendly Synthesis of Multi-Walled Carbon Nanotubes from Plant-Based Hydrocarbons for Efficient Water Purification

Hall-3,Dharsini R, Devi Sri M

15th to 16th of November 2024

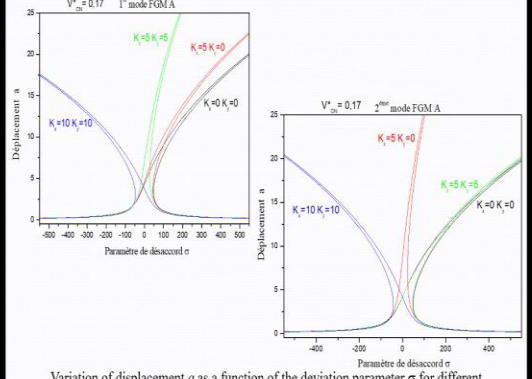
INTERNATIONAL CERAMICS AND COMPOSITE MATERIALS SYMPOSIUM, Süleyman Demirel University, Türkey

Giriş yapın Kaydediliyor... Görüntüle

Ses Video 4 Katılımcılar Sohbet Tepki ver Paylaş Uygulamalar Ara odalar Kaydı duraklat/durdur Daha fazla Odadan çık

Results and discussions

Curvature effect : CRNTC-Λ et V^*_{CN} = 17%



Variation of displacement a as a function of the deviation parameter σ for different curvatures.

27

zakia hammou

Observer- H3

Abderrahim Ait Lhaj-Session-1, Hall-3

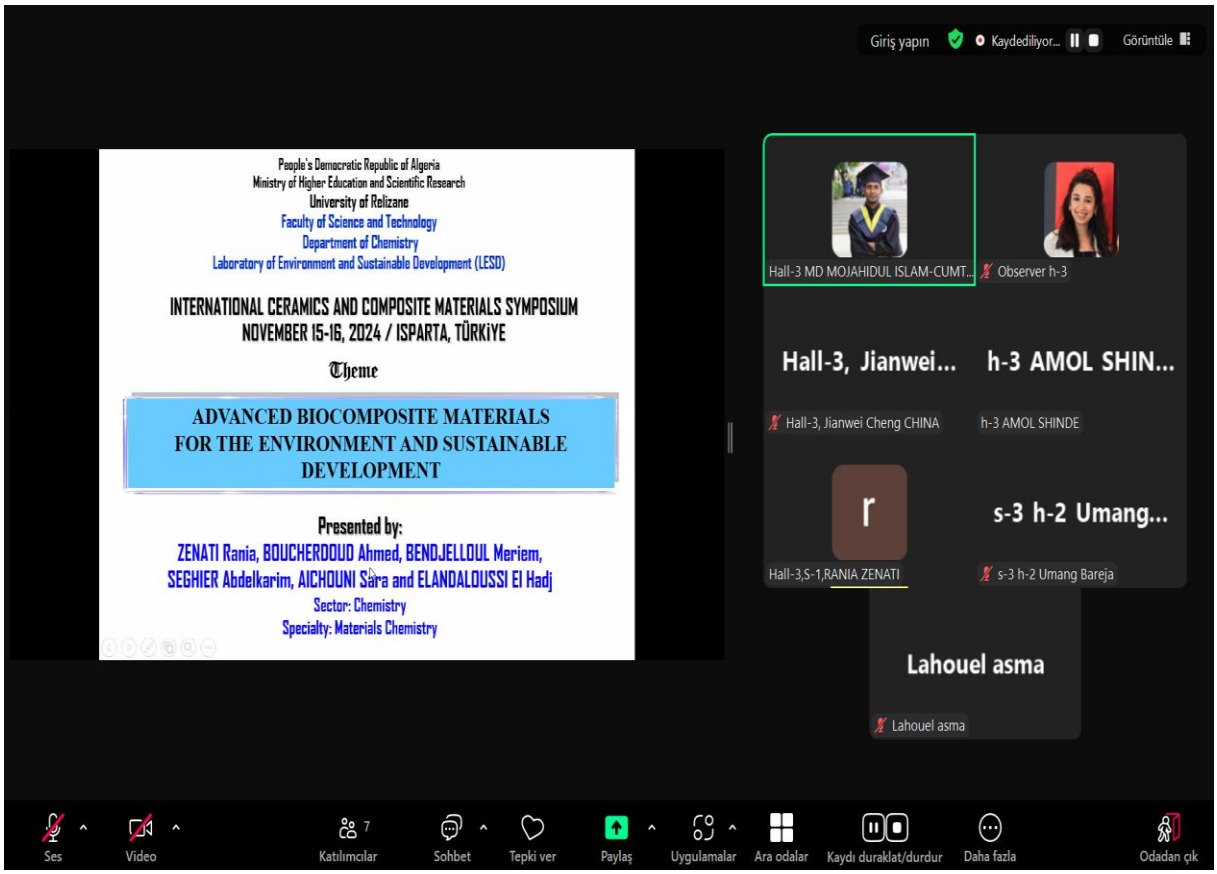
Hall-3,Dharsini R, Devi Sri M

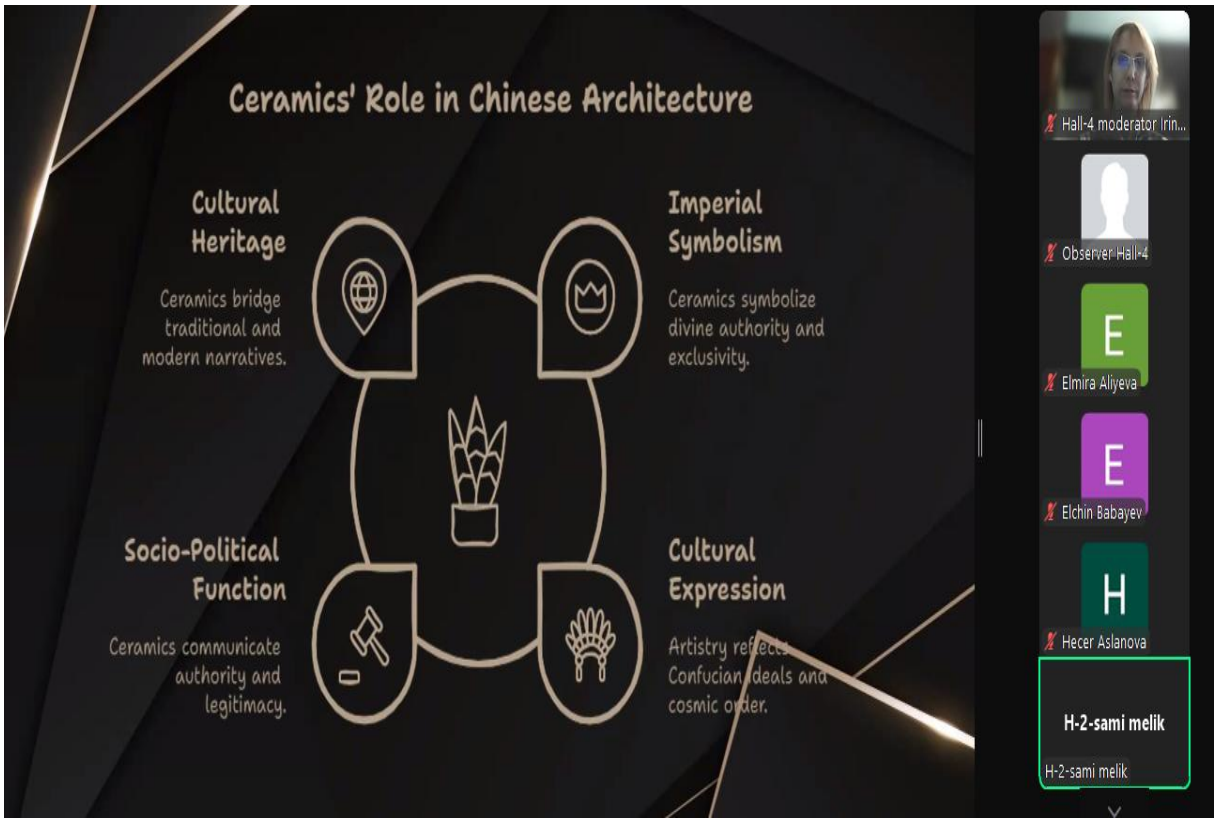
Hall 3 session 1 Aysegul UYGUN OKSUZ...

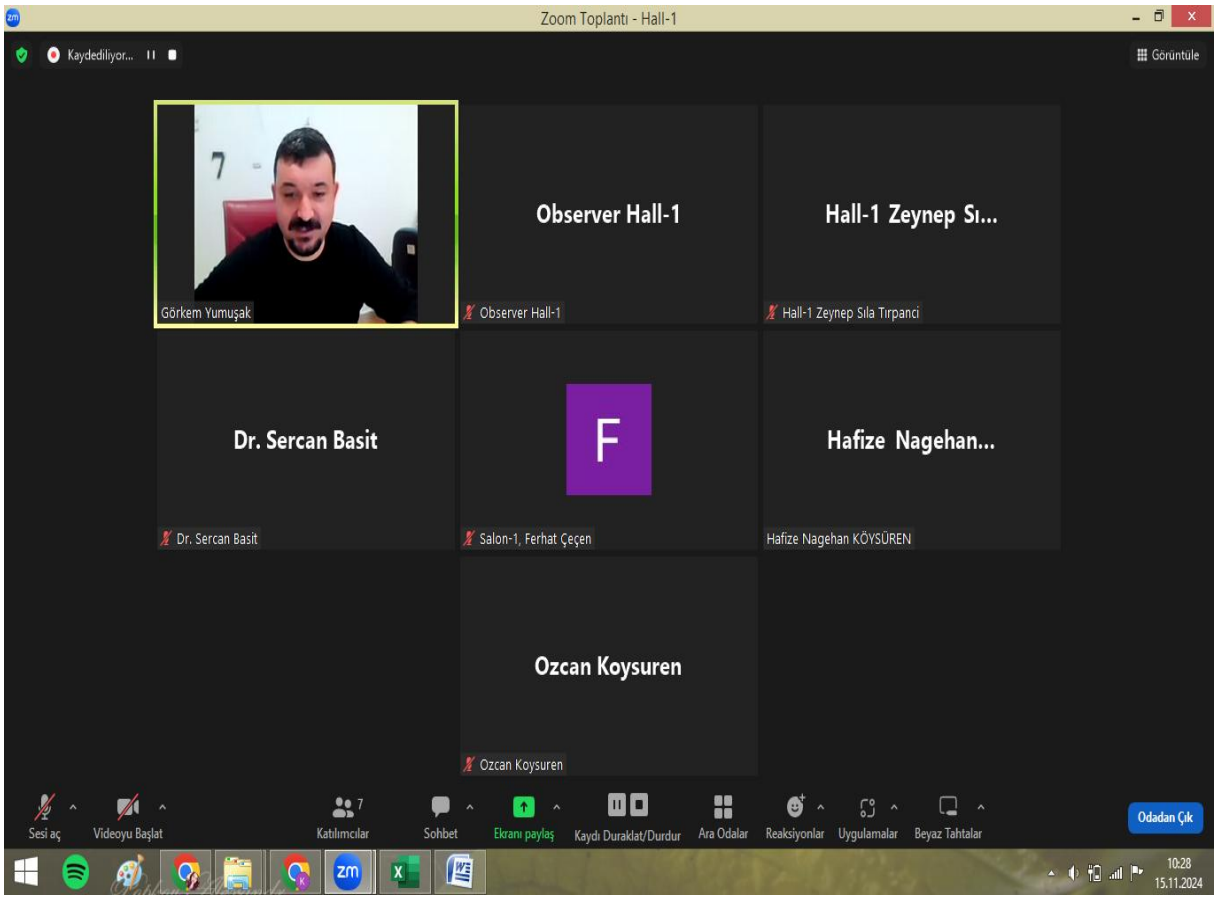
Umang Bareja

Giriş yapın Kaydediliyor... Görüntüle

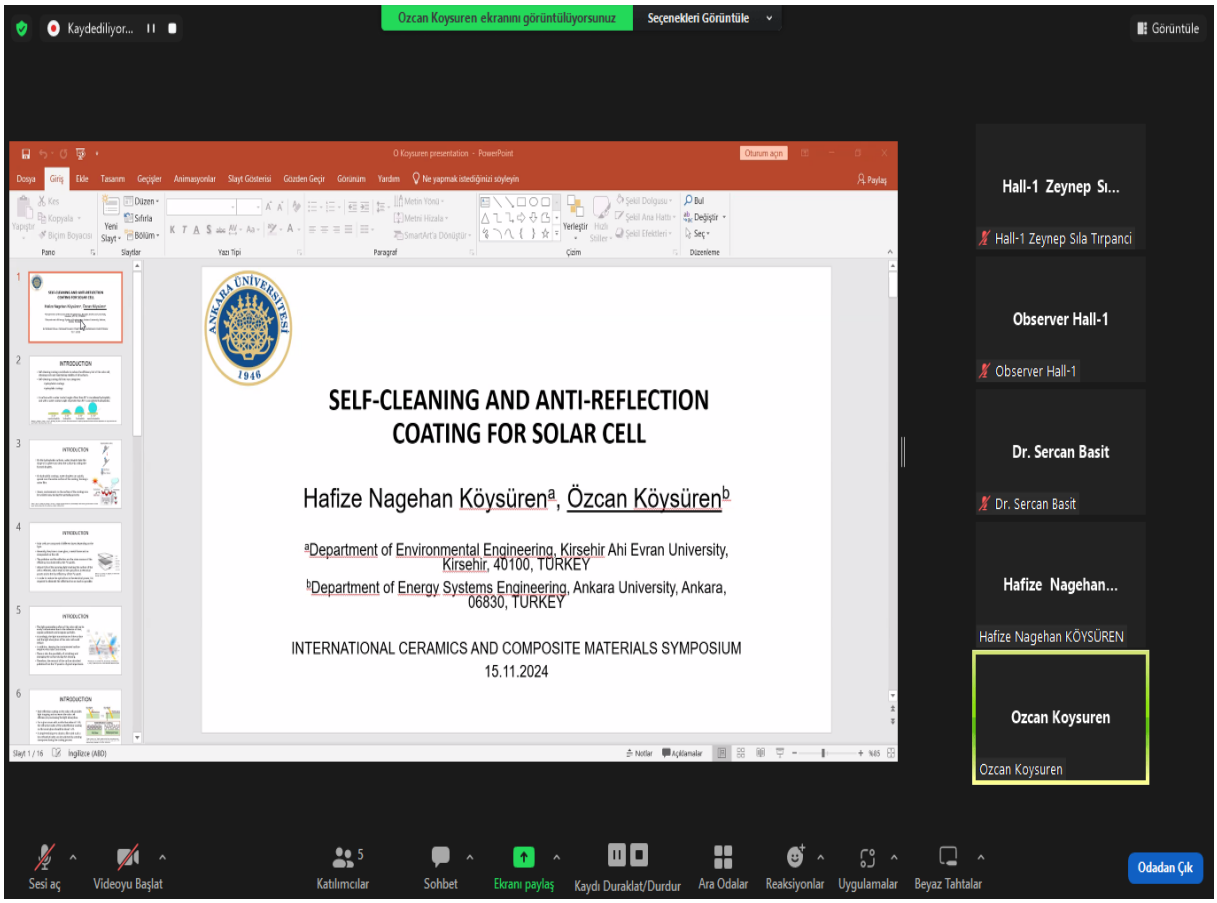
Ses Video 6 Katılımcılar Sohbet Tepki ver Paylaş Uygulamalar Ara odalar Kaydı duraklat/durdur Daha fazla Odadan çık

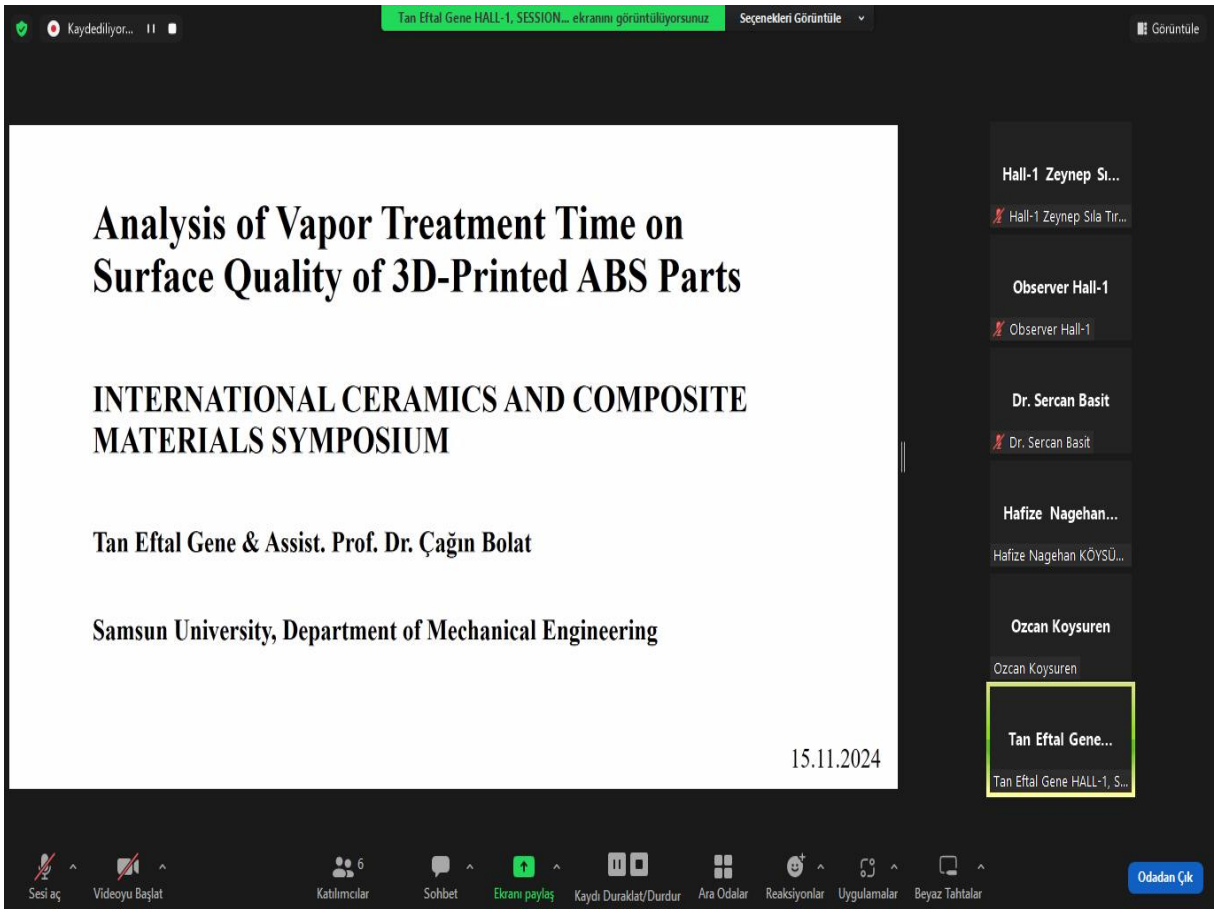

Giriş yapın
Kaydediliyor...
Görüntüle
People's Democratic Republic of Algeria
Ministry of Higher Education and Scientific Research
University of Relizane
Faculty of Science and Technology
Department of Chemistry
Laboratory of Environment and Sustainable Development (LESD)
INTERNATIONAL CERAMICS AND COMPOSITE MATERIALS SYMPOSIUM
NOVEMBER 15-16, 2024 / ISPARTA, TÜRKİYE
Theme
ADVANCED BIOCOMPOSITE MATERIALS FOR THE ENVIRONMENT AND SUSTAINABLE DEVELOPMENT
Presented by:
ZENATI Rania, BOUCHERDOUD Ahmed, BENDJELLOUL Meriem, SEGHIER Abdelkarim, AICHOUNI Sâra and ELANDALOUSSI El Hadj
Sector: Chemistry
Specialty: Materials Chemistry
Hall-3 MD MOJAHIDUL ISLAM-CUMT...
Observer h-3
Hall-3, Jianwei...
Hall-3, Jianwei Cheng CHINA
h-3 AMOL SHIN...
h-3 AMOL SHINDE
r
Hall-3,S-1,RANIA ZENATI
s-3 h-2 Umang...
s-3 h-2 Umang Bareja
Lahouel asma
Lahouel asma
Ses
Video
7
Katılımcılar
Sohbet
Tepki ver
Paylaş
Uygulamalar
Ara odalar
Kaydı duraklat/durdur
Daha fazla
Odadan çık

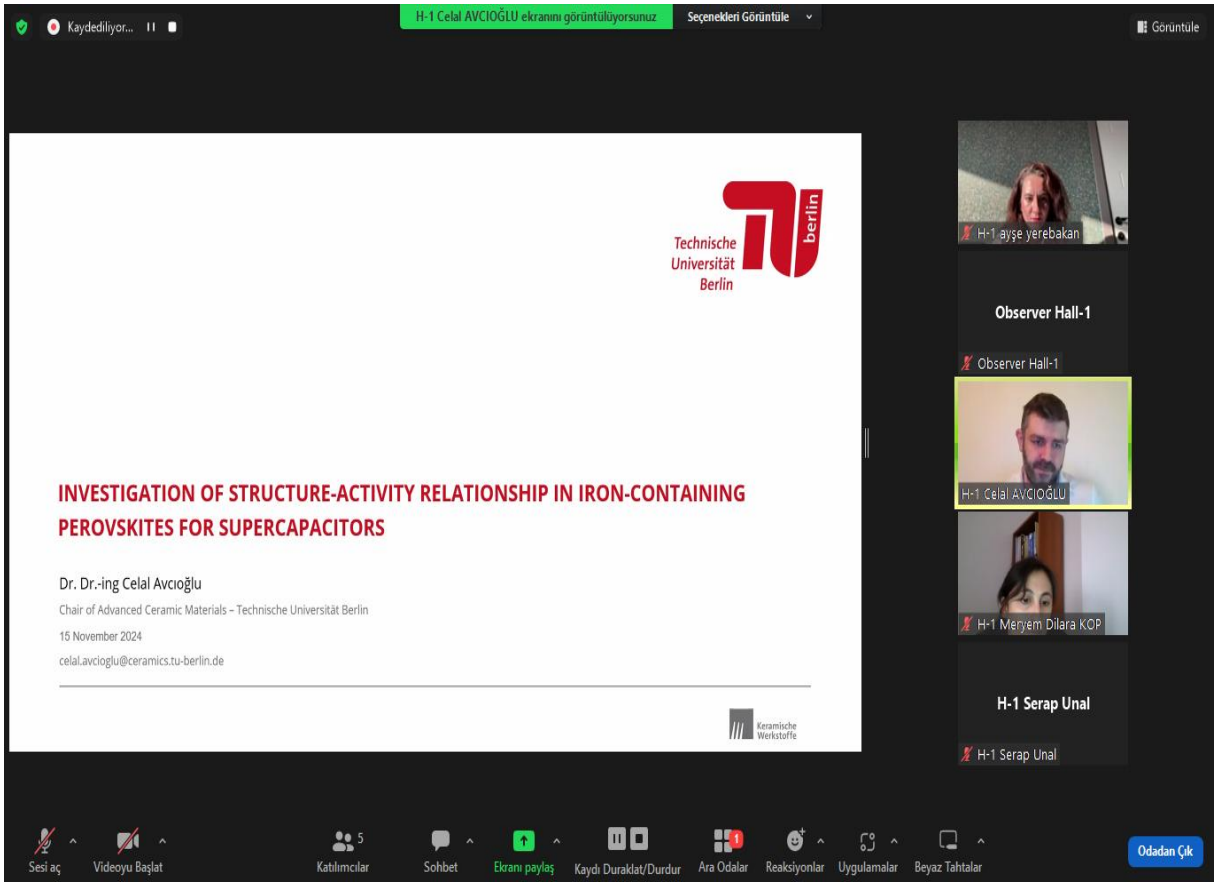

Ceramics' Role in Chinese Architecture
Cultural Heritage
Ceramics bridge traditional and modern narratives.
Imperial Symbolism
Ceramics symbolize divine authority and exclusivity.
Socio-Political Function
Ceramics communicate authority and legitimacy.
Cultural Expression
Artistry reflects Confucian ideals and cosmic order.
Hall-4 moderator Irin...
Observer Hall-4
E
Elmira Aliyeva
E
Elchin Babayev
H
Hecer Aslanova
H-2-sami melik
H-2-sami melik

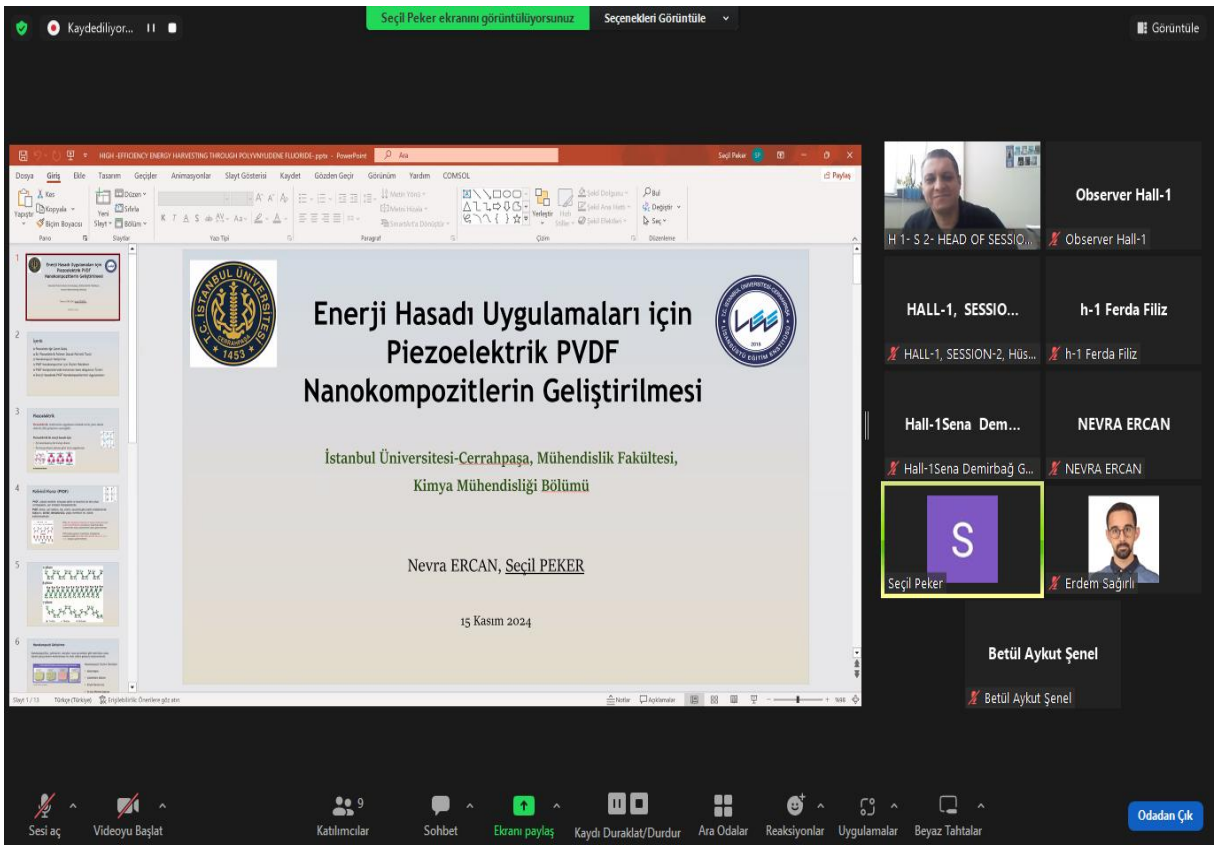

Zoom Toplantı - Hall-1
Kaydediliyor...
Görüntüle
Görkem Yumuşak
Observer Hall-1
Observer Hall-1
Hall-1 Zeynep Sı...
Hall-1 Zeynep Sıla Tırpancı
Dr. Sercan Basit
Dr. Sercan Basit
F
Salon-1, Ferhat Çeçen
Hafize Nagehan...
Hafize Nagehan KÖYSÜREN
Ozcan Koysuren
Ozcan Koysuren
Sesi aç
Videoyu Başlat
7
Katılımcılar
Sohbet
Ekranı paylaş
Kaydı Duraklat/Durdur
Ara Odalar
Reaksiyonlar
Uygulamalar
Beyaz Tahtalar
Odadan Çık
10:28
15.11.2024


Zoom Toplantı - Hall-1
Kaydediliyor...
Görüntüle
Hall-1 Zeynep Sıla Tırpancı
Observer Hall-1
Observer Hall-1
F
Salon-1, Ferhat Çeçen
Hafize Nagehan...
Hafize Nagehan KÖYSÜREN
Sesi aç
Videoyu Başlat
4
Katılımcılar
Sohbet
Ekranı paylaş
Kaydı Duraklat/Durdur
Ara Odalar
Reaksiyonlar
Uygulamalar
Beyaz Tahtalar
Odadan Çık
10:02
15.11.2024


Kaydediliyor...
Özcan Koysuren ekranını görüntülüyorsunuz
Seçenekleri Görüntüle
Görüntüle
SELF-CLEANING AND ANTI-REFLECTION COATING FOR SOLAR CELL
Hafize Nagehan Köysüren[a], Özcan Köysüren[b]
[a]Department of Environmental Engineering, Kirsehir Ahi Evran University, Kirsehir, 40100, TURKEY
[b]Department of Energy Systems Engineering, Ankara University, Ankara, 06830, TURKEY
INTERNATIONAL CERAMICS AND COMPOSITE MATERIALS SYMPOSIUM
15.11.2024
Hall-1 Zeynep Sı...
Hall-1 Zeynep Sıla Tırpancı
Observer Hall-1
Observer Hall-1
Dr. Sercan Basit
Dr. Sercan Basit
Hafize Nagehan...
Hafize Nagehan KÖYSÜREN
Ozcan Koysuren
Ozcan Koysuren
Sesi aç
Videoyu Başlat
Katılımcılar
Sohbet
Ekranı paylaş
Kaydı Duraklat/Durdur
Ara Odalar
Reaksiyonlar
Uygulamalar
Beyaz Tahtalar
Odadan Çık


Kaydediliyor...
Tan Eftal Gene HALL-1, SESSION... ekranını görüntülüyorsunuz
Seçenekleri Görüntüle
Görüntüle
Analysis of Vapor Treatment Time on Surface Quality of 3D-Printed ABS Parts
INTERNATIONAL CERAMICS AND COMPOSITE MATERIALS SYMPOSIUM
Tan Eftal Gene & Assist. Prof. Dr. Çağın Bolat
Samsun University, Department of Mechanical Engineering
15.11.2024
Hall-1 Zeynep Sı...
Hall-1 Zeynep Sıla Tır...
Observer Hall-1
Observer Hall-1
Dr. Sercan Basit
Dr. Sercan Basit
Hafize Nagehan...
Hafize Nagehan KÖYSÜ...
Ozcan Koysuren
Ozcan Koysuren
Tan Eftal Gene...
Tan Eftal Gene HALL-1, S...
Sesi aç
Videoyu Başlat
Katılımcılar
Sohbet
Ekranı paylaş
Kaydı Duraklat/Durdur
Ara Odalar
Reaksiyonlar
Uygulamalar
Beyaz Tahtalar
Odadan Çık


Kaydediliyor...
H-1 Celal AVCIOĞLU ekranını görüntülüyorsunuz
Seçenekleri Görüntüle
Görüntüle
Technische Universität Berlin
INVESTIGATION OF STRUCTURE-ACTIVITY RELATIONSHIP IN IRON-CONTAINING PEROVSKITES FOR SUPERCAPACITORS
Dr. Dr.-ing Celal Avcıoğlu
Chair of Advanced Ceramic Materials – Technische Universität Berlin
15 November 2024
celal.avcioglu@ceramics.tu-berlin.de
Keramische Werkstoffe
H-1 ayşe yerebakan
Observer Hall-1
Observer Hall-1
H-1 Celal AVCIOĞLU
H-1 Meryem Dilara KOP
H-1 Serap Unal
H-1 Serap Unal
Sesi aç
Videoyu Başlat
5
Katılımcılar
Sohbet
Ekranı paylaş
Kaydı Duraklat/Durdur
Ara Odalar
Reaksiyonlar
Uygulamalar
Beyaz Tahtalar
Odadan Çık


Kaydediliyor...
Seçil Peker ekranını görüntülüyorsunuz
Seçenekleri Görüntüle
Görüntüle
Enerji Hasadı Uygulamaları için Piezoelektrik PVDF Nanokompozitlerin Geliştirilmesi
İstanbul Üniversitesi-Cerrahpaşa, Mühendislik Fakültesi,
Kimya Mühendisliği Bölümü
Nevra ERCAN, Seçil PEKER
15 Kasım 2024
H 1- S 2- HEAD OF SESSIO...
Observer Hall-1
Observer Hall-1
HALL-1, SESSIO...
HALL-1, SESSION-2, Hüs...
h-1 Ferda Filiz
h-1 Ferda Filiz
Hall-1Sena Dem...
Hall-1Sena Demirbağ G...
NEVRA ERCAN
NEVRA ERCAN
S
Seçil Peker
Erdem Sağırlı
Betül Aykut Şenel
Betül Aykut Şenel
Sesi aç
Videoyu Başlat
9
Katılımcılar
Sohbet
Ekranı paylaş
Kaydı Duraklat/Durdur
Ara Odalar
Reaksiyonlar
Uygulamalar
Beyaz Tahtalar
Odadan Çık

INTERNATIONAL CERAMICS AND COMPOSITE MATERIALS SYMPOSIUM

November 15-16, 2024 / Isparta, Türkiye

CONGRESS PROGRAM

Süleyman Demirel University

Çünür, Süleyman Demirel Cd., 32260 Merkez- Isparta / Türkiye

Meeting ID: 859 7119 7642
Passcode: 151515

PARTICIPANT COUNTRIES (13):

Türkiye, Azerbaijan, Germany, China, Poland, Romania, Morocco, Algeria, India, Iran, Pakistan, Vietnam, Nigeria

IMPORTANT, PLEASE READ CAREFULLY

- To be able to make a meeting online, login via **https://zoom.us/join** site, enter ID instead of “Meeting ID or Personal Link Name” and solidify the session.
- The presentation will take a **maximum of 15 minutes** (including questions and answers).
- The Zoom application is free and no need to create an account.
- The Zoom application can be used without registration.
- The application works on tablets, phones and PCs.
- Speakers must be connected to the session **10 minutes before** the presentation time.
- All congress participants can connect live and listen to all sessions.
- During the session, your camera should be turned on at least %70 of session period
- Moderator is responsible for the presentation and scientific discussion (question-answer) section of the session.
-

TECHNICAL INFORMATION

- Make sure your computer has a microphone and is working.
- You should be able to use screen sharing feature in Zoom.
- Attendance certificates will be sent to you as pdf at the end of the congress.
- Moderator is responsible for the presentation and scientific discussion (question-answer) section of the session.

Before you login to Zoom please indicate your name surname and hall number,
exp. Hall-1, Salim ŞAHİN

ÖNEMLİ, DİKKATLE OKUYUNUZ LÜTFEN

- Kongremize Yazım Kurallarına uygun gönderilmiş ve bilim kurulundan geçen bildiriler için online (video konferans sistemi üzerinden) sunum imkanı sağlanmıştır.
- Sunumlar için 15 dakika (soru ve cevaplar dahil) süre ayrılmıştır.
- Online sunum yapabilmek için https://zoom.us/join sitesi üzerinden giriş yaparak “Meeting ID or Personal Link Name” yerine ID numarasını girerek oturuma katılabilirsiniz.
- Zoom uygulaması ücretsizdir ve hesap oluşturmaya gerek yoktur.
- Zoom uygulaması kaydolmadan kullanılabilir.
- Uygulama tablet, telefon ve PC’lerde çalışıyor.
- Her oturumdaki sunucular, sunum saatinden 10 dk öncesinde oturuma bağlanmış olmaları gerekmektedir.
- Tüm kongre katılımcıları canlı bağlanarak tüm oturumları dinleyebilir.
- Moderatör – oturumdaki sunum ve bilimsel tartışma (soru-cevap) kısmından sorumludur.
-

TEKNİK BİLGİLER

- Bilgisayarınızda mikrofon olduğuna ve çalıştığına emin olun.
- Zoom'da ekran paylaşma özelliğine kullanabilmelisiniz.
- Katılım belgeleri kongre sonunda tarafınıza pdf olarak gönderilecektir
- Kongre programında yer ve saat değişikliği gibi talepler dikkate alınmayacaktır

Zoom’a giriş yaparken önce lütfen adınızı, soyadınızı ve SALON numaranızı yazınız
Örnek: Salon-1, Emsal ŞAHİN

Zoom meeting link:
https://us02web.zoom.us/j/85971197642?pwd=qvFG4zD8YcWFPH7FYZqKGCBCctqVJw.1

-OPENING CEREMONY-

Date: 15.11.2024
Time (Ankara): 09:30-10:00

HEAD OF ORGANIZING COMMITTEE

Assoc. Prof. Dr. Serap ÜNAL – *Süleyman Demirel University*

HONORARY BOARD MEMBER

Dr. Mustafa Latif EMEK – *President of IKSAD Institute*

ONLINE PRESENTATIONS / 15.11.2024

	ANKARA LOCAL TIME - **10 ^{00} : 12 ^{00}**		ZOOM ID: 859 7119 7642
	HALL-1, SESSION-1		ZOOM PASSCODE: 151515

HEAD OF SESSION: Assoc. Prof. Dr. Hafize Nagehan KÖYSÜREN

AUTHORS	AFFILIATION	TOPIC TITLE
Zeynep Sıla TIRPANCI	Technology&Innovation Engineer, Epsan Plastik (Türkiye)	DEVELOPMENT OF ORANGE GLASS FIBER REINFORCED PBT COMPOSITES WITH IMPACT RESISTANCE ADDITIVES
Lect. Dr. Ferhat ÇEÇEN Assist. Prof. Dr. Ahmet ÖZBAYRAK Prof. Dr. Bekir AKTAŞ	Suleyman Demirel University, Lakes Region Technopolis, Coordinatorship, Isparta, Erciyes University, Faculty of Engineering, Civil Engineering Department, Kayseri, (Türkiye)	ASSESSING FLY ASH-BASED, HEAT-CURED GEOPOLYMER CONCRETE'S FLEXURAL STRENGTH AND DYNAMIC MODULUS RELATIONSHIP WITH NON-DESTRUCTIVE EXPERIMENTAL MODAL ANALYSIS
Assist. Prof. Dr. Görkem YUMUŞAK	Marmara University, Faculty of Engineering, Metallurgical And Material Engineering, Department of Materials (Türkiye)	PLA-BASED COMPOSITE FILAMENTS FOR 3D PRINTING: PRODUCTION PROCESSES AND MECHANICAL PERFORMANCE
Tan Etfal GENE Assist. Prof. Dr. Çağın BOLAT	Samsun University, Faculty of Engineering and Natural Sciences, Mechanical Engineering Department (Türkiye)	ANALYZING OF THE VAPOR TREATMENT TIME ON SURFACE QUALITY OF THE 3D-PRINTED ACRYLONITRILE BUTADIENE STYRENE PARTS
Assoc. Prof. Dr. Hafize Nagehan KÖYSÜREN Prof. Dr. Özcan KÖYSÜREN	Kırşehir Ahi Evran University, Engineering and Architecture Faculty, Department of Environmental Engineering, Kırşehir- Ankara University, Engineering Faculty, Department of Energy Systems Engineering, (Türkiye)	SELF-CLEANING AND ANTI-REFLECTION COATING FOR SOLAR CELL
Assoc. Prof. Dr. Hafize Nagehan KÖYSÜREN Prof. Dr. Özcan KÖYSÜREN	Kırşehir Ahi Evran University, Engineering and Architecture Faculty, Department of Environmental Engineering, Kırşehir- Ankara University, Engineering Faculty, Department of Energy Systems Engineering, (Türkiye)	APPLICATION of $CuFe_2O_4$ on the Cr(VI) PHOTOREDUCTION
Assist. Prof. Dr. Sercan BASİT	Kırşehir Ahi Evran Üniversitesi, Faculty of Engineering and Architecture, Mechanical Engineering, Kırşehir, (Türkiye)	INVESTIGATION OF THE PRODUCTION OF HEXAGONAL BORON NITRIDE / POLYAMIDE66 NANOSTRUCTURED COMPOSITE BY TEMPERATURE CONTROLLED MECHANOCHEMICAL PROCESS

ONLINE PRESENTATIONS / 15.11.2024

	ANKARA LOCAL TIME - **10 ^{00} : 12 ^{00}**		ZOOM ID: 859 7119 7642
	HALL-2, SESSION-1		ZOOM PASSCODE: 151515

HEAD OF SESSION: Assoc. Prof. Dr. Serap ÜNAL

AUTHORS	AFFILIATION	TOPIC TITLE
Metin KARAASLAN Zeynep DOĞAN	Istanbul Technical University, Faculty of Mechanical Engineering, Mechanical Engineering, Istanbul, (Türkiye)	EVALUATION OF COMPOSITE MATERIAL PRODUCTION FROM CAST IRON AND POLYMER WASTES IN MACHINING AND CASTING PROCESS
Assoc. Prof. Dr. Serap ÜNAL Res. Assist. Ayşe Melike BİRCAN	Süleyman Demirel University, Faculty of Fine Arts, Ceramics and Glass Department, Isparta, (Türkiye)	PRIMITIVE FIRING IN CERAMIC PRODUCTION
Assoc. Prof. Dr. Serap ÜNAL	Süleyman Demirel University, Faculty of Fine Arts, Ceramics and Glass Department, Isparta, (Türkiye)	FROM NEOLITHIC POTTERY TO TODAY'S CERAMIC COMPOSITES: THOUSANDS OF YEARS OF TECHNOLOGICAL EVOLUTION
Esma ÜNGÖRMÜŞ Assist. Prof. Dr. Naci Arda TANIŞ Prof. Dr. Ayşegül Ülkü METİN Prof. Dr. Recep ÇALIN	Kırıkkale University, Institute of Science and Technology, Defense Technologies, Kırıkkale, Kırıkkale University, Faculty of Engineering and Natural Sciences, Metallurgical and Materials Engineering, Chemistry, Kırıkkale, (Türkiye)	PRODUCTION OF CARBON NANOTUBE REINFORCED ALUMINUM MATRIX COMPOSITES BY INFILTRATION METHOD
Special Dr. Hüseyin Alperen SELVİ	Bilecik Oral And Dental Health Center, Bilecik, (Türkiye)	CERAMICS IN DENTISTRY
Lect. Dr. Müyesser Selda TÖZÜM	Uşak University, Faculty of Engineering and Natural Sciences, Textile Engineering, Uşak, (Türkiye)	PREPARATION AND CHARACTERIZATION OF ZnO NANOPARTICLE-COATED CHITOSAN/SODIUM ALGINATE WALLED ENERGY-STORING COMPOSITE MICROCAPSULES

ONLINE PRESENTATIONS / 15.11.2024

	ANKARA LOCAL TIME - **10 ^{00} : 12 ^{00}**		ZOOM ID: 859 7119 7642
	HALL-3, SESSION-1		ZOOM PASSCODE: 151515

HEAD OF SESSION: Prof. Dr. P. GAJALAKSHMI

AUTHORS	AFFILIATION	TOPIC TITLE
M. Sri DEVI R. DHARSINI S. KALAISELVAN	Department of Chemistry, Rathinam Technical Campus, Coimbatore, Tamilnadu, (India)	ECOLOGICAL FRIENDLY SYNTHESIS OF MULTI-WALLED CARBON NANOTUBES FROM PLANT-BASED HYDROCARBONS FOR EFFICIENT WATER PURIFICATION
Prof. Dr. P. GAJALAKSHMI Dr. A. S. MENAKA	Department of Civil Engineering B.S Abdur Rahman Crescent Institute of Science and Technology, Indian Institute of Technology, Madras, (India)	EXPERIMENTAL STUDY ON THE BEHAVIOUR OF CONCRETE FILLED STEEL TUBES SUBJECTED TO AXIAL AND LATERAL LOADING
Zahra REZAPOUR Narges FATHABADIBOZCHELOEI	Islamic Azad University, Department of Food Safety and Hygiene, Science and Research Branch, , Tehran, (Iran)	POLYCHLORINATED BIPHENYLS (PCBS) IN FOOD PACKAGING
Rania ZENATI Ahmed BOUCHERDOUD Meriem BENDJELLOUL Abdelkarim SEGHIER Sara AICHOUNI El Hadj ELANDALOUSSI	University of Relizane, Department of Chemistry, Faculty of Sciences and Technology, Laboratory of Environment and Sustainable Development (LESD). , Relizane, (Algeria)	ADVANCED BIOCOMPOSITE MATERIALS FOR THE ENVIRONMENT AND SUSTAINABLE DEVELOPMENT
Zakia HAMMOU Zakia GUEZZEN Zouaoui SEREIR Yamna HAMMOU	University of Science and Technology of Oran, Physical chemistry Department, Chemistry Faculty, USTO, Oran, University of Science and Technology of Oran, Composite Structures and Innovative Materials Laboratory, Mechanical Engineering Faculty, , USTO, Oran, (Algeria)	NONLINEAR VIBRATION ANALYSIS OF CARBON NANOTUBE-REINFORCED SHALLOW SHELLS WITH FUNCTIONALLY GRADED DISTRIBUTION
Abderrahim Ait Lhaj Brahim OUAZIK Mohamed El HASNAOUI Hassan CHAIB	Ibnou Zohr University, Materials and Energy Research Group, (Morocco)	DFT MODELING OF STRUCTURAL, ELECTRONIC, AND OPTICAL PROPERTIES OF SnO_2 SINGLE CRYSTAL: INFLUENCE OF HUBBARD CORRECTION ON BAND GAP AND REFRACTIVE INDICES

ONLINE PRESENTATIONS / 15.11.2024

	ANKARA LOCAL TIME - **10 ^{00} : 12 ^{00}**		ZOOM ID: 859 7119 7642
	HALL-4, SESSION-1		ZOOM PASSCODE: 151515

HEAD OF SESSION: Lecturer Dr. Irina-Ana DROBOT

AUTHORS	AFFILIATION	TOPIC TITLE
Lecturer Dr. Irina-Ana DROBOT	Technical University of Civil Engineering Bucharest, Faculty of Engineering in Foreign Languages, Department of Foreign Languages and Communication, Bucharest, (Romania)	THE DEVELOPMENT OF JAPANESE CERAMICS ART
Hacar ASLANOVA Chichak SEYIDOVA Nigar SHIKHVERDIYEVA Nizami ZEYNALOV	Institute of Catalysis and Inorganic Chemistry named after M. Nagiyev, Ministry of Science and Education of the Republic of Azerbaijan, Laboratory of Nanostructured metal-polymer catalysts, Baku, (Azerbaijan)	SYNTHESIS OF PD NANOPARTICLES IN POLY-4-VINYL PYRIDINE MEDIA
Elchin BABAYEV Nargiz RAHIMLI Ulviyya MAMMADOVA Dilshad BABAYEVA	Institute of Catalysis and Inorganic Chemistry named after M. Nagiyev, Ministry of Science and Education of the Republic of Azerbaijan, Laboratory of Nanostructured metal-polymer catalysts, Baku, (Azerbaijan)	SYNTHESIS OF POLYMER-BASED SILVER NANOPARTICLES, STRUCTURE AND PROPERTIES OF OBTAINED POLYMER COMPOSITE
Elmira ALIYEVA Nizami ZEYNALOV	Ministry of Science and Education Republic of Azerbaijan «Institute of Catalysis and Inorganic Chemistry named after academician of M.Nagiev», Laboratory of Nanostructured metal-polymer catalysts, (Azerbaijan)	SMART POLYMER-BASED HYDROGELS AND THEIR FIELDS OF APPLICATION
Seadet HUMBATOVA Nizami ZEYNALOV Elmira ALIYEVA Elnara NASIYYATI	Ministry of Science and Education Republic of Azerbaijan «Institute of Catalysis and Inorganic Chemistry named after academician of M.Nagiev», Laboratory of Nanostructured metal-polymer catalysts, (Azerbaijan)	IMMOBILIZATION AND STUDY OF DOXORUBICIN AND TRYPSIN IN BIOPOLYMER-Fe_3O_4 MAGNETITE NANOPARTICLE GEL SYSTEMS
Melik SAMI Khelil SARA Tallal Abdel Karim BOUZIR	Mohamed Khider Biskra University, Departement of architecture, Biskra, Blida University, Institute of Architecture and Urban Planning, Blida, (Algeria)	FROM ORNAMENT TO STRUCTURE: THE DUAL ROLE OF CERAMICS IN OTTOMAN ARCHITECTURE
Melik SAMI Khelil SARA Tallal Abdel Karim BOUZIR	Mohamed Khider Biskra University, Departement of architecture, Biskra, Blida University, Institute of Architecture and Urban Planning, Blida, (Algeria)	CERAMIC EXPRESSIONS IN ARCHITECTURE: CULTURAL SYMBOLISM ACROSS ANCIENT AND MODERN CIVILIZATIONS

ONLINE PRESENTATIONS / 15.11.2024

	ANKARA LOCAL TIME - **12 30 : 14 30**		ZOOM ID: 859 7119 7642
	HALL-1, SESSION-2		ZOOM PASSCODE: 151515

HEAD OF SESSION: Dr. Ethem İlhan ŞAHİN

AUTHORS	AFFILIATION	TOPIC TITLE
Dr. Aytaç DİNÇER Dr. Mehmet KERTMEN Dr. Gözde Özlem ÖRENTAŞ Halil İbrahim OLUCAK	İSKUR HOLDING Kahramanmaraş, (Türkiye)	INVESTIGATION OF USING SERPANTINITE, DOLOMITE AND BARITE ADDED CONCRETE AGAINST RADIATION EFFECT
Lect. Dr. Sena DEMİRBAĞ GENÇ	Uşak University, Faculty of Engineering and Natural Sciences, Textile Engineering, Uşak, (Türkiye)	PRODUCTION OF COMPOSITE MICROCAPSULE WITH GUM ARABIC/COPPER OXIDE SHELL FOR THERMAL ENERGY STORAGE AND PHOTO–THERMAL CONVERSION
Res. Assist. Ferda TAZEOĞLU FİLİZ	Selcuk Universty, Fine Art Faculty, Ceramic, Konya, (Türkiye)	THE USE OF GLOOPY GLAZE IN CONTEMPORARY CERAMIC ART
Lect. Dr. Hüseyin ÖZKAVAK Prof. Dr. Recai Fatih TUNAY	Isparta University of Applied Sciences, Isparta OSB Vocational School, Department of Mechanical and Metal Technology, Isparta, Süleyman Demirel University, Faculty of Engineering, Department of Mechanical Engineering, Isparta, (Türkiye)	INVESTIGATION OF THE COATING PROPERTIES OF AA7075 AND AZ91 MATERIALS COATED WITH DIFFERENT RATIOS OF Al_2O_3-TiO_2
Seçil Peker ADIGÜZEL Assoc. Prof. Dr. Nevra ERCAN	Istanbul University Cerrahpaşa, Engineering Faculty, Department of Chemical Engineering, Istanbul, (Türkiye)	HIGH -EFFICIENCY ENERGY HARVESTING THROUGH POLYVNYLIDENE FLUORIDE-GRAPHENE NANORIBBON COMPOSITE
Erdem SAĞIRLI Lect. Dr. Suna AVCIOGLU Prof. Dr. Figen KAYA Prof. Dr. Cengiz KAYA	Yıldız Technical University, Department of Metallurgical and Materials Engineering, Istanbul, (Türkiye)	SYNTHESIS OF BARON NITRIDE REINFORCED BORON CARBIDE NANOCOMPOSITES AND THEIR APPLICATIONS
Res. Assist. Betül Aykut ŞENEL Prof. Dr. Şehnaz Şule Kaplan BEKAROĞLU Prof. Dr. Mehmet KİTİŞ	Suleyman Demirel University, Faculty of Engineering and Natural Sciences, Department of Environmental Engineering, Isparta, (Türkiye)	NANOCOMPOSITES AND NANOADSORBENTS FOR WATER AND WASTEWATER TREATMENT: CRITICAL REVIEW OF THE CURRENT LITERATURE

ONLINE PRESENTATIONS / 15.11.2024

	ANKARA LOCAL TIME - **12 30 : 14 30**		ZOOM ID: 859 7119 7642
	HALL-2, SESSION-2		ZOOM PASSCODE: 151515

HEAD OF SESSION: Assist. Prof. Dr. Özden İŞBİLİR

AUTHORS	AFFILIATION	TOPIC TITLE
Assist. Prof. Dr. Özden İŞBİLİR	Karabük University, Engineering Faculty, Mechanical Engineering Department, Karabük, (Türkiye)	FINITE ELEMENT ANALYSIS OF OPEN HOLE COMPRESSIVE STRENGTH OF COMPOSITE MATERIALS
Assist. Prof. Dr. Özden İŞBİLİR	Karabük University, Engineering Faculty, Mechanical Engineering Department, Karabük, (Türkiye)	FINITE ELEMENT ANALYSIS OF OPEN HOLE STRENGTH OF FIBRE METAL LAMINATES
Prof. Dr. Ayşe ÖNDÜRÜCÜ Havva Nur HİÇYORULMAZ	Suleyman Demirel University, Faculty of Engineering and Natural Science, Department of Mechanical Engineering, (Türkiye)	COMPOSITE PRODUCTION FROM WASTE CERAMICS
Assist. Prof. Dr. Nazife Korkmaz MEMİŞ Prof. Dr. Sibel KAPLAN	Suleyman Demirel University, Faculty of Engineering and Natural Sciences, Textile Engineering Department, Isparta, (Türkiye)	HIERARCHICALLY POROUS NANOCOMPOSITE FILMS FOR EFFICIENT PASSIVE DAYTIME RADIATIVE COOLING
Dilay ÖZUYAR Berkay SÖZÜDOĞRU Mustafa TOSUN Gökhan ÜNAL Prof. Dr. Burak ÖZKAL	Yurtbay Seramik, R&D Center Eskişehir (Türkiye)	THE USE OF CERAMIC TILE WASTE AS A CALCITE REPLACEMENT IN DIFFERENT MORTARS
Erhan ASLAN Elif Muslu YILMAZ Assoc. Prof. Dr. Neslihan Nohut MASLAKCI Assoc. Prof. Dr. Esin EREN Prof. Dr. Ayşegül Uygun ÖKSÜZ	Suleyman Demirel University, Innovative Technologies Application and Research Center, Isparta Suleyman Demirel University, Engineering and Natural Sciences Faculty, Chemistry Department, Isparta, Isparta Applied Sciences University, Gelendost Vocational School, Pharmacy Services Department, Isparta, (Türkiye)	SYNTHESIS AND CHARACTERIZATION OF RGO-CEO_2 BASED COMPOSITE FIBERS

ONLINE PRESENTATIONS / 15.11.2024

ANKARA LOCAL TIME - **12 30 : 14 30**	ZOOM ID: 859 7119 7642
HALL-3, SESSION-2	ZOOM PASSCODE: 151515

HEAD OF SESSION: Dr. Muhammad FAISAL

AUTHORS	AFFILIATION	TOPIC TITLE
Jianwei CHENG Shuping SHENG Dezhi RAN Md Mojahidul ISLAM Marek BOROWSKİ	China University of Mining and Technology, School of Mining Engineering, Xuzhou 221116, (China) AGH University of Science and Technology, Faculty of Mining and Geoengineering, Krakow, (Poland)	GROUTING AND SEALING BED SEPARATION BY OVERLAPPING MINE GOBS IN MULTIPLE SEAMS TO IMPROVE OXYGEN FLOW IN THE LONGWALL FACE
M. A. JAFAROV V. M. SALMANOV R. M. MAMEDOV E. F. NASIROV T. A. MAMEDOVA	Baku State University, AZ1148 Baku, (Azerbaijan)	SYNTHESIS OF CdSTe NANOPARTICLES BY LASER ABLATION
A. LAHOUEL M. ADNANE S. KOUDJETI	University of Science and Technology of Oran-Mohammed Boudiaf, Department of Physics, Oran, (Algeria) University of Sciences of Abou Bekr Belkaid, Department of Physics, Tlemcen, (Algeria)	THE SYNTHESIZE OF THIN FILM VIA SOL-GEL DIP-COATING TECHNIQUE DERIVED BY SnO_2
Muhammad FAISAL	Allama Iqbal Open University MIS/IT Specialist in Ministry of Safron (Pakistan)	BUILDING A CERAMIC AND COMPOSITE MATERIALS INDUSTRIAL ZONE IN PAKISTAN A STRATEGIC RESEARCH BY DR FAISAL FOR FRAMEWORK FOR SUSTAINABLE GROWTH
Imen Yamina OMRI Zine El Abidine RAHMOUNI Nadia TEBBAL	University Mohamed Boudiaf, Faculty technolgy, Department Civil engineering, (Algeria)	GENERAL INFORMATION ON TESTS FOR QUALITY CONTROL OF ALKALINE MATERIALS BASED ON ACTIVE RESIDUES
Bhushan CHAVAN Prof. Dr. Manish POKHARNA Assoc. Prof. Dr. Sameer NANIVADEKAR Assist. Prof. Dr. Amol SHINDE	Pacific Academy of Higher Education and Research University, Udaipur, Rajasthan, A. P. Shah Institute of Technology, Thane, Maharashtra (India)	INNOVATIVE COMPOSITE MATERIALS FOR NEXT-GENERATION ELECTRIC VEHICLE BATTERIES: CHALLENGES AND OPPORTUNITIES
Bhushan CHAVAN Prof. Dr. Manish POKHARNA Assoc. Prof. Dr. Sameer NANIVADEKAR Assist. Prof. Dr. Amol SHINDE	Pacific Academy of Higher Education and Research University, Udaipur, Rajasthan, A. P. Shah Institute of Technology, Thane, Maharashtra (India)	LIGHTWEIGHTING ELECTRIC VEHICLES: THE DUAL ROLE OF COMPOSITE MATERIALS IN BATTERY AND VEHICLE INTEGRATION

ONLINE PRESENTATIONS / 15.11.2024

	ANKARA LOCAL TIME - **12 ^{30} : 14 ^{30}**		ZOOM ID: 859 7119 7642
	HALL-4, SESSION-2		ZOOM PASSCODE: 151515

HEAD OF SESSION: Assist. Prof. Dr. Kavirayani SRIKANTH

AUTHORS	AFFILIATION	TOPIC TITLE
M. R. HARROUG H. AMEDDAH H. MAZOUZ	University Batna 2, Faculty of Technology, Department of Mechanical Engineering, Batna, (Algeria)	A NEW BIOMIMETIC DESIGN BIOCERAMIC FOR BONE REGENERATION BY TPMS LATTICE STRUCTURE
Mahmoud BOUSLAH Prof. Dr. Mekki MAZA Prof. Dr. Zine EL Abidine RAHMOUNI Prof. Dr. Nadia TEBBAL	University of M'sila, Faculty of technology ,Civil engineering department, M'sila, (Algeria)	UTILIZATION OF SEWAGE SLUDGE ASH IN LIGHTWEIGHT AGGREGATE PRODUCTION FOR SUSTAINABLE CONSTRUCTION
Dr. Saad BAALI Prof. Dr. Mekki MAZA Prof. Dr. Zine El Abidine RAHMOUNI Prof. Dr. Nadia TEBBAL	Civil engineering Department, Geomaterials Development Laboratory, University of M'sila, (Algeria)	VALORIZATION OF SEWAGE SLUDGE INTO CERAMIC MATERIALS
Romaissa HACHANA Souhila AGRED Abdallah BENAROUS	Blida1 University, Faculty of Technology, Department of Mechanics, Blida University of Chlef, Faculty of Technology, Department of Mechanics (Algeria)	ASSESSING THE INFLUENCE OF WALL MATERIALS ON COMPARTMENT FIRE BEHAVIOR: A COMPARATIVE ANALYSIS WITH EUROPEAN STANDARDS
Mustapha AOUAICHIA Rachid BOUAMRANE	Faculté de physique ;université des sciences et de la technologie d'Oran-MB (Algeria)	THE INVESTIGATION OF THE EMERGENT BEHAVIIOUR OF POLYMER FILLED WITH CARBON NANOTUBE MODELED BY RANDOM RESISTOR-CAPACITOR-DIODE ELECTRICAL NETWORK
Aparna SHARMA Namrata SINGH Akanksha YADAV Shashi BALA	University of Lucknow, Department of Chemistry, Lucknow (India)	NEW SAGACITY INTO THE ENVIRONMENTAL AND THERAPEUTIC APPLICATION OF ESSENTIAL METAL NANOPARTICLES
Assist. Prof. Dr. Kavirayani SRIKANTH	Dept. of EEE, Gayatri Vidya Parishad College of Engineering(Autonomous), Visakhapatnam, Andhra Pradesh, (India)	ENHANCING COMPOSITE MATERIALS THROUGH COMPUTATIONAL INTELLIGENCE TECHNIQUES
Faiza Baghida Prof. Dr. Mourad Boughrara	Faculty of Sciences, University Moulay Ismail B.P:11201 Zitoune, Meknès, Morocoo	ELECTRONIC AND THERMOELECTRIC PROPERTIES STUDY OF Cu_2Se : DFT STUDY

ONLINE PRESENTATIONS / 15.11.2024

	ANKARA LOCAL TIME - **15 ^{00} : 17 ^{00}**		ZOOM ID: 859 7119 7642
	HALL-1, SESSION-3		ZOOM PASSCODE: 151515

HEAD OF SESSION: Dr. Celal AVCIOĞLU

AUTHORS	AFFILIATION	TOPIC TITLE
Assist. Prof. Dr. Ayşegül YÜCEL	İskenderun Technical University, İskenderun Vocational School, Department of Envıronmental Protectıon Technologies, Hatay, (Türkiye)	INVESTIGATION OF THE USE OF ARTIFICIAL INTELLIGENCE IN DETERMINING THE STRUCTURE DEFECT IN CERAMIC COMPOSITE MATERIALS
Res. Assist. Ayşe YEREBAKAN	Çukurova University, Fine Art Faculty, Ceramic Department, Adana, (Türkiye)	REDEFINING THE NEST: THE CONTRIBUTION OF ECOLOGICAL CERAMICS TO THE CONSERVATION OF NATURAL OF HABITATS
Murat Cem DURMAZ Lect. Dr. Suna AVCIOGLU Prof. Dr. Figen KAYA Prof. Dr. Cengiz KAYA	Yıldız Technical University, Department of Metallurgical and Materials Engineering, Istanbul, (Türkiye)	SOL-GEL METHOD FOR TAILORED BN-B_4C NANOCOMPOSITES: A CONTROLLED SYNTHESIS APPROACH
Meryem Dilara KOP Gökalp YILMAZ Prof. Dr. Mehmet AVCAR Assoc. Prof. Dr. Mehmet Eren UZ	Isparta Suleyman Demirel University, Graduate School of Natural and Applied Sciences, Department of Civil Engineering, Isparta, Aydın Adnan Menderes University Faculty of Engineering, Department of Civil Engineering, Aydın, (Türkiye)	EXPERIMENTAL ANALYSIS OF HAILSTONE IMPACT ON AIRCRAFT CANOPY
Dr. Celal AVCIOĞLU	Technische Universität Berlin, Faculty III Process Sciences, Institute of Materials Science and Technology, Chair of Advanced Ceramic Materials (Germany)	INVESTIGATION OF STRUCTURE-ACTIVITY RELATIONSHIP IN IRON-CONTAINING PEROVSKITES FOR SUPERCAPACITORS

ONLINE PRESENTATIONS / 15.11.2024

	ANKARA LOCAL TIME - **15 ^{00} : 17 ^{00}**		ZOOM ID: 859 7119 7642
	HALL-2, SESSION-3		ZOOM PASSCODE: 151515

HEAD OF SESSION: Tran Kim ANH

AUTHORS	AFFILIATION	TOPIC TITLE
Anil K. VASHISHTH Umang BAREJA	Kurukshetra University, Department of Mathematics Kurukshetra, Haryana, (India)	REFLECTION AND TRANSMISSION OF ACOUSTIC AND ULTRASONIC WAVES IN FUNCTIONALLY GRADED POROUS PIEZOELECTRIC MATERIALS
Zineb El HAMRI M. ALAMI M. ASSOUAG	University Moulay Ismail, Team of Innovative Materials and Mechanical Manufacturing Processes, ENSAM, Al Mansour, Meknes, (Morocco)	IMPACT OF WALNUT SHELL POWDER ON THE PROPERTIES OF POLYPROPYLENE-REINFORCED COMPOSITES
Babafemi Raphael BABANIYI Oluwaseun Adekoya ADELAJA Folorunso Patrick ALIU Monday Peter OBAGUNWA	Bioresources Development Center, National Biotechnology Research And Development Agency Abuja, (Nigeria)	CHARACTERIZATION OF PET-ACTIVATED CARBON COMPOSITES: EFFECTS OF ORANGE PEEL AND SAWDUST DERIVATIVES
Tran Kim ANH	Vietnam Academy of Science and Technology, Nghia Do, Cau Giay, Ha Noi (Vietnam)	VIETNAM WOMEN STUDIES NANOMATERIALS CONTAINING RARE EARTH IONS AND APPLICATIONS
Zineb Ait FARES Miloudi HLAIBI Noureddine KAMIL Rachid OUCHN	Laboratory of Materials Engineering for Environment and Valorization (GeMEV), Faculty of Sciences Aïn Chock, Hassan II University of Casablanca (Morocco)	POLYMERIC MEMBRANES FOR DESALINATION USING MEMBRANE DISTILLATION: A REVIEW
A. LAHOUEL M. ADNANE S. KOUDJETI	University of Science and Technology of Oran-Mohammed Boudiaf University of Sciences of Abou Bekr Belkaid, (Algeria)	SYNTHESIS OF THIN FILMS USING THE SOL-GEL DIP-COATING TECHNIQUE DERIVED FROM SnO_2

CONTENTS

CONGRESS ID	**I**
PHOTO GALLERY	**II**
PROGRAM	**III**
CONTENT	**IV**

AUTHOR	TITLE	No
Zeynep Sıla TIRPANCI	DEVELOPMENT OF ORANGE GLASS FIBER REINFORCED PBT COMPOSITES WITH IMPACT RESISTANCE ADDITIVES	1
Ferhat ÇEÇEN *Ahmet ÖZBAYRAK* *Bekir AKTAŞ*	ASSESSING FLY ASH-BASED, HEAT-CURED GEOPOLYMER CONCRETE'S FLEXURAL STRENGTH AND DYNAMIC MODULUS RELATIONSHIP WITH NON-DESTRUCTIVE EXPERIMENTAL MODAL ANALYSIS	3
Tan Etfal GENE *Çağın BOLAT*	ANALYZING OF THE VAPOR TREATMENT TIME ON SURFACE QUALITY OF THE 3D-PRINTED ACRYLONITRILE BUTADIENE STYRENE PARTS	10
Hafize Nagehan KÖYSÜREN *Özcan KÖYSÜREN*	SELF-CLEANING AND ANTI-REFLECTION COATING FOR SOLAR CELL	20
Sercan BASİT	INVESTIGATION OF THE PRODUCTION OF HEXAGONAL BORON NITRIDE / POLYAMIDE66 NANOSTRUCTURED COMPOSITE BY TEMPERATURE CONTROLLED MECHANOCHEMICAL PROCESS	27
Zahra REZAPOUR *Narges FATHABADIBOZCHELOEI*	POLYCHLORINATED BIPHENYLS (PCBS) IN FOOD PACKAGING	38
Metin KARAASLAN *Zeynep DOĞAN*	EVALUATION OF COMPOSITE MATERIAL PRODUCTION FROM CAST IRON AND POLYMER WASTES IN MACHINING AND CASTING PROCESS	39
Serap ÜNAL *Ayşe Melike BİRCAN*	PRIMITIVE FIRING IN CERAMIC PRODUCTION	71

Serap ÜNAL	**FROM NEOLITHIC POTTERY TO TODAY'S CERAMIC COMPOSITES: THOUSANDS OF YEARS OF TECHNOLOGICAL EVOLUTION**	**84**
Esma ÜNGÖRMÜŞ *Naci Arda TANIŞ* *Ayşegül Ülkü METİN* *Recep ÇALIN*	**PRODUCTION OF CARBON NANOTUBE REINFORCED ALUMINUM MATRIX COMPOSITES BY INFILTRATION METHOD**	**96**
Rania ZENATI *Ahmed BOUCHERDOUD* *Meriem BENDJELLOUL* *Abdelkarim SEGHIER* *Sara AICHOUNI* *El Hadj ELANDALOUSSI*	**ADVANCED BIOCOMPOSITE MATERIALS FOR THE ENVIRONMENT AND SUSTAINABLE DEVELOPMENT**	**106**
Hüseyin Alperen SELVİ	**CERAMICS IN DENTISTRY**	**107**
Müyesser Selda TÖZÜM	**PREPARATION AND CHARACTERIZATION OF ZnO NANOPARTICLE-COATED CHITOSAN/SODIUM ALGINATE WALLED ENERGY-STORING COMPOSITE MICROCAPSULES**	**108**
Sena DEMİRBAĞ GENÇ	**PRODUCTION OF COMPOSITE MICROCAPSULE WITH GUM ARABIC/COPPER OXIDE SHELL FOR THERMAL ENERGY STORAGE AND PHOTO–THERMAL CONVERSION**	**116**
Hafize Nagehan KÖYSÜREN *Özcan KÖYSÜREN*	**APPLICATION of $CuFe_2O_4$ on the Cr(VI) PHOTOREDUCTION**	**125**
Ferda TAZEOĞLU FİLİZ	**THE USE OF GLOOPY GLAZE IN CONTEMPORARY CERAMIC ART**	**132**
Aytaç DİNÇER *Mehmet KERTMEN* *Gözde Özlem ÖRENTAŞ* *Halil İbrahim OLUCAK*	**INVESTIGATION OF USING SERPANTINITE, DOLOMITE AND BARITE ADDED CONCRETE AGAINST RADIATION EFFECT**	**133**
Zakia HAMMOU *Zakia GUEZZEN* *Zouaoui SEREIR* *Yamna HAMMOU*	**NONLINEAR VIBRATION ANALYSIS OF CARBON NANOTUBE-REINFORCED SHALLOW SHELLS WITH FUNCTIONALLY GRADED DISTRIBUTION**	**134**
Romaissa HACHANA *Souhila AGRED* *Abdallah BENAROUS*	**ASSESSING THE INFLUENCE OF WALL MATERIALS ON COMPARTMENT FIRE BEHAVIOR: A COMPARATIVE**	**135**

	ANALYSIS WITH EUROPEAN STANDARDS	
Abderrahim Ait Lhaj Brahim OUAZIK Mohamed El HASNAOUI Hassan CHAIB	**DFT MODELING OF STRUCTURAL, ELECTRONIC, AND OPTICAL PROPERTIES OF SnO_2 SINGLE CRYSTAL: INFLUENCE OF HUBBARD CORRECTION ON BAND GAP AND REFRACTIVE INDICES**	**142**
Hüseyin ÖZKAVAK Recai Fatih TUNAY	**INVESTIGATION OF THE COATING PROPERTIES OF AA7075 AND AZ91 MATERIALS COATED WITH DIFFERENT RATIOS OF Al_2O_3-TiO_2**	**143**
Seçil Peker ADIGÜZEL Nevra ERCAN	**HIGH -EFFICIENCY ENERGY HARVESTING THROUGH POLYVNYLIDENE FLUORIDE-GRAPHENE NANORIBBON COMPOSITE**	**154**
Erdem SAĞIRLI Suna AVCIOGLU Figen KAYA Cengiz KAYA	**SYNTHESIS OF BARON NITRIDE REINFORCED BORON CARBIDE NANOCOMPOSITES AND THEIR APPLICATIONS**	**155**
Irina-Ana DROBOT	**THE DEVELOPMENT OF JAPANESE CERAMICS ART**	**156**
Betül Aykut ŞENEL Şehnaz Şule Kaplan BEKAROĞLU Mehmet KİTİŞ	**NANOCOMPOSITES AND NANOADSORBENTS FOR WATER AND WASTEWATER TREATMENT: CRITICAL REVIEW OF THE CURRENT LITERATURE**	**163**
Özden İŞBİLİR	**FINITE ELEMENT ANALYSIS OF OPEN HOLE COMPRESSIVE STRENGTH OF COMPOSITE MATERIALS**	**164**
Özden İŞBİLİR	**FINITE ELEMENT ANALYSIS OF OPEN HOLE STRENGTH OF FIBRE METAL LAMINATES**	**175**
Hacar ASLANOVA Chichak SEYIDOVA Nigar SHIKHVERDIYEVA Nizami ZEYNALOV	**SYNTHESIS OF PD NANOPARTICLES IN POLY-4-VINYL PYRIDINE MEDIA**	**190**
Elchin BABAYEV Nargiz RAHIMLI Ulviyya MAMMADOVA Dilshad BABAYEVA	**SYNTHESIS OF POLYMER-BASED SILVER NANOPARTICLES, STRUCTURE AND PROPERTIES OF OBTAINED POLYMER COMPOSITE**	**192**
Elmira ALIYEVA Nizami ZEYNALOV	**SMART POLYMER-BASED HYDROGELS AND THEIR FIELDS OF APPLICATION**	**194**
Seadet HUMBATOVA Nizami ZEYNALOV Elmira ALIYEVA Elnara NASIYYATI	**IMMOBILIZATION AND STUDY OF DOXORUBICIN AND TRYPSIN IN BIOPOLYMER-Fe_3O_4 MAGNETITE NANOPARTICLE GEL SYSTEMS**	**196**

Havva Nur HİÇYORULMAZ *Ayşe ÖNDÜRÜCÜ*	**COMPOSITE PRODUCTION FROM WASTE CERAMICS**	**199**
Nazife Korkmaz MEMİŞ *Sibel KAPLAN*	**HIERARCHICALLY POROUS NANOCOMPOSITE FILMS FOR EFFICIENT PASSIVE DAYTIME RADIATIVE COOLING**	**211**
Dilay ÖZUYAR *Berkay SÖZÜDOĞRU* *Mustafa TOSUN* *Gökhan ÜNAL* *Burak ÖZKAL*	**THE USE OF CERAMIC TILE WASTE AS A CALCITE REPLACEMENT IN DIFFERENT MORTARS**	**217**
Meryem Dilara KOP *Gökalp YILMAZ* *Mehmet AVCAR* *Mehmet Eren UZ*	**EXPERIMENTAL ANALYSIS OF HAILSTONE IMPACT ON AIRCRAFT CANOPY**	**218**
Ayşegül YÜCEL	**INVESTIGATION OF THE USE OF ARTIFICIAL INTELLIGENCE IN DETERMINING THE STRUCTURE DEFECT IN CERAMIC COMPOSITE MATERIALS**	**219**
Melik SAMI *Khelil SARA* *Tallal Abdel Karim BOUZIR*	**FROM ORNAMENT TO STRUCTURE: THE DUAL ROLE OF CERAMICS IN OTTOMAN ARCHITECTURE**	**221**
Melik SAMI *Khelil SARA* *Tallal Abdel Karim BOUZIR*	**CERAMIC EXPRESSIONS IN ARCHITECTURE: CULTURAL SYMBOLISM ACROSS ANCIENT AND MODERN CIVILIZATIONS**	**222**
Jianwei CHENG *Shuping SHENG* *Dezhi RAN* *Md Mojahidul ISLAM* *Marek BOROWSKİ*	**GROUTING AND SEALING BED SEPARATION BY OVERLAPPING MINE GOBS IN MULTIPLE SEAMS TO IMPROVE OXYGEN FLOW IN THE LONGWALL FACE**	**223**
M. A. JAFAROV *V. M. SALMANOV* *R. M. MAMEDOV* *E. F. NASIROV* *T. A. MAMEDOVA*	**SYNTHESIS OF CdSTe NANOPARTICLES BY LASER ABLATION**	**225**
A. LAHOUEL *M. ADNANE* *S. KOUDJETI*	**THE SYNTHESIZE OF THIN FILM VIA SOL-GEL DIP-COATING TECHNIQUE DERIVED BY SnO_2**	**231**
Ayşe YEREBAKAN	**REDEFINING THE NEST: THE CONTRIBUTION OF ECOLOGICAL CERAMICS TO THE CONSERVATION OF NATURAL OF HABITATS**	**232**
Saad BAALI *Mekki MAZA* *Zine El Abidine RAHMOUNI*	**VALORIZATION OF SEWAGE SLUDGE INTO CERAMIC MATERIALS**	**233**

Nadia TEBBAL		
Kavirayani SRIKANTH	**ENHANCING COMPOSITE MATERIALS THROUGH COMPUTATIONAL INTELLIGENCE TECHNIQUES**	**234**
Murat Cem DURMAZ *Suna AVCIOGLU* *Figen KAYA* *Cengiz KAYA*	**SOL-GEL METHOD FOR TAILORED BN-B_4C NANOCOMPOSITES: A CONTROLLED SYNTHESIS APPROACH**	**235**
Celal AVCIOĞLU	**INVESTIGATION OF STRUCTURE-ACTIVITY RELATIONSHIP IN IRON-CONTAINING PEROVSKITES FOR SUPERCAPACITORS**	**236**
Muhammad FAISAL	**BUILDING A CERAMIC AND COMPOSITE MATERIALS INDUSTRIAL ZONE IN PAKISTAN A STRATEGIC RESEARCH BY DR FAISAL FOR FRAMEWORK FOR SUSTAINABLE GROWTH**	**237**
Mustapha AOUAICHIA *Rachid BOUAMRANE*	**THE INVESTIGATION OF THE EMERGENT BEHAVIIOUR OF POLYMER FILLED WITH CARBON NANOTUBE MODELED BY RANDOM RESISTOR-CAPACITOR-DIODE ELECTRICAL NETWORK**	**239**
M. R. HARROUG *H. AMEDDAH* *H. MAZOUZ*	**A NEW BIOMIMETIC DESIGN BIOCERAMIC FOR BONE REGENERATION BY TPMS LATTICE STRUCTURE**	**245**
Mahmoud BOUSLAH *Mekki MAZA* *Zine EL Abidine RAHMOUNI* *Nadia TEBBAL*	**UTILIZATION OF SEWAGE SLUDGE ASH IN LIGHTWEIGHT AGGREGATE PRODUCTION FOR SUSTAINABLE CONSTRUCTION**	**246**
P. GAJALAKSHMI *A. S. MENAKA*	**EXPERIMENTAL STUDY ON THE BEHAVIOUR OF CONCRETE FILLED STEEL TUBES SUBJECTED TO AXIAL AND LATERAL LOADING**	**247**
Görkem YUMUŞAK	**PLA-BASED COMPOSITE FILAMENTS FOR 3D PRINTING: PRODUCTION PROCESSES AND MECHANICAL PERFORMANCE**	**248**
M. Sri DEVI *R. DHARSINI* *S. KALAISELVAN*	**ECOLOGICAL FRIENDLY SYNTHESIS OF MULTI-WALLED CARBON NANOTUBES FROM PLANT-BASED HYDROCARBONS FOR EFFICIENT WATER PURIFICATION**	**256**
Imen Yamina OMRI *Zine El Abidine RAHMOUNI*	**GENERAL INFORMATION ON TESTS FOR QUALITY CONTROL OF ALKALINE**	**258**

Nadia TEBBAL	**MATERIALS BASED ON ACTIVE RESIDUES**	
Erhan ASLAN *Elif Muslu YILMAZ* *Neslihan Nohut MASLAKCI* *Esin EREN* *Ayşegül Uygun ÖKSÜZ*	**SYNTHESIS AND CHARACTERIZATION OF RGO-CEO_2 BASED COMPOSITE FIBERS**	**259**
Aparna SHARMA *Namrata SINGH* *Akanksha YADAV* *Shashi BALA*	**NEW SAGACITY INTO THE ENVIRONMENTAL AND THERAPEUTIC APPLICATION OF ESSENTIAL METAL NANOPARTICLES**	**261**
Bhushan CHAVAN *Manish POKHARNA* *Sameer NANIVADEKAR* *Amol SHINDE*	**INNOVATIVE COMPOSITE MATERIALS FOR NEXT-GENERATION ELECTRIC VEHICLE BATTERIES: CHALLENGES AND OPPORTUNITIES**	**262**
Bhushan CHAVAN *Manish POKHARNA* *Sameer NANIVADEKAR* *Amol SHINDE*	**LIGHTWEIGHTING ELECTRIC VEHICLES: THE DUAL ROLE OF COMPOSITE MATERIALS IN BATTERY AND VEHICLE INTEGRATION**	**270**
A. LAHOUEL *M. ADNANE* *S. KOUDJETI*	**SYNTHESIS OF THIN FILMS USING THE SOL-GEL DIP-COATING TECHNIQUE DERIVED FROM SnO_2**	**276**
Faiza Baghida *Mourad Boughrara*	**ELECTRONIC AND THERMOELECTRIC PROPERTIES STUDY OF Cu_2Se : DFT STUDY**	**277**
Tran Kim ANH	**VIETNAM WOMEN STUDIES NANOMATERIALS CONTAINING RARE EARTH IONS AND APPLICATIONS**	**278**
Babafemi Raphael BABANIYI *Oluwaseun Adekoya ADELAJA* *Folorunso Patrick ALIU* *Monday Peter OBAGUNWA*	**CHARACTERIZATION OF PET-ACTIVATED CARBON COMPOSITES: EFFECTS OF ORANGE PEEL AND SAWDUST DERIVATIVES**	**279**
Zineb Ait FARES *Miloudi HLAIBI* *Noureddine KAMIL* *Rachid OUCHN*	**POLYMERIC MEMBRANES FOR DESALINATION USING MEMBRANE DISTILLATION: A REVIEW**	**280**
Zineb El HAMRI *M. ALAMI* *M. ASSOUAG*	**IMPACT OF WALNUT SHELL POWDER ON THE PROPERTIES OF POLYPROPYLENE-REINFORCED COMPOSITES**	**281**
Anil K. VASHISHTH *Umang BAREJA*	**REFLECTION AND TRANSMISSION OF ACOUSTIC AND ULTRASONIC WAVES IN FUNCTIONALLY GRADED POROUS PIEZOELECTRIC MATERIALS**	**282**

DARBE DAYANIMI KATKILI TURUNCU CAM ELYAF TAKVİYELİ PBT KOMPOZİTLERİNİN GELİŞTİRİLMESİ

DEVELOPMENT OF ORANGE GLASS FIBER REINFORCED PBT COMPOSITES WITH IMPACT RESISTANCE ADDITIVES

Zeynep Sıla TIRPANCI
Technology&Innovation Engineer, Epsan Plastik
ORCID NO: 0009-0000-2019-4760

ÖZET

Otomotiv endüstrisi, güvenlik, estetik ve dayanıklılık gereksinimlerini karşılamak amacıyla çeşitli malzeme teknolojilerini kullanmaktadır. Polimer ve polimer matrisli kompozitler istenilen gereksinimlerin çoğunu karşıladığı için tercih edilmektedir. Polibutilen tereftalat (PBT), yüksek mekanik dayanım, ısı direnci ve kimyasal kararlılık gibi özelliklere sahip bir termoplastik polimerdir. Termoplastik malzemeler sertlik, dayanıklılık veya esneklik gibi özelliklere sahip olabilmek için farklı katkılar ve stabilizatörlerle karıştırılarak kompozit olarak üretilebilirler. Cam elyaf, PBT'nin mekanik özelliklerini artırarak daha yüksek çekme mukavemeti ve sertlik kazandırır; darbe dayanımı katkıları, malzemenin yüksek darbe yüklerine karşı direnç göstermesini sağlar ve malzemenin kırılma noktasını geciktirir ve böylece çarpışma anındaki enerji emilimini artırır. Otomotiv sektöründe, özellikle elektrikli araçlarda kullanılan parçalar yüksek ısı dayanımı gerektiren parçalardır. Bu tür parçalar için, genellikle tercih edilen renk kodu RAL 2003'tür. Ral kartelası, boya, kaplama ve plastikler için renkleri tanımlayan bir Avrupa renk eşleştirme sistemidir. Bu sektörde, turuncu renkli malzemeler, yüksek görünürlük ve güvenlik standartlarını sağlamak amacıyla tercih edilmektedir. Bu çalışmada elde edilecek ürünlerde kontrol numunesiyle benzer, yüksek mekanik özelliklerde turuncu renkli otomotiv parçalarının üretimi hedeflenmiştir. Darbe dayanımı katkılı ve cam elyaf takviyeli renkli PBT kompozitleri, çift vidalı ekstrüderde eriyikten karıştırma yöntemiyle üretilmiştir. Üretilen örneklere yönelik mekanik testler ve renk kontrolü, enjeksiyon makinesinde basılmış test plakalarına uygulanmıştır. Üretilen malzemelerin karakterizasyonu için çekme-kopma testleri, basma-bükülme testleri, darbe dayanımı testleri, yük altında eğilme sıcaklığı tayini, erime sıcaklığı tayini ve renk kontrolü yapılmıştır. RAL 2003 renk standardına göre dE renk değişim değerinin <5 olması hedeflenmiştir. Çalışma sonucunda kontrol numunesine göre mekanik özellikler etkilenmeden istenilen turuncu renge ulaşılmıştır. Renk testleri sonucunda dE değişimi <3 olarak tespit edilmiştir. Hem mekanik özellikler hem de renk standardı açısından hedeflenen kriterler sağlanmıştır.

Anahtar kelimeler: Polibutilen tereftalat (PBT), Cam Elyaf Takviyeli PBT, RAL 2003, Otomotiv

ABSTRACT

The automotive industry utilizes various material technologies to meet the requirements for safety, aesthetics, and durability. Polymer and polymer matrix composites are preferred because they meet most of the desired requirements. Polybutylene terephthalate (PBT) is a thermoplastic polymer known for its high mechanical strength, thermal resistance, and chemical stability. Thermoplastic materials can be compounded with different additives and stabilizers to achieve desired properties such as hardness, durability, or flexibility. Glass fibers enhance the mechanical properties of PBT by providing higher tensile strength and rigidity; impact resistance additives help the material withstand high-impact loads, delay the point of fracture, and improve energy absorption during collisions. In the automotive sector, particularly for electric vehicles, parts require high thermal resistance. For such parts, the preferred color code is typically RAL 2003. The Ral chart is a European color-matching system that defines colors for paints, coatings, and plastics. Orange-colored materials are selected to ensure high visibility and meet safety standards. In this study, the aim was to produce orange automotive parts with high mechanical properties similar to the control sample. Impact-resistant and glass fiber-filled colored PBT composites were produced by the melt mixing method in a twin screw extruder. Mechanical tests and color control for the produced samples were applied to test plates molded in the injection machine. The characterization of the produced materials included tensile tests, compression-bending tests, impact resistance tests, heat deflection temperature determination, melting temperature determination, and color control. According to the RAL 2003 color standard, it was aimed for the dE color change value to be <5. As a result of the study, the desired orange color was achieved without affecting the mechanical properties according to the control sample. As a result of the color tests, dE change was determined as <3. The targeted criteria were provided in terms of both mechanical properties and color standards.

Keywords: Polibutilen tereftalat (PBT), Glass Fiber-filled PBT, RAL 2003, Automotive

UÇUCU KÜL BAZLI, ISI İLE KÜR EDİLMİŞ GEOPOLİMER BETONUN EĞİLME MUKAVEMETİ VE DİNAMİK MODÜL İLİŞKİSİNİN HASARSIZ DENEYSEL MODAL ANALİZ İLE DEĞERLENDİRİLMESİ

ASSESSING FLY ASH-BASED, HEAT-CURED GEOPOLYMER CONCRETE'S FLEXURAL STRENGTH AND DYNAMIC MODULUS RELATIONSHIP WITH NON-DESTRUCTIVE EXPERIMENTAL MODAL ANALYSIS

Öğr. Gör. Dr. Ferhat ÇEÇEN

Süleyman Demirel Üniversitesi,

Göller Bölgesi Teknokent Koordinatörlüğü, Çünür, Isparta

Dr. Öğ. Üyesi Ahmet ÖZBAYRAK

Erciyes Üniversitesi, Mühendislik Fakültesi,

İnşaat Mühendisliği Bölümü, Talas, Kayseri

Prof. Dr. Bekir AKTAŞ

Erciyes Üniversitesi, Mühendislik Fakültesi,

İnşaat Mühendisliği Bölümü, Talas, Kayseri

ÖZET

Seramik benzeri özelliklere sahip bir malzeme olan geopolimer beton, geleneksel çimento bazlı betona sürdürülebilir ve çevre dostu bir alternatif sunmaktadır. Geopolimer beton üretiminde temel olarak uçucu kül veya cüruf gibi endüstriyel yan ürünler kullanıldığından, bu beton, geleneksel üretime kıyasla daha düşük bir karbon ayak izi bırakmaktadır. Uygun şekilde tasarlanmış geopolimer beton, basınç ve çekme dayanımı ile refrakterliği açısından, geleneksel betondan daha üstün sonuçlar verebilmektedir. Her ne kadar bu avantajlar, seramiklerle karşılaştırıldığında daha sınırlı kalsa da, önemli ölçüde daha düşük üretim maliyetleri, daha az karbon emisyonu ve daha fazla esneklik sunmakta, bu da onu dinamik yüklere maruz kalan büyük hacimli altyapı projeleri için ideal hale getirmektedir. Literatürde, geopolimer betonun çekme dayanımı ile dinamik elastisite modülü arasındaki ilişki konusunda, özellikle hasarsız yöntemlerle dinamik özelliklerinin değerlendirilmesine yönelik sınırlı araştırma bulunmaktadır. Oysaki bu özellikler, dinamik yüklere karşı dayanıklılık açısından kritik öneme sahiptir. Bu çalışma, uçucu kül bazlı ve ısı ile kür edilmiş geopolimer betonun eğilme mukavemeti ile dinamik özellikleri arasında güvenilir nümerik ilişkiler kurmayı amaçlamaktadır. Çalışma kapsamında, sodyum silikat ve sodyum hidroksit dozajlarının farklı olduğu altı farklı karışım oranı ile üretilen numuneler çeşitli test ve analizlere tabi tutulmuştur. Dinamik özellikler, hasarsız deneysel modal analiz ve sonlu elemanlar geri analiz yöntemi ile değerlendirildikten sonra, eğilme mukavemetleri dört noktalı eğilme testi ile belirlenmiştir. Sonuçlar, eğilme mukavemetlerinin 3.71 ila 5.97 MPa, temel düşey rezonans frekanslarının 802.3 ila 866.8 Hz ve dinamik modüllerin 25.2 ila 31.0 GPa arasında değiştiğini göstermiştir. Ayrıca, eğilme mukavemeti ve dinamik modül ile rezonans frekansları arasında güçlü korelasyonlar ($R^2 > 0.97$)

bulunmuştur. Bu bulgular, deneysel modal analiz yönteminin, geopolimer betonun kritik mekanik özelliklerini değerlendirmek için güvenilir ve hasarsız bir yöntem olduğunu doğrulamaktadır.

Anahtar kelimeler: Geopolimer beton, eğilme mukavemeti, dinamik modül, deneysel modal analiz.

ABSTRACT

Geopolymer concrete, a material with ceramic-like properties, offers a sustainable and environmentally friendly alternative to traditional cement-based concrete. Since geopolymer concrete production primarily uses industrial by-products such as fly ash or slag, it leaves a significantly lower carbon footprint compared to traditional concrete production. Properly designed geopolymer concrete can yield superior results in terms of compressive and tensile strength, as well as refractoriness, when compared to conventional concrete. Although these advantages may be somewhat limited when compared to ceramics, it offers significantly lower production costs, reduced carbon emissions, and greater flexibility, making it ideal for large-scale infrastructure projects exposed to dynamic loads. In the literature, there is limited research on the relationship between the tensile strength and the dynamic elastic modulus of geopolymer concrete, especially regarding the evaluation of its dynamic properties using non-destructive methods. However, these properties are critical for resilience under dynamic loads. This study aims to establish reliable numerical relationships between the flexural strength and dynamic properties of fly ash-based, heat-cured geopolymer concrete. In the study, samples produced with six different mix ratios, varying in sodium silicate and sodium hydroxide dosages, were subjected to various tests and analyses. After the dynamic properties were evaluated using non-destructive experimental modal analysis and finite element back-analysis methods, the flexural strengths were determined using a four-point bending test. The results showed that the flexural strengths ranged from 3.71 to 5.97 MPa, the fundamental vertical resonance frequencies ranged from 802.3 to 866.8 Hz, and the dynamic moduli ranged from 25.2 to 31.0 GPa. Additionally, strong correlations ($R^2 > 0.97$) were found between resonance frequencies and both dynamic modulus and flexural strength. These findings confirm that experimental modal analysis is a reliable and non-destructive method for evaluating the critical mechanical properties of geopolymer concrete.

Keywords: Geopolymer concrete; Flexural strength; Dynamic modulus; Experimental Modal Analysis.

GİRİŞ

İnşaat sektöründe günümüzde en yaygın kullanılan yapı malzemelerinden biri betondur. Özellikle çimento esaslı beton, sektörde büyük bir pazar payına sahiptir [1]. Bununla birlikte, son yıllarda geopolimer beton, sürdürülebilir bir alternatif olarak ortaya çıkmıştır. Geopolimer betonun bu yaygınlaşmasında, düşük karbon ayak izi, yüksek sıcaklık ve aşınma dayanımı ile elektriksel yalıtkanlık gibi üstün özellikleri etkili olmaktadır [2, 3].

Geopolimer betonun yapısal özellikleri ile seramikler arasında bazı benzerlikler de mevcuttur. Seramik malzemeler genellikle inorganik, kristal veya amorf yapıda; oksitler, karbürler, nitrürler ve silikatlar gibi bileşiklerden oluşmaktadır [4]. Geopolimer beton da alüminosilikat

bazlı bir malzemedir ve yarı amorf-yarı kristal bir yapıya sahiptir [1]. Bu benzerlik, geopolimer betonu, kimyasal yapısı açısından seramik malzemelere yakınlaştırmaktadır. Bu yüzden geopolimer beton, bazı kaynaklarda seramik-benzeri malzeme (seramic-like material), hidro-seramik (hydroceramic) veya alkali-bağlı seramik (alkali-bonded ceramic) olarak adlandırılmaktadır [5-8]. Ancak seramikler genellikle maliyet ve emisyon artışına neden olan çok yüksek sıcaklıklarda (1200-1600°C) sinterlenirken, geopolimer beton nispeten çok daha düşük sıcaklıklarda (<90°C) kimyasal reaksiyonlarla sertleşmektedir [9]. Bu yüzden, üretim maliyeti ve karbon ayak izi seramiklere nispeten çok daha düşük kalmaktadır.

Geopolimer betonun diğer önemli avantajları, dinamik performansı ve esnekliğidir. İnşaat sektöründe çoğu yapı, dinamik yüklere maruz kaldığından, yapı malzemelerinin dinamik özellikleri de statik kapasiteleri kadar önemli olmaktadır [1]. Yapılan deneysel modal analizler ve basınç dayanımı testleri göstermektedir ki, uygun bir şekilde dizayn edilen geopolimer betonun hem statik hem de dinamik performansı, çimento esaslı betondan daha üstün sonuçlanabilmektedir [1, 10]. Tüm bu özellikler, geopolimer betonu yüksek performans gerektiren inşaat projeleri için sürdürülebilir bir alternatif haline getirmektedir [9]. Ayrıca kırılgan yapıya sahip bazı seramiklere karşı da, ekonomik ve çevreci bir alternatif olma potansiyeli söz konusudur.

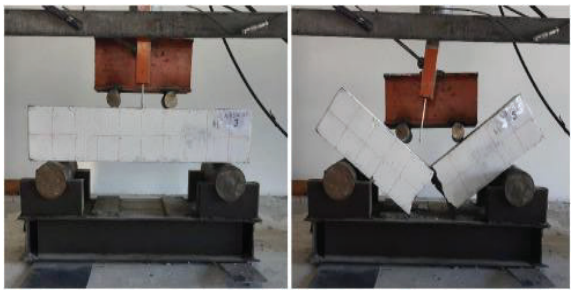
Literatürde geopolimer betonun basınç dayanımı ve dinamik özellikleri arasındaki ilişki konusunda az sayıda olsa da bazı çalışmalar mevcuttur [1, 10]. Ancak çekme dayanımı ve dinamik elastisite modülünün rezonans frekansı ile ilişkisini araştıran çalışmalar yetersizdir. Bu çalışmada, literatürdeki bu eksiklik göz önünde bulundurularak, uçucu kül bazlı, ısı ile kür edilen çeşitli geopolimer beton numunelerinin dinamik özellikleri, deneysel modal analiz ve sonlu elemanlar geri-analiz yöntemi ile değerlendirilmiş, bunun akabinde, eğilme mukavemetleri dört noktalı eğilme testi ile belirlenmiştir. Sonuçta ulaşılan değerler arasında nümerik ilişkiler araştırılmış ve bu ilişkileri ortaya koyan güvenilir modeller oluşturulmuştur.

YÖNTEM

Bu çalışmada gepolimer beton üretiminde uçucu kül kullanılmış olup, Türkiye'deki Adana Sugözü İsken Termik Santrali'nden temin edilmiştir. Geopolimer beton numunelerinin üretiminde, nehir kumu (0/4 mm), iri bazalt agregası (7/14 mm), modül oranı 2.06 olan sodyum silikat (SS) ve 14-M sodyum hidroksit (SH) kullanılmıştır.
Gepolimer beton üretildikten sonra 150x150x750 mm'lik prizma kalıplara dökülmüş ve 90°C'de 24 saat kürlenmiştir. Numuneler kalıptan çıkarıldıktan sonra 28 gün oda sıcaklığında bekletilmiştir. Bu çalışmada altı (6) farklı geopolimer beton karışımının analizlerleri gerçekleştirilmiş olup, karışım oranları ve üretim süreçleri ile ilgili diğer detaylar, yazarların önceki bir çalışmasında sunulmuştur [1]. Üretilen bazı geopolimer beton prizma numuneleri Şekil 1'de görülmektedir. Bu numuneler önce deneysel modal testlere, ardından eğilme dayanımı testlerine tabi tutulmuştur. Prizmaların eğilme dayanımlarını belirlemek için Şekil 2'de görüldüğü üzere, her karışımdan üç prizma numunesi ASTM C78'e uygun olarak dört noktalı eğilme yöntemiyle test edilmiş olup, test süreci ile ilgili diğer detaylar yazarların önceki bir çalışmasında sunulmuştur [11].

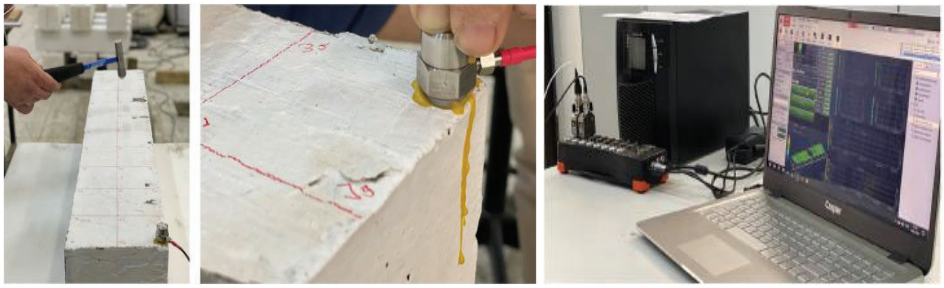


Şekil 1. Çalışmada kullanılan 150x150x750 mm prizma geopolimer beton numuneleri örnekleri [1]



Şekil 2. 150x150x750 mm'lik numunelerin dört noktalı eğilme testlerine dair örnek görseller [11]

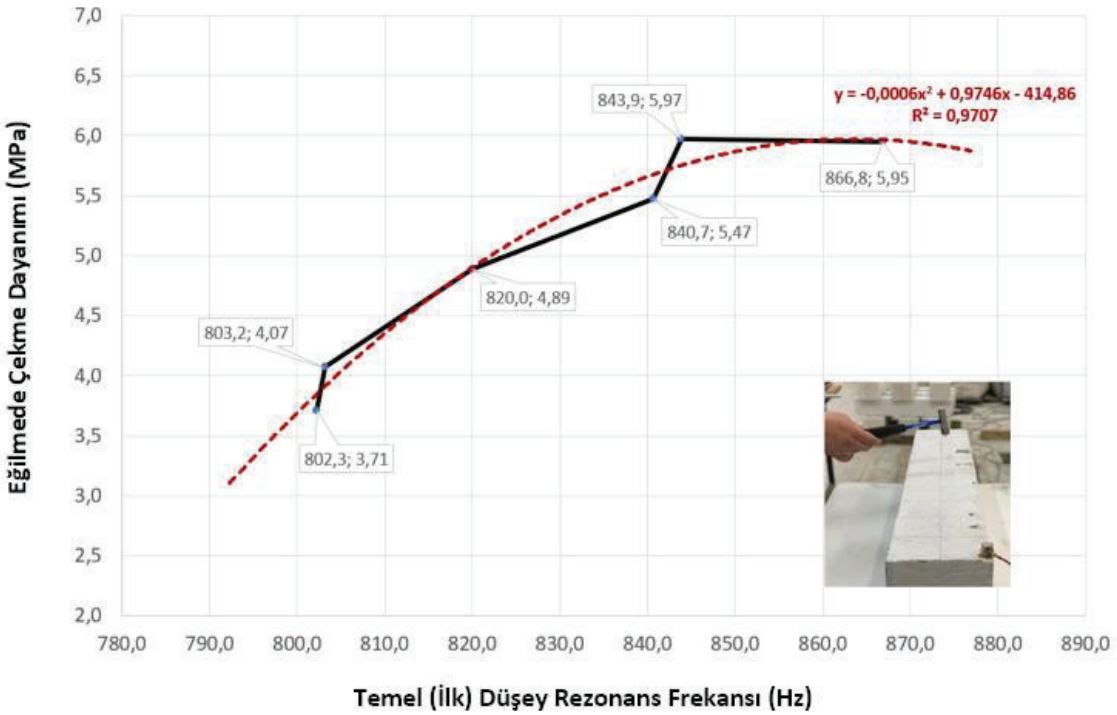
Bu çalışmada kullanılan modal test düzeneği Şekil 3'te görülmektedir [10]. Testler esnasında numuneler, serbest salınım yapabilmesi amacıyla 600 mm kalınlığında ve 70 kg/m^3 yoğunluğunda poliüretan bloklar üzerine yerleştirilmiştir. Test numuneleri, yüksek çözünürlüklü analizler için eşit uzaklıkta 33 noktaya bölünmüş ve her bir nokta, modal çekiçle 5'er kez uyarılarak etki (kuvvet) ve yanıt (ivme) değerleri ölçülmüştür. Elde edilen bu veriler modal analiz tekniklerine uygun şekilde oranlanarak Frekans Yanıt Fonksiyonları (FRF) elde edilmiştir. Bu FRF grafikleri ile rezonans frekansları belirlenmiştir. Ayrıca, numunelerin rezonans frekansları ve birim hacim ağırlıkları girdileri (input) kullanılarak sonlu eleman geri-analiz tekniğiyle (back-analysis) dinamik elastisite modülleri belirlenmiştir. Test ve analiz süreçleri hakkındaki diğer detaylar yazarların önceki çalışmalarında mevcuttur [1, 10].



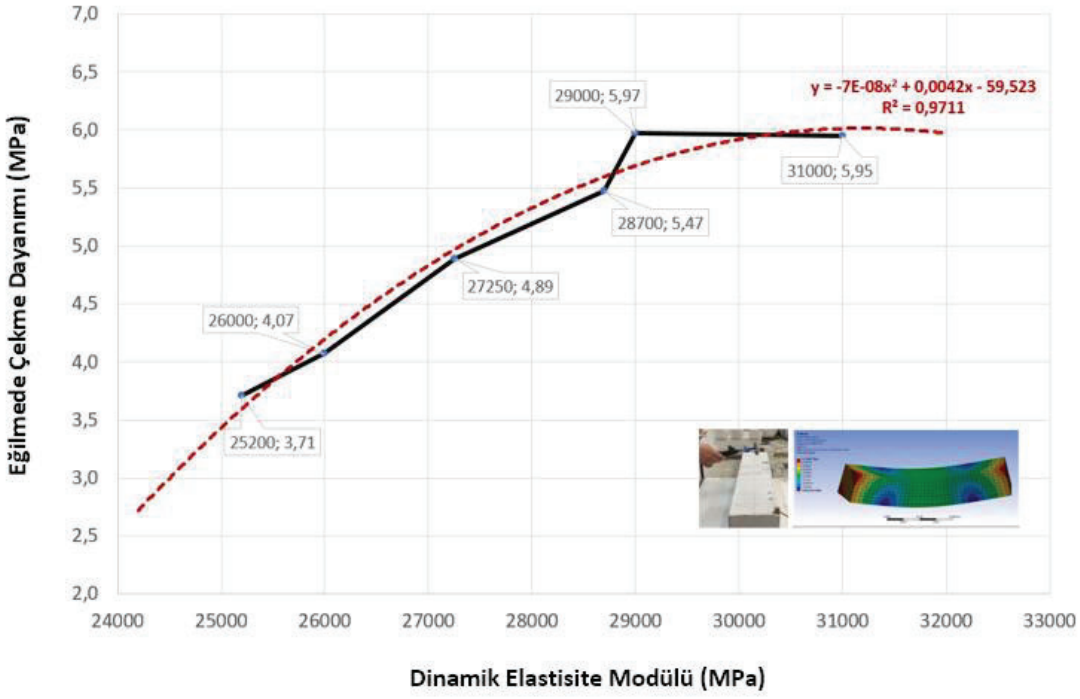
Şekil 3. Deneysel modal test ve analiz sürecine dair örnek görseller [10]

BULGULAR

Bu çalışmada analiz edilen 6 geopolimer beton numunesinin eğilmede çekme dayanımı (MPa) ile temel rezonans frekansları (Hz) arasındaki ilişki Şekil 4'te, eğilmede çekme dayanımı (MPa) ile dinamik elastisite modülü arasındaki ilişki ise Şekil 5'te gösterilmiştir.



Şekil 4. Çalışma kapsamında analiz edilen 6 farklı geopolimer beton numunesinin eğilmede çekme dayanımı (MPa) ile temel (ilk) rezonans frekansı (Hz) arasındaki ilişkiyi gösterir grafik



Şekil 5. Çalışma kapsamında analiz edilen 6 farklı geopolimer beton numunesinin eğilmede çekme dayanımı (MPa) ile dinamik eleastisite modülü arasındaki ilişkiyi gösterir grafik

TARTIŞMA VE SONUÇ

Geopolimer beton, düşük karbon ayak izi ve yüksek performansıyla çimento esaslı konvansiyonel betona sürdürülebilir bir alternatif sunmaktadır. Uygun şekilde tasarlandığında, dinamik özellikleri çimento esaslı betondan daha üstün olabilen bu malzeme, kimyasal yapısı sayesinde seramiklere benzer özellikler gösterebilmektedir. Ayrıca, seramiklere kıyasla çok daha düşük sıcaklıklarda dayanım kazanmakta ve dinamik olarak kırılgan, yüksek maliyetli ve yüksek karbon ayak izine sahip bazı seramiklere karşı ekonomik ve çevreci bir alternatif olma potansiyeli taşımaktadır.

Bu çalışmada, karışım oranları değişken altı farklı geopolimer beton numunesi üzerinde, tahribatlı ve tahribatsız, çeşitli test ve analizler yürütülmüştür. Bu kapsamda, numunelerin dinamik özellikleri, tahribatsız (non-destructive) deneysel modal analiz ve sonlu elemanlar geri analiz yöntemi ile belirlenirken, eğilme mukavemetleri dört noktalı eğilme testi (tahribatlı, destructive) ile tespit edilmiştir.

Elde edilen test ve analiz sonuçları incelendiğinde, eğilme mukavemetlerinin 3.71 ila 5.97 MPa, rezonans frekanslarının 802.3 ila 866.8 Hz ve dinamik modüllerin 25.2 ila 31.0 GPa arasında değiştiği görülmüştür. Sonuçlar arasındaki ilişki irdelendiğinde ise geopolimer beton numunelerin çekme dayanımları ve dinamik elastisite modülleri ile rezonans frekansları arasında güçlü korelasyonlar bulunduğu belirlenmiştir ($R^2 > 0.97$).

Çalışma sonucunda ulaşılan bir diğer önemli bulgu, deneysel modal analizin geopolymer betonun eğilme muakavemeti ve dinamik elastisite modülü gibi kritik mekanik özelliklerini değerlendirmek için güvenilir ve tahribatsız (non-destructive) bir yöntem olmasıdır. Bu metot sayesinde, numunelerin rezonans frekansları ölçülerek, kısa sürede ve tahribatsız bir şekilde çekme dayanımı ve dinamik elastisite modülüne ulaşılabileceği anlaşılmaktadır.

TEŞEKKÜR

Bu çalışma, TÜBİTAK (Türkiye Bilimsel ve Teknolojik Araştırma Kurumu) tarafından [proje numarası 121M236, 2021] ile desteklenmiştir. ME-KA Ltd. Şti. yetkililerine ve projeye katkıda bulunan araştırmacılara çalışmaya olan katkılarından dolayı teşekkür ederiz. Tüm yazarlar, deneylerin gerçekleştirilmesi, makalenin yazılması ve yorumlanması sürecinde birlikte iş birliği içinde çalışmıştır.

KAYNAKLAR

[1] F. Çeçen, A. Özbayrak, B. Aktaş. 2024. “Simultaneously Enhancing the Dynamic Damping and Static Strength Capabilities of Structures: A Case Study Conducted on Fly Ash-based Geopolymer Concrete Specimens using Modal, Mechanical and Microstructural Investigations,” Fırat University Journal of Engineering Science, vol. 36 (2), pp. 883-901. Doi: https://doi.org/10.35234/fumbd.1480600

[2] Y. H. M. Amran, R. Alyousef, H. Alabduljabbar, M. El-Zeadani. 2020. “Clean production and properties of geopolymer concrete; A review,” Journal of Cleaner Production, vol. 251, ID: 119679, Doi: https://doi.org/10.1016/j.jclepro.2019.119679

[3] D. Bondar. 2013. "Geo-polymer concrete as a new type of sustainable construction materials," Third International Conference on Sustainable Construction Materials and Technologies. Japan, Available [Accessed 22.10.2024]: https://www.researchgate.net/publication/263052696_Geopolymer_Concrete_as_a_New_Type_of_Sustainable_Construction_Materials

[4] K. K. Chawla. 2003. "Ceramic Matrix Materials." Ceramic Matrix Composites. Springer, Boston, MA. https://doi.org/10.1007/978-1-4615-1029-1_2

[5] J. Davidovits. 2017. "Geopolymers: Ceramic-Like Inorganic Polymers," J. Ceram. Sci. Technol., vol. 08 (3), pp. 335-350. Doi: https://doi.org/10.4416/JCST2017-00038

[6] R. Ahmad, M.M.A. Abdullah, K. Hussin, W.M.W. Ibrahim. 2021. "Fabrication of Lightweight Ceramic Materials Using Geopolymer Technology," Lecture Notes in Civil Engineering, vol 129. Springer, Singapore. https://doi.org/10.1007/978-981-33-4918-6_9

[7] E. M. Shcherban', A. N. Beskopylny, S. A. Stel'makh, L. R. Mailyan, B. Meskhi, A. A. Shilov, E. Pimenova, D. El'shaeva. 2023. "Combined Effect of Ceramic Waste Powder Additives and PVA on the Structure and Properties of Geopolymer Concrete Used for Finishing Facades of Buildings," Materials, vol. 16, ID: 3259. Doi: https://doi.org/10.3390/ma16083259

[8] S. Singh, S. K. Sharma, M. A. Akbar. 2022. "Developing zero carbon emission pavements with geopolymer concrete: A comprehensive review," Transportation Research Part D: Transport and Environment, vol. 110, ID: 103436, Doi: https://doi.org/10.1016/j.trd.2022.103436

[9] N. B. Mustapa, R. Ahmad, W. M. W. Ibrahim, M.M.A.B. Abdullah, N. Wattanasakulpong, O. Nemeş, A.V. Sandu, P. Vizureanu, I.G. Sandu, C.W. Kartikowati. 2023. "Effect of Sintering Mechanism towards Crystallization of Geopolymer Ceramic—A Review." Materials, vol. 16, ID: 4103. Doi: https://doi.org/10.3390/ma16114103

[10] F. Çeçen, A. Özbayrak, B. Aktaş. 2023. "Experimental modal analysis of fly ash-based geopolymer concrete specimens via modal circles, mode indication functions, and mode shape animations," Cement and Concrete Composites, vol. 137, ID: 104951. Doi: https://doi.org/10.1016/j.cemconcomp.2023.104951

[11] A. Özbayrak, H. Kucukgoncu, H. H. Aslanbay, Y. G. Aslanbay, O. Atas. 2023. "Comprehensive experimental analysis of the effects of elevated temperatures in geopolymer concretes with variable alkali activator ratios," Journal of Building Engineering, vol. 68, ID: 106108, Doi: https://doi.org/10.1016/j.jobe.2023.106108

ANALYZING OF THE VAPOR TREATMENT TIME ON SURFACE QUALITY OF THE 3D-PRINTED ACRYLONITRILE BUTADIENE STYRENE PARTS

3D BASKILI AKRİLONİTRİL BÜTADİEN STİREN PARÇALARININ YÜZEY KALİTESİNDE
BUHAR İŞLEM SÜRESİNİN ANALİZİ

Tan Eftal GENE

Samsun University, Faculty of Engineering and Natural Sciences,
Mechanical Engineering Department, Samsun, Turkey
ORCID:0009-0009-9646-0039

Assist. Prof. Dr. Çağın BOLAT

Samsun University, Faculty of Engineering and Natural Sciences,
Mechanical Engineering Department, Samsun, Turkey
ORCID:0000-0002-4356-4696

ÖZET

Katmanlı imalatla üretilen mühendislik polimerlerinde ikincil işlemler, son ürünün yüzey kalitesi ve mekanik tepkileri üzerindeki yeterli verimlilikleri nedeniyle son yıllarda oldukça popüler hale gelmiştir. Bu çalışmada, akrilonitril bütadien stiren (ABS) parçalarında üstün yüzey kalitesi elde etmek amacıyla bir ikincil işlem olarak buharlaştırma işlemi uygulanmıştır. Kür ortamı olarak, altı farklı maruz kalma süresi (15, 30, 45, 60, 75 ve 90 dakika) için aseton buharı kullanılmıştır. Sonuçlar, 60-75 dakika aralığının en iyi kürleme süresi olduğunu göstermiştir. 75 dakikadan sonra parlaklık daha iyi bir duruma gelse de detay oluşturma kabiliyeti azalmıştır. Ayrıca, son parçanın tasarım geometrisi, bileşenlerin yüzey kalitesi ve boyutsal kararlılığı üzerinde önemli ölçüde belirleyici olmuştur.

Anahtar Kelimeler: katmanlı imalat, buhar işlemi, yüzey kalitesi, mühendislik polimerleri, ABS

ABSTRACT

Secondary treatments have been highly popular on the additevely manufactured engineering polymers in recent years due to their sufficient efficiency on the surface quality and mechanical responses of the final product. In this work, vaporizing process was adopted as a secondary treatment on the acrylonitrile butadiene styrene (ABS) parts to obtain superior surface quality. As a curing environment, acetone vapor was used for six different exposure time (15, 30, 45, 60, 75 and 90 min). The results showed that 60-75 time interval was the best curing time. After 75 min, although the brigthness became better condition, detail-making ability dropped. Furrthermore, the design geometry of the final part was notably decisive for the surface quality and dimensional stability of the components.

Keywords: additive manufacturing, vapor treatment, surface quality, engineering polymers, ABS

Introduction

3D printing is a technology used to produce three-dimensional objects from a digital model. It is often referred to as "additive manufacturing" because the object is created by adding material layer by layer [Gojzewski, Guo, Grzelachowska, Ridwan, Hempenius, Grijpma, & Vancso 2020]. This technology is widely utilized across various industries and has revolutionized production processes due to the advantages it offers [Dodziuk, Warsaw, 2016]. This interesting production technique is utilized in different industrial sectors like medicine (prosthetics [Sandeep, Kannan, Chandradass 2021], dental implants, custom medical devices, and even bioprinting for organ production), automotive (body parts) [Romero, Pablo 2021], aerospace (prototypes) [Kalender, Murathan 2019], dentistry (temporary teeth, night guards, and occlusal splints), education (models and apparatus), and fashion (clothing, jewelry, and artistic projects). Furthermore, ability to make complex geometries, customization opportunity, rapid prototyping capability [Srivastava 2017], cost-efficiency, and material efficiency are the most significant advantages of the layer-by-layer production.

Among the all printing ways, fused deposition modeling (FDM) is the most preferred method. FDM is a 3D printing method that works by melting thermoplastic materials layer by layer [Silva, Luisa 2021]. In this process, a plastic material called filament is melted through a nozzle and deposited layer by layer onto the build platform to create objects. The process flow can be followed as; model preparation (CAD software), slicing (special slicing software for G-codes), filament melting, layer addition on the first baseline, main printing, cooling, and part separation. When the main advantages of the FDM is analyzed, cost-effectiveness, ease of use, material portfolio, and modularity can be seen. Also, this strategy does not form any hazardous chemicals and toxic gases.

In the previous scholarly studies, physical, mechanical and chemical behaviors of the 3D-printed polymers were examined by various research groups. Usually, printing parameters and target material type were investigated in terms of mechanical performance. On the other side, lately, secondary treatments were also applied to the 3D-printed polymers for higher crystalinity [Dizon, Ryan 2021]. In addition, surface modification efforts have been carried out with proper ambient treatments to improve the outer brightness of the product, detail-making on the printed sample, and better surface roughness [Demircali, Anil 2024].

The objective of this project is to investigate the effects of a surface smoothing process conducted using acetone vapor to improve the surface quality of ABS material produced by a 3D printer. The surface changes and the extent of defect remediation in samples exposed to acetone vapor for varying durations will be analyzed. This application will demonstrate the importance of how long we need to expose the surface of the print made from ABS filament to acetone vapor in order to enhance its appearance without compromising its internal structure.

Materials and Methods

ABS (Acrylonitrile Butadiene Styrene) is a polymer commonly used in molding processes due to its lightweight and rigid structure [Ergene, ŞEKEROĞLU, Bolat, & Yalçın 2021]. This copolymer is produced through the polymerization of styrene and acrylonitrile within polybutadiene. Typical component ratios vary between 15-35% acrylonitrile, 5-30% butadiene, and 40-60% styrene [Jin, Lu, Song, Pang, Zhang, Sun, & Cai, 2010]. The styrene and acrylonitrile components in its composition are sensitive to organic solvents such as acetone [Neff, Clayton, Trapuzzano, & Crane 2016]. Acetone creates a softening and dissolving effect on the material's surface by dissolving these components in the polymer structure of ABS.

This property particularly facilitates the use of ABS in 3D printing projects for surface smoothing because, when acetone is applied carefully, it dissolves the ABS surface, making it smoother. This characteristic is the primary reason for the use of ABS material in this project. These ratios determine the material's durability, flexibility, and hardness properties.

Another reason for selecting ABS for this project is its high impact resistance and good surface quality. These attributes make it popular in various industries such as automotive, electronics, toys, and home appliances. Furthermore, the ease of processing and recyclability of ABS provide advantages in production processes. The ABS filament will be supplied in the Porima brand and a thickness of 1.75 mm. The detailed specifications of the filament to be used are shared in Table 1 below.

Table 1. ABS filament properties

Feature	**Result**
Printing Temperature	220-260°C
Table Temperature	80-110°C
Print Speed	40-60 mm/sn
Diameter	1.75 mm
Diameter Tolerance	+/- 0.05 mm
Net Weight	1000 g
Reel Weight	200-220 g

In this context, the printer model used throughout the project is the Flashforge Creator 3, and no other printer was utilized during the project.

The printer model used is shown below in Figure 1. All of the printing parameters were adjusted according to the filament manufacturer's advice as also emphasized in Table 1. Layer thickness value was kept constant as 0.2 mm during the manufacturing.



Figure 1. Flashforge Creator 3 printer used within the scope of the project

The CAD representations of the sample to be produced within the scope of the project are illustrated in Figure 2, while the visual of the produced sample before exposure to acetone vapor is shown below in Figure 3. An acetone vapor chamber has been designed in the Siemens NX program to be isolated from the external environment, as depicted in Figure 4.

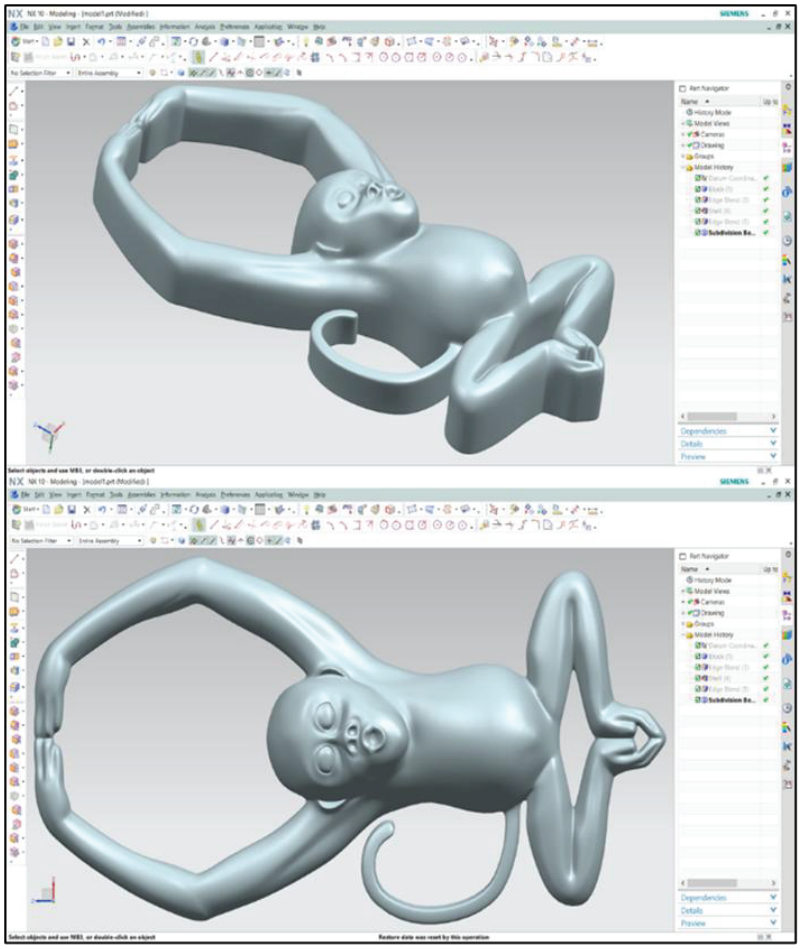


Figure 2. Different CAD views of the created part



Figure 3. Initially produced sample not interacted with acetone

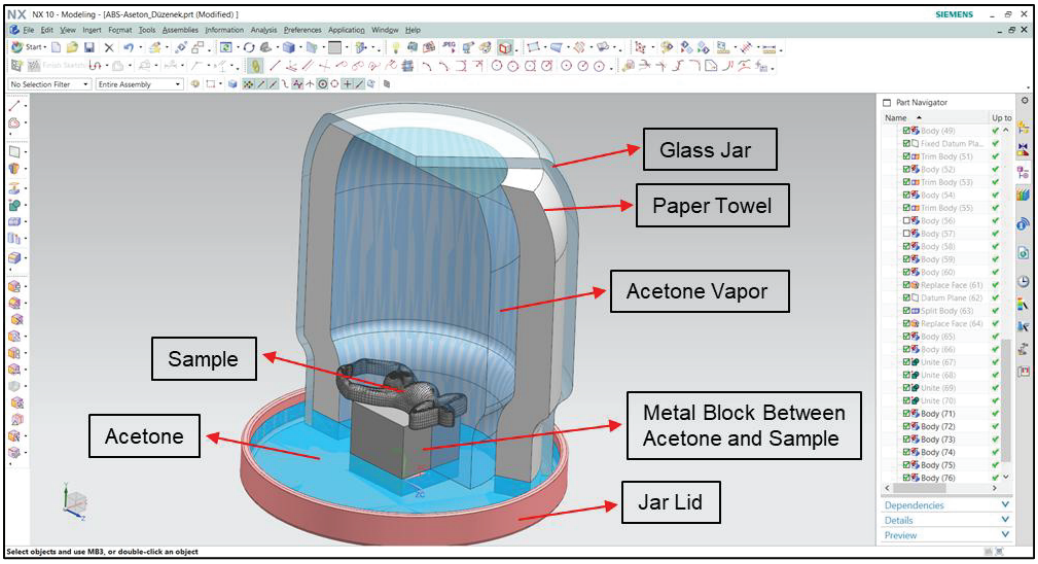
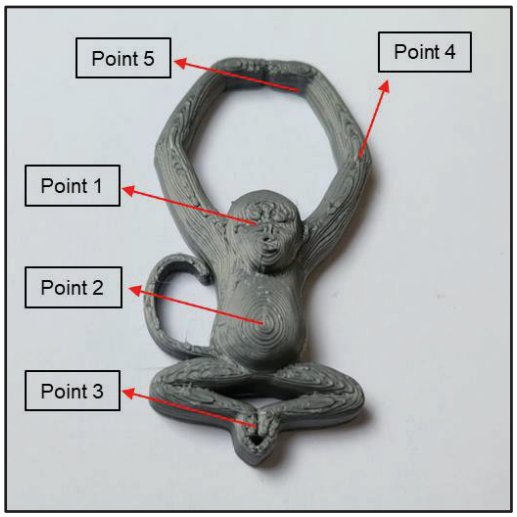


Figure 4. Acetone steam cabinet designed by CAD program

In the setup shown in Figure 4 above, the glass jar and its lid are liquid and gas-tight, and the jar's walls are wrapped with paper towels. This design allows the paper towel to vaporize the acetone more rapidly and uniformly across all sides of the jar. A small amount of acetone is poured onto the lid, and a metal block is placed directly in the center of the lid. The sample is then positioned on top of the metal block, and the glass jar, with its walls wrapped in paper towel, is inverted and closed as illustrated in Figure 4. The purpose of using a metal block is to prevent direct contact between the sample produced from ABS material and the acetone. Six identical samples were exposed to acetone vapor for varying durations (15, 30, 45, 60, 75, and 90 minutes). Changes in surface brightness and defect remediation of the samples were visually analyzed at the end of the specified durations.

Results and Discussion

Below, the effects of exposing identical samples to acetone vapor for varying durations have been analyzed and interpreted. Subsequently, five different points on the acetone-isolated sample were examined (Figure 5). The characteristics such as surface roughness, print defects,



and layer visibility were compared in Table 2. The samples exposed to acetone vapor for different durations are illustrated in Figure 6.

Figure 5. Points to look for in samples that will be exposed to acetone vapor

To better understand the relationship between ABS and acetone, five points have been identified, as shown in Figure 5. Among these points: Point 1 indicates the surface area, showcasing its details, Point 2 marks the abdominal region, where the layers are sparsely stacked, Point 3 represents the foot area, which is a region with a high concentration of defects, Point 4 indicates the arm area, characterized by both sparse and dense layers with detailed features, and Point 5 highlights areas where the layers are directly stacked on top of each other.



Figure 6. Changes of the surface quality and detail resolution depending on the vaporising time

Depending on the vapor subjecting time, some detections can be made;

- ✓ **15 minutes:** There were no visible changes on the sample surface; the effect of exposure to acetone vapor remained minimal.
- ✓ **30 minutes:** The surface of the sample began to smooth out, and print defects were partially reduced; an increase in glossiness was observed due to the vapor effect.
- ✓ **45 minutes:** The surface became smoother, with a significant reduction in print defects; the increase in glossiness continued.
- ✓ **60 minutes:** The smoothness and glossiness of the surface became even more pronounced, with print defects largely corrected.
- ✓ **75 minutes:** The surface achieved its smoothest state, with print defects nearly completely eliminated and glossiness reaching its highest level.
- ✓ **90 minutes:** Glossiness continued to increase, but losses in detail began to appear; deterioration in sample characteristics was observed due to excessive processing.

Table 2. Specific points observed on samples exposed to acetone vapor

	15 Minutes	30 Minutes	45 Minutes	60 Minutes	75 Minutes	90 Minutes
Point 1	☆	☆☆	☆☆☆	☆☆☆☆	☆☆☆☆	☆☆☆
Point 2	☆	☆☆	☆☆☆	☆☆☆☆	☆☆☆☆☆	☆☆☆☆
Point 3	☆	☆☆	☆☆☆	☆☆☆☆☆	☆☆☆☆	☆☆☆
Point 4	☆	☆☆	☆☆☆	☆☆☆☆	☆☆☆☆☆	☆☆☆☆☆
Point 5	☆	☆☆	☆☆☆	☆☆☆☆	☆☆☆☆☆	☆☆☆☆☆

The exposure of the samples to acetone vapor for varying durations has been effective in reducing surface roughness. However, excessive exposure times resulted in unwanted deformations on the surface stimulating resolution reduction. This indicates that the smoothing process using acetone vapor should be performed under controlled and optimal durations. In general, the study has been successfully completed, and the targeted surface smoothness has been achieved after a specific duration. The results of the experiments indicated that certain exposure times were effective in smoothing 3D printed ABS samples with acetone vapor. Durations of 60 to 75 minutes provided optimal results in terms of defect remediation and smoothness.

Conclusion

As a result of the conducted efforts, some conclusion remarks can be noted;

- Acetone treatment can be seen as a promising way to improve the final surface quality and brightness of the fabricated ABS parts.
- As the vapor exposure time increases, shape resolution also goes up but after 75 minutes detail making ability begins to drop.
- With the rising exposure time, dimensional deviation emerges and thin sections get larger due to the softening effect of the acetone vapor.

- Due to the chemical softening, indentation endurance of the samples diminishes with increasing exposure time.
- The body shape of the target product is significant for the effectiveness of the vapor treatment as the thin, thick, and curved sections indicate different response.
- ABS and ASA are similar thermoplastics although some differences like UV-resistance are present. In the future work, as an alternative filament, ASA can be probed in point of vapor treatment depending on changing printing parameters.
-

REFERENCES

[1] Gojzewski, H., Guo, Z., Grzelachowska, W., Ridwan, M. G., Hempenius, M. A., Grijpma, D. W., & Vancso, G. J. (2020). Layer-by-layer printing of photopolymers in 3D: How weak is the interface?. ACS applied materials & interfaces, 12(7), 8908-8914.

[2] Helena Dodziuk, Institute of Physical Chemistry PAS, Warsaw, Poland Kardiochirurgia i Torakochirurgia Polska 2016; 13 (3): 283-293 DOI: 10.5114/kitp.2016.62625

[3] B. Sandeep, T.T.M. Kannan, J. Chandradass et al., Scope of 3D printing in manufacturing industries-A review, Materials Today: Proceedings, https://doi.org/10.1016/j.matpr.2021.01.394

[4] Romero, Pablo E., et al. "Manufacture of polyurethane foam parts for automotive industry using FDM 3D printed molds." *CIRP Journal of Manufacturing Science and Technology* 32 (2021): 396-404.

[5] Kalender, Murathan, et al. "Additive manufacturing and 3D printer technology in aerospace industry." *2019 9th International Conference on Recent Advances in Space Technologies (RAST)*. IEEE, 2019.

[6] Srivastava, V. K. "A review on advances in rapid prototype 3D printing of multi-functional applications." *Sci. Technol* 7.1 (2017): 4-24.

[7] Silva, Ana Luisa, et al. "A 3D printer guide for the development and application of electrochemical cells and devices." *Frontiers in Chemistry* 9 (2021): 684256.

[8] Dizon, John Ryan C., et al. "Post-processing of 3D-printed polymers." *Technologies* 9.3 (2021): 61.

[9] Demircali, Ali Anil, et al. "Enhancing mechanical properties and surface quality of FDM-printed ABS: A comprehensive study on cold acetone vapor treatment." *The International Journal of Advanced Manufacturing Technology* 130.7 (2024): 4027-4039.

[10] Ergene, B., ŞEKEROĞLU, İ., Bolat, Ç., & Yalçın, B. (2021). An experimental investigation on mechanical performances of 3D printed lightweight ABS pipes with different cellular wall thickness. Journal of Mechanical Engineering and Sciences, 15(2), 8169-8177.

[11] Jin, F. L., Lu, S. L., Song, Z. B., Pang, J. X., Zhang, L., Sun, J. D., & Cai, X. P. (2010). Effect of rubber contents on brittle–tough transition in acrylonitrile-butadiene-styrene blends. Materials Science and Engineering: A, 527(15), 3438-3441.

[12] Neff, Clayton, Matthew Trapuzzano, and Nathan B. Crane. "Impact of vapor polishing on surface roughness and mechanical properties for 3D printed ABS." (2016).

SELF-CLEANING AND ANTI-REFLECTION COATING FOR SOLAR CELL

Assoc. Prof. Dr. Hafize Nagehan KÖYSÜREN

Kırşehir Ahi Evran University, Faculty of Engineering and Architecture, Department of Environmental Engineering, Kırşehir-Türkiye
ORCID: 0000-0002-7115-2250

Prof. Dr. Özcan KÖYSÜREN

Ankara University, Faculty of Engineering, Department of Energy Systems Engineering, Ankara-Türkiye, (Responsible Author)
ORCID: 0000-0001-7100-0399, +905353914560

ABSTRACT

The aim of this study was to prepare anti-reflection and self-cleaning coating for solar cell. SiO_2 film was synthesized by using a sol-gel technique. The as-prepared SiO_2 solution was mixed with a porogen, poly(ethylene glycol) (PEG), in the solution phase. PEG molecules were added to the SiO_2 phase to obtain nano-porous structures in the film coating. Nano-porous structures in the film coating reduce the light transmittance on the film coating, which is beneficial for the anti-reflection feature. In addition to PEG, TiO_2/WO_3 nanoparticles and ZnO/CuO nanoparticles were also added into the SiO_2 solution, respectively. TiO_2/WO_3 and ZnO/CuO nanoparticles can reduce the surface free energy of the SiO_2 coating. The self-cleaning feature can be related to the surface free energy and hydrophilic character. Hence, the surface with the hydrophilic character can play a crucial role in the enhancement of the self-cleaning feature of the film coating. For this reason, SiO_2 film was combined with certain nanoparticles (TiO_2/WO_3 and ZnO/CuO) with high surface free energy. Optical microscopy analysis, UV-Vis absorbance and transmittance measurements, and solar cell efficiency measurements were performed with the SiO_2 composite films. The morphology analysis results revealed the successful coating of the SiO_2 composite films on glass slides. Nano-porous structures endowed the SiO_2 film with a relatively lower transmittance (1%) than that of reference glass slide. The SiO_2 films became more hydrophilic with TiO_2/WO_3 and ZnO/CuO nanoparticles, respectively, favouring the self-cleaning character of the resulting film. The current-voltage measurements revealed that the SiO_2 composite films did not have a negative effect on the photovoltaic conversion efficiency of the silicon solar cell. The characterization test results demonstrated that the SiO_2/ZnO/CuO film has the potential for anti-reflection coating application on the cover glass of the solar cell.

Keywords: Anti-reflection coating, solar cell, SiO_2 film, self-cleaning coating.

INTRODUCTION

Solar energy has a crucial role in meeting energy needs of the world due to its availability all year round. Photovoltaic (PV) technology provides to generate electricity form the solar light. The efficiency of a solar cell largely depends on the number of photons passing from the air to its absorber material. When the photons of the solar light reach the surface of a solar cell including a cover glass at the top, certain part of the incoming light is reflected from the surface of the cover glass of the solar cell. Therefore, to reduce the reflection losses and enhance the solar cell efficiency, an anti-reflection coating needs to be

applied on the surface of the cover glass. Anti-reflection coating on the solar cell provides light trapping and increases the solar cell efficiency by increasing the light absorption. For a glass cover with a refractive index of 1.53, the refractive index of the antireflection-coating on the cover glass should be about 1.23. A simple technique to obtain a film with such a low refractive index can be achieved by creating nanopores during the coating process (Chandralekha et al., 2024).

On the other hand, the photovoltaic conversion efficiency of the solar cell can be significantly affected by the accumulation of dust or other kinds of contaminants soil on its cover glass. The incoming solar light can also be reflected on the cover glass of the solar cell by dust or other contaminants, which inhibits the light transmission to the absorber layer of the solar cell, and hence leads to decrease the photovoltaic conversion efficiency. A viable solution to this problem is a self-cleaning coating, preventing dust and other contaminant particles from accumulating on the cover glass (Zhou et al., 2023).

The self-cleaning film have attracted great interest recently owing to its wide application potential such as the cover glass of solar cells, roof tiles, automobile windshields, fabrics, screens of electronic instruments and window glasses. In general, the self-cleaning film can be divided into two groups: hydrophobic surfaces and hydrophilic surfaces. The hydrophobic surface effect or the hydrophilic surface effect can be obtained by altering the chemical structure or the surface morphology of the film. On the hydrophobic film surface, drops of water can roll down from the surface and remove dust or contaminants owing to the water repellent and low adhesion features of the surface. On the hydrophilic surface, drops of water can spread over the entire film surface to form a water film, which allows dust and contaminants on the surface to be washed away (Ren et al., 2020). The self-cleaning process is related to the water contact angle on the surface. As a definition, a surface whose water contact angle approaches zero is classified as superhydrophilic and a surface whose water contact angle approaches 180° is classified as superhydrophobic (Zhou et al., 2023).

Superhydrophilic and anti-reflection coatings can be prepared by using complicated coating or deposition techniques, which are not suitable for coating on large surfaces like the cover glass of solar cells. A sol-gel technique can be utilized to prepare film on the cover glass of the solar cell with the superhydrophilicity and anti-reflection properties. To enhance the anti-reflection feature of the film coating, a nano-porous surface structure needs to be obtained on the cover glass of the solar cell. In literature, Wang and his coworkers (2020) applied a simple sol mixing technique to obtain a surface coating with the nano-porous structure. Two different types of monodisperse SiO_2 solutions were prepared, and their mixture was coated as a film using the dip-coating technique (Wang et al., 2020). In another study, Zhu and his coworkers (2018) prepared a SiO_2 film with nano-porous surface structure using PEG as a porogen. PEG used a a porogen reduced the refractive index of the SiO_2 film coated on the cover glass of the solar cell. PEG molecules provided both anti-reflection property and self-cleaning feature to the SiO_2 film (Zhu et al., 2018). Within this scope, Li and his coworkers (2015) prepared a porous SiO_2 film using two types of porogens, cetyltrimethylammonium bromide and polypropylene glycol, at the same time. The as-pepared SiO_2 provided excellent optical property with a light transmittance of 99.8% (Li et al., 2015). In addition to specified techniques, spherical nanoparticles can also be added into the coating to provide nano-rough surface structures on the film, which also enhances the anti-reflection feature of the coted film. Especially, metal oxide nanoparticles like TiO_2 and ZnO in the spherical shape can enhance both the anti-reflection property and the surface hydrophilicity (Jiao et al., 2023). On the other hand, although TiO_2 and similar semiconductor metal oxides are hydrophilic, they can behave superhydrophilic under sunlight, providing complete wetting of water on the film surface including the specified metal oxide nanoparticles. The solar light can induce oxygen vacancies in the semiconductor crystal structure, giving rise to form radical species on the film surface. The active species can help to completely wet the film surface (Adachi et al., 2018).

In this study, SiO_2 composite films were prepared using a sol-gel technique. PEG was added into the SiO_2 phase as a porogen during the synthesis step of SiO_2. In addition to PEG, TiO_2/WO_3 and ZnO/CuO nanoparticles were added into the SiO_2. Both PEG, as a porogen, and semiconductor nanoparticles

(TiO_2/WO_3 and ZnO/CuO) were expected to improve the anti-reflection and self-cleaning properties of the SiO_2 film.

MATERIALS AND METHODS

SiO_2 films were coated on glass slides. Before the coating process, the glass slides were washed in an ultrasonic bath using distilled water and then left to drying at room temperature. A sol-gel technique was followed to synthesize SiO_2. In detail, tetraethylorthoxylsilicane (TEOS) (112 ml) was mixed with ethanol-water mixture (36 ml – 1090 ml) in a glass vial and stirred at room temperature. Then, HCl (0.2 ml, 36%) was added drop-wise to the as-prepared TEOS solution with a continuous magnetic stirring at room temperature. Then, polyethylene glycol (PEG), with a molecular weight of 1500 g/mol, was added to the TEOS solution. Afterward, TiO_2/WO_3 and ZnO/CuO nanoparticles, separately, were added into the final SiO_2 solution and kept stirring at room temperature for 24 h. The TiO_2/WO_3 and ZnO/CuO contents of the SiO_2 solution were adjusted to be 10% by weight of the final SiO_2 film. The as-prepared SiO_2 composite solutions were coated on the glass slides by using a dip-coating method. The coated glass slides were dried at room temperature for 24 h. Finally, they were annealed at 550°C for 1 h (Feng et al., 2022). The SiO_2 composite films were labeled as $SiO_2/PEG/TiO_2/WO_3$ and $SiO_2/PEG/ZnO/CuO$, respectively.

The surface morphology of the prepared film samples was investigated using an optical microscope (LEICA, binocular microscope). The UV-Vis absorbance and transmittance spectra of the film samples were recorded using a Thermo Scientific model spectrophotometer (Genesys 10S). The solar cell efficiency of the standard uncoated solar cells and the standard coated solar cell was measured using a solar module analyzer (PROVA 210). The water contact angle measurements were performed using an optical tensiometer (Theta Lite model)

FINDINGS AND DISCUSSION

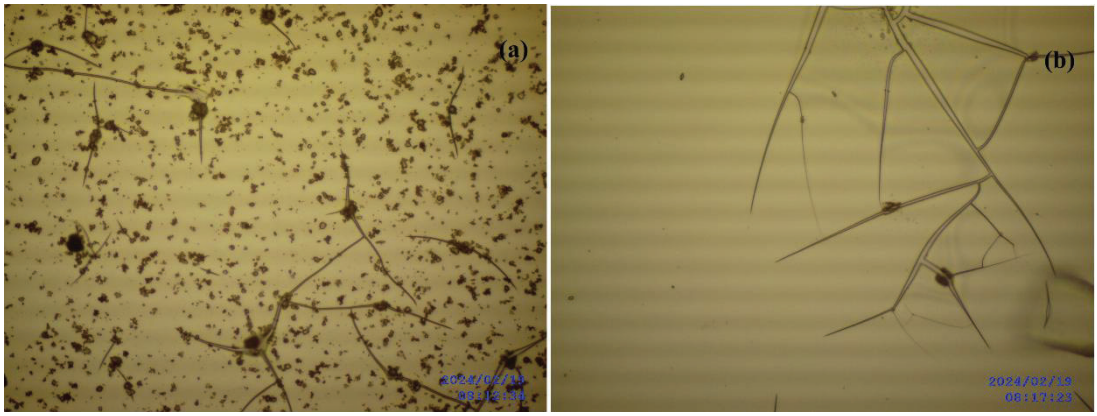


Figure 1. Optical microscopy images of (a) $SiO_2/PEG/TiO_2/WO_3$ and (b) $SiO_2/PEG/ZnO/CuO$ films

Figure 1 exhibits the optical microscopy images of the prepared film samples. There are a few crack structures on both of the film samples. There are dark regions on the microscopy image of the $SiO_2/PEG/TiO_2/WO_3$ film, which might belong to the TiO_2 and WO_3 nanoparticles in the agglomerate form. On the other hand, the $SiO_2/PEG/ZnO/CuO$ film sample includes a few dark regions in different sizes, which migh belong to ZnO and CuO nanoparticles in the agglomerate form. Both images show that the coated films have a very smooth and homogeneous structure.

Figure 2 illustrates UV-Vis absorbance spectrum of $SiO_2/PEG/TiO_2/WO_3$ and $SiO_2/PEG/ZnO/CuO$ films. Both film samples absorbed the incoming light at around 300 nm. No significant light absorption was observed in the visible light wavelength range, which is important for the application of the prepared

film samples on the solar cell under natural sunlight. By using the UV-Vis absorbance values and the Tauc's relation (1), the optical band gap energy (E_g) of the prepared film samples was estimated (Khatun et al., 2024):

$$(\alpha hv)^2 = A(hv - E_g) \quad (1)$$

where hv is the incident photon energy, α is the absorption coefficient and A is a constant, respectively. Figure 3 shows the absorbance spectrum of the prepared films transformed according to the Tauc's relation (1) plotted against the photon energy (hv) (Khatun et al., 2024). The optical band gap energy for SiO_2/PEG/TiO_2/WO_3 and SiO_2/PEG/ZnO/CuO films was estimated to be 4.20 eV. Both film samples exhibited the same optical band gap value. The major phase in the film samples was SiO_2, which dominated also the optical properties of the prepared film samples.

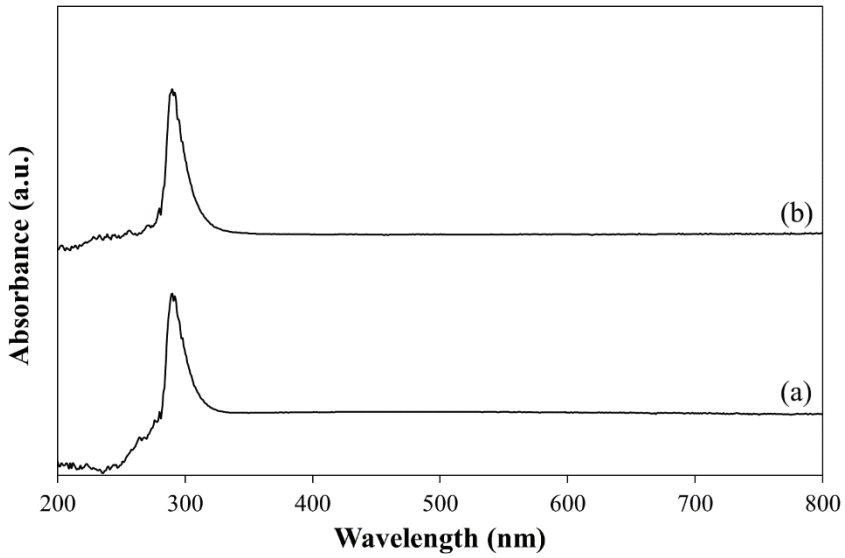


Figure 2. UV-Vis absorbance spectra of (a) SiO_2/PEG/TiO_2/WO_3 and (b) SiO_2/PEG/ZnO/CuO films

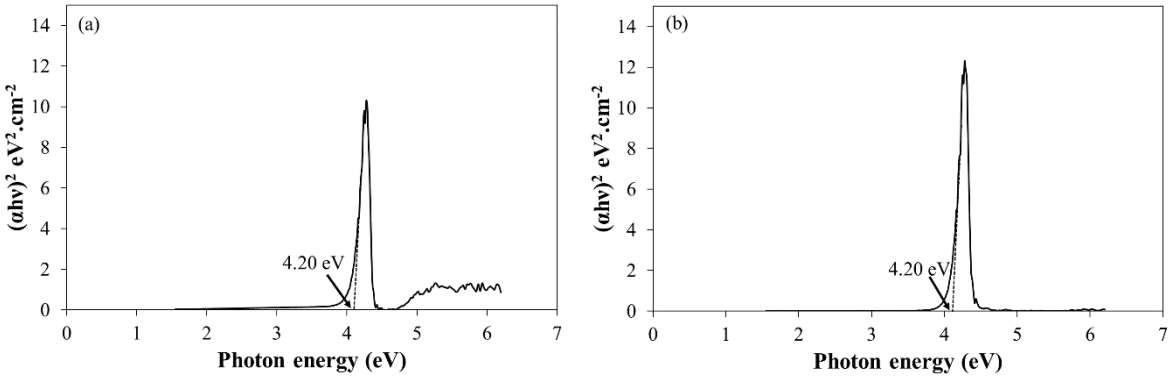


Figure 3. Tauc's plot for (a) SiO_2/PEG/TiO_2/WO_3 and (b) SiO_2/PEG/ZnO/CuO films

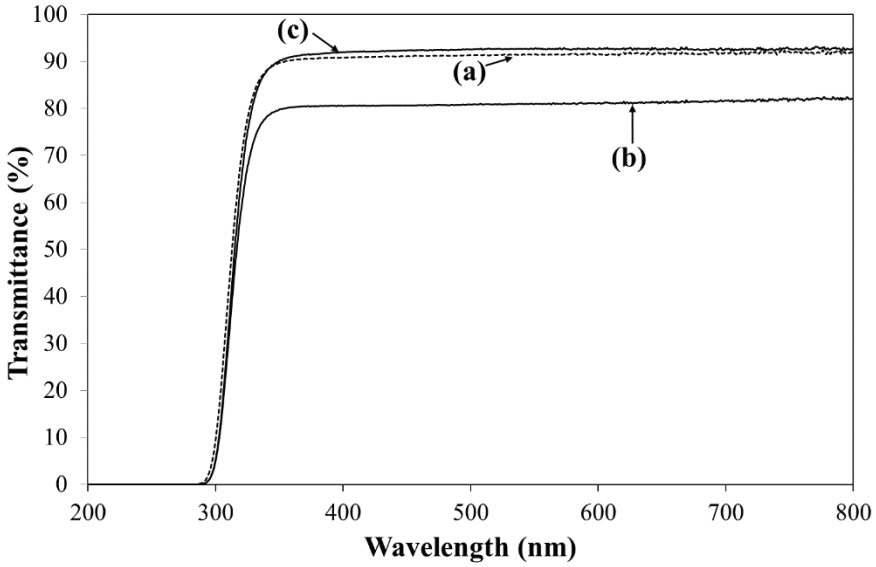


Figure 4. Transmittance spectra of (a) glass slide (standard), (b) SiO_2/PEG/TiO_2/WO_3 and (c) SiO_2/PEG/ZnO/CuO films

The transmittance spectrum of the prepared films was exhibited on Figure 4. The average transmittance of the SiO_2/PEG/TiO_2/WO_3 film between 400-800 nm was about 81.2% and the average transmittance of the SiO_2/PEG/ZnO/CuO film in the visible light region was about 92.6%, which was higher than that of standard glass slide. When compared with the average transmittance of the standard glass slide, an enhancement of about 1% in light transmittance was provided with the SiO_2/PEG/ZnO/CuO film. The light transmittance is important in terms of the solar cell efficiency.

Table 1. Water contact angle of SiO_2/PEG/TiO_2/WO_3 and SiO_2/PEG/ZnO/CuO films

Sample	Water Contact Angle (°)
SiO_2/PEG/TiO_2/WO_3	17.8
SiO_2/PEG/ZnO/CuO	16.4

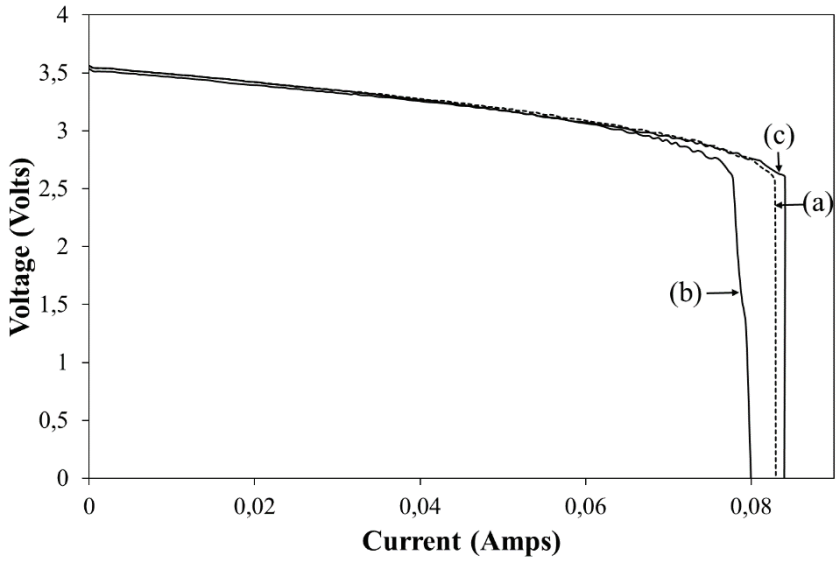


Figure 5. Current-voltage characteristics of the standard solar cell including (a) uncoated glass slide, (b) SiO_2/PEG/TiO_2/WO_3, (c) SiO_2/PEG/ZnO/CuO films

According to Table 1, the water contact angle of the SiO_2/PEG/TiO_2/WO_3 and SiO_2/PEG/ZnO/CuO film samples was measured as 17.8° and 16.4°, respectively. Both film samples approached the standard water contact angle of a superhydrophilic surface, making the coating have the self-cleaning performance. The film samples were exposed to the high temperature heat treatment. The heat treatment required to remove the PEG phase from the film resulted in the formation of a porous surface structure. The surface porosity might be the reason for the resulting water contact angle values with the film samples.

Table 2. The solar cell efficiency of the standard uncoated solar cell and the coated solar cell

Sample	V_{MP} (V)	I_{MP} (A)	V_{oc}	I_{sc}	A (m^2)	P_{in} (W/m^2)	η (%)
Standard	2.763	0.0800	3.561	0.083	0.0016	1170	11.81
SiO_2/PEG/TiO_2/WO_3	2.770	0.0757	3.562	0.080	0.0016	1170	11.20
SiO_2/PEG/ZnO/CuO	2.742	0.0811	3.536	0.084	0.0016	1170	11.88

I-V measurements were performed to investigate the effect of the prepared films on the solar cell efficiency. Using the I-V measurement values (Figure 5) and the following relation (2), the solar cell efficiency (η) was calculated.

$$\eta \text{ (efficiency)} = V_{MP}\, I_{MP} / P_{in} \quad (2)$$

at which V_{MP} indicates the voltage at the maximum power point, I_{MP} indicates the current at the maximum power point. The solar cell efficiency of the uncoated solar cell was found to be 11.81%. In addition, the solar cell efficiency of the standard solar cell coated with the SiO_2/PEG/TiO_2/WO_3 and SiO_2/PEG/ZnO/CuO film was found to be 11.20% and 11.88%, respectively. Compared with the uncoated standard solar cell, slightly higher and lower efficiencies were obtained with the standard solar cell coated with the SiO_2/PEG/ZnO/CuO and SiO_2/PEG/TiO_2/WO_3 films, respectively.

CONCLUSION AND RECOMMENDATIONS

SiO_2 composite films were prepared using a sol-gel technique in the presence of ZnO/CuO and TiO_2/WO_3 nanoparticles. Especially, the SiO_2/PEG/ZnO/CuO film exibited higher light transmittance and solar cell efficiency, which is important in terms of its application potential as a coating on the commercial solar cell. Homogenous films were obtained on glass slides. ZnO/CuO and TiO_2/WO_3 nanoparticles were dispersed in the SiO_2 phase homogeneously. It was understood that the prepared films absorbed only a small amout of the visible light. Both film samples exhibited hydrophilic behavior.

THANKS AND INFORMATION NOTE

The authors declare that no funds, grants, or other support were received during the preparation of this manuscript.

REFERENCES

Adachi, T., Latthe, S.S., Gosavi, S.W., Roy, N., Suzuki, N., Ikari, H., Kato, K., Katsumata, K.I., Nakata, K., Furudate, M. & Inoue, T. (2018). Photocatalytic, superhydrophilic, self-cleaning TiO2 coating on cheap, light-weight, flexible polycarbonate substrates. Applied Surface Science, 458, 917-923.

Chandralekha, N. R., Shanthi, J., Cathelene Antonette, L. & Anoop, K. K. (2024). Improved Efficiency of Solar Cell using Silane based SnO_2 Thin Films with Self-Cleaning and Antifogging Properties. *Silicon, 16(12)*, 5121-5134.

Feng, X., Shi, Y., Yin, X., & Wang, X. (2022). Transparent superhydrophobic film with anti-fouling and anti-scaling ability by facile method of dip-coating SiO_2 Sol. *Materials Research Express*, *9(1)*, 016404.

Jiao, Z., Wang, Z., Wang, Z. & Han, Z. (2023). Multifunctional Biomimetic Composite Coating with Antireflection, Self-Cleaning and Mechanical Stability. *Nanomaterials, 13(12)*, 1855.

Khatun, M. M., Islam, M. B., Sumona, H. J. & Al Mahmood, A. (2024). Enhanced Photocatalytic Activity of Metal-Metal-Nonmetal Multidoped TiO_2 Nanoparticles towards Visible Light. *ChemistrySelect, 9(5)*, e202304278.

Li, Y., Lv, H., Ye, L., Yan, L., Zhang, Y., Xia, B., Yan, H. & Jiang, B. (2015). Preparation of porous silica films in a binary template system for double-layer broadband antireflective coatings. RSC advances, 5(26), 20365-20370.

Ren, Y., Li, W., Cao, Z., Jiao, Y., Xu, J., Liu, P., Li, S. & Li, X. (2020). Robust TiO_2 nanorods-SiO2 core-shell coating with high-performance self-cleaning properties under visible light. Applied surface science, 509, 145377.

Wang, Y., Nie, L. & Liu, J. (2020). Preparation of hydrophobic SiO_2 film with high transmittance by sol mixing method. Chemical Physics Letters, 747, 137331.

Zhou, J., Ci, L., Hu, J., Lin, S., Hou, Y., Wang, Y., Ma, M. & Li, F. (2023). Preparation and characterization of superhydrophilic self-cleaning coating for solar cell cover glass applications. Journal of Adhesion Science and Technology, 37(17), 2524-2536.

Zhu, Y., Chen, L., Zhang, C. & Guan, Z. (2018). Preparation of hydrophobic antireflective SiO_2 coating with deposition of PDMS from water-based SiO_2-PEG sol. Applied Surface Science, 457, 522-528.

INVESTIGATION OF THE PRODUCTION OF HEXAGONAL BORON NITRIDE / POLYAMIDE66 NANOSTRUCTURED COMPOSITE BY TEMPERATURE CONTROLLED MECHANOCHEMICAL PROCESS

SICAKLIK KONTROLLÜ MEKANOKİMYASAL PROSES İLE HEKZAGONAL BOR NİTRÜR / POLİAMİD66 NANOYAPILI KOMPOZİT ÜRETİMİNİN İNCELENMESİ

Assist. Prof. Dr. Sercan BASİT

Kırşehir Ahi Evran Üniveristesi, Mühendislik-Mimarlık Fakültesi, Makine Mühendisliği Bölümü, Bağbaşı, Kırşehir
ORCID ID: https://orcid.org/0000-0002-2368-6362

ABSTRACT

It is known that melt blending, one of the most widely used processes in industry, does not provide a strong affinity between polymers and fillers. In this study, it is aimed to produce much higher quality composites for R&D or industrial production when bonding is carried out by mechanochemical pre-treatment and to minimise the loss of time and raw materials as a result of effective bonding. In the study, the method used and the material produced are intended to serve as an efficient alternative to meet the requirements of sectors such as light weapons bodies and aerospace components. In this context, polyamide 66(PA66) was chosen as the main (matrix) material and hexagonal boron nitride(h-BN) was chosen as reinforcement due to its superior properties. Initially, both materials were subjected to dehumidification in a chamber-type oven at 60°C for 30 minutes to ensure optimal processing conditions. Subsequently, the mixtures were prepared by precisely weighing PA66 and h-BN to achieve reinforcement ratios of 1% and 4% by weight using a precision balance. The total charge weight was standardized at approximately 5g, ensuring that it did not exceed 50% of the grinding vessel's volume, with a ball-to-charge ratio maintained at 10:1. The mechanochemical synthesis was conducted using a high-energy ball milling process under controlled temperature conditions. Milling speeds of 400rpm and 1200rpm were employed for durations of 15 and 30mins, respectively, with continuous operation to achieve homogeneous dispersion and enhanced interaction between the matrix and the reinforcement. The prepared samples were subjected to both visual inspection and microscopic examination to evaluate their surface morphology, homogeneity, and structural integrity. Analysis of the two series with varying reinforcement ratios revealed that milling speed plays a more critical role in achieving the homogeneous distribution of the reinforcement, its integration into the polymer structure, and enhancing the mechanochemical effects, including the formation of potential covalent bonds. A homogenous structure is clearly seen in the processes performed at 1200rpm. In addition, the relatively large PA66 granules did not undergo any deformation under these operating conditions.

Keywords: Mechanochemical, Polimer nanocomposite, Polyamide 66, Hexagonal boron nitride, Temperature controlled high energy ball mill.

ÖZET

Endüstride en yaygın kullanılan proseslerden biri olan eriyik karıştırmanın polimerler ve dolgu maddeleri arasında güçlü bir afinite sağlamadığı bilinmektedir. Bu çalışmada, bağlama işleminin mekanokimyasal ön işlem ile gerçekleştirilmesi durumunda Ar-Ge veya endüstriyel üretim için çok daha kaliteli kompozitlerin üretilmesi ve etkin bağlama sonucunda zaman ve hammadde kaybının en aza indirilmesi amaçlanmıştır. Çalışmada, kullanılan yöntem ve üretilen malzemenin, hafif silah gövdeleri ve havacılık bileşenleri gibi sektörlerin gereksinimlerini karşılamak için verimli bir alternatif olarak hizmet etmesi amaçlanmıştır. Bu bağlamda, ana (matris) malzeme olarak poliamid 66 (PA66) ve üstün özellikleri nedeniyle takviye olarak iki boyutlu(2D) altıgen bor nitrür (h-BN) seçilmiştir. Başlangıçta, her iki malzeme de optimum işleme koşullarını sağlamak için kamara tipi bir fırında 60°C'de 30 dakika boyunca nem alma işlemine tabi tutulmuştur. Daha sonra karışımlar, hassas bir terazi kullanılarak ağırlıkça %1 ve %4 takviye oranlarına ulaşmak için PA66 ve h-BN hassas bir şekilde tartılarak hazırlanmıştır. Toplam şarj ağırlığı yaklaşık 5 g olarak standartlaştırılmış, öğütme kabının hacminin %50'sini aşmaması sağlanmış ve bilye-yük oranı 10:1 olarak tutulmuştur. Mekanokimyasal sentez, kontrollü sıcaklık koşulları altında yüksek enerjili bilyalı öğütme işlemi kullanılarak gerçekleştirilmiştir. Homojen dağılım ve matris ile takviye arasında gelişmiş etkileşim elde etmek için sürekli çalışma ile sırasıyla 15 ve 30 dakikalık süreler için 400 rpm ve 1200 rpm öğütme hızları kullanılmıştır. Hazırlanan numuneler, yüzey morfolojilerini, homojenliklerini ve yapısal bütünlüklerini değerlendirmek için hem görsel hem de mikroskobik incelemeye tabi tutulmuştur. Farklı takviye oranlarına sahip iki serinin analizi yapıldığında; öğütme hızının, takviyenin homojen dağılımının sağlanmasında, polimer yapısına entegrasyonunda ve potansiyel kovalent bağların oluşumu da dahil olmak üzere mekanokimyasal etkilerin artırılmasında daha kritik bir rol oynadığını ortaya koymuştur. 1200rpm'de gerçekleştirilen işlemlerde homojen bir yapı açıkça görülmektedir. Buna ek olarak, nispeten büyük PA66 granülleri bu çalışma koşulları altında herhangi bir deformasyona uğramamıştır.

Anahtar kelimeler: Mekanokimya, Polimer nanokompozit, Poliamid 66, Hekzagonal bor nitrür, Sıcaklık kontrollü yüksek enerjili bilyalı değirmen.

INTRODUCTION

Polymer nanocomposites embedded with nanofillers have demonstrated a wide range of enhanced functionalities, encompassing mechanical, chemical, thermal, and electrical properties. The primary challenge in such composites lies in the poor compatibility between polymers and nanofillers, which has constrained the advancement of their functional properties. Nonetheless, mechanochemical processes have emerged as a promising approach to address this limitation.

Mechanochemical processes utilize mechanical energy to initiate, enhance, or regulate chemical reactions. Mechanical energy can induce structural changes at the molecular level, thereby influencing reaction mechanisms. This may enhance reaction rates, facilitate the formation of intermediate products, or reduce undesirable side reactions. These processes can be employed to modify or enhance the physical, chemical, and structural properties of materials. The effects of chemical reactions initiated by mechanical action were first observed in the late 19th century, when Carey Lea reported that grinding gold, silver, platinum, and mercury halides in a mortar

led to their decomposition into halogens and metals(Sopicka-Lizer, 2010). Thanks to its advantages, such as short reaction times, high conversion efficiencies, and the discovery of new reaction pathways, mechanochemical synthesis has established a significant role in the field of chemistry. Due to these unique characteristics, this method has been referred to as "Chemical 2.0" for its compatibility with "green chemistry" principles and its transformative potential in the discipline of chemistry. Furthermore, it has been recognized as one of the top 10 chemistry innovations that have changed the world (Gomollón-Bel, 2019; Shi et al., 2016; W. Wang et al., 2022; Y. Wang et al., 2017)

Mechanochemical methods can be performed under solvent-free, dry conditions, making them relatively simple, cost-effective, and environmentally friendly compared to other techniques. This has made mechanochemical processes an effective approach in many industries, particularly in material science and the production of advanced composite materials. The properties of pure polymers can be significantly improved by incorporating fillers; however, poor compatibility between polymers and fillers often undermines composite performance. Melt mixing, a common industrial method, struggles to achieve strong interfacial bonding, negatively impacting composite properties. Additionally, nanoscale fillers in melt-mixed systems frequently aggregate, leading to material defects (Shen et al., 2011)(Jiang et al., 2013).

Mechanochemical methods, which initiate chemical reactions through the application of mechanical energy, can significantly enhance the affinity between different types of materials (Ong, Leiding, Tao, Virshup, & Martínez, 2009)(Friščić, 2012) (Chang et al., 2014). Furthermore, these production methods are highly suitable for polymer composites as they are compatible with conventional joining processes and can effectively incorporate very small fillers, including nanomaterials(Chen, Li, & Shimizu, 2007)(Zhang, Zhang, Liang, & Lu, 2008)(Peng, Chen, & Tiwari, 2018).

In the study conducted by Jiwan You and colleagues(You et al., 2019), powders were mixed at weight ratios of 1%, 5%, 10%, and 20% and subjected to various processes, including plasma-assisted mechanochemical, non-plasma-assisted mechanochemical, and methods excluding mechanochemical treatment. The researchers concluded that they had developed a method that effectively addresses the compatibility issues between polymers and nanofillers, significantly enhancing the functionality of polymer nanocomposites. Ou and colleagues (Ou, Chen, Lu, & Lu, 2021) proposed a mechanochemical approach induced by ball milling to prepare polyimide/boron nitride (BN) films with a low coefficient of thermal expansion (CTE) and high thermal conductivity. The study emphasized that this method enables the simultaneous exfoliation of BN layers and surface covalent modification in a simple, effective, and single-step process, thereby facilitating excellent matrix dispersion and the production of high-thermal-conductivity composites. In another study(Yang, Wang, & Chen, 2020), an innovative strategy was introduced for the first time to fabricate PA12/BN thermally conductive powders suitable for selective laser sintering (SLS) 3D printing. This approach combined Solid-State Shear Milling (S^3M) technology and cryogenic pulverization techniques. The S^3M technology effectively addressed the dispersion challenges associated with a high proportion of BN particles, while the cryogenic pulverization process enhanced the spheroidization of the milled particles. The researchers highlighted that the resulting material is suitable for producing thermally conductive components using the SLS method.

In this context, polyamide 66 (PA66) was chosen as the main (matrix) material and hexagonal boron nitride (h-BN) was chosen as reinforcement due to its superior properties. The proportion of h-BN in the mixtures was determined to be 1% and 4%. The mechanochemical synthesis was

conducted using a high-energy ball milling process under controlled temperature conditions. In order to obtain homogeneous dispersion and improved matrix-reinforcement interaction, mechanochemical treatments were applied at 15 and 30 min durations and at grinding speeds of 400 and 1200 rpm without stopping the system.

MATERIAL AND METHOD

Materials

As the matrix material, transparent commercial polyamide66 in granule form (average size of 2 mm) was obtained. Since one of the aims of the study was to observe how the initial matrix size would affect the process and material properties, relatively large-sized granules were used. As reinforcement material, h-BN with 99.97% purity, average particle size of 120 nm, and a density of 2g/cm^3 was obtained from Bortek Company.

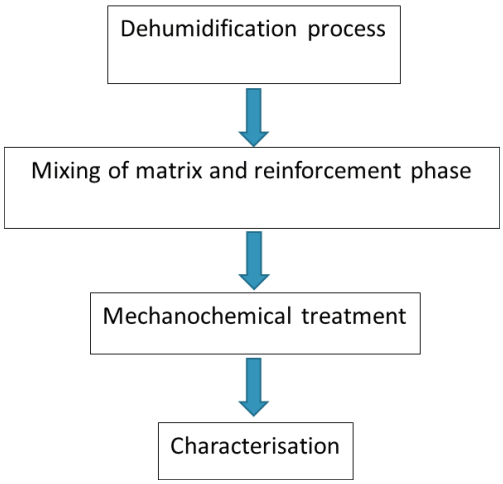


Figure 1 *Experimental flow chart*

Method

After material procurement, the experimental flow chart(figure 1) was determined, and the steps of dehumidification, mixture preparation, mechanochemical process, and examination were carried out, respectively. Initially, both materials were subjected to dehumidification in a chamber-type furnace at 60°C for 30 minutes to ensure optimal processing conditions(figüre 2a). The samples were then quickly packed so that they did not come into contact with the atmosphere.

The materials ready for the mixture were precisely prepared according to the criteria to be considered in mechanochemical processes such as charge volume, ball charge ratio and the composition ratios of the composite to be formed (1 and 4 wt%). For this purpose, a total of 5.30 g mixtures were formed with a ball charge ratio of 10:1 and a grinding jar filling rate not exceeding 50%.



Figure 2 *a. Chamber-type furnace, b. Emax high-energy ball mill, c. Grinding jars and balls*

In the current study, sufficient energy must be provided to the materials to form covalent bonds between varying amounts of h-BN reinforcement and PA66 matrix(You et al., 2019). Grinding was carried out using Retsch Emax high-energy ball mill with temperature control (integrated cooling cycle)(figure 2b) at 15-minute and 30-minute durations, and at 400 rpm and 1200 rpm speeds. Since the device is temperature-controlled, in contrast to the rest periods in the literature, the grinding process was continuously performed within the specified time parameters. Control samples were also produced with the same ratios, but without undergoing mechanochemical processing. Mechanochemical processes were carried out with stainless steel balls and in stainless steel grinding jar(figure 2c). The parameters of the prepared samples are shown in Table 1. The prepared samples were subjected to both visual inspection and microscopic examination to evaluate their surface morphology, homogeneity, and structural integrity.

Table 1 *Parameters of the prepared samples*

Sample No	h-BN Ratio (%)	Time (min)	Speed (rpm)
1	1	15	400
2	1	15	1200
3	1	30	400
4	1	30	1200
5 (Unprocessed Mixture)	1	0	0
6	4	15	400
7	4	15	1200
8	4	30	400
9	4	30	1200
10 (Unprocessed Mixture)	4	0	0
11 (PA66 Only)	0	0	0

RESULTS and DISCUSSION

Visual Inspection

The samples produced are shown in Figure 3. In the first visual inspection, it was observed that there were no problems such as overheating or burning that may occur due to non-stop grinding. The colour changes that occur as a result of the increase in grinding speed and time indicate

that the heat increases in the natural process during the grinding process. However, since temperature limits were entered in advance, a harmful temperature level for polymer or reinforcement structure was prevented. (50 °C for 15 minutes grinding and 60 °C for 30 minutes grinding).

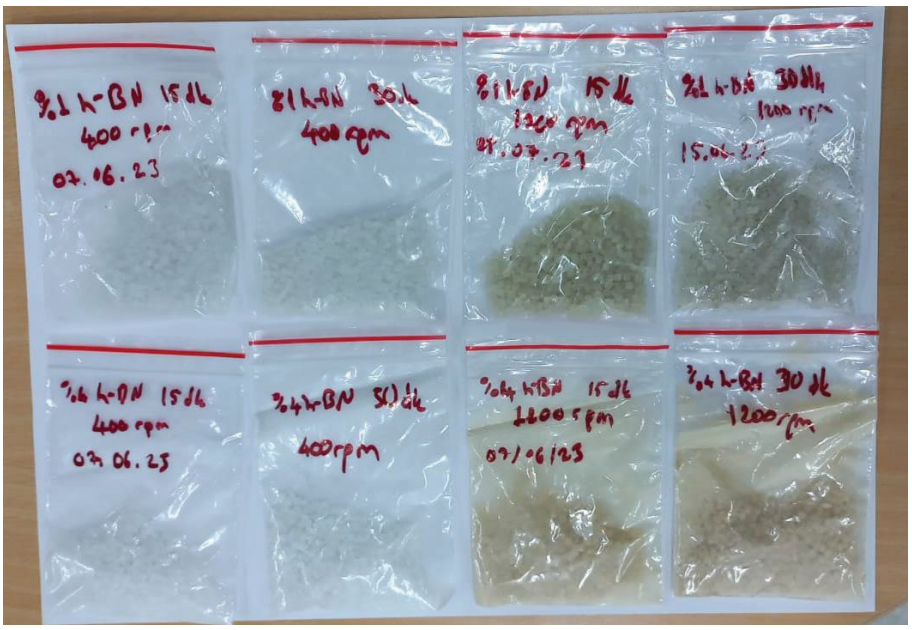


Figure 3 *Mechanochemically treated and untreated samples with different parameters*

At the end of each process, the final temperature was noted. It was observed that these final temperatures were at a level that would not damage the materials. The 400%wt increase in the mass of the reinforcing element did not cause a significant change in the final temperature (figure 4).

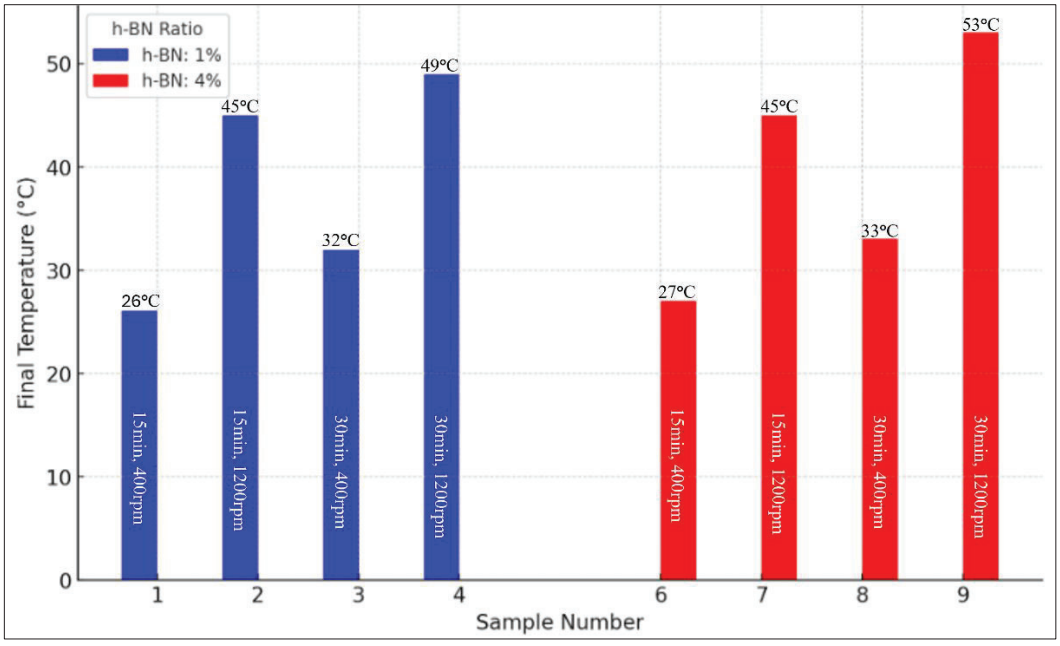


Figure 4 *Final temperatures after mechanochemistry processes*

Optical Microscope Examination

In the optical microscope examination, it was tried to observe to what extent the powder adhered to the main matrix, and the size and shape variation of large-size matrix granules were investigated. Figure 5 shows the difference between the samples containing 100% PA66 and mechanochemically treated samples containing 1% h-BN under optical microscope. The grinding process did not induce any noticeable changes in the shape or size of the matrix granules.

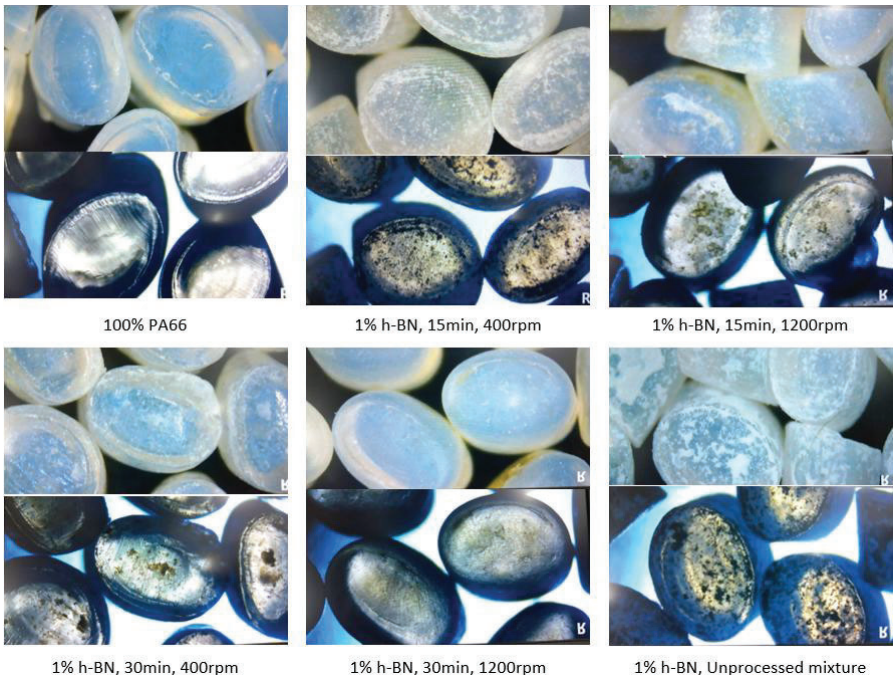


Figure 5 *Optical microscope images of 100% PA66 and 1% h-BN reinforced specimens*

Additionally, no deformation was observed as a result of unexpected sudden temperature increases during the process. It was clearly evident that as the grinding duration and rotational speed increased, agglomeration was significantly reduced, resulting in a more uniform and homogeneous mixture. In contrast, the sample containing 1% h-BN without mechanochemical treatment exhibited a non-uniform distribution of the reinforcement particles, which adhered to specific regions solely through static effects, without forming proper bonds. Figure 6 shows the difference between the samples containing 100% PA66 and mechanochemically treated samples containing 4% h-BN under optical microscope. When the figure is analysed, a similar trend is observed. As the time and rotation speed increase, it is observed that the reinforcement is more homogeneously distributed and embedded in the polymer structure.

ISBN: 978-625-378-045-6

https://doi.org/10.5281/zenodo.14537144

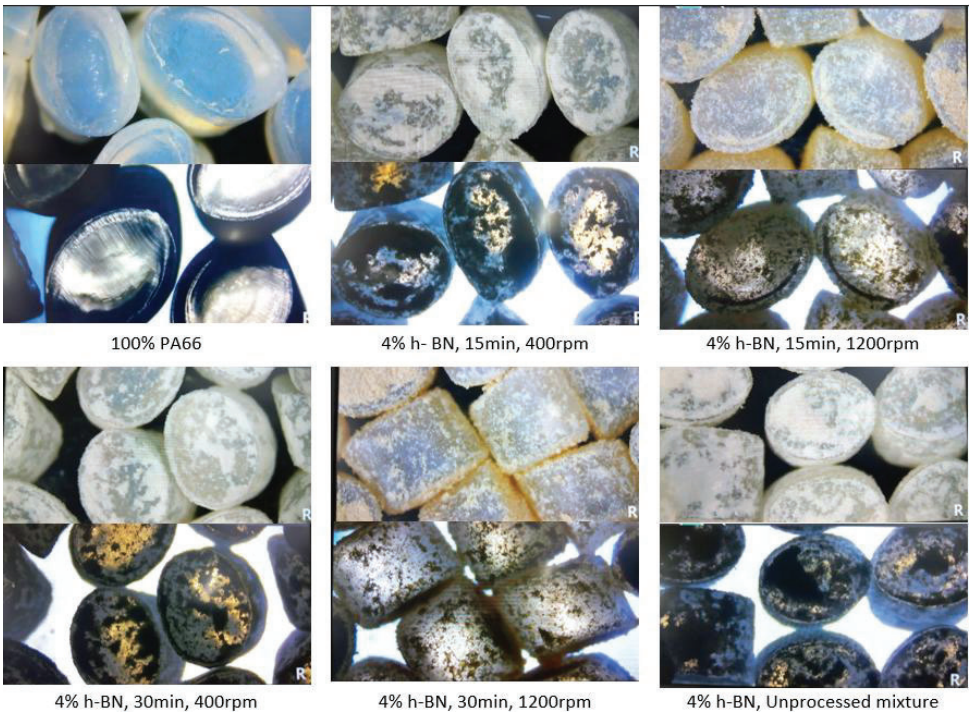


Figure 6 *Optical microscope images of 100% PA66 and 4% h-BN reinforced specimens*

CONCLUSION and SUGGESTIONS

When both series with different reinforcement ratios are analysed,

- The rotational speed is a more effective parameter for homogeneity and embedding in the polymer structure, i.e., the mechanochemical effect, i.e., possible covalent bonds.
- A homogenous structure is clearly visible in the processes performed at 1200 rpm. In both series, the most homogenous distribution is at 30 min, 1200 rpm values.
- The relatively large PA66 granules did not undergo any deformation under these operating conditions.

Future Suggestions

- In addition to the detailed characterisations, PA66 granules should be ground, and experiments should be repeated with the same parameters.
- According to the new results, it should be discussed how the initial size of the matrix material affects the performance in the mechanochemical method.
- Optimisation between the change of the predicted material properties and the increased matrix cost due to secondary grinding should be investigated.
- The proposed studies are planned to be carried out using cryogenic milling as shown in figüre 7.

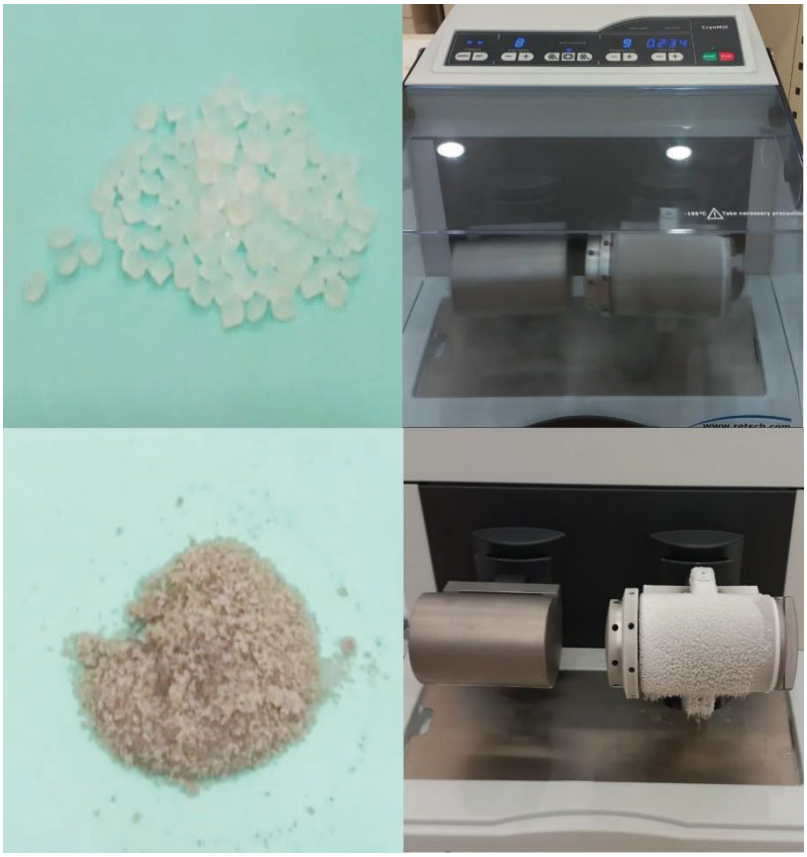


Figure 7 *Cryogenic milling process to grind the matrix*

Acknowledgments: This study was supported by Kırşehir Ahi Evran University Scıentıfic Research Projects Unıt(Project number: MMF.A4.22.001).

REFERENCES

Chang, D. W., Choi, H. J., Jeon, I. Y., Seo, J. M., Dai, L., & Baek, J. B. (2014). Solvent-free mechanochemical reduction of graphene oxide. Carbon, 77(May), 501–507. doi:10.1016/j.carbon.2014.05.055

Chen, G. X., Li, Y., & Shimizu, H. (2007). Ultrahigh-shear processing for the preparation of polymer/carbon nanotube composites. Carbon, 45(12), 2334–2340. doi:10.1016/j.carbon.2007.07.017

Friščić, T. (2012). Supramolecular concepts and new techniques in mechanochemistry: Cocrystals, cages, rotaxanes, open metal–organic frameworks. Chemical Society Reviews, 41(9), 3493–3510. doi:10.1039/c2cs15332g

Gomollón-Bel, F. (2019). Ten Chemical Innovations That Will Change Our World: IUPAC identifies emerging technologies in Chemistry with potential to make our planet more sustainable. Chemistry International, 41(2), 12–17. doi:doi.org/10.1515/ci-2019-0203

Jiang, S., Gui, Z., Bao, C., Dai, K., Wang, X., Zhou, K., … Hu, Y. (2013). Preparation of functionalized graphene by simultaneous reduction and surface modification and its polymethyl methacrylate composites through latex technology and melt blending. Chemical Engineering Journal, 226, 326–335. doi:10.1016/j.cej.2013.04.068

Ong, M. T., Leiding, J., Tao, H., Virshup, A. M., & Martínez, T. J. (2009). First principles dynamics and minimum energy pathways for mechanochemical ring opening of cyclobutene. Journal of the American Chemical Society, 131(18), 6377–6379. doi:10.1021/ja8095834

Ou, X., Chen, S., Lu, X., & Lu, Q. (2021). Enhancement of thermal conductivity and dimensional stability of polyimide/boron nitride films through mechanochemistry. Composites Communications, 23. doi:10.1016/j.coco.2020.100549

Peng, C., Chen, Z., & Tiwari, M. K. (2018). All-organic superhydrophobic coatings with mechanochemical robustness and liquid impalement resistance. Nature Materials, 17(4), 355–360. doi:10.1038/s41563-018-0044-2

Shen, B., Zhai, W., Chen, C., Lu, D., Wang, J., & Zheng, W. (2011). Melt blending in situ enhances the interaction between polystyrene and graphene through π-π Stacking. ACS Applied Materials and Interfaces, 3(8), 3103–3109. doi:10.1021/am200612z

Shi, Y. X., Xu, K., Clegg, J. K., Ganguly, R., Hirao, H., Friščić, T., & García, F. (2016). The First Synthesis of the Sterically Encumbered Adamantoid Phosphazane P4(NtBu)6: Enabled by Mechanochemistry. Angewandte Chemie - International Edition, 55(41), 12736–12740. doi:10.1002/anie.201605936

Sopicka-Lizer, M. (2010). High-energy ball milling: Mechanochemical processing of nanopowders. High-Energy Ball Milling: Mechanochemical Processing of Nanopowders. doi:10.1533/9781845699444

Wang, W., Chai, M., Bin Zulkifli, M. Y., Xu, K., Chen, Y., Wang, L., … Hou, J. (2022). Metal-organic framework composites from a mechanochemical process. Molecular Systems Design and Engineering, 8(5), 560–579. doi:10.1039/d2me00211f

Wang, Y., Wang, H., Jiang, Y., Zhang, C., Shao, J., & Xu, D. (2017). Fast, solvent-free and highly enantioselective fluorination of β-keto esters catalyzed by chiral copper complexes in a ball mill. Green Chemistry, 19(7), 1674–1677. doi:10.1039/c6gc03306g

Yang, L., Wang, L., & Chen, Y. (2020). Solid-state shear milling method to prepare PA12/boron nitride thermal conductive composite powders and their selective laser sintering 3D-printing. Journal of Applied Polymer Science, 137(23). doi:10.1002/app.48766

You, J., Choi, H. H., Lee, Y. M., Cho, J., Park, M., Lee, S. S., & Park, J. H. (2019). Plasma-assisted mechanochemistry to produce polyamide/boron nitride nanocomposites with high

thermal conductivities and mechanical properties. Composites Part B: Engineering, 164(November 2018), 710–719. doi:10.1016/j.compositesb.2019.01.100

Zhang, W., Zhang, X., Liang, M., & Lu, C. (2008). Mechanochemical preparation of surface-acetylated cellulose powder to enhance mechanical properties of cellulose-filler-reinforced NR vulcanizates. Composites Science and Technology, 68(12), 2479–2484. doi:10.1016/j.compscitech.2008.05.005

POLYCHLORINATED BIPHENYLS (PCBS) IN FOOD PACKAGING

Zahra Rezapour*

Department of Food Safety and Hygiene, Science and Research Branch, Islamic Azad University, Tehran, Iran

Narges Fathabadibozcheloei

Department of Food Safety and Hygiene, Science and Research Branch, Islamic Azad University, Tehran, Iran

*Corresponding author

ABSTRACT

Polychlorinated Biphenyls (PCBs) are a class of persistent organic pollutants (POPs) historically used in industrial applications, including plasticizers, which may persist in food packaging materials. Despite the global ban on PCB production, these compounds continue to pose significant health risks due to their persistence in the environment and ability to bioaccumulate in the food chain. This study focuses on the detection and quantification of PCBs in food packaging materials, particularly in recycled and low-cost plastics. Utilizing advanced chromatographic techniques, the research investigates the prevalence of PCB contamination and its potential migration into food products under various storage conditions. The findings are analyzed in relation to existing regulatory standards, highlighting potential gaps in current food safety regulations. Furthermore, this study explores the long-term health impacts of low-level PCB exposure, including endocrine disruption, carcinogenicity, and neurotoxicity. The presentation will conclude with a discussion of alternative packaging solutions and strategies for minimizing consumer exposure to PCBs.

Keywords: PCB, risk assessment, food packaging

EVALUATION OF COMPOSITE MATERIAL PRODUCTION FROM CAST IRON AND POLYMER WASTES IN MACHINING AND CASTING PROCESS

Metin KARAASLAN

Makina Fakültesi, Istanbul Teknik Üniversitesi, İstanbul, 34437, Türkiye

Zeynep DOĞAN

Makina Fakültesi, Istanbul Teknik Üniversitesi, İstanbul, 34437, Türkiye

ABSTRACT

In this study, it was aimed to produce recyclable composite materials by using the scraps resulting from butterfly valve manufacturing processes. Within the scope of the study, samples were produced under different manufacturing and composition conditions by using spheroidal cast iron and pig cast iron chips, filler sand and a thermoset material called aralditee, and mechanical properties were obtained as a result of compression tests. As a result of the study, it was observed that aralditee showed the highest compressive strength and toughness of the sample in which matrix, spheroidal cast-iron chips were used as fibre.

Keywords: Butterfly Valves, Composite Materials, Green Manufacturing, Cast Iron Chips, Recycling, Briquetting, Cold Forming, Polymer Matrix Composites.

1. INTRODUCTION

In today's world, especially due to the increase in energy-raw material prices and harmful gas production, the issue of reusing the materials and wastes resulting from production has gained serious importance. The use of waste materials resulting from the process of remelting causes more costs than cold pressing or sintering methods [1]. According to research conducted by the U.S. Geological Survey, the reuse of 1 ton of cast iron or steel material saves approximately 1.1 tonnes of iron ore and 0.6 tonnes of coal. In addition, remelting scrap materials is less costly than producing steel or cast iron from scratch. About 100 million tonnes of steel and cast iron chips are produced annually [2].

The most widely reported methods in the literature that enable the use of such materials resulting from production are cold / warm pressing and briquetting methods. Briquetting

allows the material in the form of billets or piles to be brought to the desired bulk density and dimensions with the help of compressive forces [3]. In their study, Torkar, Lamut and Millaku pressed their stainless steel scraps under a pressure of about 1766 kPa and then aimed to use the obtained briquette samples by melting them again in the casting pot. The main problem here is the energy costs associated with the melting process and the heating (400°C) and washing costs with organic solvents to remove chips from cutting fluids [4].

In his study, Abdelhaleem examined the properties of a mixture of recycled polypropylene and iron chips in proportions of 10%, 20% and 30%. Iron chips were heated at 100 degrees, and samples were produced with the help of plastic injection. Polypropylene was cured at 80 degrees for 2 hours [5]. The main issue that emerges in this study is the energy costs arising as a result of heating and the increase in carbon footprint. Brozek used 5 different material chips (AlSi10, AlSi9, CuZn35, CuSn10 and ZnAl4Cu1) into cylindrical specimens of 40 mm diameter and 60 mm tall and briquetted these samples at room temperature under a stress of 400 MPa [6]. The cold/warm pressing method, on the other hand, involves making the powdered or chipping material dense and high in strength before machining or sintering [3]. Briquetting and cold pressing methods allow scrap chips to be used as fibercomposite materials without any melting [7]. It is wondered how the materials planned to be produced using raw material wastes will be produced and what values their mechanical properties will have. Copper, cast iron and steel materials are generally used as waste chips. According to Demirel, Güneş and Şahin, when a mixture of 90% bronze and 10% nodular cast iron is cold pressed under a stress of 1000 MPa and sintered at 875 ° C, a compressive strength of approximately 350 MPa is obtained [8].

According to Aslan et al., the most common recycling method for scrap chips is melting and recasting, but the decrease in thermal and electrical conductivity properties as a result of oxidation of scrap chips, the energy required for smelting, and the harmful gases resulting from melting make these processes negative [8]. Another recommended method is ball milling. According to Fullenwider, chips can be obtained by the ball milling method and the desired materials can be produced again by the powder metallurgy method [9]. On the other hand, powder metallurgical methods are not preferred mainly in the reuse of waste materials due to their unsuitability for mass production and their cost compared to other methods. The main purpose of this study is to reduce the negative effects of the recent energy crises and carbon footprint increases on the earth as much as possible. Mostly with the

concept of 'Green Manufacturing', which has become an important trend in recent times, it is aimed to reduce the carbon footprint as much as possible at all stages from the design to the supply chain and production, and this indicates the importance of the use of waste materials [10].

In the continuation of this study, aralditee, filling sand, spheroidal cast iron and pig cast iron chips were used for preparing samples on different production and composition conditions. The compression test were made on the samples and mechanical properties were compared. It was discussed whether it can be used in the manufacturing of any mechanical parts or not.

2. MATERIAL & METHODS

In the production of butterfly valves, a thermoset material called aralditee is used to make the casting mould model of the butterfly valve body. For the butterfly valve body, spheroidal cast iron and pig cast iron materials are generally used. In the butterfly valve discussed in this study, which has a nominal diameter of 65 mm and operates under a pressure of 16 bar, spheroidal cast iron is used as the body material and there is a serious scrap chip production in post-casting machining operations. Filling sand material is used both in sand mould casting operations and in the mould model to reduce costs. In this study, it was tried to obtain especially a composite material, by using aralditee and cast iron chips.

Alternative materials were tried to be produced by considering waste materials separately. Casting and pressing methods were used in the study.

2.1 Sample Manufacturing

Firstly, the studies were started by experimenting with the production of an alternative material with the use of aralditee, filler sand and spheroidal cast iron chips. For this purpose, composite material productions were made by mixing aralditee, filler sand and scrap chips in certain proportions. The mass values of these materials in grams and percentages in the samples produced are given in Table 1.

Table 1 : Mass and percentage composition of samples.

MATERIALS	SAMPLE 1 [gram]	SAMPLE 1 % Mass	SAMPLE 2 [gram]	SAMPLE 2 % Mass	SAMPLE 3 [gram]	SAMPLE 3 % Mass
Aralditee	73,25	23%	55,53	21%	84	50%
Hardener	73,25	23%	55,53	21%	84	50%
Filler Sand	-	-	149,94	57%	-	-
Sphero Chips	166,5	53%	-	-	-	-
Total Mass	313	100%	261	100%	168	100%

The first produced sample is a composite material formed by a mixture of aralditee and spheroidal cast iron chips shown as sample 1 in Table 1. Aralditee material was used as a binder, while spheroidal cast-iron chips served as fiber. To cure the Aralditee and increase its strength, a commercial hardening material called "SG200" was used. The compressive strength of the supplied aralditee material is approximately 45 MPa. At the first stage of production, as a result of machining operations, wet and partially uneven cast iron chips were heated to 250 ° C with a flame in order to reduce the moisture inside and give a better form. Then, it was mixed into the aralditee and hardener mixture without any melting process. The resulting mixture was poured into the casting mould and left to cure for about 45 minutes. Approximately 73.25 grams of aralditee – hardener and 166.5 grams of spheroidal cast iron chips were used in the mixture. The total mass of the produced sample is approximately 313 grams. For total, two samples were produced.

The second sample produced is a mixture of Aralditee and filler sand. Aralditee material was used as a binder and filler sand was added to the structure. In the production stages of butterfly valves, in order to reduce the cost, filler sand is frequently used in sand mould casting processes and in the creation of mold models. In this process, similar to sample 1 production, filling sand was added to the aralditee and hardening material mixture, the mixture was poured into the casting mold and left to cure for approximately 45 minutes. Approximately 55.53 grams of aralditee-hardener and 150 grams of filler sand were used here. The mass of the material produced is approximately 261 grams.

Finally, at this stage, a sample was produced using only aralditee material and hardener. 84 grams of both materials were used and the resulting mixture was poured into the casting mold. The curing time is approximately 45 minutes.

ISBN: 978-625-378-045-6 https://doi.org/10.5281/zenodo.14537144

The 3 samples produced are cylindrical specimens with a diameter of approximately 30 mm and a length of 200 mm. Subsequently, for the experimental phases, these materials were processed by machining operations to be suitable for compression testing. The dimensions and images of the samples can be seen in Figure 1 and Figure 2 respectively.

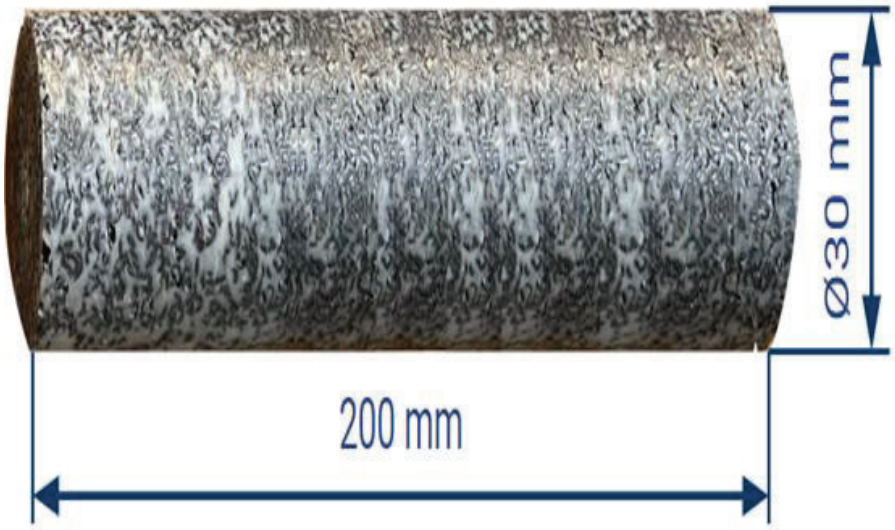


Figure 1 : Illustration of the sample dimensions.

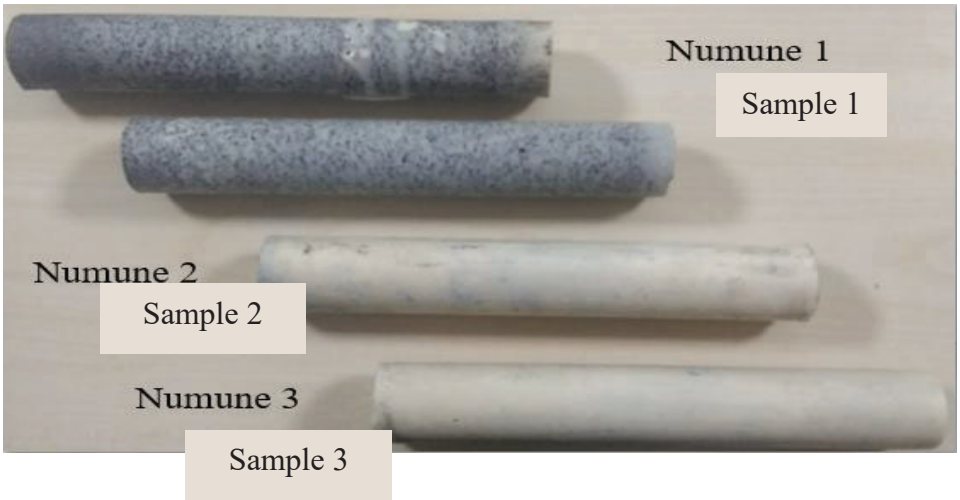


Figure 2 : Illustration of the casting samples.

After the samples were obtained by casting method and mixing processes, in order to reduce the costs arising from melting and mixing processes, the material can be produced by simply compressing the existing spheroidal cast iron scraps without any heat treatment. In this regard,

a sample production was carried out with an existing briquetting machine and mold. In the process, spheroidal cast iron chips were used and were compressed with a press force of 250 tonnes on a cylindrical mold with a diameter of about 120 mm and a height of 120 mm. During the operations, no heat input was applied to the chips and the system, and the processes were carried out entirely by cold forming. The resulting sample is shown in Figure 3.

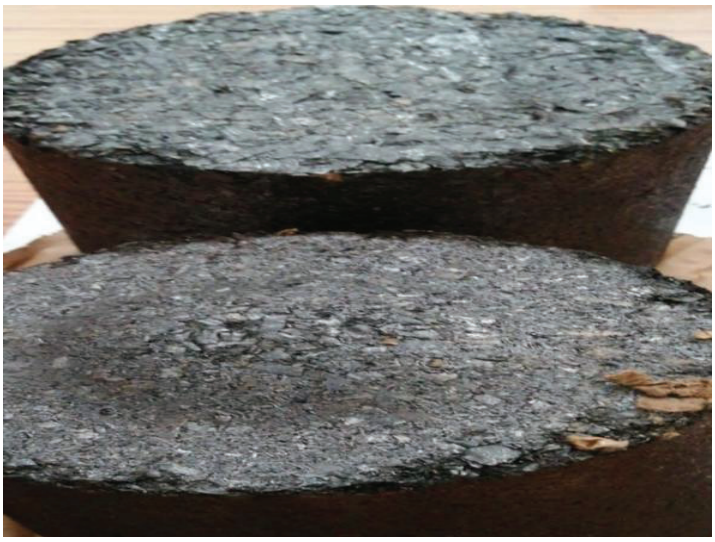


Figure 3 : The briquetting samples.

Cylindrical specimens with a diameter of 120 mm and a height of 120 mm contain a largely porous and irregular structure. The calculated approximate density of the sample is around 5 g/cm3. Due to the irregular and porosity internal structure and the tendency of the material to disperse during processing, it was decided to apply a compression test to the sample and it was desired to perform turning operations for this. With a feed rate of 400 rpm, it is realized in such a way that 1 mm of chips are removed at each step. As a result of the process, due to the inhomogeneous structure of the briquette sample, breaks occurred from the part surface during the turning operations, and therefore the diameter and length reduction operations could not be applied to the part. An image of this can be seen in Figure 4. For this reason, due to the discontinuous structure of the part, the length-shape structure of the chips being different from each other and the machinability is very low, the samples to be applied to the compression test could not be obtained.

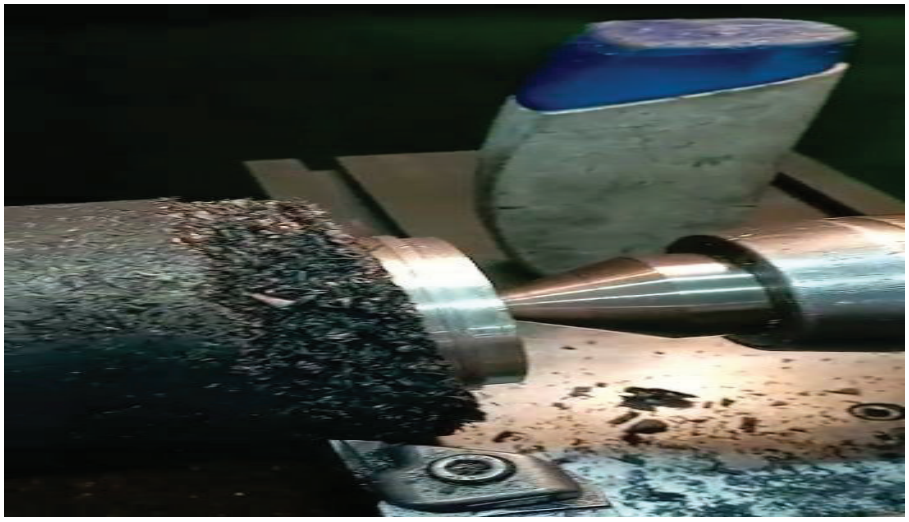


Figure 4 : Machining of the briquetting samples.

As a final alternative, due to the bonding and homogeneity problems caused by cold compression of chips, it was aimed to examine the effects of performing the process in a warm way at different press forces. In these processes, spheroidal cast iron and pig cast iron chips were used.

Reusing cast iron chips by heating them to high temperatures can make them especially easy to corrode with relatively thinner chips. For this reason, without raising the temperatures too much, spheroidal cast iron and pig cast iron chips were compressed with different press forces both at room temperature and at 260°C, resulting in cubic samples of 60mmx60mmx60mm. By increasing the pressing temperature, it is aimed to better bond the chips to each other and thus obtain a more homogeneous structure. The operations were carried out under press forces of 100 tonnes, 300 tonnes and 500 tonnes. Table 2 indicates the types of chips used and the operating parameters.

Table 2 : Pressed samples and operation parameters.

Chip Type	Press Force	Operation Temperature(°C)
Pig	100 Tonnes	25°C
Sphero	300 Tonnes	25°C
Pig	500 Tonnes	25°C
Pig	300 Tonnes	260°C
Sphero	100 Tonnes	25°C
Sphero	300 Tonnes	25°C
Sphero	500 Tonnes	25°C
Sphero	300 Tonnes	260°C

ISBN: 978-625-378-045-6

https://doi.org/10.5281/zenodo.14537144

First, the pig-cast iron chips were compressed with the help of a square mould at a press force of 100 tonnes and below 25°C, and a cubic sample was obtained. In the obtained sample, discontinuities were detected due to the low press force and process temperature, as well as chips of different sizes. The chip types used and the image of the sample are shown in Figure 5 and Figure 6 respectively. The chip sizes and types used in all samples are the same.



Figure 5 : a) Milling chips b) Turning chips.



Figure 6 : Pig cast iron chips pressed at 100 tonnes and 25°C.

Afterwards, the pig cast iron chips was compressed with 300 tonnes and 500 tonnes of press forces at a temperature of 25 ° C to observe the structure of the sample. Here, by increasing the pressing force, it is aimed to further compress the chips and eliminate the inhomogeneous

internal structure caused by size differences. Figure 7 and Figure 8 show images of samples pressed under force of 300 tonnes and 500 tonnes, respectively.



Figure 7 : Pig cast iron chips pressed at 300 tonnes and 25°C.

It has been observed that when the temperature is kept constant, with the increase of the pressing force, the chips are better compacted and the dimensionally large chips crumble. Accordingly, in order to reinforce this observation, the behavior of pig cast iron chips under a force of 500 tonnes was also examined.

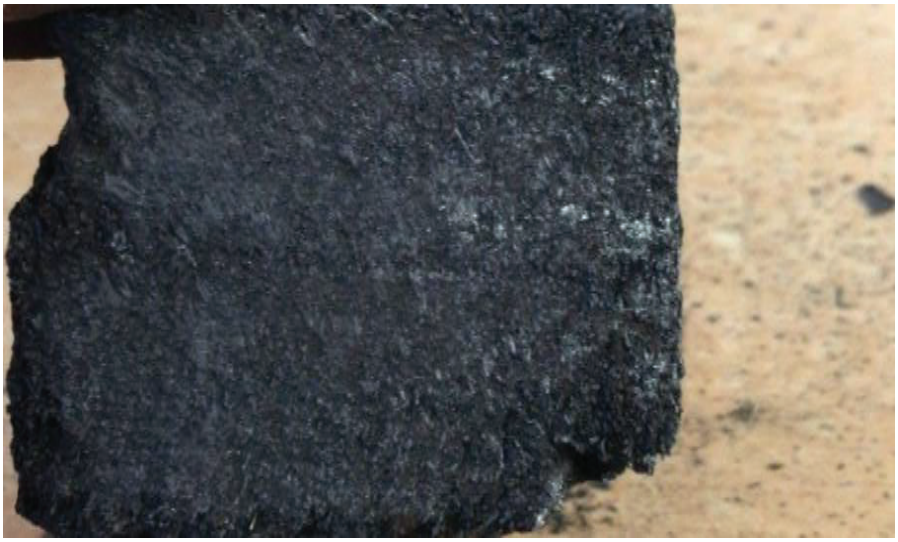


Figure 8 : Pig cast iron chips pressed at 500 tonnes and 25°C.

The process of pressing pig cast iron chips below 500 tonnes yielded better results when the temperature was kept constant than in operations of 100 tonnes and 300 tonnes, and the chips were distributed more homogeneously within the structure. In all pressing processes applied to pig cast iron chips above, the temperature value was kept constant and the press forces were changed. In the last stage, it was aimed to examine the differences that arise according to the situation where 300 tonnes of press force is applied at 260 ° C and the same force is applied at 25 ° C. Figure 9 shows an image of this specimen.



Figure 9 : Pig cast iron chips pressed at 300 tonnes and 260°C.

When the pressing force was kept constant and the temperature was increased, it was seen that the chips spread more uniformly into the structure. In addition, in the first examination of the samples, it can be interpreted that the pig cast iron chips sample, which is pressed at 300 tonnes and 260 ° C, has a harder and tougher structure than other samples.

All the steps described above, which are applied for pig cast iron chips, have been repeated for spheroidal cast iron chips and the effect of press force and temperature on the distribution and strength of chips has been examined here. Since spheroidal cast iron materials have graphite in spherical structure, they can show higher toughness and ductility. For this reason, less cracking is expected in samples produced from nodular cast iron chips. First, trials were conducted at 100 tonnes and 25°C and the resulting sample is shown in Figure 10.



Figure 10 : Sphero cast iron chips pressed at 100 tonnes and 25°C.

As can be seen in Figure 10, the pressing force and operating temperature were not fully sufficient for the homogeneous distribution of chips, nor could they ensure the crumbling of larger sized chips. Therefore, press forces of 300 tonnes and 500 tonnes respectively were also applied to spheroidal cast iron chips, and pictures of the obtained samples are presented in Figure 11 and Figure 12 respectively.



Figure 11 : Sphero cast iron chips pressed at 300 tonnes and 25°C.

It is seen that spheroidal cast iron chips with a load of 300 tonnes show a more homogeneous distribution than spheroidal cast iron chips pressed under 100 tonnes of force. In addition, the sample structure is more rigid and hard.

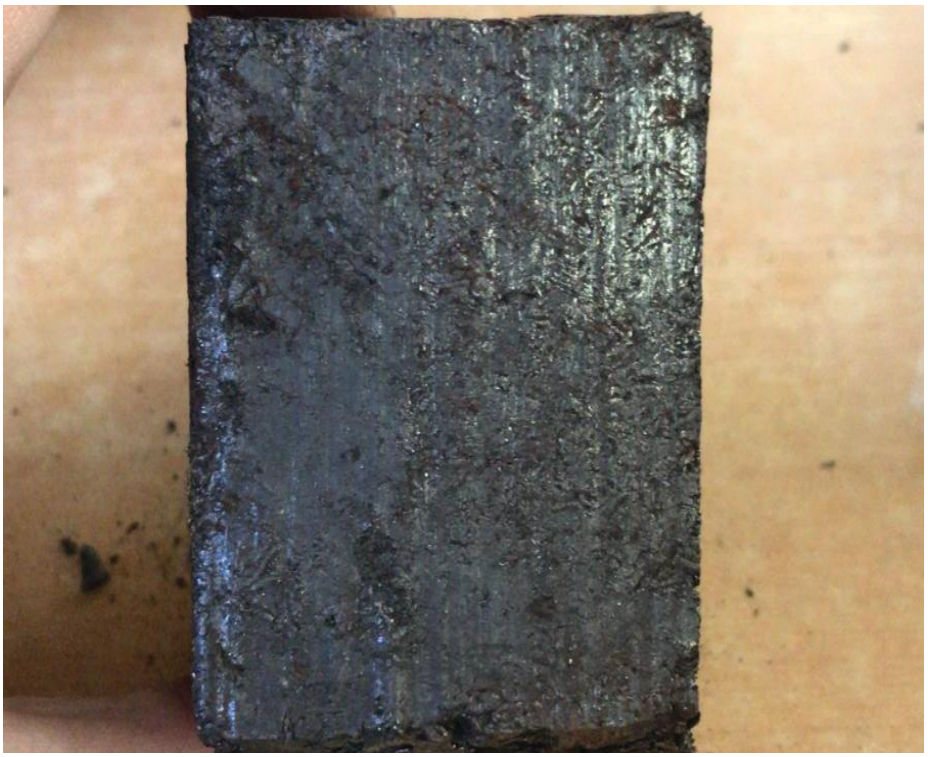


Figure 12 : Sphero cast iron chips pressed at 500 tonnes and 25°C.

In the processes performed with spheroidal cast iron chips, as in pig cast iron chips, when the temperature is kept constant and the press force is increased, it is seen that the sample shows a more homogeneous and rigid structure. In addition, due to the increased force, the chips were adhered to each other more strongly, thus achieving a tighter structure than the samples to which 100 tonnes and 300 tonnes of force were applied. In these operations, the temperature was kept constant at 25°C, only an increase in press forces was made. In order to examine the effect of temperature on the samples, spheroidal cast iron chips were pressed under 300 tonnes of force and 260°C to examine the differences from the sample produced at 300 tonnes and 25°C. The image of the nodular cast iron chips pressed at 260°C can be seen in Figure 13.

ISBN: 978-625-378-045-6 https://doi.org/10.5281/zenodo.14537144



Figure 13 : Sphero cast iron chips pressed at 300 tonnes and 260°C.

2.2 Machining of Samples

In the pressing trials with pig and spheroidal cast-iron chips, as a result of the first observations obtained without any test application to the samples, it was concluded that the pig and spheroidal cast iron chips pressed at 300 tonnes force and 260°C had a more tough and rigid structure than other samples. Later, it was considered to perform machining in order to apply tensile tests to these produced samples. The determined tensile sample dimensions, also suitable for the materials produced, are shown in Figure 14.

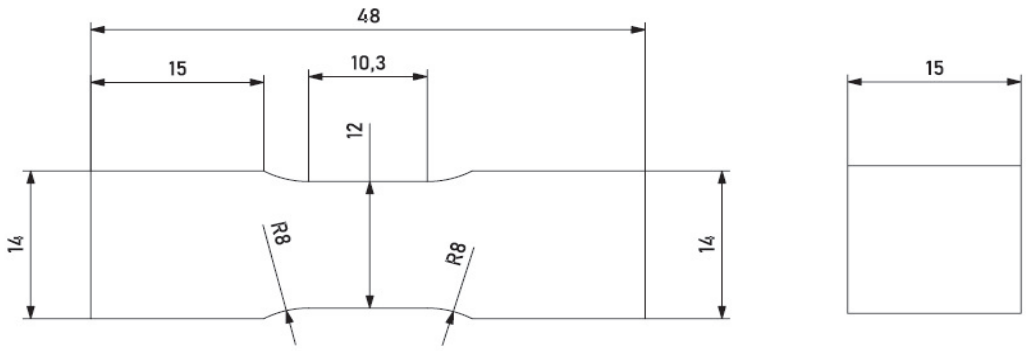


Figure 14 : Tensile specimen dimensions for pressed chips.

For this purpose, the samples produced as a result of pressing processes were wanted to be brought to the size of tensile samples by machining. For this reason, samples pressed at 300

tonnes and 260°C, which are considered to have the highest toughness value and homogeneity, are connected to the mirror for the turning operation. In order to keep the parts stable, although a small pressure was applied with the chuck, the head of the chuck continued to enter the piece. When the specimen was attached with a tailstock at different points, the same problem persisted. The gaps and irregularities in the part are thought to cause this. An example image of the situation that also occurs in pig and spheroidal cast iron samples is given in Figure 15.



Figure 15 : Machining of pressed samples at 300 tonnes and 260°C.

The mechanical properties of the samples vary considerably according to the point at which the force is applied, due to their inhomogeneous structure. For this reason, it was considered to cut the samples obtained with a hand saw without applying any machining operation, so that a tensile sample could be obtained by laser cutting operation. According to Shin et al., it is possible to effectively laser cut up to 100 mm thick [11]. However, according to the information obtained from the market for samples obtained from spheroidal cast iron and pig cast iron chips, a maximum of 25 mm can be cut.

In machining operations for all other samples produced by the pressing operation, chip breaks were observed in pieces from the samples, and some cutting could be done in the parts where there were well-interlocked chips. For this reason, it was aimed to perform cutting operations using a handsaw with a thickness of 0.62 mm in order to detect the part accuracy while cutting and to cut to a thickness that may be suitable for laser cutting.

When the sample produced from spheroidal cast iron chips pressed at 300 tonnes 260 ° C, whose surface and structure appear to be more strong, was tried to be cut with a saw, after a cutting process of about 10 mm, the piece was divided into two from the place attached with the vice, some chip fragments had a glossy surface and could be cut with a saw, while others were separated from the part in the form of breakage.

The cross-section of the cut part can be seen in Figure 16. In addition, when a tensile sample was obtained by wire erosion, it was observed that the part broke off after about 35 seconds under a water pressure of 6-8 bar.



Figure 16 : Sawing of ductile iron chips.

In Figure 16, the chips that appear dark in the area shown in red are separated from the surface. For this reason, a smooth cutting process could not be done and a surface form could not be obtained at a rate that could be processed by laser cutting.

The general view of the specimen, which is compressed in the vise and divided into two parts, is shown in Figure 17.



Figure 17 : Sample of chopped sphero cast iron chips in a clamp.

As a result of all the above-mentioned studies, cylindrical samples in sizes suitable for the compression test standard could be obtained only from the samples obtained by the casting method. Samples obtained by cold and hot pressing were subjected to compression test with the cubic shape in which they were produced, since they could not be cylindrical sampled for the reasons described in the previous sections. By further optimising chip sizes, press forces and temperature values, it may be possible to achieve more uniform structures.

3. EXPERIMENTAL STUDIES

As mentioned in the previous sections, samples that may be suitable for experimental study consist of samples produced by casting method and pressing. It has not been possible to test briquetted samples experimentally to determine their mechanical properties due to their inhomogeneous structure, the fact that chips do not adhere together completely at some points due to pressing forces and temperatures, and their unsuitability for machining. It was decided to apply the compression test to the samples obtained by casting method and pressing. In the experiments, ASTM DD695-15 standard, which is the standard for the determination of compressive properties of rigid plastics in the literature, was used as a standard. Accordingly, the diameter/aspect ratio of the samples should not exceed 0.5. The pressing speed can be taken as 1 mm/minute. Since it is not desirable to go beyond the standard, the diameter / length ratio of the tested casting samples is determined not to exceed 0.5. Thus, the samples, which initially came in length of 200 mm, were divided into three parts, one was used for compression tests,

and the remaining two were stored for hardness testing and other studies that could be carried out in the future. The table and image with the information of the samples produced can be seen in Table 3 and Figure 18.

Table 3 : Information on samples produced by casting method.

Sample	Diameter(mm)	Length(mm)	Composition
A1	29	46	Sphero-Araldite
A2	29	57	Sphero-Araldite
A3	29	57	Sphero-Araldite
B1	28	47	Araldite-Sand
B2	28	55	Araldite-Sand
B3	28	56	Araldite-Sand
C1	28	56	Araldite
C2	28	48	Araldite
C3	28	55	Araldite
D1	28	57	Sphero-Araldite
D2	28	48	Sphero-Araldite
D3	28	46	Sphero-Araldite

In the samples examined here, those shown as A1-A2-A3 and those designated as D1-D2-D3 contain the same proportion of spheroidal cast iron and araldite materials. The only difference between them is that since the chips in the D1-D2 and D3 samples were cast into the mold very early in the curing process of araldite, they collapsed to the bottom of the mold over time, so a homogeneous mixture could not be obtained. The samples denoted by A1-A2-A3 have a more homogeneous distribution.

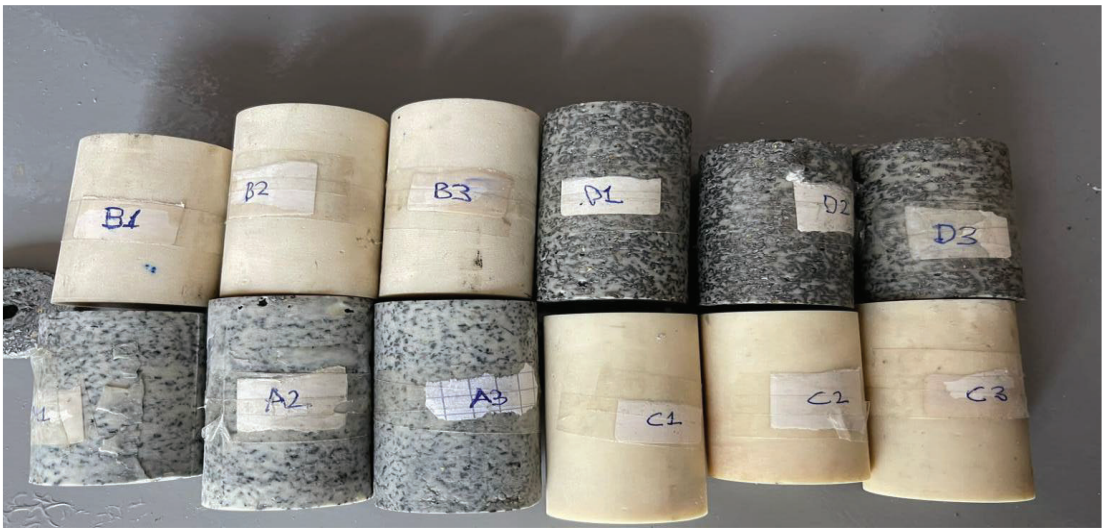


Figure 18 : Images of samples produced by casting.

Accordingly, in Figure 18, the samples shown by A1-B1-C1 were compression tested according to ASTM DD695-15. From experimental studies, it is expected to obtain mechanical properties such as compressive strength and toughness value of these samples. Then, according to the values obtained, it will be examined whether it can be used in any part of the butterfly valve. The samples obtained by pressing are 60x60x60 mm in size.

3.1 Compression Test

As mentioned in the previous sections, the compression test was applied to the samples A1, B1 and C1 detailed in Table 3. As the test standard, ASTM D695-15 is used, which determines the compressive properties of rigid plastics. According to this standard, the length/diameter ratio of the sample to be tested should not exceed 2 and a value in the range of 1 to 1.6 mm/min should be selected as the sample press rate. Depending on the test device, this value was taken as 1mm/min in the experiments. The purpose of these experiments is to determine the critical values of the material samples such as yield strength, modulus of elasticity and to understand whether they can be used at any point of the butterfly valve. Stress-unit elongation graphs of the samples will be given together. First, the C1 sample was taken for the compression test. The image of the compression damage of the C1 sample is shown in Figure 19.



Figure 19 : Compression failure for the C1 sample.

ISBN: 978-625-378-045-6

https://doi.org/10.5281/zenodo.14537144

Afterwards, the compression test of the B1 sample was performed. During the casting process, while the araldite is cured in the melt state, the filler sand is poured into the casting mold and the filling sand is adhered especially to the edge points of the mold. After the compression test, parts were torn off from the outer surface of the sample and the material was failed. Compression failure occurred as rupture where the density of filler sand was higher than the density of araldite material, and crack progression was observed on the outer surface due to the discontinuities contained in the part. The image of this situation is shown in Figure 20.



Figure 20 : Compression failure for the B1 sample.

Finally, a compression test was applied to the A1 sample. This sample is a composite structure in which araldite material acts as a matrix and spheroidal cast iron chips act as fibers. To the araldite sample produced by casting, spheroidal cast iron was added while it was in the molten state and the part was formed in this way. It was observed that a large part of the spheroidal cast iron chips fell towards the lower parts of the mold due to its density, while a small part adhered to the side walls of the mold and the middle of the material.

The spheroidal cast iron chips at the bottom of the mold are separated from the mold. Later in the compression test, crack progressions of 45 degrees were observed, especially on the outer

surface of the material, and the sample was subsequently failed by crack propagation from these points. The visual of the failure can be seen in Figure 21.



Figure 21 : Compression failure for the A1 sample.

The next section is a comparison of the stress-strain curves and mechanical properties of the samples.

3.2 Comparison of Samples' Mechanical Properties

Compression tests of A1, B1 and C1 samples were performed and as a result of the experiments, stress-strain graphs of these materials were obtained. The resulting graphs can be seen in Figure 22.

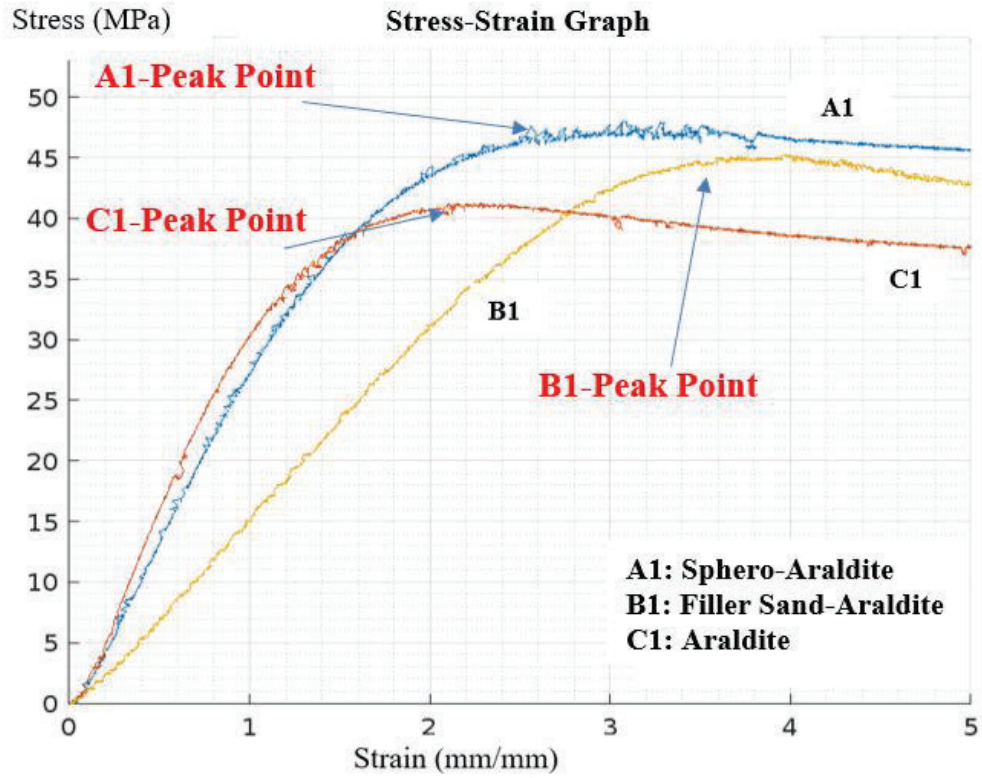


Figure 22 : The Stress-strain change graph of cast samples

As can be seen from Figure 22, the sample, consisting of spheroidal cast iron chips and araldite material mixtures, has the highest compressive strength and toughness. Secondly, the strength and toughness values of the sample consisting only of aralite material are coming. The lowest mechanical properties obtained in this study are araldite and filler sand mixture. The numerical values of these expressed properties can be seen in Table 4.

Table 4 : Mechanical properties of casting samples.

Sample	Compressive Strength [MPa]	Toughness [J/m^3]
A1	48	17,2
B1	40	13,8
C1	45	18,3

The composite material, which is formed especially with the obtained spheroidal cast iron chips and araldite material mixture, has an acceptable toughness and tightness property as well as low strength and rigidity. When these data are taken into consideration, it is determined that more

weight should be given to composite structures where spheroidal cast iron chips are used for future studies. The table comparing the properties of this material with the spheroidal cast iron used in the butterfly valve body is shown in Table 5.

Table 5 : Comparison of sphero cast iron and sphero-araldite composite [12].

Properties	Sphero Cast Iron	Sphero-Araldite Composite
Density	7300 kg/m^3	2400 kg/m^3
Young Modulus	169 GPa	2,2 GPa
Compressive Strength	250 MPa	48 MPa

In another study, samples obtained by pressing processes carried out in cold and relatively hot conditions were examined. Of these samples, the spheroidal cast iron and pig cast iron samples that were cold pressed and pressed with 100 tonnes were fragmented at the beginning of the compression test due to the low pressing force and inability to provide bind, and a graphic distribution could not be obtained. An image of this can be seen in Figure 23.



Figure 22 : 100 tons pressed with sphero and pig cast iron samples.

All remaining samples were cubic in structure and compression test was applied to these samples at a speed of 1 mm/min and stress-strain graphs were obtained to determine critical mechanical properties. First, hot-pressed pig cast iron chips under a force of 300 tonnes were put to the test and the resulting graph is shown in Figure 23.

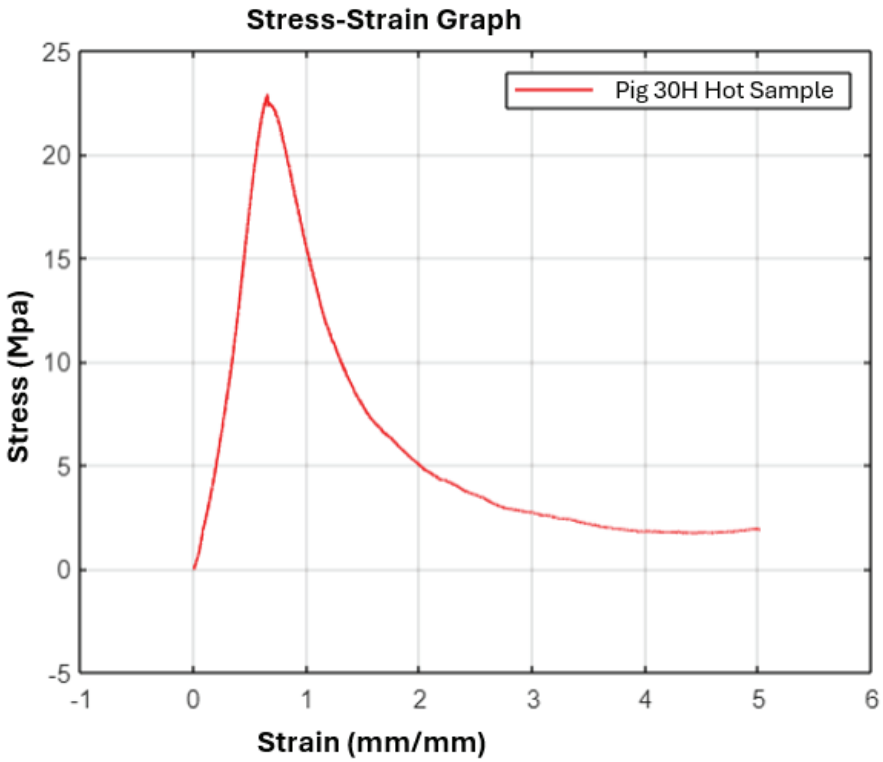


Figure 23 : Pig cast iron 300 tons hot compression sample graph.

Afterwards, pig cast iron samples, again under the same conditions, but this time cold pressed, were examined and the resulting graph is shown in Figure 24.

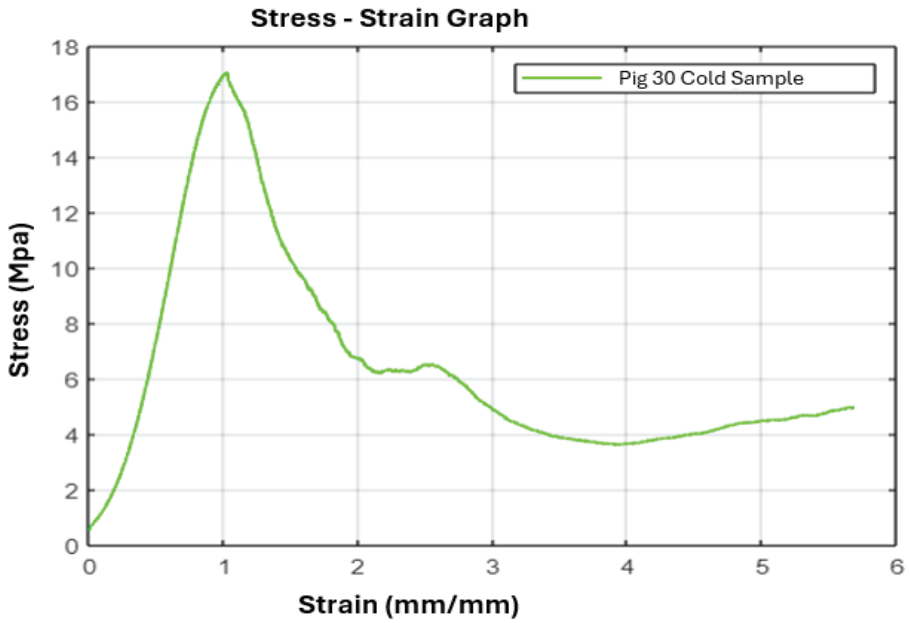


Figure 24 : Pig cast iron 300 tons cold compression sample graph.

Here, due to the inhomogeneous structure of the materials, force drop and irregularities can be seen at some points during the test, although the point where the compressive strength is maximum can be determined.

In the pig cast iron samples, the samples that were finally cold printed with 500 tonnes were put to the test and the resulting compression graph is shown in Figure 25.

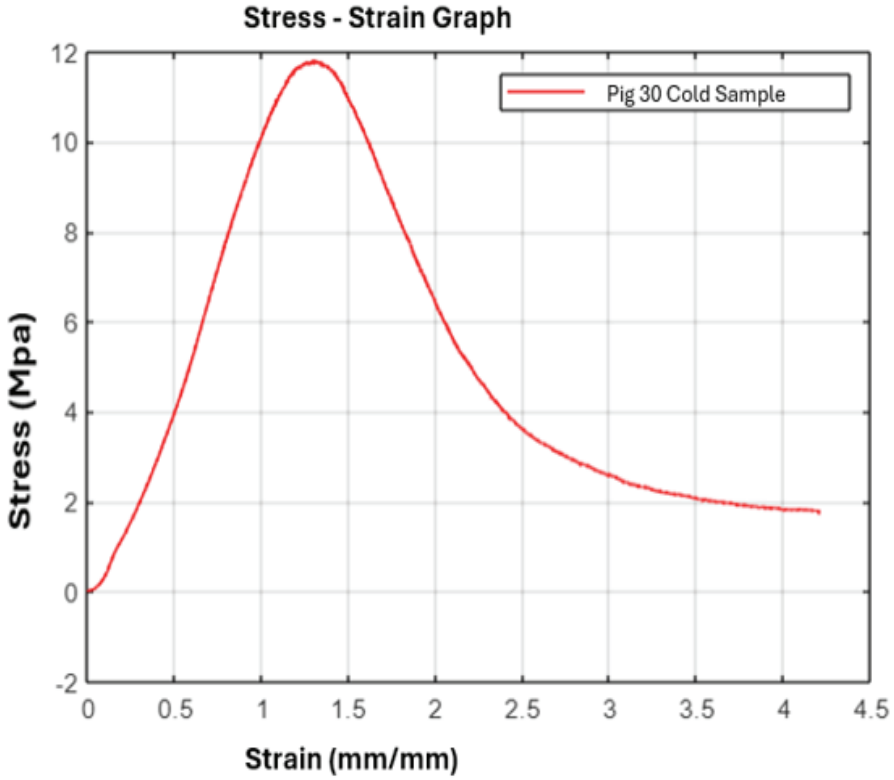


Figure 25 : Pig cast iron 500 tons cold compression sample graph.

After the experiments with the pig cast iron samples were completed, the samples containing spheroidal cast iron chips were tested at the same discharge rates and conditions.

Here, too, the process was first started with a sample compressed at 260°C under 300 tonnes of force. The resulting graph is shown in Figure 26.

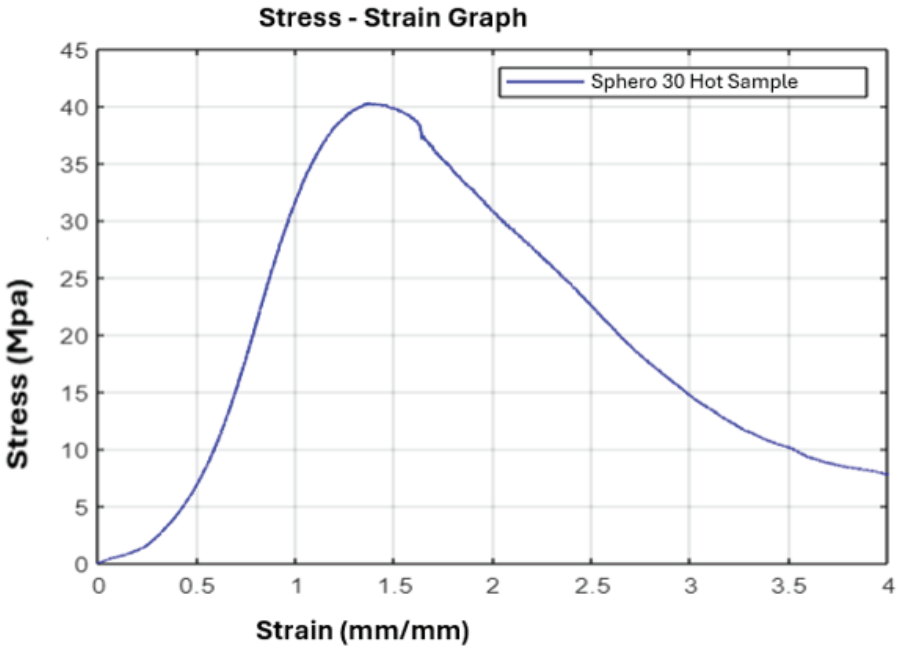


Figure 26 : Sphero cast iron 300 tons hot compression sample graph.

Subsequently, after testing 300 tonnes of nodular cast iron samples pressed under cold conditions, the resulting compression graph is shown in Figure 27.

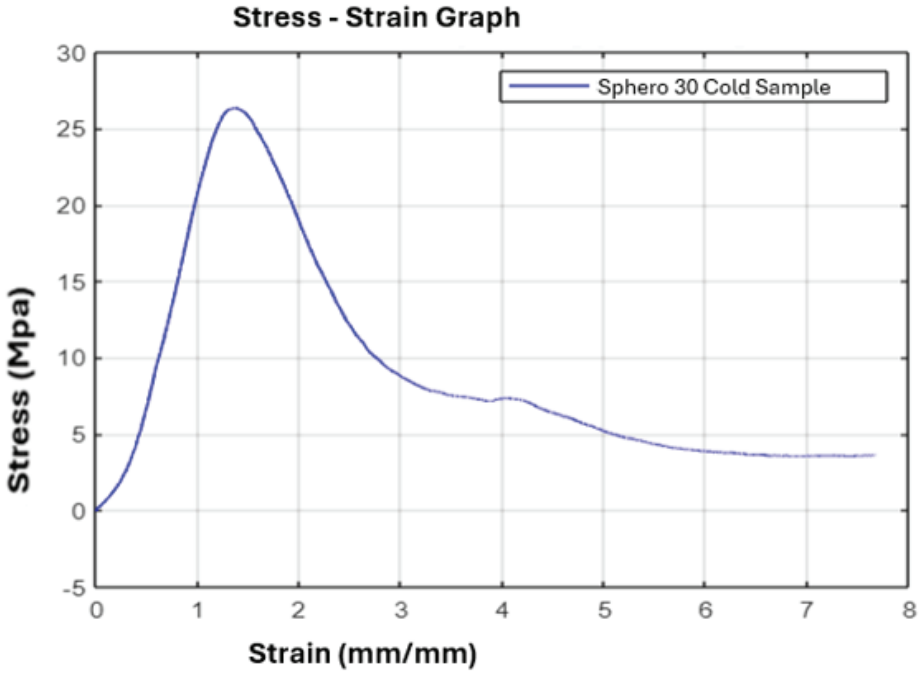


Figure 27 : Sphero cast iron 300 tons cold compression sample graph.

As can be seen in Figure 27, due to irregularities in the produced samples and the inability of the chips to fully adhere to each other under cold pressing conditions, part crack is observed at some points during the test and this situation is seen as sudden force drops in the graph. Finally, spheroidal cast iron chips pressed under 500 tonnes under cold conditions were examined and the results obtained are shown in Figure 28.

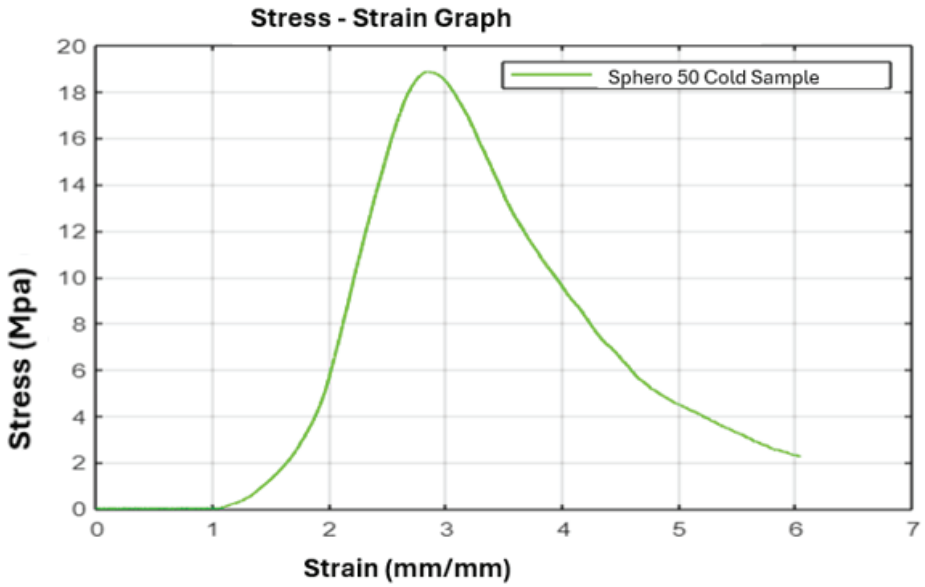


Figure 28 : Sphero cast iron 500 tons cold compression sample graph.

A total of 6 pressed samples were compression tested, and the approximate values of the mechanical properties that occur when the behavior of the samples due to the inhomogeneous structure of the samples are eliminated are shown in Table 6. The failure to the samples was not usually caused by barreling, but rather by fragment separation as a result of stress accumulation in porosite-containing areas.

Table 6 : Mechanical properties of pressed samples.

Samples	Compressive Strength[Mpa]	% Strain[mm/mm]
Pig Cast Iron 30H Hot	22	5
Pig Cast Iron 30H Cold	17	4,5

Pig Cast Iron 50H Cold	12	4
Sphero Cast Iron 30H Hot	40	4
Sphero Cast Iron 30H Cold	26	4
Sphero Cast Iron 50H Cold	19	5,5

In addition, the force-strain obtained from pig and nodular cast iron samples are shown in Figure 28 and Figure 29, respectively.

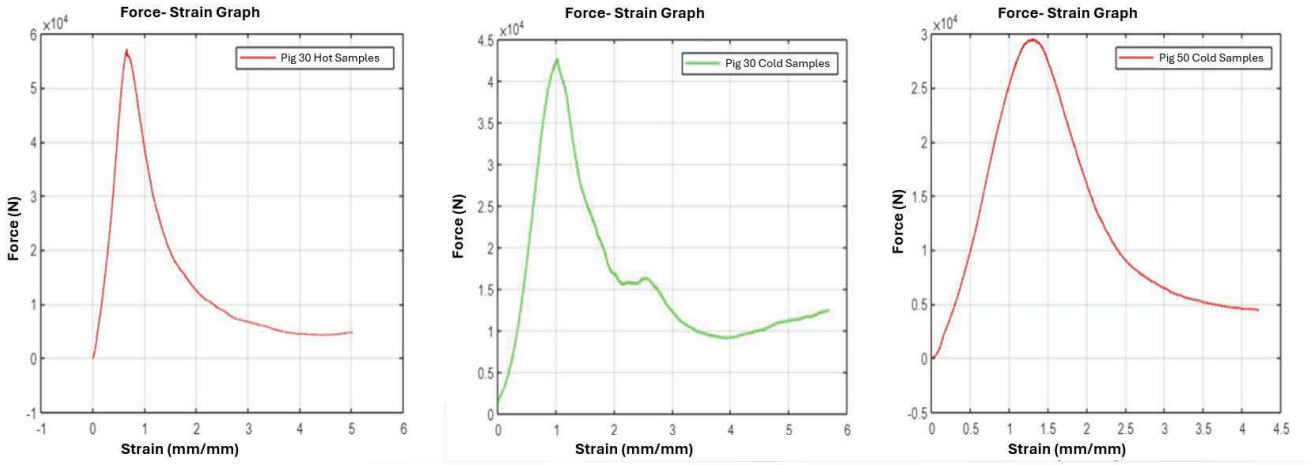


Figure 28 : a) Pig 300 tonne hot b) Pig 300 tonne cold c) Pig 500 tonne cold force graphs

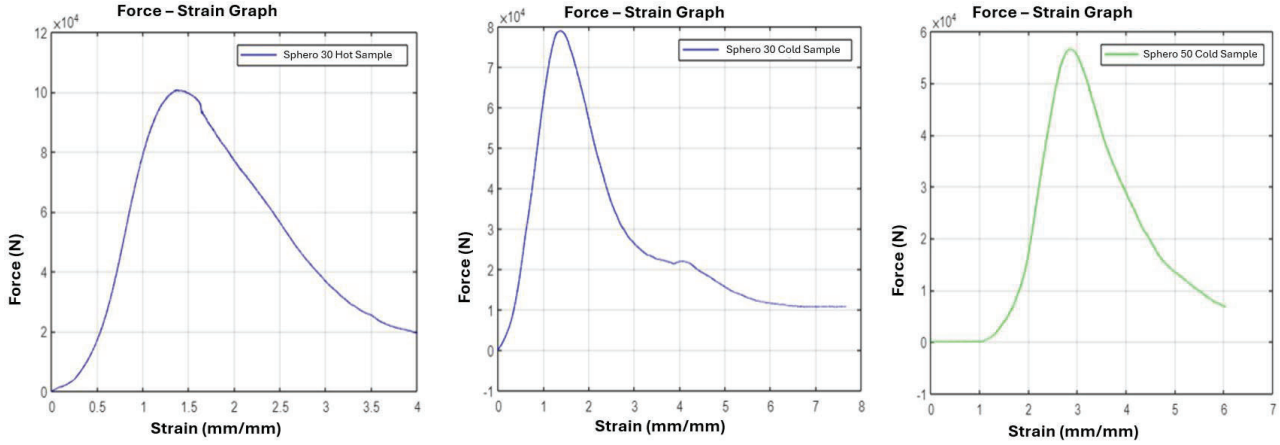


Figure 29 : a) Sphero 300 tonne hot b) Sphero 300 tonne cold c) Sphero 500 tonne cold force graphs

An image of the resulting sample failure is given in Figure 30, and this is how it has always occurred in all of the samples.

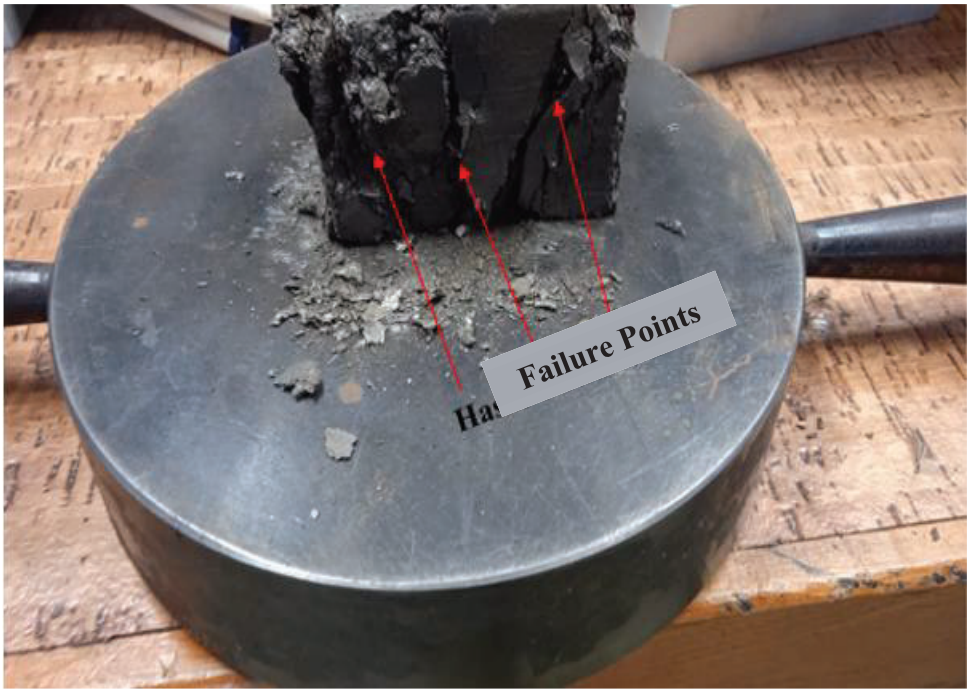


Figure 30 : Sample failures after notch effect.

When all the studies carried out in this section are examined, the samples that have been cast and pressed cannot reach the strength values of the spheroidal cast iron cast iron valve body currently in use, so it does not seem possible to use them as body materials.

When casting and pressed samples are compared, it is seen that casting materials provide higher strength. In pressed samples, when the operating temperature is increased, the strength values increase correspondingly as the chips are better bonded to each other.

The aggregate representation of the stress-strain and force-strain graphs of the samples is shown in Figure 31 and Figure 32, respectively.

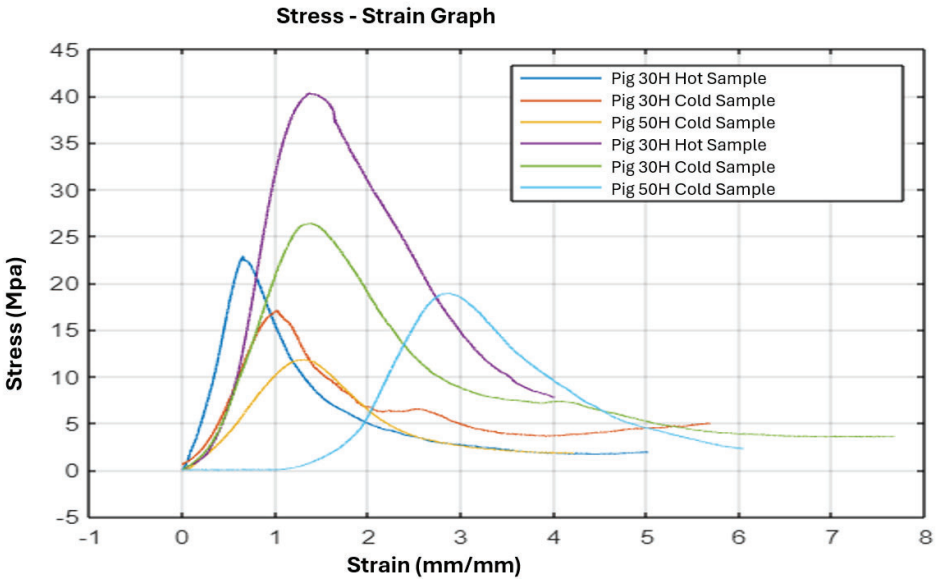


Figure 31 : Stress-strain graph of press samples.

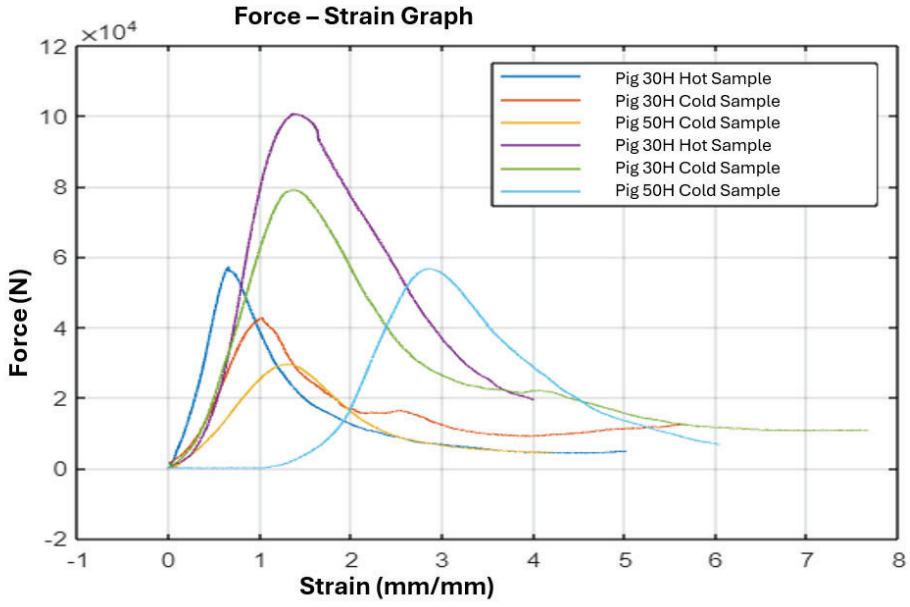


Figure 32 : Force-strain graph of press samples.

5. DISCUSSION

In this study, it is discussed to evaluate the manufacturability of alternative materials with the usage of the materials that come during and after the manufacturing process of a butterfly valve. In this manner, it is given priority to do the spheroidal cast iron scrap that comes after machining operations, the araldite used during valve body casting, and filler sand material. First, the

araldite material used in casting the valve body was produced with a mixture of filler sand and spheroidal cast iron chips. Afterward, spheroidal cast iron chips were compressed with 250 tonnes of pressing force at room temperature without using any binding material, and briquette samples were obtained. Finally, spheroidal cast iron and pig iron chips were pressed by cold and warm pressing methods, without any binder, under forces of 100, 300 and 500 tonnes, at room temperature and 260°C, and cubic samples were obtained. The samples obtained from these samples, obtained by briquetting methods, could not be turned into compression samples and their mechanical properties could not be obtained due to their discontinuous structure and poor machinability. In the first review, it has been observed that especially cold/warm pressing samples can have high strength in certain regions. In future studies, it is foreseen that more uniform and high-strength samples can be obtained by using this method. Although briquetting samples are not suitable to be used as valve material due to their dispersible and discontinuous structure, they can be used at certain points due to the ease of transportation and the convenience it provides in throwing the chips back into the casting pot.

6. RESULTS

In this study, it is desired to produce alternative materials with high strength value by using scrap materials resulting from butterfly valve production processes. For this reason, samples were obtained by using the casting method, briquetting and cold/warm pressing methods. From these samples, it was seen that araldite matrix spheroidal cast iron composite material showed more strength than other samples. It is seen that the sample with the spheroidal-araldite mixture, which can be made suitable for compression test and obtained by casting method, shows higher compressive strength and toughness than the others. It is observed that the sample with spheroidal-araldite mixture, which can be made suitable for compression test and obtained by casting method, shows higher compressive strength and toughness than the others. However, when the properties of this sample are compared with the spheroidal cast iron used in the valve body, its strength is about 1/5. In the cold/warm pressed samples tested, it has been observed that the hot-pressed spheroidal cast iron sample, especially under 300 tonnes, has the highest strength. In this type of sample, as the temperature increases, the bonding of the chips becomes easier, and the strengths also increase. However, the strength of the samples obtained by casting seems to be higher.

ISBN: 978-625-378-045-6 https://doi.org/10.5281/zenodo.14537144

Combining the resulting chips with process materials, which may vary in every plant, is likely to result in new materials with greater or equal strength. Experiments at higher temperatures and chip amounts related to samples obtained by warm and cold pressing may allow obtaining materials with higher strength for the future, but energy consumption and carbon footprint will increase accordingly.

By combining the resulting chips with process materials, which may vary according to each plant, new materials of higher or equal strength are likely to emerge. Experiments on samples obtained by warm and cold pressing, at higher temperatures and chip quantities, may allow higher strength materials to be obtained for the future, but will increase energy consumption and carbon footprint accordingly.

REFERENCES

[1] **Karadağ, H., Bahtlı, T. ve Kara, M. (**2016). The recycling of steel and brass chips to produce composite materials via cold pressing and sintering. *The International Journal of Engineering and Science (IJES),5*(5), 2319-1805.

[2] **Tuck, C.** (2020). Iron and steel scrap (Rapor No. 978-1-4113-4362-7). Amerika Birleşik Devletleri : Mineral commodity summaries.

[3] **Morris, K. J.** (1991). Cold isostatic pressing. R. J. Brook (Ed.), *Concise Encyclopedia of Advanced Ceramic Materials.* 02.03.2023 tarihinde, https://www.sciencedirect.com/ sitesinden edinilmiştir.

[4] **Torkar, M., Lamut, M. ve Millaku, A. (**2016). The recycling of steel chips. 1580-2949 *MTAEC9, 44(5), 289(2010)*

[5] **Abdelhaleem, M. (**2016). Mechanical Properties, Microstructure and Wear Resistance of Recycled Polypropylene Filled with Iron Powder. *The Egyptian International Journal of Engineering Sciences and Technology.* ISSN : 1687-1006.

[6] **Brožek, M.** (2010). Briquetting of chips from nonferrous metal..*9th International Scientific Conference Engineering for Rural Development, 9,* 236-241.

[7] **Pugaa, H., Barbosaa, J., Soares, D., Silva, F. ve Riberio, S.** (2009). Recycling of aluminium swarf by direct incorporation in aluminium melts, *Journal of Materials Processing Technology, 209*, 5195-5203.

[8] **Aslan, A., Güneş, A., Salur, E., Şahin, M. S., Karadağ, H. B., & Akdemir, A. (2018).** Mechanical properties and microstructure of composites produced by recycling metal chips. *International Journal of Minerals, Metallurgy, and Materials*, *25* (9), 1070–1079. doi:10.1007/s12613-018-1658-8

[9] **Fullenwider, B., Kiani, P., Schoenung, J.M. ve Ma, K.** (2019) From recycled machining waste to useful powders for metal additive manufacturing. G. Gaustad vd. (Editors), *The*

Minerals, Metals & Materials Series, *101,* 1-5. Rewas, Cham.: Springer. doi:/10.1007/978-3-030-10386-6_1

[10] **Zhu, J., Lu, Y., Song, Z., Shao, X. ve Xiao-Guang, Y.** (2023). The choice of green manufacturing modes under carbon tax and carbon quota*, Journal of Cleaner Production, 384,* 135336

[11] **Shin, J. S.** (2018). Laser cutting of steel plates up to 100 mm in thickness with a 6-kW fiber laser for application to dismantling of nuclear facilities. *Optics and Lasers in Engineering*, *100*, 98-104. doi:10.1016/j.optlaseng.2017.08.001

[12] **Çapanoğlu, C.** (2021). *Duyar vana DN65 vulkanize kelebek vana* [PowerPoint presentation].

SERAMİK ÜRETİMİNDE İLKEL PİŞİRİM

PRIMITIVE FIRING IN CERAMIC PRODUCTION

Doç. Dr. Serap Ünal

Süleyman Demirel Üniversitesi, Güzel Sanatlar Fakültesi, Seramik ve Cam Bölümü, Isparta, Türkiye.
ORCID ID: 0000-0003-2407-1789

Arş. Gör. Ayşe Melike Bircan

Süleyman Demirel Üniversitesi, Güzel Sanatlar Fakültesi, Seramik ve Cam Bölümü, Isparta, Türkiye.
ORCID ID: 0009-0008-2261-9222

ÖZET

Neolitik Çağ'da M.Ö. 9600-6000 yılları arasında başlayan bitkilerin kültüre alınmasına koşut olarak yerleşik düzen ile beraber insanların üretimden elde ettikleri besinlerin ergonomik bir biçimde yenilebilmesi, depolanıp saklanması gereksinimi ve amacı, dönemin ikinci yarısından itibaren de piroteknoloji ile seramik üretimini başlatmıştır. Tarihsel süreçte insanlığın gelişiminde seramik üretimi önemli bir dönüm noktası olmuştur. İnsanlığın bu gereksinimi önce taş kaplarla başlamış, ancak kilin kolayca şekillenebilir bir malzeme olduğu fark edilerek, çeşitli yöntemlerle şekillendirilen kil kaplar ilk aşamada gün ısısı ile kurutularak sertleştirilmiştir. Yaklaşık M.Ö. 7000'lerden itibaren ateşle kilin buluşmasıyla kalıcı sertlikte, değişik formlarda kaplar elde edilmiştir. Dolayısıyla bu buluş aynı zamanda seramiğin başlangıcı olarak kabul edilmektedir.

Fırın ya da benzeri yapılarla kapalı ortamlarda pişirim öncesi ilk tür seramik pişirim yöntemi açık pişirimdir. İlk tür çanak çömlek formlarının oluşturulması ve açık pişirimle sertleştirilmesi, günümüzde birçok Anadolu çömlekçilik merkezinde hala devam eden kültürel bir üretim tarzıdır. Somut Olmayan Kültürel Miras (SOKÜM) kapsamında değer ifade eden ilk üretim biçeminin Neolitik çömlekçilikle benzerlik ve örtüşümü, aynı zamanda Antropoloji, Süreçsel ve Postsüreçsel Arkeoloji gibi kültür disiplinlerine de önemli veriler sağlamaktadır.

Yapılan bu çalışmada Anadolu'da direnerek de olsa sürdürülen geleneksel çömlekçiliğin pişirim teknikleri ve evreleri, akademik ve kültürel önemi anlatılmak istenmiştir.

Anahtar Kelimeler: Çömlekçilik, Açık Pişirim, SOKÜM, Seramik

ABSTRACT

In the Neolithic Age, with the advent of plant domestication between 9600-6000 BC, the need and purpose for ergonomically consuming, storing, and preserving food obtained from production accompanied by a sedentary lifestyle initiated ceramic production with pyrotechnology from the second half of the period onwards. In the historical process, ceramic production has been a significant turning point in the development of humanity. This need of humanity initially began with stone containers, but upon realizing that clay was an easily

shapeable material, clay vessels molded by various methods were first hardened by sun heat. From around 7000 BC, the interaction of clay with fire resulted in permanently hardened vessels in various forms. Therefore, this discovery is also accepted as the beginning of ceramics.

The first type of ceramic firing method before the advent of kilns or similar structures in closed environments is open firing. The formation of the first types of pottery forms and their hardening through open firing remains a cultural production style still practiced in many pottery centers in Anatolia today. The similarity and overlap of the first production style, which is significant within the scope of Intangible Cultural Heritage (ICH), with Neolithic pottery also provides important data for cultural disciplines such as Anthropology, Processual, and Post-processual Archaeology.

This study aims to explain the academic and cultural significance of the firing techniques and phases of traditional pottery, which, though resisted, continues in Anatolia.

Keywords: Pottery, Open Firing, ICH, Ceramic.

GİRİŞ

Tarihsel süreçte insanlığın gelişiminde seramik önemli bir dönüm noktası olmuştur. M.Ö. 9600-6000 yılları arasında Neolitik Çağ'da başlayan çiftçiliğe dayalı yerleşik düzen ile beraber insanların üretimden elde ettikleri besinleri depolama ihtiyacı duymaları seramik kullanım kaplarının ortaya çıkmasında başlıca etken olarak görülmektedir. İnsanlığın toplumsal ve kültürel gelişiminde köklü değişimlerin gerçekleştiği Neolitik Dönemi Çanak-Çömleksiz (M.Ö. 9600-7000) ve Çanak Çömlekli Neolitik (M.Ö. yaklaşık 7000-6000) olarak ikiye ayıran en önemli bulgu da seramiğin bilinçli bir şekilde üretilmesidir (Ünal, 2020:930). Çanak Çömleksiz (Akeramik) Dönemde pişmiş toprak kapların altyapısını oluşturan gelişmeler yaşanmıştır. Kilin doğal ve el ile kolayca şekillendirilebilir bir hammadde olduğu keşfedilmiş ve günlük yaşamda sıklıkla kullanılan bir malzeme haline gelmiştir. İlk çanak-çömlek üretiminin kamış ve ağaçtan örülen sepetlere kil sıvanarak oluşturulduğu seramiksiz Neolitik Dönem yerleşim yerlerinde bulunan üzerinde sepet izleri olan küçük kil parçalarından anlaşılmaktadır. Güneşte kurutulan ve sertleştirilen kullanım kapları seramiğin bilinçli olarak üretilemeye başlandığı ve yaygınlaştığı Çanak-Çömlekli Neolitik Döneme bir geçiş evresi olarak görülmektedir. Seramiği daha dayanıklı hale getiren pişirme işleminin tesadüf sonucu gerçekleştiği düşünülmüş ve seramiğin ortaya çıkışı hakkında arkeolojik veriler doğrultusunda farklı görüşler öne sürülmüştür. Bu görüşlerden ilki olan 'ocak teorisi'nde ateşi daha uzun süre kullanmak amacıyla açılan çukurlarda kilin sertleşerek eski plastik halinden uzaklaşması ve seramik haline gelmesi söz konusudur. Bir diğer teori ise sepet teorisidir. Bu teoriye göre ilk kullanım kapları kamış, saz ve ağaçlardan yapılan sepetlerin kil ile sıvanarak üretildiği, böylece ateşe ve suya karşı daha sağlam bir hale geldiği öne sürülmektedir. Çanak-Çömlekli Neolitik Döneme gelindiğinde ise seramiğin hammaddesini oluşturan kilin pişirilerek daha sağlam kullanım kapları üretilebileceği anlaşılmış ve çömlek üretimi ilkel pişirimler yapılarak gerçekleştirilmiştir.

İLKEL PİŞİRİM

Seramik fırınlarının ortaya çıkışından önce yalnızca doğada bulunan malzemelerle açık ve doğal ortamda yapılan pişirimler ilkel pişirimlerdir. Tarihsel süreçte Neolitik Çağ'da yerleşik düzene geçilmesi ile beraber seramik üretimi ilk olarak ilkel pişirimler ile fırın kullanılmadan

yapılmıştır. Günümüz seramik fırınlarının temelini oluşturan ilkel pişirim ülkemizde ve dünyanın birçok yerinde seramik üretiminde kullanılmakta olup açık ateşte pişirim ve çukurda pişirim teknikleri olarak iki şekilde yapılmaktadır. Açık arazi ve çukur pişirim tekniklerine ek olarak ilerleyen dönemlerde ortaya çıkan fırın pişirimi, Anadolu' da kullanılmakta olan ilkel fırınlar ve merkezler ve günümüzde alternatif pişirim teknikleri olarak kullanılan raku, sagar ve obvara ilkel pişirimleri ele alınacaktır.

Açık Ateşte Pişirim Tekniği

Seramik üretiminin yapıldığı en ilkel pişirim tekniği olan açıkta pişirim tekniği kurutulan ürünlerin üst üste yığılıp ürünlerin alt kısmı ve üst kısmının doğal yanıcı maddeler ile (saman,



Görsel 1. Açık ateşte pişirime örnek

tezek, odun, ağaç dalları vb.) sarılarak ateşe verilmesi ile yapılmaktadır. Ateşleme süresince eklenen yanıcı maddeler ile ürünlerin pişirimi sağlanır.

Bu pişirim tekniğinde ürünlerin pişirimi oksijen dolaşımı olan ortamda (yükseltilmiş ortam) gerçekleşir (Özdoğan, 2019:271). Sıcaklık 750-800° derece arasındadır. Açık ateşte pişirimde,



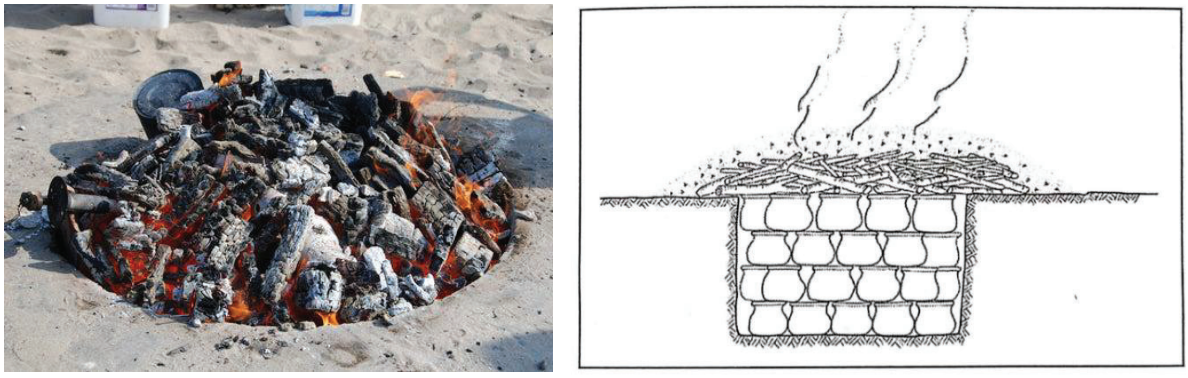
Görsel 2. Sorkun Çömlekçiliği

ateşlemenin kontrol edilememesinden ve kapların yakıtla temas etmesinden dolayı islenmesinden zarar görebilir; ayrıca hava koşullarındaki ani değişikliklere de duyarlıdır. (Nicholson, 2010:2). Kontrolsüz ve harlı ateşte pişirildikleri için seramik kaplarda renk değişimi ve çatlamalar görülebilmektedir.

Açık hava pişirimi Anadolu' da hala devam etmekte olan ilkel çömlekçilikte kullanılan pişirim türlerindendir. Manisa'nın Salihli ilçesine 40 km uzaklıkta olan Gökeyüp Köyü'nde çoğunlukla kadınlar tarafından üretilen çömleklerin pişirimi açık arazide yapılmaktadır. Güneşte iyice kuruyan, onların deyimiyle "tepinen" kaplar, "kap pişireceği yeri" adı verilen evin bahçesinin ya da avlusunun belirli bir yerinde, açıkta çalı çırpı ve odunla, güveçlerin üst üste dizilmesiyle rüzgârlı bir havada yakılan ateşte bir saat süreyle pişirilir (Güner, 1998:35). Anadolu' da açık pişirimin yapılmakta olduğu başka bir merkez Eskişehir Mihalıççık ilçesine bağlı Sorkun Köyüdür. Kadınlar tarafından geleneksel yöntemlerle üretilen çömleklerin pişirimi köyün dışında yer alan rüzgârı kesintisiz ve tek yönden alan "küllük" denilen açık arazilerde ortak bir şekilde yapılmaktadır. Güneşte çok iyi kurutulan güveçler, rüzgârlı bir havada, küllükte içlerine saman konarak, teker teker ters döndürülmüş durumda yere dizilir; aralarına konan çalı çırpı tutuşturularak bir saat süreyle pişirilir (Güner, 1998:38). Sivas-Zara (Demiryurt köyü), Elâzığ-Palu (Burgundere Köyü), Urfa-Merkez (Sırın Köyü) Anadolu' da açık pişirimin uygulandığı diğer yerlere örnektir. Açık pişirim tekniğinde oksijenli ortamda pişirilen ürünleri hava akımından korumak ve ürünlerin pişirimi sırasında meydana gelen sorunları azaltmak amacıyla pişirim tekniklerinde değişiklikler meydana gelmiştir (Sevim, 1991:18). İlerleyen dönemlerde edinilen bilgi birikimi ile çukurda pişirim tekniği geliştirilmiştir.

Çukurda Pişirim Tekniği

Çukurda pişirim yönteminde ürünler açıkta yapılan pişirimin aksine ısı kontrol altında tutulmaktadır. Bu pişirim tekniğinde çukur, ateşleme odası olarak kullanılan, yere kazılmış bir deliktir (Watkins & Wandlesss, 2004:69). Açılan çukurun tabanına ve yerleştirilen ürünlerin etrafına ve odun, talaş gibi yanıcı maddeler eklendikten sonra ateşlenir.



Görsel 3, 4. Çukur Pişirimi

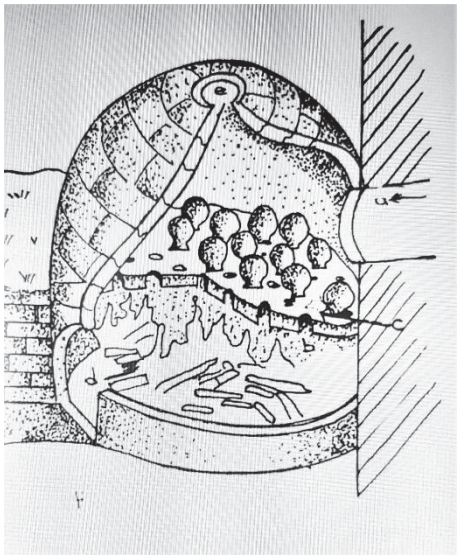
Çukurun üstü ısının korunması amacıyla toprak ile sıvanır ve eklenen yanıcı maddeler tekrar ateşe verilir. Çukur pişirimi açıkta pişirime göre daha verimlidir çünkü çukurun toprak duvarları ısıyı daha etkili bir şekilde iletir ve bunun sonucunda daha yüksek sıcaklıklar elde edilebilir (Chavarria, 1994:57). Açıkta pişirim tekniği ile arasındaki temel fark pişirimin indirgenmiş (redüksyon) ortamda yapılmasıdır. İndirgenmiş oksijensiz bir ortamda pişirim gerçekleşmektedir ve pişirim sonucunda ürünler genellikle isli, koyu renklerde çıkmaktadır. Bu

pişirim yöntemi günümüzde seramik sanatçıları tarafından eserlere isli, geçişli bir görünüm kazandırması gibi dekoratif amaçlarla kullanılmaktadır. Bakır ve metal oksitler, tuz, bitkisel maddeler ve pişirme sırasında yüzeylerde renk gölgeleri, doku ve parlama izlerinin oluşmasına ve artmasına yardımcı olacak renklendirici materyaller eklenebilir (Gregory, 2005:33).

Fırın Pişirimi

Üretilen ilk seramiklerin pişirimi açıkta, doğal ortamda ve doğal malzemelerle, ateşin ve ısının kontrolsüz bir şekilde kullanılması ile gerçekleştirilmiştir. Ateşin açık ortamdan kapalı ortama taşınması ile beraber fırın teknolojisi ortaya çıkmış ve ilkel fırınlar kullanılmaya başlanmıştır. İlkel fırınların ortaya çıkışında ilkel pişirimler sırasında kontrolsüz hava akımı sonucunda meydana gelen hataların azaltılması için ısının kontrol altında tutulması ve kişisel pişirim alanlarına duyulan ihtiyaçlar etkili olmuştur. Açık pişirimde görülen etkilerden dolayı çömleklerin etrafına duvar çevirmekle ve de kanallara ve bacaya ısı vermek yoluyla ilk fırın örnekleri oluşmaya başlamıştır (Sevim, 1991:20). İlkel fırınlar kerpiç, saman ve kum gibi malzemeler kullanılarak üretilmiş, sonraki dönemlerde tuğla gibi özel olarak üretilmiş malzemeler kullanılarak kapalı fırın üretimi yapılmıştır. Ateşleme bölmesi ve çömleklerin yerleştirildiği raflardan oluşan kapalı fırınlarda pişirim sırasında kaplar ateş ile doğrudan temas etmez. Fırınların iç tasarımı hava akışını etkileyerek pişirimin yükseltilmiş ve indirgenmiş ortamlarda yapılmasını sağlamaktadır. Sonuç olarak, açık pişirimde kullanılan ateşin kapalı ortama alınması ile çukurda pişirim tekniği ortaya çıkmış ve günümüz seramik fırınlarının altyapısını oluşturan en ilkel pişirim yöntemi olmuştur.

İlerleyen dönemlerde de farklı türlerde seramik fırınları ortaya çıkmıştır ancak ilerleyen fırın teknolojisine karşın günümüzde ilkel fırınlar hala kullanılmaya devam etmektedir. Anadolu' da kullanılan ilkel fırınlara kubbe tip, silindir tip fırın ve odunlu (kara) fırınlar örneklendirilebilir. Anadolu' da çömlekçilik geleneğinin hala sürdürülmekte olduğu öne çıkan merkezlerden biri olan Aydın'ın Karacasu ilçesinde pişirimler kubbe tip ve silindir tip fırınlarda yapılmakta olup pişirim 8-9 saat arasında gerçekleşmektedir. Bu fırınların duvarları taş örgülü olup içerden ve dışardan sıvanmıştır (Ünal, 2023:85).




Görsel 5, 6. Isparta Kubbe tipi ilkel pişirim fırını

Burdur'un Ağlasun ilçesine 15 km mesafede olan Çanaklı (Mamak) Köyü'nde de çömlek pişiriminde kubbeli yuvarlak fırınlar kullanılmaktadır. Kubbe tip de denilen bu tür fırınlar, kemerlerin üzerine oturtulmuş, üstü açık, alttan ateşlenen tipte olup, toprak kaplar üst üste yığılarak fırınlanır (Ceylan, 2014:238). Silindir tip fırınlarda ürünler fırının baca kısmından yerleştirilirken kubbe tip fırınlarda ürünler fırının pişirilmek üzere yerleştirildiği bölüme açılan boşluktan yerleştirilir. Fırın yapı malzemesi, toprak ve samandan yapılmış blokların koni şeklinde istiflenmesi ve yapının üzerine yine toprak-saman karışımından kerpiç sıva yapılması ile oluşturulmuştur (Ünal, 2022:111). Anadolu' da çömlek pişiriminin gerçekleştirildiği ilkel fırınlara başka bir örnek de odunlu (kara) fırınlardır. İç Anadolu Bölgesin'de yer alan Nevşehir' in Avanos ilçesi Anadolu' nun öne çıkan çömlekçilik merkezlerinden olup geleneksel kara fırınların kullanımının yaygın olduğu bir merkezdir. Tüm duvarları biriketlerle örülen geleneksel Avanos Kara Fırınları silindirik bir gövde yapısına sahiptir. Gövde kubbemsi bir üst yapıyla tamamlanır (Aslan, 2012:6). Kara fırınlar ateşleme (cehennemlik) bölmesi ve ürünlerin istiflendiği iki bölmeden oluşmaktadır. Bu iki bölme deliklerin açıldığı bir taban ile birbirinden ayrılır, fırının yakıtların yerleştirilip ateşe verildiği cehennemlik kapısı ve ürünlerin istiflendiği doldurma kapısı mevcuttur. Pişirimler 800-900° sıcaklığa erişir, 4-8 saat arasında gerçekleştirilir. Kara fırınlarda ürünler istiflenerek yerleştirilebildiği için çok sayıda çömlek pişirimi gerçekleştirilebilmektedir.

İLKEL PİŞİRİM TEKNİKLERİ

Raku Pişirimi

Günümüzden yaklaşık 400 yıl kadar öncesinde Japonya' da ortaya çıkan ve oldukça popüler olan Raku tekniği düşük ısıda ve hızlı pişirim sonucunda kaplarda farklı ve etkileyici yüzeysel etkiler bırakan pişirim tekniğidir. Japonya' da Momoyama Dönemin'de (1573-1615) çay ustalarının geliştirdiği bu teknik ile pişirimi yapılan Raku kapları zamanla çay törenlerinin bir parçası haline gelmiştir. Anlatılanlara göre çay ustası Rikyu, Wabi No Chado olarak bilinen Zen temelli estetik felsefeyi geliştirmiş ve değiştirmiştir (Branfman, 2012:12). Zen felsefesinin temel özellikleri doğallık, sadelik ve yalınlıktır. Çay törenlerinde kullanılan kaplar da bu felsefenin sanatsal temsilleridir. Ancak Rikyu tarafından geliştirilen Zen temelli felsefe çayın resmi bir şekilde servis edilmesine ve içilmesine karşılık estetik tepki uyandırmak için tasarlanmıştır. Raku tekniği seramik kapların yalnızca soyut güzelliği değil aynı zamanda somut estetik güzelliği yansıtması için tasarlanmış ve uygulanmıştır.

Raku pişirim tekniğinde kullanılan çamur ve sırlar farklılıklar göstermektedir. Raku kilinin temel gereksinimi, raku sürecindeki termal şoka dayanabilmesidir (Mathieson, 2005:10). Hızlı



Görsel 7, 8. Raku pişirimi

pişirim ve atmosfer değişimini kaldırabilmesi için kilin fazla miktarda kum veya şamot parçaları içermesi gerekir. Parçalar ne kadar büyük ve kalınsa kilin raku pişirimine uygunluğu ve termal şok dayanıklılığı da o kadar fazla olur (Jones, 2007:36). Şamot ve kum oranı yüksek kilden üretilen kapların bisküvi pişirimi gerçekleştirildikten sonra kaplar kurşun içeren, erime dereceleri düşük olan sırlar ile sırlanır. Raku sırlarında erime dereceleri düşüktür çünkü kullanım kaplarında uygulanan sırların sağlaması gereken yüksek teknik standartlara uyması gerekmez; bileşimleri basittir (Branfman, 2001:53). Sır pişiriminde meydana gelen çatlaklar genellikle sır ve kilin uyumsuzluğundan kaynaklanır ve kullanım kaplarında sağlık açısından sakınca oluşturması sebebiyle istenmemektedir, ancak raku tekniğinde elde edilmek istenen bir görüntüdür. Çatlaklı görünümün elde edilmesine olanak sağlayan sırlar düşük derece sırlardan oluşmaktadır.

750-950° pişirilen sırlı kaplar maşa yardımıyla akkor halde fırından alınıp talaş, kâğıt türü yanıcı malzemelerde doldurulan varillerin içine yerleştirilir ve üstü kapatılarak oksijensiz (redüksiyon) ortamda bırakılır. Böylece karbon monoksit gazına maruz bırakılan seramiklerde, üzerinde kullanılan sırın birleşimine göre farklı etkiler elde edilir (Başkırkan, 2016:16). Varillerden çıkarıldıktan sonra soğumaya bırakılır veya su ile soğutulduktan sonra yüzeyi temizlenerek sergilenmeye hazır hale getirilir.

Geleneksel raku pişirimi tuğladan inşa edilen odun yakıtlı fırınlarda yapılmaktadır. Günümüzde ise alternatif bir pişirim tekniği olarak kullanılan raku tekniğinde pişirim gazlı ve elektrikli fırınlarda yapılmaktadır ancak genellikle elektrikli fırınlar tercih edilmemektedir. Elektrikli fırınlarda yüksek ısıda 750-950° fırın kapağının açılması rezistans tellerine zarar vererek fırının ömrünü azaltır, kullanımı zordur. Elektrikli fırınlara göre daha dayanıklı olan ve daha kısa sürede yüksek derecelere ulaşan gazlı raku fırınları daha yaygın bir şekilde kullanılmaktadır.

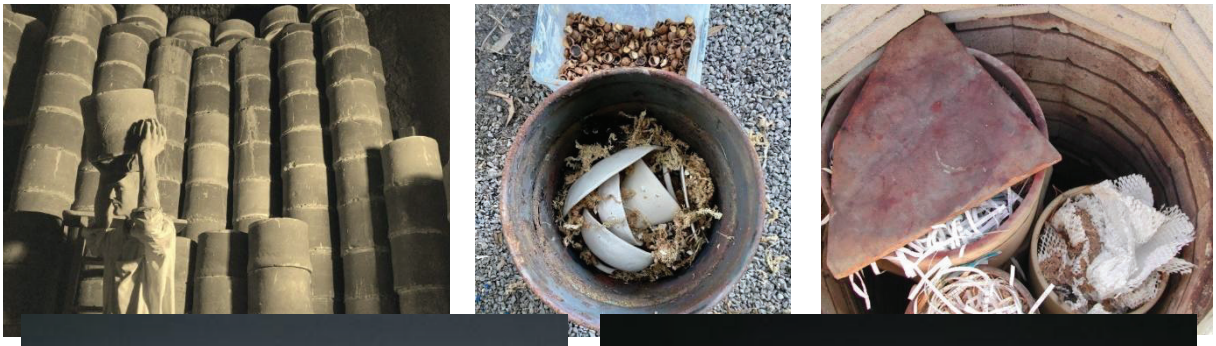


Görsel 9, 10. Raku Pişirimi Uygulanmış Örnekler

Bugün seramik sanatçılarının sıklıkla kullandığı, oldukça popüler bir pişirim tekniği olan raku kendi içinde türlere ayrılmaktadır. Raku pişiriminde redüksyon fırın dışında gerçekleşmektedir, farklı yüzeysel etkiler, renk geçişleri de bu redüksyonlar sonucunda meydana gelmektedir. Demir klorid, at kılı, balçık raku (naked raku), pas kırmızısı, terra sigillata, bakır mat-alkol redüksiyon teknikleri ile çok çeşitli sonuçlar elde edilebilmektedir.

Sagar Pişirimi

İlk olarak Çin' de Sung Hanedanı Dönemi'nde (M.S. 960-1276) geliştirilen sagar pişirim tekniği günümüzde de hala kullanılmakta olan bir tekniktir. Sagar, yüksek dayanıklılığa sahip seramik hammaddelerinden üretilmiş (refrakter) seramik veya porselen ürünlerin alevden, isten ve küllerden zarar görmeden pişirilmesini sağlayan kapaklı kutular, haznelerdir. Kömür ve odun gibi malzemeler ile ateşlenen fırınlarda pişirimi yapılan seladon sırlı porselen bünye kapların yüzeyinde oluşan hataları azaltmak için ortaya çıkmıştır. "Geleneksel anlamda sagarlar, ürünleri, odun ve kömür ile pişirim yapılırken, oluşan kül ve kalıntılardan, alevlerin direkt etkilerinden korumak amacıyla kullanılmaktadır (Dassow, 2001:46)."



Görsel 11, 12, 13. Sagar Pişiriminde Uygulama Aşamaları



Görsel 14, 15. Sagar Pişirimi Uygulanmış Örnekler

Sagar kutuları ilk olarak kilden üretilmiştir, yapımında kullanılan killer, raku pişiriminde kullanılan killer gibi şamot içeren ve yüksek sıcaklığa karşı dayanıklı olan killerdir. "Kutular iyi pekiştirilmiş %50 şamot içeren refrakter özellikli kilden yapılabilir. Fitil yöntemiyle, alçı kalıp içine sıvama yoluyla, plaka tekniğiyle ya da torna yöntemleriyle şekillendirilebilirler (Fournier, 1992:241)." Seramik üretiminde kullanılan malzeme ve şekillendirme yöntemleri ile üretilen kutular, kurutma ve pişirim işlemlerinin ardından kullanıma hale hazır hale gelir. Pişirim sırasında ürünlerin korunmasında yardımcı görev gören sagar kutuları kendi içinde ayrı ve korunaklı bir ortam yaratarak ürünlerin olası hava akımlarına veya ısı değişimlerine karşı direnç göstermesine de yardımcı olmaktadır. Kutular seramik malzemeye ek olarak yüksek sıcaklığa dayanıklı demir, çelik gibi metal malzemelerden üretilebilmekte veya ateş tuğlaları ile fırının içeresine de inşa edilebilmektedir.

Günümüz seramik sanatında sagarın kullanımının ortaya çıkışındaki temel hedeften oldukça farklı, hatta tam tersi yönde olduğu söylenebilir. "Bugün seramik sanatçıları bu terimi pişirim sırasında çömlekçinin işlerini muhafaza edecek tuğlamsı ya da ısıya dayanıklı bir malzemeden

yapılmış, herhangi bir hazne için daha geniş anlamda kullanırlar (Watkins & Wandlesss, 2004:55).” Sagar kutularının başlıca kullanımı ürünleri pişirim sırasında açığa çıkan duman, is gibi unsurlardan korumak ve olabildiğince temiz bir pişirim sonucu elde etmek iken bugünkü kullanım amacı seramik ürünleri yanıcı malzemelerle bir araya getirerek farklı yüzeysel etkiler elde etmektir. Tekniğin günümüzdeki kullanımında amaç kutu içeresine bisküvi pişirimi yapılmış seramik ürünler ile beraber yerleştirilen organik veya inorganik malzemelerin yanmasını sağlayan sınırlı bir oksijen girişinin olduğu indirgen ortam atmosferi oluşturmaktır (Bozkurt 2012: 46). Seramik ürün ile birlikte talaş, odun, gazete, saman, kuru yaprak, tuz, sülfat ve oksit gibi çeşitli yanıcı malzemeler ile doldurulan sagar kutuları fırına yerleştirilerek 750-950° arasında değişen indirgen bir kutu atmosferinde pişirim gerçekleşir. Bu atmosfer, pişirme işlemi sırasında seramik ürünün yüzeyini isleyen maddelerin yanmasıyla oluşur (Wandless, 2007:15). İsli indirgen atmosfer sagar kutusunun içinde kalarak seramik parçanın yüzeyini karbonize eder ve beraberinde çeşitli renk geçişleri ortaya çıkar. Soğumaya bırakılan ve fırından alınan sagar kutularının iç sıcaklık dereceleri düştüğünde seramik ürünler kutulardan çıkarılıp oksijensiz ortamda gerçekleşen yanma sonucunda ortaya çıkan küllerden yüzeysel kalıntılardan temizlenir, cilalanır ve sunuma hazır hale getirilir.

Gazlı, elektrikli ve raku fırınlarında genellikle sırsız seramik bünyeler ile yapılan sagar pişirim tekniği birbirinden farklı görsel etkiler ortaya çıkaran alternatif bir pişirim tekniğidir. Pişirim sonucunda seramik ürünlerde elde edilen renk geçişleri birlikte pişirim yapıldıkları malzemelerin türüne; kimyasal ve fiziksel özelliklerine ve kutu içindeki yerleşimlerine göre farklılık göstermektedir. Sagar pişirimleri; klasik toprak sagar pişirimine ek olarak alüminyum folyo sagarı, maskeleme yöntemi olmak üzere çeşitli yöntemler ile de uygulanmaktadır.

Aliminyum Folyo Sagarı

Alüminyum folyo sagarında ürünlerin yüzeyine demir klorid çözeltisi uygulanır, ardından oksit, sülfat tuz gibi organik yanıcı maddeler konulan alüminyum folyolara sarılarak pişirim yapılır. Alüminyum folyo sagarının pişirimi folyo içine eklenen sülfat ve tuzların fırın ekipmanlarını aşındırması, zarar vermesi sebebiyle elektrikli fırınlarda yapılmamaktadır. Kısa sürede yüksek sıcaklığa ulaşan ve çabuk soğuyan raku fırınlarında 650-800° düşük sıcaklıklarda yapılan pişirimler kısa bir zaman zarfında gerçekleşir.

Maskeleme Tekniği

İndirgen atmosfer pişiriminde farklı etkiler elde etmek için kullanılan başka bir sagar pişirim yöntemi de maskeleme yöntemidir. Seramik yüzeyde isli görünüm elde etmek için uygulanan bu yöntemde terra sigillata astarları kullanılarak yüzeye parlak ve kaliteli bir görünüm kazandırılması hedeflenir. Alternatif pişirim tekniklerinde sıklıkla kullanılan terra sigillata astarları Yunan ve Roma dönemi seramiklerinde ince taneli killerden üretilen ve fırınlandıklarında uygulandıkları yüzeye parlak bir görünüm kazandıran astarlardır. İndirgen ortamda yapılan isli pişirimlerde estetik açıdan olumlu sonuçlar vermektedir. Maskeleme tekniğinde bisküvi pişirimi yapılmış seramik ürünün bant ile kaplanan kısımlarına astar temas etmez ve yanıcı malzemeler ile yapılan 800-900° arasında yapılan pişirim sonucunda mat ve parlak kontrast bir görünüm elde edilir.

Obvara Pişirimi

Günümüzde de kullanılmakta olan alternatif pişirim tekniklerinden obvara 14. yüzyılda Doğu Avrupa'da ortaya çıkan geleneksel bir pişirim tekniğidir. Litvanya, Belarus, Estonya ve Rusya gibi Baltık denizine kıyısı olan ülkeler tarafından yaygın bir şekilde kullanıldığı için aynı zamanda Baltık (Beyaz Rusya) rakusu olarak da bilinmektedir. Birden çok ismi olan obvara tekniği Belarus ve Rusya'da 'haşlanmış seramik', Estonya'da 'poripott', Letonya'da 'raugo keramika (hamur mayası)', Litvanya'da 'ekşi mayalı ya da mayalı çömlek', ve dünyanın geri kalanında 'obvara' olarak bilinmektedir (Chassier, 2019).

Geçmişte evlerde tesisat sistemi kurulmadan önce, süt, haşlanmış patates suyu, elma kabukları gibi mutfak atıklarının ve atık suların lavabo kenarlarında kovalarda tutulmasıyla doğal, fermente karışımlar açığa çıkmaktaydı. Obvara tekniğinin de sıcak bir güvecin kazara bu atıkların fermente olduğu bir kovanın içine düşmesi sonucu seramiğin yüzeyinde oluşan etkinin fark edilmesi ile keşfedildiği söylenmektedir (Chassier, 2015).

Obvara pişirim tekniğinin gelenek haline gelmesinde ve kullanımının yaygınlaşmasında belli başlı unsurlar bulunmaktadır. Organik atık ile dolu kaplara daldırılarak elde edilen obvara seramiklerinde saklanan gıdaların ve içeceklerin uzun süre mevcut sıcaklığını veya



Görsel 16, 17, 18. Obvara Uygulama Aşamaları

soğukluğunu koruduğu gözlemlenmiş, bu özellik neticesinde obvara kapları uzun süre yiyecek ve içecekleri saklamak için kullanılmıştır.

Önceden işlevsel amaçlar doğrultusunda yapılan obvara pişirimi bugün seramik sanatçılarının doğal, deneysel sonuçlar elde edebileceği alternatif bir pişirim tekniği olarak kullanılmaktır. Raku tekniğine benzer bir şekilde, bisküvi pişirimi yapılmış ürünler 899°C' de fırından çıkarılır ancak raku pişiriminden farklı olarak parçayı hızlı bir şekilde soğutmak için suya batırılmadan önce obvara karışımına batırılarak tüm yüzey karışım ile kaplanır (Selsor, 2014:13).

Karışım un, şeker, süt, yulaf, maya, buğday, pirinç ve su gibi tamamen doğal malzemeler ile elde edilmektedir. Daldırma işlemiyle seramik ürünün sıcaklığı organik karışım ile temasa geçer ve yanma ve sıçramalar meydana getirerek seramik yüzeyde gözeneklere işleyen açık sarıdan koyu kahverengi, siyaha kadar doğal renk geçişleri, görsel etkiler ortaya çıkarmaktadır.

Obvara pişiriminde sıcaklık ve karışımın kalitesi yüzeysel etkilerin açığa çıkmasında önemli rol oynar, seramiklerin karışım ile tepkimeye girmesi için mevcut sıcaklık 800-900°C' den düşük olmamalıdır. Fırının 899°C' den daha soğuk olması durumunda seramikler karışımın yüzeyde yanması için yeterli sıcaklıkta olmayacaktır (Selsor, 2014:15). Sıcaklığın yanı sıra karışımın fermente olup olmaması da oldukça önemlidir. Karışım mayalanmadığı takdirde sıcak seramik yüzey ile tepkimeye girmeyecek, dolayısıyla yüzeysel etkiler elde edilemeyecektir. Malzemenin türü, çeşitliliği ve sıcaklığa bağlı olarak ürünün mayalanma süresi değişim gösterebilmektedir, karışımın en az iki gün boyunca mayalanmaya bırakılması gerekmektedir.



Görsel 19, 20. Obvara Pişirimli Seramik Örnekler

Seramik ürünlerin karışıma batırılma işlemi yüzey üzerinde oluşan renklerin tonunu doğrudan etkilemektedir. Uzun tutulduğunda koyu tonlar, kısa tutulduğunda ise açık tonlar edilir. Karşımın yoğunluğu da aynı şekilde renk oluşumunda etkendir, yoğun karışımlar ile koyu renkler, sulu karışımlar açık renkler elde edilmektedir. Diğer redüksyon pişirimlerinde olduğu gibi obvara pişirimi de gazlı fırınlarda gerçekleştirilmektedir.

SONUÇ VE DEĞERLENDİRME

Neolitik çağdan itibaren farklı kültürlerde çeşitli seramikler üretilmiştir. Açık pişirimler hem düşük teknolojili hem de çevre koşullarına uyum açısından ve kültürel açıdan önemli bir geçiş dönemi oluşturur.

Seramik tarihinin en eski pişirim yöntemi olarak, insanlıkla birlikte kültürel anlamda derin izler bırakmış ve maddi kültür değerlerinin korunmasına katkı sağlamıştır. Bu teknik, doğrudan ateşle pişirim gibi basit ve geleneksel bir yöntemle başlamış, ancak zamanla sanatın ve teknolojinin gelişimiyle çeşitlenerek günümüzde modern seramik sanatında özgün bir yere sahip olmuştur.

İlkel pişirim teknikleri sadece seramik sanatının ilk basamağını oluşturmakla kalmayıp, günümüzde de ilham verici bir miras olarak varlığını sürdürmektedir. Bu teknikler sayesinde, seramik sanatı tarih boyunca insanlar arasında kültürel bağlar kurmuş, nesiller boyu aktarılan bir miras haline gelmiştir. Modern seramik sanatında ilkel pişirime dayalı bu alternatif tekniklerin kullanımı, sanatçılara doğadan ve kültürel mirastan beslenme fırsatı sunarken, eserlerine özgün bir karakter kazandırmaktadır. Bu bağlamda ilkel pişirim, sanatsal ve kültürel anlamda sadece bir teknik değil, aynı zamanda geçmişle bugün arasında kurulan güçlü bir köprüdür.

KAYNAKÇA

Aslan, E. (2012). Avanos Çömlekçiliğinde Kaybolan Bir Değer: Kara Fırın. **İdil Dergisi**, Cilt: 1, Sayı: 4/ Volume: 1, 1-13.

Başkırkan, H. (2016). **Seramik Pişirim Teknikleri ve Fırınları: Raku Pişirimi**, Opus Basımevi, Ankara.

Bozkurt, E. (2012). **Alternatif Pişirim Tekniklerinden Sagarın Araştırılması ve Uygulanması,** Yüksek Lisans Tezi, Sakarya, Sakarya Üniversitesi, Sosyal Bilimler Enstitüsü.

Branfman, S. (2001). **Raku A Practical Approach,** Krause Publications, 700. E. State Street, Iola.

Branfman, S. (2012). **Raku Mastering**, Lark Crafts, Park Avenue South, New York.

Ceylan, S. (2015). Mamak (Çanaklı) Beldesinde (Ağlasun-Burdur) Geleneksel Yöntemlerle Sürdürülen Toprak Kap Üretiminin Kırsal Turizm Bağlamında İrdelenmesi. **Doğu Coğrafya Dergisi**, 19(32), 231-242.

Chassier, J. (2015) Obvara. **Seramik Teknik**, Haziran, 52-57.

Chavarria, J. (1994), **The Big Book of Ceramics**, Watson-Guptill Publications, 1515 Broadway, New York.

Dassow, S. V. (2001). **Barrel, Pit and Saggar Firing: A Collection of Articles from Ceramics Monthly,** Haziran.

Fournier, R. (1992). **Illustrated Dictionary of Practical Pottery,** A & C Black Publishers Ltd, 3.baskı.

Güner, G. (1988)**. Anadolu'da Yaşamakta Olan İlkel Çömlekçilik,** Ak Yayınları Kültür Serisi: 16-5, İstanbul.

Gregory, I. (2005). **Alternative Kilns**, A & C Black Publishers Ltd, London, University of Pennsylvania Press, Philadelphia.

Jones, Bill. (2007). What's a Raku Clay? **Pottery Making Illustrated.** Haziran/Ağustos, 36.

Mathieson, J. (2005), **Raku Ceramics Handbook,** A&C Black, London, American Ceramic Society, Ohio.

Nicholson, P. T. (2010). "Kilns and Firing Structures", **UCLA Encyclopedia of Egyptology,** 2**.**

Özdoğan, M. (2019). **Hammaddeden Ustalara Tarihöncesi Arkeolojisinde Malzeme**, Arkeoloji ve Sanat Yayınları, İstanbul.

Selsor, M. (2014). Obvara-Style RAKU. **Pottery Making Illustrated.** Eylül/Ekim, 13-15.

Sevim, C. (1991). **İlkel Fırınlar,** Yüksek Lisans Tezi, Eskişehir, Anadolu Üniversitesi, Sosyal Bilimler Enstitüsü.

Ünal, S. (2020). "Çağların Akışında Anadolu Pişmiş Toprak Kültürü", **USBAD Uluslararası Sosyal Bilimler Akademi Dergisi,** 930.

Ünal, S. (2023). **Anadolu Pişmiş Toprak Kültüründe Göller Bölgesi,** Arkeoloji ve Sanat Yayınları, İstanbul.

Wandless, P. (2007). It's a Wrap Saggar Firing with Aliminum Foil. **Pottery Making Illustrated.** July/August.

Watkins, C. ve Wandless, P.A. (2004). **Alternative Kilns & Firing Techniques.** Lark Crafts, Park Avenue South, New York.

İnternet Kaynakları

Chassier, J. (2019, 03 09). http://www.janicechassier.com.

http://www.janicechassier.com/Janice_Chassier/Blog/Entries/2014/3/15_Page_1_of_Obvara,_An_Eastern_European_Firing_TechniqueThe_History,_Preservation_and_Contemporary_Development.html adresinden alındı

NEOLİTİK ÇÖMLEKÇİLİKTEN GÜNÜMÜZ SERAMİK KOMPOZİTLERİNE: BİNLERCE YILLIK TEKNOLOJİK EVRİM

FROM NEOLITHIC POTTERY TO TODAY'S CERAMIC COMPOSITES: THOUSANDS OF YEARS OF TECHNOLOGICAL EVOLUTION

Doç. Dr. Serap Ünal

Süleyman Demirel Üniversitesi, Güzel Sanatlar Fakültesi, Seramik ve Cam Bölümü, Isparta, Türkiye
ORCID ID: 0000-0003-2407-1789

ÖZET

Neolitik dönemde piroteknoloji ile çömlekçiliğin başlangıcı, insanlık tarihinde önemli bir dönüm noktası oluşturmuştur. Ateşle pişirilmiş kilin sertleştirilmesi sayesinde hem günlük kullanım eşyaları hem de sanatsal objeler üretilebilmiştir. Bu üretim kültürü, çağlar boyu insanlığın gelişim sürecinde sosyal ve ekonomik düzende olduğu gibi tinsel anlayışta, sanatta ve teknolojide de önemli açılımlar ortaya koymuştur. Neolitik dönemde başlayan seramik üretimi, yüzyıllar boyunca evrimleşerek günümüz modern seramik sanatına, yüksek performanslı mühendislik malzemelerine kadar uzanarak sürdürülebilirliğini gerçekleştirmiştir.

Günümüzde seramik kompozitler, yüksek performanslı, dayanıklı ve endüstriyel üretimlerde geniş bir kullanım alanı bulan ileri teknolojilerdir. Bu gelişimin kökeni kuşkusuz yaklaşık 9000 yıl önce başlatılan ilkel çömlekçiliktir. Sanat ve iyileşmenin bu birleşimi ve sürekliliği, ilk döneminden günümüze seramik sanatında ve teknolojisinde süreklilik gösteren bir ilerleme çizgisi oluşturulmuştur. Neolitik çömlekçilik, yalnızca arkeolojik bulgular olarak değil, aynı zamanda seramik teknolojisinin de önemli bir basamağı olarak da değerlendirilmelidir. Seramik üretiminin günümüze katkısı, sadece teknolojik verilerle değil aynı zamanda yok edilemeyen bir malzeme olması nedeniyle, binlerce yıllık verileri kültür bilimcilere aktarabilmesi açısından da önem arz etmektedir. Bugün hem çağdaş seramik sanatında ve kültür bilimlerinde, hem de mühendislik seramiklerinde bu bağlantı rahatlıkla gözlemlenebilecek farklı bir bakış açısı yaratmaktadır.

Anahtar Kelimeler: Neolitik Çömlekçilik, İleri Seramik Kompozitler, Seramik Teknolojisi, Çağdaş Seramik Sanatı

ABSTRACT

The beginning of pottery with pyrotechnology in the Neolithic period constituted an important turning point in human history. Thanks to the hardening of fired clay, both daily use items and artistic objects could be produced. This production culture has revealed important expansions in the social and economic order as well as in spiritual understanding, art and technology in the development process of humanity throughout the ages. Ceramic production, which started in the Neolithic period, has evolved over the centuries and has achieved its sustainability by extending to today's modern ceramic art and high-performance engineering materials.

Today, ceramic composites are advanced technologies that are high-performance, durable and widely used in industrial production. The origin of this development is undoubtedly primitive pottery, which was started approximately 9000 years ago. This combination and continuity of

art and healing has created a continuous development line in ceramic art and technology from its early period to the present. Neolithic pottery is evaluated not only as archaeological findings but also as an important step in ceramic technology. The contribution of ceramic production to the present day is important not only with technological data but also because it is an indestructible material and can transfer thousands of years of data to cultural scientists. Today, this connection can be easily observed in both contemporary ceramic art and cultural sciences, as well as engineering ceramics, creating a different cultural area.

Keywords: Neolithic Pottery, Advanced Ceramic Composites, Ceramic Technology, Contemporary Ceramic Art

GİRİŞ

Seramiğin insanlık tarihindeki yeri, teknolojik ve kültürel anlamda çok değerli bir yere sahiptir. Neolitik dönemde çömlekçilik, yerleşik hayata geçişin simgelerinden biri olmuş, insanlar temel ihtiyaçlarını karşılamak için seramik kaplar üretmeye başlamışlardır. İlk başlarda kilin elle şekillendirilmesi ve açık ateşte pişirilmesiyle ortaya çıkan bu kaplar, zamanla daha sofistike teknikler kullanılarak üretilmiş ve seramik teknolojisi hızla gelişmiştir (Rice, 1987). Bugünkü ileri seramik kompozitleri, Neolitik dönemde başlayan bu gelişimin bir sonucudur.

Çömlekçiliğin tarihsel sürecinde, sadece işlevsel objeler üretmekle sınırlı kalınmamış, pişmiş toprak eserler aynı zamanda toplumların estetik ve sembolik değerlerini de yansıtan bir sanat formuna dönüşmüştür. İlk seramik kaplar, insan topluluklarının sosyo-ekonomik yapılarını ve kültürel pratiklerini anlamamıza olanak tanıyan önemli arkeolojik buluntular arasında yer alır (Arnold, 1985). Neolitik çömlekçilik, hem tarım toplumlarının yerleşik hayata geçişini hem de topluluklar arası ticaretin ve etkileşimin artmasını sağlamıştır (Schiffer, 1996). Bununla birlikte, seramiğin fiziksel dayanıklılığı, tarih öncesi dönemlerden günümüze kadar süregelen kültürel ve teknolojik sürekliliği belgeleyen bir malzeme olarak karşımıza çıkmaktadır.



Görsel 1. Pişmiş Toprak Yazılı Belge

Seramiğin teknolojik evrimi, insanların maddi dünyayla olan ilişkilerini ve üretim süreçlerini derinlemesine etkilemiştir. Neolitik dönemde ilk kez kontrollü ateşle pişirme teknikleri geliştirilmiş, bu teknikler seramiğin sertleştirilip dayanıklılığını artırmıştır. Zamanla, pişirme tekniklerindeki gelişmelerle birlikte, seramiğin malzeme özellikleri de çeşitlenmiş ve bu da mühendislik malzemelerine giden yolu açmıştır. Bugün ileri seramik kompozitler, bu ilk pişirme tekniklerinden yola çıkarak geliştirilmiş yüksek teknolojili ürünlerdir. Özellikle havacılık, savunma ve sağlık gibi kritik endüstrilerde kullanılan seramik kompozit malzemeler, Neolitik dönemde temelleri atılan bu teknolojik birikimin devamıdır.

Seramik, sadece günlük yaşamda kullanılan işlevsel bir malzeme olmaktan çıkmış, aynı zamanda insanların ritüel ve sanatsal ihtiyaçlarını da karşılamıştır. Neolitik dönemde seramiğin kullanımı, toplumların dünya görüşlerini ve inanç sistemlerini yansıtan sembolik bir anlam kazanmıştır (Hodder, 1990). Bugün, modern seramik sanatında bile bu tarihsel ve sembolik bağlar devam etmekte; seramik hem bir sanat eseri hem de bir teknolojik ürün olarak varlığını sürdürmektedir.

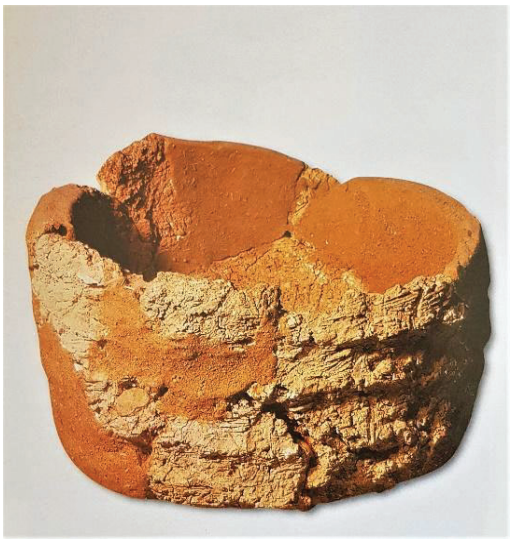
Neolitik dönemden bugüne kadar seramiğin geçirdiği evrim, sadece teknik bir ilerleme değil, aynı zamanda toplumsal ve kültürel dönüşümlerin de bir yansımasıdır. Neolitik çömlekçilik, insanoğlunun doğa ile olan ilişkisini ve maddi dünyayı şekillendirme kapasitesini gösteren en eski ve en önemli teknolojik yeniliklerden biridir (Vandiver, 1987). Bugün kullanılan seramik kompozitler, bu uzun tarihsel gelişim sürecinin en ileri örneklerini temsil etmekte ve hem sanat hem de mühendislik alanlarında dikkat çekici bir rol oynamaktadır.

Günümüzde modern seramik sanatında bile bu geleneksel ve sembolik bağlar devam etmektedir; seramik hem bir sanat eseri hem de bir teknolojik ürün olarak varlığını sürdürmektedir. Özellikle 20. yüzyıldan itibaren seramiğin sanatsal üretimi, hem çağdaş sanat formlarına hem de yeni estetik anlayışlara yön vermektedir (Cardew, 2002). Bu süreçte, sanatsal seramikler ve ileri mühendislik seramikleri, hem estetik hem de estetik anlamda dayanıklı bir dönüşüm geçirmiştir. Günümüzün modern seramik sanatında, geleneksel tekniklerin ileri seramik malzemeleriyle birleşmiş, gelişmiş ürünler üretilmekte, sanatçıların geçmişinin izlerini geleceğin teknolojileriyle birleştirmektedir (Tunalı, 2020).

Bu çalışmada, Neolitik dönemde çömlekçiliğin doğuşundan başlayarak seramiğin hem sanatsal hem de teknolojik sürecini genel olarak incelemesi amaçlanmaktadır. Seramik kompozitlerin tarihsel kökeni ve bugünkü kullanım alanlarına dair yapılan incelemeler, binlerce yıllık birikimin nasıl sürdürülebilir bir teknolojik ve sanatsal mirasa dönüştüğünü ortaya koyacaktır.

NEOLİTİK DÖNEM ÇÖMLEKÇİLİĞİ VE SERAMİK TEKNOLOJİSİNİN İLK ADIMLARI

İnsanlık, Seramikli Neolitik Dönem öncesinden kili ateş olmaksızın gün ısısı ile sertleştirerek topraktan kap ve gereç yapımını biliyordu. Bu dönemden itibaren toprak kap yapımı için kilin ateşle bütünleşmesiyle, işlevsel alanı genişleyen ve günümüze kadar devam edecek olan bir seramik süreci başlamıştır. Çömlekçilik ya da pişmiş toprak kültürü dediğimiz yapı, binlerce yıllık serüveninde insanlığın temel yaşam gereksinimlerini karşıladığı gibi, gelişerek bilimsel ve sanatsal anlamda günümüz yaşamına önemli katkılar sağlamıştır. Çağdaş seramik endüstrisinin ve modern seramik sanatının çıkış noktası unutulmamalı ki primitif çömlekçiliktir





Görsel 2, 3. Erken Neolitik Dönem çömlek örneği (Çayönü), Yaşamakta olan Anadolu çömlekçiliği ilk tür şekillendirme (Sorkun).

Anadolu ve Yakındoğu ekseninde bakıldığında; Uzun bir sürece yayılan Neolitik Dönem, Anadolu ve Yakındoğu'da çanak çömlek teknolojisine bağlı olarak iki ana evrede incelenir. Anadolu'nun Pre-Pottery Neolitihic (Akeramik) Neolitik Dönemi MÖ 9600'den 7000'e kadar devam eder ve tabakalanma ile buluntu topluluklarındaki değişim temel alınarak Çanak Çömleksiz A (Pre-Pottery Neolitihic A- PPNA), Çanak Çömleksiz Neolitik B (PPNB) ve Çanak Çömleksiz Neolitik C (PPNC) adlarıyla alt evrelere ayrılır. PPN' den sonra gelen Çanak Çömlekli Neolitik (Pottery Neolitihic-PN) ise, "ilk" ve "son" olmak üzere iki alt evreye ayrılmıştır (Sagona&Zimansky, 2015:34).

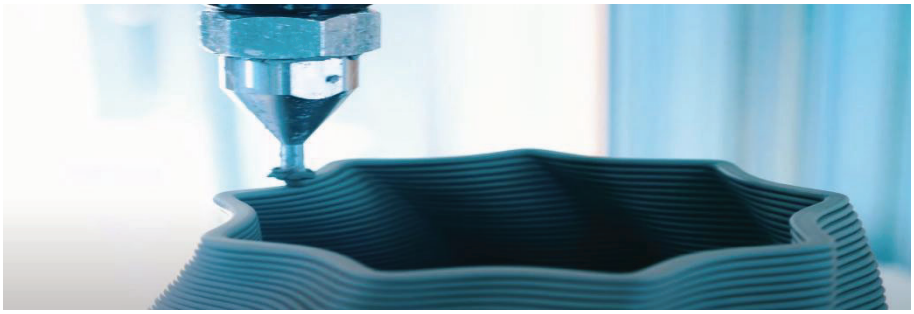
Anadolu'da MÖ 8.binyılın sonu ile 7.binyılın başına denk gelen Çanak Çömleksiz (Akeramik/ Pre-Pottery Neolitihic -PPNA) Neolitik'ten (Pottery Neolitihic-PN) Neolitik'e geçiş, ilginç bir biçimde belirsizdir. Oysaki bunu takip eden değişimler, öncü yerleşik toplulukların geleneklerini köklü bir biçimde değiştirmiştir. Her ne kadar bunun öncesinde de kilden nesneler yapılmış olsa da kilin ısıl yöntemle işlenmeye başlaması, Neolitik Çağ'ın iki ana döneme ayrılıp incelenebilmesi açısından önemli bir dönüm noktasıdır (Schmandt- Bessear, 1977: 133-150). Gordon Childe, Neolitik'i Güneybatı Asya'daki bir dizi teknolojik, ekonomik ve sosyal devrim olarak kavramsallaştırdığında, çanak çömlek yapımının belki de "insan tarafından kimyasal değişimin en erken bilinçli kullanımı" olduğu önermesini ortaya koydu (Budja, 2016:61).

Pişmiş kil teknolojisini icat etmek ve katı bir nesne, seramik bir kap yaratmak için kullanılan piroteknolojinin, modern insan düşüncesinin ve pratiğinin oluşumunda, tarım ve yerleşiklik ile birlikte ele alındığında hala devrim niteliğinde bir adım olduğu varsayılmaktadır (Gamble 2007.10-32).



Görsel 4, 5. İlkel Şekillendirme Teknikleri, çimdik tekniği (solda), sucuk (fitil) tekniği (sağda)

Prehistorik dönemlerin seramik şekillendirme teknikleri, günümüz geleneksel ve çağdaş seramik üretiminde hala kullanılmaktadır. Örneğin sucuk (fitil) tekniği ile bilinen primitif teknik, günümüz seramik şekillendirme tekniklerinden biri olarak uygulanmaktadır. Hatta buradan inovasyon kapsamında üç boyutlu yazıcılarla seramik üretimine kadar, Delta Wasp sistemli konut yapımına kadar teknolojiye esin kaynağı olmuştur.



Görsel 6. Üç Boyutlu Yazıcı ile Kilin Şekillendirilmesi



Görsel 7, 8. Delta Wasp Sistemli Konut Yapımı

Tüm öğretilerde dört temel yaşam elemanı olarak kabul edilen hava, su, toprak ve ateşin insan eliyle bütünleşmesiyle oluşan seramik, Neolitik Dönemden günümüze yaklaşık 9000 yıllık bir süreçte, ilksel gereksinimleri karşılayacak kaplardan, tinsel objelerden sanata, endüstriyel

alanlara kadar insanlığın vazgeçilmezi olmuştur. Seramik aynı zamanda, pişmiş toprak kültürü olarak binlerce yılın veri aktarımını sağlayan kıymetli bir kültür alanı oluşturmuştur.

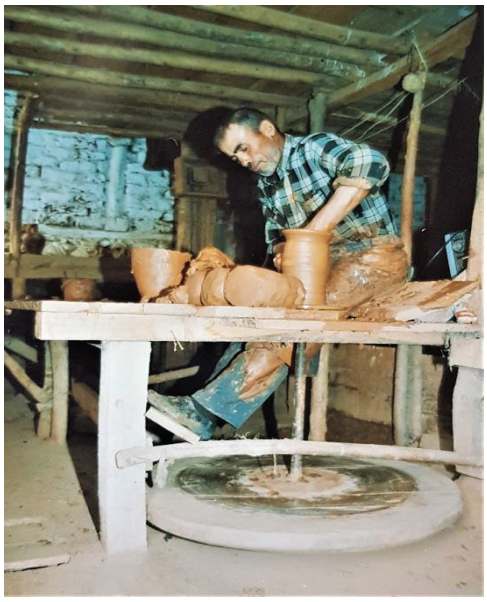
TUNÇ ÇAĞI VE SERAMİK ÜRETİMİNDE İKİNCİ TEKNOLOJİK AŞAMA

Tunç Çağı'na doğru; alet ve araç yapımı gelişimine koşut olarak, seramik üretiminde de form biçimselliğini çeşitlendiren ve daha seri üretime imkân veren çömlekçi çarkı keşfedilmiştir. Tunç Çağı'nda metal kullanımı da dâhil birçok teknolojik buluş arasında önemli bir yeri olan çömlekçi çarkı, bu çağın belki de en ilginç keşfidir. Çömlekçi çarkı, sadece kilin şekillendirmesine yaptığı üretim hızı ve estetik katkı ile kalmayıp, endüstriyel anlamda da ilk araç olma özelliğine sahiptir. Basit olarak çömlekçi çarkını, tabanlı bir mil üzerindeki tablanın (ahşap, metal, taş, seramik vb.) döndürülerek aldığı devinim ve merkezkaç kuvveti yardımıyla üzerindeki kili şekillendirmeye yarayan bir alet olarak tanımlayabiliriz.



Görsel 9. İlk Çark Örnekleri, Yaklaşık M.Ö. 3500, Uruk

Çarklı çömlekçiliğe geçişle, günümüze kadar uzanan etno-arkeolojik değerleri artıran ilk endüstriyel üretim örneği ve tarzı meydana gelmiştir. Çömlekçi çarkı öylesine değerli bir buluştur ki Childe, çömlekçi çarkının devinimli tüm araçların ilham kaynağı olduğunu öne sürer. Bugün bile çömlekçi çarkının mı tekerlekten, tekerleğin mi çömlekçi çarkından esinlendiği, yani hangisinin önce keşfedildiği bilim insanları arasında tartışma konusudur (Ünal 2023:11).





Görsel 10, 11. Anadolu'da Kullanılan İlkel Çömlekçi Çarkı (solda), Elektrikli Modern Çömlekçi Tornası (sağda)

Milsiz yivli, yivsiz disklerden, uzun milli hızlı çömlekçi çarkı ile çanak çömlek üretimine kadar arkeolojik dönemlerin en gelişmiş seramik üretim yöntemleri, günümüz Anadolu'sunda da varlığını sürdürebilen değerli bir maddi kültür unsurudur. Nitekim çarklı çömlekçilik, kültürel kapsamda günümüz geleneksel seramik üretiminde ve seramik sanatında hala önemli bir üretim tarzıdır.

SERAMİĞİN BİLİME KATKILARI

Uzun soluklu aşamalardan geçerek günümüze ulaşan seramik üretim teknolojisi, bu sürecin birikimleriyle çağdaş bilim disiplinlerine de kıymetli katkılar sunmuştur. Seramik, arkeoloji, antropoloji vb. kültür bilimlerinden mühendislik disiplinlerine kadar birçok alanda öne çıkmaktadır.

Kültür Bilimlerine Katkıları

Arkeoloji disiplininde, kalıcılık özelliği nedeniyle prehistoryadan itibaren insan ve toplumların yaşam biçimleri hakkında binlerce yıllık veriyi günümüze taşımaktadır. Özellikle son dönemde öne çıkan Süreçsel Arkeolojik yaklaşım, 20. yüzyılın ortalarında ortaya çıkan ve arkeolojik verilerin bilimsel yöntemlerle incelenmesi gerektiğini savunan bir yaklaşımdır. Bu yaklaşım, sosyal, ekonomik ve çevresel faktörlerin insan davranışları üzerindeki etkilerini analiz eder. Dean Arnold gibi araştırmacılar, seramik buluntuların bu faktörlerle ilişkisini inceleyerek, tarih öncesi toplumların yaşam biçimlerini anlamaya çalışmışlardır.

Kırsal çömlekçilik, tarih öncesi dönemlerde kullanılan tekniklerin günümüzde nasıl sürdürüldüğüne dair doğrudan bir gözlem imkânı sunar. Bu, çömlek yapımında kullanılan ham maddelerin seçimi, işlenmesi, şekillendirilmesi, kurutulması ve pişirilmesi gibi teknik detayların incelenmesine olanak tanır. Süreçsel arkeoloji, bu teknolojik süreçlerin zaman içinde nasıl evirildiğini anlamak için bu tür gözlemleri kullanabilir. Örneğin, aynı coğrafyada yüzlerce, hatta binlerce yıl boyunca sürdürülen çömlekçilik tekniklerinin karşılaştırılması, teknolojik yeniliklerin ya da değişimlerin izlenmesine olanak tanır.



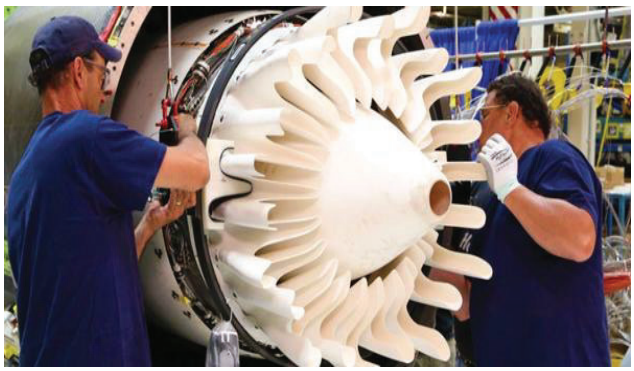
Görsel 12. Günümüzde Yaşamakta Olan İlk Tür Çömlekçilik (Gökeyüp)

Günümüzde devam eden ilkel çömlekçilik pratikleri, süreçsel arkeoloji açısından verimli bir model oluşturur.

Örneğin, Anadolu'daki Gökeyüp, Uslu ve Sorkun gibi yerleşimlerde sürdürülen çömlekçilik faaliyetleri, tarih öncesi dönemlerdeki üretim teknikleriyle büyük benzerlikler göstermektedir. Bu durum, seramik üretiminin sosyal organizasyon, ekonomik yapı ve çevresel koşullarla olan ilişkisini anlamak için önemli ipuçları vermektedir.

Malzeme Bilimi ve Seramiğin Geleceği: İleri Kompozit Malzemeler

Modern seramik kompozitler, teknoloji ve mühendislik dünyasında kilit bir rol oynar. Uzay araştırmaları, biyomedikal uygulamalar ve savunma sanayi gibi alanlarda seramiklerin yüksek dayanıklılığı, ısıya karşı direnç ve hafiflik gibi özellikleri, bu malzemelerin önemini artırmıştır. Davidge'nin modern seramik teknolojilerine dair araştırmaları, bu malzemelerin temel kökenlerinin Neolitik dönemdeki çömlekçiliğe dayandığını ortaya koymaktadır (Davidge, 1983, s. 150). Davidge, özellikle uzay sanayiinde kullanılan seramik kompozitlerin, ayrıştırılmış kilinin erken dönemlerde elde edilen rafine edilmiş versiyonları olduğunu vurgulamaktadır.





Görsel 13, 14. Havacılık ve Otomotiv Sektöründe Kullanılan İleri Seramik Örnekleri

Wachsman ve Lee, ileri mühendislik seramikleri üzerinde çalışmalarında, seramik kompozitlerin enerji üretimi ve parçaları gibi alanlarda da birleşimlerde bulunurlar. Yüksek sıcaklığa ve basınca dayanıklı seramikler, değiştirilen enerji teknolojilerinin temel yapı taşlarından biri olarak değerlendirilmektedir. Özellikle katı oksit yakıt yapısında kullanılan seramik özellikleri, enerji miktarının arttırılması için önemli bir teknoloji olarak öne çıkmaktadır (Wachsman ve Lee, 2011, s. 67).

Genel tanımıyla en az 2 farklı malzemenin birbiri içerisinde fiziksel olarak karıştırılmasıyla elde edilen yeni malzemelere kompozit malzemeler denir. Kompozit malzemeler genel olarak 'matris' adı verilen bir ana bileşen ve 'takviye elemanı' adı verilen bir başka bileşenden oluşur. Kompozit malzemeler genel olarak 'matris' adı verilen bir ana bileşen ve 'takviye elemanı' adı verilen bir başka bileşenden oluşur. Tek bir malzeme ile elde edilemeyen mekanik (dayanım, tokluk vb.) ve/veya fiziksel (elektrik iletkenliği, termal iletkenlik vb.) özelliklerin geliştirilmesi ve bir araya getirilmesidir.

Kompozit malzemeler, kullanılan matris malzemesinin cinsine göre; polimer matrisli kompozitler, metal matrisli kompozitler, seramik matrisli kompozitler, karbon/karbon matrisli kompozitler ve nano kompozitler olarak beş ana gruba ayrılmaktadırlar (Matthews ve Rawlings 1999; Sarıkaya 2019:17). Seramikler görece yüksek mukavemet ve rijitliğe sahiptirler fakat gevrektirler. Buna bağlı olarak, seramik matrisli kompozitlerin geliştirilme ve üretilme amaçlarının başında tokluklarını arttırmak gelir. Böylelikle seramiklerin yüksek mukavemet ve rijitliğinden yararlanıp gevrekliği minimize etmek amaçlanır (Matthews ve Rawlings 1999). Seramik matrisli kompozitlerin diğer kullanım alanları askeri ekipmanlar, uzay araçları ve zırhlardır. Seramik matrise eklenen takviyeler; karbon, cam ve seramiktir.

Seramik matrisin seramik fiber ile takviye edildiği malzemelerde gevreklik azalmakta, mukavemeti yüksek ve tok bir malzeme ortaya çıkmaktadır (Sarıkaya 2019:18). Bu özelliklerinden dolayı ileri seramik malzemeler, diğer kompozitlere nazaran biraz daha öne çıkmaktadır. Dolayısıyla seramiğin yaklaşık 9000 yıl önce başlayan serüveni günümüzün ileri teknolojileriyle devam etmektedir.

SANAT VE TEKNOLOJİ ARASINDA SERAMİK: ESTETİK VE ÇÖZÜMÜN BULUŞMASI

Seramik sadece bir mühendislik malzemesi değil, aynı zamanda bir sanat formülüdür. Neolitik dönemden itibaren çömlekçilerin geliştirdiği teknikler, tarihte sanat seramiklerinin yaratımına reel katkılar sağlamıştır. Read 'in sanayi ve sanatın buluşması üzerine yaptığı çalışmalar, seramiklerin iyileşmesi ile birlikte nasıl bir arada olduklarını gösterir **(**Read, 1954, s. 134). Read, seramiği hem teknolojik hem de sanatsal bir malzeme olarak kayıtlı ve tarih boyunca bu iki tarafın nasıl birbirini tamamladığını inceler.

Bugün sanat dünyasında seramik sanatı, hem geleneksel tekniklerden hem de ileri teknolojiden faydalanmaktadır. Bernstein ve Mirviss, modern seramik sanatında hem geleneksel el teknikleri hem de modern endüstriyel tekniklerin etkili olduğunu belirtirler (Bernstein & Mirviss, 2016, s. 78). Bu sistemin seramik sanatı, estetik ve teknoloji arasındaki sınırları, aşan bir ifade biçimi olarak sürdürülebilir. Deleuze ve Guattari'nin "çizgisel olmayan" sanat anlayışına göre, seramikler, sürekli bir dönüşüm ve yeniden yapılanma süreci ürünüdür (Deleuze ve Guattari, 1987, s. 215). Bu bakış açısı, seramiğin hem geleneksel hem de modern tekniklerle nasıl birleştirilebileceğini gösterir ve sanatsal yeniliğin, teknolojik ilerlemeyle nasıl iç içe geçişin mümkün olduğunu gösterir.

SONUÇ VE DEĞERLENDİRME

Bu çalışmada, seramiğin Neolitik dönemdeki yolculuğu genel olarak incelenmiş ve bu sürecin günümüzdeki toplumsal, kültürel ve teknolojik yansımaları ele alınmıştır. Neolitik dönemde başlayan pişmiş toprak üretimi, sadece insanlığın günlük hayatını iyileştirmesiyle kalmamış, aynı zamanda medeniyetlerin estetik anlayışlarına, ticaretine ve teknolojik gelişmelerine de etki etmiştir. Bugün modern seramik sanatında ve ileri teknoloji seramiklerinde yaşanan yenilikler, binlerce yıl önce atılan bu temellere dayanmaktadır. Neolitik çömlekçiliğin teknik ve estetik özelliklerinin geleneksel kırsal çömlekçilikte benzer tekniklerle sürdürülmesi de değerli bir maddi kültürdür. Bu devamlılığın günümüzde hem kültürel hem de inovasyon bağlamında görünür olması, farklı disiplinlerdeki çalışmalara önemli katkılar vermektedir. Çağdaş seramik kompozitlerin üretimi hala yaşamaktadır. Bu üretim bulunduğumuz çağda öylesine hızlı gelişmektedir ki; bugün inovasyon kapsamında seramiğin en uç noktası sayılabilecek uzay aracı başlıklarına kadar uzanan bir süreci yaşamaktayız.

Hem mühendislik seramiklerinde hem de sanat dünyasında seramiğin bu sürekliliği, geçmişten günümüze bir köprü anlayışta ve insanlığın maddi dünyaya dair anlayışını yeniden şekillendirmektedir. Geçmişin izlerini taşıyan bu kadim malzeme, geleceğin ileri teknolojilerinde de yer alarak, insanlığın tarihindeki vazgeçilmez bir rol oynamaya devam edecektir.

Seramiğin hem kültürel bir miras hem de modern teknolojilerin temel yapı taşlarından biri olduğu gerçeği, bu çalışmanın ana çıkış noktasıdır. Yıllar önce ateşle şekillenen kilinin hikâyesi, bugün hala insanlığın ve ileri teknolojik başarılarının arka planında yaşamaktadır.

KAYNAKÇA

Arnold, Dean. (1985). Ceramic Theory and Cultural Process. Cambridge: Cambridge University Press.

Bauer, S. (1999). *Erken Toplumlarda Çömlekçiliğin Rolü.* Cambridge: Cambridge University Press.

Bernstein, S. ve Mirviss, J. (2016). *Çağdaş Seramik Sanatı: Tarihsel Bir Perspektif.* New York: Wiley.

Budja, M. (2016). Ceramics among Eurasian hunter-gatherers: 32 000 years of ceramic technology use and the perception of containment. Documenta Praehistorica XLIII, 61-86.

Cardew, M. (2002). Öncü Çömlekçilik. Londra: Bloomsbury Yayıncılık.

Davidge, R. (1983). *Modern Seramik Mühendisliği: Bir İnceleme.* Malzeme Bilimi Dergisi, 18(3), 150-160.

Deleuze G. and Guattari F. (1987) [1980] A Thousand Plateaus: capitalism and schizophrenia, (trans. Massumi B.) Athlone Press, London.

Gamble, C. (2007) Origins and Revolutions. Human Identity in Earliest Prehistory. Cambridge University Press. Cambridge.

Gerrard, C. (2000). *Neolitik Dönem Arkeolojisi.* Londra: Routledge.

Hodder, I. (1990). Avrupa'nın Evcilleştirilmesi: Neolitik Toplumlarda Yapı ve Olasılık. Oxford: Blackwell Yayıncıları.

Kingery, WD (1976). *Seramiklere Giriş.* New York: John Wiley & Sons.

Matthews, F. L. and Rawlings, R. D., (1999) Composite Materials: Engineering and Science, Washington: CRC Press, (1999).

Read, H. (1954) The Meaning of Art, Penguin Books, London

Rice, PM (1987). Çömlek Analizi: Bir Kaynak Kitabı. Chicago: Chicago Üniversitesi Yayınları.

Sagona, A. and Zimansky, P. (2015) Türkiye'nin En Eski Kültürleri, Arkeoloji ve Sanat Yayınları, İstanbul

Sarıkaya, E. (2019) Doğal Fiber Takviyeli Kompozit Üretimi Ve Mekanik Özelliklerinin Tespiti Doktora Tezi, Denizli, Haziran – 2019

Schiffer, S. (1996) The hidden-indexical theory's logical-form problem: a rejoinder, https://doi.org/10.1111/j.0003-2638.1996.00092.xCitations: 2, Article Linker

Schmandt-Besserat, D. (1977) The beginnings of the use of clay in Turkey. Anatolian Studies, 27, 133–150.

Schreiber, A. (2011). *İleri Seramik Mühendisliği: İlkeler ve Uygulamalar.* Materials Today, 14(4), 204-210.

Tunalı, A. (2020). Çağdaş Sanat ve Seramik: Gelenekselden Modern Seramiklere. İstanbul: Remzi Kitabevi.

Ünal, S. (2023) Anadolu Pişmiş Toprak Kültüründe Göller Bölgesi, Arkeoloji ve Sanat Yayınları, İstanbul.

Vandiver, P. B. (1987). Sequential Slab Construction: A Conservative Southwest Asiatic Ceramic Tradition, ca. 7000-3000 B. C. Paleorient 13, 9-35.

Wachsman, E.D. and K.T. Lee. (2011) Lowering the temperature of solid oxide fuel cells, Science, 2011. 334(6058): p. 935- 939

KARBON NANOTÜP TAKVİYELİ ALÜMİNYUM MATRİSLİ KOMPOZİTLERİN VAKUM İNFİLTRASYON YÖNTEMİ İLE ÜRETİMİ

PRODUCTION OF CARBON NANOTUBE REINFORCED ALUMINUM MATRIX COMPOSITES BY VACUUM INFILTRATION METHOD

Esma ÜNGÖRMÜŞ

Kırıkkale Üniversitesi, Fen Bilimleri Fakültesi, Savunma Teknolojileri, Kırıkkale-Türkiye

Dr. Öğr. Üyesi Naci Arda TANIŞ

Kırıkkale Üniversitesi, Mühendislik ve Doğa Bilimleri Fakültesi, Metalurji ve Malzeme Mühendisliği, Kırıkkale- Türkiye

Prof. Dr. Ayşegül Ülkü METİN

Kırıkkale Üniversitesi, Mühendislik ve Doğa Bilimleri Fakültesi, Kimya Bölümü, Kırıkkale-Türkiye

Prof. Dr. Recep ÇALIN

Kırıkkale Üniversitesi, Mühendislik ve Doğa Bilimleri Fakültesi, Metalurji ve Malzeme Mühendisliği, Kırıkkale- Türkiye

ÖZET

Bu çalışmada sodyum aljinat ile kaplanmış çok tabakalı karbon nanotüplerin alüminyum matrisli kompozitlerin sertlik ve porozitelerine etkisi araştırılmıştır. Bu amaçla, alüminyum matrisli kompozitlerin üretim yöntemi olarak vakum infiltrasyon yöntemi tercih edilmiş, çok tabakalı karbon nanotüp öncelikle farklı oranlarda (%10, %20 ve %30 oranında) bir biyopolimer olan sodyum aljinat ile kaplanmıştır. Aljinat kaplı çok tabakalı karbon nanotüp malzemeler 710 ºC sıcaklıkta infiltrasyon yöntemi ile üretilen alüminyum matrisli kompozit malzemede takviye elemanı olarak tercih edilmiştir. İnfiltrasyon süresinin (2,3 ve 5 dakika) ve farklı oranlarda çok tabakalı karbon nanotüp içeren takviye elemanın etkisi araştırılmıştır. Üretilen kompozit malzemeler metalografik işlemlerin ardından optik mikroskop, taramalı elektron mikroskobu (SEM), element dağılım spektrometresi (EDS) analizi yapılmıştır. Alüminyum matrisli karbon nanotüp takviyeli kompozit malzemenin sertliği ise Vickers (HV0.2) mikro sertlik ölçüm yöntemi kullanılarak ölçülmüştür. Yapılan çalışmalar sonucunda infiltrasyon süresi arttıkça üretilen kompozitin porozitesinin düştüğü, karbon nanotüp miktarı arttıkça da kompozitin porozitesinin arttığı belirlenmiştir. Sertlik değerinin çok tabakalı karbon nanotüp takviye oranının artmasıyla arttığı, %30 karbon nanotüp içeren numunelerde ise karbon nanotüplerin kümeleşmesinden dolayı sertlik değerinde azalma görülmüştür.

ISBN: 978-625-378-045-6 https://doi.org/10.5281/zenodo.14537144

Anahtar Kelimeler: Çok Tabakalı Karbon Nanotüp, Alüminyum Matrisli Kompozit, İnfiltrasyon

ABSTRACT

In this study, the effect of multi walled carbon nanotubes coated with sodium alginate on the hardness and porosity of aluminum matrix composites was investigated. For this purpose, the vacuum infiltration method was preferred as the production method of aluminum matrix composites, and multi walled carbon nanotubes were coated with sodium alginate, a biopolymer, at different ratios (10%, 20%, and 30%). Alginate-coated multi walled carbon nanotube materials were preferred as reinforcing elements in aluminum matrix composite material produced by infiltration method at 710℃. The effect of infiltration time (2, 3, and 5 minutes) and reinforcing elements containing different ratios of multi walled carbon nanotubes were investigated. The composite materials produced were analyzed by optical microscope, scanning electron microscope (SEM), and elemental dispersion spectrometry (EDS) after metallographic processes. The hardness of the aluminum matrix carbon nanotube-reinforced composite material was measured using the Vickers (HV0.2) micro hardness measurement method. As a result of the studies, it was determined that the porosity of the composite decreased as the infiltration time increased and the porosity of the composite increased as the amount of carbon nanotubes increased. The hardness value increased with increasing multi walled carbon nanotube reinforcement ratio, while the hardness value decreased in samples containing 30% carbon nanotubes due to the clustering of carbon nanotubes.

Keyword: Multi Walled Carbon Nanotube, Aluminum Matrix Composite, Infiltration

GİRİŞ

Kompozit malzemeler en az 2 malzemenin en iyi özelliklerini yeni malzemede oluşturmak amacıyla biraraya gelmesi ile oluşmaktadır. Kompozit malzemeler matris ve takviye elemanından oluşur ve oluşan kompozit malzemenin özellikleri onu meydana getiren malzemelerden farklıdır [1]. Kompozit malzemelerde matris malzemesi olarak metal, seramik, ve polimerler tercih edilirler [2]. Metal matrisli kompozitler düşük yoğunluk, yüksek sertlik ve mukavemete sahip malzemelerdir [3]. Metal matrisli kompozitlerde matris malzemesi olarak alüminyum, bakır, magnezyum ve alaşımları tercih edilmektedir [4]. Kompozit malzemelerde takviye elemanı yükü taşıyıp matrisin rijitliğini ve dayanımı artırmaktadır [5,6]. Matris malzemenin görevi ise uygulanan kuvveti takviye elemanlarına iletmek ve kompozit malzemenin şeklinin korunmasını sağlamaktır [5]. Alüminyum matrisli kompozitler; verimliliğinin yüksek olması, enerji kazanımının yüksekliği ve bakım maliyetlerinin düşük olmasında mühendislik uygulamalarında tercih edilmektedir [7]. Bor(B), karbon nanotüp (KNT), zirkonyum dioksit(ZrO_2), alüminyum oksit (Al_2O_3),tungsten karbür (WC), silisyum karbür (SiC) metal matrisli kompozitlerde takviye elemanı olarak tercih edilmektedir [4,8]. Karbon nanotüpler dayanıklılığının yüksek, elektrik iletkenliğinin iyi olması ve üstün mekanik özelliklerinden dolayı nanoteknoloji, nanokompozit ve elektronik gibi yaygın bir alanda kullanılmaktadır [9].

Metal matrisli kompozitlerin üretiminde katı faz ve sıvı faz üretim yöntemleri tercih edilmektedir [10]. Kompozitlerin üretim yönteminde sıvı faz üretim yöntemlerinin katı faz üretim yöntemlerinden daha ucuz olması ve daha kolay şekillendirilebilir olmaları sayesinde çeşitli şekillerde üretime elverişli olması daha tercih edilir olmasını sağlamaktadır [11]. İnfiltrasyon yöntemi gözenekli gövdeden erimiş metalin

infiltre edilmesi yöntemidir [12]. İnfiltrasyon yönteminin adımları: ergimiş metal ve takviye elemanının preform olan yüzeye teması, negative basınç altında erimiş metalin preform boyunca akması ile infiltrasyonun başlaması ve katılaşmanın gerçekleşmesi şeklinde özetlenebilir [13] . Literatürde karbon nanotüplerin takviye elemanı olarak kullanıldığı çok sayıda çalışma rapor edilmiştir. Sridhar Alüminyum matrisli kompozitlere KNT'lerin etkisine baktığında, çok duvarlı karbon nanotüplerin (ÇDKNT) Alüminyum matrisli kompozitte ağırlıkça artmasının kompozit parçanın sertliğini arttırdığının gözlemlemiştir. %2 'lik ÇDKNT ilavesinin kompozit malzemenin akma mukavemetini ortalama %90 arttırdığını görmüşlerdir [14] .Güllüoğlu ve diğerleri ise yaptıkları çalışmada aşınma direnci ile takviye edilen KNT oranı arasındaki ilişkiyi incelemişlerdir ve aşınma direncinin hacimce takviye edilen KNT oranı ile doğrudan etkili olduğu sonucına varmışlardır. Ancak %5 KNT oranından sonra bu özelliklerde azalış olduğunu görmüşlerdir [11]. Safa KNT takviyeli Alüminyum matrisli kompozitlerin sertlik değerlerini ve iletkenliklerini araştırmıştır. En iyi sertlik sonucuna %0.50 KNT içerikli numunede ulaştığını, bu değer üzerine çıkıldığında ise sertlik değerinde azalma görüldüğünü bildirmiştir. KNT'lerin yüksek elektriksel iletkenliklerinden dolayı artan KNT miktarı elektriksel iletkenliği arttırdığı bildirilmiştir [15]. Karaman ve diğerleri mekanik alaşımlama yöntemini kullanarak ÇDKNT'lerin kompozitlerin aşınma davranışlarını nasıl etkilediğini araştırmışlardır ve artan ÇDKNT oranı ile aşınma özelliğinin iyileştiğini görmüşlerdir [16]. Şenel ise yaptığı çalışmada ÇDKNT takviyeli Alüminyum kompozitin basma dayanımı inceleyip, %0.3 katkılı kompozitin basma dayanımının %72, Vickers sertliğinin %38, deneysel yoğunluğunun %2 oranında iyileştiğini tespit etmiştir. Ağırlıkça %0.30 katkı oranın üzerinde ise mekanik dayanımın kötüleştiğini gözlemlemiştir [17].

Bu çalışmada da karbon nanotüp takviyeli alüminyum matrisli kompozit malzemenin infiltrasyon yöntemi kullanılarak üretilmesiyle karbon nanotüplerin ve infiltrasyon sürelerinin üretilen kompozit malzeme üzerindeki etkileri araştırılmıştır. Takviye hacim oranın, infiltrasyon süresinin, gözeneklilik ve sertlik değerinin üretilen kompoziti nasıl etkilediği belirlenmiştir.

DENEYSEL ÇALIŞMALAR

Takviye elemanı olarak çok tabakalı karbon nanotüp, matris elemanı olarak Alüminyum 356 (A356) alaşımı kullanılmıştır. A356 alaşımının kimyasal özellikleri Tablo 1'de gösterilmiştir.

Si	Fe	Cu	Mn	Mg	Zn	Ti	Diğerleri	Al
6,5-7,5	0,15	0,20	0,10	0,30-0,35	0,10	0,20	0,15	Kalan

Tablo 1 Matris A356 Malzemesinin Kimyasal Bileşimi

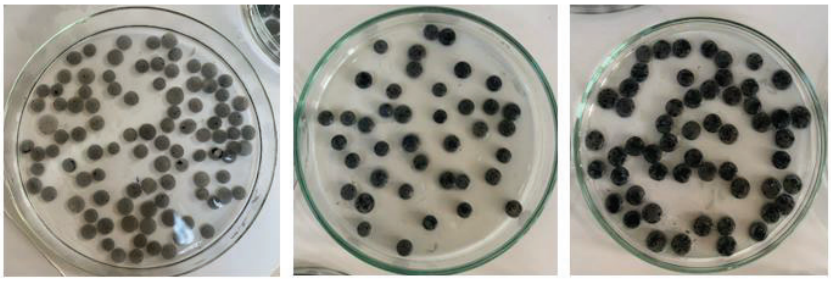
İnfiltrasyon işleminden önce karbon nanotüpler sodyum aljinat ile kaplanmıştır. Bunun için %2'lik sodyum aljinat çözeltisi ve %5'lik $AlCl_3$ çözeltisi hazırlanmıştır. Hazırlanan bu sodyum aljinat çözeltisinin içerisine farklı hacim oranlarında KNT'ler ilave edilerek homojen olarak karıştırılması

sağlanmıştır. Şekil 1'de sodyum aljinat çözeltisi ve KNT ilave edilmiş sodyum aljinat karışımı verilmiştir.



Şekil 1: Sodyum Aljinat Çözeltisi ve Sodyum Aljinat+KNT Çözeltisi

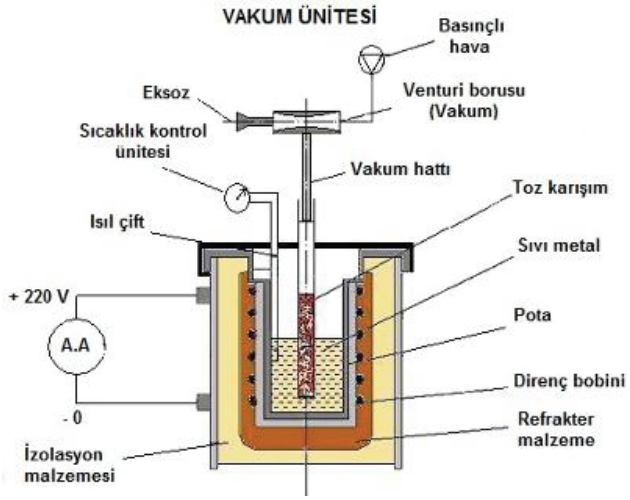
Şekil 2'de Sodyum aljinat + KNT çözeltisinin $AlCl_3$ çözeltisine damlatılmış durumu gösterilmiştir.



Şekil 2: Sodyum Aljinat Kaplanmış KNTlerin AlCl3 Çözeltisine Damlatılması

Hazırlanan numuneler çalkalayıcılı karıştırıcıda 40 ℃'de kurutulmuştur ve infiltrasyon sürecine geçilmiştir. İnfiltrasyon deneyi için dış çapı 10 mm et kalınlığı 0,5 mm ve 250 mm yüksekliğinde paslanmaz çelik borular kullanılmıştır. Çelik tüplerin alt kısımlarına alüminyum folyo ile sarılmış çelik filtreler kullanılmıştır. Hazırlanan tozlar 60 mm yükseklik oluşturacak şekilde çelik tüplere doldurulmuştur. Tozların vakum hattına gitmesini engellemek için tozların üzerine alüminyum folyo ile sarılmış çelik filtreler yerleştirilmiştir. Çelik boruların gösterimi Şekil 3'te verilmiştir. Alüminyum matrisin erimesi için Çalın'ın geliştirdiği ergitme ocağı kullanılmıştır. Bu ergitme ocağı Şekil 4'te gösterilmiştir. Vakum infiltrasyon yönteminde vakum değeri manometre yardımıyla ölçülmüştür. Vakum ünitesinin oluşan yüksek sıcaklıktan etkilenmemesi için vakum ünitesi ile çelik tüp arasında bakır boru yerleştirilmiştir. İnfiltrasyon sırasında basınç 600 mmHg değerindeki vakum 2-3 ve 5 dakika süre boyunca uygulanmıştır. Belirtilen süre sonunda çelik borular sıvı metal içerisinden çıkarılıp soğuması için oda sıcaklığındaki kum içerisine bırakılmıştır. Soğuyan borular kesilip kompozit malzemeler çıkarılmıştır. Çıkarılan numuneler metalografik süreçlerden sonra optik mikroskop altında SEM ile incelenmiştir. Numunelerin yoğunlukları ise Arşimet prensibi kullanılarak bulunmuştur ve Tablo 2'de verilmiştir.





Şekil 3: İnfiltrasyona Hazır Çelik Boru İçindeki KNTler

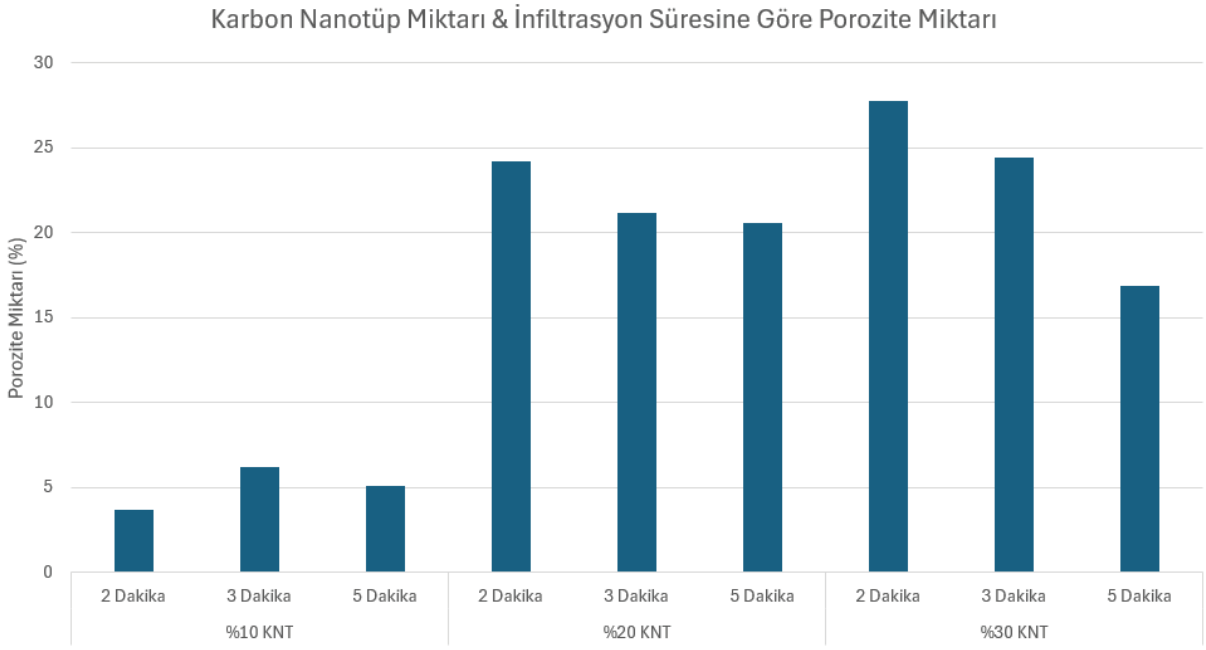
Şekil 4: İnfiltrasyon Deney Düzeneği

DENEYSEL SONUÇLAR VE TARTIŞMA

Farklı hacim oranlarında KNT içeren numuneler farklı infiltrasyon sürelerine tabii tutulmuştur. Değişen karbon miktarının oluşan kompozit malzemenin gözenekliliği üzerinde nasıl bir etkisi olduğu araştırılmıştır. Tablo 2'de porozite hesabının sonuçları verilmiştir.

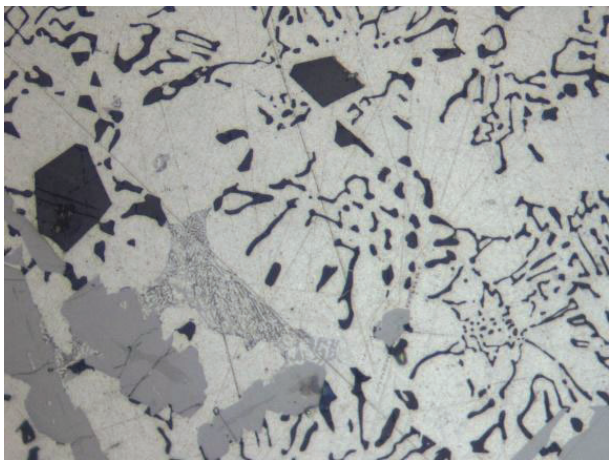
Takviye Hacim Oranı/ İnfiltrasyon Süresi	2 dk	3 dk	5 dk
%10 KNT	3,66	6,18	5,11
%20 KNT	24,19	21,16	20,61
%30 KNT	27,76	24,45	16,85

Tablo 2: Karbon Nanotüp Miktarı & İnfiltrasyon Süresine Göre Sertlik Miktarı



Şekil 5: Porozite-Takviye Hacim Oranı Arasındaki İlişki

-İnfiltrasyon süresi ve porozite arasında ters orantı vardır. Aynı miktarda KNT içeren (%20) ama infiltrasyon süreleri birbirinden farklı olan numunelerin SEM görüntüleri de infiltrasyon süresi azaldıkça porozitenin arttığını destekler niteliktedir. Şekil 6'da bu numunelerden birine ait SEM görüntüsü verilmiştir.

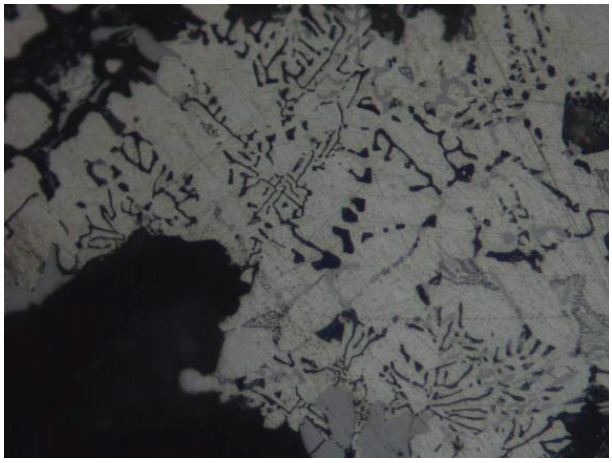


Şekil 6: 2 dk İnfiltrasyon Süresine Sahip %20 KNT

-KNT miktarının porozite üzerindeki etkisini görmek için farklı oranda KNT içeren numunelerin aynı infiltrasyon süresindeki görüntülerini incelediğimizde ise numunelerdeki KNT miktarı arttıkça daha poroz görüntü elde edilmiştir.

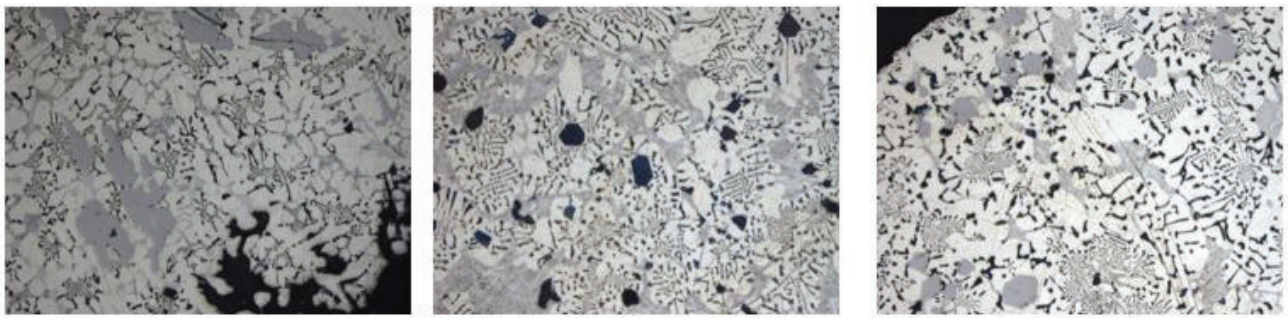
ISBN: 978-625-378-045-6

https://doi.org/10.5281/zenodo.14537144

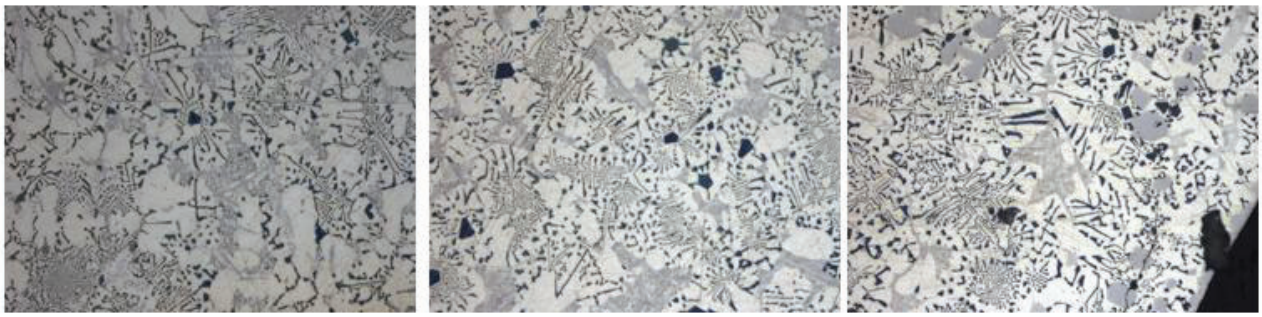


Şekil 7: 2 dk İnfiltrasyon Süresi %30 KNT Numune 50X

-Porozite miktarının eklenen KNT miktarı ile arttığı, artan infiltrasyon süresi ile azaldığı sonucu elde edilmiştir. Şekil 8'de ve Şekil 9'da farklı KNT miktarlarına ve artan infiltrasyon sürelerine ait optik mikroskop görüntüleri de bu durumu desteklemektedir.



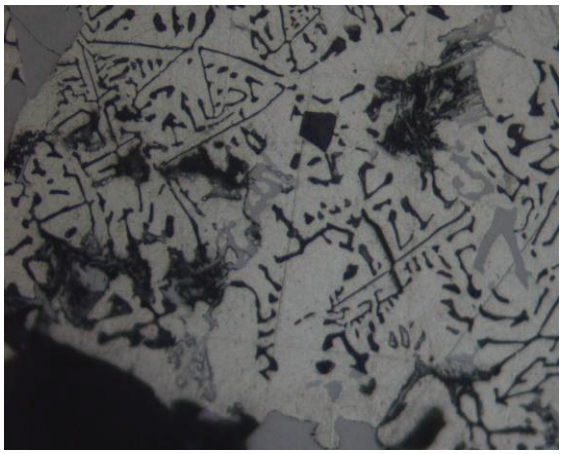
Şekil 8: %10- %20 ve %30 KNT İçeren Numunelerin 3dk İnfiltrasyon Süresine Ait Optik Mikroskop Görüntüleri

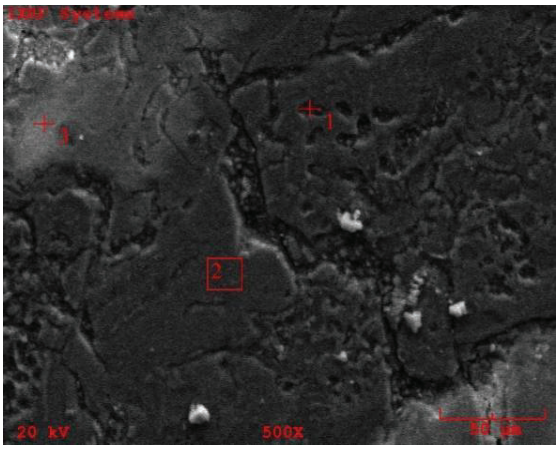


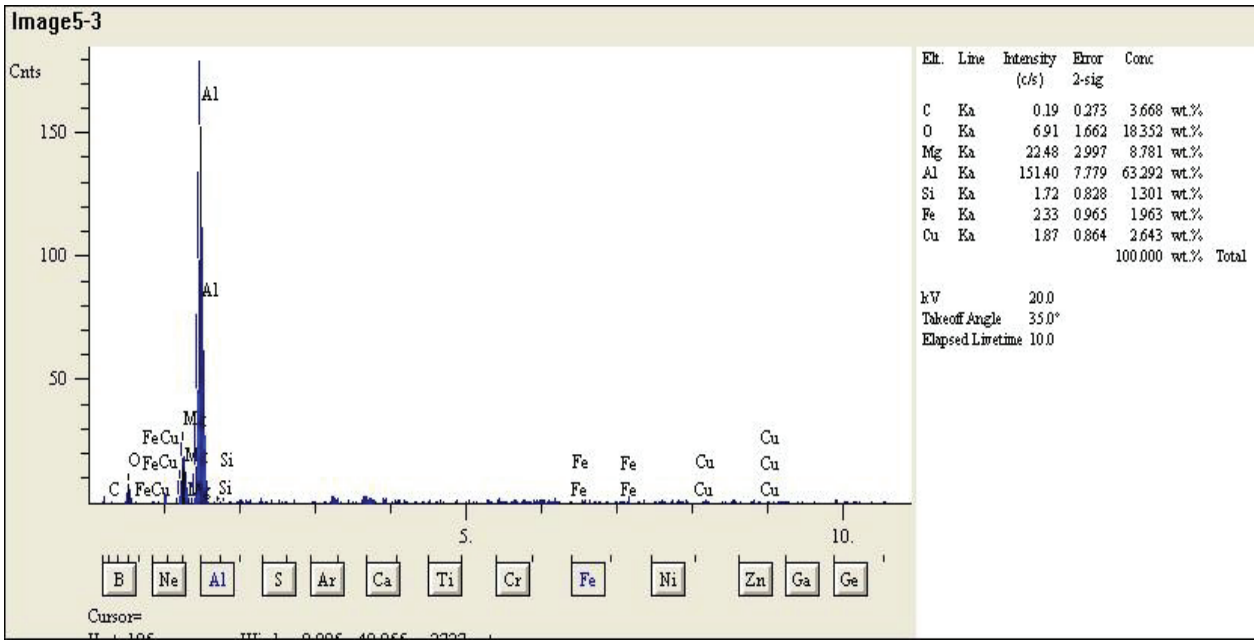
Şekil 9: %20 KNT İçeren Numunenin 2-3 ve 5dk İnfiltrasyon Süresindeki Optik Mikroskop Görüntüleri

-%10 KNT ve 3 dk infiltrasyon süresine sahip olan numunenin SEM görüntülerine baktığımızda 3 ile numaralandırılmış bölgede beyazlık olduğu görülmüştür. Bu bölgedeki beyazlığın alüminyum oksit olduğunu tahmin etmekteyiz. EDS analizlerinde de bu bölgedeki alüminyum miktarının % 63 çıkması

tahminlerimizi doğrulamaktadır. Bu numunede polimer uzaklaşması sırasında porozite meydana gelmiştir.

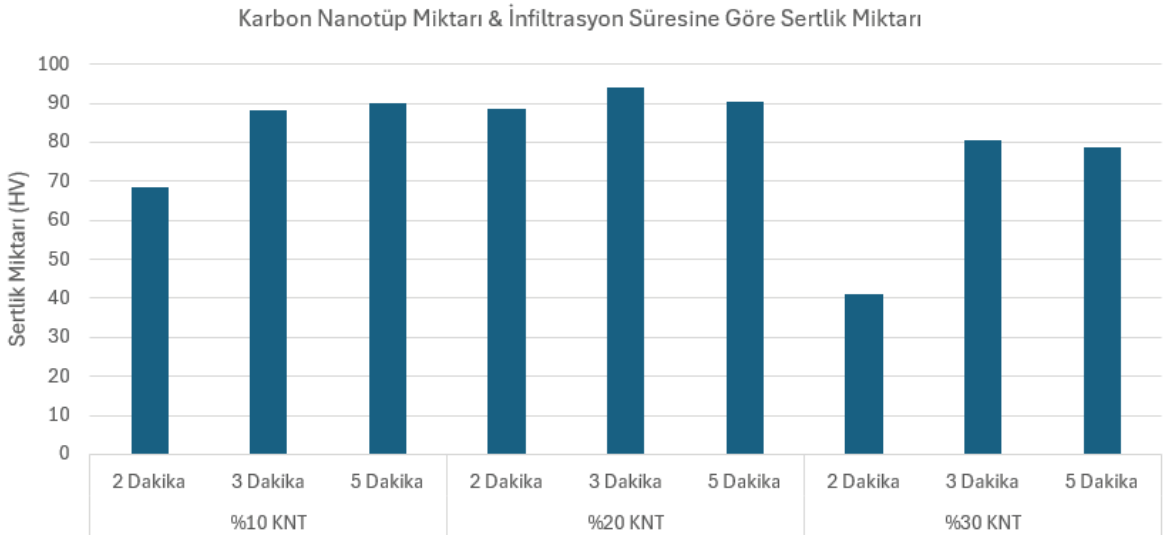






Şekil 10: %20 KNT İçeren Numunenin SEM ve EDS Görüntüleri

-Numunelerin sertlikleri Vickers sertlik cihazı ölçülmüştür. %10 ve %20 KNT içeren numunelerin sertlik değerlerine baktığımızda KNT miktarı arttıkça sertliğin de arttığını söyleyebiliriz. %30 KNT içeren numunelerde ise kümeleşmeden dolayı sertlik değerinde azalma görülmüştür. Şekil 11'de sertlik değerinin şematik gösterimi verilmiştir.



Şekil 11: Numunelerin Sertlik Ölçümlerinin Sonuçları

SONUÇ VE DEĞERLENDİRME

Bu çalışmada elde edilen sonuçlar aşağıda özet olarak verilmiştir:

- İnfiltrasyon süresi azaltıkça porozite miktarı artmaktadır. Bunun nedeni zaman yetersiz kalmıştır ve doldurulamamıştır.
- Porozite miktarının artan KNT miktarı ile arttığı gözlemlenmiştir.
- %10 KNT içeren numunelerde ise kalıntı polimer miktarının fazla olduğu görülmüştür.
- Sertlik değerinin de karbon miktarı ile arttığı söylenebilir. Fakat %30 KNT içeren numunelerde kümeleşmeden dolayı sertlik değerinde azalma olmuştur.

KAYNAKLAR

[1] Çalın R. (2006), "Magnezya Parçacik Takviyeli Al Matrisli Kompozitin Vakum Infiltrasyon Yöntemi Ile Üretilmesi ve Özelliklerinin Incelenmesi", Doktora Tezi, Gazi Üniversitesi

[2] Duran O. (2019), "Vakum İnfiltrasyon Yöntemiyle Üretilen Pirinç Çeltiği ve Alümina Takviyeli AA7075 Hibrit Kompozitlerin Mikroyapısal ve Mekanik Özelliklerinin İncelenmesi", Yüksek Lisans Tezi, Kırıkkale

[3] Kalemtaş, A. (2014), "Metal Matrisli Kompozitlere Genel Bir Bakış", Putech & Composites, 22, 18-30.

[4] Kayabaşı I. (2016), "Metal Matrisli Kompozit Malzeme Üretim Sistemi İmalati ve Performansinin İncelenmesi", Yüksek Lisans Tezi, Karabük Üniversitesi

[5] Sahin Y., (2015), "Kompozit Malzemelere Giriş", Ankara: Seçkin

[6] Kaya, A. İ. (2016), "Kompozit Malzemeler ve Özellikleri" Putech & Composite Poliüretan ve Kompozit Sanayi Dergisi, 29, 38-45.

[7] Bedir F. (2006), "Alüminyum Kompozitlerin Üretimi, Karakteristik Özellikleri Ve Endüstriyel Uygulamaları, Mühendis ve Makina, 47-554

[8] Şenel, M. C., Gürbüz, M., & Koç, E. (2018), "Toz Metalürjisi Metoduyla Üretilen Al-Si3N4 Metal Matrisli Kompozitlerin Mekanik Özelliklerinin İncelenmesi", Mühendis ve Makina, *59*(693), 33-46.

[9] Düşükcan I. (2018), "Kopolimer/Karbon Nanotüp Kompozitlerinin Sentezi, Karakterizasyonu ve Dielektrik Özelliklerinin İncelenmesi", Yüksek Lisans Tezi, Fırat Üniversitesi

[10] Parıltan M.Ç. (2018), "Al2024-316l Metal-Metal Matrisli Kompozitlerin Üretimi Ve Özelliklerinin İncelenmesi", Yüksek Lisans Tezi, Trabzon

[11] Topçu İ., Güllüoğlu A., Bilici M., Gülsoy H., Karbon Nanotüp Takviyeli Ti-6Al-4V/ KNT Kompozitlerin Aşınma Davranışlarının İncelenmesi, Journal of the Faculty of Engineering and Architecture of Gazi University (2018), https://doi.or./10.17341/gazimmfd.460542

[12] Küçükyıldırm B. (2012), "Fabrication And Investigation Of Carbon Nanotube Reinforced Aluminum Matrix Composite Material" ,Doctoral Thesis, Istanbul

[13] Tanış, N. A., Okur, O., Jafaar, C. N. A., Ariff, A. H. M., & Çalin, R. (2022). "Investigation On The Wear Behaviour And Properties Of RHA Reinforced 7075 Aluminium T6 Composites Produced By Vacuum Infiltration" Malaysian Journal of Microscopy, 18(2), 10-22

[14] Shridhar I, Karthic R.Narayanan (2009), Processing and characterization of MWCNT reinforced aluminum matrix composite, Springer Science & Business Media, 44:1750–1756

[15] Safa H., Güler S., Aksoy M., Şeker S., Al/KNT Nanokompozitlerin Toz Metalurjisi Yöntemiyle Üretimi ve Özelliklerinin Araştırılması, Fırat Üniversitesi Fen Bil. Dergisi 32(2), 31-36, 2020

[16] Topçu I., Karaman E. (2019), "Çok Duvarlı Karbon Nanotüp Takviyeli Düzenli/ Düzensiz Şekilli Ti 6Al-4V Kompozitlerin Aşınma Davranışlarının İncelenmesi", Düzce Üniversitesi Bilim ve Teknoloji Dergisi, 1249-1260

[17] Şenel M. (2021), "Çok Duvarlı Karbon Nanotüp Takviyeli Alüminyum Esaslı Kompozitlerin Mekanik Özellik ve Mikroyapı İncelemesi", Engineering Sciences (NWSAENS), 16(1):39-48

ADVANCED BIOCOMPOSITE MATERIALS FOR THE ENVIRONMENT AND SUSTAINABLE DEVELOPMENT

ZENATI Rania [1*]
BOUCHERDOUD Ahmed [1]
BENDJELLOUL Meriem [1],
SEGHIER Abdelkarim [1]
AICHOUNI Sara [1]
ELANDALOUSSI El Hadj [1]

[*1]University of Relizane, Faculty of Sciences and Technology,
Laboratory of Environment and Sustainable Development (LESD),
Department of Chemistry, Relizane, Algeria

[*1]ORCID ID: https://orcid.org/0009-0008-7369-2075

ABSTRACT

Biocomposite materials have demonstrated remarkable efficiency in treating industrial wastewater contaminated with pollutants, offering a sustainable and cost-efficient alternative to traditional treatment methods. Our research primarily explored the adsorption kinetics, with a focus on the valorization of natural waste to promote environmental protection and the conservation of water resources. This forward-thinking approach not only underscores the effectiveness of biocomposites but also highlights their potential role in advancing sustainable water resource management practices.

Keywords: biocomposite, materials, kinetics, adsorption, water.

CERAMICS IN DENTISTRY

Hüseyin Alperen SELVİ

Bilecik Oral And Dental Health Center,Bilecik, Turkey

ORCID ID: 0009-0003-6475-1348

ABSTRACT

A ceramic is an inorganic, non-metallic solid composed of metal or non-metal compounds that are shaped and hardened by heating to high temperatures.
Today, ceramics find applications in various fields, including the automotive and aerospace industries, computer and machinery manufacturing, electrical transmission systems, household appliances, and electronic equipment. They are also used in medicine and dentistry, construction, tableware, and artistic works.
Dental ceramics are a special group known for their different properties from ceramics. Porcelain, a common type of ceramic, is composed of heat-resistant vitreous materials that include a glass matrix and crystalline particles. Dental porcelains represent a specific subgroup of dental ceramics.
Ceramics have been utilized in dentistry for many years because of their aesthetic qualities, biocompatibility, and low thermal conductivity. Recent studies have expanded the applications of dental ceramic materials, leading to changes in their composition and types.
Dental ceramics can be produced using various methods, including slip casting, CAD/CAM technology, powder-liquid layering, and pressing.
Ceramic materials are used in various dental applications, including dental crowns, dental implants, dental implant abutments, ceramic posts, inlays, and other restorations, all of which have demonstrated long-term clinical success.
This report compiles and presents information about the history of dental ceramics in dentistry, their basic composition, areas of application, and classifications.

Keywords: Ceramics, Dentistry, Dental Ceramics

PREPARATION AND CHARACTERISATION OF ZnO NANOPARTICLE-COATED CHITOSAN/SODIUM ALGINATE WALLED ENERGY-STORING COMPOSITE MICROCAPSULES

Müyesser Selda TÖZÜM
Uşak University, Faculty of Engineering and Natural Sciences, Textile Engineering Department, Uşak 64200, Turkey
ORCID ID: 0000-0003-2887-5637

ABSTRACT

The use of phase change microcapsules as energy storage materials for a wide range of applications is becoming increasingly important. In this study, the production of chitosan/sodium alginate walled energy-storing composite microcapsules coated with metal oxide nanoparticles was carried out using the complex coacervation method. The objective of this study is to enhance the thermal response to temperature of microcapsules by coating metal oxide on their external surface. For this aim, inorganic zinc oxide (ZnO) metal oxide nanoparticles were employed as the coating material, while 1-tetradecanol was utilized as the core material for the capsules. 1-tetradecanol, a fatty alcohol act as a phase change material. Microcapsules have thermal energy storage properties due to the latent heat energy storage/release of 1-tetradecanol in their structure. The morphology and chemical structures of the produced microcapsules were investigated using scanning electron microscopy (SEM) and Fourier transform infrared spectroscopy (FTIR), respectively. The latent heat storage and release properties of the microcapsules were determined by differential scanning calorimetry (DSC). The thermoregulation properties of microcapsules and their thermal response against temperature increase were analyzed by thermal history (T-history) test method. Leakage prevention performances of microcapsules were examined by photographs taken after heating.

Keywords: chitosan, sodium alginate, ZnO, energy storage, thermal response

1. INTRODUCTION

Phase change materials (PCMs) are known as substances that absorb/release energy during the phase transition process (Niu et al., 2023; Kang et al., 2023). When the ambient temperature is above the PCMs' melting temperature, they absorb latent heat from the ambient during the melting period. In the reverse phase change, the heat stored in the melting process is released to the ambient at a temperature below the solidification temperature of the PCMs (Mondal, 2008). The main categories of PCMs are organic and inorganic. Organic PCMs are paraffin, poly ethylene glycol, fatty acid and fatty alcohols. Organic PCMs are have the potential to be used in a wide range of applications such as thermal protection of electronic components, thermal systems of spacecraft, cooling systems, thermal storage of solar energy and thermal protection of food. (Javadi et al., 2020). PCMs, which have the capacity to increase the efficiency of thermal energy utilization, have some disadvantages such as having low thermal conductivity. Since these disadvantages greatly limit the thermal energy conversion and operational durability of PCMs, research has been carried out on this topic. There are numerous techniques that can be employed to enhance the thermal conductivity of PCMs. Some of them

are impregnation of metal and metal oxide nanoparticles or carbon nanotubes and addition of metal matrices to PCMs. However, these enhancements do not eliminate leakage, diffusion and flow problems. The microencapsulation technique has been demonstrated to be an effective method for preventing the leakage of PCMs during the solid-liquid phase transition. With microencapsulation, not only leakage and corrosion problems can be solved, but also mechanical strength and thermal resistance properties can be gained (Liu et al., 2019; Zhu et al., 2016).

In this study, it was aimed to prepare thermal energy storing microcapsules with chitosan/sodium alginate walls coated with ZnO nanoparticles. The speed at which the capsules respond to changes in temperature has been increased by coating the outer surface of the microcapsules with ZnO nanoparticles. In study, fatty alcohols are much cheaper about 4 times than the most preferred paraffin and can be microencapsulated with higher heat storage capacity was used as core material of microcapsules. The morphology and chemical characterization of the microcapsules were performed by SEM and FTIR analysis, respectively. Thermal and thermo-regulation features of the microcapsules were determined by DSC and T-history test method. Leakage prevention performances of microcapsules were evaluated by photographs taken after heating.

2. MATERIAL AND METHOD

2.1. MATERIAL

1-tetradecanol (>97%, Alfa Aesar) which was also a PCM was used as the core material of the microcapsules. Chitosan (Sigma Aldrich) as a cationic polymer and sodium alginate (Sigma Aldrich) as an anionic polymer were used as the wall materials of the microcapsules. Cetyl trimethyl ammonium bromide (CTAB, Sigma Aldrich) was employed as cationic surfactant. Glutaraldehyde (25%, Sigma Aldrich) was used as a cross-linker to stabilize the microcapsules and acetic acid (10%) and sodium hydroxide (5%) solutions for pH adjustments during the microcapsule production process. Zinc oxide (ZnO, Sigma Aldrich) nanoparticles were used as coating material of microcapsules.

2.2. PRODUCTION OF MICROCAPSULES

The production of chitosan/sodium alginate walled energy-storing microcapsules coated with metal oxide nanoparticles was carried out using the complex coacervation method. 1-tetradecanol, a phase change material, was encapsulated in a chitosan/sodium alginate wall structure. In the presence of 0.10 g of CTAB surfactant, 2.5 g of 1-tetradecanol was dispersed in 50 ml of 1.25% (w/v) chitosan solution. Then, 50 ml of 1.25% (w/v) sodium alginate solution were added to the prepared emulsion and pH was adjusted to 4 in order to initiate polymer-polymer complex formation. After one and a half hour, pH was adjusted to 9 and the complex formation was stopped. After that, emulsion system temperature was decreased to 4 °C and 0.8 g of glutaraldehyde was added dropwise to stabilize the microcapsules. At the last stage of microcapsule production, the microcapsules were treated with 5% (w/v) aqueous solution of tannic acid for 15 minutes. In the ZnO nanoparticle coating process of the prepared

microcapsules, 1% ZnO nanoparticle solution was added dropwise to the tannic acid-treated microcapsule solution and the pH was adjusted to 4. The mixing was maintained at 70 °C for 4 hours at 750 rpm and then left overnight. In the last step, the microcapsule sample coated with ZnO nanoparticles was subjected to washing and filtration. The production procedure of the microcapsules was shown in Figure 1.

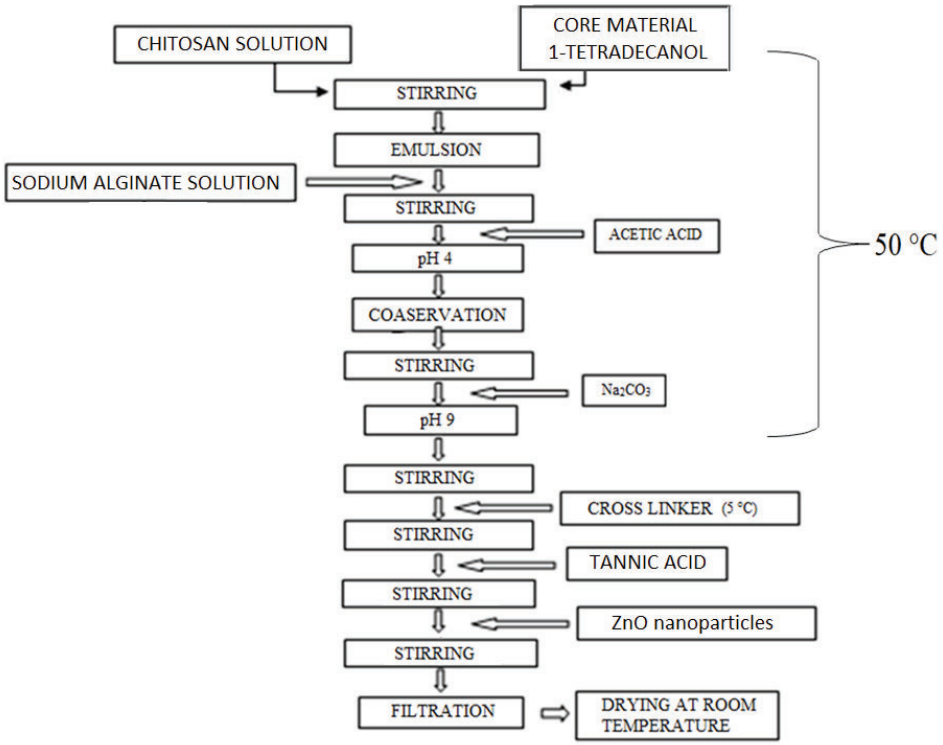


Figure 1. Process of microcapsule production

2.3. CHARACTERIZATION OF MICROCAPSULES

The microcapsules were analyzed morphologically by SEM (ZEISS GEMINI 500 model). ATR-FTIR (Perkin Elmer) analysis was performed in the range of wave number from 4000 to 400 cm^{-1}. To investigate phase transition temperatures and enthalpies of microcapsules, differential scanning calorimetry (Perkin-Elmer, DSC 400) analysis was made under nitrogen gas flow at 60 mL/min, at a heating rate of 1 °C/min and between the temperature of 0 °C and 60 °C. In the leaking test, 0.5 g of microcapsule were placed in the center of a 5 cm diameter filter paper. The sample was heated in an oven at 65 °C for 60 minutes. The images of the sample before and after the test were studied in order to observe whether it leaked. The thermoregulation property of the microcapsules was investigated by T-history test. In this test, thermoregulation property of the microcapsules was associated with the temperature change caused by the latent heat energy absorption or releasing of the 1-tetradecanol which forms the core substance of the microcapsules (Tözüm et al., 2022). The measurement was made in an insulated polyurethane foam box whose indoor temperature was controlled by a lamp connected to a thermostat. Before the test, the samples were conditioned in a cold medium. The test was started when the conditioned samples were placed in the heated box, and their surface temperature during the heating of the sample in the box was measured with a thermal camera

(Fluke TiX500 9Hz Thermal Imager) (Alay-Aksoy et al., 2017). Measurements were repeated for the produced ZnO coated microcapsules and ZnO uncoated reference microcapsules, and the change in their surface temperatures was compared.

3. RESULTS AND DISCUSSIONS

SEM analysis was performed to determine the morphology of microcapsules. Figure 2 shows the SEM images of microcapsules. According to the SEM images, it was seen that the produced microcapsules were spherical in shape and their particle size were smaller than 1 µm.

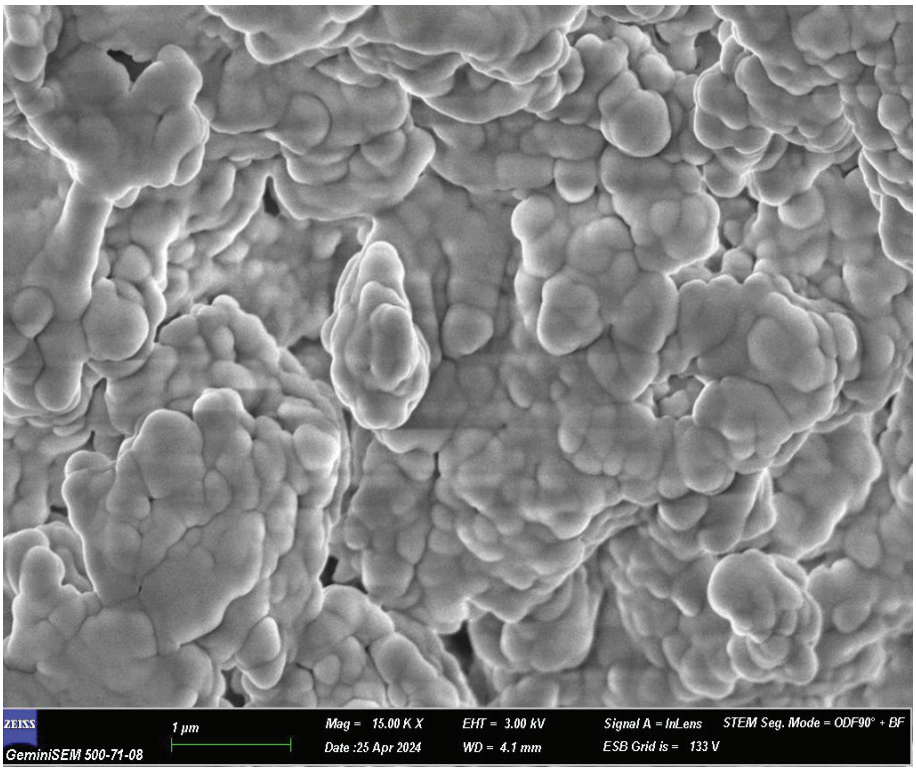


Figure 2. SEM images of microcapsules

Figure 3 illustrates the IR spectra of microcapsules coated with ZnO nanoparticles, 1-tetradecanol, chitosan, sodium alginate and ZnO nanoparticles. The broad band seen at 3270 cm^{-1} in the spectra of microcapsules belongs to the combination of hydrogen bonded -OH stretching and -NH stretching peaks of chitosan polymer, -OH stretching peaks of sodium alginate and -OH stretching peaks of 1-tetradecanol. In the spectra of chitosan polymer, the amide I and amide II peaks of the chitosan polymer were observed at wavelengths of 1650 cm^{-1} and 1592 cm^{-1}, respectively (Ahn et al., 2001). The peaks were observed at wavelengths of 1690 cm^{-1} and 1599 cm^{-1} in the spectra of microcapsule (Genç and Alay Aksoy, 2016). The peaks at 2849 cm^{-1}, 2917 cm^{-1} and 2957 cm^{-1} in the microcapsule spectra were characteristic C-H stretching peaks of 1-tetradecanol and proved the presence of 1-tetradecanol in the structure. Besides, the strong and sharp peaks at 1472 cm^{-1} and 1463 cm^{-1} in the spectra of microcapsules were the C-H bending peak of 1-tetradecanol. The characteristic Zn-O band of ZnO nanoparticles was observed between 720 cm^{-1} and 575 cm^{-1} wavenumbers in the spectrum of ZnO and appeared as a small peak at approximately 683 cm^{-1} wavenumbers in the IR spectra

of microcapsules. The observed peak was indicative of the presence of ZnO nanoparticles in the microcapsule structure.

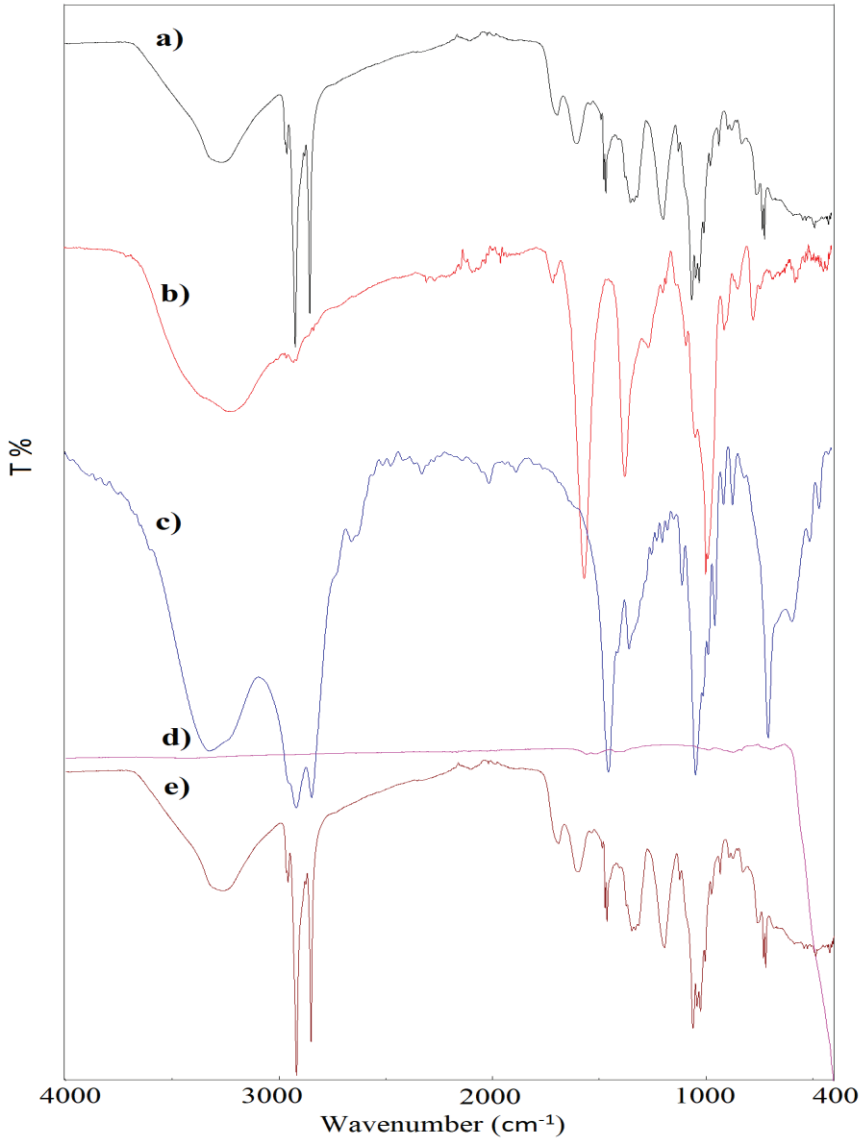


Figure 3. FT-IR ATR spectra of chitosan a), sodium alginate b), 1-tetradecanol c), ZnO nanoparticle d), CS/TD/ZnO microcapsules

The phase transition characteristics of microcapsules were quantified by DSC analysis. The resulting DSC thermogram is presented in Figure 4. According to DSC thermogram, the latent heat stored by microcapsules was found to be 61.26 J/g at 35.94 °C. Their crystallization enthalpies were measured as -61.28 J/g at 35.36 °C. It was possible to say the microcapsules' energy storage temperatures were close to body temperature and suitable for thermal energy applications.

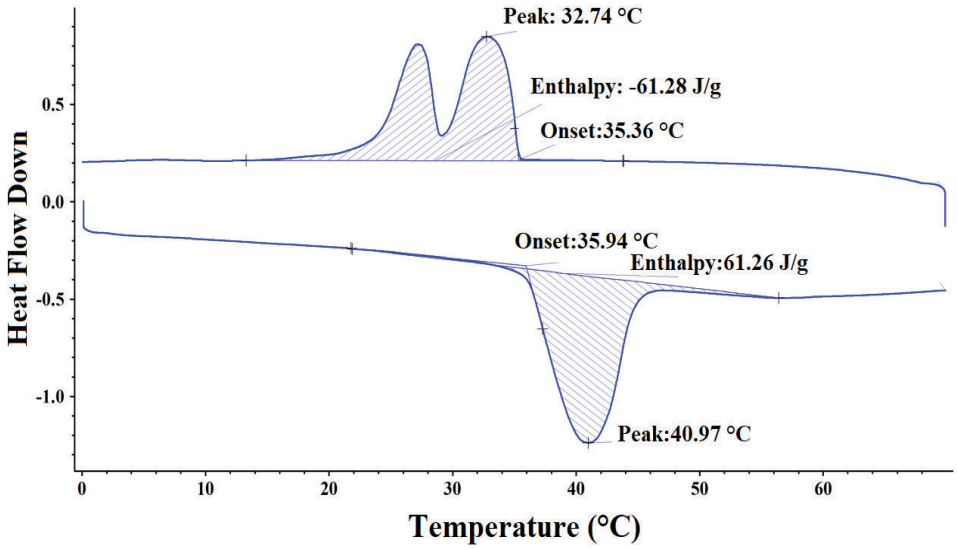


Figure 4. DSC thermogram of the produced microcapsules

Figure 5 shows the photographs of the microcapsules before and after heating. According to the photographs, there was no leakage from the filter paper on which the microcapsules were placed.

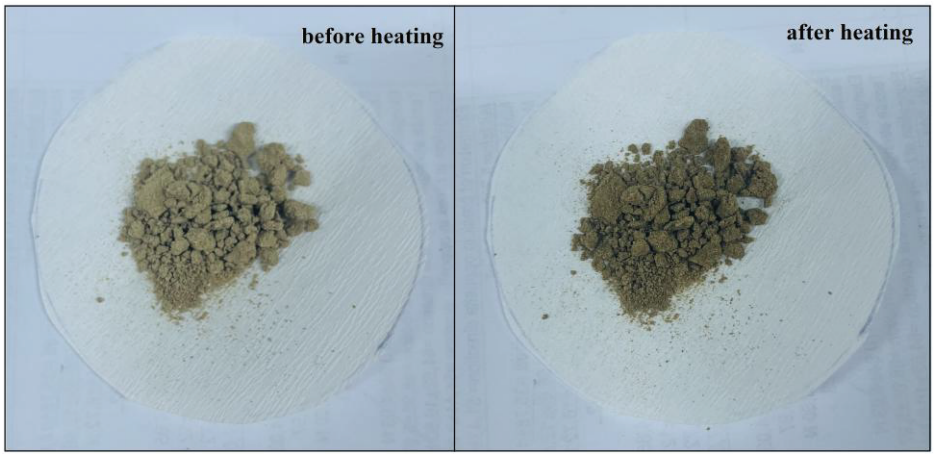


Figure 5. Leakage test of microcapsules

The thermo-regulation properties of the microcapsules due to the PCM in their structure were determined using the T-History Test. Figure 6 shows time-dependent temperature change graphs of microcapsules which is obtained at the end of the test. According to Figure 6, it was seen that the surface temperature of the microcapsules coated with ZnO nanoparticles reached the phase change temperature faster than the reference capsules without ZnO nanoparticles. The temperature of the reference capsules increased to 34.8°C in approximately five minutes, whereas the ZnO coated capsules reached 34.4 °C in three and a half minutes. This rapid increase was thought to be due to the ZnO nanoparticles increasing the speed of thermal response of the capsules. In addition, the temperature range of 34 °C and 40 °C for both capsules showed the temperature range in which 1-tetradecanol started to melt and finish melting, demonstrating that the capsules had thermo-regulation properties.

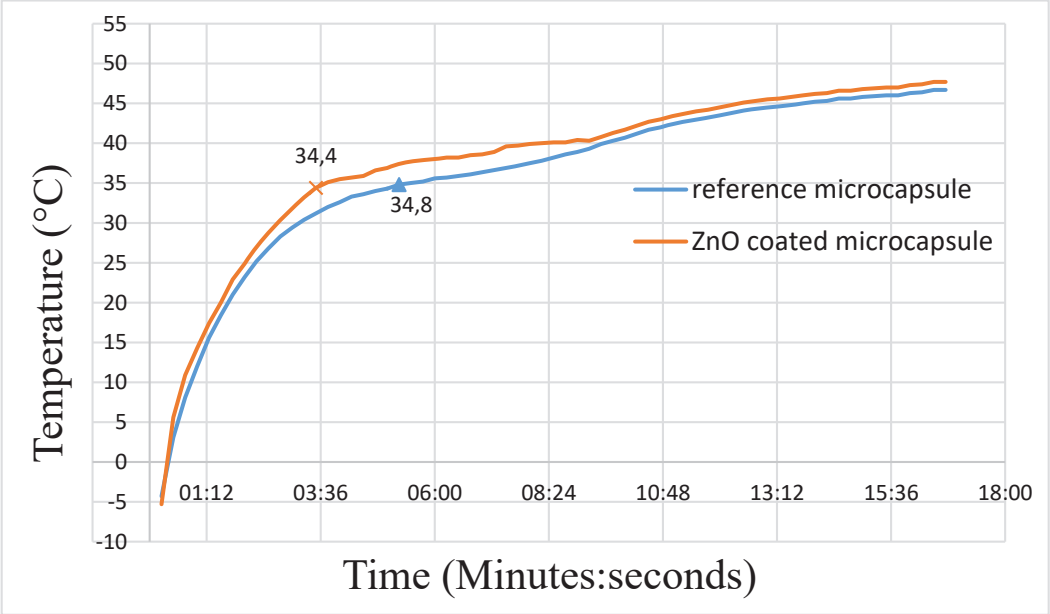


Figure 6. T-History results of the microcapsules

4. CONCLUSION

In this study, chitosan/sodium alginate walled energy-storing composite microcapsules coated with metal oxide nanoparticles was successfully produced by the complex coacervation method. Regarding to SEM images, it was seen that the prepared microcapsules had almost spherical particles with smooth surface. Microencapsulation of 1-tetradecanol into chitosan/sodium alginate shell was proven by FT-IR spectroscopy. According to the DSC analysis results, the melting and crystallization temperatures of the microcapsules were suitable for use in thermal energy sensors and applications. T-history results showed that the produced microcapsules exhibited thermoregulation properties and ZnO nanoparticles accelerated the thermal response of the microcapsules against temperature. Leakage test results showed that no leakage was recorded on the filter paper on which the microcapsules were placed.

REFERENCES

Ahn, J.S, Choi, H-K, Cho, C.S. (2001). A Novel Mucoadhesive Polymer Prepared by Template Polymerization of Acrylic Acid in The Presence of Chitosan, Biomaterials, 22 (9), 923-928.

Alay Aksoy, S., Alkan, C., Tözüm, M.S., Demirbağ, S., Altun Anayurt, R., Ulcay Y. (2017). Preparation and textile application of poly (methyl methacrylate-co-methacrylic acid)/n-octadecane and n-eicosane microcapsules. The Journal of The Textile Institute, 108, 30-41. https://doi.org/10.1080/00405000.2015.1133128

Genç, E., & Aksoy, S. A. (2016). Fabrication of microencapsulated PCMs with nanoclay doped chitosan shell and their application to cotton fabric. Textile and Apparel, 26(2), 180-188.

Javadi, F.S., Metselaar, H.S.C., & Ganesan, P. (2020). Performance improvement of solar thermal systems integrated with phase change materials (PCM), a review. Solar Energy, 206, 330-352.

Kang, M., Liu, Y., Lin, W., Liang, C., Qu, W., Li, S., Wang, Y., Zhang, F., & Cheng, J. (2023). Thermal comfort and flame retardant performance of novel temperature-control coatings with modified phase change material microcapsules. Progress in Organic Coatings, 181, 107579.

Liu, H., Wang, X., Wu, D., & Ji, S. (2019). Fabrication and applications of dual-responsive microencapsulated phase change material with enhanced solar energy-storage and solar photocatalytic effectiveness, Solar Energy Materials and Solar Cells, 193, 184-197.

Mondal, S., 2008. Phase Change Materials for Smart Textiles-an Overview. Applied Thermal Engineering, 28, 1536-50

Niu, S., Kang, M., Liu, Y., Lin, W., Liang, C., Zhao, Y., & Cheng, J. (2023). The preparation and characterization of phase change material microcapsules with multifunctional carbon nanotubes for controlling temperature. Energy, 268, 126652.

Tözüm, M.S., Alkan, C., & Alay Aksoy, S. (2022). Developing of thermal energy storing visual textile temperature indicators based on reversible color change, Journal of Industrial Textiles, 51:1964S-1988S.

Zhu, Y.L., Liang, S.E., Wang, H., Zhang, K., Jia, X.R., Tian, C.R., Zhou, Y.L., & Wang, J.H. (2016). Morphological control and thermal properties of nanoencapsulated n-octadecane phase change material with organosilica shell materials, Energy Conversion and Management, 119, 151–162.

PRODUCTION OF COMPOSITE MICROCAPSULE WITH GUM ARABIC/COPPER OXIDE SHELL FOR THERMAL ENERGY STORAGE AND PHOTO–THERMAL CONVERSION

Sena Demirbağ Genç

Uşak University, Faculty of Engineering and Natural Sciences, Textile Engineering, Uşak, Türkiye.

ORCID ID: 0000-0003-1634-6391

ABSTRACT

In recent years, the fact that fossil fuels are limited, and their widespread use causes environmental problems such as air pollution and global warming has led people to the use of renewable energy sources and the development of energy efficient technologies. In the present era, there is a significant interest in the development of efficient photothermal conversion materials that can collect solar energy, a clean and sustainable energy source, and convert it directly into usable energy. In this study, it was aimed to produce phase change material (PCM) containing composite microcapsules capable of photo-thermal energy conversion and energy storage. For this aim, the 1-tetradecanol fatty alcohol was encapsulated into the gum arabic/ copper (II) oxide nanoparticles shell structure by the complex coacervation method. The morphological properties and chemical structure of the microcapsules were investigated using scanning electron microscopy (SEM) and Fourier transform infrared spectroscopy (FTIR), respectively. The phase change temperatures and heat storage energies of the composite microcapsules were examined by differential scanning calorimetry (DSC) analysis. The leakage-proof performance of microcapsules was assessed by images taken after heating at 60 °C for 60 minutes. Furthermore, the photo-thermal conversion performance was determined through the utilization of an experimental setup comprising a polyurethane box, a thermal camera and a UV lamp.

Keywords: microcapsule, photo-thermal conversion, phase change material, complex coacervation.

INTRODUCTION

Recently, the demand for renewable and sustainable energy sources has been increasing rapidly due to the increase in fossil fuel consumption. The importance of sustainability of energy systems is increasing in order to provide efficient energy while minimizing the damage caused by fossil fuels to the environment. Thermal energy storage is an important solution for energy efficiency. Phase change materials (PCMs) have the ability to store and release large amounts of latent heat during phase change. Their ability to store energy at a constant temperature makes PCMs an effective solution for balancing energy production and consumption in sustainable energy systems (Maithya et al., 2021; Fan et al., 2022; Zhao et al., 2022).

There is more than one source of energy in nature, and among renewable and sustainable energy sources, solar energy is recognized as one of the most efficient and effective options in terms

of direct conversion into thermal energy (Chen et al.,2020). In this respect, the development of materials and technologies for the efficient use of solar energy is one of the most interesting energy topics for researchers. Photo-thermal conversion is the conversion of solar radiation (sunlight) into thermal energy, and in recent years it has become an important area of research among the technologies mentioned for the effective use of solar energy. The use of photothermal materials in combination with phase change energy storage materials allows efficient use of solar energy. Microencapsulation technology has the advantage of solving the known disadvantages of solid-liquid organic PCMs such as leaching, low thermal conductivity and also provides a good solution for combining photothermal materials with phase change materials with the ability to convert solar absorbed light energy into heat energy (Maithya et al., 2021). In the production of photo-thermal conversion microcapsules, hybrid shell with polymer/light-heat conversion material or light-heat conversion material is used as shell material. Materials such as graphene oxide (Zhao et al., 2019; Maithya et al., 2020; Yuan et al., 2018; Liu et al., 2017), silicon carbide (Wang et al., 2021; Wang et al., 2018), titanium oxide (Li et al., 2022; Ma et al., 2018), zinc oxide (Huang et al., 2020; Liu et al., 2022) were used as light-heat converting materials. In this study, 1-tetradecanol fatty alcohol was encapsulated in a gum arabic/copper (II) oxide hybrid shell structure using a complex coacervation method and characterized. The morphology, chemical structure, heat storage/release properties, photo-thermal conversion and leakage-proofing performance of the prepared microcapsules were examined.

MATERIAL AND METHOD

Material

In this study, 1-tetradecanol (>97%, Alfa Aesar) was used as the core material to produce microcapsules, while gum arabic polymer (Sigma Aldrich) and copper (II) oxide nanoparticles (CuO, Sigma Aldrich) were used as shell and light-heat converting material. Hexadecyltrimethylammonium bromide (CTAB, Sigma Aldrich) was used as surfactant. Glutaraldehyde (25%, Sigma Aldrich) was used to stabilize the microcapsules. Acetic acid and sodium hydroxide were used to adjust the pH in production.

Production of microcapsules

Gum arabic/copper (II) oxide/ 1-tetradecanol (GA/CuO/TD) microcapsules were produced using the complex coacervation method. In the initial phase of the process, the core substance, 1-tetradecanol, was emulsified using CTAB (0.1) in a gum arabic polymer solution (2.5 %). In the second step, CuO nanoparticles solution (2.5%) was added to the mixture and adjusted to pH 4 to initiate the formation of a complex between the gum arabic polymer and the CuO nanoparticles. Following an hour of reaction time, the pH of the mixture was adjusted to 9, thereby halting the complex formation process. In the final stage of the process, the temperature of the mixture was reduced to 4°C, after which the microcapsule was stabilized by the addition

of glutaraldehyde (0.8 g). The microcapsule production process was conducted at a rate of 1000 rpm, with a core-to-wall ratio of 1:1.

Characterization of microcapsule

The morphological characteristics of the microcapsules were investigated using a scanning electron microscope (SEM- ZEISS GEMINI 500). The attenuated total reflectance-fourier transform infrared spectroscopy (ATR-FTIR) analysis was performed to examine the chemical structure of microcapsule. The phase change temperatures and heat storage/release capacities of the microcapsules were determined by differential scanning calorimetry (DSC) analysis. The photo-thermal conversion performance of the prepared microcapsule was investigated using an experimental setup consisting of an insulated box, a UV lamp (25 Watt), a thermal camera and a computer. Before the test, microcapsule samples were compressed into a 2x2 cm polyurethane based insulated box and kept in the refrigerator to cool down to temperatures below the melting temperature of the capsules. In the test, the cooled microcapsule samples were subjected to ultraviolet (UV) radiation for a period of 15 minutes, after which the UV light was switched off to allow cooling. The temperature change on the surface of the microcapsule sample was monitored with a thermal camera, and a time-dependent temperature change graph was obtained. The photo-thermal conversion efficiencies of the microcapsules were calculated using the formula presented in Equation 1. In the equation, the following variables are defined: m is the mass of the microcapsule, ΔH is the melting enthalpy of the microcapsule obtained from DSC analysis, P is the light radiation intensity, S is the measured surface area, and tme and tmo are the start and end times of the phase transition, respectively.

$$n = \frac{m.\Delta H}{P.S.(tme - tmo)} * 100$$

Equation 1

In order to examine the leakage-proofing performance of the produced composite microcapsules, the microcapsule sample was placed on filter paper and heated at 60°C in an oven for one hour. The photographs taken before and after the heating process were evaluated visually (Tian et al., 2020).

RESULTS AND DISCUSSION

SEM analysis results

The SEM analysis was performed to examine the morphological properties of G/GA/LA-SA microcapsules, and the resulting SEM micrograph is presented in Figure 1. According to SEM micrograph, G/GA/LA-SA microcapsules had spherical morphology and smooth surface. Additionally, the particles were observed to be below 1 μm in diameter.

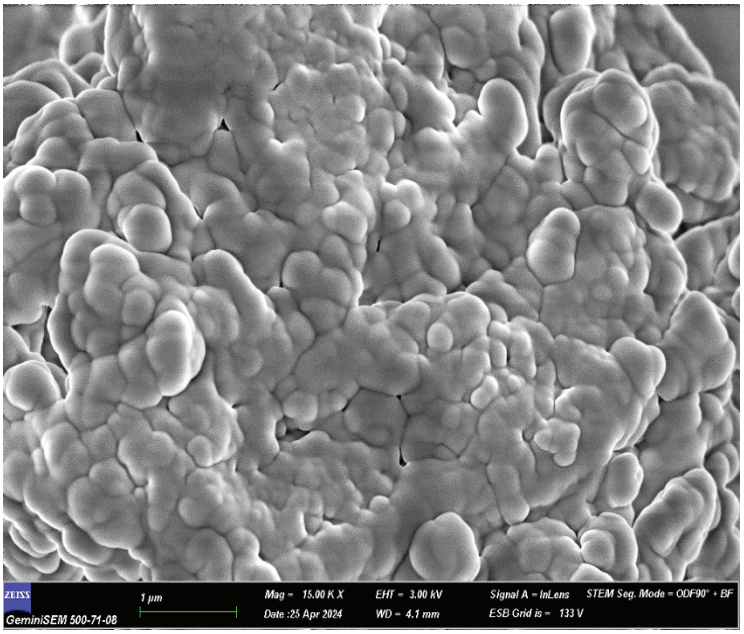


Figure 1. SEM micrograph of G/GA/LA-SA microcapsules

FTIR- ATR Results

The chemical structure of the microcapsules was investigated using attenuated total reflection (ATR) spectroscopy. The IR spectra of the core, shell materials and microcapsules were presented in Figure 2. In the IR spectrum of the microcapsule, the peak at 3294 cm^{-1} was attributed to the OH stretching peak of gum arabic and 1-tetradecanol. The peaks observed at 2920 and 2850 cm^{-1} in the IR spectrum of 1-tetradecanol were identified as C-H stretching peaks. Furthermore, the pronounced peaks observed at 1472 cm^{-1} and 1463 cm^{-1} in the IR spectrum of the microcapsule were attributed to the C-H bending peak of 1-tetradecanol, while the double peak at 730 cm^{-1} and 720 cm^{-1} was the characteristic peak of 1-tetradecanol (Tozum et al., 2020).

On the other hand, the Cu (II)-O vibration peak observed at wavelengths of 471 and 416 cm-1 in the IR spectrum of CuO nanoparticles was revealed at wavelengths of 525 and 484 cm^{-1} in the IR spectrum of microcapsules. These findings indicate that 1-tetradecanol was successfully encapsulated within the gum arabic/CuO wall structure.

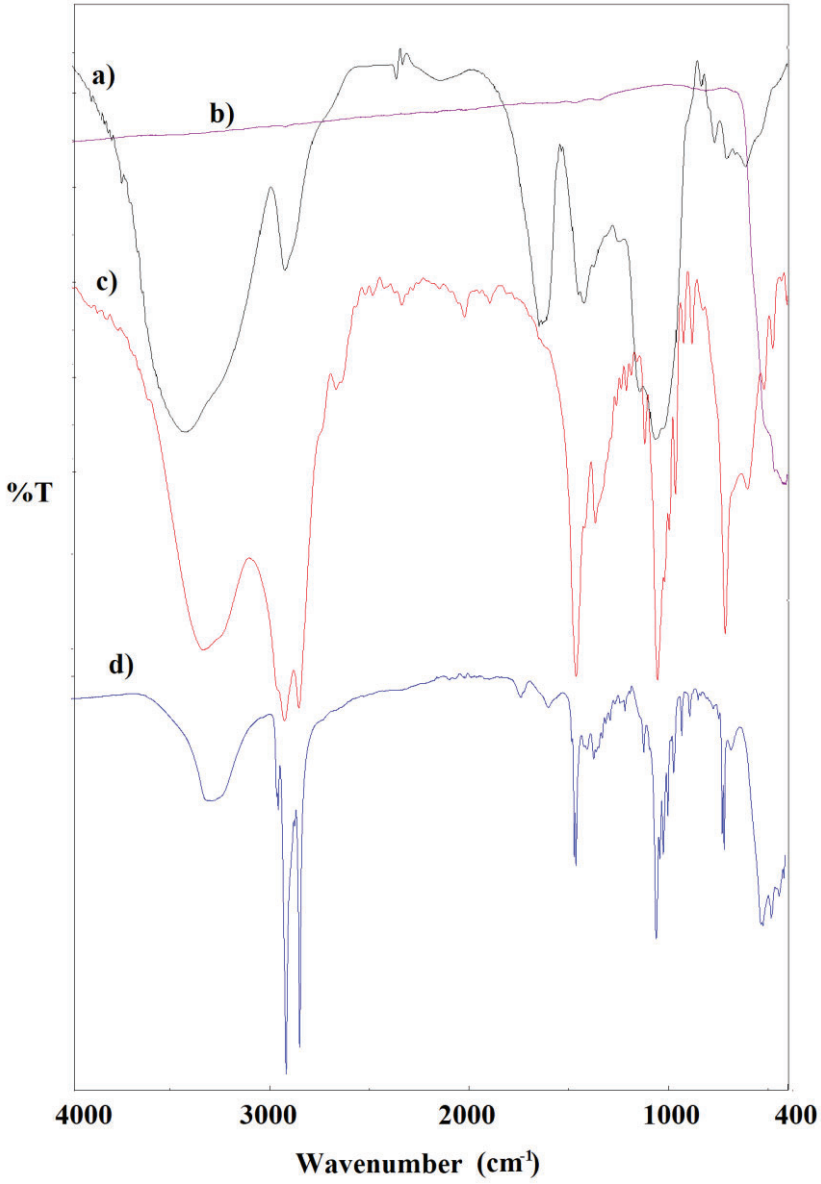


Figure 2. IR spectrum of gum Arabic (a), CuO (b), 1-tetradecanol (c) and G/GA/LA-SA microcapsules

DSC Results

The phase change temperatures and heat storage properties of the microcapsule were analyzed by differential scanning calorimetry (DSC), and the resulting DSC graph was presented in Figure 3. The capsule sample exhibited a heat storage capacity of 146.8 J/g at 36.60 °C, while it demonstrated a heat release capacity of -143.3 J/g at 35.24 °C. The findings indicated that the manufactured microcapsules exhibited an exceptionally high heat storage capacity, with the storage temperatures close to body temperature.

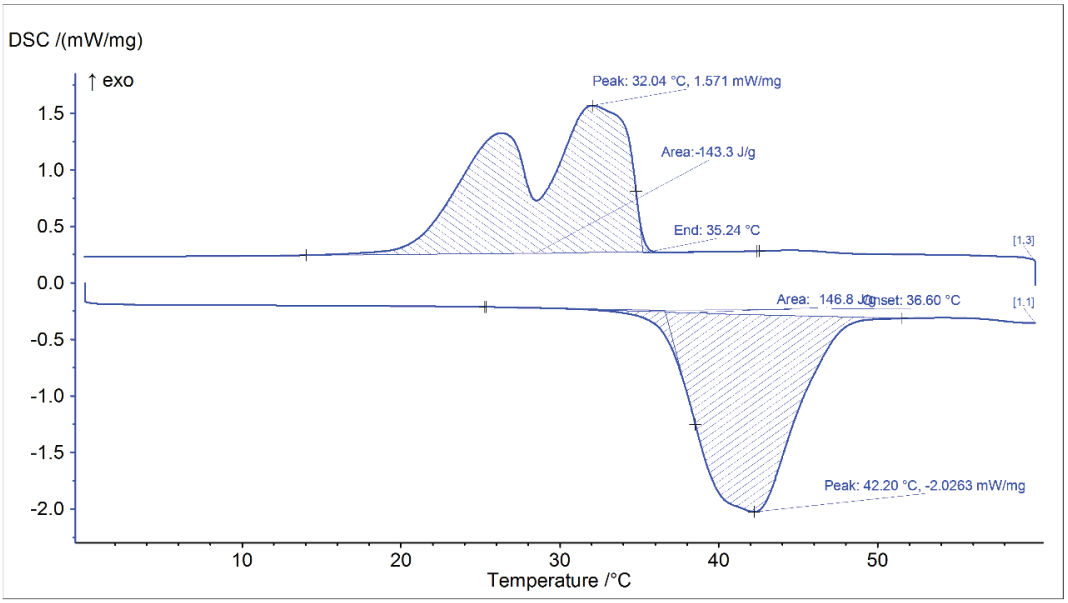


Figure 3. DSC graph of GA/CuO/TD microcapsule

Evaluation of Photo-thermal Conversion Performances

The photothermal conversion efficacy of the microcapsules was evaluated through the utilization of a configuration comprising a UVA lamp, thermal camera and a polyurethane box. The resulting temperature-time graph was presented in Figure 4. It was determined that the phase transition of GA/CuO/TD microcapsules exposed to UVA light commenced at approximately 36°C, concluded in 810 seconds, and attained a maximum temperature of 49.9°C. The photo-thermal conversion efficiency of the microcapsule was calculated to be %79.95. The findings indicate that GA/CuO/TD microcapsule samples are capable of capturing UV light and converting it into heat energy.

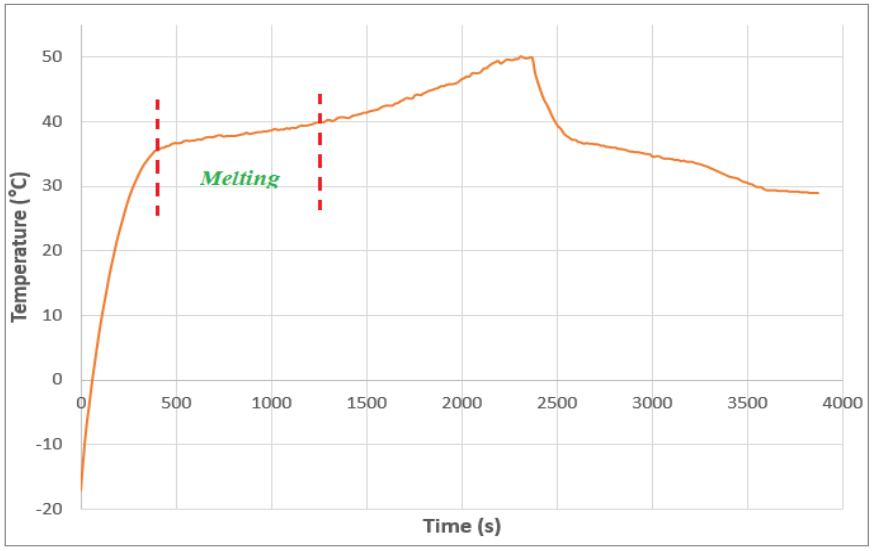


Figure 4. Temperature–time curves of GA/CuO/TD microcapsules

The Leakage Proofing Test Results

The leakage performance of the microcapsules was evaluated through a leakage test, and the resulting images were presented in Figure 5. Upon completion of the test, no wetting was observed on the filter paper on which the microcapsules were placed following an hour of heating. This means that the microcapsules do not leak the core material they contain. In other words, despite the heating the microcapsule shell effectively prevented the core material from escaping and provided robust leakage-proof.

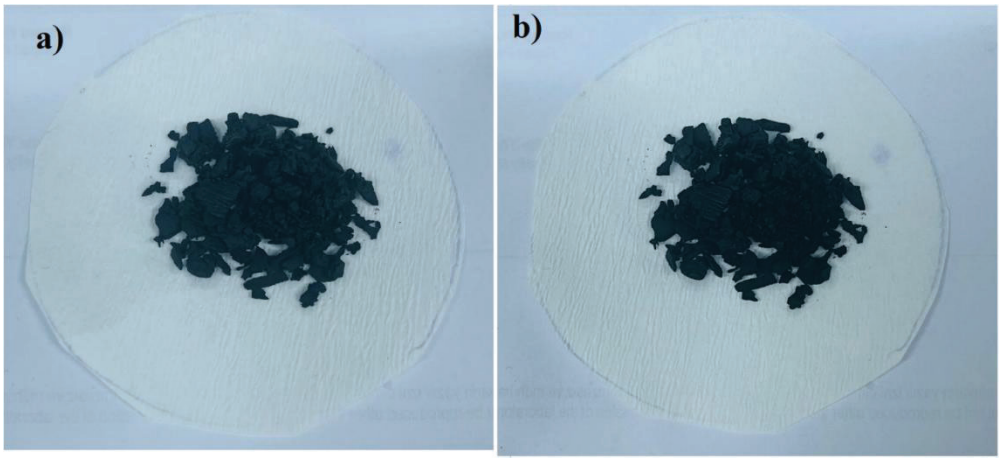


Figure 5. Leakage test of GA/CuO/TD microcapsules (a: before heating; b: after heating for 1 hour)

CONCLUSIONS

In this study, GA/CuO/TD composite microcapsules were prepared using the complex coacervation method. SEM analysis revealed the formation of capsules with a diameter below 1 µm and a spherical morphology. Furthermore, the composite microcapsules demonstrated a noteworthy capacity for heat storage, reaching 146.8 J/g, and exhibited a notable photothermal conversion efficiency of 79.9% when subjected to solar radiation. The findings indicated that the GA/CuO/TD microcapsules have the potential to be employed as a thermal energy storage material.

REFERENCES

Chen, X., Tang, Z., Gao, H., Chen, S. & Wang, G. (2020). Phase change materials for electro-thermal conversion and storage: from fundamental understanding to engineering design. Iscience, 23(6), 101208

Fan, R., Zheng, N. & Sun, Z. (2022). A modified method to quantify the photo-thermal conversion efficiency of shape-stable phase change materials. Solar Energy Materials and Solar Cells, 237, 111572.

Huang, M., Luo, Y., Zhong, Y., Xiao, M. & Hu, J. (2017). Preparation and characterization of microencapsulated phase change materials with binary cores and poly (allyl methacrylate) (PALMA) shells used for thermo-regulated fibers. Thermochimica Acta, 655, 262-268.

Li, S., Ji, W., Zou, L., Li, L., Li, Y. & Cheng, X. (2022). Crystalline TiO2 shell microcapsules modified by Co3O4/GO nanocomposites for thermal energy storage and photocatalysis. Materials Today Sustainability, 19, 100197.

Liu, L., Miao, X., Cheng, X., Wang, H., Guo, M., Cheng, F. & Zhang, M. (2022). Preparation and characterization of ZnO/SiO2@ n-octadecane nanocapsule for ultraviolet absorbing and photothermal conversion energy storage. Journal of Energy Storage, 54, 105363.

Liu, J., Chen, L., Fang, X. & Zhang, Z. (2017). Preparation of graphite nanoparticles-modified phase change microcapsules and their dispersed slurry for direct absorption solar collectors. Solar energy materials and solar cells, 159, 159-166.

Ma, X., Liu, Y., Liu, H., Zhang, L., Xu, B. & Xiao, F. (2018). Fabrication of novel slurry containing graphene oxide-modified microencapsulated phase change material for direct absorption solar collector. Solar energy materials and solar cells, 188, 73-80.

Maithya, O. M., Zhu, X., Li, X., Korir, S. J., Feng, X., Sui, X. & Wang, B. (2021). High-energy storage graphene oxide modified phase change microcapsules from regenerated chitin Pickering Emulsion for photothermal conversion. Solar Energy Materials and Solar Cells, 222, 110924.

Maithya, O. M., Li, X., Feng, X., Sui, X. & Wang, B. (2020). Microencapsulated phase change material via Pickering emulsion stabilized by graphene oxide for photothermal conversion. Journal of materials science, 55(18), 7731-7742.

Tian, Y., Liu, Y., Zhang, L., Hua, Q., Liu, L., Wang, B., & Tang, J. (2020). Preparation and characterization of gelatin-sodium alginate/paraffin phase change microcapsules. Colloids and Surfaces A: Physicochemical and Engineering Aspects, 586, 124216.

Tözüm, M. S., Alkan, C., & Alay Aksoy, S. (2020). Preparation of poly (methyl methacrylate-co-ethylene glycol dimethacrylate-co-glycidyl methacrylate) walled thermochromic microcapsules and their application to cotton fabrics. Journal of Applied Polymer Science, 137(24), 48815.

Wang, X., Zhang, C., Wang, K., Huang, Y. & Chen, Z. (2021). Highly efficient photothermal conversion capric acid phase change microcapsule: Silicon carbide modified melamine urea formaldehyde, Journal of Colloid and Interface Science, 582, 30-40.

Wang, X., Li, C. & Zhao, T. (2018). Fabrication and characterization of poly (melamine-formaldehyde)/silicon carbide hybrid microencapsulated phase change materials with enhanced

thermal conductivity and light-heat performance. Solar Energy Materials and Solar Cells, 183, 82-91.

Yuan, K., Liu, J., Fang, X. & Zhang, Z. (2018). Novel facile self-assembly approach to construct graphene oxide-decorated phase-change microcapsules with enhanced photo-to-thermal conversion performance, Journal of Materials Chemistry A, 6(10), 4535-4543.

Zhao, Q., He, F., Zhang, Q., Fan, J., He, R., Zhang, K., Yan,H., & Yang, W. (2019). Microencapsulated phase change materials based on graphene Pickering emulsion for light-to-thermal energy conversion and management. Solar Energy Materials and Solar Cells, 203, 110204.

Zhao, K., Wang, J., Xie, H., & Guo, Z. (2022). Enhanced photothermal conversion and thermal conductivity of phase change n-Octadecane microcapsules shelled with nano-SiC doped crosslinked polystyrene. Energy Storage and Saving, 1(4), 284-292.

APPLICATION of $CuFe_2O_4$ on the Cr(VI) PHOTOREDUCTION

Assoc. Prof. Dr. Hafize Nagehan KÖYSÜREN

Kırşehir Ahi Evran University, Faculty of Engineering and Architecture, Department of Environmental Engineering, Kırşehir-Türkiye

ORCID: 0000-0002-7115-2250

Prof. Dr. Özcan Köysüren*

Ankara University, Faculty of Engineering, Department of Energy Systems Engineering, Ankara-Türkiye

(Responsible Author*) ORCID: 0000-0001-7100-0399

ABSTRACT

Among heavy metals, hexavalent chromium (Cr(VI)) is considered one of the most dangerous pollutants. It is not only a highly corrosive element, but also a carcinogenic substance. Cr(VI) is very mobile in nature because it has very weak adhesion to inorganic surfaces. The rapid development of industries such as electroplating, leather and chromate manufacturing caused serious wastewater problems, and Cr(VI), which has high toxicity and high solubility features, has begun to be widely seen in industrial wastewater. Therefore, it is important to remove Cr(VI) ions from the wastewater environment. In this study, Cr(VI) removal was carried out by photoreduction technique. For this purpose, copper ferrite ($CuFe_2O_4$) was synthesized through a facile citric acid assisted auto combustion process. The synthesized product was exposed to a heat treatment at 800°C for 3 h. FTIR and XRD analysis showed that $CuFe_2O_4$ was synthesized successfully. The transmittance peak belonging to the Fe-O bond was observed on the FTIR spectrum, and on the XRD diffractogram of $CuFe_2O_4$, the diffraction peaks of the spinel crystal phase were observed. A considerably higher magnetic saturation value was obtained with the as-prepared product. According to SEM images, $CuFe_2O_4$ nanoparticles in the range of about 200-400 nm are estimated to be obtained. It was understood that $CuFe_2O_4$ absorbed the incoming light between 200–250 nm and 400–800 nm, respectively. According to the Tauc plot analysis using UV-Vis absorption data, the optical band gap energy was determined as 1.0 eV. 10.9% of Cr(VI) removal was obtained with $CuFe_2O_4$ under the visible light irradiation within 120 min.

Keywords: Cr(VI) removal, photoreduction, $CuFe_2O_4$, photocatalyst.

INTRODUCTION

Hexavalent chromium (Cr(VI)) has considered one of the most dangerous heavy metal ions and pollutants. It is not only a highly corrosive heavy metal ion, but also a carcinogenic element (Feng et al., 2019). The development of certain industries such as electroplating, leather, chromate manufacturing and metallurgy industries has caused serious wastewater problems, and Cr(VI) with high toxicity and high solubility properties has begun to be widely observed in industrial wastewater. Various traditional methods such as flotation, coagulation-flocculation, chemical precipitation, ion exchange and adsorption are used to remove Cr(VI) ions from the wastewater environment. As an alternative to the mentioned methods, photocatalysis process is an environmentally friendly, low energy consumption, simple and non-secondary pollution method. The photocatalysis process allows the reduction of highly toxic Cr(VI) ions in aqueous solutions to less toxic Cr(III) ions using only UV light or sunlight energy (Wu et al., 2021).

The net reactions estimated to occur for the reduction of Cr(VI), which is mostly present as dichromate ($Cr_2O_7^{2-}$) ion in water at standard conditions (pH ~ 7), oxidation of water and reduction of oxygen molecule are shown by the following equations (Cheng et al., 2015):

$$\text{Semiconductor} + hv \rightarrow h^+ + e^- \quad (1)$$

$$H_2O + h^+ \rightarrow \cdot OH + H^+ \quad (2)$$

$$O_2 + e^- \rightarrow \cdot O_2^- \quad (3)$$

$$Cr_2O_7^{2-} + 14H^+ + 6e^- \rightarrow 2Cr^{3+} + 7H_2O \quad (4)$$

For the recovery and separation of photocatalysts from the solution medium after the Cr(VI) photoreduction reactions, a semiconductor photocatalyst with magnetic feature can be utilized. In the literature, Mohagheghian et al. (2018) synthesized magnetic semiconductor Fe_3O_4 nanostructures by precipitation method and combined the magnetic nanoparticles with WO_3 in the composite structure. 99% of Cr(VI) was reduced at the end of 300 min under visible light with the magnetic composite photocatalyst. Thanks to the magnetic Fe_3O_4, the composite photocatalyst could be easily separated from the solution medium by magnetic separation technique after the Cr(VI) removal process (Mohagheghian et al., 2018). As a different example of the application of magnetic semiconductor as photocatalyst, Zhang et al. (2020) synthesized magnetic $ZnFe_2O_4$ nanoparticles and combined with g-C_3N_4 nanoparticles, and approximately 95% Cr(VI) removal was achieved with the obtained heterostructure under visible light after 60 min (Zhang et al., 2020). In a different study, Nasrallah et al. (2011) synthesized magnetic $CuFe_2O_4$ nanoparticles and combined with CdS nanoparticles in the composite structure. They achieved approximately 60% of Cr(VI) photoreduction after 240 min under a light source at 650 nm wavelength (Nasrallah et al., 2011).

Copper ferrite ($CuFe_2O_4$) is a strong magnetic semiconductor with a saturation magnetization value of 31.92 emu/g at room temperature (Kurian and Mathew, 2018). $CuFe_2O_4$, which is also a material with high catalytic activity and thermal stability, is widely used in photocatalysis and solar water splitting processes. In this study, magnetic $CuFe_2O_4$ nanoparticles were synthesized and the Cr(VI) photoreduction efficiency of the as-prepared magnetic nanoparticles was studied.

MATERIALS AND METHODS

1 mmol of copper (II) nitrate trihydrate ($Cu(NO_3)_2.3H_2O$) and 2 mmol of iron nitrate ($Fe(NO_3)_3.9H_2O$) were dissolved in 10 ml of distilled water. Then, 2 mmol of citric acid ($C_6H_8O_7$) was added to theas-prepared solution under stirring using a magnetic stirrer. The pH of the as-prepared solution was adjusted to 8 using HCl or NH_3. Then, the prepared solution was heated to 100°C under continuous stirring. After all the water was evaporated, the solution was expected to turn into a gel form. The gel structure that emerged with the continuation of heating turned into a powder form by a spontaneous combustion reaction. The composite particles obtained in powder form were heat treated at 800°C for 3 hours. Pure $CuFe_2O_4$ was obtained after following the specified reaction steps.

Fourier transform infrared (FTIR) spectroscopy analysis of $CuFe_2O_4$ nanoparticles was carried out using Nicolet 6700 (Thermo Scientific) model spectrophotometer. FTIR spectrum of $CuFe_2O_4$ nanoparticles was used to characterize the chemical bond structures of the magnetic semiconductor. X-ray diffraction (XRD) pattern of the as-prepared sample was recorded using Riguku Ultima IV model X-ray diffraction device. The crystal structure of the magnetic semiconductors was investigated by XRD analysis. FTIR and XRD analyses are important in terms of showing that the magnetic semiconductor can be synthesized successfully. The morphology of the synthesized photocatalyst samples was examined using QUANTA 400F model field emission scanning electron microscope (FE-SEM). In addition, the elemental structure of the photocatalyst samples was investigated by energy dispersive X-ray (EDX) spectroscopy (JXA-8230 EDX Microanalyzer). The saturation magnetization value of $CuFe_2O_4$

nanoparticles was measured by a vibrating sample magnetometer (VSM, Cryogenic Limited PPMS) under a magnetic field at room temperature.

A visible light lamp (Osram Ultravitalux) with a power of 300 W was used in the Cr(VI) photoreduction experiment. Simulated Cr(VI) solution (20 mg/l) was prepared by dissolving 2 mg of potassium dichromate ($K_2Cr_2O_7$) in 100 ml of distilled water. 50 mg of photocatalyst was dispersed in the 100 ml Cr(VI) solution. The solution was stirred with a magnetic stirrer in the dark for half an hour to provide adsorption-desorption equilibrium between the photocatalyst and Cr(VI) ions. Then, the Cr(VI) solution was exposed to visible light radiation. While visible light radiation was applied, 2 ml of simulated Cr(VI) solution was sampled every 20 min and centrifuged to separate from the solid particles. Diphenylcarbazide (DPC) photometric technique was applied to the solution separated from the photocatalyst to determine the Cr(VI) concentration in the simulated solution (Sun et al., 2022). During the DPC technique, 1 ml of sulfuric acid (0.2 M) and 1 ml of 1.5-diphenylcarbazide (0.5% w/v) were added to the 2 ml centrifuged sample and mixed. After approximately 5 min, the sample solution was analyzed using a UV-Vis spectrophotometer (Genesys 10S, Thermo Scientific). Cr(VI) photoreduction efficiency was calculated by comparing the absorbance values obtained at 543 nm using the following equation (5):

$$\text{Cr(VI) photoreduction efficiency (\%)} = (C_0 - C)x100 / C_0 \quad (5)$$

In the equation, C_0 and C correspond to the Cr(VI) concentration values before and after the Cr(VI) photoreduction reaction.

FINDINGS AND DISCUSSION

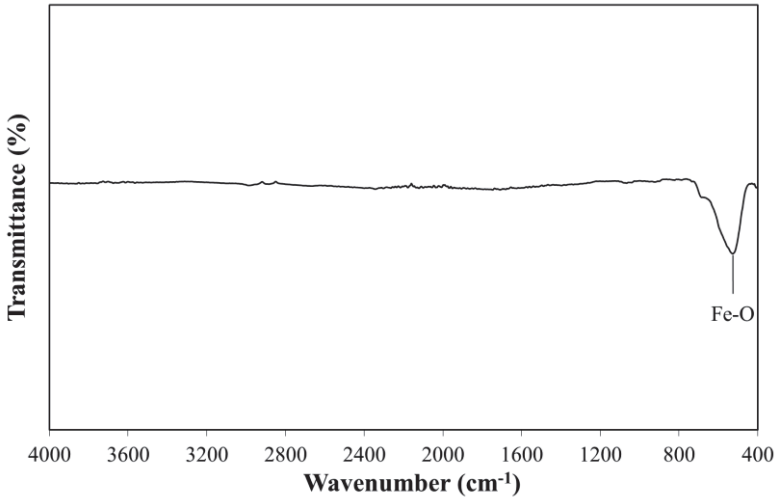


Figure 1. FTIR spectrum of $CuFe_2O_4$ nanoparticles

The spectrum of $CuFe_2O_4$ on Figure 1 exhibits a strong transmittance peak at 527 cm^{-1}, which is attributed to the symmetric vibration of the metal oxide (Cu-O and Fe-O) (Amuthan et al., 2022). Ferrites in spinnel structure exhibit two transmittance peaks in the range of 400-600 cm^{-1}, which are attributed to the vibration of the bond between oxygen ions and cations in the tetrahedral and octahedral regions in the crystal unit cell. The FTIR spectrum of $CuFe_2O_4$ confirms the presence of spinel phase in the synthesized photocatalyst (Othman et al., 2019). Figure 2 shows the XRD diffractogram of $CuFe_2O_4$, which is in good agreement with the standard data (JCPDS 34-0425) (Zhao et al., 2017). The diffraction peaks belonging to the (112), (220), (103), (311), (222), (400), (312), (511), (440) planes of spinel $CuFe_2O_4$ are observed at the diffraction angle values of 29.9º, 30.6º, 34.7º, 35.9º, 37.2º, 43.9º, 54.1º, 58.0º and 62.2º, respectively. The XRD diffractogram of $CuFe_2O_4$ also reveals that the synthesized product was successfully obtained.

Figure 3a shows the optical properties of the synthesized samples. According to the UV-Vis absorption spectrum, it is understood that pure $CuFe_2O_4$ can absorb the incident light between 200-250 nm and 400-800 nm, respectively. The optical band gap of the sample was determined by the Tauc plot method using the following equation (Jiao et al., 2023):

$$(\alpha hv)^2 = A(hv - E_g) \quad (6)$$

where A is a constant, hv represents the photon energy, α represents the absorption coefficient and Eg represents the optical band gap (Jiao et al., 2023). The optical band gap value is determined by a line extended to the x-axis from the $(\alpha hv)^2$-hv curve drawn using UV-Vis absorbance data (Figure 3b). The optical band gap of $CuFe_2O_4$ was determined to be 1.00 eV.

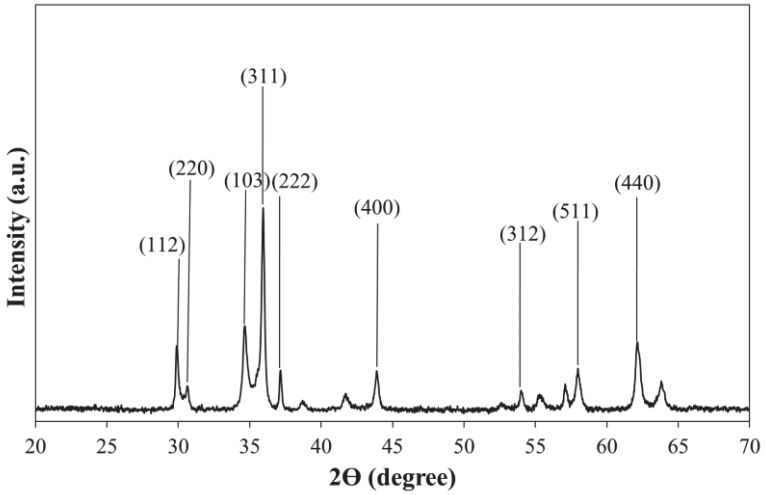


Figure 2. XRD pattern of $CuFe_2O_4$

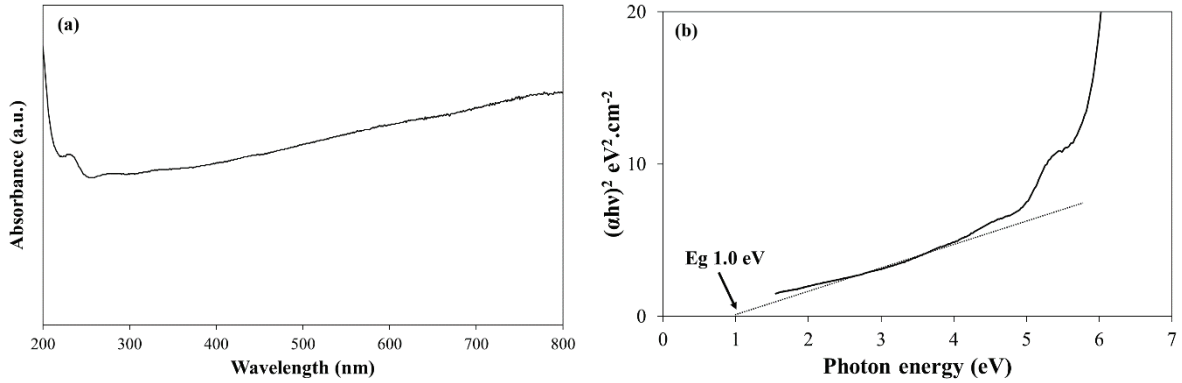


Figure 3. (a) UV-Vis absorbance spectrum of $CuFe_2O_4$, (b) Tauc's plot for $CuFe_2O_4$

The morphology of the synthesized sample was examined by field emission scanning electron microscopy (FESEM) (Figure 4). According to FESEM images, $CuFe_2O_4$ samples were obtained in nanoparticle structure with a size of 200–400 nm.

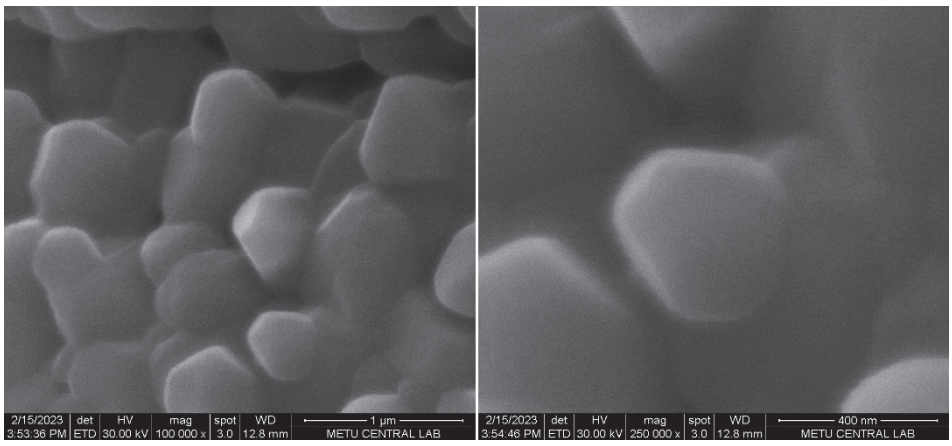


Figure 4. FESEM images of $CuFe_2O_4$ nanoparticles

The EDX spectrum shows the presence of Cu, Fe and O atoms in the structure (Figure 5). It was confirmed by EDX analysis that $CuFe_2O_4$ was synthesized successfully.

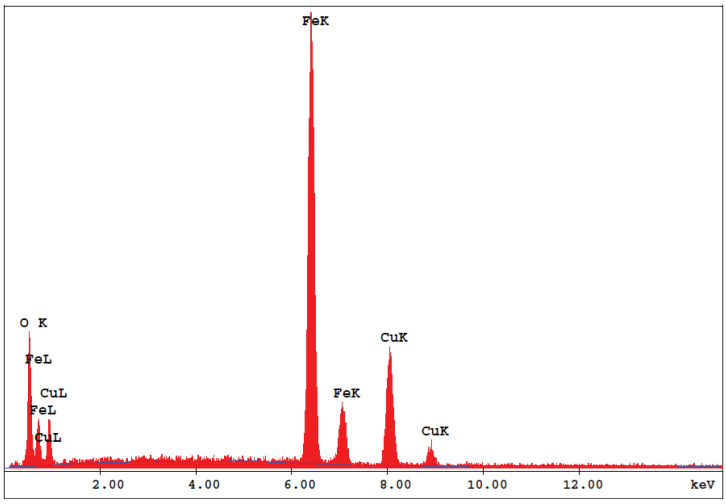


Figure 5. EDX spectrum of $CuFe_2O_4$

Figure 6a shows the UV-Vis absorption spectrum of Cr(VI) in the presence of $CuFe_2O_4$. The intensity of the absorption peak at 543 nm decreases with time under visible light radiation. The Cr(VI) photoreduction efficiency of pure $CuFe_2O_4$ was calculated as 10.9% after 120 min of visible light irradiation (Figure 6b). Relatively low Cr(VI) photoreduction efficiency was obtained with pure $CuFe_2O_4$. This can be attributed to the high recombination rate of photogenerated electron-hole pairs formed on the semiconductor photocatalyst under visible light.

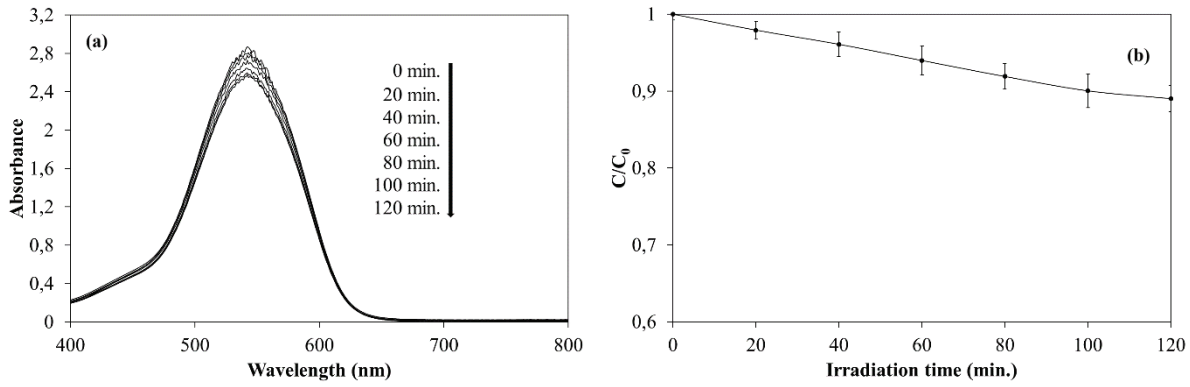


Figure 6 (a) Time dependent change of UV-Vis absorption spectrum of Cr(VI) solution in the presence of $CuFe_2O_4$, **(b)** time-dependent photoreduction rate of Cr(VI) under visible light source in the presence of $CuFe_2O_4$

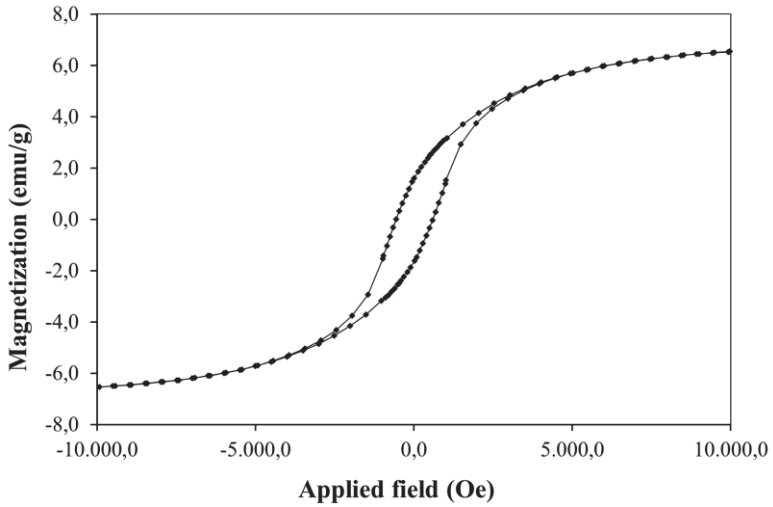


Figure 7. Magnetic hysteresis loop of $CuFe_2O_4$

The magnetic hysteresis loop of pure $CuFe_2O_4$ is shown in Figure 7. The saturation magnetization value of pure $CuFe_2O_4$ was measured to be 6.55 emu/g. Magnetic hysteresis loops revealed the ferromagnetic property of the prepared sample. Therefore, the as-prepared sample can be easily removed from the reaction medium by magnetic separation, which is important for the reusability of the prepared photocatalyst.

CONCLUSION AND RECOMMENDATIONS

$CuFe_2O_4$, a visible light driven photocatalyst, was synthesized through a facile sol-gel technique. The highest Cr(VI) removal, 10.9%, was achieved with $CuFe_2O_4$ nanoparticles within 120 min of visible light irradiation. FTIR, XRD and EDX analyzes confirmed the successful synthesis of $CuFe_2O_4$ nanoparticles. According to FESEM images, $CuFe_2O_4$ in spherical shape between 200-400 nm were obtained. The saturation magnetization value of pure $CuFe_2O_4$ was found out to be 6.55 emu/g.

THANKS AND INFORMATION NOTE

This research was supported by Kırşehir Ahi Evran University Scientific Research Projects Coordination Unit. Project Number: MMF.A4.23.002, 2023.

REFERENCES

Amuthan, T., Sanjeevi, R., Kannan, G. R., Sridevi, A. (2022). A novel p-CuFe2O4/n-ZnS heterojunction photocatalyst: Co-precipitation synthesis, characterization and improved visible-light driven photocatalytic activity for removal of MB and CV dyes, *Physica B*, 638, 413842.

Cheng, Q., Wang, C., Doudrick, K., Chan, C. K. (2015). Hexavalent chromium removal using metal oxide photocatalysts, *Applied Catalysis B-Environmental*, 176, 740-748.

Feng, M., Liu, Y., Zhao, Z., Huang, H., Peng, Z. (2019). The preparation of Fe doped triclinic-hexagonal phase heterojunction WO3 film and its enhanced photocatalytic reduction of Cr(VI), *Materials Research Bulletin*, 109, 168-174.

Jiao, Y. X., Wang, S., Liu, Y. P., Li, X., Yang, W. L., Han, S., Zhang, H., Jiang, J. X. (2023). A novel Zn0.5Cd0.5S/WO3middotH2O S-scheme heterostructures with one-pot synthesis for significant photodegradation of toxic Cr(VI) and organic RhB pollutants: Kinetics, degradation mechanism and photocatalytic evaluation, *Journal of Alloys and Compounds*, 938, 168576.

Kurian, J., Mathew, M. J. (2018). Structural, optical and magnetic studies of CuFe2O4, MgFe2O4 and ZnFe2O4 nanoparticles prepared by hydrothermal/solvothermal method, *Journal of Magnetism and Magnetic Materials*, 451, 121-130.

Mohagheghian, A., Ayagh, K., Godini, K., Shirzad-Siboni, M. (2018). Photocatalytic reduction of Cr(VI) from synthetic, real drinking waters and electroplating wastewater by synthesized amino-functionalized Fe3O4-WO3 nanoparticles by visible light, *Journal of Industrial and Engineering Chemistry*, 59, 169-183.

Nasrallah, N., Kebir, M., Koudri, Z., Trari, M. (2011). Photocatalytic reduction of Cr(VI) on the novel hetero-system CuFe2O4/CdS, *Journal of Hazardous Materials*, 185 (2-3), 1398-1404.

Othman, I., Abu Haija, M., Banat, F. (2019). Catalytic Properties of Phosphate-Coated CuFe2O4 Nanoparticles for Phenol Degradation, *Journal of Nanomaterials* 2019, 3698326.

Sun, J, Sun Y. Q., Zhang, L., Cao, F. M. (2022). The highly enhanced Cr(VI) photoreduction removal by oxalic acid coordinated with iron-loaded waste Loofah, *Environmental Research* 205,112456.

Wu, Y., Chen, C., He, S., Zhao, X., Huang, S., Zeng, G., You, Y., Cao, Y., Niu, L. (2021). In situ preparation of visible-light-driven carbon quantum dots/NaBiO3 hybrid materials for the photoreduction of Cr(VI), *Journal of Environmental Sciences*, 99, 100-109.

Zhang, H., Zhu, C., Zhang, G., Li, M., Tang, Q., Cao, J. (2020). Palladium modified ZnFe2O4/g-C3N4 nanocomposite as an efficiently magnetic recycling photocatalyst, *Journal of Solid State Chemistry*, 288, 121389.

Zhao, Y. L., Lin, C. P., Bi, H. J., Liu, Y. G., Yan, Q. S. (2017). Magnetically separable CuFe2O4/AgBr composite photocatalysts: Preparation, characterization, photocatalytic activity and photocatalytic mechanism under visible light, *Applied Surface Science,* 392, 701-707.

THE USE OF GLOOPY GLAZE IN CONTEMPORARY CERAMIC ART

Ferda Tazeoğlu Filiz

Selcuk Universty, Fine Art Faculty, Ceramic, Konya, Turkey

ORCID ID: 0000-0002-3411-2575

ABSTRACT

Glaze is a type of coating material used in ceramic art and industry to provide various properties to ceramic surfaces. Glazes can be shiny, matte, or opaque, with various additives included to achieve desired effects. Among these, “artistic glazes” are primarily applied to flat surfaces and are continually developed by both commercial manufacturers and artists. Artistic glazes can be classified into categories such as crackle glazes, ash glazes, celadon glazes, copper red glazes, crystal glazes, crater glazes, metallic glazes, dot effect glazes, drippy glazes, and fluid glazes.

Additionally, there are glazes referred to as “gloopy glazes” in international sources, which currently lack a national literature equivalent. These glazes resemble a gloop due to their sticky structure, high alumina, and silicium content, and have become increasingly popular among artists for their versatility and impact on shaping forms. Gloopy glazes are more viscous than standard glazes but possess a higher melting ability compared to clays at elevated temperatures. They can be applied in thicker layers than other glazes.

Unlike artistic glazes, gloopy glazes can be used not only as a surface coating but also as a material that influences the shape of the form itself. This unique characteristic sets them apart from other glaze types. Research has been conducted to identify artists using gloopy glazes in their works, evaluating the differences in their usage patterns and the contributions this glaze type makes to contemporary ceramic art.

Keywords: Gloop, Gloopy Glaze, Glaze, Ceramic, Art, Contemporary ceramic.

INVESTIGATION OF USING SERPANTINITE, DOLOMITE AND BARITE ADDED CONCRETE AGAINST RADIATION EFFECT

Aytaç Dinçer[1]

ORCID ID: https://orcid.org/0009-0009-4767-4794

Mehmet Kertmen[1]

ORCID ID: https://orcid.org/0000-0003-1661-7219

Gözde Özlem Örentaş[1]

ORCID ID: https://orcid.org/0000-0001-9656-2638

Halil İbrahim Olucak[1]

ORCID ID: https://orcid.org/0009-0009-4767-4794

[1]**İSKUR HOLDING Kahramanmaraş / Türkiye**

ABSTRACT

As long as radiation sources exist, people are affected by radiation. People have been and continue to be exposed to many harmful radiation events. The harmful effects of radiation last for decades. Apart from nuclear power plants and weapons, nuclear power is used in many areas of technology, including medicine. This situation requires human beings to take precautions against the harmful effects of radiation. In this study, it is aimed to minimize the harmful effects of radiation sources by absorbing them through building elements. In this study, the ability of concrete samples containing serpentinite, dolomite and barite to absorb harmful radioactivity was investigated. Additionally, some mechanical and durability properties of mortar and concrete samples produced with the same additives were examined. In addition to the mechanical properties of the mortar samples such as 7, 28 and 90-day compressive and bending strengths, the sulphate resistance of the samples kept in 10% Na2SO4 solution for 90 days was examined. 7, 28, 90 day compressive strength of concrete samples were found by pressure press, ultrasonic test and Schmidt Hammer methods. In addition, abrasion resistance, permeability, freeze-thaw resistance and microstructures were examined. The samples were sized 10x10x10~~2~~ cm and measured at 100 Kv 2.5 mm Al. In the study, it was determined that serpentinite, dolomite and barite added concrete samples significantly increased the radiation shielding feature, but caused decreases in strength and durability properties after certain rates.

Keywords: Serpentinite, Dolomite, Barite, Linear absorption coefficient, Concrete Durability

NONLINEAR VIBRATION ANALYSIS OF CARBON NANOTUBE-REINFORCED SHALLOW SHELLS WITH FUNCTIONALLY GRADED DISTRIBUTION

Zakia Hammou[1], Zakia Guezzen[2], Zouaoui Sereir[2] and Yamna Hammou[3]

[1] Physical chemistry Department, Chemistry Faculty, University of Science and Technology of Oran, USTO, Oran, Algeria.

[2] Composite Structures and Innovative Materials Laboratory, Mechanical Engineering Faculty, University of Science and Technology of Oran, USTO, Oran, Algeria.

[3] Maritime Sciences and Engineering Laboratory, Mechanical Engineering Faculty, University of Science and Technology of Oran, USTO, Oran, Algeria

ABSTRACT

In this paper, we investigate the nonlinear vibration behavior of shallow shells reinforced with carbon nanotubes (CNTs). The reinforcement is modeled as functionally graded (FG) along the radial direction of the shell. The material properties of these functionally graded carbon nanotube-reinforced composites (FG-CNTRCs) are assumed to vary through the shell thickness, estimated via a micromechanical model. Nonlinear partial differential equations are derived using the Von Karman geometric nonlinear theory, assuming the shell follows classical shell theory. The problem is reduced using the Galerkin technique, leading to a system of nonlinear equations with quadratic and cubic terms. These equations are solved using the method of multiple scales (MMS) for simply supported boundary conditions. Our findings indicate that the distribution of carbon nanotubes, mode shapes and the shell's curvature significantly influence the natural frequencies.

Keywords: Galerkin method; Functionally Graded Carbon Nanotube; Fundamental Linear Frequency, resonance.

ASSESSING THE INFLUENCE OF WALL MATERIALS ON COMPARTMENT FIRE BEHAVIOR: A COMPARATIVE ANALYSIS WITH EUROPEAN STANDARDS

Romaissa HACHANA

Blida 1 University, Algeria
ORCID NO: 0009-0002-1384-3333

Souhila AGRED

Chlef University, Algeria

Abdallah BENAROUS

Blida 1 University, LISICPE Laboratory Chlef, Algeria

SUMMERY

This study investigates the impact of wall material type on the characteristics of compartment fires by combining a parametric temperature-time (T-t) curve with the European standards. The study focuses on the effect of various wall materials not only on the temperature curves during the development of the fire but also on the evolution of the upper smoke layer within the enclosure. This impacts directly the openings to be incorporated in the building structure in order to enhance the natural smoke evacuation. The outcomes are discussed in the context of European regulations, to incorporate relevant safety measures. It has been established that the type of wall construction materials plays a crucial role in fire dynamics; therefore, there is a need for careful consideration in the compartment design and ventilation systems. These results are of practical interest for fire safety engineers and reduce the risks of fire in the construction developments, focusing on fire resisting materials and efficient natural ventilation in buildings.

Keywords: Fire engineering, Wall material, SHEVS, Compartment fire, European standards.

INTRODUCTION

Fire engineering is a field positioned at the interface between reactive fluid mechanics, heat transfer, and structural analysis. It has transcended the boundaries of academic research to become an essential prerequisite in professional practice, for firefighters, urban planning engineers, and even fire safety regulation experts [1]. Fire safety strategies are specifically mandated during the design or preliminary studies of industrial compartments, public buildings, and residential complexes [2]. It is therefore crucial to conduct sizing calculations for Smoke and Heat Exhaust Ventilation Systems (SHEVS) to evacuate or at least control the flow of these substances [3]. These calculations are based on correlations adopted by regional fire safety authorities and utilize thermal loads such as the ISO-834 standard [4].

Several attempts have been made to consider scenarios of ultra-fast fire development in large compartments [5]. These studies employed field models without accounting for the effects of natural ventilation. More recent research has focused on comparative analyses between

European and American correlations, where extreme temperatures were derived from numerical models [6]. Updated analyses have leaned towards discussing the validity of thermal load types in the Eurocodes concerning the heating of structures [7], without considering the suitability or effectiveness of natural ventilation. A critical analysis of a parametric fire thermal load (EPFC) was conducted for a large compartment constructed with commercial concrete [8]. The study revealed the influence of wall heat transfer on the temperature evolution history within the compartment.

Based on the literature review, the authors noted a lack of additional studies on the effects of the construction material type on the temperature evolution within the compartment. Moreover, the sizing calculations for openings for natural ventilation (NV) are never correlated with the conditions of thermal loading (Temperature-Time curve) or the heat transfer to the walls (thermal properties of materials) of the compartment. The objective of this paper is to evaluate the impact of wall material type on the development of temperature and smoke layer in a large, naturally ventilated compartment.

MATERIALS AND METHODS

A. Thermal characterization of smoke

A zone model approach assumes that the entire convective heat release rate $\dot{Q}_c$ of the fire is converted into a temperature rise ΔT which induces among other things, a mass flow rate of smoke $\dot{M}$, stratifying at a vertical distance Y_s from the floor. This formalism is derived from analytical relationships established by Merci et al [9]:

$$\dot{M}_s = \dot{Q}_c / c\Delta T \quad (1)$$

$$Y_s = \left(\dot{M}_s / C_e P_f\right)^{2/3} \quad (2)$$

Here, c is the specific heat of smoke, and $\Delta T = T_s - T_\infty$ represents the temperature rise compared to the ambient temperature. P_f is the perimeter of the fire load, and C_e is an empirical coefficient equal to 0.19 for compartments with a floor area exceeding 500 m² [9].

B. Sizing of openings for natural ventilation

Based on the basic configuration of the compartment, the fire development results in the release of smoke, which may or may not be naturally evacuated through existing openings. The verification procedure involves estimating the total area A_{NV} of openings required for smoke extraction. The European standard expresses this quantity as [9].

$$A_{NV}^t C_v = \dot{M}_s T_s / [2\rho_\infty^2 g \delta_s T_\infty \Delta T - \dot{M}_s^2 T_s . T_\infty / (A_i C_i)^2]^{1/2} \quad (3)$$

C. Prediction of temperature evolution over time

In engineering calculations, the transient temperature within the compartment is predicted using correlations that involve the ventilation factor (effect of openings) and the type of wall material (effect of wall heat transfer). Curve 'A' provides an expression for the temperature during the fire development phase as [10].

$$T(t) = T_{max} . (t/t_{max}) . exp\left[1 - \left(\frac{t}{t_{max}}\right)\right] \quad (4)$$

$$t_{max} = q/(a.O);\ T_{max} = b + c[1 - \exp(d.O)] . q^{m - n \times O} \quad (5)$$

The overall opening factor of the compartment is given by [10]:

$$O = A_V.\sqrt{H_{eq}}/A_t \; ; \; H_{eq} = \sum h_i A_i \, / A_V \tag{6}$$

Here, A_V, A_t and h_i denote the total surface area of openings (doors, windows), the total area of partitioning (walls, floor, ceiling), and the height of each opening, respectively. The coefficients a, b, c, d, m, n, vary depending on the nature of the wall material and have specific numerical values [10].

CASE STUDY

The building considered (32 m × 21 m × 5 m) is the same as the one examined in the work of Santarpia et *al*. [10]. It is classified as a large compartment and has five 5 windows (1.2 m × 2 m) positioned 2 meters above the floor, and two 2 large doors (3.2 m × 3.5 m, 2.4 m × 3.5 m). The combustible load (wood) is spread over an area of 100 m², with a heat density of 973.5 MJ/m² [10]. The compartment is naturally ventilated, with walls constructed from commercial concrete (type 1). Given this heat load, the compartment falls under the REI 90 class (5400 s) for structural fire resistance. Figure 1 presents a 3D schematic of the compartment studied.

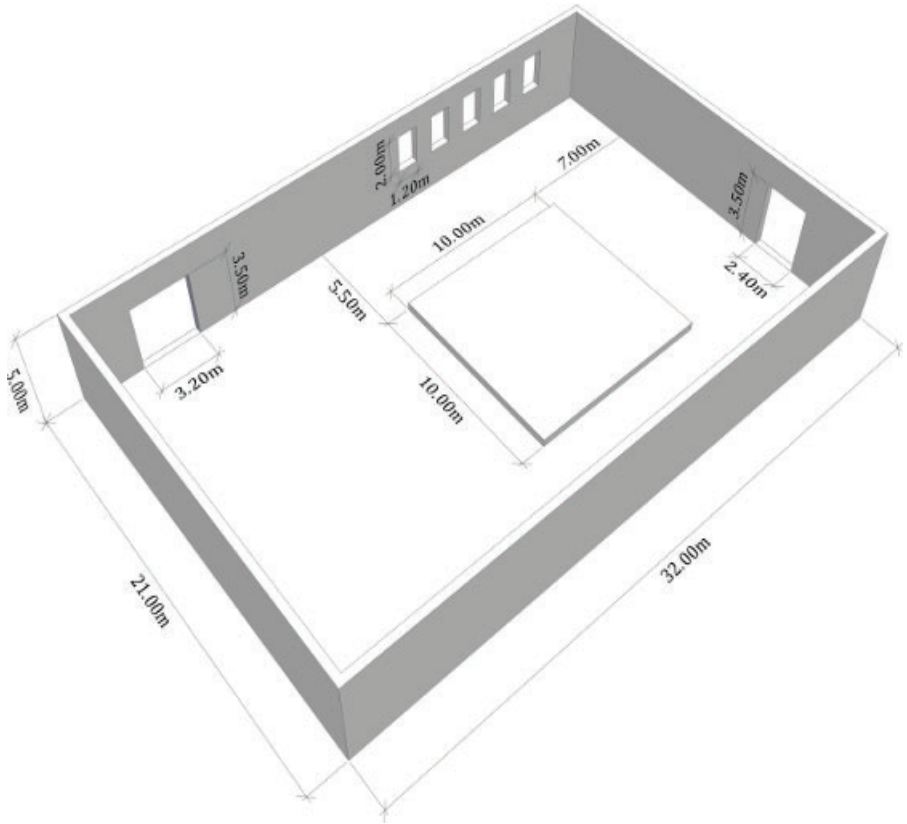


Fig. 1. 3D sketch of the study area [10]

FINDINGS AND DISCUSSION

The walls of the compartment are made from standard commercial concrete (type 1). Two other variants will be examined: lightweight concrete (type 2) and brickwork (type 3). The material properties are shown in the table below (Table I).

Table 1. Materials used (walls)

Concrete	Thermal properties		
	Density (Kg.m^{-3})	*Specific heat (J. Kg^{-1}.K^{-1})*	*Thermal conductivity (W.m^{-1}.K^{-1})*
Type 1	2300	913	1.45
Type 2	1600	840	0.60
Type 3	1900	1000	0.78

Given the significant heat density, it is appropriate to predict the temporal evolution of temperature within the compartment as a function of the natural ventilation rate. The opening factor *O* may vary between a minimum value O_{min}=0.0018 m$^{0.5}$, corresponding to the opening of a single window, and a maximum value reflecting the opening of all doors and windows (O_{max}=0.0289 m0.5). The transition from one limit configuration to another could occur deliberately via human agents (e.g., firefighters' interventions) or naturally during fire development (e.g., breaking of windows, obstruction of openings).

A. Maximum opening factor

As predicted by the European standard curve 'A', the development phase lasts for almost 1 hour (t_{max}=3852 s), indicating that fire resistance will be assessed during the decay phase. The curve in Figure 2 predicts a critical temperature (at t_{REI}=5400 s) of 535°C, which is 6% lower than the flashover temperature. The high thermal levels reveal that the fire, according to this model, is ventilation-controlled, favoring combustion in a well-ventilated regime. Maintaining the same heat load while changing the compartment wall material can be justified by economic or environmental requirements. Lightweight concrete (type 2), though economically attractive, results in a critical temperature of 1083°C, significantly higher (+103%) than its value for standard concrete. In the case of brickwork concrete (type 3), the critical temperature exceeds its reference value by only 22%, even though the material is heavier but has higher thermal conductivity (Fig. 2).

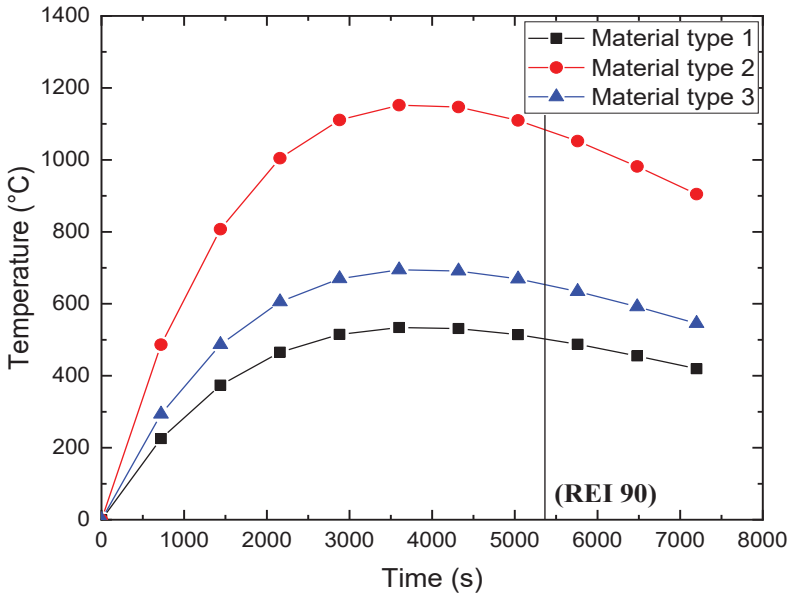


Fig. 2. Temperature-time curve (O=O_{max})

B. Minimum opening factor

The abundance of the heat load significantly prolongs the fire's development phase under sub-ventilation. Thus, the time to reach flashover is t_{max}=17.23 h, indicating that the critical temperature evaluation will occur during the pre-flashover phase. The thermal level at the critical time remains low (59°C for type 1 concrete), but the maximum temperature can reach 271°C during 17 hours of fire (Fig. 3), representing a relative increase of +300% compared to its critical value. These increases become more significant when using lightweight or interlocking concrete (+360%).

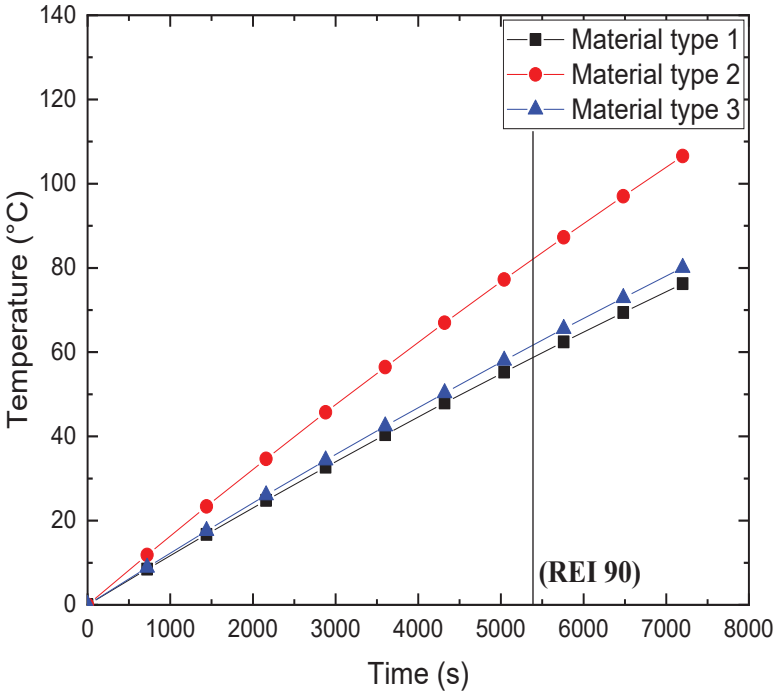


Fig. 3. Temperature-time curve ($O=O_{min}$)

C. Stratification and natural ventilation

In the absence of mechanical ventilation, thermal stratification is inevitable. The average thickness of the smoke layer is an indicator for evaluating scenarios and designing additional openings for smoke evacuation. With a constant heat load, a proportional relationship between the temperature level and the smoke layer thickness is observed.

In a sub-ventilated regime, this thickness increases from 0.33 m during the critical phase (5400 s) to 3.75 m during flashover. The consequent increase (+1030% over 17 hours of fire) indicates a need to size the smoke extraction systems during the post-flashover phase. The wall material has a decisive impact on the average smoke layer thickness. The stratification increases by +75% when switching from standard concrete to brickwork concrete (type 3), while it exceeds +420% for lightweight concrete (type 2), as shown in Figure 4.

ISBN: 978-625-378-045-6

https://doi.org/10.5281/zenodo.14537144

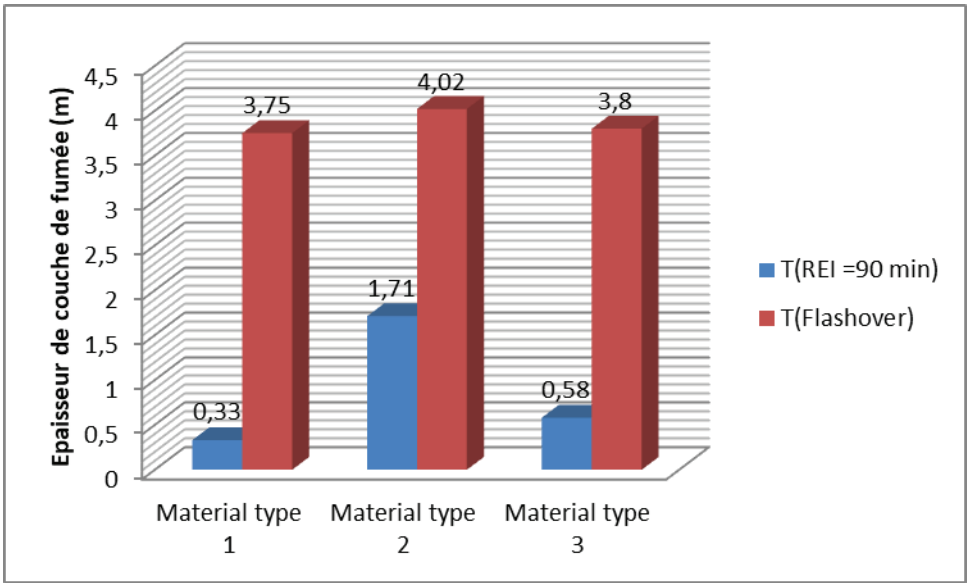


Fig. 4. Average thickness of the smoke layer

In the sub-ventilated configuration ($O=O_{min}$) of the compartment, the smoke layer thickness remains relatively limited compared to the ceiling height at the critical time (t_{REI}=5400 s). The relationship (3) yields an indeterminate result, indicating that existing openings are sufficient for smoke evacuation. However, the additional surface area required for smoke evacuation at flashover time is 2.35 m² (equivalent to 1 additional window) for standard concrete, while it reaches 3.50 m² (equivalent to 2 additional windows) for lightweight concrete. This calculation should be taken with caution as it reproduces a limit situation where the ventilation factor is fixed, knowing that its value may change during fire development.

CONCLUSION

The presented work is an attempt to characterize the thermal behavior of a fire in a large, naturally ventilated compartment. The approach used involves applying a standard parametric temperature-time curve and coupling it with the European standard, which characterizes stratification and smoke and heat exhaust ventilation systems (SHEVS). The results highlight the influence of wall material not only on the temporal evolution of temperature within the compartment but also on the development of the smoke layer, and consequently, on the sizing of openings intended for natural ventilation.

REFERENCES (Apa)

[1] Jian-qiang, W., Lei, Z., & Guo-qing, Z. (2011). Performance-based Evaluation on the Logistics Warehouse. Procedia Engineering, 11, 522–528.

https://doi.org/10.1016/j.proeng.2011.04.691

[2] Denoël, I. (n.d.). Fire Safety and Concrete Structures. Retrieved September 15, 2024, from https://www.febelcem.be/fileadmin/user_upload/autres-publications/en/docref_feu_en.pdf

[3] Merci, B., & Shipp, M. (2013). Smoke and heat control for fires in large car parks: Lessons learnt from research, Fire Safety Journal, 57, 3–10.

https://doi.org/10.1016/j.firesaf.2012.05.001

[4] Lucherini, A., Balša Jovanović, Torero, J. L., Ruben Van Coile, & Merci, B. (2024). Thermal characterisation of the cooling phase of post-flashover compartment fires. International Journal of Thermal Sciences, 199, 108933–108933.

https://doi.org/10.1016/j.ijthermalsci.2024.108933

[5] Du, Y., & Li, G. (2012). A new temperature–time curve for fire-resistance analysis of structures. Fire Safety Journal, 54, 113–120.

https://doi.org/10.1016/j.firesaf.2012.07.004

[6] S. Agred, A. Benarous, L. Loukarfi, A. Liazid, P.O. Logerais, & J.F. Durastanti. (2016). On the thermal characterization of a fire induced smoke-layer in semi-confined compartments. International Journal of Hydrogen Energy, 41(45), 21030–21035.

https://doi.org/10.1016/j.ijhydene.2016.03.212

[7] Lucherini, A., Jovanović, B., Van Coile, R., & Merci, B. (2021). Background and limitations of the Eurocode parametric fire curves, including the fire decay phase. In ASFE'21: Applications of Structural Fire Engineering. Proceedings (pp. 330–335). University of Ljubljana.

[8] Benarous, A., Hachana, R., Roudane, M., & Piloto, P. (2023). On the derivation of temperature-time curves for large-scale compartment fires. In the 53th International Conference on Advances in Sciences, Engineering and Technology, proceedings, Istanbul, Turkiye.

[9] Merci, B., & Vandevelde, P. (2007). Comparison of calculation methods for smoke and heat evacuation for enclosure fires in large compartments. Thermal Science, 11(2), 181–196.

https://doi.org/10.2298/tsci0702181m

[10] Santarpia, L., Bologna, S., Ciancio, V., Golasi, I., & Salata, F. (2019). Fire Temperature Based on the Time and Resistance of Buildings—Predicting the Adoption of Fire Safety Measures. Fire, 2(2), 19.

https://doi.org/10.3390/fire2020019

DFT MODELING OF STRUCTURAL, ELECTRONIC, AND OPTICAL PROPERTIES OF SNO_2 SINGLE CRYSTAL: INFLUENCE OF HUBBARD CORRECTION ON BAND GAP AND REFRACTIVE INDICES

Abderrahim Ait Lhaj[1*]

Brahim Ouazik[1,]

Mohamed El Hasnaoui[1,]

Hassan Chaib[2]

[1*]Materials and Subatomic Physics, Faculty of Sciences, Ibn Tofail University, Morocco.
[2] Materials and Energy Research Group, Polydisciplinary Faculty of Ouarzazate, Ibnou Zohr University, Morocco.

ABSTRACT

In this work, we modeled the structural, electronic, and optical properties of the SnO_2 single crystal, which crystallizes in the quadratic rutile phase at ambient temperature, with space group $P4_2/mnm$ (136). The calculations were performed using the Quantum Espresso code based on Density Functional Theory (DFT), employing norm-conserving pseudopotentials and the PBEsol exchange-correlation functional.

The optimized structural parameters are in good agreement with experimental values. However, the theoretical band gap is underestimated at 0.45 eV, compared to the experimental value of 3.56 eV. Through projected density of states (PDOS) analysis, we found that the O-2p orbitals dominate the valence band, while the Sn-5p orbitals are most prominent in the conduction band. This observation led us to apply the Hubbard correction to these orbitals to increase the band gap and improve the study of optical properties, particularly the ordinary and extraordinary refractive indices.

Keywords: DFT; DFT+U; PBEsol ; Energy band gap; SnO_2

FARKLI ORANLARDA Al_2O_3-TiO_2 KAPLANMIŞ MALZEMELERİN KAPLAMA ÖZELLİKLERİNİN İNCELENMESİ

INVESTIGATION OF THE COATING PROPERTIES OF AA7075 AND AZ91 MATERIALS COATED WITH DIFFERENT RATIOS OF Al_2O_3-TiO_2

Hüseyin ÖZKAVAK*

*Isparta Uygulamalı Bilimler Üniversitesi, Isparta OSB MYO,Makine ve Metal Teknolojileri Bölümü,Isparta,Türkiye, ORCID ID: 0000-0003-2857-4500

Recai Fatih TUNAY

Süleyman Demirel Üniversitesi, Mühendislik ve Doğa Bilimleri Fakültesi, Makine Mühendisliği Bölümü, Isparta, Türkiye, ORCID ID: https:0000-0002-9877-9379

ÖZET

Hafiflik, yüksek elektrik ve termal iletkenlik, iyi sönümleme, biyouyumluluk gibi birçok üstünlüğü sahip Magnezyum alaşımları günümüzde otomotiv, uzay, endüstriyel ve biyomedikal gibi birçok alanda kullanım alanı bulmaktadır. Ancak düşük tokluk, elastisite modülü ve yüksek kimyasal reaktiflik magnezyum alaşımlarının kullanımını zorlaştırmaktadır. Alüminyum alaşımları düşük yoğunluğunun tanında kolay üretim, dayanım/yoğunluk oranının yüksek olması ve düşük maliyetten dolayı çeliğin yerine tercih edilebilir hal almıştır. Ancak atmosferik nem gibi düşük aktiviteli ortamlarda korozyona uğramasından dolayı kullanımı sınırlanmaktadır. Bu kadar üstün özelliğe sahip malzemelerin yüzey özellikleri iyileştirilerek negatif özelliklerinin ortadan kaldırılması ve kullanımlarının daha da yaygınlaştırılması hedeflenmektedir. Bu amaçla bu malzemelere yüzey kaplama işlemleri uygulanmaktadır. Plazma Püskürtme yöntemi malzemelerin kaplanmasında yaygın olarak kullanılan bir kaplama yöntemidir. Plazma kaplama işlemine etki eden birçok parametre bulunmakta olup bu parametrelerden bazıları kontrol edilebilirken bazıları kontrol edilememektedir. Kaplama karakteristiğine etki eden en önemli parametrelerin başında kaplama öncesi yüzey hazırlığı gelmektedir. Bu nedenle kaplama öncesi numunelere kaplama öncesi yapılan yüzey hazırlığı önem arz etmektedir. Bu çalışmada plazma püskürtme yöntemi kullanarak farklı oranlarda Al_2O_3 ve TiO_2 seramik malzemeler AA7075 alüminyum alaşımı alt malzeme ile AZ91 magnezyum alaşımı alt malzeme üzerine kaplanmış ve yapılan kaplamaların kaplama karakteristikleri incelenmiştir. Çalışma sonunda AZ91 ve AA7075 alt malzemeler üzerine farklı oranlarda Al_2O_3-TiO_2 ‘nin başarılı bir şekilde kaplandığı belirlenmiştir. Elde edilen

kaplamalarda boşluk, çatlak gibi hataların bulunmadığı gözlemlenmiştir. Çalışmada ayrıca kaplama işlemi sonrası kaplama kalınlık değerleri incelenmiştir. Her iki alt malzeme grubunda da en yüksek kaplama kalınlık değerinin %13 TiO_2 %87 Al_2O_3 ilave edilmiş numunelerde elde edildiği belirlenmiştir. Bunun yanında AZ91 alt malzeme üzerine yapılan kaplamaların kaplama kalınlık değerlerinin AA7075 alt malzeme üzerine yapılan kaplama kalınlık değerlerinden daha düşük olduğu belirlenmiştir.

Anahtar Kelimeler: Kaplama, plazma püskürtme, TiO_2, Al_2O_3, kaplama karakteristiği

ABSTRACT

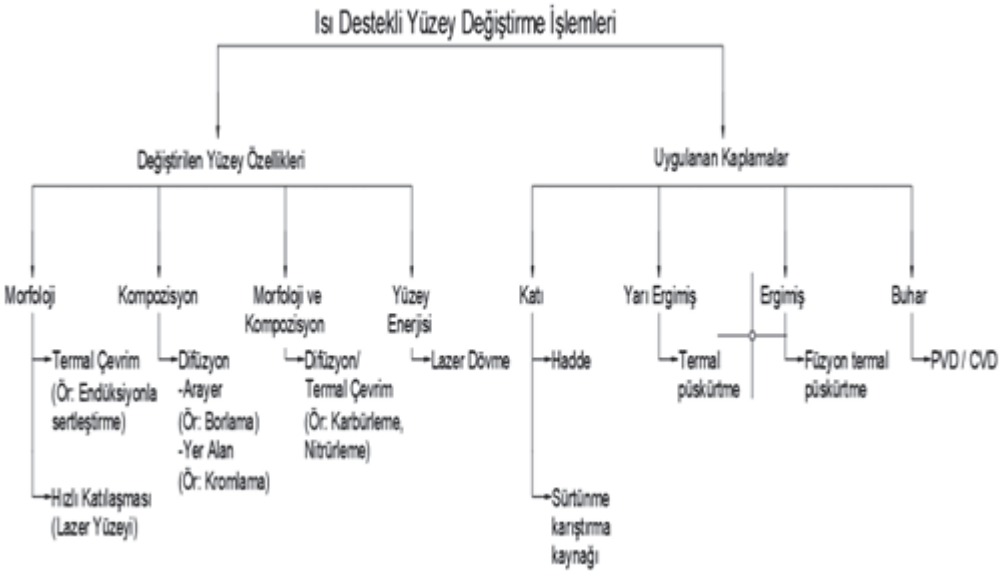
Magnesium alloys, which have many advantages such as lightness, high electrical and thermal conductivity, good damping, biocompatibility, are used in many areas such as automotive, aerospace, industrial and biomedical. However, low toughness, elasticity modulus and high chemical reactivity make the use of magnesium alloys difficult.Aluminum alloys have become preferable instead of steel due to their low density, easy production, high strength/density ratio and low cost. However, its use is limited due to its corrosion in low-activity environments such as atmospheric humidity.It is aimed to eliminate the negative features of materials with such superior properties by improving their surface properties and to make their use more widespread.For this purpose, surface coating processes are applied to these materials.Plasma Spraying method is a coating method widely used in coating materials. Here are many parameters affecting the plasma coating process, some of which can be controlled while others cannot. The most important parameter affecting the coating characteristics is the surface preparation before coating. Therefore, the surface preparation applied to the samples before coating is important.In this study, different ratios of Al_2O_3 and TiO_2 ceramic materials were coated on AA7075 aluminum alloy substrate and AZ91 magnesium alloy substrate using the plasma spray method and the coating characteristics of the coatings were examined. At the end of the study, it was determined that Al_2O_3-TiO_2 was successfully coated on AZ91 and AA7075 substrates at different ratios.It was observed that there were no defects such as gaps and cracks in the obtained coatings.In addition, the coating thickness values after the coating process were examined in the study.It was determined that the highest coating thickness value in both substrate groups was obtained in samples to which 13% TiO_2 and 87% $Al2O_3$ were added.In addition, it was determined that the coating thickness values of the coatings made on AZ91

substrate were lower than the coating thickness values of the coating made on AA7075 substrate.

Keywords: Coating, plasma spraying, TiO_2, $Al2O_3$, coating characteristic

GİRİŞ

Mühendislikte malzeme seçimi hem parça ömrü hem de maliyet açısından önem arz etmektedir. Seçilen malzemelerin çevresel koşullar ile etkileşime girmesi malzemelerde bozulmalara yol açacaktır. Bu nedenle var olan malzemelerin yüzey özelliklerinin geliştirilmesi gerekmektedir. Malzemenin değiştirilmesi gereken temel yüzey özellikleri yüzey enerjisi, yüzey morfolojisi, bileşimi ve sertliğidir. Bu özeliklerin değiştirilmesi için yüzey mühendisliğine ihtiyaç duyulmaktadır. Yüzey mühendisliği ile hali hazırda kullanılan mühendislik malzemeler kaplanarak yüzey özelliklerinde iyileşme elde edilmektedir. Yüzey kaplama işlemi ısı enerjisi yardımı ile malzeme yüzey özelliklerinin değiştirilmesi esasına dayanmaktadır. Isı enerjisi kullanarak uygulanan yüzey kaplama yöntemleri Şekil 1'de verilmektedir.



Şekil 1. Isı enerjisi kullanarak uygulanan yüzey modifikasyon işlemleri (Chattopadhyay,2007)

Plazma püskürtme yöntemi tel, akışkan veya toz halindeki kaplama malzemesinin plazma yardımı ile gaz haline dönüştürülerek alt malzeme üzerine püskürtülmesi esasına dayana bir termal kaplama yöntemidir (Özkavak,2024). Plazma püskürtme yöntemine etki eden kontrol edilebilen ve edilemeyen birçok parametre bulunmaktadır. Tanecik şekli ve boyutu, toz besleme oranı, ark, giriş gücü, gaz basıncı, püskürtme mesafesi gibi birçok faktör plazma işlemine etki etmektedir (Heimann,2006).

Magnezyum 1,74 g/cm^3 yoğunluğa sahip yüksek özgül dayanım, yüksek dayanım/ağırlık oranı, düşük özgül ağırlık, yüzsek hızda tornalanma ve frezelenme kabiliyeti, biyouyumluluk gibi birçok üstün özelliğinden dolayı uzay, biyomedikal, elektronik, otomotiv gibi birçok sektörde kullanılmaktadır. Ancak magnezyumun kullanımına düşük tokluk ve elastisite modülü, soğuk şekillendirme kabiliyetinin sınırlı olması ve yüksek reaktiflik gibi olumsuz özellikleri kullanım alanını sınırlandırılmaktadır. Benzer şekilde 2,7 g/cm^3 yoğunluğa sahip, düşük maliyet, dayanım/yoğunluk oranı oldukça yüksek olan alüminyum yine benzer şekilde düşük aktiviteye sahip ortamlarda bile gerilmeli korozyona karşı dayanıksız olması kullanımda farklı çözümlere başvurulmaya neden olmuştur. Bu kadar üstün özelliğe sahip bu malzemelerin yüzey özellikleri iyileştirilerek kullanımını daha da yaygın hale getirilmesi amaçlanmaktadır. Bu amaçla çalışmalar bu malzemelere yüzey kaplama işlemleri uygulayarak yüzey özelliklerini iyileştirmek üzerine yoğunlaşmıştır. Seramik malzemeler arasında ergime noktası sertlik, aşınma ve korozyon dayanımı yüksek olan Al_2O_3 yüzey kaplama yöntemleri için tercih edilen bir malzemedir (Kumar vd., 2004). TiO_2 benzersiz bir kristal yapıda olan ve Al_2O_3 içerisine ilave edildiğinde aşınma ve korozyon direncini daha da artırmaya sağlayan seramik malzemeler arasındadır. Bu özellikleri dikkate alındığında farklı alt malzemeler üzerine farklı kaplama yöntemleri kullanarak kaplanarak elde edilen kaplamaların aşınma ve korozyon davranışları belirlenmeye çalışılmıştır. Bu amaçla yapılan çalışmalar incelenmiştir.

Kim ve arkadaşları (2001), yaptıkları çalışmada plazma püskürtme yöntemiyle Al_2O_3-%13 TiO kaplaması polimere bağlı olarak belirlenen üç ticari dolgu malzemesi kullanılmış ve sızdırmazlık sağlanmıştır. Çalışmada işlemden önceki ve sonraki mekanik özellikleri incelemiştir. Çalışma sonunda kaplama işlemi ile mikrosertlik, abrazif aşınma direnci, bağ kuvveti ve yüzey pürüzlülüğü değerlerinin dolgu malzemesine bağlı olarak iyileştiği gözlemlenmiştir. Ya-Li ve arkadaşları (2007), yaptıkları çalışmada plazma kaplama ile lazer eritme plazma püskürtme yöntemi kullanarak, AZ91HP Mg alaşımı üzerine Al_2O_3 seramik kaplamışlardır. Çalışma sonunda yazarlar; lazer yöntemi ile yapılan kaplamaların korozyon ve aşınma direnci kaplama yapılmayan Mg alaşımlarına göre daha yüksek olduğu belirlenmiştir. Plazma püskürtme yöntemi kullanılarak Al_2O_3-Al kompozit kaplama uygulayan Yin vd. (2008) elde ettikleri kaplamaların mikroyapı ve mekanik özelliklerini incelemişlerdir. Yazarlar Al_2O_3-Al kompozit kaplamalar; Al_2O_3 kaplamalarla kıyaslandığında düşük sertlik gösterdiği ve aşınma direncinin daha yüksek olduğu sonucuna ulaşmışlardır.

Çalışmalarında plazma püskürtülmüş Al_2O_3/TiO_2 kompozit kaplamaların mikro yapısına nozul çapının etkisini incelemeyi amaçlayan Morks ve Akimoto (2008) 7,5mm ve 8mm nozul çapını çalışmaları için seçmişlerdir. Çalışma sonunda yazarlar ,5 mm nozul çapı kullanılarak yapılan Al_2O_3/TiO_2 kaplamaların 8 mm nozul çapına göre daha yoğun bir yapıya, yüksek sertlik aşınma direnci ve düşük gözenekliliğe sahip olduğu sonucun ulaşmışlardır. Marcinauskas vd. (2010), çalışmalarında atmosferik plazma jet

parametrelerinden olan plazma tabancasının çıkışı ile altlık malzeme arasındaki mesafenin ile karbon kaplamalar üzerine etkisini incelemişlerdir. Marcinauskas ve arkadaşları çalışmalarının sonunda kaplama işlemi için plazma gazı olarak argon ve asetilen; altlık malzeme arasındaki mesafe 5-20 mm ve 1200 dk. işlem süresi parametrelerini belirlemişlerdir. Islak ve Buytoz (2011), çalışmalarında AISI 304 çelik üzerine ZrO_2/ Al_2O_3/TiO_2 kompozit malzeme kaplanmış numunelerin mikro yapılarını araştırmışlardır. Islak ve Buytoz çalışmaları sonunda lamelli ve tabakalı bir mikro yapı elde ettikleri; kaplama kalınlığı oksit kaplama tabakası ve bağlayıcı tabaka (Ni-20Cr) olarak sırasıyla 100 µm ve 20 µm olarak ölçtükleri ve kaplama yapısında az miktarda ergimemiş partiküller, kısmi ve tamamen ergimiş bölgeler ile gözenek varlığını sonucuna varmışlardır. Jıa ve arkadaşları (2015), çalışmalarında 6061 alüminyum alaşımı üzerine farklı TiO_2 içeriklerine sahip Al_2O_3 termal bariyer kaplamaları, plazma püskürtme yöntemi ile kaplamış, kaplamaların korozyon direnci, ısı yalıtım özelliği ve faz bileşimlerini incelemişlerdir.

Yazarlar tüm hammadde tozlarının püskürtme işlemi sırasında faz dönüşümü sergilediği ve tozdaki TiO_2 içeriğinin artmasıyla kaplamanın korozyon direncinin arttığı, ısı yalıtım özelliğinin ise azaldığı sonucuna ulaşmışladır. Basha vd. (2020), yaptıkları çalışmada atmosferik plazma yöntemi kullanarak Al_2O_3-TiO_2 kaplama işlemini incelemişlerdir. Çalışmada İnce katmanlı mikro yapıya sahip nano yapılı tozlar kullanılmıştır. Yazarlar aşınmaya karşı nano büyüklükte alümina-titanyanın topaklanmış tozlarından elde edilen kaplamaların, geleneksel tozların kaplamalarına göre daha üstün direnç gösterdiği sonucuna ulaşmışlardır. Bu çalışmalar dikkate alındığında kaplama oranlarının belirli değerler arasında kaldığı ve genel olarak yapısal inceleme yapılmadığı belirlenmiştir.

Bu amaçla bu çalışmada daha önce belirlenen %3 TiO_2 +%97 Al_2O_3 ve %13 TiO_2 +%87 Al_2O_3 oranlarına ilave olarak %40 TiO_2 +%60 Al_2O_3 , %100 TiO_2 ve%100 Al_2O_3 oranları kullanarak plazma püskürtme yöntemi kullanarak kaplama işlemi gerçekleştirilmiş ve yapılan kaplamaların karakteristik özelliklerinin belirlenmesi amaçlanmıştır.

MATERYAL METOT

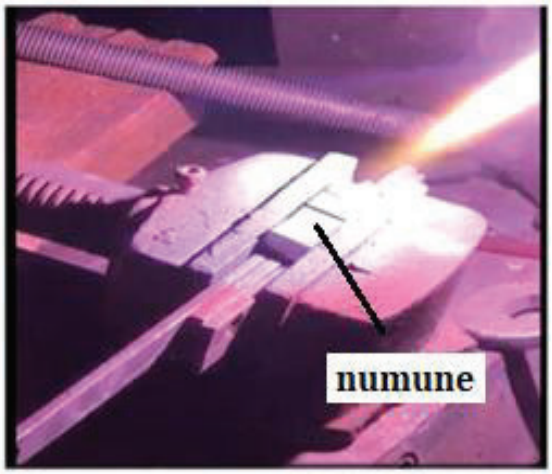
Bu çalışmada AZ91 magnezyum alaşımı ve AA7075 Alüminyum alaşımından oluşan alt malzeme üzerine plazma püskürtme yöntemi kullanarak farklı oranlarda Al_2O_3 ve TiO_2 seramik malzemeleri kaplanmıştır. Yapılan kaplamaların kaplama karakteristikleri belirlenmesi amaçlanmıştır. Çalışmada kullanılan alt malzeme ve kaplama malzeme oranları Tablo 1'de verilmektedir.

Tablo 1. Çalışmada kullanılan alt malzeme ve kaplama malzeme oranları

Malzeme	Kullanım Amacı
AA7075 Alüminyum alaşımı	Alt malzeme
AZ91 Magnezyum alaşımı	Alt malzeme
%100 Al_2O_3	Kaplama malzemesi
%100 TiO_2	Kaplama malzemesi
%97 Al_2O_3 +%3 TiO_2	Kaplama malzemesi
%87 Al_2O_3 +%13 TiO_2	Kaplama malzemesi
%60 Al_2O_3 +%40 TiO_2	Kaplama malzemesi

Al_2O_3 seramik malzeme korozyon ve aşınma direncine oldukça dayanıklı bir malzeme olup bu özelliğinden dolayı tercih edilen bir malzemedir. Bu malzemeye TiO_2 ilave edilmesi ile aşınmanın yanında korozyon dayanımı ve tokluk gibi özelliklerde iyileşme elde edilmektedir (Simbar, 2020; Buytoz, 2012; Kuşoğlu 2005). Bu nedenle çalışmada Al_2O_3 ve TiO_2 seramik malzemeler farklı oranlarda karıştırılarak kaplanmıştır. Çalışma için belirlen oranlardaki tozlar plazma tabancasına toz halinde gönderilmektedir. Bu nedenle kaplama tozlarının homojenlik ve boyut açısından birbirine yakın olması amacıyla bilyeli öğütme tekniği kullanılarak karıştırılmıştır.

Çalışmada ayrıca için %100 Al_2O_3 ve %100 TiO_2 kaplama oranları da seçilerek bu oranların kaplama karakteristikleri belirlenmiştir. Çalışmada plazma kaplama yöntemi kullanılmış olup numunelerin kaplama işleminin uygulanması Şekil 2'de verilmektedir. Çalışmada plazma kaplama işlem parametreleri olarak daha önce firma tarafından optimize edilen parametreleri kullanılmıştır.



Şekil 2. Numunelere kaplama işleminin uygulanması

Yüzey kaplama işlemlerinde kaplama karakteristiğine etki eden ve kontrol edilebilen faktörlerden bir tanesi alt malzemenin yüzey hazırlığı olarak ifade edilebilir. Bu nedenle kaplama işlemi öncesi numunelerin yüzey hazırlığı önem arz etmektedir.

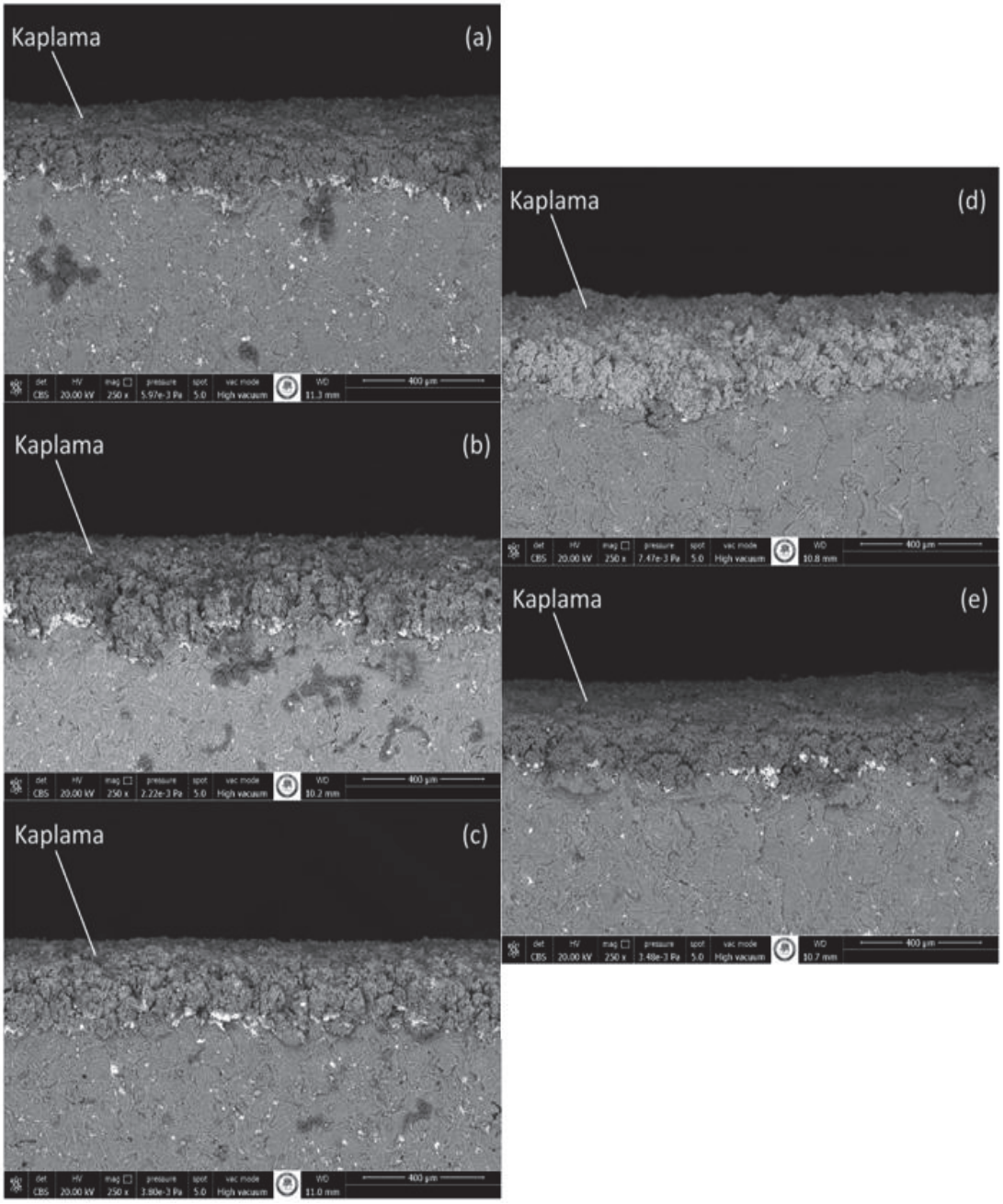
Bu amaçla çalışmada alt malzemelere kaplama işlemi öncesi yüzey hazırlığı işlemi yapılmıştır. Çalışmada yüzey hazırlığı kumlama işlemi ile başlamıştır. Kumlama işlemi sonrası numuneler ultrasonik temizleme işlemine tabi tutulmuştur. Bu işlem ile kaplama sırasında meydana gelecek adezyon direncini artırmak amaçlanmıştır. Yüzey hazırlık işlemi kumlama ve ultrasonik temizleme işlemi uygulana numunelere Ni-Cr astar malzemesi kullanarak kaplama ince astarlama işlemi ile sonlandırılmıştır.

Çalışmada numunelerin kaplama öncesi ve sonrasında yüzey pürüzlülük değerleri TIME marka TR200 model yüzey pürüzlülük ölçüm cihazı kullanılarak yapılmıştır (Özkavak,2024). Kaplama karakteristiğinin belirlenmesi amacıyla kaplanmış numunelerin yapısal incelemeleri için Fei Quanta Feg 250 marka Taramalı elektron mikroskobu (TEM) kullanılmıştır. Kaplama karakteristik incelemelerin yanı sıra kaplama kalınlıkları da ölçülmüştür. Ölçümler birkaç noktadan yapılmış ve aritmetik ortalaması alınarak hesaplanmıştır.

SONUÇ

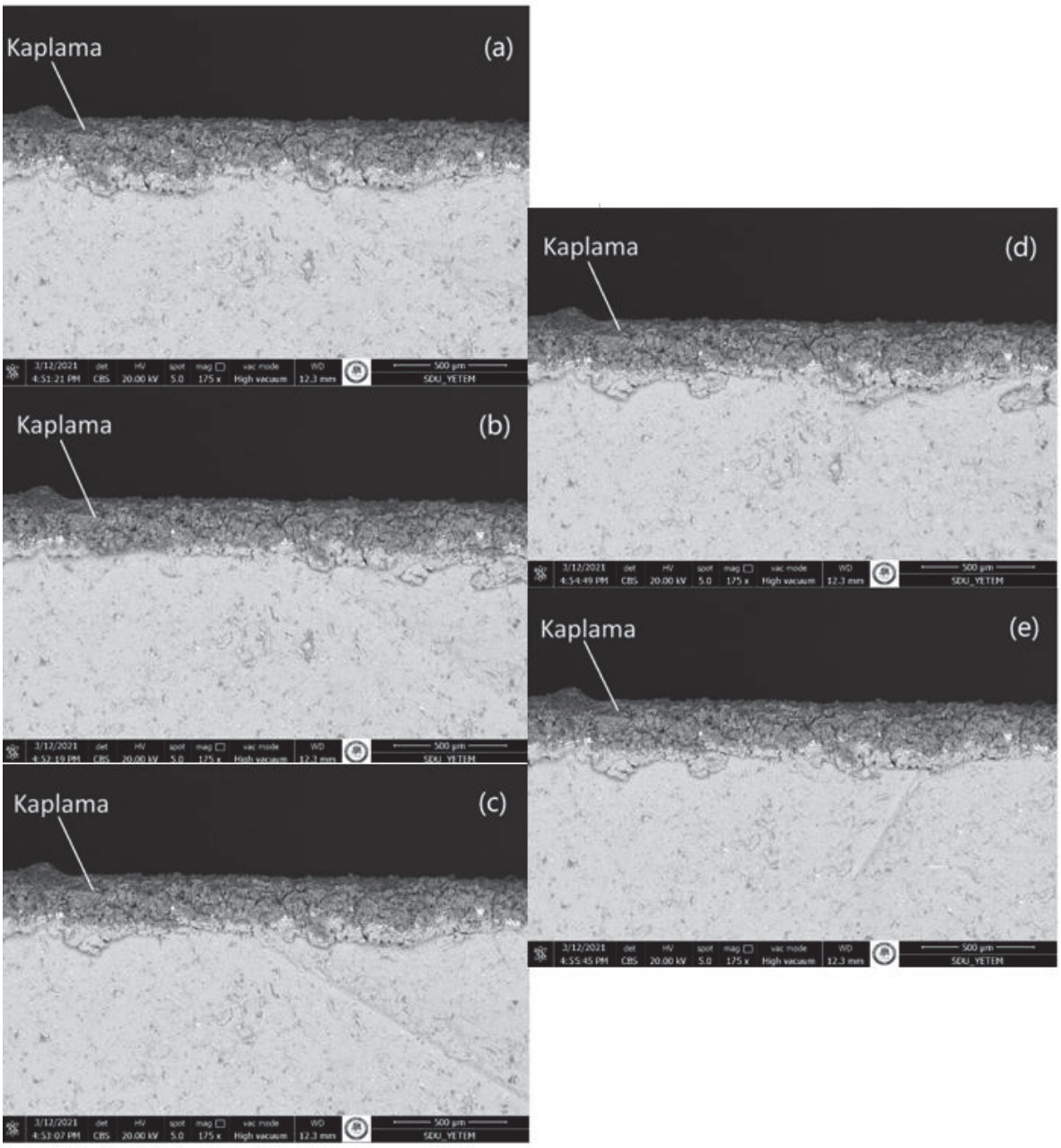
Bu çalışmada plazma püskürtme kaplama yöntemi kullanarak AZ91 magnezyum alaşımı alt malzeme ile AA7075 alüminyum alaşım alt malzeme üzerine farklı oranlarda Al_2O_3 ve TiO_2 seramik malzemeler kaplanmış ve kaplamanın karakteristiği incelenmiştir. Kaplama karakterizasyonu yapılırken çatlak, porozite gibi süreksizliklerin olup olmadığı, alt malzeme üzerine uygulanan kaplama malzemesinin rejiminin düzenli olup olamadığı noktaları belirlenmiştir. Ayrıca kaplama öncesi ve sonrası yüzey pürüzlülük değerleri ölçülerek kaplama karakterizasyonuna etkisi belirlenmiştir.

Çalışmada kaplama işlem öncesi numunelerin pürüzlülük değerleri AZ91 alt malzeme için (Ra) 0,219 µm ve AA7075 alt malzeme için de (Ra) 0,195 µm olarak ölçülmüştür. Kaplama sonrası elde edilen pürüzlülük değerleri ise her iki alt malzeme grubu için de 6,5-7,5 µm olarak ölçülmüştür. Kaplama işlemi sonrası yüzey pürüzlülük değerlerinin birbirine yakın elde edilmesi kaplamaların homojen olduğunun bir göstergesidir.



Şekil 3. AZ91 alt malzeme üzerine yapılan kaplamaların TEM görüntüleri (a) %97 Al_2O_3 +%3 TiO_2 (b) 87 Al_2O_3 +%13 TiO_2 % (c) %60 Al_2O_3 +%40 TiO_2 (d) %100 TiO_2 (e)%100 Al_2O_3

AZ91 alt malzeme üzerine farklı oranlarda Al_2O_3, TiO_2 kaplanmış numunelerin TEM görüntüleri Şekil 3'te verilmektedir. Şekil 3 incelendiğinde kaplama işlemi sonrası kaplama ara yüzeylerinde boşluk, çatlak gibi hataların bulunmadığı açıkça gözlemlenmiştir.



Şekil 4. AA7075 alt malzeme üzerine yapılan kaplamaların TEM görüntüleri (a) %97 Al_2O_3 + %3 TiO_2 (b) +%87 Al_2O_3+ %13 TiO_2 (c) %60 Al_2O_3 +%40 TiO_2 (d) %100 TiO_2 (e)%100 Al_2O_3

AA7075 alt malzeme üzerine farklı oranlarda Al_2O_3, TiO_2 kaplanmış numunelerin TEM görüntüleri ise Şekil 4'te verilmektedir. AZ91 alt malzeme üzerine yapılan kaplamalara benzer kaplama işlemi sonrası kaplama ara yüzeylerinde boşluk, çatlak gibi hataların bulunmadığı açıkça gözlemlenmiştir. Bu durum alt malzeme üzerine uygulanan kaplamaların başarılı bir şekilde gerçekleştiğinin bir göstergesidir. Ayrıca altlık-kaplama malzemesinin ksusursuz kaplandığı birbiri arasında herhangi bir tutunma sorununun olmadığı da yine Şekil 3 ve 4'ten net bir şekilde anlaşılmaktadır. Ayrıca yapılan kaplamaların

Al_2O_3, TiO_2 kaplanmış malzeme karakteristiklerine benzer olduğu gözlemlenmiştir. Bunun yanında Alt malzeme ile kaplama malzemesi arasındaki yapışma rejiminin düzenli olduğu da gözlemlenmiştir.

Çalışmada yapılan kaplamaların yüzey pürüzlülük değerlerinin birbirine yakın elde edilmesi kaplama kalınlık değerlerinin de birbirine yakın olmasını sağlamaktadır. 0 yüzey pürüzlülük değerlerinin yanında yapılan kaplamaların kaplama kalınlıkları ölçülmüştür.

AA7075 alt malzeme üzerine yapılan kaplama kalınlık değerleri incelendiğinde %13 TiO_2 +%87 Al_2O_3 oranında kaplanan numunelerde 257,9µm olarak en yüksek ölçülmüştür. Bu kalınlık değerini sırası ile %40 TiO_2 +%60 Al_2O_3 oranında kaplanmış numunede 220,3µm ; %100 TiO_2 kaplanmış numunede 215,2µm; %3 TiO_2 +%97 Al_2O_3 oranında kaplanan numunede 208,8µm; %100 Al_2O_3 kaplanmış numunede ise 203,2µm olarak ölçülmüştür. Kaplama işlemi sonrası kalınlık değerleri incelendiğinde yapılan kaplama işleminde kaplama işlemi sırasında TiO_2 ile Al_2O_3 reaksiyo$_{na}$ girerek Al_2TiO_5 fazını oluştururlar. Meydana gelen Al_2TiO_5 fazının kaplama kalınlığı değerlerini etkilediği düşünülmektedir. AA7075 alt malzemelerin kaplanması ile kaplama kalınlıklarında elde edilen benzer durum AZ91 alt malzeme üzerine yapılan kaplamalarda elde edilmiştir. AZ91 kaplanmış numunelerin kaplama kalınlıkları sırası ise %13 TiO_2 +%87 Al_2O_3 oranında kaplanan numunelerde 253,3 µm olarak en yüksek ölçülmüştür. Bu kalınlık değerini sırası ile %40 TiO_2 +%60 Al_2O_3 oranında kaplanmış numunede 218,7µm ; %100 TiO_2 kaplanmış numunede 214,7µm; %3 TiO_2 +%97 Al_2O_3 oranında kaplanan numunede 258,8µm; %100 Al_2O_3 kaplanmış numunede ise 202,3µm olarak ölçülmüştür.

Her iki alt malzeme üzerine yapılan kaplama kalınlıkları karşılaştırıldığında AZ91 alt malzeme üzerine yapılan kaplamaların AA7075 alt malzeme üzerine yapılan kaplamalara nazaran daha düşük çıktığı belirlenmiştir. Bu durum AZ91 alt malzeme üzerine tutunmanın AA7075 alt malzemeden daha düşük olduğunun bir göstergesi olarak açıklanabilir.

SONUÇLAR VE DEĞERLENDİRME

Çalışmada Plazma püskürtme kaplama yöntemi kullanarak AZ91 magnezyum alaşımı alt malzeme ile AA7075 alüminyum alaşım alt malzeme üzerine farklı oranlarda Al_2O_3 ve TiO_2 seramik malzemeler kaplanmış ve kaplamanın karakteristiği belirlenmiştir. Çalışma sonunda her iki alt malzeme üzerine uygulanan kaplamalarda boşluk, porozite gibi hataların bulunmadığı ve alt malzeme ile kaplama malzemesinin yapışma rejiminin düzenli olduğu belirlenmiştir. Bu durum Az91 ve AA7075 alt malzemeler üzerine yapılan kaplamaların başarılı bir şekilde gerçekleştiğinin kanıtıdır. Yapılan kaplamaların yüzey pürüzlüklerinin birbirine yakın olduğu belirlenmiştir. Benzer durum kaplama kalınlıkları değerlerinde de elde edilmiştir. Bu durum yapılan kaplamaların homojen olduğunun bir göstergesidir.

TEŞEKKÜR

Bu çalışma, Süleyman Demirel Üniversitesi Bilimsel Araştırma Projeleri Koordinasyon Birimi tarafından FDK-2019-7386 proje numarası kapsamında desteklenmiştir.

KAYNAKLAR

Basha, M. T., Srikantha, A., Venkateshwarlua, B., 2020. A Critical Review on Nano structured Coatings for Alumina-Titania (Al_2O_3-TiO_2) Deposited by Air Plasma Spraying Process (APS). Materials Today: Proceedings 22, 1554–1562.

Chattopadhyay, R., 2000. Advanced Thermally Assisted Surface Engineering Process. Mumbai, Kluwer Academic Publishers, 500p, London.

Heimann, R.B., 2006. Plasma Spray Coating. Münden, Wiley-VCH, 427p, Germany.

Islak S., Buytoz, S., 2011. Plazma Püskürtme Yöntemiyle AISI 304 Paslanmaz Çelik Yüzeyinde Elde Edilen ZrO_2/Al_2O_3-%13 TiO_2 Kompozit Kaplamasının Mikroyapı Özellikleri. 6th International Advanced Technologies Symposium, 16-18 May, Elazığ, 6-12.

Jia, S., Zou, Y., Xu, J., Wang, J., Yu, L., 2015. Effect of TiO_2 Content on Properties of Al_2O_3 Thermal Barrier Coatings by Plasma Spraying. Transactions of Nonferrous Metals Society of China, 25, 175-183.

Kumar, L.G., Thirumalaikumarasamy, D., Karthikeyan, K., Mathanbabu, M., Ashokkumar, M., Ramachandran, C.S., 2023. An overview of recent trends and challenges of post treatments on magnesium alloys. Materials Today: Proceedings 78, 700–707.

Marcinauskas, L., Silinskas, M., Grigonis, A.,2010. Influence of Stand Off Distance on the Structure and Properties of Carbon Coatings Deposited by Atmospheric Plasma Jet. Applied Surface Science, 257(7), 2694-2699.

Morks, M., Akimoto, K., 2008. The Role of Nozzle Diameter on the Microstructure and Abrasion Wear Resistance of Plasma Sprayed Al_2O_3/TiO_2 Composite Coatings. Journal of Manufacturing Processers, 10, 1-5.

Özkavak,2024. Seramik Malzemelerle Kaplanmış AA7075 Ve AZ91 Alaşımlarının Korozyon Direnci Ve Yüzey Özelliklerinin İncelenmesi. Süleyman Demirel Üniversitesi, Fen bilimleri Enstitüsü, Doktora tezi,180s,Isparta.

Simbar, A.R., Shanaghi, A., Moradi, H., Chu, P.K., 2020. Corrosion Behavior of Functionally Graded and Self-Healing Nanostructured TiO_2–Al_2O_3-Benzotriazole Coatings Deposited on AA 2024-T3 by the Sol-Gel Method. Materials Chemistry and Physics, 240, 122-233.

Ya-li G., Cun-shan, W., Man, Y., Hong-bin, L., 2007. The Resistance to Wear and Corrosion of Laser-Cladding Al_2O_3 Ceramic Coating on Mg Alloy. Applied Surface Science, 253, 5306-5311.

Yin, Z., Tao, S., Zhou, X., Ding, X., 2008. Microstructure and mechanical properties of Al_2O_3–Al composite coatings deposited by plasma spraying. Applied Surface Science, 254, 1636–1643.

HIGH -EFFICIENCY ENERGY HARVESTING THROUGH POLYVNYLIDENE FLUORIDE-GRAPHENE NANORIBBON COMPOSITE

Seçil Peker Adıgüzel

Istanbul University Cerrahpaşa, Engineering Faculty, Department of Chemical Engineering, Istanbul, Turkey

ORCID ID: 0000-0003-4438-00896

Nevra Ercan

Istanbul University Cerrahpaşa, Engineering Faculty, Department of Chemical Engineering, Istanbul, Turkey

ORCID ID: 0000-0001-9927-0315

ABSTRACT

Piezoelectric nanogenerators possess the ability to convert mechanical energy into electrical energy, making them particularly promising for applications in areas such as wearable electronic devices, sensors, and energy harvesting systems. Their unique design allows for the efficient capture of energy from everyday activities, such as walking or bending, which can be transformed into usable electrical power. This capability is especially beneficial for self-powered devices that require minimal external energy sources. Nanogenerators created by integrating carbon-based nanoparticles with polymer materials like polyviniylidine fluoride (PVDF), which possess piezoelectric properties, offer several advantages including higher energy density, improved flexibility, and extended lifespan. The approach enables the conversion of ambient mechanical energy into usable electrical energy, contributing to the development of sustainable energy sources. In this study, the piezoelectric behavior of composites obtained by incorporating graphene nanoribbons (GNRs), which are member of carbon-based nanomaterials, into a polyvinylidene fluoride (PVDF) polymer has been investigated. Unzipping multi-walled carbon nanotubes is an effective and scalable strategy for synthesizing graphene nanoribbons. The synthesized GNRs are employed to prepare nanometer-scale piezoelectric polymer composite films showing higher piezoelectric performance than neat PVDF. The structural, surface morphology, crystal properties of the synthesized materials were examined by Fourier-Transform Infrared Spectroscopy (FTIR), Scanning Electron Microscopy, Transmission electron microscopy (TEM), X-ray Diffraction (XRD), respectively. Additionally, the piezoelectric performance was evaluated by testing the output voltages under specific mechanical forces.

Keywords: energy harvesting, graphene nanoribbon, piezoelectric nanogenerator, polyvinylidene fluoride composite

SYNTHESIS OF BARON NITRIDE REINFORCED BORON CARBIDE NANOCOMPOSITES AND THEIR APPLICATIONS

Erdem SAĞIRLI

Suna AVCIOGLU

Figen KAYA

Cengiz KAYA

Department of Metallurgical and Materials Engineering, Yıldız Technical University, Istanbul, TURKEY

ABSTRACT

Boron carbide (B_4C) is one of the hardest ceramic materials, second only to diamond and cubic boron nitride. Its remarkable mechanical properties—including extreme hardness, low density, a high melting point of 2450 °C, excellent wear resistance, superior chemical stability, and high neutron absorption capacity—make it invaluable in numerous industries, particularly in defense. However, to optimize B_4C for defense applications, enhancements in fracture toughness are essential. In this study, a sol-gel method was employed to develop an ammonium salt-modified polymeric precursor for synthesizing BN-B_4C nanocomposites. The primary goal was to achieve uniform distribution of BN particles within B_4C grain boundaries to improve fracture toughness. Ammonium salt and various carboxylic acid sources were used in different quantities in the sol-gel process to produce precursors with diverse structures. By adjusting the ammonium salt added during synthesis, the ratio of boron nitride in the final composite structure was effectively controlled. Four distinct powder samples were obtained and characterized. XRD analysis was conducted to determine phase ratios, while FT-IR analysis was used to assess the chemical structure of the gel precursors. SEM imaging provided insights into the BN distribution within B_4C particles and their morphological characteristics. The analysis of these precursors revealed that increasing the initial ammonium salt concentration resulted in larger, more heterogeneous grain sizes. XRD results showed a decline in the purity of B_4C and BN as ammonium salt concentration increased. SEM images indicated that higher ammonium salt levels caused BN particles to cluster, leaving some B_4C grains uncoated. In summary, BN-B_4C nanocomposites were successfully synthesized via the sol-gel method. Findings show that BN particle distribution and morphology on B_4C grains can be modulated by varying the amount of ammonium salt introduced during synthesis. This study demonstrates that BN ratio and distribution within B_4C structures can be finely tuned through careful control of citric acid diammonium salt proportions in the sol-gel process.

Acknowledgments: The authors are grateful for the financial support from TUBITAK under contract number of 122M836.

Keywords: Boron carbide, Boron nitride, Sol-gel

THE DEVELOPMENT OF JAPANESE CERAMICS ART

Lecturer, PhD Irina-Ana DROBOT

Technical University of Civil Engineering Bucharest, Faculty of Engineering in Foreign Languages, Department of Foreign Languages and Communication, Bucharest, Romania
ORCID ID: 0000-0002-2556-6233

ABSTRACT

The purpose of this paper is to trace the development of Japanese ceramics art. We may consider other cultures' influence, based on their taking over the utilitarian, practical use of Chinese ceramics. The ceramics are just an example of cultural product taken over from Chinese culture and then individualized and turned into a specific cultural product for and by the Japanese culture. The Japanese have developed their distint style and also use of ceramics in their tea ceremony, as well as in their Buddhist rituals. This taking over of ceramics form China happened starting from the Kamakura period (around 1185-1333). However, this was just an influence and this is not the only contribution to the development of the Japanese ceramics art. The practice and the presence of these objects begins even earlier on for the Japanese culture, with the Jomon period (10 500-300 BC), when the first earthenwares were created. This means that Japan has, in fact, one of the oldest such practices. It was the tea ceremony that assigned to the ceramics an aesthetic and artistic note and tradition to ceramics. There was also the influence of Korea, when, during the fifth century, Japan imported a new techique for pottery, involving firing in high temperature of the stoneware in a reduced atmosphere, resulting in natural ash glaze. Green glazed ware was around during the periods of Asuka and Nara, influenced by the techniques from China and Korea. Ceramics art is still being created today, and present in exhibitions all over the world, with world of artists such as Aya Murata, Yuri Takemura, Mikiko Tomita, Sayaka Shingu, Sayaka Oishi, Mayumi Nakamura, Seito Tamura, who were part of an Exhibition in Bucharest, Romania, Dıversıty Of Sensıtıvıty And Expressıon (September 12 - October 31, 2022).

Keywords: Soft Power, Culture, Contemporary Art.

INTRODUCTION

The cultural contact between Japan and China is a well-known one throughout history. While Japan has taken over in its beginnings cultural products from China, starting with the writing system, and continuing with painting, with Buddhism, and the way it was included in the everyday mindset, as well as its cultural identity manifestations, which includes values, symbols, rituals, traditions, practices and personalities (Baciu, 2012), it has developed a distinct culture of its own.

When it comes to ceramics, Japan has both its own, age-old tradition, and its borrowings from cultural contact with China and Korea, resulting in further adaptations of them. The ceramic tradition starts in Japan during the Jomon period (10 500-300 BC) (Habu & Hall, 1999). Japan has, therefore, a long lasting ceramics tradition starting from the Jomon period (Bausch, 2016) and continuing into the Heian period (Sinopoli, 1992). During this time, the first earthenwares were created. Later on, Japan took over the ceramics style from China when

developing their traditions and rituals of the tea ceremony. During the Kamakura period (1185-1333), Japan took over the elaborate style of Chinese ceramics. This was the time when the artistocratic classes of Japan were fascinated by Chinese culture, and at the time Chinese cultural traditions and practices, as well as objects, together with the writing system were considered to make a Japanese culture member refined. Knowing Chinese poetry and owning Chinese ceramics was considered to make Japanese members of the elite refined in their tastes.

These Chinese ceramics, which were so elaborate, were not only imported to Japan (Rousmaniere, 1998; Tregear, 1976), but later on imitations of them also started being produced in Japan.

Later on, in the fifth century, Japan was influenced by Korea (Johnson, 1999), when not only a new technique for creating pottery appeared, but also a new style for the tea bowls used in the tea ceremony, a style which was a much more simple one. The technique taken over from Korea meant using firing in high temperature of the stoneware in a reduced atmosphere, which resulted in natural ash glaze. During the periods of Asuka and Nara in Japan, green glazed ware could be found, and this technique was influenced from the techniques of creating ceramics taken over from China and Korea.

This history of cultural contact, as well as of its own tradition, makes us better understand the culture of Japan regarding its use of tea bowls in the tea ceremony we Western culture members know as an example of simplicity and austerity specific to Zen Buddhist beliefs and rituals. We are familiar with concepts such as ephemerality, and wabi-sabi, or accepting the beauty of simplicity and imperfection.

What is significant about ceramics in Japanese culture is that not only is it part of its own tradition, of its own past, of its cultural contacts with China and Korea, and of its specific way of adapting and making cultural products that are taken over from other culturues into their own recognizable cultural products, but it is also an example of tradition that continues until today. Japanese ceramics is one of those cultural objects which shows that culture is dynamic (Baciu, 2012), always in the making, as well as the way in which it is still a practice and a symbol that are still so much relevant nowadays. Japanese ceramics is not a cultural products and practice restricted to the past. It is of actual concern to the members of its culture nowadays, as much as it has been in the past, since its beginnings and during the time when it considered being open to influences from the cultural contact with China and Korea.

Japanese culture uses other cultures for inspiration and as opportunities to select those cultural products, or the features of those cultural products they consider appealing.

Nowadays, Japanese women artists are renowned in art exhibitions all over the world with their ceramic art. In Bucharest, Romania, where the author of the present paper lives, Galateea Contemporary Art organized the art exhibition called *Dıversıty of Sensıtıvıty And Expressıon*, which ran during September 12 - October 31, 2022, and which presented ceramic artworks by Aya Murata, Yuri Takemura, Mikiko Tomita, Sayaka Shingu, Sayaka Oishi, Mayumi Nakamura, and Seito Tamura. These contemporary artists show the same style of starting from the traditional past, and then building upon the tradition, reinterpreting it, and adding their own contribution to it. This fits in with the idea of certain cultures' members contributing to the tradition of their own culture, by adding up to the horizon of expectations (Baciu, 2012), meaning that each member of a certain culture, once he or she assimilates it, and acquires knowledge about it, can start bringing his or her own contribution to it. These

women artists bring their creative contribution to the ceramic tradition and practice of Japanese culture.

MATERIAL AND METHOD

According to Moeran (1990), “It is often claimed that the Japanese indulge in the 'worship of tradition' (dento suhai).” Moeran (1990) considers that “the Japanese have made much of their ceramic 'art' precisely because pottery (and note the difference in terminology) has not until very recently been seen as an art form in the West.”

We are aware of the very strong differences between Asian worlds and the Western world. These difference fascinate, since it is challenging to find that the world as we view it is not the only possible way to see it, as other cultures see it so very differently. Objects have different purposes, or some objects that are purely utilitarian in our understanding of the within our culture are considered art in the context of other cultures. Japanese ceramics are considered art, while for the Western world ceramic are just considered utilitarian pottery or, at least, it was considered like this until relatively recently. However, this is still part of the traditional mindset.

While for the Japanese the tea ceremony is an elaborate ritual and ceremony, which is still practiced today by Buddhist monks and geisha, for the Western world it is mostly a socializing, secular ritual. For the Japanese, it has a spiritual dimension next to the social dimension, and it can be had in both personal homes, or in secular contexts, in traditional tea houses, helping us connect to the atmosphere of the old Japanese ways of life, and spiritual, as it can be practiced in the setting of temples by Buddhist monks.

It is only by means of cultural differences and comparisons that we get to have access to an entirely different perpective on life and on the world, as well as on our way of thinking and understanding not only a certain object, but the way in which it can make for us a certain ritual spiritual or secular, or simply tied in with the mindset that is specific to a certain culture.

We notice how Japan, like each and every other country and nation, after all, has struggled to create a distinct identity for itself while coming into contact with various cultures. It has also considered that cultural products and traditions at some point need both to be preserved and respected, as well as continued, which is what contemporary Japanese ceramic artists are doing. These artists show that the tradition serves as a foundation for their work. It is from where they start, and afterwards they bring their own contribution.

Historical sources have shown how the basis for the way in which ceramics and pottery were created were established and, from then on, came the time for considering aesthetics. First of all, we witness the influence of Chinese ceramics, with its elaborate patters and also elaborate accompanying tea ritual, and afterwards the Japanese culture members changed their tastes and considered simple to be the best aesthetics for tea bowls and for the tea ceremony itself.

This preference goes in line with the overall tendencies of Japanese culture towards minimalism and austerity. The Japanese Zen gardens are very simple, with a few symbolic elements, such as ponds suggesting lakes, and stones suggesting mountains. In its turn, the Japanese traditional interior design involved very few pieces of furniture, and empty spaces which stimulate creativity and allow for personal contact, with no pieces of furniture as obstacles in the way of two people connecting, and free movement.

Throughout their history of taking over ceramics art and inspiration from other cultures and building their own understanding of ceramics art and sense of aesthetics, the Japanese culture has hesitated in-between a usual difference, which has preocuppied all cultures and all people: between elaborate style and simple, even austere style. This hesitation is still visible in the work of contemporary Japanese ceramics artists.

As an example, in the work of one single artist, Yuri Takemura, we see under Fig. 1, a, a tea bowl which is closest to the simple austere style, yet has still a creative spin to it:

a.  b.  c. 

Fig. 1. a. Yuri Takemura, Tea Bowl "Kanchubai", 2022. b. Yuri Takemura,Tea Bowl "Yugyo", 2022. c. Yuri Takemura, Tea Bowl "Nigimitama", 2017. Image sources: Galateea Contemporary Art (2022)

When it comes to the tea bowls in figure 1 b and c, we can notice a more visible tendency towards creativity and elaborate details. The bowl in Fig 1 a suggests a more simple pattern than the bowls in Fig 1 b and c. The bowl in Fig 1 a reminds of a very simple material which is combined based on two colours, yet does not have the elaborate technique in the last two bowls, and seems closer to the aesthetics of imperfection.

The creative tendency has been visible, suprisingly, in Japanese culture ever since old days, when, according to Watanabe (2007), “tea masters such as Rikyu altered traditional notions of beauty to create a new sensibility,” which was done by shattering bowls and cracking them on purpose. It is said that “Furuta Oribe (1543-1615)” had “cracked an old Korean bowl into several pieces, using those fragments to make a smaller bowl, one more in tune with his taste.” These, however, are just unverifiable accounts of tea master’s exploits and may as well be simple examples of fiction.

However, Western culture members recognize the wabi-sabi aesthetics. At the same time, the mindset fits in with what we notice about the Japanese sense of creativity and specificity of taste.

The work by contemporary artist Sayaka Oishi below, shown in Fig. 2, presents a bowl with elaborate design which can make us Western culture members think of the elaborate Chinese ceramics tradition:



Fig. 2. Sayaka Oishi, Tea Bowl Ryuryoku Kakou, 2022. Image sources: Galateea Contemporary Art (2022)

In the bowls shown in Fig. 3 below (Kogei Standard, 2024), we notice a comparative look at Chinese, Korean, and Japanese bowls from the past:

a.  b.  c. 

Fig. 3. a. Title: Tenmoku Tea Bowl with a "Hare's-Fur" Glaze. Country/Origin: Jian ware, China. Period/Century: Southern Song dynasty, 12th-13th century. Holder: Tokyo National Museum. b. Title: Tea Bowl, Named "Uraku Ido". Country/Origin: Korea. Period/Century: Joseon dynasty, 16th century. Holder: Tokyo National Museum. c. Title: Tea Bowl, Named "Furisode (Swinging Sleeves)". Country/Origin: Japan, Mino ware, Shino type. Period/Century: Azuchi-Momoyama-Edo period, 16th-17th century. Holder: Tokyo National Museum

The Chinese bowl has a refined aspect, the Korean bowl a simple one, and the Japanese bowl combined a rough aspect with a deliberately sought artistic aspect, showing the aesthetics of the beauty of imperfection.

We witness the changes that Japanese ceramics art has gone through, and its continuously innovative aspect, which is still visible today.

RESULTS

The analysis of Japanese ceramics has focused around the practice of the tea ceremony, of which it can be seen as a symbol. While Japan has taken over the practice, ritual and tradition of the tea ceremony from Chinese culture, and has found inspiration in their ceramics art, and further on in Korean ceramics and tea bowls, we notice the changing tastes of Japanese culture from elaborate aesthetics to simple aesthetics. The simple aesthetics is a recognized feature of this culture by Western culture members, as it marks the differences between the

two large cultural spaces in a very distinct way. What is significant is how such an age-old tradition, that of ceramic art, continues until today in Japan and is continuosly subject to creativity.

DISCUSSION AND CONCLUSION

The history and development of Japanese ceramics art presents us with an interplay between cultural preservation and adaptation. Japan's ceramics tradition, which began in the Jomon period, has undergone changes through interactions with Chinese and Korean cultures. These cultural contacts show Japan's tendency to assimilate and reinterpret external influences, transforming them into distinctly Japanese cultural products. The influence of Chinese ceramics during the Kamakura period and the later integration of Korean techniques show this process of cultural adoption and adaptation. This cultural adaptation underlines Japan's tendency to balance respect for tradition with a tendency to innovation.

We notice the shift in Japanese taste, from the elaborate designs of Chinese ceramics to the minimalism inspired by Zen Buddhism.

Contemporary Japanese ceramics art continues this tradition of creativity. The works of artists such as Yuri Takemura and Sayaka Oishi illustrate how contemporary artists start from historical practices and afterwards as personal and creative elements. This continuity is a proof of the dynamic nature of Japanese culture, where historical traditions serve as a foundation for contemporary artistic works.

We notice, by examining, briefly, the history of Japanese ceramics art, how it reflects, throughout the ages, interaction with other cultures, adaptation, creativity, and continuity of tradition. While rooted in tradition, Japanese ceramics also incorporates other cultures' influences and reshapes them tin order to conform to the Japanese mindset and sense of aesthetics. Ceramics art has adapted and it was likely because of this adaptation that it has remained relevant in time, starting with the Jomon period and still continuing with our contemporary times.

The tea ceremony includes ceramics as its central element, and, for that matter, symbolic object. This object has gone through transformations from elaborate artistic taste to simple artistic taste, and nowadays we notice the conflict between the two expressed by the contemporary artists while creating tea bowls.

REFERENCES

Baciu, S. (2012). Culture: An Awareness-Raising Approach. Cavallioti Publishing House, Bucharest, Romania.

Bausch, I. (2016). The splendour of the middle jomon culture: ceramics from the central Japanese highlands. *Aziatische Kunst*, *46*(2), 42-49.

Galateea Contemporary Art. (2022). *Dıversıty of Sensıtıvıty And Expressıon*. Aya Murata, Yuri Takemura, Mikiko Tomita, Sayaka Shingu, Sayaka Oishi, Mayumi Nakamura, Seito Tamura. September 12 - October 31, 2022. https://www.galateeagallery.com/diversity-of-sensitivity-and-expression.html

Habu, J., & Hall, M. E. (1999). Jomon pottery production in central Japan. *Asian Perspectives*, 90-110.

Johnson, E. J. (1999). *Korean influence on Japanese ceramics*. California State University, Dominguez Hills.

Kogei Standard. (2024). The Art of Appreciating Tea Bowls. A Bowl Trusted for Peaceful a Sip of Tea. https://www.kogeistandard.com/insight/serial/column-how-to-appreciate-tea-bowls/2024-06-03/

Moeran, B. (1990). Japanese Ceramics and the Discourse of'Tradition'. *Journal of Design History*, *3*(4), 213-225.

Rousmaniere, N. C. (1998). *Vessels of influence: Chinese ceramics imported into Japan and the formation of the porcelain industry*. Harvard University.

Sinopoli, C. (1992). [Review of *The Rise of a Great Tradition: Japanese Archaeological Ceramics from the Jomon through Heian Periods (10,500 B.C.-1185 A.D.)*]. *Asian Perspectives*, *31*(1), 105–107. http://www.jstor.org/stable/42928262

Tregear, M. (1976). Chinese Ceramic Imports to Japan between the Ninth and Fourteenth Centuries. *The Burlington Magazine*, *118*(885), 816-825.

Watanabe, T. (2007). From Korea to Japan and Back Again: One Hundred Years of Japanese Tea Culture through Five Bowls, 1550-1650. *Yale University Art Gallery Bulletin*, 82–99. http://www.jstor.org/stable/40514680

NANOCOMPOSITES AND NANOADSORBENTS FOR WATER AND WASTEWATER TREATMENT: CRITICAL REVIEW OF THE CURRENT LITERATURE

Betul Aykut Senel[1]

ORCID ID: 0000-0003-3674-5525

Sehnaz Sule Kaplan Bekaroglu[1]

ORCID ID: 0000-0003-0917-7219

Mehmet Kitis[1]

ORCID ID: 0000-0002-6836-3129

[1]Suleyman Demirel University, Faculty of Engineering and Natural Sciences, Department of Environmental Engineering, Isparta, Turkey

ABSTRACT

The discharge of toxic pollutants from untreated water and wastewater remains a pressing environmental issue worldwide. Pollutants such as heavy metals, herbicides, personal care products, pharmaceuticals, dyes, and various chemicals can severely impact ecosystems, environmental quality, and human health when released untreated into the environment without adequate treatment. Conventional water treatment methods often lack the capacity to remove these contaminants effectively. In this context, nanotechnology has emerged as a transformative solution in pollutant removal. Multifunctional nanocomposite adsorbents environmentally friendly materials offer advanced properties and innovative approaches, making them particularly valuable in water and wastewater treatment. Nanoadsorbents, as a subcategory of these materials, are considered next-generation adsorbents due to their remarkable efficiency in capturing pollutants. Their high surface area, significant capacity, non-toxic nature, and reusability make them ideal for water treatment applications. This study aims to consolidate recent research and advancements in the application of nanocomposites and nanoadsorbents for water and wastewater treatment. It presents examples to illustrate the roles and benefits of metal, polymer, and ceramic matrix nanocomposites in removing pollutants. Additionally, a distinct focus is given to the use of nanoadsorbents within water and wastewater treatment systems. Findings indicate that nanocomposites offer substantial potential as next-generation technologies for addressing toxic pollutants in water/wastewater. With their ability to target specific pollutants, nanocomposites and nanoadsorbents present promising solutions for achieving sustainable water quality and effective management.

Keywords: Nanoadsorbent, nanocomposite, toxic pollutant, wastewater treatment, water quality.

FINITE ELEMENT ANALYSIS OF OPEN HOLE COMPRESSIVE STRENGTH OF COMPOSITE MATERIALS

Assist. Prof. Dr. Özden İŞBİLİR

Karabük University, Engineering Faculty, Mechanical Engineering Department, Karabük, Türkiye

ORCID ID: 0000-0002-2526-602X

ÖZET

Yapısal bileşenler genellikle montaj amacıyla kullanılan delik ve/veya çentikler içerir, ancak bu delikler kablo ve hidrolik hatlar için geçiş noktası olarak da işlev görebilir. Bu tür gerilme arttırıcılar, fibrelerin mikro burkulmasından dolayı özellikle basma yükleri altında kompozit yapıların dayanımını önemli ölçüde zayıflatmaktadır. Bu çalışmada, karbon fibre takviyeli polimer (KFTP) kompozit laminatların çentik basma dayanımı ve hasar analizi üzerine sayısal bir inceleme gerçekleştirilmiştir. Referans malzeme olarak merkezinde 6.35 mm çapında delik bulunan, toplamda 24 çapraz tabaka içeren T300/976 karbon fibre epoksi laminat kompozit sistemi seçilmiştir. Hasar başlangıcı ve gelişimini içeren üç boyutlu kademeli hasar modeli ile üç boyutlu sonlu elemanlar modeli geliştirilmiştir. Hasar başlangıcı modelinde üç boyutlu Hashin ve Puck kriterleri kullanılmıştır. Analizler için gerekli olan elastik malzeme özellikleri ve kompozit sistemin dayanım değerleri literatürden elde edilmiştir. Bu parametreler kullanılarak laminat kompozit malzemenin mekanik davranışı sonlu elemanlar modelleri için hesaplanmış, hasar modları incelenmiştir. Her iki hasar başlangıç modeli için sonlu eleman modelleri, maksimum basma yükü, ilgili hasar gerinmesi ve ortalama çentik basma dayanımını deneysel verilerle yakın uyum içinde hesaplamıştır. Bu çalışma, önerilen modelin araştırma ve geliştirmede maliyetli ve zaman yoğun deneysel prosedürlere bağımlılığı azaltma potansiyelini vurgulamaktadır.

Anahtar kelimeler: Sonlu elemanlar analizi, Karbon fibre takviyeli polimer kompozitler, Çentik basma dayanımı, Kademeli hasar modelleme, Hasar analizi

ABSTRACT

Structural components often include open holes or notches, which are mainly for assembly purposes, however, they can be also access for cables and hydraulic lines. These stress concentrators notably weaken the strength of composite structures, particularly under compressive loads due to the micro buckling of the fibres. In this present paper, a numerical investigation has been carried out for the open-hole compressive (OHC) strength and failure analysis of carbon fibre-reinforced epoxy laminates. 24 layers of cross-ply T300/976 carbon fibre-epoxy laminated composite system with a 6.35 mm diameter centre hole was selected as reference material. A three-dimensional finite element (FE) model was developed with a three-dimensional progressive damage model including the damage initiation and propagation. Three-dimensional Hashin and Puck failure criteria have been utilized for damage initiation. Mechanical and material properties of the composite system were derived from the literature. The mechanical response of the laminated composite material was estimated for all finite element models using these parameters and the damage modes were examined. Finite element

models for both damage initiation models predicted the ultimate load, corresponding failure strain, and average notch compressive strength in close agreement with the literature. The study highlights the model's potential for reducing reliance on costly and time-intensive experimental procedures in research and development.

Keywords: Finite element analysis, Progressive damage modelling, Failure analysis, Carbon fibre-reinforced epoxy composites, Open-hole compressive strength,

INTRODUCTION

The open-hole compressive strength of composite materials is a critical parameter in the design and application of composite structures, particularly in industries such as aerospace, automotive, and civil engineering. This strength metric is essential for understanding how composite materials behave under compressive loads when they contain holes, which are often introduced for functional purposes such as fastening, assembly, access, or weight reduction. Holes can significantly weaken the strength of composite structures and alter the stress distribution within the material, leading to potential failure modes that must be carefully evaluated during the design process.

One of the primary reasons for the importance of open-hole compressive strength is its direct impact on the structural integrity and performance of composite components. Holes in composite laminates can lead to stress concentrations that significantly reduce the overall compressive strength of the material (Zhou et al., 2017a). This reduction can be as much as 40% compared to unnotched materials, which emphasizes the need for accurate predictions of open-hole strength in engineering applications (Casavola et al., 2012). Understanding these effects is crucial for ensuring that composite structures can withstand the loads they will encounter in service without experiencing catastrophic failure.

The mechanical response of a composite material under compressive loads with open holes is affected by different factors, such as the geometry of the holes, the stacking sequence of the laminate, and the material properties. For instance, Liu et al. highlighted that the size and shape of open holes can lead to different failure mechanisms, which need to be accounted for in design and analysis (Zhang et al., 2010). Additionally, the interaction between the hole and the surrounding material can lead to complex stress states that require advanced modelling methods, such as finite element analysis, to accurately estimate the material's response (Zhou et al., 2017b). The use of progressive damage models allows for a more nuanced understanding of how damage evolves in composite materials under load. This approach has been shown to provide more accurate predictions of strength degradation in the presence of holes, as demonstrated by Khedkar et al. in their analysis of CFRP laminates with interacting holes (Khedkar et al., 2014). Such models are invaluable for engineers seeking to optimize composite designs for specific applications.

The implications of open-hole compressive strength extend beyond individual components to the overall design of composite structures. As Gupta et al. pointed out, aerospace and automotive industries often rely on open-hole strength evaluations as part of their qualification procedures for composite components (Gupta et al., 2023). This is particularly important in applications where safety is paramount, as the failure of a single component can lead to catastrophic consequences. Therefore, understanding and accurately predicting open-hole compressive strength is essential for stress engineers who design safe and effective composite structures.

The importance of open-hole compressive strength in composite materials cannot be overstated. It is a critical factor that influences the design, performance, and safety of composite structures across various industries. Understanding the effects of hole size, geometry, and damage mechanisms is essential for engineers tasked with developing reliable and efficient composite materials. In this present study, a numerical investigation has been carried out for the open-hole compressive (OHC) strength and failure analysis of carbon fibre-reinforced plastic (CFRP) composite by the integration of advanced modelling

techniques. A three-dimensional FE model has been developed with a progressive damage model including the estimation of the damage initiation and propagation. Three-dimensional Hashin and Puck damage onset models have been utilized in the FE model. The mechanical response of the laminated composite material has been estimated for all models. The ultimate load, OHC strength, and damage modes were calculated for each model, and compared with the literature.

MATERIALS and METHODS

Constitutive Relation

In a static stress analysis, a carbon fibre-reinforced laminated composite is treated as a homogeneous, linear, elastic, and orthotropic material. Therefore, the constitutive model is expressed as follows:

$$\{\sigma\} = [C]\{\epsilon\}$$

The elastic stress-strain constitutive relation for three-dimensional orthotropic models can be written as follows:

$$\begin{Bmatrix}\sigma_{11}\\ \sigma_{22}\\ \sigma_{33}\\ \sigma_{12}\\ \sigma_{13}\\ \sigma_{23}\end{Bmatrix} = \begin{bmatrix}C_{11} & C_{12} & C_{13} & 0 & 0 & 0\\ C_{12} & C_{22} & C_{23} & 0 & 0 & 0\\ C_{13} & C_{23} & C_{33} & 0 & 0 & 0\\ 0 & 0 & 0 & C_{44} & 0 & 0\\ 0 & 0 & 0 & 0 & C_{55} & 0\\ 0 & 0 & 0 & 0 & 0 & C_{66}\end{bmatrix} \begin{Bmatrix}\epsilon_{11}\\ \epsilon_{22}\\ \epsilon_{33}\\ \gamma_{12}\\ \gamma_{13}\\ \gamma_{23}\end{Bmatrix}$$

Where;

$$C_{11} = (1-df) * E_{11}(1 - v_{23}v_{32})\Delta$$
$$C_{22} = (1-dm) * E_{22}(1 - v_{13}v_{31})\Delta$$
$$C_{33} = (1-dm) * E_{33}(1 - v_{12}v_{21})\Delta$$
$$C_{12} = (1-df) * (1-dm) * E_{11}(v_{21} - v_{31}v_{23})\Delta$$
$$C_{13} = (1-df) * (1-dm) * E_{22}(v_{32} - v_{12}v_{31})\Delta$$
$$C_{23} = (1-df) * (1-dm) * E_{33}(v_{31} - v_{21}v_{32})\Delta$$
$$C_{44} = (1-ds) * G_{12}$$
$$C_{55} = (1-ds) * G_{13}$$
$$C_{66} = (1-ds) * G_{23}$$
$$\Delta = \frac{1}{1 - v_{12}v_{21} - v_{23}v_{32} - v_{31}v_{13} - 2v_{21}v_{32}v_{13}}$$

In the equations above, C_{ij} is the material stiffness tensors, v_{ij} is the Poisson ratios, E_{ij} is Young's moduli, G_{ij} is the shear moduli, and d_f, d_m, d_s are fibre, matrix, and shear damage parameters, respectively (where 0 indicates no damage and 1 indicates complete damage in the affected mode). In the constitutive relationship, the damage parameters are initially set to zero before the onset of damage.

Damage Initiation Criteria

Predicting intralaminar damage onset involves a systematic process where stress analysis is performed, followed by evaluating failure initiation using the chosen criteria. Plenty of the failure criteria are two-dimensional since most of the time fibre-reinforced laminated structures are subjected to in-plane loads. However, in the case of three-dimensional loading scenarios, such as impact, bird strike, drilling, etc; the performance of these criteria are arguable. From this point of view, it must be noted that selecting

the suitable damage model is a significant challenge. The selection process is heavily influenced by the availability of experimental data for validation purposes and the expertise of the design engineer. In the present study, three-dimensional Hashin and Puck failure models were implemented in the progressive damage model. The performance of each model was evaluated in terms of failure strain, ultimate load, and OHC strength prediction.

The Hashin model (Hashin, 1980) identifies four different modes of failure for the composite material, namely fibre tensile failure (FI_{ft}), fibre compressive failure (FI_{fc}), matrix tensile failure (FI_{mt}), matrix compressive failure (FI_{mc}), and expressed as below.

$$FI_{ft} = \left(\frac{\sigma_{xx}}{X_T}\right)^2 + \frac{\sigma_{xy}^2 + \sigma_{xz}^2}{S_{xy}^2} \quad \text{if } \sigma_{11} \geq 0$$

$$FI_{fc} = \left(\frac{\sigma_{xx}}{X_C}\right)^2 \quad \text{if } \sigma_{11} < 0$$

$$FI_{mt} = \left(\frac{\sigma_{yy} + \sigma_{zz}}{Y_T}\right)^2 + \frac{\sigma_{yz}^2 - \sigma_{yy}\sigma_{zz}}{S_{yz}^2} + \frac{\sigma_{xy}^2 + \sigma_{xz}^2}{S_{xy}^2} \quad \text{if } (\sigma_{22} + \sigma_{33}) \geq 0$$

$$FI_{mc} = \frac{1}{Y_C}\left[\left(\frac{Y_C}{2S_{yz}}\right)^2 - 1\right](\sigma_{yy} + \sigma_{zz}) + \left(\frac{\sigma_{yy} + \sigma_{zz}}{2S_{yz}}\right)^2 + \frac{\sigma_{yz}^2 - \sigma_{yy}\sigma_{zz}}{S_{yz}^2} + \frac{\sigma_{xy}^2 + \sigma_{xz}^2}{S_{xy}^2}$$

$$\text{if } (\sigma_{22} + \sigma_{33}) < 0$$

In the above Hashin criteria; σ_{xx} is the stress in the fibre direction, σ_{yy} and σ_{zz} are the normal stresses in the transverse directions in the ply; σ_{xy}, σ_{xz}, and σ_{yz} are longitudinal/transverse shear stress, longitudinal/transverse shear stress, and transverse/transverse shear stress, respectively; X_T and X_C are the tensile and compressive strengths of the ply in the fibre direction, respectively; Y_T, and Y_C are the tensile and compressive strengths of the ply in the transverse directions, respectively; S_{xy} and S_{yz} are the shear strengths of the ply in the longitudinal/transverse and transverse/transverse directions, respectively.

The Puck failure model (Puck and Schürmann, 2002) identifies four different modes of failure for the composite material, namely fibre tensile failure (FI_{ft}), fibre compressive failure (FI_{fc}), inter fibre tensile failure (FI_{mt}), inter fibre compressive failure (FI_{mc}) and expressed as follows:

$$FI_{ft} = \frac{1}{R_{\parallel}^{(+)}}\left[\sigma_{11} - \left(v_{\perp\parallel} - v_{\perp\parallel f}.\, m_{\sigma f}\frac{E_{\parallel}}{E_{\parallel f}}\right)(\sigma_{22} + \sigma_{33})\right] \quad \text{if } \sigma_{11} \geq 0$$

$$FI_{fc} = \frac{1}{-R_{\parallel}^{(-)}}\left[\sigma_{11} - \left(v_{\perp\parallel} - v_{\perp\parallel f}.\, m_{\sigma f}\frac{E_{\parallel}}{E_{\parallel f}}\right)(\sigma_{22} + \sigma_{33})\right] \quad \text{if } \sigma_{11} < 0$$

$$FI_{mt} = \sqrt{\left[\left(\frac{1}{R_{\perp}^{(+)}} - \frac{p_{\perp\psi}^{(+)}}{R_{\perp\psi}^{A}}\right)\sigma_n\right]^2 + \left(\frac{\tau_{nt}}{R_{\perp\perp}^{A}}\right)^2 + \left(\frac{\tau_{n1}}{R_{\perp\parallel}}\right)^2} + \frac{p_{\perp\psi}^{(+)}}{R_{\perp\psi}^{A}}\sigma_n \quad if\ \sigma_n \geq 0$$

$$FI_{mc} = \sqrt{\left(\frac{\tau_{nt}}{R_{\perp\perp}^{A}}\right)^2 + \left(\frac{\tau_{n1}}{R_{\perp\parallel}}\right)^2 + \left(\frac{p_{\perp\psi}^{(-)}}{R_{\perp\psi}^{A}}\sigma_n\right)^2} + \frac{p_{\perp\psi}^{(-)}}{R_{\perp\psi}^{A}}\sigma_n \quad \text{if } \sigma_n < 0$$

Where,

$$\begin{Bmatrix}\sigma_n\\ \tau_{nt}\\ \tau_{n1}\end{Bmatrix}=\begin{bmatrix}c^2 & s^2 & 2sc & 0 & 0\\ -sc & sc & (c^2-s^2) & 0 & 0\\ 0 & 0 & 0 & s & c\end{bmatrix}\begin{Bmatrix}\sigma_{22}\\ \sigma_{33}\\ \tau_{23}\\ \tau_{31}\\ \tau_{21}\end{Bmatrix},\qquad c=cos\theta \quad and \quad s=sin\theta$$

$$\frac{p_{\perp\psi}^{(\pm)}}{R_{\perp\psi}^{A}}=\begin{cases}\dfrac{p_{\perp\perp}^{(\pm)}}{R_{\perp\perp}^{A}}\cos^2\psi+\dfrac{p_{\perp\parallel}^{(\pm)}}{R_{\perp\parallel}^{A}}\sin^2\psi & if\ \tau_{nt}^2+\tau_{n1}^2>0\\ 0 & if\ \tau_{nt}^2+\tau_{n1}^2=0\end{cases}$$

$$\cos^2\psi=1-\sin^2\psi=\frac{\tau_{nt}^2}{\tau_{nt}^2+\tau_{n1}^2}$$

$$R_{\perp\perp}^{A}=\frac{R_{\perp}^{(-)}}{2(1+p_{\perp\perp}^{(-)})}$$

In the above Puck criteria; $R_{\parallel}^{(+)}$ and $R_{\parallel}^{(-)}$ are the tensile and compressive strengths of the ply in the fibre direction, respectively; $R_{\perp}^{(+)}$, $R_{\perp}^{(-)}$ and $R_{\perp\parallel}$ are the tensile strength perpendicular to the fibre direction, the compressive strength perpendicular to the fibre direction, and the in-plane shear strength, respectively; $R_{\perp\perp}^{A}$ is the fracture resistance due to transverse/transverse shear stressing; σ_{11} is the stress in the fibre direction, σ_{22} and σ_{33} are the stresses in the transverse and stacking directions in the ply, respectively; σ_n, τ_{nl}, and τ_{nt} are the normal, transverse/longitudinal shear and transverse/transverse shear stresses on the fracture plane with the fracture angle (θ), respectively; $v_{\perp\parallel}$ and $v_{\perp\parallel f}$ are the major Poisson's ratio of the ply and of the carbon fibres, respectively; $E_{\parallel}$ and $E_{\parallel f}$ are the longitudinal elasticity modulus of the ply and the carbon fibres, respectively. $m_{\sigma f}$ is the stress magnification factor for transverse stresses in the fibres; $p_{\perp\perp}^{(\pm)}$, $p_{\perp\parallel}^{(\pm)}$ are the inclination parameters; ($\parallel$) and ($\perp$) denote parallel and transverse to the fibre direction, respectively.

Damage Progression

When a damage mode has initiated in any element, the damage progression was simulated as the last part of the progressive damage model. In this study, sudden degradation law was chosen over continuum degradation law for its simplicity. The stiffness of the damaged element was suddenly decreased by setting the corresponding damage variable (d_f and/or d_m) to 0.9999. The shear damage variable, d_s, was determined using the equations provided below.

$$d_f=\begin{cases}d_{ft} & \text{if } FI_{ft}\geq 1\\ d_{fc} & \text{if } FI_{fc}\geq 1\end{cases}\qquad d_m=\begin{cases}d_{mt} & \text{if } FI_{mt}\geq 1\\ d_{mc} & \text{if } FI_{mc}\geq 1\end{cases}$$

$$d_s=1-(1-d_{ft})(1-d_{fc})(1-d_{mt})(1-d_{mc})$$

Finite Element Model

Three-dimensional FE models were developed by incorporating the geometries of the open-hole compressive test specimen, loading, and progressive damage models; and the ultimate load, open-hole compressive strength, and damage modes were predicted. Figure 1 displays the proposed mesh discretisation of the model. A fine, uniform mesh structure around the hole vicinity is required for accurate predictions due to high stress/strain gradients. The element size around the hole vicinity was set to the same value as the thickness of each ply, 0.1429 mm.

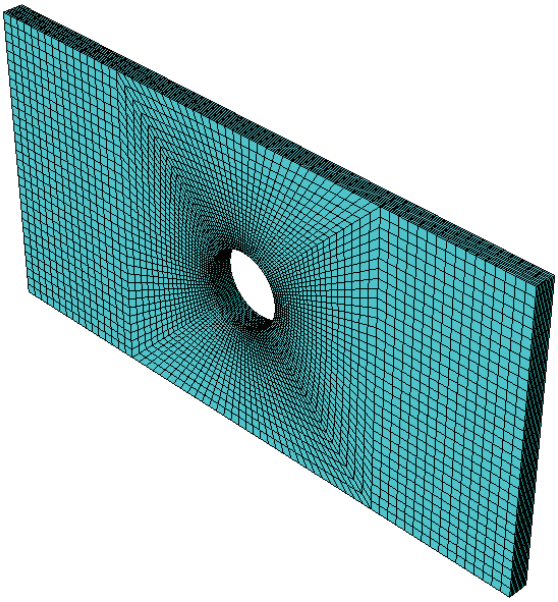


Figure 1. The proposed mesh of the FE model

24 layers of cross-ply T300/976 carbon fibre-epoxy laminated composite system with a 6.35 mm diameter (D) centre hole was selected as the reference test system. The length (L) and width (W) of the laminated CFRP are 50.8 mm and 25.4 mm, respectively. The material and dimensions were selected the same as the experimental literature (Lessard and Chang, 1991) for validation purposes. Each 0.1429 mm-thick laminated CFRP plies was modeled with a single element per ply through the thickness, utilizing three-dimensional linear cubic elements with a reduced integration formulation. Adjacent plies shared nodes at their interfaces, implying a perfect bond assumption. This means interlaminar failure, delamination, is excluded from the analysis.

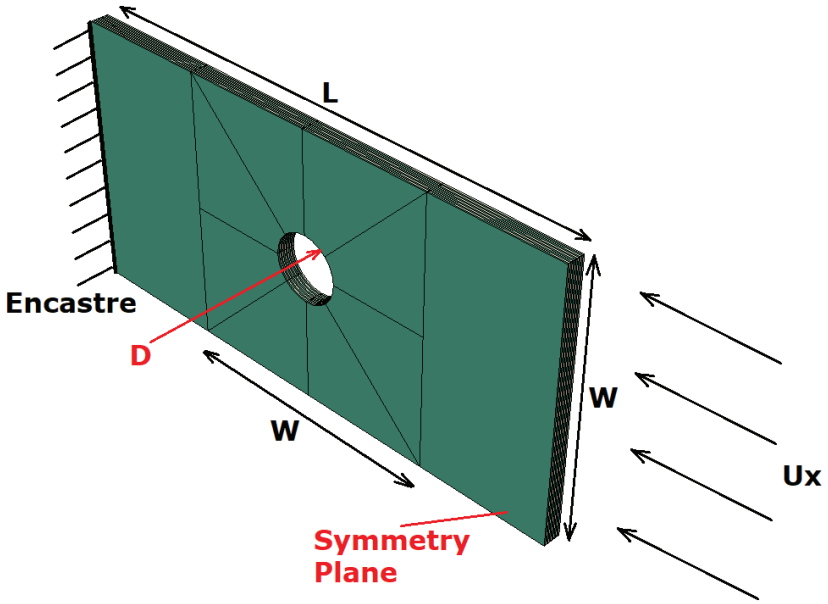


Figure 2. Boundary Conditions the laminated CFRP

Figure 2 displays the boundary conditions of the model. The left end of the laminate was fully fixed to simulate a fully clamped end boundary. To improve the computational efficiency, symmetrical boundary conditions were applied in the FE model.

This is a common and essential practice to reduce the computational time without sacrificing accuracy. A half model was generated along the thickness direction, with symmetric conditions applied to the nodes on the front face plane, which is the mid-plane of the composite structure. An incremental displacement was imposed to the right end of the laminate, through a reference node to ensure all the nodes on the right side of the laminate moved simultaneously. In total negative displacement of 1 mm was applied in the x-direction (0° fibre direction) to induce compression. The load-displacement curve was plotted by using the reference node, and the average open-hole compressive (OHC) strength was predicted based on the ultimate load from the curve.

Equivalent homogeneous, linear, elastic orthotropic material properties were assigned to each unidirectional composite ply, based on the corresponding individual orientation angle. The mechanical properties and damage parameters of T300/976 carbon fibre-reinforced epoxy laminated composite material system are provided in Table 1.

Table 1: Mechanical Properties and Damage Properties of T300/976 CFRP Composite System (Lessard and Chang, 1991; Puck, Kopp and Knops, 2002)

E_{11} (GPa)	$E_{22} = E_{33}$ (GPa)	$G_{12} = G_{13}$ (GPa)	G_{23} (GPa)	$\nu_{12} = \nu_{13}$	ν_{23}
156.512	12.962	6.964	4.470	0.23	0.45
X_T (MPa)	X_C (MPa)	$Y_T = Z_T$ (MPa)	$Y_C = Z_C$ (MPa)	$S_{XY} = S_{YZ} = S_{ZX}$ (MPa)	
1516.85	1592.69	44.54	253.04	106.87	
$p^{-}_{\perp\parallel}$		$p^{+}_{\perp\parallel}$		$p^{\pm}_{\perp\perp}$	
0.30		0.35		0.30	
$E_{\parallel f}$ (GPa) of carbon fibre		$\nu_{\perp\parallel f}$ of carbon fibre		$m_{\sigma f}$	
230		0.22		1.1	

RESULTS and DISCUSSIONS

The predicted total displacement at ultimate failure was 0.32 mm, an equaivalent failure strain of approximately 0.63%, which closely matches the experimental failure strain of approximately 0.6%. Figure 3 illustrates the load-displacement curves derived from the numerical analysis for the compression of a cross-ply T300/976 CFRP composite system with a 6.35 mm hole, based on Puck and Hashin failure criteria. Both curves exhibit a linear response up to approximately 90% of the ultimate load, corresponding to the onset of the fibre compressive damage.

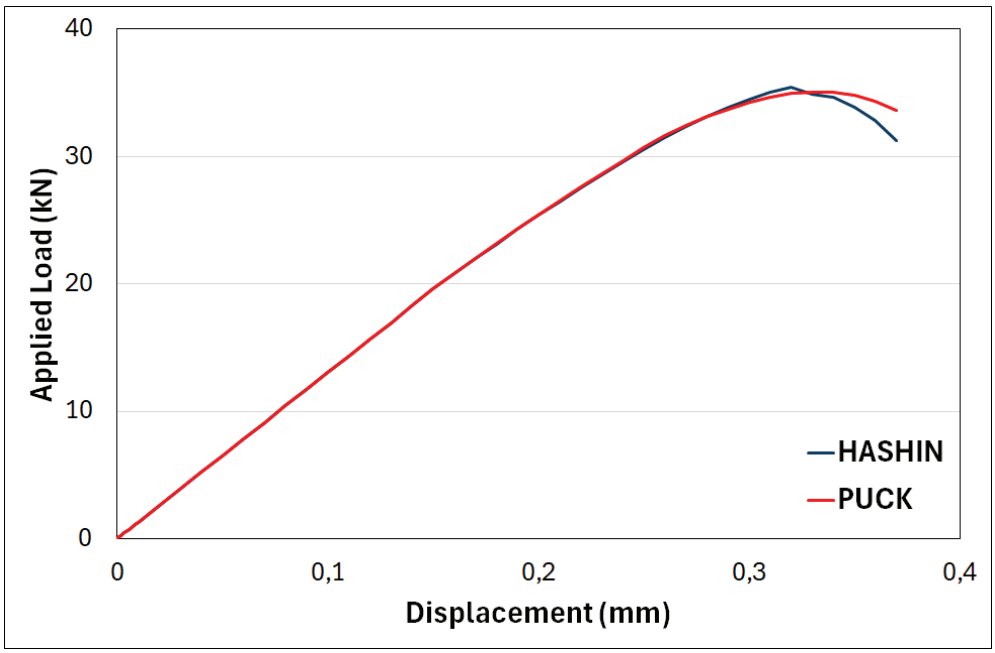


Figure 3. FEA based load-displacement curve of T300/976 subjected to Open Hole Compression

Table 2 compares the ultimate load and average OHC strength predicted by the FEA models with experimental results reported by Lessard and Chang (1991). The model employing the Hashin failure criteria slightly outperformed the Puck model in terms of accuracy, with the predicted ultimate load deviating by -4.47% from the experimental value compared to -5.44% for the Puck model.

The average open-hole compressive (OHC) strength of the laminates was calculated using the equation, $\sigma_{OHC} = P_{max}/Wt$, where P_{max} represents the ultimate load derived from the load-displacement plot of the numerical analysis displayed in Figure 4, W and t denote the width and thickness of the CFRP laminate, respectively. Similar to the ultimate load, the predicted OHC strength using the Hashin model was within 4.47% of the experimental value, highlighting the robustness of the developed FEA models.

Table 2. Comparison of Ultimate Load and Average OHC Strength of T300/976

	Ultimate Load (kN)	**Error (%)**
Experimental (Lessard and Chang, 1991)	37,09	
FEA with Hashin Failure Model	35,43	-4,47
FEA with Puck Failure Model	35,07	-5,44
	Average OHC Strength (MPa)	**Error (%)**
Experimental (Lessard and Chang, 1991)	425,77	
FEA with Hashin Failure Model	406,75	-4,47
FEA with Puck Failure Model	402,62	-5,44

Figures 4 through 7 present the damage modes predicted by the Hashin and Puck failure models at critical layers of the composite laminate. Figure 4 illustrated the damage modes by the Puck failure model at the central 90° ply (first layer from the symmetry plane of the laminate) induced at the ultimate load. Since the majority of the compressive load in the composite laminate is carried by the 0° plies, no fibre damage was observed in the central 90° ply. However, matrix damage was estimated as presented

in Figure 4 (c) and (d) even in lower load on this ply. Overall, matrix damage dominated, without any induced fibre damage. The 0° plies carries majority of the compressive load in composite system.

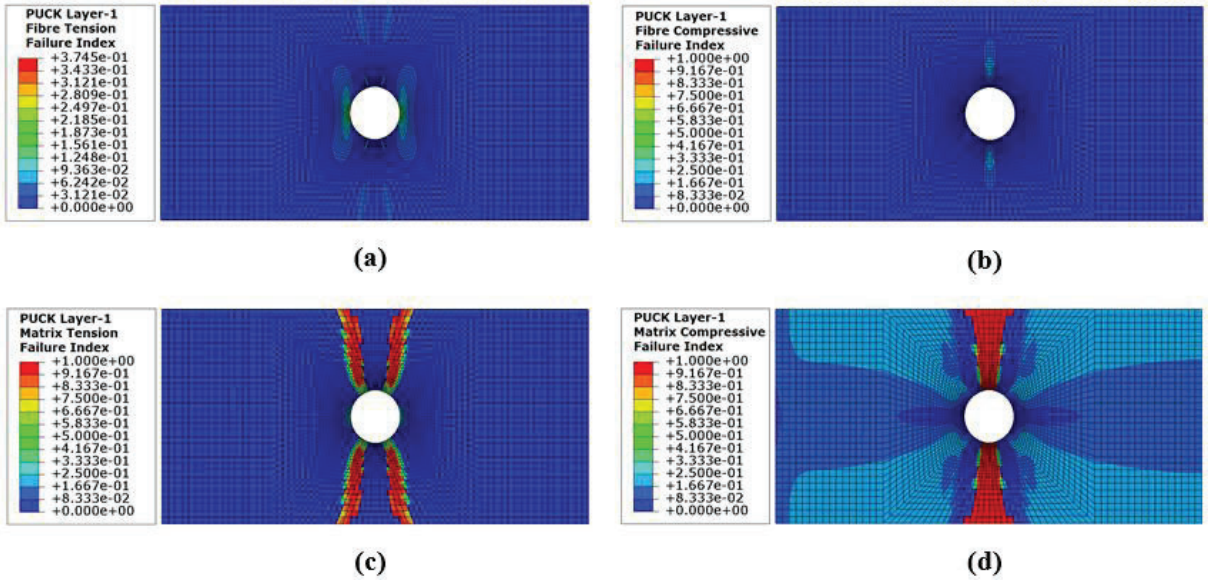


Figure 4. Puck Damage Modes in Layer-1 (90°) of T300/976 subjected to Open Hole Compression a) Fibre Tension b) Fibre Compression c) Matrix Tension d) Matrix Compression

Figure 5 illustrates the damage modes predicted by the Puck failure model in the second layer (0°) from the symmetry plane of the laminate. Since the majority of the compressive load is carried by these 0° plies, the damage modes in these plies are of interest. As can be noticed easily, there was complete fibre damage (Figure 5 (b)) in the ply attributed to micro buckling under compressive loading. Additionally, the matrix damage in tension (Figure 5 (c)) was observed in the transverse direction at $\theta=\pm 90°$ angles. This damage is likely caused by the poisson ratio after the damage induced in the fibre mode.

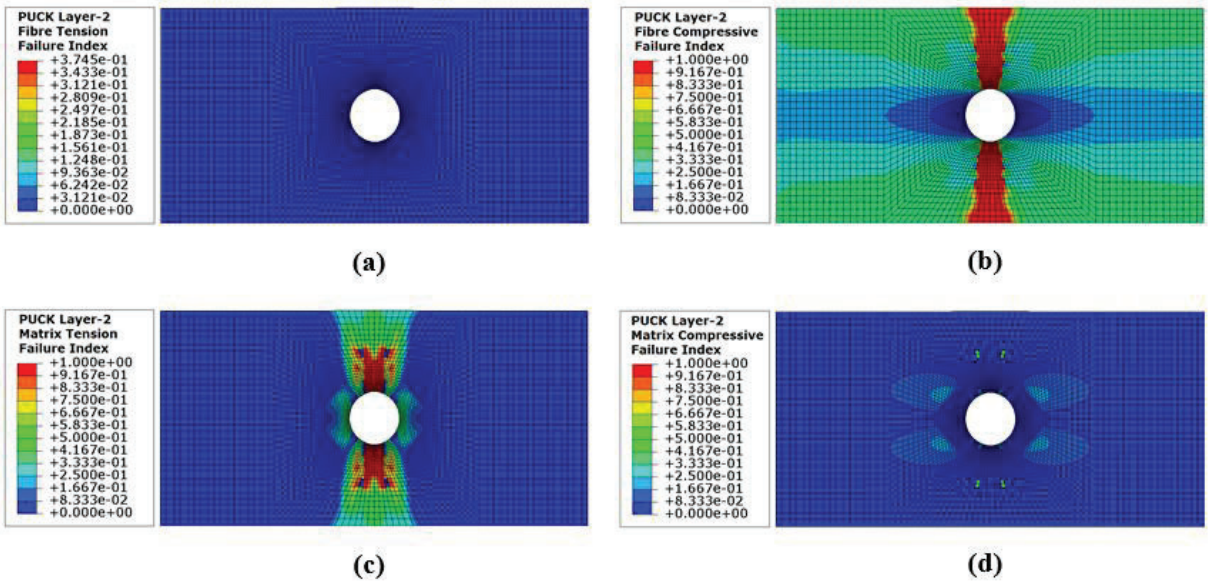


Figure 5. Puck Damage Modes in Layer-2 (0°) of T300/976 subjected to Open Hole Compression a) Fibre Tension b) Fibre Compression c) Matrix Tension d) Matrix Compression

Figure 6 represents the damage modes estimated by the Hashin failure model in the 90° ply, which is the first layer from the mid-plane of the laminate. As previously discussed, most of the compressive

load is carried by the 0° plies. Consequently, the finite element (FE) model did not predict any fibre damage in the central 90° ply. However, matrix compressive damage was identified (Figure 6(d)), particularly at θ=**±90°** angles, even under relatively lower loading conditions in this ply.

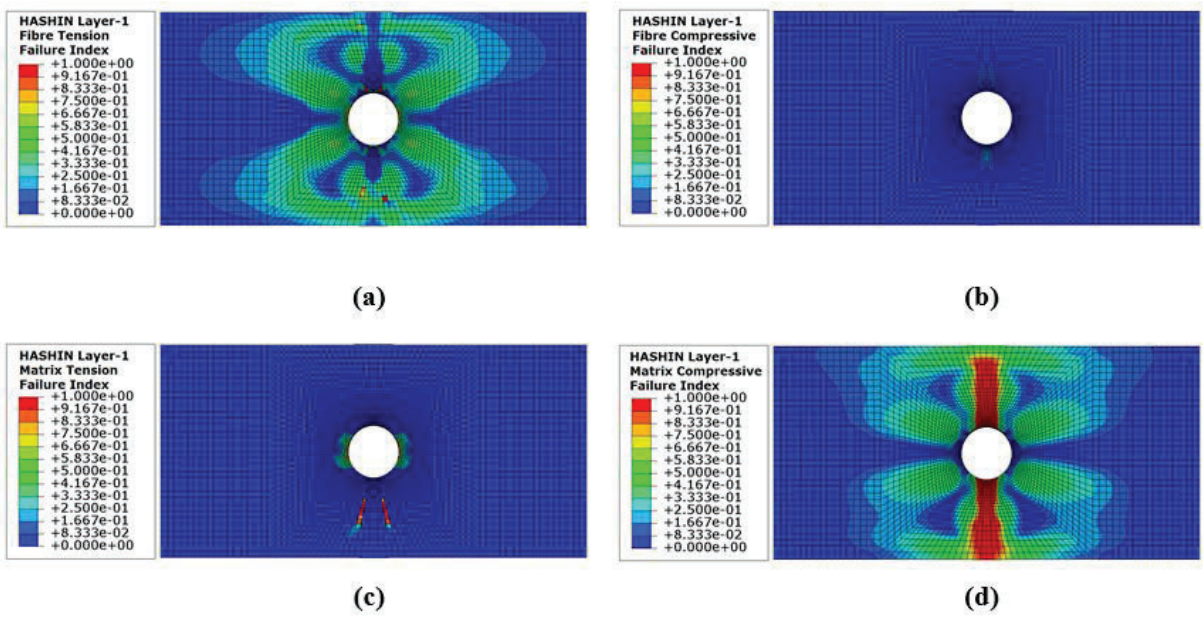


Figure 6. Hashin Damage Modes in Layer-1 (90°) of T300/976 subjected to Open Hole Compression a) Fibre Tension b) Fibre Compression c) Matrix Tension d) Matrix Compression

Figure 7 depicts the damage modes calculated by the Hashin damage model in the second layer (0°) from the symmetry plane of the laminate. Complete fibre damage in the ply, attributed to micro buckling under compressive loading, is observed in Figure 7(b). Matrix damage resulting from tension in the transverse direction was also identified, occurring between 0° and ±45° angles due to the influence of shear stresses in the matrix tension mode (Figure 7(c)). Additionally, matrix compressive damage was estimated at θ=±90° angles (Figure 7(d)), likely driven by poisson ratio following the fibre damage.

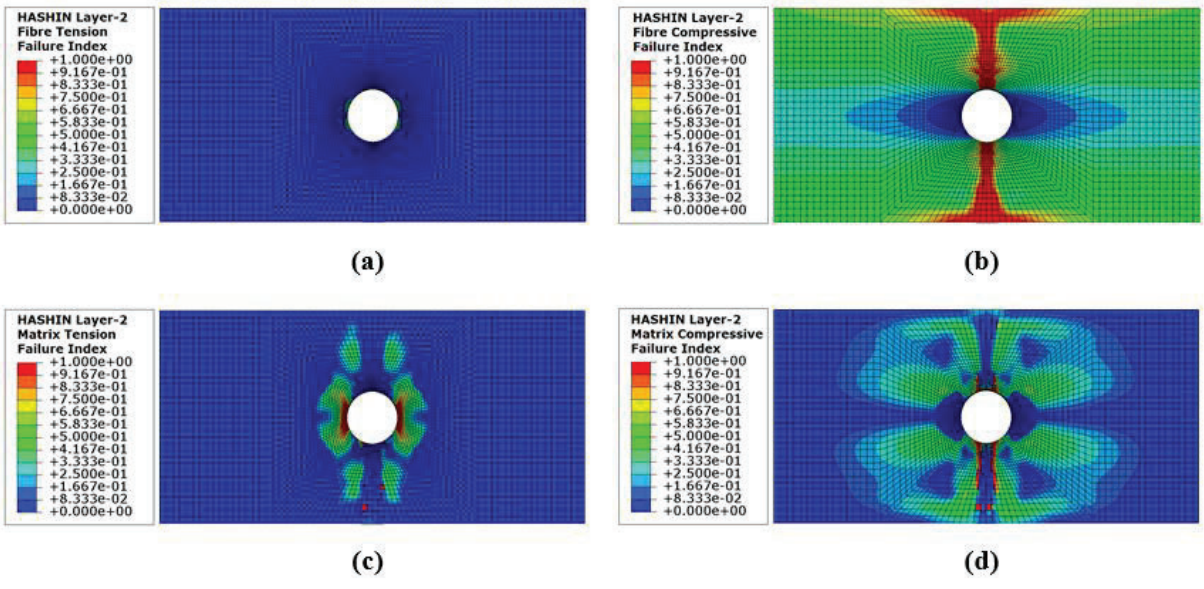


Figure 7. Hashin Damage Modes in Layer-2 (0°) of T300/976 subjected to Open Hole Compression a) Fibre Tension b) Fibre Compression c) Matrix Tension d) Matrix Compression

CONCLUSION

This study investigated the open-hole compressive (OHC) strength of the $[(0/90)_6]_S$ T300/976 carbon fibre-epoxy laminated composite system with a 6.35 mm diameter central hole. The primary objective was to evaluate the ultimate load, average OHC strength, and damage modes within the laminated composite material system. A three-dimensional FE model was developed, incorporating a three-dimensional progressive damage framework capable of predicting both damage onset and propagation. The model employed three-dimensional Hashin and Puck damage initiation criteria. The study can yield the following key findings:

- The developed model accurately predicted the failure strain.

- The ultimate load predictions demonstrated strong correlation with experimental data from the literature.

- The estimated average OHC strength closely aligned with published experimental results.

- As expected, the main damage mode was fibre compressive mode in 0° layers of the laminated composite system. Matrix failure was also observed in both 0° and 90° layers.

- The proposed FE model offers significant potential for further development in research and development (R&D) applications. It can serve as a valuable tool to reduce the dependency on costly and time-intensive experimental testing for composite materials.

REFERENCES

Casavola, C., Giannoccaro, R., Pappalettere, C., & Soutis, C. (2012). Open hole compressive strength of composite laminates and sandwich panels: comparison between budiansky–fleck–soutis model and experiments. Plastics Rubber and Composites, 41(4-5), 199-208.

Gupta, S., Pal, S., & Ray, B. (2023). An overview of mechanical properties and failure mechanism of frp laminates with hole/cutout. Journal of Applied Polymer Science, 140(20).

Hashin, Z. (1980). Failure Criteria for Unidirectional Fibre Composites. Journal of Applied Mechanics, 47, 329–334.

Khedkar, S., Chinthapenta, V., Madhavan, M., & Ramji, M. (2014). Progressive failure analysis of cfrp laminate with interacting holes under compressive loading. Journal of Composite Materials, 49(26), 3263-3283.

Lessard, L.B., Chang, F-K. (1991) Damage Tolerance of Laminated Composites Containing an Open Hole and Subjected to Compressive Loadings: Part II—Experiment. Journal of Composite Materials, 25(1), 44-64.

Puck, A., Kopp, J., Knops, M. (2002) Guidelines for the determination of the parameters in Puck's action plane strength criterion. Composites Science and Technology, 62, 371-378.

Puck, A., Schürmann, H. (2002). Failure Analysis of FRP Laminates by Means of Physically Based Phenomenological Models. Composites Science and Technology, 62, 1633–1662.

Zhang, C., Zhang, J., Qu, M., & Zhang, J. (2010). Toughness properties of basalt/carbon fibre hybrid composites. Advanced Materials Research, 150-151, 732-735.

Zhou, S., Sun, Y., & Chen, B. (2017a). Material orthotropy effects on progressive damage analysis of open-hole composite laminates under tension. Journal of Reinforced Plastics and Composites, 36(20), 1473-1486.

Zhou, S., Sun, Y., Ridha, M., & Chen, B. (2017b). Progressive damage simulation of scaling effects on open-hole composite laminates under compression. Journal of Reinforced Plastics and Composites, 36(18), 1369-1383.

FINITE ELEMENT ANALYSIS OF OPEN HOLE STRENGTH OF FIBRE METAL LAMINATES

Özden İŞBİLİR

Karabük University, Engineering Faculty, Mechanical Engineering Department, Karabük, Türkiye

ORCID ID: 0000-0002-2526-602X

ÖZET

Fiber metal laminatlar (FML'ler), geleneksel lamime kompozit malzemelerle birleştirilmiş ince metal katmanlardan oluşur. Bu hibrit kompozitin önemli bir örneği, ince alüminyum levhaların cam elyafla güçlendirilmiş epoksi laminatlarla birleştiği GLARE'dir. Bu malzemeler, monolitik alüminyum alaşımlarına kıyasla gelişmiş yapısal davranışları, yüksek mukavemet, yüksek kırılma tokluğu ve daha düşük yoğunluk gibi üstün mekanik özellikleri nedeniyle modern havacılık endüstrisinde büyük ilgi görmektedir. Bununla birlikte, bu tür yapıların montajı sıklıkla çok sayıda delik gerektirir ki bu da kompozit yapıların mukavemetini önemli ölçüde azaltır. Bu çalışma, fiber metal laminat yapıların çentik mukavemeti ve hasar davranışlarına ilişkin sayısal bir araştırma sunmaktadır. İnce monolitik alüminyum alaşım levhaları ve cam elyaf takviyeli epoksi laminat içeren üç boyutlu bir sonlu eleman modeli geliştirildi. Katmanlar arası ve katman içi hasar için hem hasarın başlamasını hem de ilerlemesini tahmin edebilen üç boyutlu bir aşamalı hasar modeli uygulandı. Katman içi hasar başlangıcı modelinde üç boyutlu Hashin ve Puck kriterleri kullanılmıştır. Elastik ve plastik mekanik özellikler, bileşen mukavemet değerleri de dahil olmak üzere analiz için gerekli olan malzeme özellikleri literatürden elde edilmiştir. Fiber metal laminatların çentik çekme ve çentik basma altındaki mekanik davranışları, bu parametreler kullanılarak sonlu eleman modellerinde değerlendirilmiştir. Her iki hasar başlangıç modeli için sonlu eleman modelleri, maksimum yükü, karşılık gelen hasar gerinimini ve ortalama çentik çekme ve basma dayanımlarını, tabakalar arası ve tabaka içi hasar modellerini hesaplamıştır. Bu sonuçlar literatürde yer alan deneysel sonuçlarla karşılaştırıldı. Bu çalışma, önerilen modelin kompozit malzemelerin araştırılması ve geliştirilmesinde maliyetli ve zaman yoğun deneysel prosedürlere olan bağımlılığı azaltma potansiyelini vurgulamaktadır.

Anahtar kelimeler: Sonlu elemanlar analizi, Fiber metal laminat, Hibrid kompozit, Cam fiber takviyeli kompozitler, Çentik dayanımı, Hasar analizi

ABSTRACT

Fibre metal laminates (FMLs) consist of laminated thin metal layers bonded with traditional composite materials. An important example of this hybrid composite is GLARE, which combines thin aluminium layers with glass fibre-reinforced epoxy laminates. These materials are of significant interest in the modern aerospace industry due to their enhanced structural capabilities and superior mechanical properties, such as high strength, elevated fracture toughness, and lower density compared to monolithic aluminium alloys. However, the assembly of such structures frequently necessitates numerous holes, which significantly reduces the strength of composite structures. This study presents a numerical investigation into the open-hole strength and failure characteristics of fibre metal laminate structures. A three-dimensional finite element model was developed, incorporating thin layers of monolithic aluminium alloy and glass fibre-reinforced

epoxy plies. The model employed three-dimensional progressive damage framework designed to predict damage initiation and propagation for interlaminar and intralaminar failures. Three-dimensional Hashin and Puck failure criteria have been utilized for intralaminar damage initiation. Material properties essential for analysis, including elastic and plastic characteristics and constituent strength values, were derived from the literature. The mechanical response of the fibre metal laminates under OHT and OHC was evaluated across all finite element models using these parameters. Finite element models for both damage initiation models predicted the ultimate load, corresponding failure strain, and average notch tensile and compressive strengths, interlaminar and intralaminar damage patterns. These numerical results were compared with the experimental results reported in the literature. The study highlights the model's potential for reducing reliance on costly and time-intensive experimental procedures in the research and development of composite materials.

Keywords: Finite element analysis, Fibre metal laminate, Hybrid composite, Glass fibre reinforced composites, Open hole strength, Failure analysis

INTRODUCTION

Fibre metal laminates (FMLs) are advanced composite materials composed of alternating layers of metal and fibre-reinforced polymer. Their unique combination of properties, including high strength-to-weight ratios, excellent fatigue resistance, and superior impact performance, makes them highly suitable for a diverse range of applications across various industries. One of the most significant application fields for FMLs is the aerospace industry. FMLs, particularly GLAREs (Glass Fibre Reinforced Aluminium Laminate), have been extensively utilized in aircraft structures, including the fuselage skin of the Airbus A380. This widespread adoption is mainly attributed to their outstanding damage tolerance, low weight, and high fatigue resistance, which are critical for maintaining structural integrity in the demanding aerospace environment (Zhu et al., 2012). Furthermore, the ability of FMLs to absorb impact energy while maintaining mechanical performance under various loading conditions makes them an ideal material choice for aircraft components that are subjected to dynamic stresses and potential impacts, such as bird strikes (Zhu et al., 2014).

In addition to aerospace, the automotive industry has increasingly adopted FMLs due to their lightweight properties and superior mechanical performance. Weight reduction is a critical factor in enhancing fuel efficiency and lowering vehicle emissions, making FMLs an attractive choice for modern automotive design. These materials are employed in various automotive components, such as body panels and structural elements, where their high strength and stiffness significantly contribute to enhanced safety and performance (Kali and Korla, 2022). Moreover, the integration of FMLs in automotive applications is further supported by their excellent resistance to fatigue and impact loads, which are common in demanding automotive environments (Awi and Abdullah, 2023).

The open-hole strength of fibre metal laminates is a critical focus of research, particularly in aerospace and automotive applications where achieving weight reduction while maintaining mechanical performance is a paramount. The tensile and compressive strengths of FMLs are substantially reduced under open-hole conditions compared to unnotched specimens, which requires a deeper understanding of their mechanical behaviour. He et al. (2020) carried out an experimental study on the tensile mechanical behaviour of multihole FMLs, demonstrating that the energy dissipation during tensile loading can be correlated with the failure mechanisms observed. Their findings indicated that the failure modes including fibre breakage, matrix cracking, and delamination, were influenced by the arrangement and number of holes. Similarly, Jiang et al. (2021) investigated the open-hole tensile behaviour of GLARE laminates, employing both experimental and numerical approaches. Their study highlighted that progressive damage mechanisms, such as fibre pull-out and interfacial debonding, were critical in determining the tensile strength of the laminates. Authors reported that the open-hole tensile strength

was significantly lower than that of unnotched specimens, emphasizing the need for careful design considerations in applications where holes are unavoidable.

The influence of hole size and shape on compressive strength has also attracted significant research attention. Tuo et al. (2017) investigated the compressive properties of laminated composites with central holes and revealed that larger holes significantly reduced the compressive strength. Their findings are consistent with those of Hu et al. (2020), who employed finite element modelling to analyze the damage mechanisms in open-hole laminates. The authors concluded that the stress distribution around the hole is a critical factor influencing the compressive performance of these materials.

The strength of the FML structure is strongly influenced by the presence and characteristics of holes, making them a crucial consideration in the design, performance, and safety of these advanced composite materials. Understanding the associated damage mechanisms is essential for engineers to develop reliable and efficient composite designs. In this study, a numerical investigation was carried out to evaluate the open-hole strength, including both tensile (OHT) and compressive (OHC) strengths, as well as the failure analysis of fibre metal laminates (FMLs). A three-dimensional finite element (FE) model was developed, incorporating a progressive damage framework to predict damage initiation and propagation. The model implemented three-dimensional Hashin and Puck failure criteria to simulate damage initiation, and cohesive elements to simulate delamination. The mechanical behaviour of FMLs was analyzed using these models, with ultimate load, OHT and OHC strengths, and damage modes calculated for each case. The results were then compared with experimental data reported in the literature.

MATERIALS and METHODS

Constitutive Relation

A glass fibre-reinforced laminated composite in a static stress analysis is considered as a homogeneous linear, elastic, and orthotropic material, hence the constitutive model is expressed as follows:

$$\{\sigma\} = [C]\{\epsilon\}$$

The elastic stress-strain constitutive relation for three-dimensional orthotropic material can be expressed as follows:

$$\begin{Bmatrix}\sigma_{11}\\ \sigma_{22}\\ \sigma_{33}\\ \sigma_{12}\\ \sigma_{13}\\ \sigma_{23}\end{Bmatrix} = \begin{bmatrix}C_{11} & C_{12} & C_{13} & 0 & 0 & 0\\ C_{12} & C_{22} & C_{23} & 0 & 0 & 0\\ C_{13} & C_{23} & C_{33} & 0 & 0 & 0\\ 0 & 0 & 0 & C_{44} & 0 & 0\\ 0 & 0 & 0 & 0 & C_{55} & 0\\ 0 & 0 & 0 & 0 & 0 & C_{66}\end{bmatrix} \begin{Bmatrix}\epsilon_{11}\\ \epsilon_{22}\\ \epsilon_{33}\\ \gamma_{12}\\ \gamma_{13}\\ \gamma_{23}\end{Bmatrix}$$

Where;

$$C_{11} = (1-df) * E_{11}(1 - v_{23}v_{32})\Delta$$

$$C_{22} = (1-dm) * E_{22}(1 - v_{13}v_{31})\Delta$$

$$C_{33} = (1-dm) * E_{33}(1 - v_{12}v_{21})\Delta$$

$$C_{12} = (1-df) * (1-dm) * E_{11}(v_{21} - v_{31}v_{23})\Delta$$

$$C_{13} = (1-df) * (1-dm) * E_{22}(v_{32} - v_{12}v_{31})\Delta$$

$$C_{23} = (1-df) * (1-dm) * E_{33}(v_{31} - v_{21}v_{32})\Delta$$

$$C_{44} = (1-ds) * G_{12}$$

$$C_{55} = (1-ds) * G_{13}$$

$$C_{66} = (1 - ds) * G_{23}$$

$$\Delta = \frac{1}{1 - v_{12}v_{21} - v_{23}v_{32} - v_{31}v_{13} - 2v_{21}v_{32}v_{13}}$$

In the equations above, C_{ij} is the material stiffness tensors, v_{ij} is the Poisson ratios, E_{ij} is Young's moduli, G_{ij} is the shear moduli, and d_f, d_m, d_s are fibre, matrix, and shear damage parameters (0:no damage; 1:complete damage in the affected mode), respectively. In the constitutive relationship, the damage parameters are zero before the onset of damage.

The interlaminar failure, delamination, can be modelled by the use of cohesive-type bonded interfaces. The elastic behaviour of a cohesive interface can be expressed through the linear traction–separation law, as outlined below.

$$K_{nn} = \frac{E}{t}, \quad K_{ss} = \frac{G}{t}, \quad K_{tt} = \frac{G}{t}$$

$$\begin{Bmatrix} t_n \\ t_s \\ t_t \end{Bmatrix} = \begin{bmatrix} K_{nn} & 0 & 0 \\ 0 & K_{ss} & 0 \\ 0 & 0 & K_{tt} \end{bmatrix} \begin{Bmatrix} \varepsilon_n \\ \varepsilon_s \\ \varepsilon_t \end{Bmatrix} = K\varepsilon$$

It should be noted that this relation applies to uncoupled behaviour. In the equations above; E, G and t denote Young's modulus, shear modulus and thickness of the interface, respectively; t_n, t_s, t_t represent the nominal tractions in the normal and two local shear directions; while ε_n, ε_s, and ε_t represent the corresponding nominal strains (separations). K represents the elastic stiffness matrix.

The homogeneous and isotropic aluminium alloy 2024-T3 can be modelled with linear elastic and plastic behaviour with isotropic hardening. The true stress and true strain can be calculated using the corresponding nominal values as below.

$$\sigma_{true} = \sigma_{nom}(1 + \varepsilon_{nom})$$

$$\varepsilon_{true} = ln(1 + \varepsilon_{nom})$$

Damage Initiation Criteria

Predicting intralaminar damage involves a systematic process where stress analysis is performed, followed by evaluating failure initiation using the chosen criteria. Plenty of the failure criteria are two-dimensional since most of the time fibre-reinforced laminated structures are subjected to in-plane loads. However, in the case of three-dimensional loading scenarios, such as impact, bird strike, drilling, etc; the performance of these criteria are arguable. From this point of view, it must be noted that selecting the suitable damage model is a significant challenge. The selection process is heavily influenced by the availability of experimental data for validation purposes and the expertise of the design engineer In this present study, three-dimensional Hashin and Puck failure initiation crtieria were implemented in the progressive damage model. Their performance was evaluated in terms of failure strain, ultimate load, OHC and OHT strength prediction.

The Hashin model (Hashin, 1980) identifies four different modes of failure for the composite material, namely fibre tensile failure (FI_{ft}), fibre compressive failure (FI_{fc}), matrix tensile failure (FI_{mt}), matrix compressive failure (FI_{mc}), and expressed as below.

$$FI_{ft} = \left(\frac{\sigma_{xx}}{X_T}\right)^2 + \frac{\sigma_{xy}^2 + \sigma_{xz}^2}{S_{xy}^2} \quad \text{if } \sigma_{11} \geq 0$$

$$FI_{fc} = \left(\frac{\sigma_{xx}}{X_C}\right)^2 \quad \text{if } \sigma_{11} < 0$$

$$FI_{mt} = \left(\frac{\sigma_{yy}+\sigma_{zz}}{Y_T}\right)^2 + \frac{\sigma_{yz}^2 - \sigma_{yy}\sigma_{zz}}{S_{yz}^2} + \frac{\sigma_{xy}^2+\sigma_{xz}^2}{S_{xy}^2} \quad \text{if } (\sigma_{22}+\sigma_{33}) \geq 0$$

$$FI_{mc} = \frac{1}{Y_C}\left[\left(\frac{Y_C}{2S_{yz}}\right)^2 - 1\right](\sigma_{yy}+\sigma_{zz}) + \left(\frac{\sigma_{yy}+\sigma_{zz}}{2S_{yz}}\right)^2 + \frac{\sigma_{yz}^2 - \sigma_{yy}\sigma_{zz}}{S_{yz}^2} + \frac{\sigma_{xy}^2+\sigma_{xz}^2}{S_{xy}^2}$$

$$\text{if } (\sigma_{22}+\sigma_{33}) < 0$$

In the above Hashin criteria; σ_{xx} is the stress in the fibre direction, σ_{yy} and σ_{zz} are the normal stresses in the transverse directions in the lamina; σ_{xy}, σ_{xz}, and σ_{yz} are longitudinal/transverse shear stress, longitudinal/transverse shear stress, and transverse/transverse shear stress, respectively; X_T and X_C are the tensile and compressive strengths of the lamina in the fibre direction, respectively; Y_T, and Y_C are the tensile and compressive strengths of the lamina in the transverse directions, respectively; S_{xy} and S_{yz} are the shear strengths of the lamina in the longitudinal/transverse and transverse/transverse directions, respectively.

The Puck failure model (Puck and Schürmann, 2002) identifies four different modes of failure for the composite material, namely fibre tensile failure (FI_{ft}), fibre compressive failure (FI_{fc}), inter fibre tensile failure (FI_{mt}), inter fibre compressive failure (FI_{mc}) and expressed as follows:

$$FI_{ft} = \frac{1}{R_{\parallel}^{(+)}}\left[\sigma_{11} - \left(\nu_{\perp\parallel} - \nu_{\perp\parallel f}.\, m_{\sigma f}\frac{E_{\parallel}}{E_{\parallel f}}\right)(\sigma_{22}+\sigma_{33})\right] \quad \text{if } \sigma_{11} \geq 0$$

$$FI_{fc} = \frac{1}{-R_{\parallel}^{(-)}}\left[\sigma_{11} - \left(\nu_{\perp\parallel} - \nu_{\perp\parallel f}.\, m_{\sigma f}\frac{E_{\parallel}}{E_{\parallel f}}\right)(\sigma_{22}+\sigma_{33})\right] \quad \text{if } \sigma_{11} < 0$$

$$FI_{mt} = \sqrt{\left[\left(\frac{1}{R_{\perp}^{(+)}} - \frac{p_{\perp\psi}^{(+)}}{R_{\perp\psi}^{A}}\right)\sigma_n\right]^2 + \left(\frac{\tau_{nt}}{R_{\perp\perp}^{A}}\right)^2 + \left(\frac{\tau_{n1}}{R_{\perp\parallel}}\right)^2} + \frac{p_{\perp\psi}^{(+)}}{R_{\perp\psi}^{A}}\sigma_n \quad if\ \sigma_n \geq 0$$

$$FI_{mc} = \sqrt{\left(\frac{\tau_{nt}}{R_{\perp\perp}^{A}}\right)^2 + \left(\frac{\tau_{n1}}{R_{\perp\parallel}}\right)^2 + \left(\frac{p_{\perp\psi}^{(-)}}{R_{\perp\psi}^{A}}\sigma_n\right)^2} + \frac{p_{\perp\psi}^{(-)}}{R_{\perp\psi}^{A}}\sigma_n \quad \text{if } \sigma_n < 0$$

Where,

$$\begin{Bmatrix}\sigma_n\\ \tau_{nt}\\ \tau_{n1}\end{Bmatrix} = \begin{bmatrix} c^2 & s^2 & 2sc & 0 & 0\\ -sc & sc & (c^2-s^2) & 0 & 0\\ 0 & 0 & 0 & s & c\end{bmatrix}\begin{Bmatrix}\sigma_{22}\\ \sigma_{33}\\ \tau_{23}\\ \tau_{31}\\ \tau_{21}\end{Bmatrix}, \qquad c = cos\theta \quad and \quad s = sin\theta$$

$$\frac{p_{\perp\psi}^{(\pm)}}{R_{\perp\psi}^{A}} = \begin{cases}\dfrac{p_{\perp\perp}^{(\pm)}}{R_{\perp\perp}^{A}}\cos^2\psi + \dfrac{p_{\perp\parallel}^{(\pm)}}{R_{\perp\parallel}^{A}}\sin^2\psi & if\ \tau_{nt}^2 + \tau_{n1}^2 > 0\\ 0 & if\ \tau_{nt}^2 + \tau_{n1}^2 = 0\end{cases}$$

$$\cos^2\psi = 1 - \sin^2\psi = \frac{\tau_{nt}^2}{\tau_{nt}^2 + \tau_{n1}^2}$$

$$R_{\perp\perp}^{A} = \frac{R_{\perp}^{(-)}}{2(1+p_{\perp\perp}^{(-)})}$$

In the above Puck criteria; $R_{\parallel}^{(+)}$ and $R_{\parallel}^{(-)}$ are the tensile and compressive strengths of the lamina in the fibre direction, respectively; $R_{\perp}^{(+)}$, $R_{\perp}^{(-)}$ and $R_{\perp\parallel}$ are the tensile strength perpendicular to the fibre direction, the compressive strength perpendicular to the fibre direction, and the in-plane shear strength, respectively; $R_{\perp\perp}^{A}$ is the fracture resistance due to transverse/transverse shear stressing; σ_{11} is the stress in the fibre direction, σ_{22} and σ_{33} are the stresses in the transverse and stacking directions in the lamina, respectively; σ_n, τ_{nl}, and τ_{nt} are the normal, transverse/longitudinal shear and transverse/transverse shear stresses on the fracture plane with the fracture angle (θ), respectively; $v_{\perp\parallel}$ and $v_{\perp\parallel f}$ are the major Poisson's ratio of the lamina and of the carbon fibres, respectively; $E_{\parallel}$ and $E_{\parallel f}$ are the longitudinal elasticity modulus of the lamina and the carbon fibres, respectively. $m_{\sigma f}$ is the stress magnification factor for transverse stresses in the fibres; $p_{\perp\perp}^{(\pm)}$, $p_{\perp\parallel}^{(\pm)}$ are the inclination parameters; ($\parallel$) and ($\perp$) denote parallel and transverse to the fibre direction, respectively.

The damage initiation for the cohesive interfaces can be defined by the quadratic nominal stress criterion as follows.

$$\left\{\frac{\langle t_n \rangle}{t_n^0}\right\}^2 + \left\{\frac{t_s}{t_s^0}\right\}^2 + \left\{\frac{t_t}{t_t^0}\right\}^2 = 1$$

where t_n, t_s and t_t represent the fracture strength of Mode I, II and III, respectively.

Damage Progression

When a damage mode has initiated in any element, the damage propagation was simulated as the last part of the progressive damage model. In this study, sudden degradation law for intralaminar behaviour was chosen over continuum degradation law for its simplicity. The stiffness of the damaged element was suddenly decreased by setting the corresponding damage variable (d_f and/or d_m) to 0.9999. The shear damage variable, d_s, was determined using the equations provided below.

$$d_f = \begin{cases} d_{ft} & \text{if } FI_{ft} \geq 1 \\ d_{fc} & \text{if } FI_{fc} \geq 1 \end{cases} \qquad d_m = \begin{cases} d_{mt} & \text{if } FI_{mt} \geq 1 \\ d_{mc} & \text{if } FI_{mc} \geq 1 \end{cases}$$

$$d_s = 1 - (1 - d_{ft})(1 - d_{fc})(1 - d_{mt})(1 - d_{mc})$$

The propagation of the damage for the interlaminar behaviour can be described by the mixed mode fracture energy, based on a power-law fracture criterion, as shown below.

$$\left\{\frac{G_n}{G_N}\right\}^2 + \left\{\frac{G_s}{G_S}\right\}^2 + \left\{\frac{G_t}{G_T}\right\}^2 = 1$$

G_N, G_S and G_T represent the critical fracture energies in the normal, first shear and second shear directions, respectively.

Finite Element Model

Three-dimensional FE models were developed by incorporating the geometries of the open-hole tensile and compressive test samples, loading, and progressive damage models; and the ultimate load, open-hole tensile (OHT) strength, open-hole compressive (OHC) strength, and damage modes were predicted numerically. Fig. 1 shows the mesh structure and the dimensions of the specimen. A fine, regular mesh structure around the hole vicinity is required to predict high-stress/strain gradients accurately. The element size around the hole vicinity was set to 0.125 mm (the thickness of the glass fibre-reinforced composite ply).

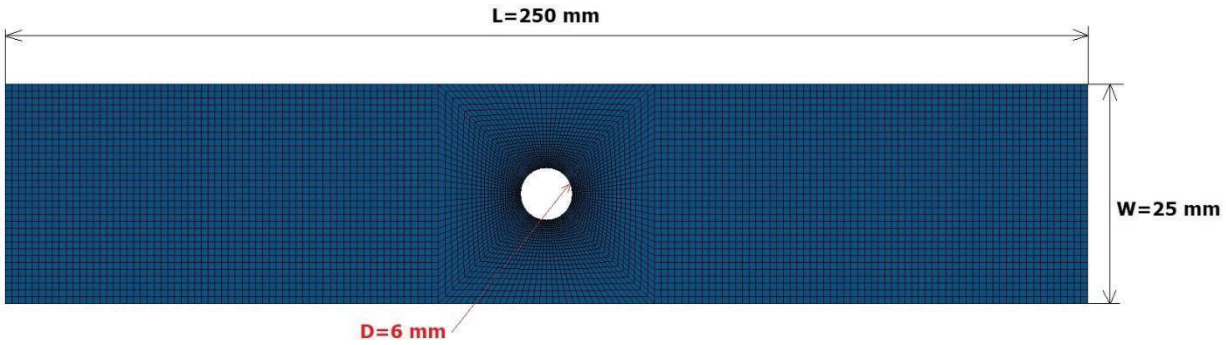


Figure 1. The proposed mesh and dimensions of the FE model

GLARE 3- 3/2-0.5 Al2024-T3 composite system with a 6 mm diameter central hole was selected for validation purposes with the published literature. 3 layers of 0.5 mm thick Al2024-T3 and between them cross-ply S-glass reinforced epoxy (GFRP) laminated composite system was used. The stacking information of the composite system is represented in Figure 2. Each 0.125 mm-thick laminated GFRP plies was modeled with a single element per ply through the thickness, utilizing three-dimensional linear cubic elements with a reduced integration formulation. The aluminium layers were also modelled with the same elements and mesh sizes. For the interfaces between the adjacent layers, 0.001 mm cohesive elements are employed to model interlaminar failure in the analysis.

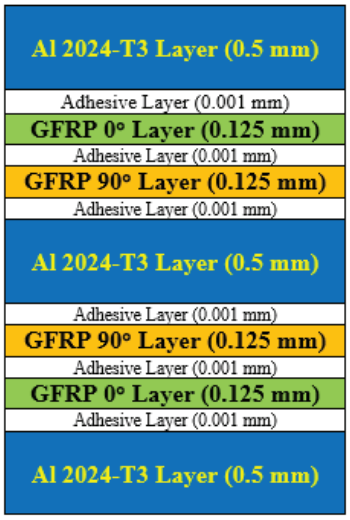


Figure 2. Stacking Information of GLARE 3- 3/2-0.5 Al2024-T3 composite system

Figure 3 shows the boundary conditions of the FE models. The left end of the laminates was completely fixed to simulate the fully clamped end. To improve the computational efficiency, symmetrical boundary conditions were applied in the FE model. A half model was generated along the thickness direction, with symmetric conditions applied to the nodes on the front face plane, which is sytemmetry plane of the composite structure. An incremental displacement was imposed to the right end of the laminate, through a reference node to ensure all the nodes on the right side of the laminate moved simultaneously. In total negative displacement of 1 mm was applied in the x-direction (0° fibre direction) to induce compression in OHC while a positive displacement of 1 mm was applied in the x-direction (0° fibre direction) to induce tensile in OHT simulations. The load-displacement plots were obtained by using the reference node, and the average open-hole tensile (OHT) and open-hole compressive (OHC) strength values were predicted based on the ultimate load from the curves.

ISBN: 978-625-378-045-6

https://doi.org/10.5281/zenodo.14537144

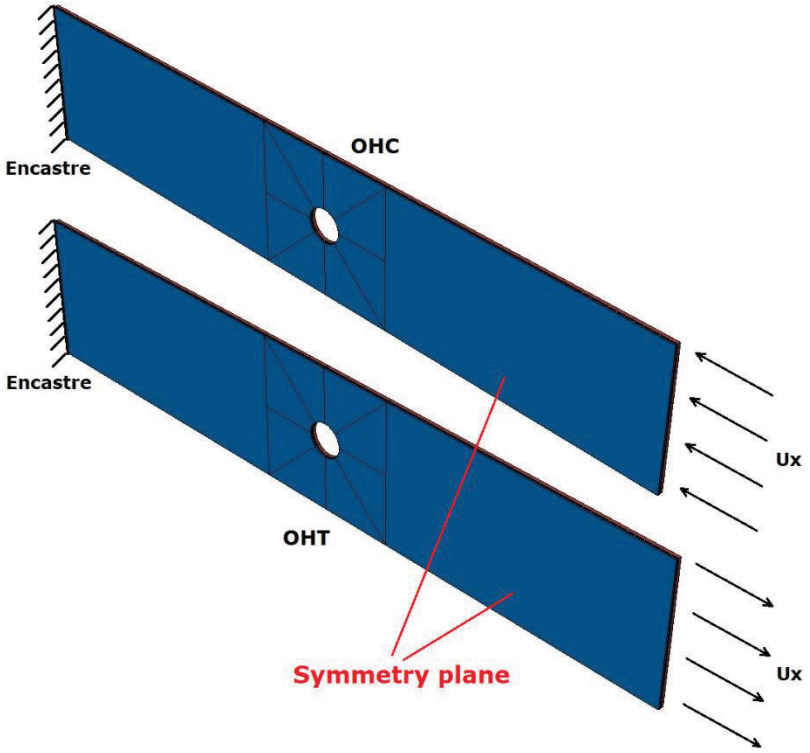


Figure 3. Boundary Conditions of GLARE 3- 3/2-0.5 Al2024-T3 composite system for Open Hole Compressive and Open Hole Tensile Models

Equivalent homogeneous, linear, elastic orthotropic behaviour was assigned to each unidirectional GFRP plies according to the appropriate individual orientation angle. The mechanical properties and damage parameters of GFRP are given in Table 1.

Table 1: Mechanical Properties and Damage Properties of GFRP (Jiang et.al, 2022; Puck, Kopp and Knops, 2002)

E_{11} (GPa)	$E_{22} = E_{33}$ (GPa)	$G_{12} = G_{13}$ (GPa)	G_{23} (GPa)	$\nu_{12} = \nu_{13}$	ν_{23}
49	14	4.6	4.6	0.3	0.3
X_T (MPa)	X_C (MPa)	$Y_T = Z_T$ (MPa)	$Y_C = Z_C$ (MPa)	$S_{XY} = S_{YZ} = S_{ZX}$ (MPa)	
1158	379	59	137	40	
$p^{-}_{\perp\parallel}$		$p^{+}_{\perp\parallel}$		$p^{\pm}_{\perp\perp}$	
0.25		0.30		0.2	
$E_{\parallel f}$ (GPa) of carbon fibre		$\nu_{\perp\parallel f}$ of carbon fibre		$m_{\sigma f}$	
86.9		0.23		1.3	

Linear uncoupled elastic traction-separation behaviour was assigned to each cohesive interface between the Al2023 and GFRP, cross-ply GFRP layers. The mechanical properties of these adhesive layers are given in Table 2.

ISBN: 978-625-378-045-6 https://doi.org/10.5281/zenodo.14537144

Table 2: Mechanical Properties of Adhesive (Jiang et.al, 2022)

E (GPa)	G (GPa)	t_N (MPa)	t_S (MPa)	t_T (MPa)	G_N (J/m^2)	G_S (J/m^2)	G_S (J/m^2)
2	0.75	65	38	38	2	4	4

Linear elastic and plastic with isotropic hardening behaviour were assigned to each Al2023-T3 layer. The mechanical properties of Al2023-T3 are given in Table 3.

Table 3: Mechanical properties of Aluminum 2024-T3(Jiang et.al, 2022)

E (GPa)	ν	σ_y (MPa)	ε_p (%)
72	0.33	300.4	0
		310.2	0.018
		320	0.044
		330.2	0.09
		340.1	0.228
		350.1	0.48
		360.2	0.783
		370.2	1.097
		380.2	1.467
		390.1	1.918
		400.1	2.376
		410	2.902
		420.1	3.431
		430.2	3.965
		440.2	4.585
		450	5.243
		460.2	5.954
		473.6	7.028
		480	7.761
		490.2	8.582
		500.1	9.651
		520.4	12.314

RESULTS and DISCUSSIONS

Figure 4 illustrates the load-displacement curves obtained from the finite element analysis for the open-hole tension (OHT) and open-hole compression (OHC) of GLARE 3- 3/2-0.5 Al2024-T3 with a 6 mm diameter central hole. The results are based on the Puck and Hashin failure criteria.

In OHT analysis, both models exhibit a linear load response up to a displacement of 0.4 mm, after which damage initiation occurs. The Puck model predicted premature failure at a displacement of 0.6 mm of displacement, corresponding to a strain of 0.48%. In contrast, the Hashin model estimated failure at a displacement of approximately 0.98 mm, with a corresponding strain of 0.78%. Both models underestimated the failure strain compared to the experimental failure strain of approximately 1.5%, with the Hashin model providing closer predictions.

For the OHC analysis, the displacement at failure was lower than that for OHT. The Puck model predicted failure at a displacement of 0.49 mm (strain: 0.39%), while the Hashin model estimated failure at 0.55 mm (strain: 0.44%).

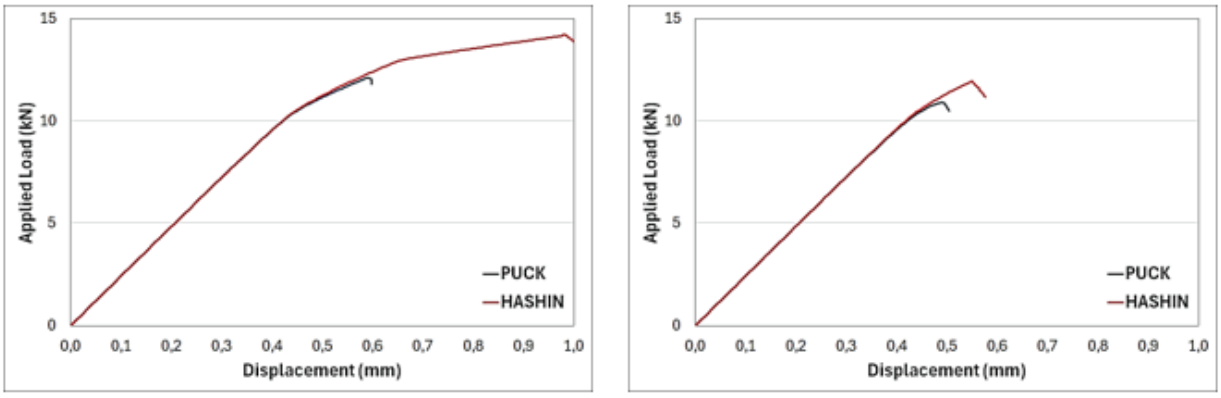


Figure 4. FEA based load-displacement curve of GLARE
a) Open Hole Tension b) Open Hole Compression

Table 4 compares the ultimate load and average OHT strength predicted by the FEA models to experimental data reported by Jiang et al. (2022). The Hashin model outperformed the Puck model, with a deviation of -5% from the experimental ultimate load, compared to -19.27% for the Puck model. The average open-hole tensile (OHT) strength of the FML was calculated using the equation, $\sigma_{OHT} = P_{max}/Wt$, where P_{max} represents the ultimate load derived from the load-displacement plot of the FE model presented Figure 4 (a), W and t denote the width and thickness of the FML, respectively. The ultimate load trend was consistent for the predicted average OHT strength, with the Hashin model showing an error of -5%, further underscoring the accuracy of this approach.

Table 4. Comparison of Ultimate Load and Average OHT Strength of GLARE 3- 3/2-0.5 Al2024-T3

	Applied Load (kN)	
Experimental (Jiang et.al, 2022)*	15.00	
FEA with Hashin Failure Model	14,25	-5,00
FEA with Puck Failure Model	12,11	-19,27
	Average OHT Strength (MPa)	**Error (%)**
Experimental (Jiang et.al, 2022)	300,00	
FEA with Hashin Failure Model	285,00	-5,00
FEA with Puck Failure Model	242,20	-19,27

* Experimental Ultimate load information was derived from the stress and cross-section information.

In the OHC analysis (in Table 5), the Hashin model also performed better, predicting a slightly higher ultimate load and average OHC strength than the Puck model. The Hashin model deviated by 9.52% from the experimental value for OHC strength, demonstrating reasonable accuracy for compressive behaviour.

Table 5. Comparison of Ultimate Load and Average OHC Strength of GLARE 3- 3/2-0.5 Al2024-T3

	Applied Load (kN)
FEA with Hashin Failure Model	11,97
FEA with Puck Failure Model	10,93
	Average OHC Strength (MPa)
FEA with Hashin Failure Model	239,40
FEA with Puck Failure Model	218,60

In the above OHT results, the model with the Hashin failure model predicted more accurate results compared to the Puck failure model. Therefore, the damage modes predicted by the Hashin failure model under OHT for GLARE 3-3/2-0.5 Al2024-T3 are displayed in Figure 5.

The Hashin model identified fibre tension damage in both the 90° (Figure 5a) and 0° (Figure 5b) GFRP layers. These failure modes are primarily attributed to tensile loading along the respective fibre orientations.

The failure in ±45° angles are due to the effect of the shear stresses in the fibre tension mode. Interlaminar damage was also observed across multiple interfaces between Al2023-GFRP 90° layers in Figures 5c, GFRP 90°-GFRP 0° layers in Figures 5d and GFRP 0°- Al2023 layers in Figures 5e. These images reflected delamination between adjacent composite layers owing to the stress concentrations around the hole. The highest zone was observed between GFRP 0°- Al2023 layers in Figure 5e due to the higher stresses carried by the 0° ply. When interlaminar damage occurs, the plies are debonded from each other, thus it can affect stress distribution in both plies.

ISBN: 978-625-378-045-6

https://doi.org/10.5281/zenodo.14537144

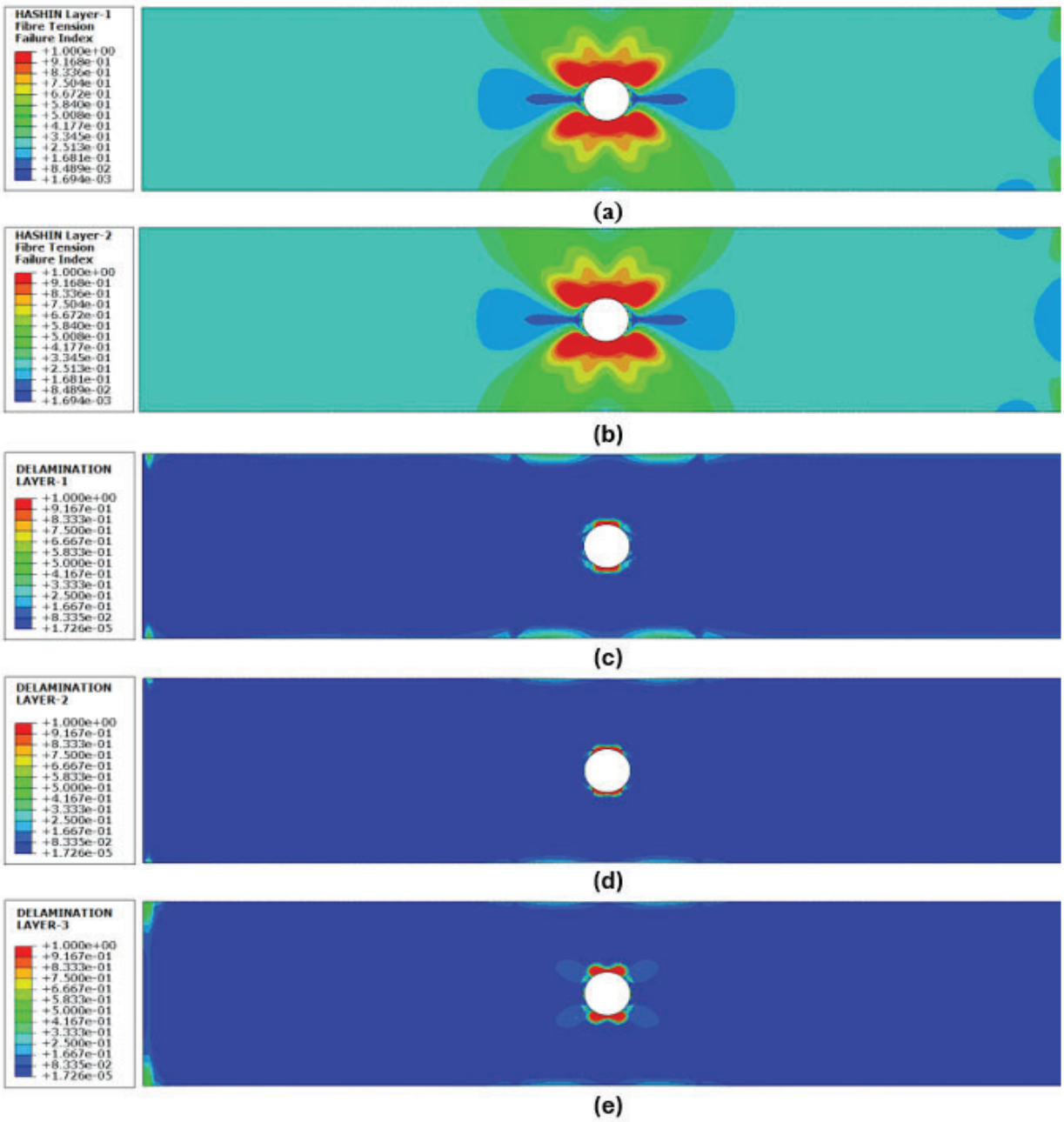


Figure 5. Damage Modes in GLARE 3 under Open Hole Tension
a) Hashin Fibre Tension in 90° GFRP b) Hashin Fibre Tension in 0° GFRP c) Interlaminar Failure in Cohesive Layer-1 d) Interlaminar Failure in Cohesive Layer-2 e) Interlaminar Failure in Cohesive Layer-3

Figure 6 illustrates the damage modes predicted by the Puck failure models under OHC for GLARE 3-3/2-0.5 Al2024-T3. No fibre damage was observed in the 90° ply (Figure 6a), but the Puck model identified fibre compression damage in the 0° ply of GFRP (Figure 6b). This failure mode is primarily attributed to compressive loading along the respective fibre orientations. Similar to the Hashin model in OHT, interlaminar damage was predicted across cohesive layers (Figures 6c, 6d, and 6e). However, the extent and location of delamination zones varied slightly in different layers. Interlaminar damage was predicted more severe at interfaces between GFRP 90°-GFRP 0° layers in Figures 5d, and GFRP 0°-

Al2023 layers in Figures 5e. This could be due to the micro buckling of the 0° ply GFRP under compressive load.

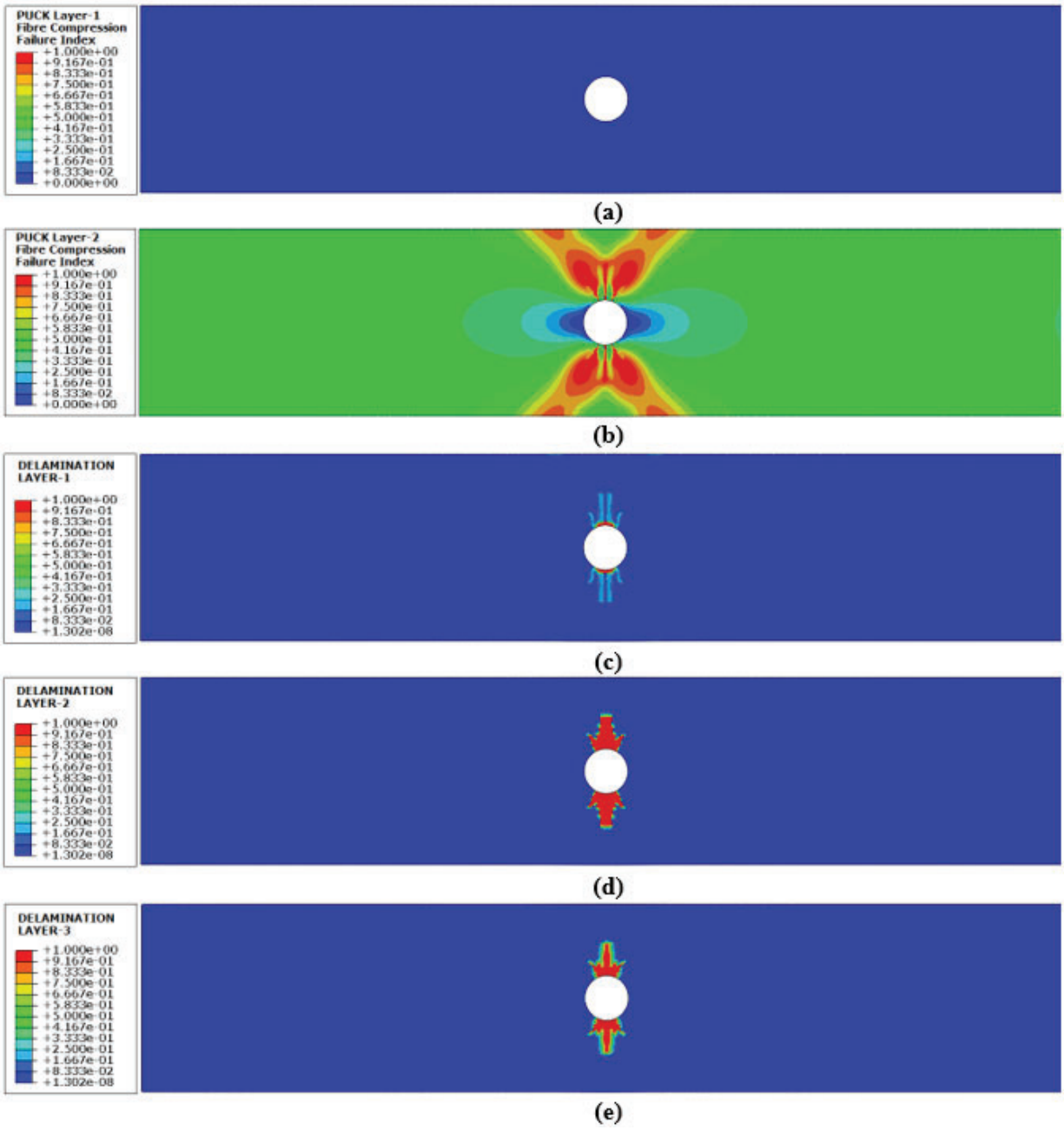


Figure 6. Damage Modes in GLARE 3 under Open Hole Tension
a) Puck Fibre Tension in 90° GFRP b) Puck Fibre Tension in 0° GFRP c) Interlaminar Failure in Cohesive Layer-1 d) Interlaminar Failure in Cohesive Layer-2 e) Interlaminar Failure in Cohesive Layer-3

CONCLUSION

This study investigated the open-hole tensile (OHT) and open-hole compressive (OHC) strength of the GLARE 3-3/2-0.5 Al2024-T3 fibre metal laminate system with a 6 mm diameter central hole. The primary objective was to evaluate the ultimate loads, average OHT and OHC strength, and intralaminar and interlaminar damage modes within the fibre metal laminate composite system. A three-dimensional FE model was developed, incorporating a three-dimensional progressive damage framework capable of predicting both damage onset and propagation for both intralaminar and interlaminar failure modes. The model utilized three-dimensional Hashin and Puck failure criteria to simulate damage initiation, as well as traction-separation behaviour to model delamination. The key findings of the study are as follows:

- The Hashin failure model demonstrated strong agreement with reported data from the literature in predicting ultimate loads and average OHT strength.

- As anticipated, the dominant damage modes were fibre tensile failure in the 0° GFRP plies during OHT and fibre compressive failure in the same plies during OHC.

- Interlaminar damage was observed in both OHC and OHT, induced at the interfaces between the Al2023 and GFRP plies. Delamination was predicted more severe in OHC due to microbuckling in the 0° ply of GFRP.

- The proposed FE exhibit valuable potential for further development in research and development (R&D) applications. It offers a valuable tool to reduce reliance on expensive and time-consuming experimental testing for composite structures.

REFERENCES

Awi, M. and Abdullah, A. (2023). A review on mechanical properties and response of fibre metal laminate under impact loading (experiment). Evergreen, 10(1), 111-129.

Hashin, Z. (1980). Failure Criteria for Unidirectional Fibre Composites. Journal of Applied Mechanics, 47, 329–334.

He, W., Wang, C., Wang, S., Lu, Y., Wu, J., & Xie, D. (2020). Tensile mechanical behavior and failure mechanisms of multihole fibre metal laminates—experimental characterization and numerical prediction. Journal of Reinforced Plastics and Composites, 39(13-14), 499-519.

Hu, J., Zhang, X., Chen, Z., Guo, W., Li, H., and Deng, X. (2020). Experimental and numerical research on open-hole strength and damage mechanism of regularly arrayed short fibre reinforced polymer composite. Polymers, 12(7), 1622.

Jiang, S., Gao, L., Xie, B., Li, K., & Wu, C. (2021). Open-hole tensile behavior and progressive damage of hybrid fibre metal laminates. Applied Composite Materials, 29(2), 547-563.

Jiang, S., Gao, L., Xie, B., Li, K., and Wu, C. (2022). Open-Hole Tensile Behavior and Progressive Damage of Hybrid Fibre Metal Laminates. Applied Composite Materialsi 29, 547–563.

Kali, N. and Korla, S. (2022). Numerical studies on mode i delamination and its effect on the vibrational characteristics in fibre metal laminates. Iop Conference Series Materials Science and Engineering, 1225(1), 012039.

Puck, A., Kopp, J., Knops, M. (2002) Guidelines for the determination of the parameters in Puck's action plane strength criterion. Composites Science and Technology, 62, 371-378.

Puck, A., Schürmann, H. (2002). Failure Analysis of FRP Laminates by Means of Physically Based Phenomenological Models. Composites Science and Technology, 62, 1633–1662.

Tuo, H., Lu, Z., and Ma, X. (2017). Effects of environment on compressive properties of laminated composites containing a central hole. International Conference on Material Science, Energy

and Environmental Engineering (MSEEE 2017), Advances in Engineering Research, volume 125335, 335-339

Zhu, G., Xiao, Y., Yang, Y., Wang, J., Sun, B., and Boom, R. (2012). Degradation behavior of epoxy resins in fibre metal laminates under thermal conditions. Journal of Shanghai Jiaotong University (Science), 17(3), 257-262.

Zhu, S., Wang, Y., Tong, M., & Xiong, P. (2014). Numerical simulation of bird impact on fibre metal laminates. Polymers and Polymer Composites, 22(2), 147-156.

SYNTHESIS OF PD NANOPARTICLES IN POLY-4-VINYL PYRIDINE MEDIA

Hacar Aslanova
Institute of Catalysis and Inorganic Chemistry named after M. Nagiyev, Ministry of Science and Education of the Republic of Azerbaijan, Laboratory of Nanostructured metal-polymer catalysts, Baku, Azerbaijan
[1]ORCID ID: 0000-0002-5579-1802

Chichak Seyidova
Institute of Catalysis and Inorganic Chemistry named after M. Nagiyev, Ministry of Science and Education of the Republic of Azerbaijan, Laboratory of Nanostructured metal-polymer catalysts, Baku, Azerbaijan.
[2]ORCID ID: 0000-0002-4286-0135

Nigar Shikhverdiyeva
Institute of Catalysis and Inorganic Chemistry named after M. Nagiyev, Ministry of Science and Education of the Republic of Azerbaijan, Laboratory of Nanostructured metal-polymer catalysts, Baku, Azerbaijan.
[3]ORCID ID: 0009-0007-6863-9715

Nizami Zeynalov
Institute of Catalysis and Inorganic Chemistry named after M. Nagiyev, Ministry of Science and Education of the Republic of Azerbaijan, Laboratory of Nanostructured metal-polymer catalysts, Baku, Azerbaijan.
[4]ORCID ID: 0000-0002-7889-6594

ABSTRACT

The use of palladium catalyst precursors among various transition metals as well as nanosized palladium particles in organic synthesis has become widespread, especially in the last decade [1]. At this time, the application of heterogenized catalysts is one of the current trends of recent years due to several superior properties [2]. Considering the importance of applying synthetic polymers as carriers for heterogeneous catalysts, obtaining catalysts based on poly-4-vinyl pyridine (P-4VP) is very important. [3].

However, P-4VP also has several drawbacks. Modifying the polymer (quaternization) helps to significantly overcome the limitations that may arise during its application. Quaternized polymers have several superior properties over primary polymers.

Considering all this, P-4VP was quaternized with methyl iodide based on the appropriate methodology during the study [4]. Then the obtaining of a catalyst based on a quaternized polymer was considered. Initially, the polymer sample was dissolved in a low-concentration alcohol solution, and then PdCl2 was added to the reaction medium.

After the Me/polymer solution was stirred on a magnetic stirrer for several hours, $NaBH_4$ was added to the medium as a reducing agent, and a darkening of the color in the solution was observed. In the last stage, the obtained nanocomposite was cross-linked using a cross-linking agent. It should be noted that Me/Pol plays a decisive role in the synthesis of nanocatalysts. N, N`-methylene bis acrylamide (MBA) was used as a cross-linking agent in this context. MBA was dissolved in distilled water and added to the reaction medium. After stirring for 2 hours, the reaction product was washed successively with diethyl ether and distilled water and purified from unreacted residues. After the obtained precipitate is dried at room temperature (21°C), it is cross-linked under a UV quartz lamp at 40°C for 4 hours. Finally, the obtained reaction product was studied by the FTIR analysis method and it was found that the process was successfully implemented during the analysis of their spectra.

Keywords: Pd nanoparticles, heterogenized catalysts, polymer, poly-4-vinyl pyridine

References

1. H.Z. Liu, T. Jiang, B.X. Han, S.G. Liang, Y.X. Zhou, Science 326 (2009) 1250–1252.
2. Meemken, F.; Baiker, A. Recent Progress in Heterogeneous Asymmetric Hydrogenation of C-O and C-C Bonds on Supported Noble Metal Catalysts. Chem. Rev. 2017, 117, 11522−11569.
3. Zhao X, Chang Y, Chen WJ, Wu Q, Pan X, Chen K, Weng B. Recent Progress in Pd-Based Nanocatalysts for Selective Hydrogenation. ACS Omega. 2021 Dec 20;7(1):17-31. doi: 10.1021/acsomega.1c06244. PMID: 35036674; PMCID: PMC8756445.
4. H.F.Aslanova, N.A.Zeynalov, D.B.Tağıyev. Metil-yodid mühitində poli-4-vinilpiridinin kvaternizasiyası. Ümummilli Lider Heydər Əliyevin anadan olmasının 101-ci ildönümünə həsr olunmuş: "Dayanıqlı Kimya və Kimya mühəndisliyinə doğru" Tələbə və Gənc Tədqiqatçıların V Beynəlxalq Elmi Konfransı. Bakı. 23-25 aprel 2024. S.230-231

SYNTHESIS OF POLYMER-BASED SILVER NANOPARTICLES, STRUCTURE AND PROPERTIES OF OBTAINED POLYMER COMPOSITE

Elchin Babayev
Institute of Catalysis and Inorganic Chemistry named after M. Nagiyev, Ministry of Science and Education of the Republic of Azerbaijan, Laboratory of Nanostructured metal-polymer catalysts, Baku, Azerbaijan.
ORCID ID: 0009-0004-8602-9951

Nargiz Rahimli
Institute of Catalysis and Inorganic Chemistry named after M. Nagiyev, Ministry of Science and Education of the Republic of Azerbaijan, Laboratory of Nanostructured metal-polymer catalysts, Baku, Azerbaijan.
ORCID ID: 0000-0003-4097-7302

Ulviyya Mammadova
Institute of Catalysis and Inorganic Chemistry named after M. Nagiyev, Ministry of Science and Education of the Republic of Azerbaijan, Laboratory of Nanostructured metal-polymer catalysts, Baku, Azerbaijan.
ORCID ID: 0000-0003-3197-0918

Dilshad Babayeva
Institute of Catalysis and Inorganic Chemistry named after M. Nagiyev, Ministry of Science and Education of the Republic of Azerbaijan, Laboratory of Nanostructured metal-polymer catalysts, Baku, Azerbaijan.
ORCID ID: 0009-0007-3490-0428

ABSTRACT

In recent years, Ag nanoparticles have attracted great attention due to their unique properties in nanoscale materials and their wide range of applications for optical, catalytic, magnetic, electrical, and antimicrobial devices. Silver nanoparticles are widely used as antibacterial agents in the medical industry, textile coatings and many environmental processes. In addition, due to the biocidal properties of silver-based compounds, non-toxic inorganic antibacterial agents have many applications, including tree protection, water treatment in hospitals, and wound or burn dressings [1,2].

Recent advances in nanoparticle synthesis have had a strong impact on many scientific fields, and the synthesis of silver nanoparticles has followed this trend. In fact, silver-based compounds are much cheaper than gold-based compounds, and silver nanoparticles (AgNPs) are now

considered an important class of nanomaterials. Currently, they are used as catalysts and antibacterial agents [2].

At the same time, silver is a nanoparticle with unique physical and chemical properties that enable the development of new polymer/metal materials. Ag-based polymers have been recognized as an effective method for developing new materials with broad-spectrum properties, including long-term antimicrobial and catalytic activity. Thus, these nanocomposites have a wide range of applications. [3].

Considering the above, polymer/Ag-based nanocomposites were synthesized in the presented work. Natural polymer gelatin was used as a carrier in the experiment. For this purpose, 0.5 g of gelatin is placed in 50 mL of distilled water a day before use, which is important for the swelling of the polymer. It is mixed in an 'IKA RCT standard safety control' magnetic mixer for 6 hours at a temperature of 65°C. Then Ag metal salt ($AgNO_3$) is added to the solution and mixed again for 3 hours. The resulting composite is reduced with $NaBH_4$ to obtain Ag nanoparticles, then washed with ether (diethyl ether) and distilled water. At the end, an N, N'-methylene-bis-acrylamide solution, which acts as a crosslinking agent, is added to enhance the durability of the nanocomposite in various environments. The structure and properties of the synthesized nanocomposite were studied by analysis methods such as FTIR, X-Ray, DLS.

Keywords: Ag nanoparticles, polymer composites, application

References

1. Kholoud M.M., Abou El-Nour, Ala Eftaiha, Abdulrhman Al-Warthan, Retla A.A.Ammar/Synthesis and applications of silver nanoparticles// Arabian Journal of Chemistry, 2010, 3, 135-140.
2. D.B.Tagiyev, N.A.Zeynalov, Sh.Z.Tapdigov, S.F.Humbatova, S.M.Mammadova, M.Kh.Hasanova//Synthesıs of sılver nanopartıcles ın the presence of natural and synthetıc polymers and the ınvestıgatıon of theır morphologıcal structures//Azərbaycan Kimya Jurnalı № 3 2016.
3. LauraTamayo, HumbertoPalza, JuliánBejarano, Paula A.Zapata /8 - Polymer Composites With Metal Nanoparticles: Synthesis, Properties, and Applications// Polymer Composites with Functionalized Nanoparticles Synthesis, Properties, and Applications Micro and Nano Technologies 2019, Pages 249-286.

SMART POLYMER-BASED HYDROGELS AND THEIR FIELDS OF APPLICATION

Elmira Aliyeva
Ministry of Science and Education Republic of Azerbaijan «Institute of Catalysis and Inorganic Chemistry named after academician of M.Nagiev», Laboratory of Nanostructured metal-polymer catalysts, Baku, Azerbaijan
ORCID ID: 0009-0008-2767-3949

Nizami Zeynalov
Ministry of Science and Education Republic of Azerbaijan «Institute of Catalysis and Inorganic Chemistry named after academician of M.Nagiev», Laboratory of Nanostructured metal-polymer catalysts, Baku, Azerbaijan
ORCID ID: 0000-0002-788967-6594

ABSTRACT

Recently, the pharmaceutical industry has been paying great attention to the development of drug delivery systems that precisely target specific sites, optimize effect of drug use, minimize the use of excipients, and reduce side effects. Smart polymers hold great promise in the design of innovative formulations tailored for drug delivery with high precision, efficacy and therapeutic benefit while minimizing adverse effects. In drug delivery systems, smart polymers show exceptional potential in achieving controlled and targeted profiles, delivering drugs to specific receptors, and minimizing off-target effects. Smart polymer-based materials offer various applications by intelligently responding to external stimulation and enable their use in modern pharmaceutical research [1].

Smart polymers are a class that differs from conventional polymers by their rapid transition in physico-chemical state in response to the external environment. The main focus of these polymers are related to their turnable structural and functional potential. The classification of smart polymers is based on different environmental effects such as temperature, pH, light, enzymatic reaction, pressure, electric/magnetic field, etc. The properties of these compounds can be changed during polymer synthesis by changing the chain structure. The intelligent behavior of these polymers enables their application in many fields, including drug delivery, tissue engineering, tissue repair, and various sensors. Although significant progress has been made with smart polymers, there are still several limitations in their application due to pre-use resolution. This includes rapid response in vivo, dose measurement during drug delivery, biocompatibility, and biodegradation [2].

At the time, smart polymers have the ability to strongly react to relatively weak external influences. External influences that change the properties of smart polymers can be temperature, humidity, acidity of the environment, light radiation, electric and magnetic fields,

etc. Taking into account above-mentioned, our main goal in research is the synthesis of polymer gels sensitive to the pH of the environment and the processes of their immobilization to pharmaceuticals. Encapsulated polymers, both natural and synthetic, can deliver immobilized biologically active compounds and drugs to a pH-medium in which they can work, and are therefore called smart polymers.

Keywords: smart polymer, composite materials, application

References

1. Avinash Kumar Seth, Ghanshyam Parmar, Chintan Aundhia, Nirmal Shah and Dipti Gohil//Smart Polymer Systems: A Futuristic Approach to Enhance Therapeutic Efficacy// Current Organic Chemistry 2024, Volume 28, Issue 15, p.1164-1178.
   https://doi.org/10.2174/0113852728305580240429100851
2. Deepti Bharti, Indranil Banerjee, Preetam Sarkar, Doman Kim, Kunal Pal// Smart polymers for biomedical applications//Advances in Biomedical Polymers and Composites Materials and Applications, 2023, Chapter 9, Pages 223-24.
   https://doi.org/10.1016/B978-0-323-88524-9.00010-3.

IMMOBILIZATION AND STUDY OF DOXORUBICIN AND TRYPSIN IN BIOPOLYMER-Fe_3O_4 MAGNETITE NANOPARTICLE GEL SYSTEMS

Seadet Humbatova
Ministry of Science and Education Republic of Azerbaijan «Institute of Catalysis and Inorganic Chemistry named after academician of M. Nagiev», Laboratory of Nanostructured metal-polymer catalysts, Baku, Azerbaijan
ORCID ID: https://orcid.org/0009-0004-8197-6714

Nizami Zeynalov
Ministry of Science and Education Republic of Azerbaijan «Institute of Catalysis and Inorganic Chemistry named after academician of M.Nagiev», Laboratory of Nanostructured metal-polymer catalysts, Baku, Azerbaijan
ORCID ID: https://orcid.org/0000-0002-788967-6594

Elmira Aliyeva
Ministry of Science and Education Republic of Azerbaijan «Institute of Catalysis and Inorganic Chemistry named after academician of M.Nagiev», Laboratory of Nanostructured metal-polymer catalysts, Baku, Azerbaijan
ORCID ID: https://orcid.org/0009-0008-2767-3949

Elnara Nasiyyati
Ministry of Science and Education Republic of Azerbaijan «Institute of Catalysis and Inorganic Chemistry named after academician of M.Nagiev», Laboratory of Nanostructured metal-polymer catalysts, Baku, Azerbaijan
ORCID ID: https://orcid.org/0009-0003-1520-2588

ABSTRACT

Through immobilization of biologically active substances, including antibiotics, in polymer-metal gel complexes, it has become possible to develop innovative drug forms in medicine that offer prolonged effects and targeted delivery[1-2]. Using doxorubicin and the enzyme trypsin as model agents, polymer gel systems were created and thoroughly investigated. [3-4].Research was conducted to determine the effect of magnetite nanoparticle size on the drug-loading capacity of previously synthesized hydrogel samples based on natural polymers.

In this study, a sorption method was used to load trypsin and the antibiotic doxorubicin into each Fe_3O_4 nanogel sample to determine their capacity for biologically active agents. After being kept in the appropriate preparation medium for 24 hours, the Fe_3O_4 nanogels were separated from the system, and the concentration of the drug was measured to determine the immobilization degree of trypsin and doxorubicin for each gel, as well as the drug-loading capacity of the gel (Table 1).

Table 1.

Immobilization Degree and Capacity of Natural and Synthetic-Based Magnetite Nanogels for Trypsin and Doxorubicin.

Fe_3O_4 nanoparticle carrier gel	The size of nanoparticle, nm	According to trypsin		According to doxorubicin	
		Immobiliza-tion rate, %	Protein capacity, mg/g	Immobiliza-tion rate, %	Antibiotic capacity, mg/g
*GA-nanoFe_3O_4	39.16	66.12	3.29	21.32	42. 65
*AG-nanoFe_3O_4	38.45	63.43	3.17	21.78	43.57
GA-*PVP-nanoFe_3O_4	33.27	58.80	2.94	23.20	46.39
GA-PVP(5%)-*MBAA	–	74.96	3.73	25.46	50.92
AG-PVP-nanoFe_3O_4	34.58	54.80	2.74	24.69	49.38
AG-PVP(5%)-MBAA	–	73.27	3.66	27.94	55.88
*CHS-nanoFe_3O_4	32.46	75.52	3.77	26.87	53.74

*GA- gum arabic, *AG-arabinogalactan, *PVP-polyvinylpyrrolidone, *CHS-chitosan, *MBAA-methylene-bis-acrylamide

As seen in Table 1, the incorporation of magnetite nanoparticles into the gel matrix somewhat increases its capacity for both trypsin and doxorubicin. This can be explained by two factors:

- The functional groups in the gel that can form chemical bonds with biologically active compounds are surrounded by Fe_3O_4 nanoparticles;
- The swelling degree is relatively high.

The higher capacity and immobilization degree compared to other nanoparticles is also due to the presence of magnetite nanoparticles in the form of mixed oxides of divalent and trivalent iron, which allows coordination rather than in a zero-valent metal state. Despite this, the capacity and immobilization degree of magnetite nanogels make them suitable for transporting biologically active compounds. The presence of magnetite nanoparticles in the hydrogel structure enhances the potential for targeted delivery of physiologically active substances. Additionally, preliminary experimental results indicate that gels formed with doxorubicin immobilized in magnetite nanogels release the antibiotic faster. In contrast, trypsin retains its biological activity for a longer period compared to samples without Fe_3O_4.

ISBN: 978-625-378-045-6

https://doi.org/10.5281/zenodo.14537144

Keywords: immobilization, doxorubicin, trypsin, polymer, magnetite, nanoparticle, gel systems

References:

1. Aseri.A., Garg.S.K., Nayak.A., Sanket.K., Ahsan.M.J. Magnetic nanoparticles: Magnetic nano-technology using biomedical applications and future prospects. International Journal of Pharmaceutical Sciences Review and Research. 2015. 31. p.119-131.
2. Karchoubi.F., Ghotli.R.A., Pahlevani.H., Salehi.M.B. New insights into nanocomposite hydrogels; a review on recent advances in characteristics and applications. Advanced Industrial and Engineering Polymer Research. 2024.Vol.7. p.54-78.
3. Tapdiqov.Sh.Z., Zeynalov.N.A., Taghiyev.D.B., Humbatova.S.F., Mammedova.S.M., Nasiyyati.E.F., Babayeva.D.T. Hydrogels for immobilization of trypsine based on poly-N-vinylpyrrolidone and arabinogalactan graft copolymers. J.Chem.Soc.Pak., 2015. 37..6. p.1112-1118.
4. Virmani. M., Deshpande. N.U., Pathan.Sh.,Jayakannan.M. Self-reporting polysaccharide polymersome for doxorubicin and cisplatin delivery to live cancer cells. ACS Polymers Au. 2022. Vol. 2. p.181–193.

SERAMİK ATIKLARI İLE KOMPOZİT ÜRETİMİ

COMPOSITE PRODUCTION FROM WASTE CERAMICS

Havva Nur HİÇYORULMAZ
Süleyman Demirel Üniversitesi, Fen Bilimleri Enstitüsü, Makine Mühendisliği Anabilim Dalı,Isparta, Turkey.
0000-0001-7462-624X

Prof. Dr. Ayşe ÖNDÜRÜCÜ
Süleyman Demirel Üniversitesi, Mühendislik ve Doğa Bilimleri Fakültesi, Makine Mühendisliği Bölümü, Isparta, Turkey.
0000-0002-0319-4256

ÖZET

Türkiye, kil kaynaklarının zenginliği ve geleneksel seramik üretim teknikleriyle seramik çamuru üretiminde önemli bir konuma sahiptir. Birçok alanda kullanılan seramik, beraberinde seramik atıklarını da getirmektedir. Günümüzde sıkça duyduğumuz "sıfır atık" kavramı ile birlikte seramik alanında da geri dönüşüm çalışmaları önemli hale gelmiştir. Seramik bazlı geri dönüşüm çalışmaları, estetik ve dayanıklılık açısından geliştirilmeye uygun sonuçlar vermektedir. Atölyelerde fırından çıkan fakat hasar görmüş ürünler, dış mekanda kullanılan seramik yapıların kırılan parçaları gibi atıklar, polyester ve poliüretan ile karıştırılarak hızlı ve verimli ürünler üretilebilmektedir. Böylelikle geri dönüşüme katkı sağlanırken kullanıma uygun, suya dayanıklı, hafif, sağlam ve şekil verilebilen ürünler elde edilebilmektedir.

Bu çalışmada, atık seramik parçalarının verimli bir şekilde değerlendirilmesi amaçlanmıştır. Atık pişmiş seramik ürün parçaları, polyester ve polimer ile karıştırılarak elde edilen yeni numuneler şekil verilebilirlik ve endüstriyel kullanıma uygunluk açısından kıyaslanmış ve verimliliği artırmak hedeflenmiştir. Pişmiş seramik parçaları kırılarak 1000 µm ve 300µm elekten geçirilerek toz haline getirilmiştir. 1000 µm filtreden geçirilen seramik tozları, hassas terazide tartılarak polyester ile %25, %50 ve %75 oranlarında, polietilen ile %30, %50 ve %75 oranlarında karıştırılmıştır. 300 µm filtreden geçirilen seramik tozları, hassas terazide tartılarak polyester ile % 25 ve %50 oranlarında, poliüretan ile %30 ve %50 oranlarında karıştırılmıştır. Döküm yöntemiyle seramik kompozit malzemeden numuneler elde edilmiş ve kıyaslanmıştır.

Anahtar kelimeler: Kompozit Malzeme, Atık Seramik, Seramik Geri Dönüşümü, Seramik Polyester, Seramik Polimer.

ABSTRACT

Turkey holds a significant position in the production of ceramic clay due to its rich clay resources and traditional ceramic production techniques. Ceramic products, used in various fields, also bring along ceramic waste. With the current emphasis on the "zero waste" concept, recycling efforts in the ceramic industry have become increasingly important. Ceramic-based

recycling studies yield results suitable for improvement in terms of aesthetics and durability. Waste materials, such as kiln-fired but damaged products from workshops and broken pieces of ceramic structures used outdoors, can be quickly and efficiently transformed into new products when mixed with polyester and polyurethane. This process contributes to recycling by producing usable, water-resistant, lightweight, durable, and moldable products.

This study aims to efficiently utilize waste ceramic pieces. New samples, obtained by mixing waste fired ceramic pieces with polyester and polymer, were compared in terms of moldability and suitability for industrial use to enhance efficiency. The fired ceramic pieces were ground and passed through a 1000 µm and 300µm sieve to obtain powder form. The passed through a 1000 µm sieve ceramic powders were weighed with precision scales and mixed with polyester at ratios of 25%, 50%, and 75%, and with polyethylene at ratios of 30%, 50%, and 75%. The passed through a 300 µm sieve ceramic powders were weighed with precision scales and mixed with polyester at ratios of 25% and 50%, and with polyethylene at ratios of 30% and 50%.Samples of ceramic composite material were obtained and compared using the casting method.

Keywords: Composite Material, Waste Ceramic, Ceramic Recycling, Ceramic Polyester, Ceramic Polymer.

GİRİŞ

Seramik, insanlık tarihinin en eski malzemelerinden biridir ve geçmişten günümüze pek çok farklı alanda kullanılmıştır. İlk seramik malzemesi depolama kapları, süs eşyaları, kültürel ve dini figürlerde kullanılırken ateş ile seramiğin sertleştirilmesi sağlandığında kullanım alanları giderek artmıştır. Sanayi devrimi ile seramik üretimi gelişerek, teknoloji ve seramik kompozit üretimleri ile hayatımızın birçok alanında kullanılmaya başlanmıştır. Geleneksel seramik ve İleri teknoloji seramikleri olarak ikiye ayırabileceğimiz seramikler günümüzde; endüstriyel tasarım, inşaat, yer ve duvar kaplamaları, çatı kiremitleri, elektrik yalıtkanları, mutfak ve banyo seramikleri, fayanslar, yemek takımları, otomotiv, kimya endüstrisi, tıpta kullanılan protezler, havacılık ve uzay araçları gibi hem teknolojik hem geleneksel alanlarda kullanılmaktadır. Geleneksel seramikler kil, kuvars gibi doğal hammaddelerden oluşurken, ileri teknoloji seramikleri Al_2O_3, SiC, Si_3N_4, B_4C, Z_rO_2 benzeri hammaddelerden oluşur. Genel olarak seramikler hammadde olarak bulunması kolay, sertliği yüksek, uzun ömürlü, geliştirilmeye açık olmakla beraber, düşük ısı iletkenliğine, yüksek elektriksel dirence, hem saydam hem opak çeşitliliğine, biyouyumluluğa ve gözenekliliğe sahip olmaları tercih sebeplerindendir.

Türkiye kil kaynakları zenginliği ve geleneksel seramik üretim teknikleriyle seramik çamurunda önemli konuma sahiptir. Türkiye'de en fazla Şile kili, Afyon kili, Doğanhisar kili, Söğüt kili kullanılmakla beraber en fazla ithal edilen Ukrayna kilidir. Kullanım açısından Ukrayna ve Şile kili en fazla tercih edilenlerdir. Günümüzde tedariki zorlaşan ithal killer yerine yerli killere ihtiyaç artmıştır.

Kullanım kolaylığı, geliştirilebilir olması, mekanik ve kimyasal özellikleri sebebiyle birçok alanda kullanılan seramik beraberinde seramik atıklarını da getirmiştir. Türkiye'de seramik atıklarının geri dönüşümüne yönelik yasal düzenlemeler ve farkındalık çalışmaları giderek artmaktadır. Çevre ve Şehircilik Bakanlığı'nın uyguladığı "Atık Yönetimi" projeleri ve çeşitli belediyelerin yürüttüğü geri dönüşüm faaliyetleri, bu konuda önemli adımlar atılmasına olanak sağlamaktadır.

Dünyamızın ihtiyaç duyduğu geri dönüşüm projelerinde süreklilik kazanmak için en önemli davranışımız günlük alışkanlıklarımızı gözden geçirmektir. Geri dönüşüm adına attığımız her küçük adımı günlük yaşantımıza, küçük iş yerlerimizden büyük üretim tesislerine kadar yayabilirsek fark yaratabiliriz. Seramik atıkları yoğun olarak beton ve harç üretimi, dolgu malzemesi, yalıtım malzemesi gibi alanlarda inşaat sektöründe kullanılmaktadır. Birçok sektörde kendine yer bulabilen seramik atıkları çağdaş seramik sanatçısı David Binns ve Bremner'in yaptığı gibi agrega ve seramik camdan oluşan malzemelerle farklı kullanım alanlarını geliştirerek geri dönüşümlü sanatsal üretimler yapmaktadır. Dünyanın her neresinde olursak olalım, çevremize verdiğimiz olumsuz etkiyi azaltmak için çaba göstermemiz gerektiğini ifade eden Binns seramik sanatçılarını, yapmış oldukları seramik uygulamalarında çevreye karşı daha sorumlu bir yaklaşım benimsemeleri gerektiğini ifade etmektedir (Poyraz, 2018).

Kompozit malzemeler, iki veya daha fazla malzemenin kendi özelliklerini kaybetmenden birbiri içerisine katılmasıyla elde edilen bir malzeme türüdür. İçerisinde yer alan hacimce fazla olan yapı matris olarak adlandırılırken, içerisine ilave edilen malzemeye ise takviye denilmektedir (Kaw, 2014; Şahin, 2022). Uçakların hafifletilmesi ve performanslarının arttırılması amaçlarıyla gerçekleştirilen araştırmalarla, uçak motorlarında yoğunluğu daha düşük seramik, metal ve plastik kompozitlerin kullanımına odaklanılmaktadır. Günümüzde seramik matrisli kompozitler, mükemmel fiziksel ve mekanik özellikleri nedeniyle otomotiv, haberleşme, uzay havacılık ve savunma sanayi, tıp, kimya ve daha bir çok alanda kullanım alanı bulan geniş malzeme grubunu oluşturmaktadır. Seramik özelliklerini (yüksek mukavemet, sertlik ve sıcaklık stabilitesi), takviye fazının yapısına bağlı olarak özel uyarlanmış özelliklerle (tokluk, kendi kendini iyileştirme veya işlevsellik) birleştirir. Seramik kompozit malzemeler en iyi ısıl dayanımlara sahip olmakla beraber, en büyük dezavantajları işlemesi zor ve pahalı olmasının yanı sıra oldukça kırılgan malzemelerdir. Yüksek sıcaklıklara dayanımları yüksek olsa dahi parçaya etki eden darbe anında kırılma yaşanması oldukça yüksektir. İşleme anında bile parçaya gelen kesme kuvvetleri sonucunda da kırılmalar yaşanmaktadır. Seramik kompozitler kırılgan oldukları için kırılma tokluklarını arttırmaya yönelik malzemeler geliştirilmeye çalışılmaktadır (Yudar, 2023).

Seramik üretimi ve tüketimi her geçen yıl artmakta ve bunu on milyonlarca ton seramik atığı takip etmektedir. Seramik atık kaynaklarını yeniden kullanmanın iki ana yolu vardır. Bunlardan biri, çeşitli atık seramik malzemeleri dekorasyonlarda yeniden birleştirmek için doğrudan işlemedir. Diğeri ise bunları farklı ürünler yapmak için hammadde olarak geri dönüştürmektir. Geri dönüşüm kullanılmış üretimlerin daha iyi kalitede veya çevreye daha az zarar verecek şekilde dönüştürülmesi anlamına gelmektedir. Seramik Kaplama üretiminin farklı aşamalarında (şekillendirme, pişiririm, sırlama, parlatma, taşlama) ortaya çıkan kırık ya da alt standart üretimler sonucu çok yüksek miktarda atık oluşmaktadır. Üretim işlemleri esnasında seramik malzemenin bileşimlerinden kaynaklanan değişiklikler nedeniyle (boya ve sır gibi) önemli bir yüzdesi tekrar kullanılamaz hale gelmektedir. Pişmiş ıskarta karoların yeniden kullanımı depolanması ya da imha edilmesi zor atıklar sınıfına girmektedir (Poyraz, Yılmaz).

Mobilya üretimin tekniklerine göre poliüretan ve polyester dökümün, çerçeveler, ev mobilyalarında ahşap yerine, ve mobilya oymalarında sıkça kullanıldığı görülmüştür. Polyester ve poliüretan döküm yöntemleri kullanılan mobilya üretimi, klasik mobilya üretim tekniklere göre şekil alabilirlik, uzun ömürlü olması, ürünlerin hafifliği, taşıma kolaylığı, çevre şartlarına dirençli olması, üretim kolaylığı ve hızı özellikleriyle avantaj sağlamaktadır (Tosun, Altınok ve Küreli, 2023).

Bu çalışmada; pişmiş seramik atık parçalarını kısa sürede ve basitçe geri dönüştürüp dayanıklı dekorasyon ürünler üretilmesi amaçlanmıştır. Bu kapsamda, filtreden geçirilen seramik tozları hassas terazide tartılarak farklı oranlarda, polyester ve poliüretan ile karıştırılarak döküm yöntemiyle kompozit numuneler elde edilmiştir. Atölyede fırınlanarak üretilen kompozit ürünlerden yaklaşık %5'i kırılmıştır. Bu kırılmaların nedeninin yanlış sırlanma ve tasarım hatalarından dolayı meydana geldiği sonucuna varılmıştır. Seramik atıklarının en verimli üretim için kullanım oranları incelenmiştir. Seramik kompozit üretimi için elyaf tipi polyester ve A (poliol) ile B (izosiyanat) bileşenli poliüretan seçilmiştir.

YÖNTEM

Bu çalışmada; pişmiş fakat hatalı tasarım, yanlış sırlama, çatlama veya kırılma meydana gelmiş kullanılmaz durumdaki seramik objelerin hızlı ve kolay bir şekilde dönüştürülmesi amaçlanmıştır. Bunun için önce kırık ve atılacak bir seramik obje (Şekil 1) çekiç ile kırılıp filtrelemeye hazır hale getirilmiştir. Seramik tozları öncelikle 1000µm filtreden geçirilmiştir (Şekil 2).



Şekil 1. Atık haldeki seramik parça



Şekil 2. 1000µm filtreden geçirme

Elde edilen seramik tozu hassas terazi ile tartılıp üç farklı oranda elyaf tipi polyester, sıvı kobalt ve metil etil keton peroksit (MEKP) ile karıştırılmıştır. Sıvı kobalt ve mekp, polyesterin katılaşmasında hızlandırıcı olarak aynı oranlarda kullanılmıştır. Karışım oranları ve kullanıldıkları kalıp çeşitleri Tablo 1'de verilmiştir.

Tablo 1. 1000µm Filtreden Geçirilen Seramik Tozu ile Polyester Karışım Oranları

Kalıp çeşitleri	Numuneler	Seramik tozu (%)	Polyester (%)	Kobalt + MEKP (%)
Çiçek kalıbı için	S_1	25	70	5
	S_2	50	45	5
	S_3	75	20	5
	S_a	-	100	-
Çekmece kulbu için	S_4	25	70	5
	S_5	50	45	5
	S_b	-	100	-

ISBN: 978-625-378-045-6

https://doi.org/10.5281/zenodo.14537144

Şekli, doku ayrıntıları, köşeleri ve inceliği bakımında seçilen iki farklı numuneye döküm yapıldı. Özellikle çekmece kulpu, karışımın ince desenlere elde edilebilirliğini görmek için seçilmiştir.



Şekil 3. Çiçek kalıbı



Şekil 4. Çekmece kulpu kalıbı

Karışım için elde ettiğimiz seramik tozları 1000 µm filtreden geçirilerek 3 farklı oranda poliüretan ile karıştırılmıştır. Çiçek kalıbına ve çekmece kulpu kalıbına dökülmüştür. Kullanılan oranlar Tablo2'de verilmiştir.

Tablo 2. 1000µm Filtreden Geçirilen Seramik Tozu ile Poliüretan Karışım Oranları

Kalıp çeşitleri	Numuneler	Seramik tozu (%)	Poliüretan (%) A Katmanı	Poliüretan (%) B Katmanı
Çiçek kalıbı	P_1	30	35	35
	P_2	50	25	25
	P_3	75	12.5	12.5
	P_a	-	50	50
Çekmece kulpu	P_4	30	35	35
	P_b	-	50	50

Seramik tozları Şekil 5'de verilen 300 mikrometre filtreden geçirilerek tekrar polyester, kobalt ve met ile karıştırılmıştır. 300µm filtreden geçirilen seramik tozu ile polyester karışım oranları Tablo 3'de verilmiştir.

ISBN: 978-625-378-045-6

https://doi.org/10.5281/zenodo.14537144



Şekil 5. 300 µm filtre

Tablo 3. 300µm Filtreden Geçirilen Seramik Tozu ile Polyester Karışım Oranları

Numuneler	Seramik tozu (%)	Polyester (%)	Kobalt + MEKP (%)
R_1	25	70	5
R_2	50	45	5

Seramik tozları 300 mikrometre filtreden geçirilerek tekrar polyester, kobalt ve MEKP ile karıştırıldı. 300µm filtreden geçirilen seramik tozu ile poliüretan karışım oranları Tablo 4'te verilmiştir.

Tablo 4. 300µm Filtreden Geçirilen Seramik Tozu ile Poliüretan Karışım Oranları

Numuneler	Seramik tozu (%)	Poliüretan (%)	Poliüretan (%)
T_1	30	35	35
T_2	50	25	25

BULGULAR VE TARTIŞMA

Seramik tozu, elyaf tipi polyester, kobalt ve MEKP karışımın dökümünden elde edilen çiçek numuneleri Şekil 6- Şekil 9'da verilmiştir.



Şekil 6. S_1 numunesi



Şekil 7. S_2 numunesi



Şekil 8. S_3 numunesi



Şekil 9. S_a numunesi

Çiçek numuneleri incelendiğinde seramik tozu oranı arttıkça gözeneklenme artışı görülmüş, sertleşme sürelerinin arttığı gözlemlenmiştir. %25 seramik tozu oranından sonraki artışlarda sertliğin azalıp, S_2 (şekil 10) ve S_3 (şekil 11) numunelerinde kolayca kırılmaların oluştuğu gözlemlenmiştir.



Şekil 10. Kırılan S_2 numunesi



Şekil 11. Kırılan S_3 numunesi

ISBN: 978-625-378-045-6

https://doi.org/10.5281/zenodo.14537144

Şekil 12-Şekil 14'te seramik tozu, elyaf tipi polyester, kobalt ve MEKP karışımının dökümünden elde edilen çekmece kulbu numuneleri görülmektedir.



Şekil 12. S_4 numunesi



Şekil 13. S_5 numunesi



Şekil 14. S_b numunesi

Numuneler incelendiğinde doküm malzemesinin kulp köşelerine ulaşamadığı görülüyor. S_4 ve S_5 numunesi Sap kısımlarında kırılmalara uğruyor. S_b numunesi esnek iken %25 seramik tozu içeren S_4 numunesi daha serttir.

Şekil 15-Şekil 18'de elde seramik tozu, poliüretan reçinesi karışımı dökümünden elde edilen çiçek numuneleri görülmektedir.



Şekil 15. P_1 numunesi



Şekil 16. P_2 numunesi



Şekil 17. P_3 numunesi



Şekil 18. P_a numunesi

Numuneler incelendiğinde seramik oranı arttıkça gözeneklenme artışı (Şekil 18) ve hammaddelerin girdiği tepkime oranının artığı görülüyor.



Şekil 19. P_3 numunesinde oluşan tepkime

Kalıbın her ayrıntısı, seramik oranının en çok olduğu P_3 numunesi de dahil olmak üzere tüm ürünlerde sorunsuzca alınabiliyor. Yüzeylerdeki küçük kırıklar Seramik oranı arttıkça daha fazla görünüyor. Seramik içermeyen P_a numunesi ile P_1 numunesi kıyaslandığında %30 seramik tozu içeren P_1 numunesi daha sert bir yapı oluşturuyor.

Şekil 20 ve Şekil 21'de elde seramik tozu, poliüretan reçinesi karışımı dökümünden elde edilen P_4 ve P_b çekmece kulpu numuneleri görülmektedir.



Şekil 20. P_4 numunesi



Şekil 21. P_b numunesi

%50 ve %75 seramik tozu oranındaki karışım, tepkime oluşumu nedeniyle bu ince kalıba uygulanmadı. P4 numunesinde akışkan kalıbın her köşesine ulaştığı için köşelerde boşluk oluşmadı. Desenler iki numunede de net olarak alındı.

Şekil 22 ve Şekil 23'te 300 µm filtreden geçirilen seramik tozları ile polyester, kobalt ve met karışımı dökümünden elde edilen R_1 ve R_2 çiçek numuneleri verilmiştir.



Şekil 22. R_1 numunesi



Şekil 23. R_2 numunesi

R_1 ve R_2 numuneleriyle aynı hammaddelerden fakat farklı toz boyutlarından üretilen S numune serisi arasında gözle görülür farklar oluşmuştur. S_2 numunesindeki kırılma R_2 de görülmemesiyle beraber R_2 numunesi oldukça serttir. Burada da seramik oranının artmasıyla gözenek oluşumu çok az miktarda artmıştır. R_2 numunesinde yaprak kenarlarında küçük kırılmalar gözlenmektedir.

300 µm filtreden geçirilen seramik tozları ile elyaf tipi poliüretan karışımı dökümünden elde edilen çiçek numuneleri Şekil 24 ve Şekil 25'te verilmiştir.



Şekil 24. T_1 numunesi



Şekil 25. T_2 numunesi

T_1 ve T_2 numunesi kıyaslandığında seramik tozu oranı artınca gözeneklenme artmıştır, yaprak kenarlarında küçük boşluklar oluşmuştur. Poliüretan ile tepkime seramik oranı arttıkça yükselmiştir. T_1 numunesi ile saf poliüretan numunesi olan P_a pürüzsüzlüğü elde edilmiştir.

Tarımsal atıkların değerlendirilmesi için şeftali çekirdeği kabuğunun farklı oranlarda eklenmesiyle elde edilen polyester esaslı kompozit üretme çalışmasında, eklenen oranlar yüksek olduğunda kompozitin mekanik özelliklerinde düşüş görülmüştür. Polyester esaslı kompozit numunelerine ait SEM görüntüsünde %5'lik şeftali kabuğu takviyeli numunenin SEM görüntüsünde fazla değişiklik görülmemiştir. %20 ve özellikle %40 katkılı numunelerin SEM görüntülerinde kabarcık oluşumu artmış, homejenizasyonun azaldığı görülmüştür. %20 maliyet düşürmek amacıyla şeftali çekirdeği tozunun düşük oranlarda kullanılması uygun görülmüştür (Topuz ve Orhan 2022). Bu çalışmada da benzer şekilde Polyester reçinesine max. 1000µm boyutunda seramik tozlarının eklenerek üretilen kompozit numunelerde, seramik tozu oranı arttıkça gözenek görünümü artmıştır. Gözenek görünümü %25'lik numunede ihmal edilebilir düzeyde iken %75'lik numunede oldukça fazladır. Polyester reçinesine max. 300µm

boyutunda ve %25 oranında seramik tozu eklenerek üretilen kompozit numune ile en iyi yüzey görünümü elde edilmiştir.

SONUÇ VE ÖNERİLER

Bu çalışmada; pişmiş seramik parçaları kırılarak 1000 µm ve 300µm elekten geçirilerek toz haline getirilmiştir. 1000 µm filtreden geçirilen seramik tozları hassas terazide tartılarak; polyester ile %25, %50 ve %75 oranlarında, polietilen ile %30, %50 ve %75 oranlarında karıştırılmıştır. 300 µm filtreden geçirilen seramik tozları hassas terazide tartılarak; polyester ile % 25 ve %50 oranlarında, poliüretan ile %30 ve %50 oranlarında karıştırılmıştır. Daha sonra her karışım oranı için döküm yöntemiyle kompozit numuneler üretilmiş ve üretilen bu numuneler kıyaslanmıştır. Çalışma sonucu elde edilen sonuçlar aşağıda sunulmuştur:

- Çekmece kulpu için S serisi ve P serisi numuneleri incelendiğinde bu ince ve köşeli yapıdaki kalıp için şekil alma bakımından en iyi numune sonucunu %30 seramik oranında poliüretan karışımı olan P4 numunesi vermiştir. S numune serisinde seramik miktarı arttıkça ürünlerde yumuşama görülmüştür. % 100 polyester içeren Sb numunesi dahil çekmece kulplarının dar kesitlerinde kırılmalar gerçekleşmiştir. S4 ve S5 numunelerinin kare köşelerine karışım tam yayılma yapamamıştır. Boşluk olan köşelerin farklı olması bunun sebebinin kalıp değil karışım içeri olduğunu gösteriyor. Çünkü aynı mikrometrelik filtreden geçen P4 numunesi, S4 numunesinden daha fazla seramik tozu içermesine rağmen şekli tam almıştır. Poliüretan ile seramik tepkimesinin artması sebebiyle %50lik ve %75lik seramik oranları ile bu kalıpta çalışılmamıştır. Şekil alma bakımından en verimli sonuç P4 numunesinde görülse de %100 poliüretan numunesi olan Pb daha sert ve dayanıklıdır. Burada dayanıklılığı ve sertliği arttırmak için % 30'dan daha düşük seramik oranları, daha küçük seramik tozu boyutları ve basınçlı döküm kullanılabilir.

- Tüm çiçek numuneleri incelendiğinde; öncelikle 1000 µm filtreden geçen polyester numuneleri S2 ve S3 zamanla yumuşamış ve parçalanmakla beraber gözenek görünümü yüksektir. S1 numunesi ise %100 polyester numunesi olan Sa gibi gözeneksiz bir yüzey çıkartmıştır fakat Sa numunesinden daha esnektir. Buradaki esneklik kesici aletlerle şekil verilmek istenirse bir avantaj olarak kullanılabilir. 300 µm filtre kullanılarak üretilen R serisi numunelerde ise gözenek görünümü olmadan pürüzsüz bir yüzeye ulaşılmıştır. Seramik tozu boyutlarının küçülmesi kopmaların önüne geçmiştir ve Sa numunesinden daha sert ürün üretilmesini sağlamıştır. R2 numunesinde yaprak kenarlarında küçük boşluklar oluştuğu için burada en verimli sonucu R1 numunesi vermiştir.

- 1000 µm filtreden geçen poliüretan içerikli P numune serisinde seramik oranı arttıkça tepkime artarak kalıptan taşmalar görülmüştür. Genleşme sebebiyle bu karışım hasarlı ürünlerin yarıklarını doldurmak için değerlendirilebilir. Seramik oranı arttıkça sertleşme sağlanmış fakat yüzeyde gözenek görünümü artmıştır. Özellikle P3 numunesinde gözenekler oldukça yoğun görünmektedir. 300 µm filtre kullanılarak üretilen T serisinde ise gözeneksiz görünüm elde edilmiş özellikle T1 numunesinde pürüzsüz bir yüzey görülmüştür. Burada en verimli sonucu, % 100 poliüretan içerikli Pa numunesinden daha sert olmasının yanı sıra gözeneksiz bir yüzeye sahip olduğu için T1 vermiştir.

- Sertleşme süreleri ise poliüretan içerikli kompozit numunelerinde, polyester içerikli kompozit numunelerine göre oldukça avantajlıdır. Poliüretan içerikli P ve T numune

serisinde 8-10 dakika içinde donma, 30 dakikada sonunda da kürleşme görülmüştür. Seramik tozu oranı arttıkça katılaşma süresi ihmal edilecek düzeyde artıyor. Polyester içerikli S ve R numune serisinde 30-40 dakika donma, 24 saat sonunda kürleşme görülmüştür. Seramik oranı arttıkça kürleşme süresinde uzama gerçekleşmiştir.

- Poliüretan A ve B reçinesi tepkimeye girdiğinde koku yaymakta ve sonrasında kokusuz bir kompozit ürün sağlamıştır. Polyester ise kokulu olduğundan kapalı alanlarda üretimi ve depolanması zor bir malzemedir.

- Şekil alabilirlik, sertlik, üretim kolaylığı, hafiflik, insan ve çevre sağlığı göz önüne alındığında; en verimli sonucu 300µm filtreden geçirilen %30 seramik %70 poliüretan içeren T_1 numunesi vermiştir.

Yapılan bu çalışma ile seramik özelliklerini taşıyan, seramikten daha hafif, dış ortamlara da uyum sağlayabilecek, saf poliüretandan daha sert, heykel yada dekorasyon ürünlerinde kullanılmak üzere seramik atıkları geri dönüşüme kazandırılabileceği sonucuna varılmıştır.

KAYNAKÇA

Kaw, A.K. (2014). Kompozit malzeme mekaniği, 1. Basım, Ankara: Efil Yayınevi.

Poyraz, M. (2018). Pişmiş seramik atıkların artistik yüzeylerde geri dönüşümü ve çağdaş seramik sanatçısı David Binns. İnönü Üniversitesi Kültür ve Sanat Dergisi İnönü University Journal of Culture and Art, 4(2), 17-27.

Poyraz, M., Yılmaz, Z. Seramik karo sektöründe sürdürülebilirlik ve geri dönüşüm.

Anadolu Üniversitesi, Sanat & Tasarım Dergisi, 256-270.

Şahin, Y. (2022). Kompozit malzemelere giriş, 4. Basım, Ankara: Seçkin Yayıncılık Topuz, S., Orhan, R. (2022). Şeftali çekirdeği kabuğunun polyester esaslı kompozitinbazı mekanik özellikleri üzerine etkisi. Fırat Üniversitesi Mühendislik Bilimleri Dergisi, 34(2), 565-577.

Tosun, Ö., Altunok, M., & Küreli, İ. (2023). Polyester ve poliüretan döküm teknikleriyle klasik tarz mobilya üretim teknolojilerinin incelenmesi. Gazi Üniversitesi Fen Bilimleri Dergisi Part C: Tasarım Ve Teknoloji, 11(3), 572-581.

Yudar, S. (2023). The examination of composite materials as alternatives to superalloys in aircraft engines. Gazi Journal of Engineering Sciences, 9(3), 585-595. doi:10.30855/gmbd.0705089.

HIERARCHICALLY POROUS NANOCOMPOSITE FILMS FOR EFFICIENT PASSIVE DAYTIME RADIATIVE COOLING

Nazife Korkmaz Memiş
Suleyman Demirel University, Faculty of Engineering and Natural Sciences, Textile Engineering Department, Isparta, Türkiye
ORCID ID: 0000-0003-1605-0670

Sibel Kaplan
Suleyman Demirel University, Faculty of Engineering and Natural Sciences, Textile Engineering Department, Isparta, Türkiye
ORCID ID: 0000-0002-7247-135X

ABSTRACT

Passive daytime radiative cooling materials with simultaneous high solar reflectance and infrared thermal emittance, hold enormous potential for addressing the energy crisis and global warming through advantages of zero energy consumption and low carbon emissions. Herein, novel hierarchically porous nanocomposite films with randomly distributed heterogeneous pores and nanoparticles are fabricated in a low-cost and simple method known as non-solvent-induced phase separation method with two solvents and water, employing polyvinylidene fluoride (PVDF) (10%) and zinc oxide (ZnO) (90 nm, 2%) nanoparticles. Utilizing the regulation of structural parameters such as pore size and film thickness (200-600 µm) to control multi-scattering of light by the films, hence cooling performance is achieved. The porous structure of the films was evaluated by SEM analysis as well as cooling performances were measured by a hotplate apparatus combined with a halogen lamb as a sun simulator. SEM images show that the most obvious heterogeneous pore structure was obtained in the samples with a film thickness of 400 µm. However, it has been determined that as the film thickness increases, there are macro and nano-micro heterogeneous pores in the film structure, but the number and size of macro pores decrease. The trend regarding pore formation, size and number of pores was also detected in the cross-sectional images of the films. Under exposure to a solar intensity of 600 Wm^{-2}, compared to non-porous PVDF films, an effective passive cooling effect was achieved due to a higher temperature drop in porous PVDF films in the range of 2.14-5.6°C. The porous nanocomposite films lower the temperature effectively especially at a film thickness of 600 µm by an average of 6.5°C. This work opens up a simple, cost-effective, and scalable route for achieving efficient radiative cooling nanocomposite films with excellent cooling performance based on multi-scattering effect with controllable porous structure and ZnO.

Keywords: Radiative cooling, porous nanocomposite structure, PVDF, nonsolvent-induced phase separation.

INTRODUCTION

Today, as global warming is now one of the greatest crises faced by all races on earth, the increasing trend in outdoor temperatures, increasing energy requirements for insulation/cooling systems and the world's limited energy reserves have brought the novel thermal management materials and technologies with low to zero carbon emissions to the agenda. Recently, radiative

cooling, which is an electricity- free cooling technology, by dissipating an object's heat to the cold outer space through an atmospheric transparency window (8–13 μm) without any energy consumption or greenhouse gas release, are attracting attention with advantages of environmental impact, energy savings, and total wellbeing of the population (Liu et al., 2022). Moreover, passive radiative cooling materials enable effective cooling performance by reflection sunlight in UV–Vis-NIR band and emitting thermal radition in MIR band. Many materials including inorganic materials (Lin et al., 2023), multilayer photonic crystal/coating (Lee et al., 2023; Meng et al., 2023), composite materials with particles, bio-inspired materials, metamaterials (Tsang et al., 2024), etc. were developed. Despite their wide application potential, these materials were manufactured using complicated and costly process which makes these materials unsuitable for large-scale production.

As a solution, porous radiative cooling materials especially polymer-based ones are attracting attention due to the simplicity, applicability, economical efficiency, and effective cooling performance (Wang et al., 2021). Solar reflectance and emissivity could be enhanced by rationally adjusting the porous structure and refrective particles as well as using polymer having higher emisivity with appropriate chemical bonding. In this manner, designing a composite/nanocomposite material having refractive particles such as ZnO, TiO_2, MgO, Al_2O_3, SiO_2 in the porous film to establish reflection interface and to improve emissivity (Du et al., 2023), attract attention. Recently, polymer based porous composite materials could be produced by phase separation especially non-solvent induced phase separation (NIPS) method which enables tunable micro-nano hierarchical porous structure in polymer films by varying polymer content, non-solvent: solvent content etc. with low-cost and large production scale.

In this study, PVDF nanocomposite films with varying thickness reinforced by ZnO particles, were succefully produced by NIPS method forming a hierarchical morphology. By controlling structural parameters such as pore size and film thickness (200-600 μm), the multi-scattering of light by the films is controlled.

MATERALS AND METHODS

Materials

PVDF chips (Kynar® 721, melting temperature: 168°C, glass transition temperature: -40°C) were kindly provided by Arkema, France. PVDF polymer, with high MIR emission properties owing to the C-F bonds stretching and deforming vibrations in the atmospheric window range (Yu et al., 2021), was used as matrix material. ZnO (90 nm, Nanografi, Türkiye) nanoparticles were used for sunlight reflecting with refractive index $n \approx 2$ and little absorption value from visible wavelength to MIR wavelengths (Zhu and Feng, 2021). In one-step phase separation film formation method, N, N dimethyl acetamide (Sigma Aldrich, DMAc), acetone (Acros Organics, ACE), and deionized water, were used as solvents. A non-ionic surfactant (sorbitan monostearate, Span60, Sigma Aldrich) was used for getting more homogenous nanoparticle dispersion.

Methods

Nanocomposite film preparation

PVDF-ZnO nanocomposite films with hierarchical micro-nano porous structure were produced through NIPS method including binary solvent system (solvent, co-solvent) (DMAc, ACE) and

non-solvent (water). First, 10 wt. % PVDF polymer chips were dissolved in a blended solvent consisting of DMAc and ACE at the same ratio at 50°C for 6 h. Subsequently, ZnO particles at

2 wt. % content and Span60 at a ratio of 1:2 with respect to the nanoparticle, were incorporated into the PVDF solution at 50°C while being agitated magnetically for another 1 h followed by 2 h of ultrasonic mixing. Following the ultrasonic mixing, 7% amount of water determined in previous studies (Korkmaz Memiş and Kaplan, 2024a; b) for optimum pore formation was added dropwise into the PVDF-ZnO dispersion by a syringe pump at a 0.2 mL/min feeding rate. Finally, the prepared nanocomposite casting solutions were drop-cast to the petri-dishes and dried at 20°C for 24 h at different thicknesses (200, 400, and 600 µm).

Characterizations

Morphology

Scanning electron microscope (SEM, Fei Quanta FEG 250) with an accelerating 20 kV voltage and 10 µA current was used for examining porous structure of the film surfaces.

Outdoor cooling performances

Cooling performance of the films was measured by a self-made hotplate system simulating skin with K-type sensors and data acquisition system. The film was placed on the hot plate plate that can precisely remain constant at the skin surface temperature of 34°C under a sun simulator halogen lamb at a distance of 25 cm and the irradiation intensity on the surface of the sample was controlled at 600 Wm^{-2} with environment temperature at 22-26°C and relative humidity at 50%. The actual temperature of the films were measured at every 5 s for 1 min stabilization stage followed by 20 min lamp-on (sunny) and lamp-off stages (shady) in turn.

RESULTS and DISCUSSIONS

The SEM images of the PVDF and PVDF-ZnO nanocomposite films are shown in Fig. 1. As seen in SEM images, the porous structure was obtained by adding water as non-solvent into the binary solvent system. Porous structure formation can be explained by three stages such as; rapid evaporation of ACE enabling phase separation, slow exchanging of DMAc, and water evaporation which formed pores in different sizes. As depicted in Fig. 1, different thicknesses reveal that more porous structure formation as a result of ZnO incorporation in PVDF matrix is enabled, which effect continuity of the polymer-enriched phase (Ma et al., 2024).

Unlike porous PVDF films, ZnO particles led to form many uneven surfaces and more nanosize pores resulted in hierarchically porous structure through slowing down of solvent evaporation and delaying the phase inversion process with higher viscosity (Qi et al., 2022). Besides micro-nano pores, macro voids formed in the nanocomposite films by surface-driven phase separation and crystallization induction. Among nanocomposite films with varying thickness, the most obvious heterogeneous porous structure belongs to the samples of 400 µm.

ISBN: 978-625-378-045-6 https://doi.org/10.5281/zenodo.14537144

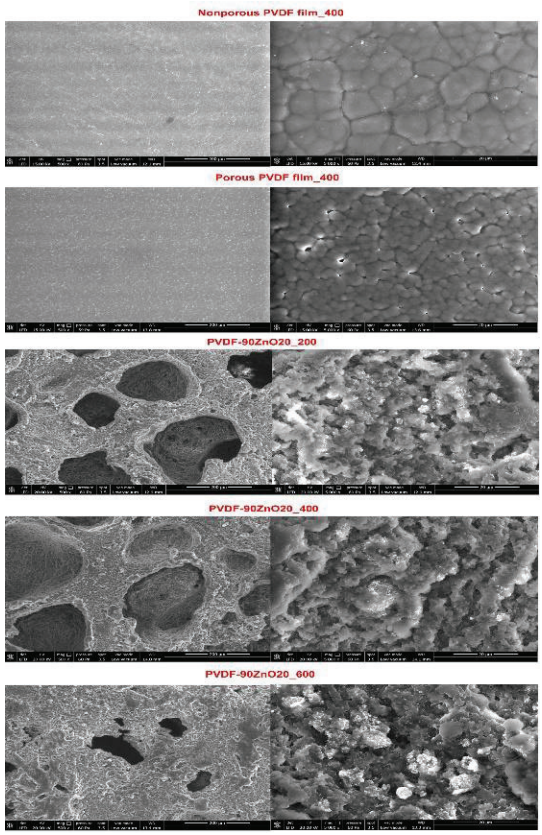


Fig. 1. Surface morphology of PVDF and nanocomposite films

The real-time temperature curves created as a result of cooling performance measurements by the developed hotplate system and temperature differences of the films were given in Fig. 2 and Table 1, respectively. According to temperature measurement under exposure to a solar intensity of 600 Wm^{-2} simulating outdoor conditions, temperature of the porous PVDF films with varying thicknesses were lower in the range of 2.14-5.6°C than the nonporous ones (Table 1). The hierarchically porous structure seen in SEM images enhanced the total solar scattering efficiency and mid-infrared emissivity (Qi et al., 2022), resulted in passive radiative cooling effect.

Beside porous structure, high MIR emission properties based on the functional group vibrations (C-F stretching and deforming vibrations) of PVDF polymer through the atmospheric window (Yu et al., 2021) may improve the thermal emissions of the films.

With ZnO particle addition into PVDF matrix, the nanocomposite films especially at a film thickness of 600 µm exhibited a maximum temperature decrease of 6.5°C (Fig. 2b) followed by 6.28°C at 200 µm thickness (Fig. 2a, Table 1) due to the synergistic scattering effect of the richer porous structure and high refractive index $n \approx 2$ and little absorption value (Zhu and Feng, 2021) of ZnO particles. The same nanocomposite film samples demonstrated lower temperature by an average of 9.6°C as compared to the blank hotplate surface simulating the body without clothing in outdoor conditions.

ISBN: 978-625-378-045-6 https://doi.org/10.5281/zenodo.14537144

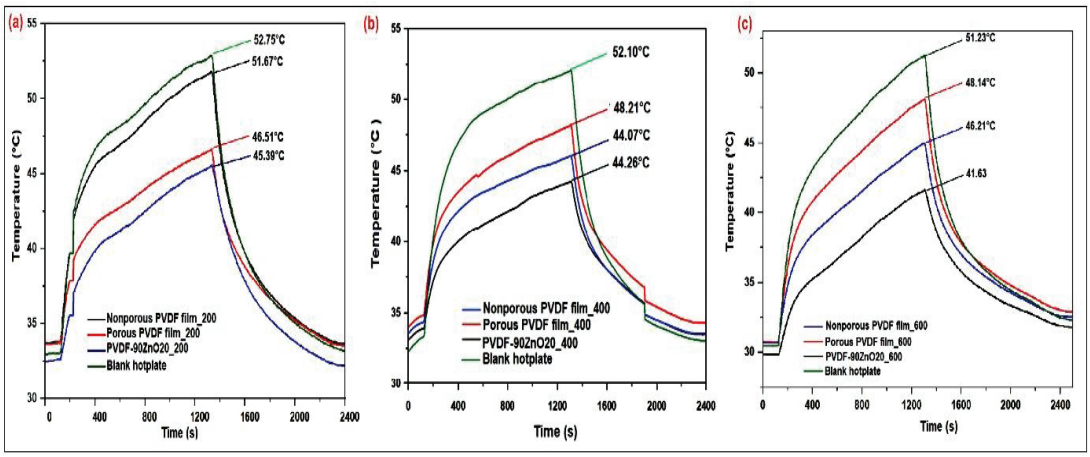


Fig. 2. Temperature profiles measured for cooling performance of the films with varying thickness

Table 1. Temperature changes of the films

Film thickness (µm)	PVDF-90ZnO20 ΔT(°C)		
	1-2	2-3	1-3
200	5.16	1.12	6.28
400	2.14	1.8	3.94
600	3.14	3.6	6.50
Bare hotplate-nanocomposite films			
200	1.08	6.23	7.35
400	3.9	6.03	7.83
600	3.10	6.24	9.60

*1: Nonporous PVDF film, 2: Porous PVDF film, 3: PVDF-ZnO nanokompozit film

CONCLUSIONS

This study presents a hierarchically porous nanocomposite films at varying thickness with effective passive passive daytime radiative cooling performance, including PVDF matrix and ZnO particles through NIPS method. The nanocomposite films exhibit impressive outdoor cooling performance especially at the thickness of 600 µ followed by 200 µm ones by temperature drop of 6.5°C and 6.28°C, respectively, compared with nonporous films. This may be attributed the hierarchically porous structure and ZnO particles which ensured high solar reflection and infrared emissivity resulting from the unique structure of PVDF. In addition to its porous film structure and relatively high cooling performance, the nanocomposite film at 200 µm including 2 wt.% ZnO particles may be selected as a radiative cooling material due to practical economic considerations. In summary, PVDF-ZnO nanocomposite films with varying thickness with higher passive radiative daytime cooling performance and scale-up production method are expected to open up new prospects thermal management and practical application range of radiative cooling materials.

ACKNOWLEDGEMENT

The authors are grateful for the financial support of The Scientific and Technological Research Council of Türkiye (TÜBİTAK) (grant agreement no: 123M553) and Arkema, France for the polymer supply.

REFERENCES

Du, L., Zhou, Z., Li, J., Hu, B., Wang, C., Zheng, J., Chen, W. (2023). Highly efficient subambient all-day passive radiative cooling textiles with optically responsive mgo embedded in porous cellulose acetate polymer. Chemical Engineering Journal, 469, 143765.

Korkmaz Memiş, N., Kaplan, S., (2024a). PVDF films with optimized porous structure using non-solvent induced phase separation for passive radiative cooling. 7th International Scientific Conference "CONTEMPORARY TRENDS AND INOVATIONS IN TEXTILE INDUSTRY"-CT&ITI 2024, 19-20th Semptember, 2024, Belgrade, Serbia.

Korkmaz Memiş, N., Kaplan, S., (2024b). Drying temperature optimizatıon of PVDF-ZnO porous passive radiative cooling films. 14th International Conference "Textile Science and Economy - TNP2024, 25th October, 2024, Zrenjanin, Serbia.

Lee, M., Kim, G., Jung, Y., Pyun, K. R., Lee, J., Kim, B. W., Ko, S. H. (2023). Photonic structures in radiative cooling. Light: Science & Applications, 12(1), 134.

Lin, K., Zhu, Y., Ho, T. C., & Tso, C. Y. (2023). Cellular ınorganic ceramic for highly efficient daytime passive radiative cooling. Energy Sustainability.

Liu, J., Tang, H., Jiang, C., Wu, S., Ye, L., Zhao, D., Zhou, Z. (2022). Micro-nano porous structure for efficient daytime radiative sky cooling. Advanced Functional Materials, 32(44), 2206962.

Ma, C.Q., Xue, C. H., Guo, X.J., Shi, W., Wang, H. D., Huang, M. C., Cheng, J. (2024). Fabrication of passive cooling fabric as thermal management curtain for building energy-saving. Chemical Engineering Journal, 497, 154431.

Meng, X., Chen, Z., Qian, C., Li, Q., Chen, X. (2023). Durable and mechanically robust superhydrophobic radiative cooling coating. Chemical Engineering Journal, 478, 147341.

Qi, M., Wang, Y., Chang, G., Li, R. (2022). Energy-saving cooling coated fabric with robust solar reflection and water repellent properties. Fibers and Polymers, 23(7), 1881-1887.

Tsang, Y. C. A., Varghese, N. J., Degeorges, M., Mandal, J. (2024). Porous polymer bilayer with near-ideal solar reflectance and longwave infrared emittance. Nanophotonics, 13(5), 669-677.

Wang, T., Wu, Y., Shi, L., Hu, X., Chen, M., & Wu, L. (2021). A structural polymer for highly efficient all-day passive radiative cooling. Nature communications, 12(1), 365.

Yu, X., Chan, J., Chen, C. 2021. Review of radiative cooling materials: performance evaluation and design approaches. Nano Energy, 106259.

Zhu, F.L., Feng, Q.Q. (2021). Recent advances in textile materials for personal radiative thermal management in ındoor and outdoor environments. International Journal of Thermal Sciences, 165, 106899.

THE USE OF CERAMIC TILE WASTE AS A CALCITE REPLACEMENT IN DIFFERENT MORTARS

Dilay Özuyar
Yurtbay Seramik, R&D Center Eskişehir/Türkiye
ORCID ID: https://orcid.org/0000-0002-9780-5723
dilay.ozuyar@yurtbay.com

Berkay Sözüdoğru
Yurtbay Seramik, R&D Center Eskişehir/Türkiye
ORCID ID: https://orcid.org/0009-0000-3581-2373

Mustafa Tosun
Yurtbay Seramik, Eskişehir/Türkiye
ORCID ID: https://orcid.org/ 0009-0009-0596-1752

Gökhan Ünal
Yurtbay Seramik, Eskişehir/Türkiye
ORCID ID: https://orcid.org/ 0009-0006-7949-477X

Burak Özkal
Yurtbay Seramik, R&D Center Eskişehir/Türkiye
ORCID ID: https://orcid.org/000-0003-3431-2304

ABSTRACT

In this study, potential use of waste ceramic tiles in powder form instead of calcite were studied for different mortar compositions. Aiming for both environmental and economic benefits a series of detailed experiments were conducted to see how this replacement affects the mechanical, thermal, and physical properties of three different mortars: (i) ceramic adhesive mortar, (ii) bricklaying mortar, and (iii) insulation adhesive mortar. For this purpose, waste ceramic tiles were converted to powder form and added to mortar compositions as calcite replacement in different amounts and standart production route was followed. After preparation all samples including control ones were tested in order to obtain tensile adhesion strength, compressive strength, water absorption %, and thermal conductivity value. According to characterization results certain improvements were observed compared to control samples having no replacement. For instance, ceramic adhesive mortar having 3% replacement achieved a tensile adhesion strength of 0.57 N/mm², bricklaying mortar having 100% replacement reached to compressive strength of 185 N/mm², along with a 17% reduction in water absorption. The insulation adhesive mortar, having 100% replacement gave a compressive strength of 185 N/mm² and decreased the water absorption by 13%. These results show that the replacement of calcite with waste ceramic tile in powder form has a potential to enhance the durability of mortar materials, reduce water permeability, and improve energy efficiency staying in the borders of industrial standarts from other expectations

Keywords: Waste Ceramic Tiles, Mortars, Calcite Replacement, Sustainability, Recycling.

EXPERIMENTAL ANALYSIS OF HAILSTONE IMPACT ON AIRCRAFT CANOPY

Meryem Dilara KOP
Isparta Suleyman Demirel University, Graduate School of Natural and Applied Sciences, Department of Civil Engineering, Isparta, Turkey
ORCID ID: 0000-0001-6428-5744

Gökalp YILMAZ
Aydın Adnan Menderes University Faculty of Engineering, Department of Civil Engineering, Aydın, Turkey
ORCID ID: https://orcid.org/0000-0003-2183-586X

Mehmet AVCAR
Isparta Suleyman Demirel University, Faculty of Engineering and Natural Sciences, Department of Civil Engineering, Isparta, Turkey
ORCID ID: https://orcid.org/0000-0002-0689-0601

Mehmet Eren UZ
Aydın Adnan Menderes University Faculty of Engineering, Department of Civil Engineering, Aydın, Turkey
ORCID ID: https://orcid.org/0000-0002-4466-5536

ABSTRACT

Hailstones can vary in diameter and strike objects at different velocities related to airflow. The damage caused by hailstorms depends on the diameter and velocity of the hailstones. Simulating hailstones is critical for impact tests. In this study, polyvinyl acetate (PVA) additive artificial hailstones were used. Previous studies have shown that mixtures of 12% PVA and 88% demineralized water are more successful in simulating natural hailstone behavior. The aim of the study is to design an experimental test setup for investigating aircraft canopy impact tests. In line with this purpose, requirements for impact tests were developed. Two aircraft dimensions were used in dynamic impact tests. Artificial hailstones with diameters of 20 mm and 50 mm were produced for use in the experiments. These dimensions of artificial hailstones were produced successfully. The targeted velocities of the artificial hailstones are 20 m/s, 30 m/s, 60 m/s, and 120 m/s. To achieve this, the required air pressures were determined. Experiment results showed that different diameters of artificial hailstones can be produced successfully, and they impacted the targeted points on the aircraft canopies. Another observation from the study is that artificial hailstones traveling at velocities over 120 m/s could not cause visible deformation on aircraft canopies.

Keywords: Impact tests, Artificial hailstone, Aircraft canopy

INVESTIGATION OF THE USE OF ARTIFICIAL INTELLIGENCE IN DETERMINING THE STRUCTURE DEFECT IN CERAMIC COMPOSITE MATERIALS

Assist. Prof. Dr. Aysegul Yucel
İskenderun Technical University, İskenderun Vocational School, Department of Envıronmental Protectıon Technologies, Hatay, Türkiye
ORCID ID: 0000-0001-7069-7518

ABSTRACT

Ceramic composite materials have a very wide range of usage temperatures, from marine to aviation, to automobiles with infrastructure and even energy. This increase is observed in the expected performance properties according to the usage temperature. These performance properties cover chemical, mechanical, thermal, optical, magnetic and electrical components. Obtaining the desired properties starts with the synthesis of the ceramic composite material. In the synthesis phase, the types, quantities, temperature increase rate, reaction temperatures of the initial classes, such as the product structural properties to be obtained are quite nice. This effect affects the size and phase composition of the ceramic composite ratios and may naturally cause the desired material to not be produced. Artificial intelligence can classify problems such as defects, grain boundary incompatibilities, phase separations in the synthesis of ceramic composite components. Microstructure distances obtained with scanning electron microscope (SEM) or transmission electron microscope can be trained with artificial intelligence with deep learning models such as separation convolutional neural networks and thus image analysis can be performed. Artificial intelligence can use XRD patterns to determine data such as crystallinity, lattice defects and phase formation. Phase inconsistencies, lattice defects and divisions can be interpreted with artificial intelligence by using machine operation and various XRD logs. In this context, it will be beneficial to change the substitutes used in the synthesis method of composites in the ceramic sector. In addition, the probability of defects can be predicted by the degradation analysis related to the studied effect and payments, and this information allows financial financial parameter suggestions.

The benefits of AI in the production phase of ceramic and ceramic composite materials are significant. The ability to identify and predict defects using parameters such as microstructural defects, crystallinity, phase compositions, and defect defects, and the formation of defect prediction models is a practical and applicable use of AI. These materials offer considerable benefits, especially in terms of time and cost. This study focuses on the predictability of defect evaluation with AI during the production of ceramic and ceramic composite materials, highlighting the practical implications of this research and its relevance to the field.

Keywords: Ceramic, ceramic composite, artificial intelligence, material characterization

ÖZET

Seramik kompozit malzemler denizcilikten havacılığa, alt yapı endüstrisinden otomobile ve hatta yenilenebilir enerjide olmak üzere çok geniş kullanım alanlarına sahiptir. Kullanım alanlarına göre bu malzemelerden beklenen performans özellikleri de değişiklik göstermektedir. Bu performans özellikleri kimyasal, mekanik, termal, optik, manyetik ve elektriksel yönleri kapsamaktadır. İstenen özelliklerin elde edilmesi seramik kompozit malzemenin sentezlenmesi ile başlamaktadır. Sentezleme aşamasında başlangıç maddelerinin türleri, miktarları, sıcaklık artış hızı, reaksiyon sıcaklığı gibi parametreler elde edilecek ürünün yapısal özelliklerini oldukça etkilemektedir. Bu parametreler seramik kompozit yapının parçacık boyutu ve faz bileşimini etkileyerek yapısal kusurların oluşmasına dolayısıyla istenen malzemenin üretilememesine neden olabilir.

Yapay zeka ise seramik kompozit malzemelerin sentezinde kusurların tespiti, tane sınırı uyumsuzlukları, faz ayrılıkları gibi sorunları belirleyerek sınıflandırabilir. Taramalı elektron mikroskobu (SEM) ya da transmisyon elektron mikroskobu ile elde edilen mikroyapı görüntüleri örneğin evrişimli sinir ağları gibi derin öğrenme modelleri ile kullanılarak yapay zeka eğitilebilir ve böylece görüntü analizi yapılabilir. Yapay zeka kristalinite, kafes kusurları ve faz bileşimi gibi verilerin belirlenmesi amacıyla XRD desenlerini kullanabilir. Makine öğrenimi algoritmaları ve çeşitli XRD kütüphaneleri kullanılarak faz tutarsızlıkları, kafes yapısındaki kusurlar ve düzensizlikler yapay zeka ile yorumlanabilir. Bu yorumlar doğrultusunda seramik kompozitlerin sentezlenme yönteminde kullanılan parametrelerin değiştirilmesinde fayda sağlayabilecektir. Ayrıca çalışılan parametreler ile oluşturulan kombinasyonlar ile ilgili verilerin analizi yapılarak kusurların oluşma olasılığı tahmin edilebilir, bu bilgi doğrultusunda önleyici parametre önerilerine olanak sağlayabilir.

Mikroyapısal kusurlar, kristalinite, faz bileşimi ve kafes kusurları gibi parametrelerin geliştirilen algoritmalar ile tespit edilmesi, kusur tahmin modellerinin geliştirilmesi yapay zeka ile imkansız görünmemektedir. Böyle malzeme üretim aşamasında özellikle zaman ve maliyet açısından oldukça fazla fayda sağlayacaktır. Bu çalışma seramik ve seramik kompozit malzemelerin üretimi esnasında oluşabilecek kusurların yapay zeka kullanılarak tahmin edilmesinin araştırılmasını kapsamaktadır.

Anahtar Kelimeler: Seramik, seramik kompozit, yapay zeka, malzeme karakterizasyonu

FROM ORNAMENT TO STRUCTURE: THE DUAL ROLE OF CERAMICS IN OTTOMAN ARCHITECTURE

Melik Sami[1]

Khelil Sara[2]

Tallal Abdel Karim Bouzir[3]

[1,2] Departement of architecture, Mohamed Khider Biskra University, Biskra, Algeria /LACOMOFA Biskra laboratory

[3] Institute of Architecture and Urban Planning, Blida University, Blida, Algeria

ABSTRACT

It analyzes ceramics in Ottoman architecture where their ornamental and structural functions intersect in order to enhance both the aesthetic and pragmatic dimensions of the architectural design. In this research we focus on iconic structures such as the Blue Mosque, Topkapi Palace, and Rustem Pasha Mosque, which show how ceramics were combined to simultaneously generate visual splendor through color variation and differentiation, as well as provide climate control, acoustic optimization, and structural integrity through thermal mass. The study also shows how Ottoman architects changed ceramics from mere decorative elements to consequential components vital to building resilience and environmental comfort through the detailed analysis of ceramic tiles, especially Iznik tiles ceramic tiles with abounding floral and geometric motifs. The findings demonstrate the intersection of beauty and functionality through the lens of materiality, demonstrating invaluable lessons for current sustainable design practices. This article bridges traditional architectural wisdom and the most modern innovations by studying the historic applications and technical properties of Ottoman ceramics advocating for a design paradigm that values cultural heritage and environmental responsiveness.

Keywords: Ottoman architecture; Ceramic tiles; Dual functionality; Structural integrity; Aesthetic design.

.

CERAMIC EXPRESSIONS IN ARCHITECTURE: CULTURAL SYMBOLISM ACROSS ANCIENT AND MODERN CIVILIZATIONS

Melik Sami[1]

Khelil Sara[2]

Tallal Abdel Karim Bouzir[3]

[1,2] Departement of architecture, Mohamed Khider Biskra University, Biskra, Algeria /LACOMOFA Biskra laboratory

[3] Institute of Architecture and Urban Planning, Blida University, Blida, Algeria

ABSTRACT

Ceramics were, and remain, fundamental to architectural design not only as a functional but also as a symbol, of socio/political order, spirituality, and cultural identity. In this paper, we explore ceramic expressions in architecture from Ancient and Modern civilizations, specifically how ceramics convey cultural symbolism, resonating with time. And we show how, at such sites as the Great Mosque of Kairouan, Forbidden City, and La Alhambra, ceramic motifs, colors and materials are painstakingly chosen to reveal in codes the active value of the society in which they are employed: from religious devotion to imperial authority. The ceramics of this comparative study can speak the identity and memory that are both the foci for modernism and the vehicle for continuity, adapting to and synthesizing artistic and technological innovation in ways that protect cultural heritage. In applying to contemporary uses, we suggest ceramics as a means of bridging architectural narrative and existing design frameworks through historical traditions. Perhaps most importantly, this research ultimately underscores ceramics as indispensible to architectural discourse, and as a means to further explore ceramics' enduring significations of collective cultural narrative in a variety of culturally specific contexts.

Keywords: Ceramic symbolism; Architectural ceramics; Cultural identity; Ancient architecture; Modern architecture.

.

INTERNATIONAL CERAMICS AND COMPOSITE MATERIALS SYMPOIUM
November 15-16, 2024 / Süleyman Demirel University, Isparta, Türkiye

GROUTING AND SEALING BED SEPARATION BY OVERLAPPING MINE GOBS IN MULTIPLE SEAMS TO IMPROVE OXYGEN FLOW IN THE LONGWALL FACE

Jianwei Cheng[1]*

Shuping Sheng[1]

Dezhi Ran[1]

Md Mojahidul Islam[2]

Marek Borowski[3]

[1]School of Safety Engineering, China University of Mining and Technology, Xuzhou 221116, China

[2]School of Mining Engineering, China University of Mining and Technology, Xuzhou 221116, China

[3]Faculty of Mining and Geoengineering, AGH University of Science and Technology, Krakow, Poland, 30001

Corresponding Author*

ABSTRACT

The conditions under which coal production bases occur are characterized by shallow burial and the presence of multiple coal seams. This leads to the overlying strata being repeatedly disturbed, causing increased deformation and the formation of cracks that result in air leakage. The air leakage allows gases to escape into the upper gob, leading to low oxygen levels in the working areas of various mines within the region. The primary cause of these low oxygen levels is the leakage of harmful gases from the upper gob to the lower working face. To address this problem, a 'man-made isolation layer' was proposed, involving the grouting and sealing of the interlayer separation. A rock movement model was used to perform precise calculations of the primary deformation in the interlayer rock layers, while secondary movement deformation patterns of the overlying rock during multi-coal-seam mining were also determined. Mathematical models and numerical simulations were employed to study changes in deformation, porosity, and permeability in the overlying rock before and after filling the separation in the overlapping gob bed. The study

also investigated gas transport behavior and the impact of grouting and filling on this separation. The findings demonstrated that grouting and filling can effectively reduce the subsidence of the overlying strata, lower porosity and permeability, and limit the development of interlayer cracks that act as communication pathways. This method significantly contributed to the physical isolation of the upper and lower sections of the overlapping gob, resulting in a 40.9% and 32.8% reduction in interlayer air leakage, respectively, compared to the original levels.

Keywords: Overlapping gob; Mitigate Low Oxygen; Bed separation; Oxygen flow; Air leakage; Grouting; Underground mine.

SYNTHESIS OF CdSTe NANOPARTICLES BY LASER ABLATION

M. A. Jafarov

V. M. Salmanov

R. M. Mamedov

E. F. Nasirov

T. A. Mamedova

Baku State University, AZ1148 Baku, Azerbaijan

CdSTe nanoparticles were synthesized in solution using the reactive laser ablation method. Highly pure $CdCl_2$ (99.9 % pure from Sigma Aldrich), $Na_2S_2O_3$ (99.95 % pure from Sigma Aldrich) and TeO_2 (99.99 % pure from Sigma Aldrich) powders mixed with distilled water were used as initial raw materials. Immediately after irradiation with a laser pulse, CdSTe nanoparticles were formed. The ablation process was performed by laser radiation with a wavelength of λ=1064 nm, with a pulse energy of 135 mJ and an ablation time of ~10 min. The radiation source was a pulsed Nd:YAG laser with built-in generators of the 2nd and 3rd harmonics, designed to generate radiation with a wavelength of 1064, 532, and 335 nm. The laser pulse duration was 10 ns with a maximum power of ~12 MW/cm^2. The radiation intensity was varied using calibrated neutral light filters. The optical absorption and luminescence spectra of CdSTe nanoparticles were studied using an automatic M833 double dispersion monochromator (spectral resolution ~0.024 nm at a wavelength of 600 nm), with computer control and a detector that records radiation in the wavelength range of 350–2000 nm. The scheme of the experimental setup for ablation of CdSTe nanoparticles is shown in Fig.1.

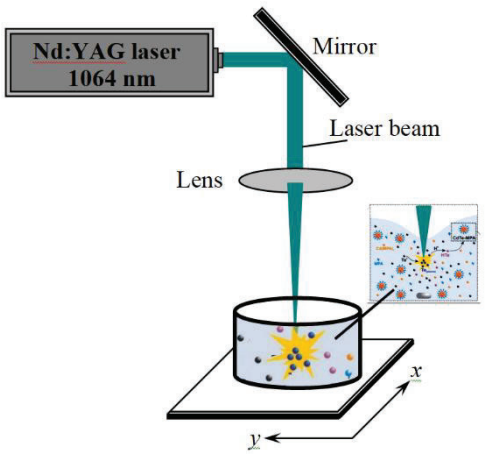


Fig.1. Scheme of the experimental setup.

Materials and Methods

On fig. Figure 2 shows the diffraction pattern (XRD) of nanoparticles from drops of a colloidal solution of CdSTe dried on a clean glass substrate. CuKα, λ=1.544178A^0 SSFOM: F17-610.0.5.10.60 were used as the radiation source. It is shown that the diffraction planes (111), (200),

(220), (311), (222), (400), (331), (422), and (511) at 2θ diffraction angles 23.620, 27.890, 38.970, 45.280, 49.340, 56.750, 63.600, 73.220, and 76.840, respectively, correspond to the cubic (zinc blende) structure of the bulk CdSTe crystal [14], which confirms the crystal structure of the synthesized nanoparticles, which is the same as that of the bulk material. Based on the X-ray diffraction patterns, using the Debye–Scherer formula [1-9], the sizes of the obtained nanoparticles were calculated:

$$D = \frac{k\lambda}{\beta \cos\theta}$$

where D-sizes of nanoparticles, k = 0.9 – line shape factor (shape factor), β = 0.035 A0 – intensity maximum half-width (FWHM- Full Width at Half Maximum), λ – X-ray wavelength, λ=1.54 A0, θ-Bragg angle, cos θ=0.727.

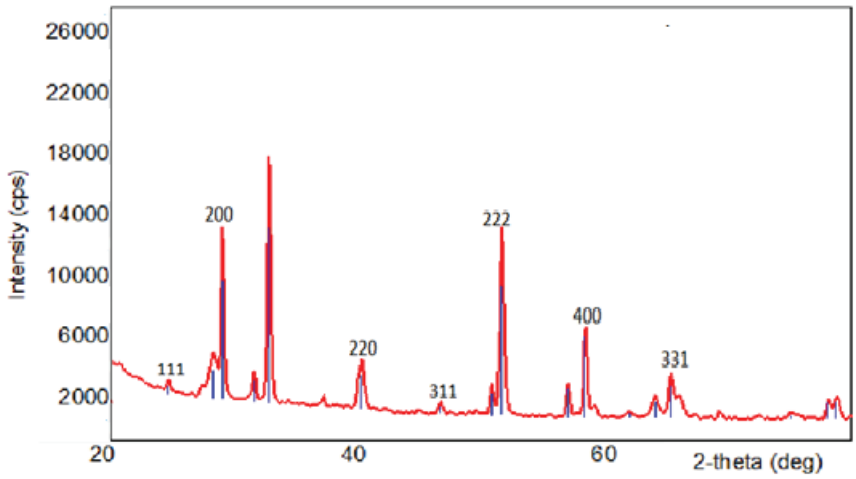


Fig.2. Diffraction pattern (XRD) of CdSTe nanoparticles on a glass substrate.

Estimates show that the average size of CdSTe crystallites is 27.434 nm (see Table).

2 theta	**Crystallite size**
23.62(3) 111	28.27 nm
27.891(9) 200	34.91 nm
38.97(3) 220	16.31 nm
45.28(5) 311	23.66 nm
49.347(14) 222	39.72 nm
56.75(8) 400	47.17 nm
63.60(5) 331	20.78 nm
73.2(2) 422	10.87 nm
76.84(3) 511	25.22 nm

average crystallite size:	**27.434 nm**

Morphologists. The surfaces of the synthesized CdSTe nanoparticles were studied using AFM analysis. Figure 3 shows a 3D AFM image of CdSTe nanoparticles on a glass substrate. As can be seen from the figure, a homogeneous distribution of particles in the presented figure is not observed.

The histogram of particle size distribution is shown in fig. 4. The average particle size estimated using the software was about 40-50 nm. The particle size value is higher than calculated by X-ray diffraction analysis. This is due to the fact that XRD depends on the free volume of dimensional defects, while AFM directly visualizes the grain without taking into account the degree of defectiveness of the crystal.

The absorption curve from a colloidal solution of CdSTe nanoparticles is shown in Figure 5a. The onset of absorption at ~500 nm is consistent with the absorption of an ensemble of nanoparticles whose maximum diameter is ~50 nm. Taking into account that CdSTe is a semiconductor with a direct band gap, from the dependence , the band gap of the studied samples was determined, which turned out to be equal to Eg = 2.46 eV (Fig. 5b). This value is 0.97 eV larger than the band gap of a bulk undoped CdSTe crystal, (eV (~827 nm) [1]. It should be noted that the shift of the red absorption band of nanoparticles to the short-wavelength region of the spectrum compared to a bulk crystal is a characteristic feature of semiconductor nanoparticles, which is related to the quantum size effect

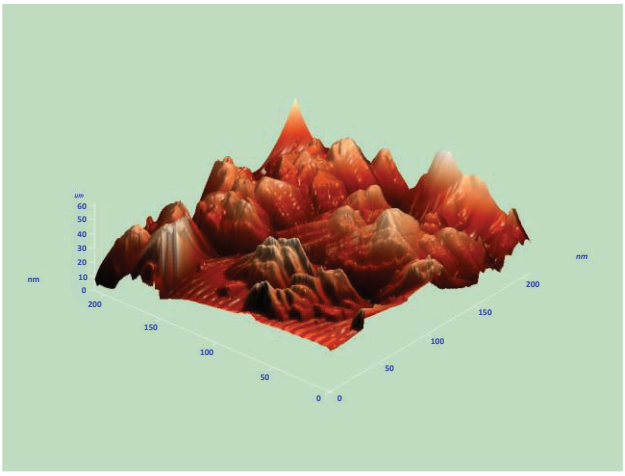


Fig.3. AFM image of CdSTe nanoparticles on a glass substrate.

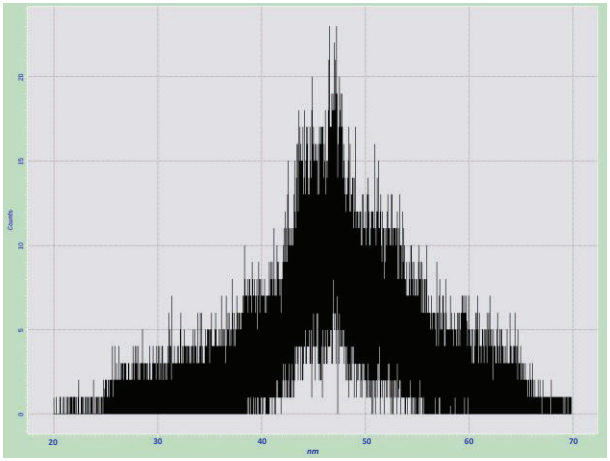
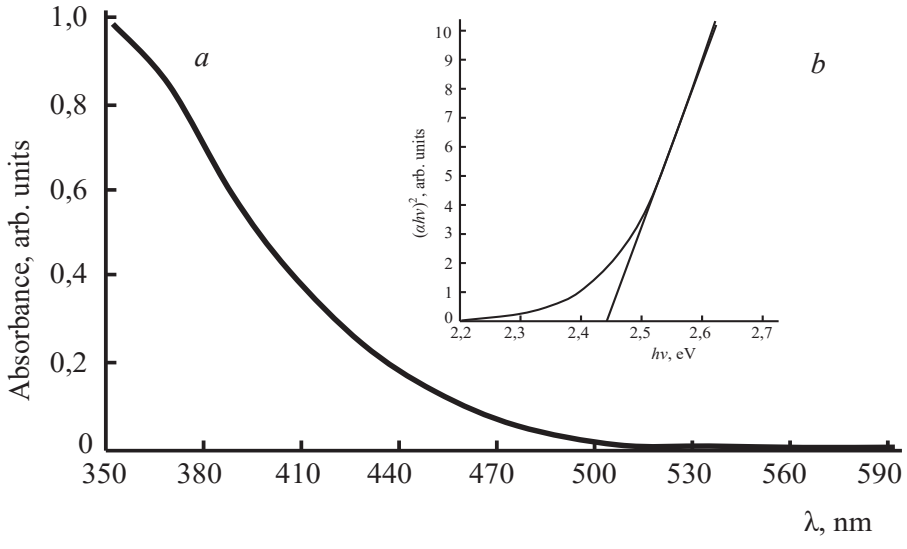


Fig.4. Histogram of particle size distribution.

Figure 6 shows the photoluminescence spectra of CdSTe nanoparticles excited by the second harmonic of the Nd:YAG laser (eV). As can be seen from the figure, the emission maximum of nanoparticles corresponds to wavelengths ~ 510 nm (2.43 eV). An increase in the laser light power by 1.2 times does not affect the position of the spectra, but leads to an increase in the radiation intensity by ~2.1 times. As regards the nature of the observed radiations, in our opinion they are due to the radiative recombination of free excitons.



.

Fig.5. Optical absorption spectrum (a) and dependence $\alpha^2 \sim f(h\nu)$ (b) of CdSTe nanoparticles obtained in a colloidal solution.

Knowing the energy of free excitons in CdSTe (~29 meV), it is possible to determine the band gap of nanoparticles, which is equal to 2.46 eV, which is in satisfactory agreement with the value determined from the absorption spectrum.

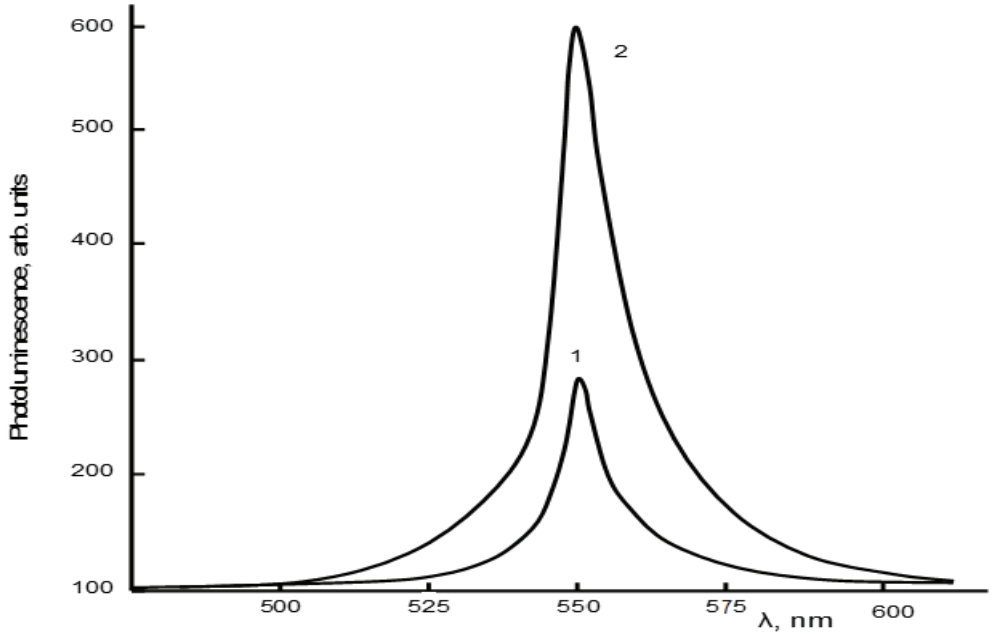


Fig.6. Photoluminescence spectra of CdSTe nanoparticles at two different excitation powers, the second harmonic of a neodymium laser (eV): 1 – 1 MW/cm^2; 2 – 10 MW/cm^2.

Conclusion

A new method for synthesizing CdSTe nanoparticles by laser radiation is proposed. Highly pure $CdCl_2$, $Na_2S_2O_3$ and TeO_2 powders mixed with distilled water were used as initial raw materials. The ablation process was performed by laser radiation with a wavelength of 1064 nm, with a pulse energy of 135 mJ and an ablation time of ~10 min. Under these ablation conditions in a colloidal solution, the formation of nanoparticles with diameters from ~10 to ~50 nm was observed. It is shown that the synthesized nanoparticles retain the crystalline structure of the bulk material and emit photoluminescence at 560 nm associated with the radiative recombination of free excitons [1-15].

Conflict of interst.

The authors of this work declare that they have no conflicts of interest.

References

[1]. *N.G. Semaltianos, S. Logothetidis, W. Perrie, S. Romani, R.J. Potter, M. Sharp, G. Dearden and K.G. Watkins.* CdSTe nanoparticles synthesized by laser ablation. Applied physics letters. 95, 2009, 033301-033306.

[2]. M. A. Jafarov, E. F. Nasirov, S. A. Jahangirova, R. Jafarli, NanoZnS thin films for solar cell. Nanosystems: physıcs, chemıstry, mathematıcs, 2015, 6 (5), P. 644–649

[3]. M. A. Jafarov, E. F. Nasirov, R. Mammadov, R. Jafarli. Fabrıcatıon and characterızatıon ZnCdS nanowıre. Nanosystems: physıcs, chemıstry, mathematıcs, 2014, 5 (6), P. 796–802

[4]. *A.V. Bulqakov, A.B. Yevtushenko, Yu.Q. Shukhov, I. Ozerov, V. Marin.* Pulsed laser ablation of binary semiconductors: evaporation mechanisms and cluster generation. «Quantum electronics», 40, № 11, 2010, 1021-1033.

[5]. *M.A.Jafarov, E. F. Nasirov* Nanoscale Structures based on the $Zn_{1-x}Cd_xS$. Nanosystems: physics, chemistry, mathematics, 2013, 4 (5), P. 680-689

[6]. *A. Morales-Acevado*. Thin film CdS/CdSTe solar cells: research perspectives. Solar Energy, 80, 2006, 675.

[7]. K. Zweibel. Engineering. The impact of tellurium supply on cadmium telluride photovoltaics. Science, 328, 2010, 699.

[8]. *R.L. Johnston.* Atomic and Molecular Clusters. London: CRC Press, 2002. 256.

[9]. *B.M. Smirnov.* Generation of cluster beams. Advances in the physical sciences, 173, 2003,609.

[10]. *Q.N. Makarov.* Extremal processes in clusters in collision with a solid surface. Advances in the physical sciences, 176, 2006,121.

[11]. *Z.A. Peng and X. Peng.* Formation of High-Quality CdSTe, CdSe, and CdS Nanocrystals Using CdO as Precursor. J. Am. Chem. Soc. 123, 2001, 183.

[12]. *M. Marc-Oliver Piepenbrock, Tom Stirner, Mary O'Neill and Stephen M. Kelly*. Growth dynamics of CdSTe nanoparticles in liquid and crystalline phases. J. Am. Chem. Soc. 129, 24, 2007, 7674.

[13]. *Martin Sharp.* CdSTe nanoparticles synthesized by laser ablation. Applied Physics Letters. 95, 2009, 033302.

[14]. *A.R. Albert, A.Y. John, A. Young.* Generation of CdSe and CdTe nanoparticles by laser ablation in liquids. Colloids and Surfaces A: Physicochemical and Engineering Aspects . 279, 1-3, 2006, 121.

[15]. *L. Patrone, D. Nelson, V.I. Safarov, M. Sentis, W.J. Marine.* Photoluminescence of silicon nanoclusters with reduced size dispersion produced by laser ablation. Appl. Phys., 87, 2000, 3829.

THE SYNTHESIZE OF THIN FILM VIA SOL-GEL DIP-COATING TECHNIQUE DERIVED BY SnO_2

A. Lahouel[1]*

M. Adnane[1]

S. Koudjeti[2]

[1]University of Science and Technology of Oran-Mohammed Boudiaf, Department of Physics, Oran, Algeria,

[2]University of Sciences of Abou Bekr Belkaid, Department of Physics, Tlemcen, Algeria
*Corresponding

ABSTRACT

Transparent conductive oxides (TCO) are smart materials with a wide band gap, transparenct in the visible region (400-700 nm) and have high electrical conductivity and are used variety of areas such as in photovoltaic cells, light-emitting diodes, gas sensors, flat panel displays (FPD) etc. Sol-gel is. These coatings can change the properties of surfaces and improve protection and surface functions in the intelligent system technologies. The sol-gel coating method is used in smart technology applications as it is a cost-effective and simple method and also suitable for large-scale production to synthesize homogeneous and conformal TCO film coatings. In this work, to obtain the sol-gel solution, firstly, oxide solutions of copper, aluminum, zinc, tin and titanium are synthesized (0,1 M) by using sol-gel method. Then the solution prepared to examine the changing characteristics. The films were coated by dip-coating technique to make 10 layers and annealed at 500˚C for 1 hour. Contact angle measurements were applied to these thin films and thin film samples exhibited the properties at the point of contact with the water droplet.

Keywords: Thin films, TCO, Sol-gel method, Contact angle

REDEFINING THE NEST: THE CONTRIBUTION OF ECOLOGICAL CERAMICS TO THE CONSERVATION OF NATURAL OF HABITATS

Ayşe Yerebakan
Çukurova University, Fine ArtFaculty, Ceramic Department, Adana, Turkey
ORCID ID: 0000-0002-6611-8218

ABSTRACT

Ecological degradation, one of the biggest problems of our age, negatively affects natural life, ecosystems, biodiversity, resource continuity and climate balance. Those most affected by these ecological problems are living creatures struggling to survive in their natural habitats. These creatures lose or are damaged in the habitats they call “home”. However, the nest is not only a shelter but also a living space where all kinds of security, reproduction and protection needs are met. These areas need to be rebuilt to protect living things and increase their numbers. At this point, ceramic stands out as a material that is compatible with the life of living things with its natural and inorganic structure. The durable and environmentally friendly properties of ceramics make it a suitable material for ecological designs. Thanks to the adaptation of ceramic structures to natural habitats, it is possible to protect the populations of living things and biodiversity. In this study, we investigate how the classic bird nests can be redefined with more durable and safer ceramic bird nests, how ground nest bees can have a sustainable habitat in ceramic hives, and how coral reefs can thrive on ceramic tiles. These ecological designs offer innovative solutions to preserve the natural balance and sustainably support biodiversity.

Keywords: Ecological ceramics, ecological design, ecological design, ecological degradation, wildlife conservation, natural habitat

VALORIZATION OF SEWAGE SLUDGE INTO CERAMIC MATERIALS

Dr. Saad BAALI
Civil engineering Department, Geomaterials Development Laboratory, University of M'sila, Algeria

Prof. Dr. Mekki MAZA
Civil engineering Department, Geomaterials Development Laboratory, University of M'sila, Algeria

Prof. Dr. Zine EL Abidine RAHMOUNI
Civil engineering Department, Geomaterials Development Laboratory, University of M'sila, Algeria

Prof. Dr. Nadia TEBBAL
Civil engineering Department, Geomaterials Development Laboratory, University of M'sila, Algeria

ABSTRACT

The valorization of sewage sludge into ceramic materials is an innovative method to recycle wastewater treatment residues into construction products, thus contributing to more sustainable waste management. This process begins with the dewatering of the sludge, reducing its water content to facilitate its handling. The sludge is then mixed with traditional raw materials, such as clay, to form a homogeneous mixture. This mixture is shaped into bricks, tiles or other ceramic shapes, then fired at high temperatures (usually between 900 and 1200°C). Firing stabilizes the potentially toxic components of the sludge, such as heavy metals, and gives the materials their mechanical, aesthetic and durability properties. The use of sewage sludge in the manufacture of ceramics has several advantages: it significantly reduces the volume of waste to be disposed of, reduces the consumption of natural raw materials, and produces materials with properties comparable to, or even superior to, those of traditional ceramics. However, challenges remain, including the variability of sludge composition depending on its origin, and the need to strictly control contaminants to ensure the safety of finished products.

In short, this recovery is part of a circular economy approach, promoting the reduction of the ecological footprint of sewage sludge while contributing to the production of sustainable and environmentally responsible construction materials.

Keywords: valorization, sewage sludge, ceramic materials, environment.

ENHANCING COMPOSITE MATERIALS THROUGH COMPUTATIONAL INTELLIGENCE TECHNIQUES

Assist. Prof. Dr. Kavirayani Srikanth

Dept. of EEE,Gayatri Vidya Parishad College of Engineering (Autonomous), Visakhapatnam, Andhra Pradesh-530017, India

ABSTRACT

The pursuit of advanced composite materials with superior mechanical properties and performance characteristics has become increasingly critical in various engineering applications. This study presents a novel approach that leverages computational intelligence algorithms—specifically particle swarm optimization and flower pollination—to optimize the design and performance of composite materials used in dynamic systems, such as in the geometry and design of complex structures of airplane and bioreactor applications. By integrating computational intelligence with material science, we developed a framework to predict and enhance the properties of composite materials under various operational conditions. The proposed method involves a single objective and multi-objective optimization process that simultaneously considers factors such as weight reduction, tensile strength, and thermal stability. Through simulations and experimental validations, we demonstrate how the optimization of fiber orientation, matrix selection, and layering configurations can lead to significant improvements in the performance of composite materials. Additionally, we explore the application of sensor fusion techniques to monitor real-time performance metrics of these materials in dynamic environments, allowing for adaptive responses to varying operational conditions. The results indicate a marked improvement in the resilience and functionality of composite materials, paving the way for their enhanced application in aerospace engineering and bioprocessing. This work underscores the potential of computational intelligence in revolutionizing the design and application of composite materials, offering promising pathways for future research and industrial implementation.

Keywords: Composite, Matrix selection, Mechanical properties

SOL-GEL METHOD FOR TAILORED BN-B_4C NANOCOMPOSITES: A CONTROLLED SYNTHESIS APPROACH

Murat Cem DURMAZ[1]

Suna AVCIOGLU[1]

Figen KAYA[1]

Cengiz KAYA[1]

[1]Department of Metallurgical and Materials Engineering, Yıldız Technical University, Istanbul, TURKEY

ABSTRACT

Boron carbide (B_4C) is an advanced ceramic material widely used in sectors such as the defense industry, owing to its remarkable physical and chemical properties, including high hardness, low density, high melting point, excellent wear resistance, chemical stability, and strong neutron absorption capacity. However, alongside its many advantages, low fracture toughness of B_4C remains a limitation that warrants improvement.

In this study, polymeric precursors modified with various ammonium salts for the synthesis of BN-B_4C nanocomposites was developed. The influence of the molecular structure of these ammonium salts on the BN-B_4C phase ratio, particle morphology, particle size, and size distribution was investigated.

SEM analysis of the powders revealed that B_4C particles reached a maximum size of 9 microns, while BN particles were approximately 0.1 microns. FT-IR and NMR analyses were conducted to examine the chemical structure of the synthesized precursors and to assess borate ester (B-C-O) formation yields. XRD analyses provided insights into the phase composition of the synthesized powders.

The results demonstrated that BN-B_4C nanocomposites with tunable phase ratios and particle sizes could be successfully synthesized via the sol-gel method, with variations controlled by the type and concentration of ammonium salts. Therefore, the present work offers new approaches for enhancing the properties of B_4C ceramics, broadening their applicability in various technological fields, such as defense and radiation shielding.

Acknowledgments: The authors are grateful for the financial support from TUBITAK under contract number of 122M836.

Keywords: Sol-gel, Ammonium salt, Boron Nitride, Boron Carbide

INVESTIGATION OF STRUCTURE-ACTIVITY RELATIONSHIP IN IRON-CONTAINING PEROVSKITES FOR SUPERCAPACITORS

Dr. Celal AVCIOĞLU
Technische Universität Berlin, Faculty III Process Sciences, Institute of Materials Science and Technology, Chair of Advanced Ceramic Materials, Straße des 17. Juni 135, Berlin 10623, Germany

ABSTRACT

This study explores the structure-activity relationship in iron-containing perovskites for supercapacitor applications, focusing on their unique energy storage and rapid charge/discharge capabilities. Iron-based perovskites are promising due to their high theoretical capacitance, environmental stability, and cost-effectiveness. In this research, iron-containing perovskites were synthesized using a cost-effective molten salt method, yielding materials with high crystallinity. X-ray diffraction (XRD) was used to confirm the crystalline phases and structural integrity of the materials, with the phase compositions further verified through Rietveld refinement. The oxidation states of the elements, particularly focusing on the B-site cations, were examined using X-ray photoelectron spectroscopy (XPS), providing insights into the chemical environment. Morphological analysis was conducted using Scanning Electron Microscopy (SEM) and Transmission Electron Microscopy (TEM), allowing for detailed observation of particle size, shape, and surface characteristics. Additionally, UV-Vis Spectroscopy was utilized to investigate the optical properties and bandgap of the materials, which is crucial for understanding their electronic behavior and potential contributions to energy storage performance. The study evaluates the influence of key structural factors, including, crystal structure, oxygen vacancy concentration and oxidation states of B-site cations, band gap, charge transfer resistance on the electrochemical charge storage performance of these materials. This research underscores the potential of iron-containing perovskites in advancing supercapacitor technology and provides insights into structuring these materials for improved energy storage applications.

Keywords: Energy storage, perovskite, iron-based supercapacitors, electrochemical performance.

BUILDING A CERAMIC AND COMPOSITE MATERIALS INDUSTRIAL ZONE IN PAKİSTAN A STRATEGIC RESEARCH BY DR FAISAL FOR FRAMEWORK FOR SUSTAINABLE GROWTH

MUHAMMAD FAISAL
Allama Iqbal Open University
MIS/IT Specialist in Ministry of Safron Pakistan
ORCID: 0000-0002-5797-766X

ABSTRACT

Dr Faisal structuring a production zone narrowly focused on ceramics and composites in Pakistan will be a substantial help for the country's long-term development as a materials industry leader and will be in line with the ongoing technological progression in the world. This report describes the main components of the concept that will enable the setting up of an industrial zone, the areas of infrastructure, technological capabilities, skilled workforce, and government support being the main points of focus. At the same time, Pakistan has abundant mineral resources like clay and silica which can be used in the making of ceramics. Thus, a solid supply chain system and import facilitation need to be built to tackle the shortage in the field of advanced composite materials. Modern manufacturing facilities that would include super temperature kilns and high precision CNC machines could be acquired as direct investments into the sector and thus, the production of the parts will be very efficient. Furthermore, central points that are engaged in cooperative research and development can stimulate innovation in areas that are related to, for instance, bio-composites, and lightweight materials, with the multiplication of this whole process in construction, automotive, and renewable energy sectors being just three of the possible segments. The skill development framework program focuses on instructing and training a large batch of students who will then be able to be efficient workers in industries requiring advanced materials engineering. Reduction of taxes, simple regulations, and the establishment of special economic zones to attract the potentials of both local and foreign investors. Finally, observance of environmental regulations and the implementation of green practices will now allow Pakistan to gain an advantage and company in the world market. Educatively meeting these strategic needs of Pakistan, the country can create such a sustainable, competitive industrial zone that, besides fulfilling the national requirement, can still be in touch with the global perspective in ceramics and composites. Setting up a ceramic and composite materials only industrial area in Pakistan would be assisting various technologies, thus boosting from industrial development, and also diversifying and helping climbing to the top in global markets, making the industry more competitive in the state. Pakistan can use its local resources and benefit from supply chain networks to create a solid basis for the ceramics industry as well as cover the present gap in the production of advanced composite materials by means of the international alliances and imports. Investing in advanced manufacturing equipment and automation, along with having a workforce skilled in using modern materials, will boost productivity and encourage new ideas. Government help, such as special benefits, simpler rules, and creating special areas for business, will bring in more investment. The plan to set up research centers and education programs will create a steady supply of skilled workers and promote a culture of always finding better ways

in material science. By using environmentally friendly methods in production, the industry can meet both local and global demand for green materials. This complete plan will help Pakistan become an important player in the ceramics and composites industries, supporting long-term growth and economic strength.

Keywords: structuring, substantial, capabilities, Reduction of taxes, environmentally.

THE INVESTIGATION OF THE EMERGENT BEHAVIIOUR OF POLYMER FILLED WITH CARBON NANOTUBE MODELED BY RANDOM RESISTOR-CAPACITOR-DIODE ELECTRICAL NETWORK

Dr. Mustapha AOUAICHIA
University of Science and Technology Mohamed Boudiaf
LEPM, Faculty of Physics, Oran, Algeria.
ORCID ID: 0009-0009-7282-8329

Prof. Rachid Bouamrane
University of Science and Technology Mohamed Boudiaf
LEPM, Faculty of Physics Oran, Algeria.
ORCID ID: 0000-0002-9162-7399

ABSTRACT

The purpose of this research was the investigation of the power law behaviour of Jonscher known as "the Universal Dielectric Response" for the polymer-carbon nanotube composites. The electrical and dielectric properties of polymer matrices filled with carbon nanotubes (CNTs) are studied using resistor-capacitor-diode (RCD) network models. Above the percolation threshold, CNT networks dominate, with conductivity increasing and permittivity decreasing due to resistive losses. Below this threshold, tunnelling resistance and capacitive effects govern the response, while at low CNT concentrations, isolated CNTs contribute primarily to capacitive behaviour. These results offer insights into the role of CNT dispersion and connectivity, with applications in energy storage, electromagnetic shielding, and flexible electronics. Experimental validation is proposed to link theoretical predictions with practical outcomes.

Keywords: Carbon nanotube, Percolation, Random networks RCD, UDR

INTRODUCTION

Materials modelling is a broad field and essential for designing and understanding the behaviour of complex materials, where interactions between multiple components give rise to new phenomena at the system level [1]. Heterogeneous materials such as polymer composites loaded with a variety of conductive fillers, glassy materials, and carbon nanotube (CNTs) polymer [2,3] that contain two phases, conductive or semi-conductive and insulating (dielectric) are widely modelled by random electrical network [3,4].

These systems exhibit a frequency dependence of conductivity and permittivity, which is known as the universal dielectric response (UDR) [5]. Examples of UDR behaviour in ceramic materials are in Fig. 1 [2], which show the ac conductivity of an Al_2O_3–TiO_2 ceramic composite and a doped zirconia at a variety of temperatures. At low frequencies the bulk (real) ac conductivity $\sigma(\omega)$ is frequency independent, but at higher frequencies the ac conductivity increases, following a power law behavior such that [2]:

$$\sigma(\omega) = \sigma(0) + A\omega^n$$

Where ω is angular frequency (2πf) and n is typically 0.6 < n < 1.0. The dielectric permittivity exhibits a frequency independence at high frequency can be expressed by a power law decay such that:

$$\varepsilon(\omega) = B\omega^{n-1} + \varepsilon_{\infty}$$

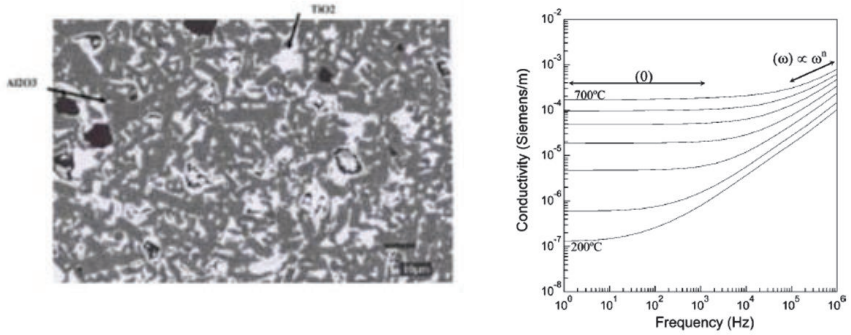


Fig.1. Ac conductivity of an Al_2O_3 (insulator) TiO_2 (conductor) composite[2].

In Our previous work, we use a large random resistor, capacitor to investigate the power-law scaling of the conductance and the percolation and saturation limit at high and low frequency [3]. This paper presents a diode to simulate the semiconducting phase of single-walled carbon nanotubes. Bychanok et al. [6] used Kirchhoff's circuit laws to model the carbon nanotube-filled polymer using an RCD random network at low frequencies in order to investigate low frequency dispersion. Our work focusses on the universal dielectric response of this material at middle frequencies.

METHODE

One third of single-walled (SW) CNT nanocylinders have metallic behavior while the rest behave as semiconductors leading to the study of a 3-phase system [6,7]. The electromagnetic properties of CNTs polymer composite can be modelled by random resistor-capacitor-diode electrical networks (RCD) Fig.2. The conducting phase is represented by a $p_r = 1 - p_c - p_d$ proportion of resistance, the insulator phase is represented by a p_c proportion of the capacitance and the semiconducting phase is represented by a p_d proportion of diode. The impedance of each component in the network is R for the resistor, $\frac{1}{i\omega C_0}$ for the capacitor and $\frac{1}{(i\omega)^m C_1}$ for the diode [6, 8].

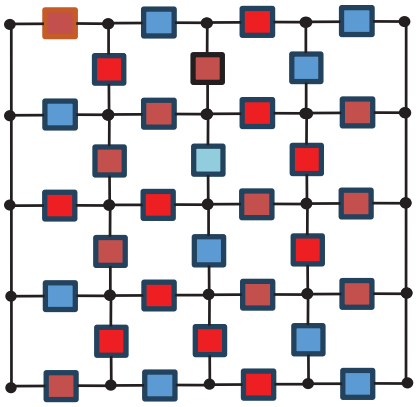


Fig.2. Example of random square network containing 32 components S=4. The resistors are in brown, capacitors in red, diode in blue.

Numerical Calculation Process:

The principal method to calculate the equivalent impedance of electrical random network that contains resistors, capacitors and diodes is Frank-Lobb reduction scheme, by applying a sequence of triangle-star transformation. A details demonstration method calculation is in [3]. We consider a square network composed by the parameter of $R = 10^3 kw$, $C_0 = 0.1nF$, $C_1 = 50nF$, $m = 0.1$, randomly positioned. The network size is the total of N= $2S^2$ components, where S is the node on the horizontal side. The dielectric response $\varepsilon(\omega)$ and the conductivity $\sigma(\omega)$ of a mixture random network RCD is determined by calculating the equivalent impedance from the following relation:

$$\varepsilon(\omega) = \varepsilon'(\omega) + i\varepsilon''(\omega) = \frac{1}{i\varepsilon_0 \omega Z_{eq}(\omega)}, \sigma(\omega) = \omega\varepsilon_0\varepsilon''$$

RESULTS

We present in this work three configuration possible of random RCD networks; we consider percolation under the diode over the resistor (i), percolation under the resistor over the diode (ii), percolation under the resistor-diode (iii).

(I) **in regions under the diode percolation threshold but over the resistor percolation threshold**, the network can behave in a way that AC conductivity is influenced by the proportion of capacitors and diodes present. We show in Fig.3, that the conductivity follows the power law such as $\sigma(\omega) \propto \omega^n$, where n=0.480518= $p_c + p_d$ is the proportion of capacitors and diode.

The permittivity decreases with frequency according to a power law $\varepsilon(\omega) \propto \omega^{n-1}$, where $n - 1 = -0.519482$ is the proportion of resistor, this aligns with some theoretical and empirical observations in complex networks. This suggests that the network behaves like a loss dielectric where resistive effects cause energy dissipation and frequency-dependent polarization.

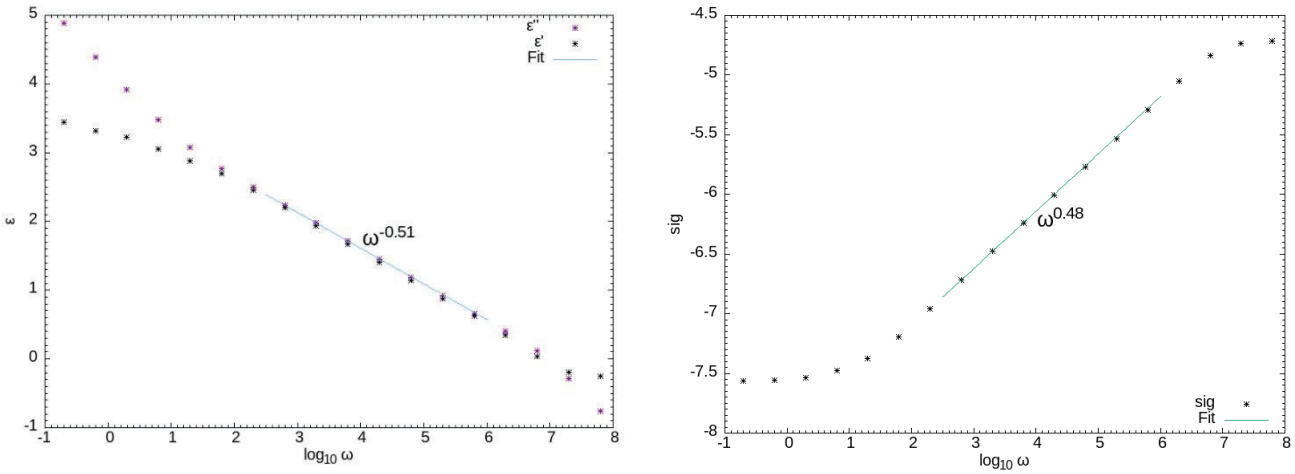


Fig.3. The effective permittivity and conductivity of random RCD networks for the case under diode over resistor percolation.

(ii) In this region, the network likely transitions from primarily resistive to capacitive behaviour (**under resistor percolation but over diode percolation**).

The Fig.4 shows that the permittivity decreasing and following the power law ω^{n-1}, where $n-1=-0.43304$ is the proportion of diode p_d, this could indicate that the diodes introduce a specific type of frequency-dependent response. Since diodes in our model act similarly to capacitors but with a non-linear behaviour due to the power law $\frac{1}{(i\omega)^m C_1}$, their proportion might influence how the permittivity scales with frequency. While the conductivity increases with a power law ω^n , n=0.56696 is the sum of the proportions of resistors and capacitors, suggests that these two components dominate the conductivity pathways. This makes sense, because capacitors introduce frequency-dependent behaviour, while resistors contribute direct current pathways.

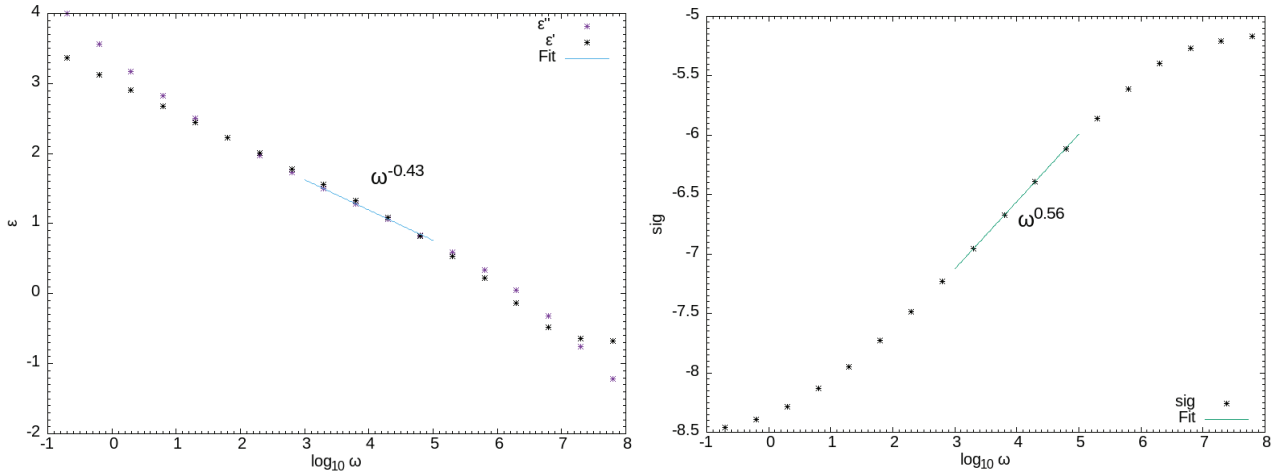


Fig.4. The effective permittivity and conductivity of random RCD networks for the case under resistors over diode percolation.

(iii) In the Fig.5 shows **the case under R-D percolation**, which the conductivity is increasing with power of n=0.537664 that equals the proportion of capacitors p_c, this suggests that capacitors are the primary conductive pathways at the frequencies analysed. This behaviour is consistent with the capacitive response at higher frequencies, where capacitors contribute to the overall current flow due to their impedance decreasing with frequency$\frac{1}{i\omega C_0}$. The permittivity decreasing with a power of $n-1=-0.462336$ is the proportion of p_r+p_d, indicates that the dielectric storage capability decreases as frequency increases. This is characteristic when non-linear or resistive elements do not contribute

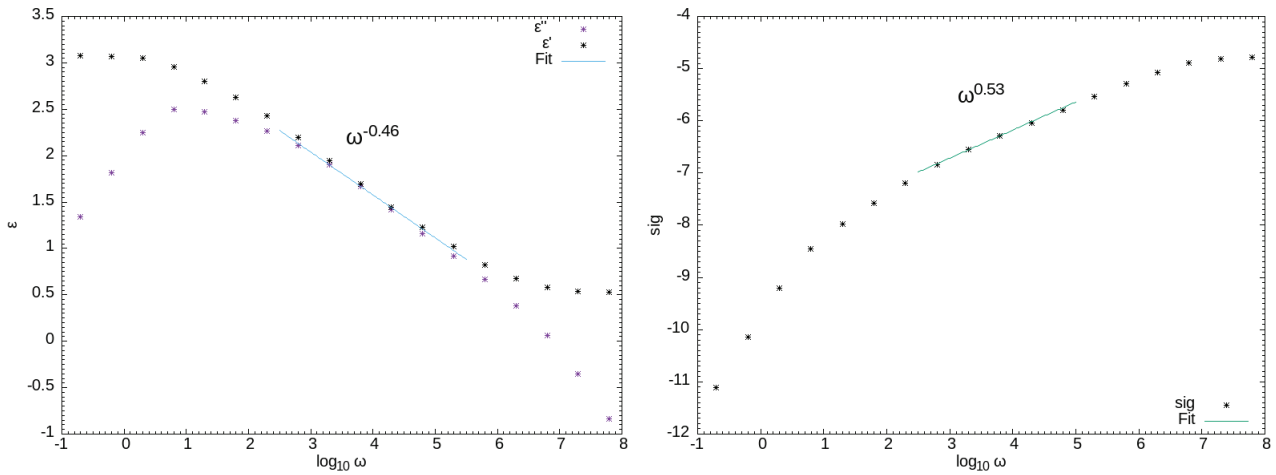


Fig.5. The effective permittivity and conductivity of random RCD networks for the case under resistors - diode percolation

effectively to the storage of electric charge at these frequencies. The presence of diodes, which can introduce non-linearity, and resistors, which dissipate energy, may reduce the effective permittivity in this regime.

CONCLUSION

Polymers filled with carbon nanotubes (CNTs) is both relevant and insightful because such composites are excellent examples of disordered systems where percolation theory and dielectric scaling laws often govern the observed properties. Carbon nanotubes (CNTs) are highly conductive, and when dispersed in a polymer matrix, they introduce percolate networks where the conductivity and permittivity of the composite depend on: The proportion of CNTs, dispersion, connectivity, and Interactions with the polymer matrix.

For the first case (i), in a polymer-CNT composite above the percolation threshold, CNT networks dominate conductivity, which the conductivity follows a positive power law with CNT concentration. While permittivity decreases due to resistive losses within the conductive network, aligning with the observation $n - 1 = -$ proportion of resistors.

The second case (ii), under resistor percolation but over diode percolation, in this regime, tunnelling resistance or semi-continuous CNT pathways could act as diodes or capacitive elements: Conductivity may scale positively with capacitive effects as CNTs interact with the polymer matrix through tunnelling gaps. Permittivity could decrease due to partial conductive behaviour influenced by the diode-like tunnelling junctions.

In the last case (iii), where the resistor and the diode are under percolation threshold, the composites with low CNT content, individual CNTs may act as capacitive elements. The conductivity scales with capacitive pathways and Permittivity decreases as resistive and diode-like contributions fade, leaving only the capacitive response of isolated CNTs.

REFERENCES

[1] McCullen, N.J., Almond, D.P., Budd, C.J., Hunt, G.W.(2009). The robustness of the emergent scaling property of random RC network models of complex materials. J. phys. D:Appl. Phys, 42 064001.

[2] Bowen, C.R., Almond, D.P.(2006). Modelling the ‘universal’ dielectric response in heterogeneous materials using microstructural electrical networks. Materials Science and Technology, Vol. 22 No. 6.

[3] Aouaichia, M., McCullen, N., Bowen, C.R., Almond, D.P., Budd, C., Bouamrane, R.(2017). Understanding the anomalous frequency responses of composite materials using very large random resistor-capacitor networks. Eur. Phys. J. B 90, 39.

[4] Almond, D.P., Vainas, B. The dielectric properties of random r-c networks as an explanation of the ’universal’ power law dielectric response of solids.(1999). J. Phys.: Condens. Matter ,11, 9081.

[5] Jonscher, A. K. The Universal Dielectric Response.(1990). Part I. IEEE Electrical Insulation Magazine.Vol. 6, No. 2.

[6] Bychanok, D.S., Paddubskaya, A.G., Kuzhir, P.P., Maksimenko, S.A., Brosseau, C. A study of random resistor-capacitor-diode networks to assess the electromagnetic properties of carbon nanotube filled polymers.(2013). Applied Physics Letters 103,243104 .
[7] Saito, R., Dresselhaus, G., Dresselhaus, M.S.(1998). Physical Properties of Carbon Nanotubes.Imperial College Press, London.
[8] Donahue, M., Lubbers, B., Kittler, M., Mai, P., Schober, A.(2013).Impedance characterization of AlGaN/GaN Schottky diodes with metal. contacts Appl. Phys. Lett. 102, 141607.

A NEW BIOMIMETIC DESIGN BIOCERAMIC FOR BONE REGENERATION BY TPMS LATTICE STRUCTURE

M. R. Harroug *
University Batna 2, Faculty of Technology, Department of Mechanical Engineering, Batna, Algeria.
ORCID ID: 0000-0000-0000-0000

H. Ameddah
University Batna 2, Faculty of Technology, Department of Mechanical Engineering, Batna, Algeria.
ORCID ID: 0000-0003-2572-7372

H. Mazouz
University Batna 2, Faculty of Technology, Department of Mechanical Engineering, Batna, Algeria. ORCID ID: 0000-0000-0000-0000

ABSTRACT

Bone regeneration is a major challenge in surgery. Complex fractures and loss of bone substance pose serious health problems. Current grafting techniques, although widely used, have their limitations: limited availability of grafts, risks associated with surgery, and sometimes insufficient quality of reconstituted tissue. Tissue engineering, an innovative approach, offers new prospects by combining cells, biomaterials and biological signals to stimulate bone regeneration. However, many challenges remain: the design of biocompatible materials that promote bone growth. The aim of this study is to develop a new therapeutic approach based on the design of new biomimetic materials capable of mimicking the extracellular matrix of bone to enhance bone regeneration. The TMPS method is used to manufacture scaffolds for tissue engineering based on mathematical equations, 3D printed with interconnected pores and appropriate biomorphic surfaces. The material chosen for the bone, LithaCon ATZ 980, an alumina-hardened zirconia supplied by Lithoz with Young's Young of 220 GPa and a theoretical density of 5.48 g/cm3, a compressive strength of 2200 MPa and a Poisson's ratio of 0.27. The numerical development is using Ansys workbench for lattice configuration and meshing, this design undergoes a comprehensive stress analysis using finite element analysis (FEA). The scaffolds exhibited comparable stiffness and tensile strength to cortical bone, mitigating the risk of failure and suggesting their suitability for bone replacement.

Keywords: Bone regeneration, bone defects, biomimetic materials, bioceramics, TPMS.

UTILIZATION OF SEWAGE SLUDGE ASH IN LIGHTWEIGHT AGGREGATE PRODUCTION FOR SUSTAINABLE CONSTRUCTION

BOUSLAH Mahmoud
University of M'sila, Faculty of technology , Civil engineering department, M'sila, Algeria.
ORCID ID: 0009-0007-2645-6160

MAZA Mekki
University of M'sila, Faculty of technology, Civil engineering department, M'sila, Algeria.
ORCID ID: 0000-0002-4742-4711

RAHMOUNI Zine EL Abidine
University of M'sila, Faculty of technology, Civil engineering department, M'sila, Algeria.
ORCID ID: 0000-0001-8551-2715

TEBBAL Nadia[4]
[4]University of M'sila, Faculty of technology, Civil engineering department, M'sila, Algeria.

ABSTRACT

This paper investigates the alternative use of sewage sludge ash (SSA) for the production of light weight aggregate (LWA) for sustainable construction The main objective is to investigate how SSA can be successfully reused to produce construction materials without reducing environmental contributions. The study examines the processes for converting SSA into lightweight aggregates, focusing on the technological processes and factors that make this application possible. Key benefits include significant reductions in the overall weight of concrete structures, reduced transportation and housing costs, and improved thermal insulation, which improves energy efficiency in buildings to the sky

In addition, the paper discusses the environmental benefits of implementing SSA in LWA operations, such as waste disposal reduction, greenhouse gas emission reduction, natural a will be preserved and also discusses technical challenges including the need for continuous quality improvement and compliance with regulatory standards. Research emphasizes the importance of quality qualitative and strategic approaches to ensure the reliability and efficiency of SSA-based LWAs.

Overall, this study presents SSA as a promising alternative for small aggregates, promoting a circular economy in the construction industry. In producing LWA by turning waste into a value-added product, SSA is a sustainable way to model modern construction practices, contributing to greener and more efficient industries.

Keywords: Sewage Sludge Ash (SSA), Lightweight Aggregates (LWA), Sustainable Construction, Eco-friendly Building Materials, Environmental Impact.

EXPERIMENTAL STUDY ON THE BEHAVIOUR OF CONCRETE FILLED STEEL TUBES SUBJECTED TO AXIAL AND LATERAL LOADING

Prof. Dr. P. Gajalakshmi
Department of Civil Engineering
B.S Abdur Rahman Crescent Institute of Science and Technology, Chennai

Dr. A. S. Menaka
Indian Institute of Technology, Madras, Chennai

ABSTRACT

Concrete-filled steel tubular (CFST) columns offer a viable alternative to reinforced concrete structures. Circular composite concrete-filled tubular (CCFT) columns, comprising a steel tube filled with concrete, are extensively utilized in structures requiring substantial moment resistance and ductile deformation capacity. In contrast to conventional steel and concrete structures, CFST columns exhibit enhanced strength and stiffness while also streamlining costs through reduced construction materials and shallower floor depths. This study delves into the theoretical examination of hollow and CCFT columns under axial loading, comparing their performance using various standards including AISC LRFD - 1999, Eurocode 4 – 1994, AS 4100 (1998), NZS - 4600 (1998), and BS 5400 – 1979. Subsequent experimental investigations involve subjecting the columns to axial loading and comparing the results with theoretical predictions. Furthermore, experimental analysis extends to studying the behavior of circular concrete-filled tubular columns under lateral loading, encompassing both static and dynamic tests.

Keywords: Steel tubes, deformation, concrete

PLA-BASED COMPOSITE FILAMENTS FOR 3D PRINTING: PRODUCTION PROCESSES AND MECHANICAL PERFORMANCE

Asst. Prof. Dr. Görkem YUMUŞAK
Marmara University, Turkey
ORCID NO: 0000-0002-5047-4357

ABSTRACT

This research examines PLA-based composite filaments using iron powder. The goal is to make materials used in Fused Deposition Modeling (FDM) 3D printing better in terms of their mechanical and thermal properties. The incorporation of iron particles into the PLA matrix alters the composite material's characteristics to satisfy the requirements of high-performance applications. The research involves filament fabrication by extrusion, tensile and thermal assessments, and heat treatment to analyze performance enhancements. A close look is given to the outcomes of differential scanning calorimetry (DSC) and tensile tests done before and after annealing. The findings indicate notable improvements in thermal stability. The tensile strength value, which decreased after the addition of iron, was tried to be improved by applying heat treatment. This study advances the creation of sustainable, high-performance composite materials for sophisticated additive manufacturing applications.

Keywords: PLA-based composite filaments, Iron powder doping, Additive manufacturing

INTRODUCTION

Additive manufacturing, also referred to as 3D printing, signifies a revolutionary advancement in contemporary production and prototyping. Fused Deposition Modeling (FDM) has achieved extensive popularity among the many approaches in this category due to its simplicity, affordability, and adaptability (Ian Gibson, 2015). The core principle of FDM is the layer-by-layer deposition of thermoplastic filaments to create intricate shapes, providing exceptional precision and accessibility for industrial and personal applications. The efficacy of FDM is significantly affected by the characteristics of the filament material employed. Material development is a crucial priority area to expand the capabilities of FDM technology (Chua & Leong, 2014).

Polylactic acid (PLA), a biodegradable and eco-friendly polymer sourced from renewable resources, is among the most extensively utilized materials for Fused Deposition Modeling (FDM). PLA is preferred due to its low processing temperature, simplicity of printing, and capacity to produce a high-quality surface finish. Moreover, its biodegradability corresponds with the worldwide movement toward more sustainable production techniques (Jamshidian, Tehrany, Imran, Jacquot, & Desobry, 2010). Still, PLA can only be used in less demanding situations because of its mechanical and thermal properties, such as its low glass transition temperature, low elongation at break, and low tensile strength. These constraints have prompted researchers and materials scientists to investigate methods for improving PLA's performance.

A promising method entails the creation of composite materials through the integration of additives into the PLA matrix. Metal powders, including aluminum, copper, and iron, have proven to be excellent fillers that can alter the characteristics of PLA to satisfy the demands of more rigorous applications (Koukouviti, Economou, & Kokkinos, 2024). Iron powder is noteworthy for its magnetic characteristics, thermal conductivity, and cost-effectiveness. Incorporating iron powder into PLA may enhance its thermal stability, tensile strength, and overall durability. Nonetheless, attaining a homogeneous distribution of metal particles inside the polymer matrix presents a problem, as particle aggregation may result in inconsistencies in the material's properties.

A multitude of studies has examined the advantages of metal-polymer composites in several manufacturing applications (Antoniac et al., 2019; Pušnik Črešnar et al., 2021; Ulkir, 2024). These composites exhibit substantial enhancements in heat conductivity, stiffness, and mechanical strength, rendering them appropriate for applications in automotive, aerospace, and medical devices. The inclusion of metal fillers might improve the functional characteristics of printed items, such as electrical conductivity or magnetic responsiveness, thereby expanding the range of FDM applications. Even so, these studies have given us a better understanding of metal-polymer composites. However, adding things like iron powder to PLA is still an area of research that is still being developed.

In addition to the initial development of PLA's qualities by additives, post-processing processes like annealing are essential for further increasing the material's performance (Chien & Yang, 2024; Jayanth, Jaswanthraj, Sandeep, Mallaya, & Siddharth, 2021). Annealing, a thermal treatment method, can augment the crystallinity of the PLA matrix, thereby improving its tensile strength and thermal stability. Because adding metals and heating up PLA together changes its properties, we need to do a lot of research to make these methods better so they can be used in real life.

This study seeks to fill these gaps by investigating the manufacture and characterization of PLA-based composite filaments infused with iron powder. The study examines the mechanical and thermal characteristics of the filaments in both their as-extruded condition and post-annealing. Differential Scanning Calorimetry (DSC) is utilized to examine the thermal transitions of materials, whereas tensile testing offers insights into their mechanical properties. This study aims to enhance the existing knowledge of composite filaments for FDM and provide a framework for developing high-performance, sustainable materials for 3D printing applications through a systematic investigation of these features.

MATERIALS AND METHODS

The fabrication and assessment of PLA-based composite filaments infused with iron powder employed a methodical strategy aimed at guaranteeing consistency and dependability in outcomes. The process comprised four primary phases: material preparation, filament extrusion, sample manufacturing, and property characterization.

Materials

Polylactic acid (PLA) pellets were picked as the main polymer matrix because they are commonly used in Fused Deposition Modeling (FDM) and are safe for the environment. The PLA utilized in this investigation was commercially obtainable, with a melting point range of 160–180°C and a density of around 1.25 g/cm³. Fine iron powder was selected as the reinforcing component. The iron powder was provided with a purity of 99% to reduce contamination. Prior to processing, the PLA pellets were desiccated in a vacuum oven at 60°C for 4 hours to remove residual moisture, which could cause flaws during extrusion. The iron powder was combined with the dry PLA pellets in a 99:1 weight ratio (PLA: Fe). The blending was conducted using a mechanical mixer for 20 minutes to attain initial homogeneity.

Filament Extrusion

The composite mixture was introduced into a twin-screw extruder (Figure 1) engineered for thermoplastic processing. The parameters of the extrusion process were meticulously tuned to guarantee the uniform distribution of iron particles throughout the PLA matrix. The extruder barrel comprised four heating zones, with temperatures established at 170°C, 180°C, 190°C, and 200°C from the feeding zone to the die. The screw rotation speed was sustained at 10 rpm, and the filaments were extruded using a die with a diameter of 1.75 mm.



Figure 1. Extruder

The extruded filaments were chilled in a 60°C water bath, facilitating quick solidification to preserve dimensional precision. The filaments were subsequently wound onto reels for additional processing. The filament's diameter was measured using a micrometer during the extrusion operation to guarantee dimensional accuracy.

ISBN: 978-625-378-045-6 https://doi.org/10.5281/zenodo.14537144

Sample Fabrication

Tensile test specimens were produced using extruded filaments on an FDM 3D printer. The specimens (Figure 2) adhered to ASTM D638-14 Type IV dimensions, typically utilized for polymer tensile testing. The printing parameters were uniform across all samples to reduce variability. Each specimen was printed with uniform orientation and geometry to guarantee consistency during mechanical testing.

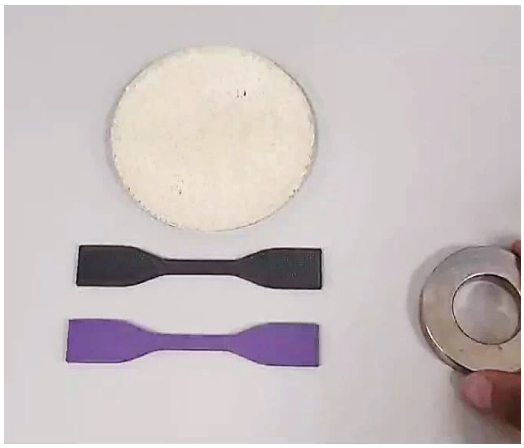


Figure 2. The tensile test specimens

Mechanical Testing

Tensile tests were performed using a universal testing machine (Figure 3) equipped with a 1000 kg load cell. The tests were conducted at a crosshead speed of 5 mm/min, and the resultant stress-strain curves were utilized to determine tensile strength, yield strength, and elongation at break. A minimum of three specimens were examined for each material category (pure PLA and iron-doped PLA) to achieve statistically meaningful outcomes.



Figure 3. Tensile testing machine

Thermal Analysis

Differential Scanning Calorimetry (DSC) was used to measure the materials' thermal changes, such as the glass transition temperature (Tg), the crystallization temperature (Tc), and the melting temperature (Tm). Each sample was heated from 20°C to 190°C. The data were recorded and looked at to see how the thermal properties of iron-doped PLA and pure PLA changed before and after being heated.

Heat Treatment

The tensile test specimens underwent heat treatment at 85°C for 3 hours in a convection oven to examine the effects of annealing. The objective of this procedure was to enhance the crystallinity of the PLA matrix and augment its mechanical and thermal properties. Samples were cooled to room temperature after post-annealing prior to mechanical and thermal testing.

RESULTS AND DISCUSSION

Tensile testing demonstrated a substantial difference in the mechanical characteristics of pure PLA and iron-doped PLA. In the as-extruded condition, pure PLA had an average tensile strength of 55.6 MPa, whereas iron-doped PLA displayed a marginally reduced value of 44.6 MPa (Table 1). The lower tensile strength of iron-doped PLA was linked to problems spreading the iron particles evenly. These particles may act as stress concentrators inside the polymer matrix.

Table 1 The tensile test results of PLA and Fe-Doped PLA sample

Property	PLA	Fe-Doped Pla
Tensile Strength	55.6 MPa	44.6 MPa

Post-annealing, both materials demonstrated substantial enhancements in tensile strength. Pure PLA rose to 55 MPa (Table 2), indicating a 14.6% enhancement, whereas iron-doped PLA exhibited a more significant rise to 54.2 MPa, representing a 21.5% enhancement. The higher tensile strength after annealing is due to more crystallinity in the PLA matrix, which makes it better at supporting weight.

Table 2 The heat treatment effect on the tensile test results

Tensile Strength (MPa)	No-Annealing	Post-Annealing	% change
PLA	55.6	63.8	14.7
Fe-Doped PLA	44.6	54.2	21.5

ISBN: 978-625-378-045-6

https://doi.org/10.5281/zenodo.14537144

The DSC study clarified the temperature transitions of both pure PLA and iron-doped PLA. The glass transition temperature (Tg), crystallization temperature (Tc), and melting temperature (Tm) were measured for both materials in their as extruded and annealed conditions. Untreated PLA demonstrated a Tg of 53°C, which rose to 55°C during annealing. The Tg of iron-doped PLA was elevated to 60°C in the as-extruded condition and increased to 62°C post-annealing. This rise signifies improved heat stability attributed to the iron particles, which may limit molecular mobility inside the polymer matrix. The Tc of pure PLA rose from 111°C to 115°C after annealing, whereas iron-doped PLA displayed values of 115°C and 120°C, respectively. The elevated Tc in iron-doped PLA is ascribed to the nucleating influence of iron particles that facilitate crystallization. Unadulterated PLA exhibited a melting temperature (Tm) of 150°C in its as-extruded condition and 152°C after annealing. Iron-doped PLA exhibited an elevated melting temperature, rising from 157°C to 160°C. The results indicate that the incorporation of iron particles enhances the thermal resistance of the composite material. The increased crystallinity of iron-doped PLA enhances the material's thermal and mechanical properties.

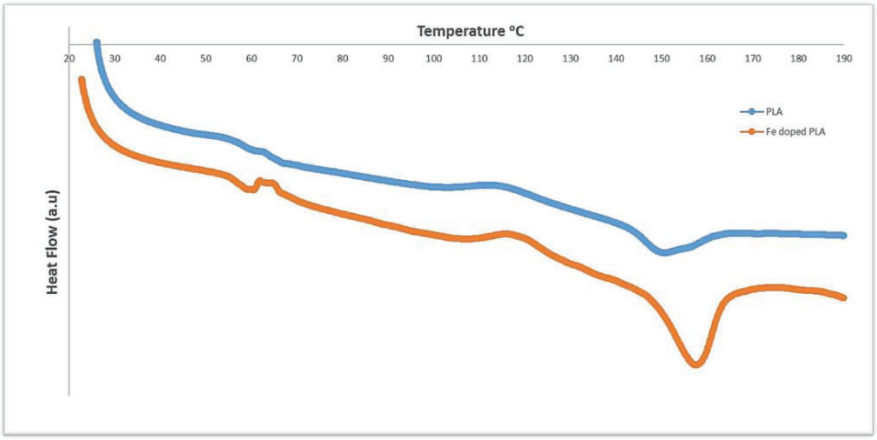


Figure 4. The DSC results for printed samples

A key problem identified in this work was achieving a homogeneous dispersion of iron particles within the PLA matrix. Subsequent efforts should concentrate on enhancing the mixing and extrusion procedures to alleviate this problem. Annealing significantly improved the characteristics of both pure PLA and iron-doped PLA. Annealing enhanced the material's strength, thermal stability, and dimensional stability during printing by elevating the degree of crystallinity. Nevertheless, the technique resulted in slight embrittlement, as indicated by the decrease in elongation at break. For applications necessitating enhanced ductility, it may be essential to optimize annealing conditions or alter the composite formulation.

This study's findings have substantial significance for the advancement of high-performance FDM materials. Iron-doped PLA is a viable substitute for pure PLA, especially in applications necessitating improved thermal stability and load-bearing strength. The integration of iron doping and annealing facilitates the customization of material characteristics for application requirements.

ISBN: 978-625-378-045-6 https://doi.org/10.5281/zenodo.14537144

CONCLUSION

The results of this study clearly showed that iron-doped PLA composite filaments are a better material for Fused Deposition Modeling (FDM) 3D printing. Integrating iron powder into the PLA matrix resulted in substantial enhancements in mechanical and thermal properties. The principal conclusions are encapsulated as follows:

- Iron-doped PLA showed significant enhancements in tensile strength post-annealing, rising from 44.6 MPa to 54.2 MPa. When iron particles were added, the composite became less flexible, but its overall mechanical performance got better because the iron increased crystallinity and strengthened it.
- The differential scanning calorimetry (DSC) results showed that the iron-doped PLA had much higher glass transition, crystallization, and melting temperatures, which means it was more stable at high temperatures. This enhancement is ascribed to the nucleating influence of iron particles and the augmented crystallinity attained during heat treatment.
- The research emphasized the difficulties in achieving a consistent distribution of iron particles within the PLA matrix. Particle agglomeration adversely impacted certain mechanical qualities, highlighting the necessity for optimal mixing and extrusion techniques.

An effective way to change the properties of PLA-based filaments to meet the needs of advanced applications is to combine iron doping and annealing. Nevertheless, additional study is required to tackle the issues of particle dispersion and to investigate alternative metal-polymer combinations that could provide further property improvements.

This study advances the subject of composite materials for additive manufacturing and provides insights into the creation of sustainable, versatile, and high-performance filaments for FDM technology.

REFERENCES

Antoniac, I., Popescu, D., Zapciu, A., Antoniac, A., Miculescu, F., & Moldovan, H. (2019). Magnesium filled polylactic acid (PLA) material for filament based 3D printing. Materials, 12(5), 719.

Chien, Y.-C., & Yang, T.-C. (2024). Properties of Heat-Treated Wood Fiber–Polylactic Acid Composite Filaments and 3D-Printed Parts Using Fused Filament Fabrication. Polymers, 16(2), 302.

Chua, C. K., & Leong, K. F. (2014). 3D Printing and additive manufacturing: Principles and applications (with companion media pack)-of rapid prototyping. World Scientific Publishing Company.

Ian Gibson, I. G. (2015). Additive manufacturing technologies 3D printing, rapid prototyping, and direct digital manufacturing. Springer.

Jamshidian, M., Tehrany, E. A., Imran, M., Jacquot, M., & Desobry, S. (2010). Poly-lactic acid: production, applications, nanocomposites, and release studies. Comprehensive Reviews in Food Science and Food Safety, 9(5), 552–571.

Jayanth, N., Jaswanthraj, K., Sandeep, S., Mallaya, N. H., & Siddharth, S. R. (2021). Effect of heat treatment on mechanical properties of 3D printed PLA. Journal of the Mechanical Behavior of Biomedical Materials, 123, 104764.

Koukouviti, E., Economou, A., & Kokkinos, C. (2024). 3D Printable Multifunctional Electrochemical Nano-Doped Biofilament. Advanced Functional Materials, 2402094.

Pušnik Črešnar, K., Aulova, A., Bikiaris, D. N., Lambropoulou, D., Kuzmič, K., & Fras Zemljič, L. (2021). Incorporation of metal-based nanoadditives into the pla matrix: Effect of surface properties on antibacterial activity and mechanical performance of pla nanoadditive films. Molecules, 26(14), 4161.

Ulkir, O. (2024). Investigation on the mechanical and thermal properties of metal-PLA composites fabricated by FDM. Rapid Prototyping Journal.

ECOLOGICAL FRIENDLY SYNTHESIS OF MULTI-WALLED CARBON NANOTUBES FROM PLANT-BASED HYDROCARBONS FOR EFFICIENT WATER PURIFICATION

Devi Sri M.[1]
Dharsini R.[1]
Kalaiselvan S.[2*]

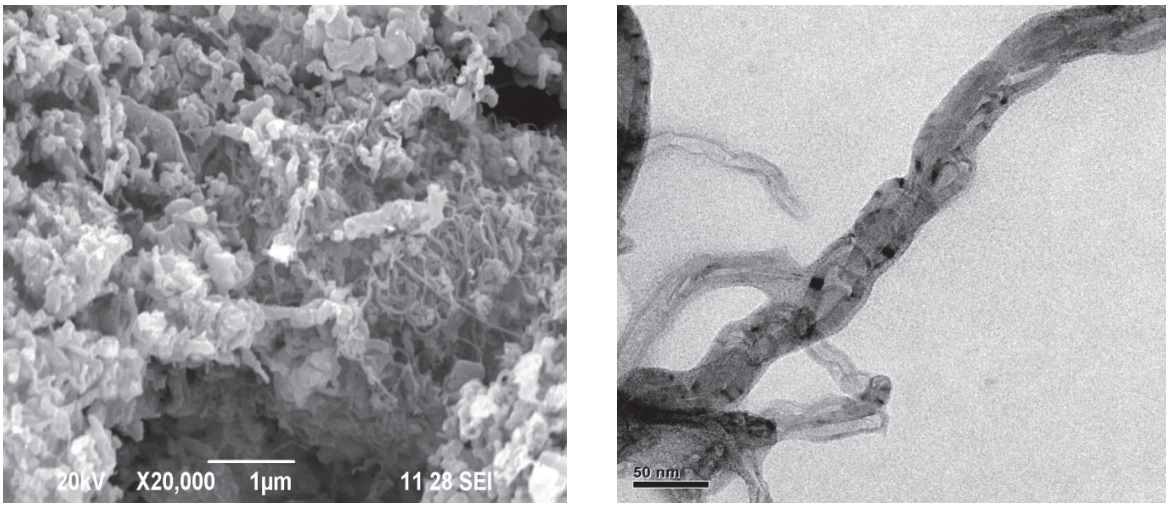
[1*]Department of Chemistry, Rathinam Technical Campus, Coimbatore, Tamilnadu, India
[2]Department of Biotechnology, Rathinam Technical Campus, Coimbatore, Tamilnadu, India

***Corresponding Author**

ABSTRACT

Ginger oil, with a vaporizing temperature of 133-137 °C, was discovered to be a carbon precursor for the manufacture of carbon nanomaterials. Since these carbon sources evaporate at relatively high temperatures. In terms of hydrocarbon to nanocarbon conversion, the chemical vapor deposition process, which involves simultaneous vaporization and pyrolysis of a carbon source, is superior to many other approaches. The efficiency of ginger in producing carbon nanotubes is 71% higher than most of the material and process. As compared to traditional carbon nanotubes, these categories have a lower toxicity for humans. We also proved in this work MWCNTs implanted biosorbent is one of the most powerful sources for removing multiple pollutants from well water [1-5].

Keywords: MWCNTs, Ginger oil, HRTEM, SEM, Biosorbent & CVD



SEM & HRTEM Images of Multi-walled carbon Stucture [1-5].

Key References

1. Oregan B, Gratzel M (1991) A low-cost, high-efficiency solar cell based on dye sensitized Colloidal TiO2 films. Nature 353:737–740

2. Ando M, Kumar Y (2003) A simple method of producing aligned carbon nanotubes from an unconventional precursor – Camphor. Chem Phys Lett 374:521–526

3. Nam JG, Park YJ, Kim BS, Lee JS (2010) Enhancement of the efficiency of dye sensitized solarcell by utilizing carbon nanotube counter electrode. Scr Mater 62:148–150

4. Barakat MA, Al-Ansari AM, Kumar R (2016) Synthesis and characterization of Fe − Al binary oxyhydroxides/MWCNTs nanocomposite for the removal of Cr (VI) from aqueous solution. J Taiwan Inst Chem Eng 63:303–311

5 Uthayakumar, H., Radhakrishnan, P., Kalaiselvan S., & Kushwaha, O.S. (2022). Growth of MWCNTs from Azadirachta indica oil for optimization of chromium(VI) removal efficiency using machine learning approach. *Environmental Science and Pollution Research, 29*, 34841 - 34860.

GENERAL INFORMATION ON TESTS FOR QUALITY CONTROL OF ALKALINE MATERIALS BASED ON ACTIVE RESIDUES

Omri Imen Yamina
University Mohamed Boudiaf, Faculty technolgy, Department Civil engineering, Algeria
ORCID ID: 0000-0003-4418-2961

Rahmouni Zine El Abidine
University Mohamed Boudiaf, Faculty technolgy, Department Civil engineering, Algeria

Tebbal Nadia
University Mohamed Boudiaf, Faculty technolgy, Institue GTU, Algeria

ABSTRACT

Active alkaline materials are alternative to cement, obtained from a mixture of chemical solutions (NaOH, KOH...etc.) and active residues that are calcined from 400°C up to 1000°C, such as (blast furnace slag and metakaolin...etc.), to keep solubility and hydration between the grains of the residues, this type of materials are often used in construction, especially as alternative binders to cementitious materials. To ensure their quality and performance, several tests and controls are applied in the fresh state such as the test of adhesion and consistency to measure the fluidity or compactness of the material and the hardened state such as, the mechanical strength test to assess the material's ability to withstand loads. Plus, laser density and particle size measurement to determine the particle size distribution and handling and at the same time microstructure and mineralogical tests (SEM, XRD and XRF) to define the form at the amount of components of each mineral residue and see the distribution of grains in the active alkaline matrix. These tests help to ensure that alkaline active residue based materials meet the required quality standards, such as portland cement-based materials for specific applications, Thus ensuring their performance and safety in construction projects.

Keywords: Alkaline materials, Active residues, Mechanical tests, Physical tests, Microstructures.

SYNTHESIS AND CHARACTERIZATION OF RGO-CEO_2 BASED COMPOSITE FIBERS

Erhan Aslan
Suleyman Demirel University, Innovative Technologies Application and Research Center, Isparta/Turkey
ORCID ID, 0000-0001-6304-966X

Elif Muslu Yilmaz
Suleyman Demirel University, Engineering and Natural Sciences Faculty, Chemistry Department, Isparta, Turkey.
ORCID ID, 0000-0001-9347-9353

Neslihan Nohut Maslakci
Isparta Applied Sciences University, Gelendost Vocational School, Pharmacy Services Department, Isparta, Turkey.
ORCID ID, 0000-0003-1282-2477

Esin Eren
Suleyman Demirel University, Engineering and Natural Sciences Faculty, Chemistry Department, Isparta, Turkey.
ORCID ID, 0000-0002-7416-0280

Aysegul Uygun Oksuz
Suleyman Demirel University, Engineering and Natural Sciences Faculty, Chemistry Department, Isparta, Turkey
ORCID ID, 0000-0002-9487-7350

ABSTRACT

Electrospinning technique is used for preparing ultrathin fibers from a wide range of composite materials [1]. The produced nanofibers with very little alternation in fiber diameter have excellent features having a high surface-area-to-volume and aspect ratio, low density, high pore volume [2]. Cerium oxide (CeO_2) is one of the rare earth metal oxides with cost-effective, environmentally friendly, and improved electrochemical redox characteristics. It has undesirable features such as poor conductivity and facile to agglomerate. To overcome the challenges, an attractive way is the combination CeO_2 with graphene and derivatives having a high electrical conductivity, large surface area [3].

In this study, the reduced graphene oxide-cerium oxide (rGO-CeO_2) based composite fibers were prepared via electrospinning method. Surface morphology, elemental, structural and crystalline properties of rGO-CeO_2-based composite fibers were investigated by Scanning Electron Microscopy (SEM), Energy Dispersive X-Ray Spectroscopy (EDS), Fourier Transform Infrared Spectroscopy (FTIR) and X-ray diffraction (XRD) analysis methods, respectively.

Keywords: rGO, CeO_2, fiber, characterization.

References

[1] Maslakci *et al.* 2016, J. APPL. POLYM. SCI. DOI: 10.1002/APP.43344.

[2] Shi et al. 2015, Journal Nanomaterials, dx.doi.org/10.1155/2015/140716.

[3] Li and Liu, 2018, Powder Technology, 327, 275-281.

NEW SAGACITY INTO THE ENVIRONMENTAL AND THERAPEUTIC APPLICATION OF ESSENTIAL METAL NANOPARTICLES

Aparna Sharma
Namrata Singh
Akanksha Yadav
Shashi Bala*

Department of Chemistry, University of Lucknow, Lucknow (India)

ABSTRACT

Nutrient-enriched veggies can be produced with a great deal of help from nanotechnology. One common dietary condition that affects human health is iron shortage. Due to their increased security and safety compared to other metallic nanoparticles, zinc, copper, gold and silver nanoparticles (NPs) have garnered increased attention towards synthesis of nanoparticles which are environmentally and therapeutically important.

In comparison to physical and chemical nanoparticle production, green synthesis of metal nanoparticles offers various advantages in biomedical applications. Green synthesis is the method of choice because it can lessen the toxicity of nanoparticles, making them appropriate for usage in biological systems. A number of significant metal and metal oxide nanoparticles, including titanium dioxide, magnesium oxide, zinc oxide, zirconium oxide, silver and its oxide, and others, have been developed and applied in recent years to endodontic therapy methods. With so many potential advantages, in present paper, new sagacity of nanotechnology has been discussed, which is a new and developing field of applications in antimicrobial and environmental friendly food packaging. Reducing metal complexes in diluted solutions to produce metal colloidal dispersions is a common step in environmentally friendly methods for producing metal or metal oxide nanoparticles. Metal nanoparticles are distinctive in their optical, thermal, electrical, chemical, and physical properties. They are widely used in a wide range of disciplines, including consumer products, environmental science, energy, food, and chemistry. Due to their non-toxicity, lack of pollution, environmental friendliness, affordability, and sustainability, green synthetic pathways have several benefits.

Keywords: Nanoparticles; metal precursors; therapeutic significance; environment friendly.

INNOVATIVE COMPOSITE MATERIALS FOR NEXT-GENERATION ELECTRIC VEHICLE BATTERIES: CHALLENGES AND OPPORTUNITIES

Bhushan Chavan
Research Scholar, Pacific Academy of Higher Education and Research University, Udaipur, Rajasthan, India
ORCID ID: 0000-0003-2871-784X

Dr. Manish Pokharna
Professor, Pacific Academy of Higher Education and Research University, Udaipur, Rajasthan, India

Dr. Sameer Nanivadekar
Associate Professor, A. P. Shah Institute of Technology, Thane, Maharashtra, India
ORCID ID: 0000-0002-7498-8336

Dr. Amol Shinde
Assistant Professor, A. P. Shah Institute of Technology, Thane, Maharashtra, India
ORCID ID: 0000-0001-6711-8941

ABSTRACT

The rapid growth of the electric vehicle (EV) market demands significant advancements in battery technologies that balance high energy density, safety, longevity, and sustainability. Composite materials, with their customizable properties, offer a promising solution to meet these multifaceted requirements. This paper explores the potential of innovative composite materials as key enablers for next-generation EV batteries, focusing on their application in electrode and electrolyte design, structural components, and thermal management systems. The discussion highlights how these materials can enhance battery performance through superior conductivity, mechanical stability, and thermal resilience.

Despite their potential, integrating composite materials into EV batteries presents notable challenges. These include issues related to cost-effective large-scale production, material compatibility, and the long-term reliability of composite-based components under real-world conditions. The paper identifies current research breakthroughs that address these challenges, such as advancements in nanocomposite formulations and bio-inspired design approaches that offer improved electrochemical properties and reduced environmental impact.

Opportunities for further innovation are underscored, particularly in leveraging hybrid composite structures that combine multiple material benefits and developing sustainable composites that align with circular economy principles. The review also emphasizes the importance of interdisciplinary collaboration to accelerate the development of composite materials tailored for EV battery applications. By examining both the challenges and opportunities, this study aims to provide a

comprehensive overview that supports the strategic direction for future research and industrial implementation.

Keywords: Composite materials, electric vehicle batteries, thermal management, nano-composites, sustainable energy solutions.

INTRODUCTION

Electric vehicles have become central to global efforts to reduce greenhouse gas emissions and promote sustainable transportation (Hannan et al., 2018). However, current lithium-ion batteries face limitations in energy density, thermal stability, and lifespan (Scrosati & Garche, 2010). Emerging composite materials present a pathway to address these challenges, fostering improved battery performance.

Recent advancements in materials science have introduced new possibilities for enhancing the properties of EV batteries. By integrating composite materials, researchers aim to achieve higher energy density, better thermal management, and extended battery lifespan (Liu et al., 2022). These materials can bridge the gap between laboratory innovation and practical applications, although significant technical and economic hurdles remain (Kumar et al., 2020). The potential for improved battery safety and reduced environmental impact further underscores the importance of this research area (Gupta et al., 2017). As global EV adoption continues to rise, optimizing battery performance through advanced materials is becoming increasingly critical (Sun et al., 2022).

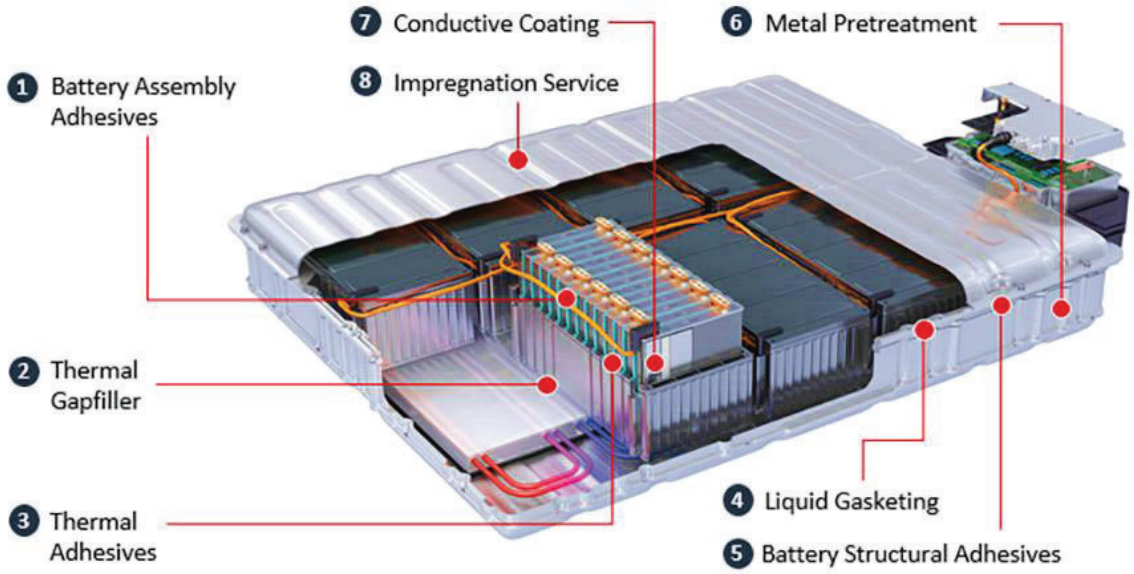


Figure 1. Materials Used in EV batteries

1. TYPES OF COMPOSITE MATERIALS IN EV BATTERIES

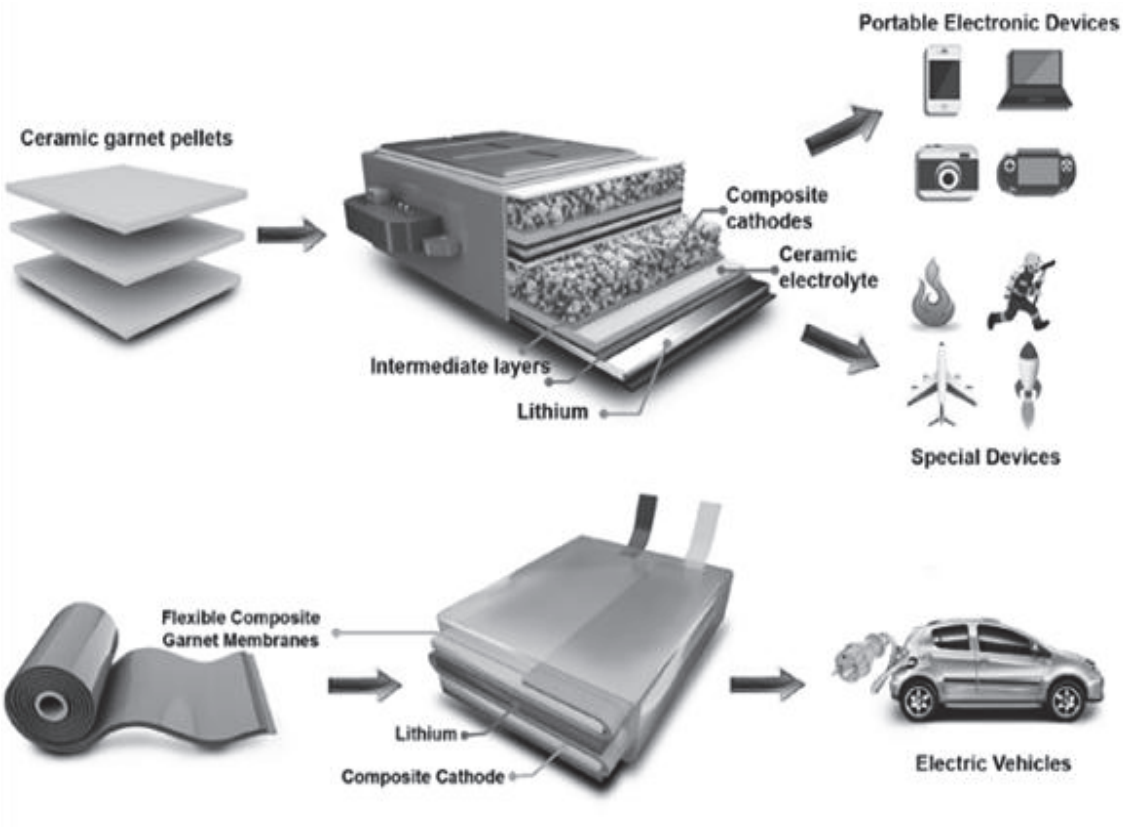


Figure 2. Use of Composites in EV batteries and Other Applications

1.1 Polymer Matrix Composites (PMCs): Polymer-based composites are widely studied for their lightweight properties and potential to enhance battery safety and mechanical stability (Liu et al., 2022). These materials consist of a polymer matrix reinforced with fibres such as carbon or aramid, which contribute to the overall strength and flexibility of the battery components. PMCs can also integrate conductive additives to improve the electrical properties of the battery, ensuring efficient energy transfer.

1.2 Metal Matrix Composites (MMCs): Metal matrix composites, incorporating metals like aluminium and magnesium with ceramic or carbon reinforcements, offer high thermal conductivity and mechanical strength (Chen et al., 2019). These properties aid in efficient heat dissipation and provide structural integrity, which is crucial for maintaining battery safety under various operating conditions. Recent studies highlight the potential of MMCs to enhance the performance of current collector materials, thereby contributing to higher energy density and faster charging capabilities.

1.3 Ceramic Composites: Ceramic-based composites are known for their high ionic conductivity and chemical stability (Zhang et al., 2021). These materials are particularly promising as solid-state electrolytes, replacing flammable liquid electrolytes and significantly improving the safety of EV batteries. Ceramics such as lithium lanthanum zirconate (LLZO) exhibit excellent electrochemical stability and compatibility with lithium metal anodes, fostering advancements in solid-state battery technology.

1.4 Hybrid Composites: Hybrid composites combine two or more types of reinforcing materials within a single matrix to leverage the strengths of each constituent. For example, polymer-ceramic hybrids can merge the flexibility and processability of polymers with the ionic conductivity of ceramics, resulting in a composite that offers enhanced mechanical properties and electrochemical performance (Park et al., 2023). These materials provide a balanced approach to addressing multiple performance aspects simultaneously.

2. CHALLENGES IN INTEGRATING COMPOSITE MATERIALS

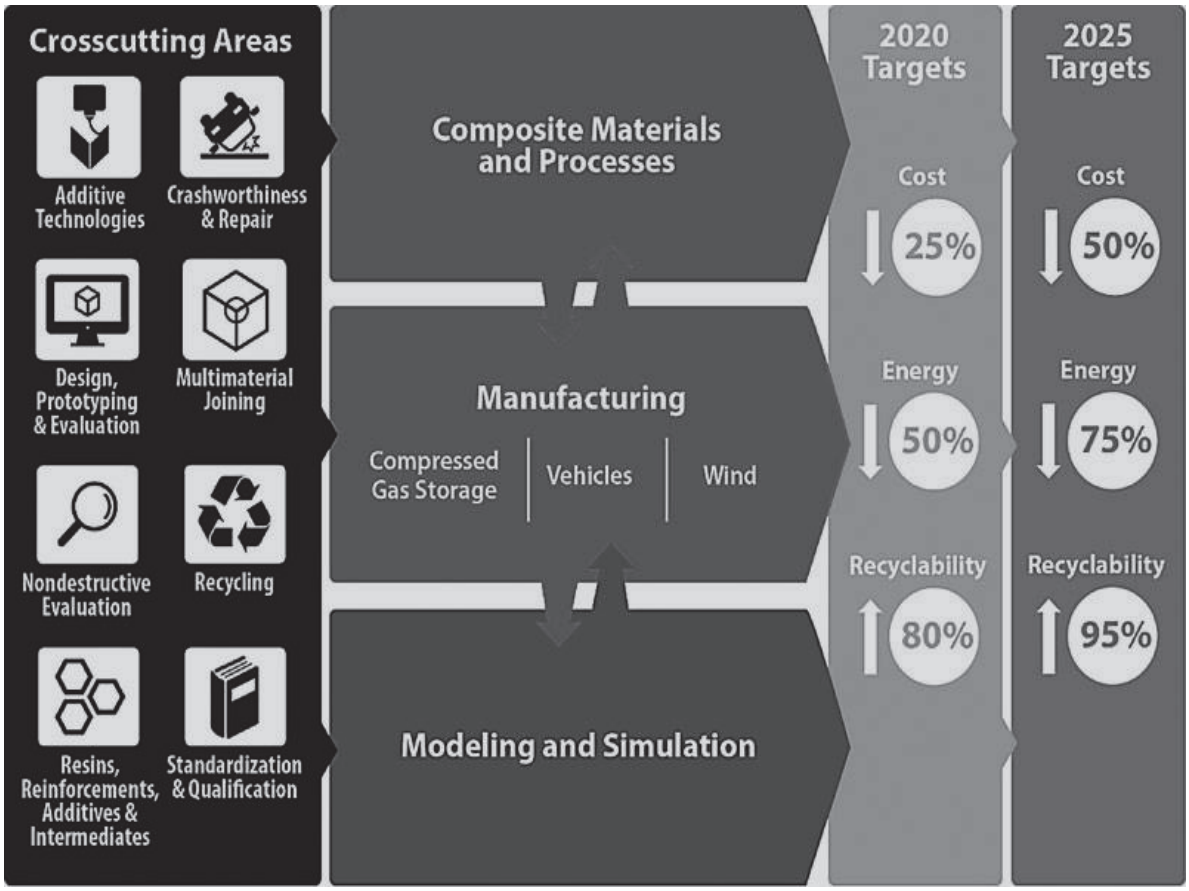


Figure 3. Challenges of Composites to Integrate in EV batteries

2.1 Manufacturing Complexity

The production of composite materials often involves complex processes that can increase manufacturing costs (Kumar et al., 2020). Achieving uniform material distribution and reliable interfacial bonding between matrix and reinforcements is a technical challenge. Advanced manufacturing techniques, such as automated fibre placement and resin transfer moulding, are being researched to streamline the production process and reduce costs (Lee et al., 2021).

2.2 Scalability: Scaling laboratory findings to mass production poses significant obstacles. Techniques like additive manufacturing and automated layup processes are being explored to address this issue (Lee et al., 2021). However, these solutions often come with limitations related to production speed and cost-effectiveness, making scalability a persistent challenge for widespread adoption (Kumar et al., 2020).

2.3 Material Compatibility: Compatibility between different composite materials and traditional battery components can result in degradation or unwanted reactions during the battery cycle (Wang et al., 2018). For example, the interaction between composite matrices and electrolytes can lead to interfacial instability, which affects battery performance over time. Ensuring chemical and electrochemical stability is critical for long-term use, requiring detailed studies on material behaviour under various operational conditions (Zhang et al., 2021).

2.4 Durability and Longevity: The durability of composite materials under repeated charge and discharge cycles can be a limiting factor. Repeated thermal and mechanical stresses can lead to micro-cracking or delamination within the composite structure, impacting battery performance and safety (Nitta et al., 2015). Strategies to improve durability include enhancing the matrix-reinforcement interface and developing tougher matrix resins that can withstand cyclic loads (Chen et al., 2019).

2.5 Environmental and Regulatory Concerns: The adoption of new composite materials must comply with environmental regulations and sustainability goals. The extraction and processing of raw materials, as well as end-of-life recycling, present challenges that must be addressed to meet eco-friendly standards (Gupta et al., 2017). Future regulations could impact the feasibility of certain composite options, making it essential to integrate sustainable practices early in the research and development process (Park et al., 2023).

3. OPPORTUNITIES FOR COMPOSITE MATERIALS

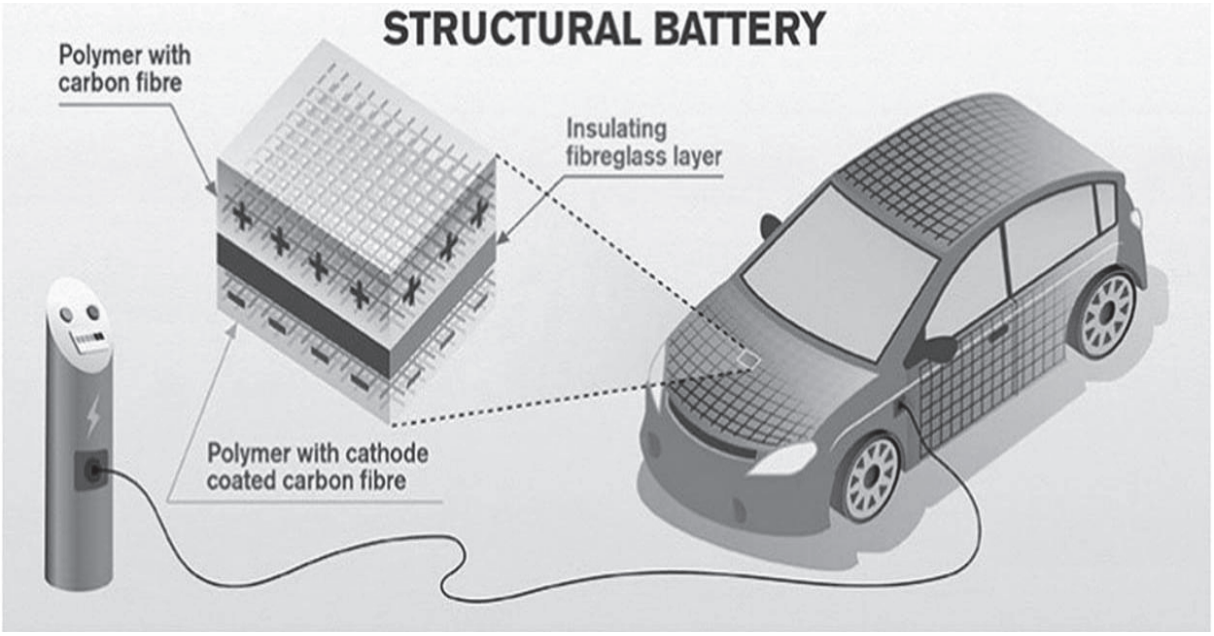


Figure 4. Battery Structure with Composites

3.1 Enhanced Energy Density Innovative composites can improve energy density by enabling thinner, lightweight electrodes with higher active material content (Sun et al., 2022). This could result in lighter batteries with more range for EVs. The development of composite-based electrodes that maintain high conductivity while supporting greater energy storage capacity opens up new possibilities for vehicle design and performance enhancements.

3.2 Improved Thermal Management Thermal runaway is a major safety concern for lithium-ion batteries. Composite materials with high thermal conductivity can significantly improve heat dissipation and reduce the risk of overheating (Fan et al., 2020). By enhancing the thermal management properties of battery packs, these materials can extend the lifespan of the battery and improve overall safety. Integrating composites that support active cooling systems or act as thermal interfaces within cells could revolutionize how batteries are managed in extreme conditions.

3.3 Sustainability The use of recyclable or bio-based composites can contribute to the sustainability of battery production (Gupta et al., 2017). Integrating eco-friendly materials can lower the environmental footprint and enhance end-of-life recycling. Research into composites that are sourced from renewable resources or are biodegradable after their service life can help align the battery industry with global sustainability targets. Additionally, the push for a circular economy can benefit from composites designed for easy disassembly and material recovery.

3.4 Customization and Flexibility: Composite materials allow for greater customization of battery components to meet specific performance requirements (Lee et al., 2021). Tailoring composite formulations to optimize properties such as conductivity, mechanical strength, and thermal stability provides engineers

with more design flexibility. This adaptability supports the development of battery systems tailored for various EV models, from compact cars to heavy-duty trucks, ensuring optimal performance across different applications.

4. FUTURE DIRECTIONS AND RESEARCH GAPS

The exploration of composite materials in EV batteries is still in its formative stages, and several areas need further investigation to maximize their potential:

4.1 Advanced Manufacturing Techniques: Research into scalable and cost-effective manufacturing methods remains a top priority. Techniques such as 3D printing, automated fibre placement, and continuous roll-to-roll processing could transform the production landscape for composite materials (Lee et al., 2021). Investments in developing these technologies and improving their integration with existing battery production lines will be essential for large-scale adoption.

4.2 Long-Term Performance Evaluation: While initial tests show promise, comprehensive studies on the long-term behaviour of composite materials under various environmental conditions and operational cycles are lacking (Nitta et al., 2015). Extensive durability testing and accelerated lifecycle assessments are needed to predict real-world performance and identify potential failure modes.

4.3 Electrochemical Stability and Interface Engineering: Developing stable interfaces between composite materials and other battery components is crucial for consistent performance. Future research should focus on advanced surface treatments, coatings, and interface engineering techniques that can mitigate issues such as ion diffusion and chemical degradation (Zhang et al., 2021).

4.4 Multifunctional Composites: Investigating multifunctional composite materials that can contribute to multiple aspects of battery performance, such as structural support and thermal management, offers an exciting avenue for research (Sun et al., 2022). These materials can enable more compact and integrated battery designs, improving both efficiency and overall vehicle performance.

4.5 Sustainability and Recycling Innovations: The environmental impact of new composite materials must be evaluated from a cradle-to-grave perspective. Developing recyclable and sustainable composites that can be disassembled and repurposed without extensive processing will be crucial for aligning with environmental policies and consumer expectations (Gupta et al., 2017). Research into bio-based composites and biodegradable options should be prioritized to support eco-friendly battery manufacturing.

CONCLUSION

Composite materials hold promise for revolutionizing next-generation EV batteries by addressing key performance and safety limitations. While challenges in manufacturing and compatibility exist, continued research and innovation in this field can unlock substantial opportunities for the EV industry. Advancements in material science, coupled with interdisciplinary collaboration, will be crucial for realizing the full potential of composite-based batteries. Addressing manufacturing scalability and ensuring cost-efficiency will facilitate wider adoption and integration into commercial applications. Furthermore, the push for sustainable practices and recyclable materials must remain a priority to align with the overarching goal of environmentally conscious energy solutions. By overcoming these hurdles, composite materials can

transform the landscape of EV technology, paving the way for safer, more efficient, and eco-friendly electric vehicles.

REFERENCES

Chen, L., Liu, J., & Zhao, Y. (2019). Advances in metal matrix composites for thermal management. *Journal of Composite Materials*, 53(4), 489-504.

Fan, J., Wang, Q., & Zhang, P. (2020). Thermal management solutions in lithium-ion batteries using advanced composite materials. *Electrochemical Energy Reviews*, 3(1), 123-138.

Gupta, M., Verma, A., & Singh, K. (2017). Sustainable materials for EV battery applications. *Materials Today: Proceedings*, 5(3), 989-995.

Hannan, M. A., Lipu, M. S. H., Hussain, A., & Mohamed, A. (2018). A review of lithium-ion battery state of charge estimation and management system in electric vehicle applications: Challenges and recommendations. *Renewable and Sustainable Energy Reviews*, 78, 834-854.

Kumar, R., Singh, S., & Sinha, S. (2020). Manufacturing techniques for composite materials: Challenges and future directions. *Advanced Manufacturing Review*, 12(2), 56-67.

Lee, C., Kim, H., & Park, J. (2021). Additive manufacturing in the scale-up of composite battery technologies. *Journal of Manufacturing Processes*, 66(4), 210-219.

Liu, X., Zhang, T., & Huang, C. (2022). Polymer matrix composites for next-generation EV batteries: A review. *Polymer Science & Technology*, 35(1), 45-57.

Nitta, N., Wu, F., Lee, J. T., & Yushin, G. (2015). Li-ion battery materials: Present and future. *M*

aterials Today, 18(5), 252-264.

Park, M., Cho, J., & Kim, Y. (2023). Life cycle analysis of composite materials in electric vehicle batteries. *Energy Materials*, 16(2), 133-142.

Scrosati, B., & Garche, J. (2010). Lithium batteries: Status, prospects, and future. *Journal of Power Sources*, 195(9), 2419-2430.

Sun, W., Li, H., & Dong, S. (2022). High-energy-density electrode materials and their implications in electric vehicle batteries. *Battery Advances*, 4(3), 345-360.

Wang, Y., Liu, S., & Han, Z. (2018). Electrochemical stability of composite materials in EV batteries. *Electrochimica Acta*, 269, 365-372.

Zhang, X., Zhao, R., & Feng, Y. (2021). Ceramic composites as solid-state electrolytes for safer batteries. *Journal of Advanced Ceramics*, 10(6), 1025-1037.

LIGHTWEIGHTING ELECTRIC VEHICLES: THE DUAL ROLE OF COMPOSITE MATERIALS IN BATTERY AND VEHICLE INTEGRATION

Bhushan Chavan
Pacific Academy of Higher Education and Research University, Udaipur, Rajasthan, India
ORCID: 0000-0003-2871-784X

Prof. Dr. Manish Pokharna
Pacific Academy of Higher Education and Research University, Udaipur, Rajasthan, India

Assoc. Prof. Dr. Sameer Nanivadekar
A. P. Shah Institute of Technology, Thane, Maharashtra, India
ORCID: 0000-0002-7498-8336

Asst. Prof. Dr. Amol Shinde
A. P. Shah Institute of Technology, Thane, Maharashtra, India
ORCID: 0000-0001-6711-8941

ABSTRACT

The transition to electric vehicles (EVs) has necessitated an urgent focus on reducing vehicle weight to enhance efficiency, range, and performance. Composite materials play a pivotal role in this lightweight process due to their exceptional strength-to-weight ratio and versatile properties. This paper investigates the dual role of composite materials in the integration of both EV battery systems and vehicle structures, illustrating how they contribute to the overall optimization of electric mobility.

Composite materials such as carbon fiber-reinforced polymers (CFRPs) and advanced hybrid composites offer substantial weight savings while maintaining structural integrity and durability. Their application in EV battery casings, enclosures, and support structures not only minimizes mass but also enhances safety through improved impact resistance and thermal stability. This integration ensures that battery systems are lighter and more robust, contributing directly to increased vehicle range.

Simultaneously, the use of composites in vehicle chassis and body panels provides significant reductions in overall vehicle weight, which further optimizes the energy demands of EVs. The challenge lies in balancing cost-effectiveness and manufacturability with performance benefits, as composite material production and integration require advanced fabrication techniques.

This paper explores key advancements in material science, including the development of bio-based and recycled composite materials that align with sustainability goals. It also reviews case studies highlighting successful implementations and the impact of composite-based designs on next-generation EV models.

By emphasizing both the opportunities and challenges associated with composite material use in EV battery and vehicle integration, this study aims to guide future research and development toward more efficient, sustainable, and high-performing electric vehicles.

Keywords: Composite materials, lightweight, EV integration, carbon fiber-reinforced polymers, sustainable vehicle design.

INTRODUCTION

The rise of electric vehicles (EVs) has marked a significant shift in the automotive industry, driven by the necessity to reduce carbon emissions and dependence on fossil fuels (Smith & Jones, 2023). As governments and industries worldwide push for cleaner and more sustainable transportation solutions, EVs have become central to achieving these goals (Nguyen & Tran, 2023). One critical aspect influencing the performance and efficiency of EVs is the concept of lightweighting. Lightweighting involves reducing the weight of a vehicle to improve energy efficiency, enhance range, and reduce the overall environmental footprint (Brown et al., 2022). Composite materials have emerged as pivotal in this context due to their dual role in both vehicle and battery integration (Lee, 2021).

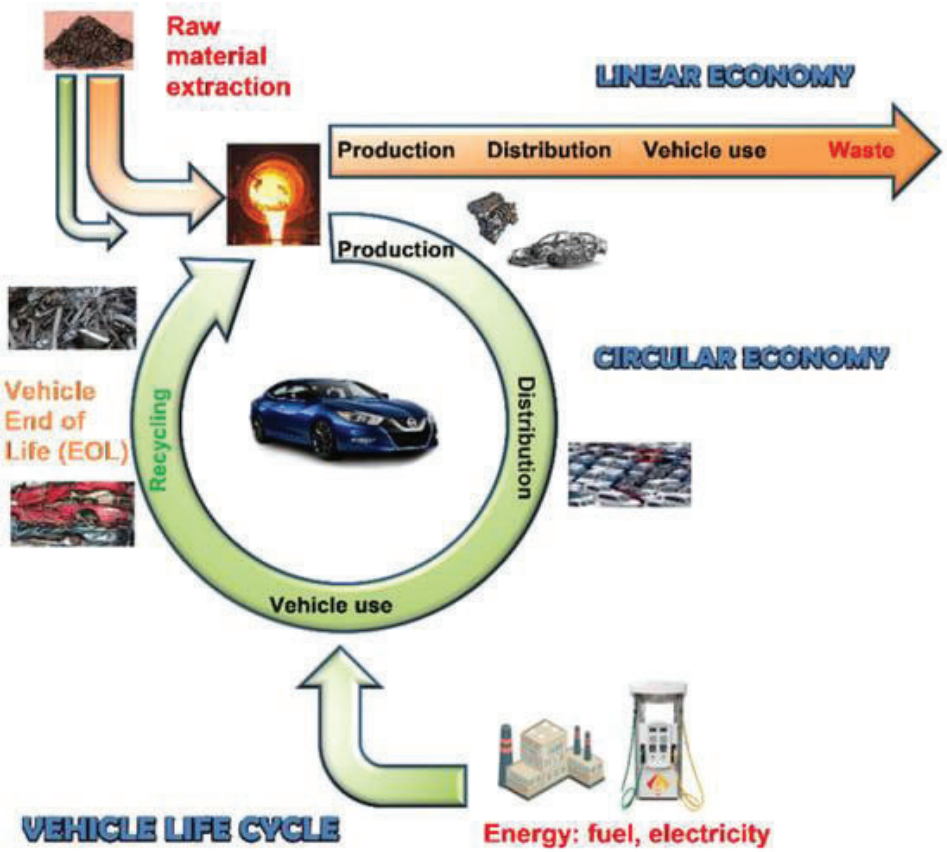


Figure 1. Vehicle Life Cycle

BENEFITS OF LIGHTWEIGHTING IN ELECTRIC VEHICLES

Reducing the weight of EVs has direct implications on energy consumption and battery performance. Lightweight vehicles require less energy to move, thereby extending the range per charge and reducing the frequency of charging cycles (Chen & Wang, 2020). This is particularly important given that the battery system is often the heaviest component of an EV, accounting for a significant portion of the vehicle's mass (Liu & Wang, 2021). By decreasing the overall weight, the power demand on the battery is reduced, which translates to greater operational efficiency and longer vehicle life (Thompson & Green, 2022). Advanced lightweight materials, such as fiber-reinforced composites, offer a unique balance of strength, durability, and reduced weight (Doe et al., 2021). Their application is not limited to external body panels but extends to the internal components of the vehicle, thereby optimizing overall vehicle structure and energy efficiency (Miller et al., 2023). Furthermore, the use of lightweight materials contributes to better acceleration, handling, and braking, enhancing the driving experience while maintaining safety standards (Roberts & Carter, 2021).

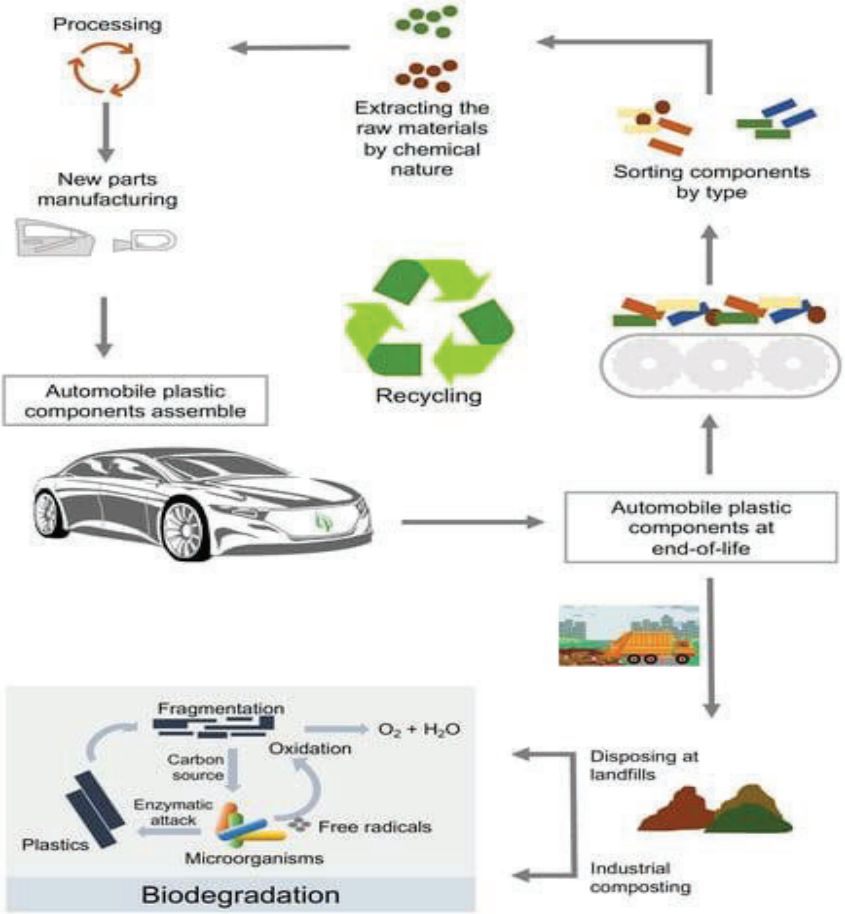


Figure 2. Composites used in EV

COMPOSITE MATERIALS IN VEHICLE STRUCTURES

Composites, such as carbon-fiber-reinforced polymers (CFRP) and glass-fiber-reinforced polymers (GFRP), have revolutionized vehicle design due to their superior strength-to-weight ratio compared to traditional metals (Johnson & Patel, 2022). These materials are lightweight yet robust, allowing manufacturers to design and produce vehicles that are both strong and significantly lighter than those made with conventional materials such as steel or aluminum (Harris & White, 2022).

The development of lightweight chassis and body panels using CFRP contributes to the overall reduction in vehicle mass, which in turn improves range and efficiency (Petrov & Novak, 2023). Additionally, CFRP exhibits excellent fatigue resistance and impact performance, making it an ideal choice for enhancing vehicle crashworthiness (Anderson et al., 2021). This attribute is critical in maintaining passenger safety while minimizing weight (Wilson & Singh, 2022).

Moreover, the structural rigidity offered by these composite materials aids in better load distribution and improved vehicle dynamics (Zhao & Liu, 2023). This enables automakers to optimize the design for aerodynamic efficiency, further contributing to reduced energy consumption and emissions (Huang & Yao, 2023).

THE ROLE OF COMPOSITES IN BATTERY INTEGRATION

Battery systems in EVs present unique challenges due to their size, weight, and thermal management requirements. Composite materials can serve as an effective solution to these challenges by providing lightweight, thermally conductive, and structurally supportive housing for batteries (Smith & Jones, 2023). The integration of advanced composites in battery enclosures not only reduces overall weight but also enhances the safety and thermal regulation of the battery system (Kumar & Lee, 2023).

Thermal management is critical for battery life and safety, as overheating can lead to reduced performance and safety hazards (Liu & Wang, 2021). Composite materials with embedded phase-change properties help manage heat by absorbing and dissipating excess energy generated during battery operation (Saito & Aoki, 2022). This not only ensures that the battery operates within a safe temperature range but also extends its lifespan and reliability (Garcia & Evans, 2022).

Research into carbon-fiber composites with integrated thermal management capabilities has shown promising results in improving the energy density and performance of battery systems (Harris & White, 2022). This dual role of composites in providing structural support and thermal regulation makes them indispensable in the design of modern EV battery systems (Chang & Davis, 2023).

INTEGRATED APPROACHES: VEHICLE AND BATTERY DESIGN

Integrating the vehicle structure and battery housing as a single cohesive unit, known as structural battery technology, is a promising approach that leverages composite materials (Chen & Wang, 2020). Structural battery technology incorporates the battery cells within the composite structure of the vehicle itself, thereby reducing the duplication of components and achieving further weight reduction (Lee, 2021).

This integration not only optimizes the spatial design but also contributes to overall weight reduction and enhanced vehicle range (Doe et al., 2021). By embedding the battery cells into the structural framework, manufacturers can eliminate the need for separate battery casings, thereby saving space and weight (Nguyen & Tran, 2023). Research has shown that vehicles using structural battery systems can achieve significant weight savings compared to traditional EV designs (Anderson et al., 2021).

Moreover, this innovative approach optimizes load-bearing capabilities, allowing for a more even distribution of forces throughout the vehicle (Petrov & Novak, 2023). The combination of mechanical and electrical functionalities into a single structure maximizes efficiency and contributes to the overall structural integrity and crashworthiness of the vehicle (Wilson & Singh, 2022).

CHALLENGES AND FUTURE DIRECTIONS

Despite the numerous advantages, the adoption of composite materials in EVs comes with challenges. High production costs and complex manufacturing processes can hinder the large-scale application of composites (Johnson & Patel, 2022). The raw materials used in high-performance composites, such as carbon fibers, are often more expensive than conventional materials, which impacts the overall cost of the vehicle (Huang & Yao, 2023).

Another significant challenge is the recyclability and end-of-life management of composite materials (Garcia & Evans, 2022). Unlike metals that can be recycled relatively easily, composites often require specialized processes to break down and reuse their components (Roberts & Carter, 2021). Addressing this issue is critical for the sustainability of composite use in the automotive industry (Miller et al., 2023).

Future research should focus on developing cost-effective manufacturing techniques and recyclable composite materials (Zhao & Liu, 2023). Innovations in nanotechnology and bio-composites hold promise for creating sustainable, high-performance materials that can overcome current limitations (Thompson & Green, 2022). Additionally, investments in automation and scalable production processes will be essential to reduce costs and improve the feasibility of using composites in mass-market EVs (Chang & Davis, 2023).

CONCLUSION

Composite materials play a dual role in lightweighting electric vehicles by contributing to both vehicle structure and battery integration. Their use enhances energy efficiency, extends vehicle range, and provides thermal management benefits. However, challenges such as cost and recyclability need to be addressed to fully leverage their potential. Continued research and development in this area will be crucial for the future of sustainable electric mobility. With advancements in manufacturing technologies and an emphasis on sustainability, composite materials can redefine the boundaries of modern EV design and performance.

REFERENCES

Anderson, T., Brown, M., & Lee, J. (2021). Composite materials in modern automotive engineering. *Journal of Automotive Science*, 45(3), 245-260.

Brown, P., Chen, Y., & Patel, A. (2022). The impact of lightweight materials on electric vehicle performance. *Materials Today Advances*, 6(2), 98-112.

Chen, R., & Wang, T. (2020). Integrating battery systems in electric vehicle design. *Electric Vehicle Technology Journal*, 10(4), 340-356.

Doe, J., Smith, R., & Patel, L. (2021). Structural battery technology and its implications. *Journal of Electrochemical Applications*, 29(1), 122-134.

Johnson, L., & Patel, R. (2022). The future of composite materials in automotive design. *International Journal of Vehicle Materials*, 12(1), 34-50.

Kumar, A., & Lee, H. (2023). Enhancing battery safety with composite thermal management systems. *Energy Solutions*, 14(5), 301-317.

Lee, S. (2021). Advancements in carbon-fiber composites for automotive applications. *Composite Engineering Review*, 9(3), 189-202.

Miller, D., Zhao, X., & Liu, Q. (2023). Challenges in the application of composite materials in electric vehicles. *Sustainable Automotive Materials*, 8(2), 112-128.

Smith, J., & Jones, K. (2023). Lightweighting strategies in the EV industry. *Automotive Innovations Journal*, 15(1), 56-78.

Zhao, W., & Liu, Y. (2023). Nanotechnology and the future of recyclable composites. *Journal of Advanced Materials*, 7(4), 210-230.

Synthesis of Thin Films Using the Sol-Gel Dip-Coating Technique Derived from SnO_2

A. Lahouel[1]*

M. Adnane[1]

S. Koudjeti[2]

[1]University of Science and Technology of Oran-Mohammed Boudiaf, Department of Physics, Oran, Algeria,

[2]University of Sciences of Abou Bekr Belkaid, Department of Physics, Tlemcen, Algeria
*Corresponding

ABSTRACT

Transparent conductive oxides (TCOs) are advanced materials with a wide band gap, transparent in the visible region (400-700 nm), and highly electrically conductive. They are utilized in various applications, such as photovoltaic cells, light-emitting diodes, gas sensors, and flat panel displays (FPDs). These coatings have the ability to change surface properties and can also increase protection and functionality in smart system technologies. The sol-gel coating method is favored in smart technology applications due to its cost-effectiveness, simplicity, and suitability for large-scale production, enabling the synthesis of homogeneous and conformal TCO film coatings.
In this study, to prepare the sol-gel solution, oxide solutions of copper, aluminum, zinc, tin, and titanium (0.1 M) were synthesized using the sol-gel method. The solution was then used to investigate the changing characteristics of the films. The films were coated using the dip-coating technique, creating 10 layers, and annealed at 500°C for 1 hour. Contact angle measurements were performed on these thin films, and the samples exhibited specific properties at the point of contact with water droplets.

Keywords: TCO, Sol-gel procedure, Contact angle

ELECTRONIC AND THERMOELECTRIC PROPERTIES STUDY OF CU_2SE : DFT STUDY

Faiza Baghida

Prof. Dr. Mourad Boughrara

ABSTRACT

The ever-increasing energy problem gives strong impetus to restore efficiency and convert heat into electrical energy, in which thermoelectric materials play a central role. These materials provide a simple and environmentally friendly solution to thermal conversion. Density functional theory (DFT) is an indispensable method for predicting and calculating material properties based on quantum mechanical considerations. Copper selenide (Cu2Se) is a simple binary compound that exhibits very remarkable thermoelectric properties, which is why it has been widely studied. Until very recently. In this work, we studied the structural, electronic and thermal properties of Cu2Se. We also removed Cu for the first time and also removed Se for the purpose of knowing the effect of vacuum on the thermal properties. Seebeck modulus, electrical conductivity, thermal conductivity, and figure of merit were calculated using the BoltzTraP2 tool based on Quantum Espresso code. We used Molecular Dynamics and Lammps with the help of SchengBTE (Boltzmann transport equation) to calculate Kappa.

Keywords: Thermoelectric; Copper-selenide; Density functional theory; Thermal conductivity; Electrical conductivity; SchengBTE

VIETNAM WOMEN STUDIES NANOMATERIALS CONTAINING RARE EARTH IONS AND APPLICATIONS

Tran Kim Anh
Vietnam Academy of Science and Technology, 18 Hoang Quoc Viet, Nghia Do, Cau Giay, Ha Noi Vietnam

ABSTRACT

Review of studies nanomaterials containing rare earth ions and applications poteltial in lighting technology and medical. Tb^{3+}, Eu^{3+}, Er^{3+}, Yb^{3+} ions were doped in some host such as Y_2O_3, Gd_2O_3. $NaYF_4$ synthesis, structure study, luminescent properties were detail studies. We have some NAFOSTED projects and more than 20 international papers in ten years. Energy transfer, upconversion luminescence and life time were presented. Upconverting nanomaterials for bioimaging by the rare earth ions are well known to produce infrared to visible green or red by a two photon of mechanism discussed. The upconversion processes in rare earth ions exhibit a strong power dependence on excitation intensity of 975 nm diod laser. An advantage ofered by the two photon excited. We can use a low power continuos wave diode laser excited. Nanomedicine is an emerging field Er-Yb doped Y_2O_3, Gd_2O_3 or $NaYF_4$ nanoparticles and nanospheres which asbsord infrared light by multistep multiphoton absorption to produce upconversion in green or red provide opportunity for background free bioimaging and deper penetration in cells and tisues,

Keyworks: Women Vietnam, Nanomaterials, Rare earth, Application Poteltial

INTERNATIONAL CERAMICS AND COMPOSITE MATERIALS SYMPOIUM
November 15-16, 2024 / Süleyman Demirel University, Isparta, Türkiye

CHARACTERIZATION OF PET-ACTIVATED CARBON COMPOSITES: EFFECTS OF ORANGE PEEL AND SAWDUST DERIVATIVES

Babafemi Raphael Babaniyi [1*]

Oluwaseun Adekoya Adelaja[2]

Folorunso Patrick Aliu[1]

Monday Peter Obagunwa[1]

[1]Bioresources Development Center, National Biotechnology Research And Development Agency Abuja, Nigeria

[2]Department of Chemistry, School of physical sciences, Federal University of Technology Akure, P.M.B. 704, Akure, Nigeria

ABSTRACT

This study investigates the mechanical, optical, and chemical properties of polyethylene terephthalate (PET) composites reinforced with activated carbon (AC) derived from orange peel and sawdust. The effects of varying AC concentrations on the tensile and flexural properties of the composites were evaluated. The incorporation of AC into the PET matrix resulted in a notable reduction in tensile strength and elongation at break, particularly for composites with higher AC content. Interestingly, composites with orange peel-derived AC exhibited an increase in tensile strength at specific AC concentrations, suggesting a stronger interfacial bonding between the PET matrix and AC. Conversely, the sawdust-derived AC samples showed a progressive decrease in both tensile strength and elongation at break. Flexural tests indicated an initial increase in strength with the incorporation of AC, followed by a subsequent decrease, particularly in samples with higher AC content. Optical properties assessed by UV-Vis spectroscopy revealed shifts in absorption peaks, indicating changes in the conjugation of the PET matrix due to AC addition. Fourier Transform Infrared (FTIR) spectroscopy further confirmed the interaction between the AC particles and the PET matrix, highlighting the presence of functional groups such as N-H, C-H, and C=O. These findings suggest that the type and amount of AC, as well as the nature of the derived material, significantly influence the mechanical and chemical properties of PET-AC composites, which provide an insights for potential applications in material engineering and environmental sustainability.

Keywords: Polyethylene terephthalate (PET), activated carbon (AC), composites, mechanical properties, environmental sustainability.

POLYMERIC MEMBRANES FOR DESALINATION USING MEMBRANE DISTILLATION: A REVIEW

Zineb Ait Fares [1],
Miloudi Hlaibi[1],
Noureddine Kamil [1,2]
Rachid Ouchn[1] .

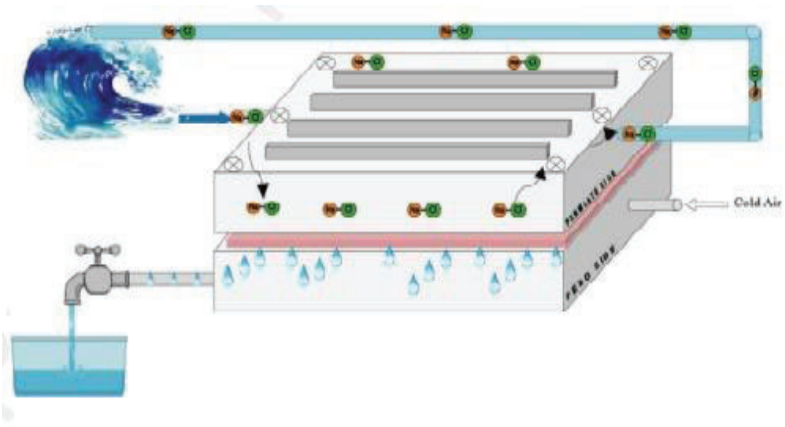
[1] Laboratory of Materials Engineering for Environment and Valorization (GeMEV), Faculty of Sciences Aïn Chock, Hassan II University of Casablanca

[2]Higher School of Technology Casablanca ESTC,

ABSTRACT

Membrane distillation (MD) is considered an emerging technology for seawater desalination. The hydrophobic polymers commonly used for this process are polytetrafluoroethylene (PTFE), polyvinylidene fluoride (PVDF), and polypropylene (PP). An ideal membrane for MD should exhibit characteristics such as high liquid entry pressure, low fouling rate, high permeability, and excellent mechanical resistance. Polymeric membranes, being more cost-effective than ceramic membranes, are considered a more affordable alternative and have dominated the research conducted so far on membrane distillation (MD). This review aims to provide a brief introduction to MD, summarize the research efforts to achieve the desired properties in polymeric membranes used in MD for desalination purposes and focus on the fabrication methods for these membranes

Keywords : Membrane distillation, direct contact membrane distillation DCMD, desalination, polymeric



https://www.sciencedirect.com/science/article/abs/pii/S0142941814002141

IMPACT OF WALNUT SHELL POWDER ON THE PROPERTIES OF POLYPROPYLENE-REINFORCED COMPOSITES

Zineb El Hamri*

M. Alami

M. Assouag

Team of Innovative Materials and Mechanical Manufacturing Processes, ENSAM, University Moulay Ismail, B.P. 15290, Al Mansour, Meknes, Morocco.

*Corresponding

ABSTRACT

The study examined the impact of particle size and filler concentration on the mechanical and functional properties of polypropylene composites reinforced with walnut shell powder. Composites were produced using filler levels from 0 to 20 wt% and particle sizes of 0.100, 0.200, and 0.300 mm, with melt-blending and injection molding employed to achieve uniform distribution. Findings revealed that higher walnut shell filler content consistently led to reductions in tensile strength, elongation at break, and flexural strength for all particle sizes. In contrast, increased filler levels and larger particle sizes resulted in greater hardness and specific gravity. Water absorption was also found to increase with higher filler content, although smaller particle sizes helped to limit this effect. However, the addition of walnut shell powder did not significantly reduce the rate of flame propagation in polypropylene.

Keywords: Polypropylene, Composite, Mechanical and End-Use Properties, Walnut shell.

REFLECTION AND TRANSMISSION OF ACOUSTIC AND ULTRASONIC WAVES IN FUNCTIONALLY GRADED POROUS PIEZOELECTRIC MATERIALS

Anil K. Vashishth

Department of Mathematics, Kurukshetra University, Kurukshetra-136119, Haryana, India

Umang Bareja

Department of Mathematics, Mukand Lal National College, Yamunanagar-135001, Haryana, India

ABSTRACT

The phenomenon of reflection transmission provides crucial insights into the internal composition of structures. This paper investigates the reflection and transmission characteristics of acoustic and ultrasonic waves in a functionally graded half-space (FGPPHS) situated beneath a fluid half-space (FHS). The gradual variation in the substrate's functional properties enhances the model's applicability in fields like ocean acoustics, acoustic devices, and nondestructive evaluation. When waves from the FHS incident upon the FGPPHS, five waves are transmitted into the FGPPHS. The general solution for displacements and stresses is calculated in terms of eigenvalues and eigenvectors. The amplitude and energy ratios have been derived analytically. Numerical analysis explores the effects of incidence angle, frequency, porosity, and graded coefficients on reflection and transmission characteristics, as well as on critical angles. Furthermore, various materials are selected for the FGPPHS, and their impact on material parameters is examined. It is observed that the choice of materials significantly affects the critical angle. The effects of porosity, frequency and grade parameter on the leaky wave velocity are also studied. The findings from this study offer valuable insights applicable to diverse fields such as geophysics, ocean acoustics, acoustic devices, and nondestructive evaluation.

Keywords: Ultrasonic, acoustic, structure

T.C.
SÜLEYMAN DEMİREL ÜNİVERSİTESİ
Genel Sekreterlik
Yazı İşleri Şube Müdürlüğü

Sayı :E-70038785-903.07-838879 Tarih: 17.09.2024
Konu :Uluslararası Seramik ve Kompozit Malzemeler Sempozyum Düzenleme Kurulu

DAĞITIM YERLERİNE

Üniversitemiz tarafından 15-16 Kasım 2024 tarihlerinde düzenlenmesi planlanan *"Uluslararası Seramik ve Kompozit Malzemeler Sempozyumu"* na yazımız ekinde yer alan öğretim üyeleri ve ögretim elemanları, sempozyum düzenleme kurulu üyesi olarak görevlendirilmesi uygun görülmüştür.

Gereğini rica ederim.

Prof.Dr. Mehmet SALTAN
Rektör

Ek: Liste (1 Sayfa)

DAĞITIMLAR:
Gereği
Mühendislik Ve Doğa Bilimleri Fakültesi
Dekanlığına
Güzel Sanatlar Fakültesi Dekanlığına
Isparta Sağlık Hizmetleri Meslek Yüksekokulu
Müdürlüğüne

Bu evrak 5070 sayılı Elektronik İmza Kanununun 5. maddesi gereğince güvenli elektronik imza ile imzalanmıştır.

Belge Doğrulama Kodu: 77927D6D Belge Takip Adresi: https://www.turkiye.gov.tr/sdu-ebys
SDÜ Batı Yerleşkesi ÇÜNÜR/ISPARTA Bilgi İçin:Servet KAPLAN
Tel No:(246) 211-8046 Faks No:(246) 211-1069 Şef
E-Posta:yaziisleri@sdu.edu.tr İnternet Adresi:http://genelsekreterlik.sdu.edu.tr/ Tel No:1745
Kep Adresi: sdu@hs01.kep.tr

ULUSLAR ARASI SERAMİK VE KOMPOZİT MALZEMELER SEMPOZYUMUNA GÖREVLENDİRİLEN PERSONEL

Sıra No	Ünvanı	Adı Soyadı	Görevli Olduğu Birim
1	Prof. Dr.	Ayşe ÖNDÜRÜCÜ	Mühendislik ve Doğa Bilimleri Fakültesi Dekanlığı
2	Prof. Dr.	Ayşegül ÖKSÜZ	Mühendislik ve Doğa Bilimleri Fakültesi Dekanlığı
3	Prof. Dr.	Bilgehan İlker HARMAN	Mühendislik ve Doğa Bilimleri Fakültesi Dekanlığı
4	Prof. Dr.	Gülcan ÖZKAN	Mühendislik ve Doğa Bilimleri Fakültesi Dekanlığı
5	Prof. Dr.	Mehmet AVCAR	Mühendislik ve Doğa Bilimleri Fakültesi Dekanlığı
6	Prof. Dr.	Mustafa GENÇ	Güzel Sanatlar Fakültesi Dekanlığı
7	Prof. Dr.	Recai Fatih TUNAY	Mühendislik ve Doğa Bilimleri Fakültesi Dekanlığı
8	Prof. Dr.	Serdal TERZİ	Mühendislik ve Doğa Bilimleri Fakültesi Dekanlığı
9	Doç Dr.	Serap ÜNAL	Güzel Sanatlar Fakültesi Dekanlığı
10	Dr. Öğr. Üyesi	Ekinhan ERİŞKİN	Isparta Sağlık Hizmetleri Meslek Yüksekokulu Müdürlüğü
11	Araştırma Görevlisi	Ayşe Melike BİRCAN	Güzel Sanatlar Fakültesi Dekanlığı

INTERNATIONAL CERAMICS AND COMPOSITE MATERIALS SYMPOSIUM

NOVEMBER 15-16, 2024 / ISPARTA, TÜRKİYE

Süleyman Demirel University

20.12.2024

REF: Akademik Teşvik

İLGILI MAKAMA;

Uluslararası Seramik ve Kompozit Malzemeler Sempozyumu, 15-16 Kasım 2024 tarihleri arasında Süleyman Demirel Üniversitesi'nde 13 (Türkiye, Azerbaycan, Almanya, Çin, Polonya, Romanya, Fas, Cezayir, Hindistan, İran, Pakistan, Vietnam, Nijerya) farklı ülkenin (Türkiye 31 bildiri- Diğer ülkeler 34 bildiri) akademisyen/araştırmacılarının katılımıyla gerçekleşmiştir.

Kongre 16 Ocak 2020 Akademik Teşvik Ödeneği Yönetmeliğine getirilen "Tebliğlerin sunulduğu yurt içinde veya yurt dışındaki etkinliğin uluslararası olarak nitelendirilebilmesi için Türkiye dışında en az beş farklı ülkeden sözlü tebliğ sunan konuşmacının katılım sağlaması ve tebliğlerin yarıdan fazlasının Türkiye dışından katılımcılar tarafından sunulması esastır." değişikliğine uygun düzenlenmiştir.

Bilgilerinize arz edilir,

Saygılarımla

Assoc. Prof. Dr. Serap ÜNAL

Süleyman Demirel University

HEAD OF ORGANIZING COMMITTEE

DÜZENLEME KURULU BAŞKANI